
Novel Applications of α -Diazocarbonyl Compounds and
Enabling Technologies in Stereoselective Synthesis



A Thesis Submitted to Cardiff University
in Fulfilment of the Requirements for the
Degree of Doctor of Philosophy by

Micol Santi

PhD Thesis, May 2020

Cardiff University

Acknowledgments

Words will never fully express the gratitude I have for everyone who has spent their time to help and support me during my PhD.

First of all, I would like to thank my supervisor Prof. Thomas Wirth, for giving me the opportunity to work in his research group, for his constant interest and availability, despite his busy schedule. He has always encouraged me to develop my own ideas and supported even the most creative ones.

Next, I would like to thank all the past and present members of the Wirth group, who I had the pleasure to share some time with, in and outside the laboratory. Special thanks to Tobi for his remarkable support. Since day one, he has celebrated my achievements and helped me getting over the most disappointing days. Thank you for reminding me what I am capable of when I am not able to see it myself, and for making sure I was getting to work on time in the morning. Thanks to Ana who was literally by my side from the very beginning and who had to cope with hundreds of my daily questions. Next, I would like to thank Filipa for keeping me motivated to go to the gym during lunch breaks and for that walk in the park when everything felt a bit too much. A huge thanks to Marina. Since she has joined the group, she has improved my working days with her positive vibes. Also, she has kindly read and corrected every piece of work I have written so far including my job applications, so I really owe her big time. Thanks to Matt for being always so energetic and truly one of my favourite people to spend a night out with. Having him in the group was a blast, especially because his messy desk made mine look nicer. Thanks to Ziyue for being a great example in the lab and for being someone to look up to. Also, thank you for your hilarious straight-to-the-point comments and for teaching me some cool dance moves. A sincere thanks to Doc. After a first rough start, we became very good friends and there has been nothing he has not helped me with. Thanks to Donya for always sharing her honest opinion. She helped me growing as a researcher and prevented my presentations from going too wild. I would also like to thank the "electrochemistry squad": Jakob, Nasser and Beth who introduced me to the whole wild world of flow-electrochemistry. Thank you for your time and your help. Special thanks are due to all the students I had the pleasure to supervise during this time: Niklas, Alex, Weronika (twice!), Dorothea, Stefano, Adele, Tom and Ben. They taught me more than they can possibly imagine. Thanks to Kurt and Ben for entertaining a typical day in the lab with their creative playlists.

I would also like to thank Dr Rebecca Melen, and her group members. In particular Darren, Jamie, Jan and Yashar for their help in the borane project and the moral support. Moreover, I would like to thank Dr Daniel Tray and Simon Bate from GSK UK, for our discussions about Design-of-Experiment. Their advice was extremely helpful, in particular for the last project. A special mention to my monitoring panel, Dr Duncan Browne and Dr Louis Morrill, for our interesting and inspiring discussions about my projects. Thanks to all the technicians from Cardiff University. Their work and friendly chats were much appreciated. An additional thanks to Doc, Ana, Alex, my dad, Marina, Jamie and Tobi for correcting and proof-reading this thesis.

Big shout out to all amazing people I met that kept the party going, even with social-distancing: Deborah, Rhiannon, Alexandra, Alex, Jamie, Flo, Nicolò, Davide, Martin, Tom, Riccardo, Kim, Mike, Antoine, Jake, Nicolas, Melina, Rodolfo, Joey, Chrissy and James. Thank you for the great time!!

Thanks to Dieter and Kerstin for welcoming me, allowing me finish writing up in a quiet place far away from the chaos.

Obviously, a “Grazie” is due to all the support “from home”. Grazie alle vere amicizie, quelle che nonostante il tempo e la distanza, ancora chiamano, scrivono, si interessano e si ricordano. Ai CTFini, che non dicono mai di no ad una reunion quando torno. Grazie Laura che ancora ascolta tutti i miei messaggi vocali, anche quelli di otto minuti. Grazie Gioia per rendere ogni mio piccolo traguardo una “big deal” ed una ragione in più per celebrare con me con un bicchiere di vino.

Alla mia famiglia son grata per tante cose. In particolare, per avermi spronato ad andare ma soprattutto a restare quando io volevo prendere e partire. Grazie Elen per i thè delle 5 e le lezioni di yoga su Skype. Grazie per rendermi sempre partecipe facendomi sentire leggermente meno il peso dei chilometri di distanza. Grazie mamma, per tutte le volte che hai ascoltata lamentarmi troppe volte delle stesse cose per ore di fila. Grazie papà per tutti i consigli e per aver trovato sempre il tempo di leggere le mie bozze. Grazie per tutto il vostro costante supporto ed incoraggiamento.

This PhD-journey would have been a lot harder without each and every one of you. Thank you.

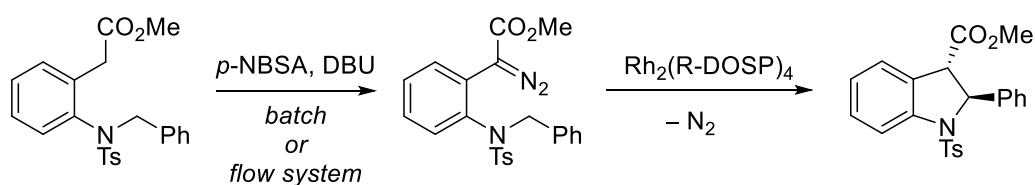
Micol

A mia madre, mio padre ed Elen

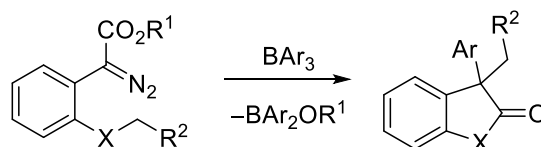
Abstract

α -Diazocarbonyl compounds are widely used in organic chemistry as versatile carbene precursors which enable concise synthesis towards complex asymmetric molecules. Due to their intrinsic highly energetic nature, flow technology can be applied to ensure safer, scalable and efficient protocols. Other modern enabling tools such as Design of Experiment (DoE) and online analysis, provide great advantages to achieve faster analysis and optimisations of chemical transformations.

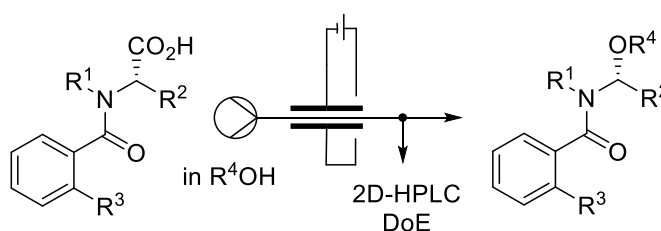
In the first part of this work, α -diazocarbonyl compounds have been used in the enantioselective synthesis of novel *trans*-indolines.¹



The synthesis of the diazo precursors, previously investigated in batch, was translated into a flow system and optimised following a DoE-approach. Moreover, highly Lewis acidic boranes were found to enable related α -diazocarbonyl compounds to undergo a metal-free transfer/rearrangement cascade reaction towards asymmetric benzofuran-3*H*-ones.²



The focus in the final part of this work was on the development of a faster analytical method for an accelerated optimisation of stereoselective reactions. The reactions were performed in a continuous flow electrochemical reactor directly coupled to a 2D-HPLC for immediate online analysis, which allowed a fast screening of reaction conditions using DoE.³



Publications

- 1 M. Santi, S. T. R. Müller, A. A. Folgueiras-Amador, A. Uttry, P. Hellier, T. Wirth, *Eur. J. Org. Chem.* **2017**, 1889–1893.
- 2 M. Santi, D. M. C. Ould, J. Wenz, Y. Soltani, R. L. Melen, T. Wirth, *Angew. Chem. Int. Ed.* **2019**, 58, 7861–7865.
- 3 M. Santi, J. Seitz, R. Cicala, T. Hardwick, N. Ahmed, T. Wirth, *Chem. Eur. J.* **2019**, 25, 16230–16235.

List of Abbreviations

°C	Degree Celsius
λ	Wavelength
δ	Chemical Shift
¹ D	First dimension (2D-HPLC)
² D	Second dimension (2D-HPLC)
1D-LC	One-dimensional Liquid Chromatography
2D-LC	Two-dimensional Liquid Chromatography
2D-HPLC	Two-dimensional High Performance Liquid Chromatography
2FI	Two-factor Interaction
Ac	Acetyl
A	Ampere
AN	Acceptor Number
APCI	Atmospheric Pressure Chemical Ionisation
API	Active Pharmaceutical Ingredient
Ar	Aryl
ASAP	Atmospheric Solid Analysis Probe
BDD	Boron Doped Diamond
BPR	Back-pressure Regulator
calc.	calculated
cat.	catalytic
CCD	Circumscribed Composite Design
CCF	Central Composite Faced design
conv.	conversion
CV	Cyclic Voltammetry
DBU	1,8-Diazabicycloundec-7-ene
dec.	decomposition
DFT	Density Functional Theory
DIAD	Diisopropyl azodicarboxylate
DMAP	4-Dimethylaminopyridine
DIPEA	<i>N,N</i> -diisopropylethylamine
DOSP	Dodecylphenylsulfonylprolinate
DMF	<i>N,N</i> -Dimethylformamide
DMSO	Dimethyl sulfoxide
DoE	Design of Experiments

<i>d.r.</i>	diastereomeric ratio
EDA	Ethyl diazoacetate
EDG	Electron Donating Group
<i>ee</i>	enantiomeric excess
<i>e.r.</i>	enantiomeric ratio
EI	Electron Ionisation
equiv.	equivalent
ES	Electrospray Ionisation
Et	Ethyl
EWG	Electron Withdrawing Group
F	Faraday
FD	Full Design
FFD	Full Factorial Design
FLPs	Frustrated Lewis Pairs
g	gram
GC	Gas Chromatography
h	hour
HPLC	High Performance Liquid Chromatography
HRMS	High Resolution Mass Spectrometry
HTC	Hard-To-Change
HTS	High-Throughput-Screening
Hz	Hertz
Ile	Isoleucine
<i>i</i> -Pr	<i>iso</i> -Propyl
IR	Infrared
<i>J</i>	coupling constant
L	litre
LC	Liquid Chromatography
LCxLC	Comprehensive two-dimensional Liquid Chromatography
LC-LC	Heart-cutting two-dimensional Liquid Chromatography
LDA	Lithium diisopropylamide
LiHMDS	Lithium bis(trimethylsilyl)amide
M	molarity
m	meter
m.p.	melting point
m/z	mass over charge ratio
Me	Methyl
X	

MS	Mass Spectrometry
Ms	Mesyl
min	minute
mol	mole
MRC	Metallo-radical Catalysis
<i>n</i> -BuLi	normal butyllithium
NBR	<i>N</i> -bromosuccinimide
NHS	<i>N</i> -hydroxysuccinimide
NMR	Nuclear Magnetic Resonance
NP-LC	Normal-phase Liquid Chromatography
NSI	Nanospray Ionisation
<i>p</i> -ABSA	<i>p</i> -Acetamidobenzenesulfonyl azide
PET	Positron Emission Tomography
Ph	Phenyl
PMP	<i>p</i> -Methoxyphenyl
<i>p</i> -NBSA	<i>p</i> -Nitrobenzenesulfonyl azide
ppm	parts per million
PTAD	<i>N</i> -Phthalimido-1-adamantyl acetate
PTFE	Polytetrafluoroethylene
PTTL	<i>N</i> -phthamido-1- <i>tert</i> -leucinate
Pyr	Pyridine
R_f	Retention factor
RP-LC	Reverse-phase Liquid Chromatography
RSM	Response Surface Model
rt	room temperature
<i>t</i> -Bu	<i>tert</i> -Butyl
TEA	Triethylamine
TFA	Trifluoroacetic acid
THF	Tetrahydrofuran
TLC	Thin-Layer Chromatography
Ts	Tosyl
<i>vs</i>	<i>versus</i>
V	Volt

Table of Contents

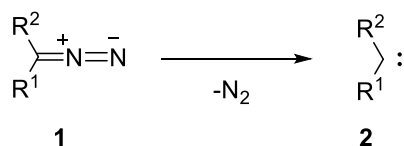
Abstract	VII
List of Abbreviations	IX
CHAPTER 1: Introduction	1
1.1 α -Diazocarbonyl Compounds in Organic Synthesis	1
1.1.1 Synthesis of α -Diazocarbonyl Compounds	3
1.1.2 Reactivity of α -Diazocarbonyl Compounds	9
1.2 General Introduction on Enabling Technologies	23
1.2.1 Flow Chemistry	23
1.2.2 Design of Experiment	32
References	37
CHAPTER 2: Synthesis of Novel <i>trans</i> -Dihydroindoles	47
2.1 Introduction	47
2.2 Results and Discussion	53
2.2.1 Synthesis of the Starting Materials	53
2.2.2 Synthesis of α -Diazocarbonyl Precursors	58
2.2.3 Optimisation of the C–H Insertion Reaction	72
2.3 Conclusion and Outlook	78
References	79
CHAPTER 3: Synthesis of Fluorinated Benzofuranones	83
3.1 Introduction	83
3.2 Results and Discussion	88
3.2.1 α -Functionalisation of Esters	89
3.2.2 Synthesis of α,α -Disubstituted Benzofuranones	98
3.3 Conclusion and Outlook	116
References	118
CHAPTER 4: Synthesis of <i>N,O</i> -acetals in a Flow Electrochemical Microreactor	121
4.1 Introduction	121
4.1.1 Continuous Flow Setup and 2D-HPLC	128
4.1.2 2D-HPLC	129
4.2 Results and Discussion	133

4.2.1	Synthesis of the Starting Materials and Racemates	133
4.2.2	Optimisation of Asymmetric non-Kolbe Oxidation	136
4.2.3	Substrate Scope	144
4.3	Conclusions and Outlook	149
	References	150
	CHAPTER 5: Experimental Part	153
5.1	General Methods	153
5.2	Experimental Data for Chapter 2.....	156
5.2.1	Synthesis of Starting Materials.....	156
5.2.2	Diazo-transfer Reaction in Batch	171
5.2.3	Diazo-transfer in Flow and DoE	179
5.2.4	Synthesis of Dihydroindoles.....	184
5.2.5	<i>In Situ</i> ¹ H NMR Experiment: Temperature Effect	194
5.2.6	Evidence for Triazene 167	195
5.3	Experimental Data for Chapter 3.....	196
5.3.1	Synthesis of Diazo Precursors	196
5.3.2	Synthesis of α -Aryl Esters.....	223
5.3.3	Synthesis of Cyclised Products.....	236
5.3.4	Characterisation of Phenol Side Product 230	249
5.4	Experimental Data for Chapter 4.....	251
5.4.1	Synthesis of Starting Materials.....	251
5.4.2	Synthesis of <i>N,O</i> -acetals	256
5.4.3	DoE-assisted Optimisation.....	264
5.4.4	Cyclic Voltammetry	269
	References	270
	Appendix A: Glossary of DoE Terminology	273
	Appendix B: Kinetic Data Table for 185a Formation	279

CHAPTER 1: Introduction

1.1 α -Diazocarbonyl Compounds in Organic Synthesis

Diazo compounds are a class of neutral organic reagents presenting a terminal dinitrogen moiety (Scheme 1.1).

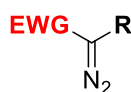


Scheme 1.1: Diazo compound **1** as precursor for carbene species **2**.

The highly energetic carbon-nitrogen bond can be cleaved, releasing molecular nitrogen N_2 and generating the reactive carbene species **2**. For this reason, since their discovery in 1858 by Peter Griess,¹ diazo compounds are widely used in organic chemistry as versatile building blocks. However, due to their intrinsic reactivity, diazo intermediates are also highly toxic and explosive.² Several explosions due to diazomethane have been reported as result of its fast decomposition at higher temperatures or in contact with scratched glassware.³ This high reactivity has limited their applications especially in industrial setting.

Diazo compounds can be classified into three groups according to the electronic properties of their substituents (Figure 1.1).⁴

Class I



- "acceptor/acceptor", R = EWG
- "acceptor", R = H, alkyl

used for: cyclopropanation, intramolecular X–H insertion (X=C,N,O), carbonyl ylides generation

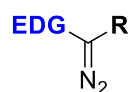
Class II



- "donor/acceptor"

used for: cyclopropanation, intra- and intermolecular X–H insertion (X = C,N,O)

Class III

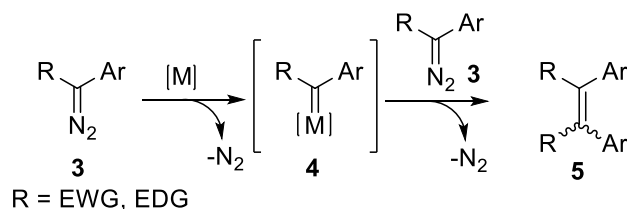


- "donor/donor", R = EDG
- "donor", R = H, alkyl

used for: intramolecular C–H insertion

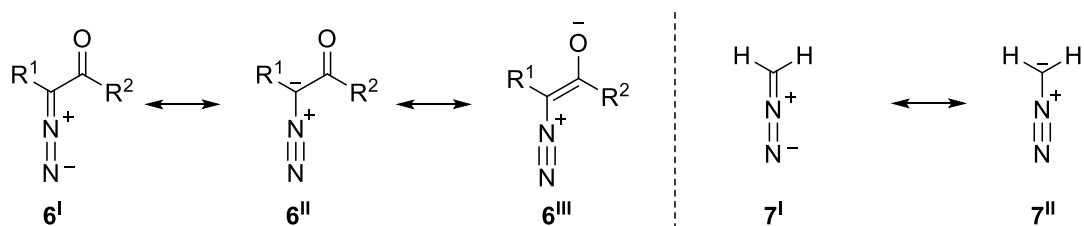
Figure 1.1: Diazo compounds classified according to the electronic properties of the substituents: EWG = carbonyl, sulfonyl, cyano, nitro, phosphonate group; EDG = aryl, heteroaryl, vinyl group.

Early works in the area of diazo chemistry focused on the first class of diazo compounds bearing one (“acceptor”) or two (“acceptor/acceptor”) electron-withdrawing groups (EWG) such as dicarbonyl diazo or α -diazo ester. These electrophilic molecules generate highly reactive carbene intermediates that found applications in a wide range of transformations from cyclopropanation⁵ to X–H insertion (X = C, O, N)⁶ and generation of ylides.⁷ However, due to the high electrophilic nature of the carbon atom and the inability of the EWG to stabilise the carbene centre, this class of compounds is characterised by low selectivity especially in intermolecular insertions, therefore they are mainly used for intramolecular processes. Subsequently, Davies and co-workers explored how proximal electron-donating groups (EDG), such as aryl or vinyl moieties, provide more stable carbene precursors (Class II). For this reason, and due to their slightly attenuated reactivity, “donor/acceptor” diazo compounds can be engaged in more selective intermolecular reactions.⁸ While these first two classes have received more attention, just a few examples have been reported using the third class of diazo compounds. The “donor/donor” carbene precursors have been known for many years but their electron-rich character makes their isolation problematic and an *in situ* generation is often required.^{4a,9} Furthermore, these types of diazo compounds are reported to be highly explosive and they are subjected to a fast dimerisation which limits their applicability (Scheme 1.2).



Scheme 1.2: Dimerisation of “donor/acceptor” and “donor/donor” diazo compounds.

This work of thesis mainly focuses on the synthesis and reactivity of donor/acceptor diazo compounds such as **6**, that are generally preferred over diazoalkane intermediates because of their higher stability (Scheme 1.3). The additional resonance structure **6^{III}** presents a negative charge located on the more electronegative oxygen atom which stabilises the dipole of the diazo functional group. On the contrary, when the negative and the positive charge are located next to each other as in diazomethane (**7**), the loss of N₂ is thermodynamically favoured and therefore the compound is less stable.



Scheme 1.3: Resonance structures for α -diazocarbonyl compound **6** and diazomethane (**7**).

The thermal properties of diazo compounds are the reason why large-scale syntheses are still scarce, despite the advantages on selectivity of “donor/donor” carbene and the increased stability of “donor/acceptor” carbenes. Nevertheless, in the last two decades, continuous flow chemistry has proven to be a safer alternative for the synthesis of diazo compounds. As discussed later in this chapter, due to the better control of the temperature and the possibility to generate *in situ* highly energetic diazo precursors, flow chemistry enables “safer” protocols for the synthesis of diazo compounds, even in large-scale reactions.^{10,11}

1.1.1 Synthesis of α -Diazocarbonyl Compounds

Diazocarbonyl compounds are widely used as valuable intermediate in organic chemistry and some diazo-containing compounds such as the kinamycins and Lomaiviticin A were also isolated from natural products (Figure 1.2).¹²

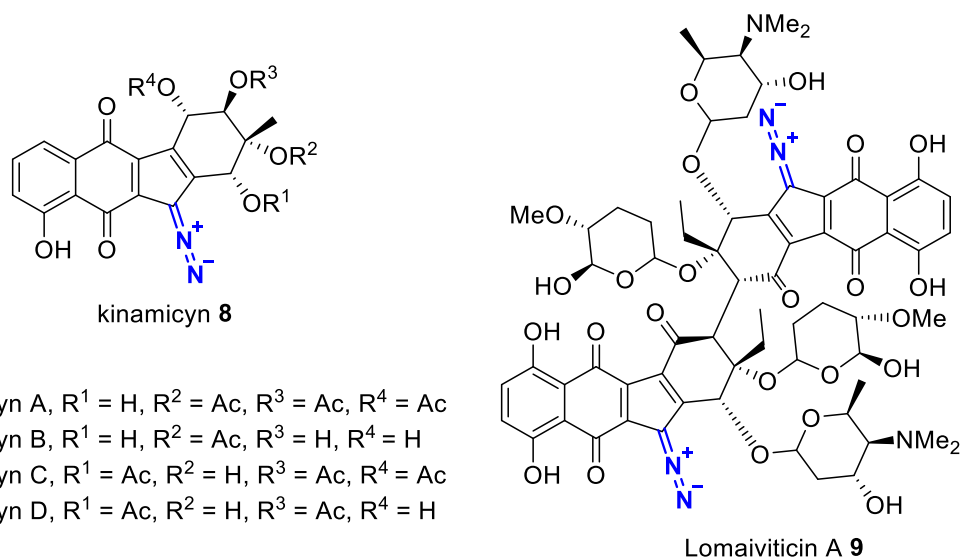
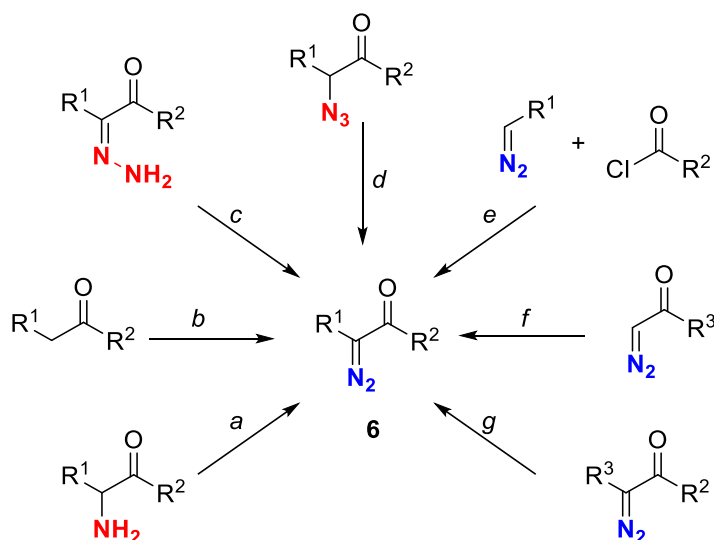


Figure 1.2: Examples of natural products containing the diazo moiety.

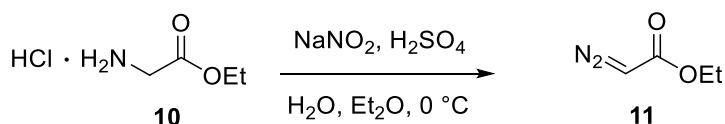
The broad use of diazocarbonyl compounds relies on well-established and efficient synthetic methods depicted in Scheme 1.4: diazotisation of amino acids (a), diazo-transfer reactions (b), dehydrogenation of hydrazones (c), modification of azides

(d), acylation of diazoalkanes (e), substitution/cross-coupling (f) and substituent modification (g).¹³



Scheme 1.4: Classic routes to α -diazocarbonyl compounds (**6**): a) diazotisation of amino acids; b) diazo-transfer reactions; c) dehydrogenation of hydrazones; d) modification of azides; e) acylation of diazoalkanes; f) substitution/cross-coupling; g) substituent modification.

The first reported approach toward diazo compounds dates back to 1883, with the pioneering work of Curtius on the diazotisation of amino acids as a way of preparing ethyl diazoacetate (EDA, **11**) from ethyl glycine ester (**10**) hydrochloride (Scheme 1.5).¹⁴ Nowadays, this reaction is mainly used for the synthesis of diazonium salts¹⁵ and azides,¹⁶ while the introduction of a diazo moiety *via* diazotisation is less common.

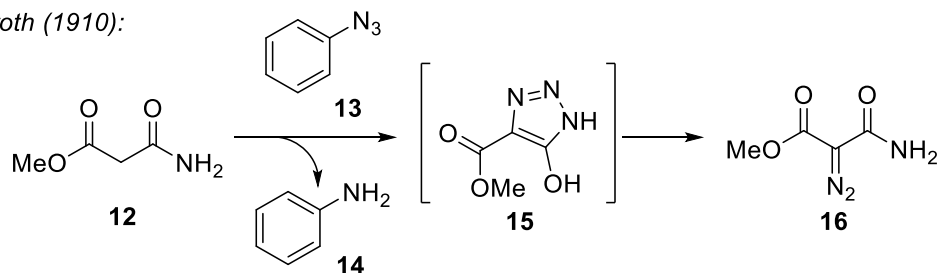


Scheme 1.5: First reported synthesis of ethyl α -diazoacetate **11** *via* diazotisation of amino acid **10**.¹⁴

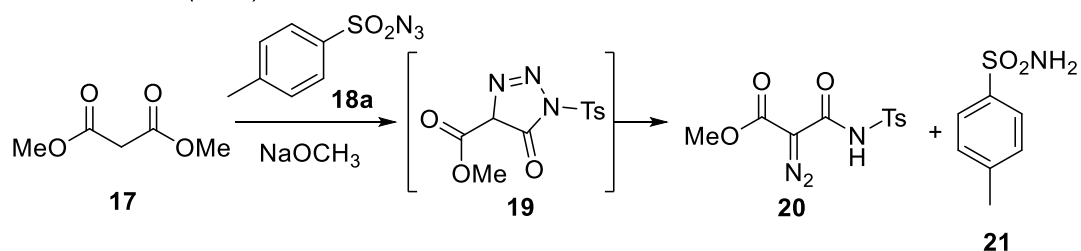
In 1910, Dimroth reported the reaction between the malonic ester amide (**12**) and phenyl azide (**13**) to give diazomalonic ester (**16**) *via* triazole intermediate **15** (Scheme 1.6).¹⁷ A few years later Curtius and Klavehn prepared methyl diazo-*N*-tosylamide **20** from dimethyl malonate **17** using *p*-toluenesulfonyl azide **18a** and suggesting **19** as intermediate.¹⁸ However, these reactions remained unacknowledged until 1964 when Regitz, inspired by the above-mentioned works, investigated the reaction between the sulfonyl azide **18a** and the ketone anthrone (**22**) in pyridine/ethanol and isolated the corresponding diazocarbonyl **23** and tosylsulfonamide **21** as the side product.¹⁹ This base-promoted transfer of a diazo group from a sulfonyl azide reagent onto an activated

methyl or methylene group carries the name of Regitz diazo-transfer, in honour of the German chemist who first explained the mechanism in 1964.²⁰

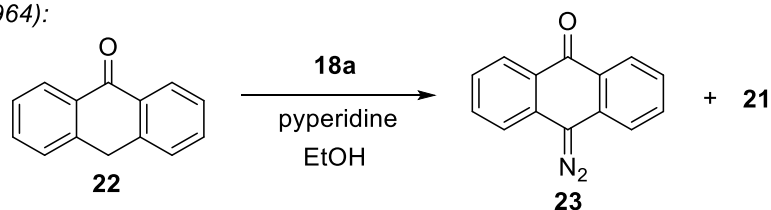
Dimroth (1910):



Curtius and Klavehn (1926):

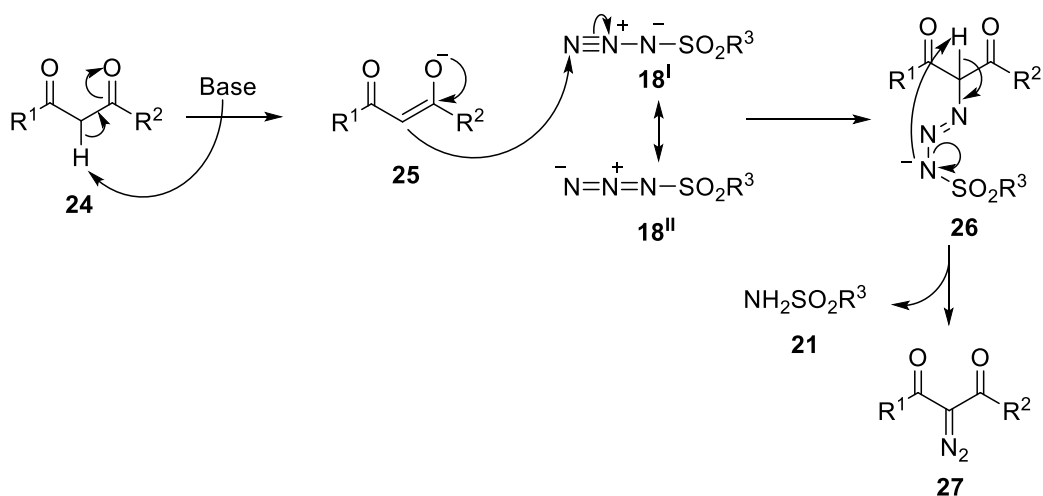


Regitz (1964):



Scheme 1.6: First examples of diazo-transfer reactions.

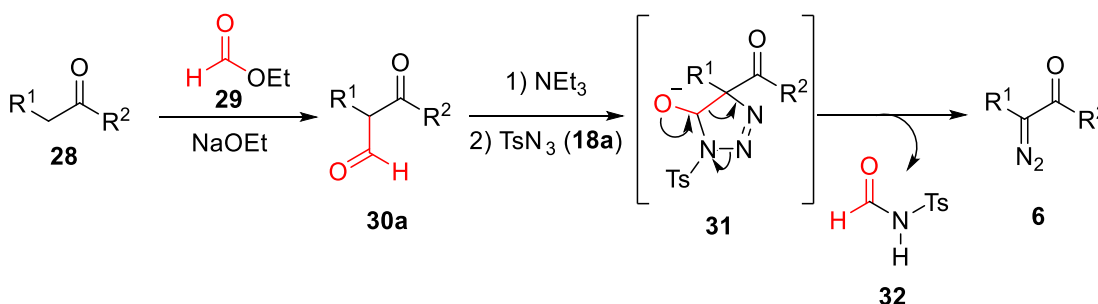
According to the general mechanism, the diazo group is transferred from a diazo-transfer reagent **18**, which is generally a sulfonyl azide, to the desired substrate bearing an activated methylene moiety such as the 1,3-dicarbonyl **24** under basic conditions (Scheme 1.7).



Scheme 1.7: General mechanism of the α -diazo-transfer between the 1,3-dicarbonyl **24** and a sulfonyl azide **18**.

The activated substrates **24** bearing one or more EWG can be deprotonated in the α -position by a relatively weak base such as triethylamine (TEA), diethylamine or pyridine forming the enolate **25**. This reacts with the sulfonyl azide **18** generating the triazene **26** that decomposes into the α -diazo- β -dicarbonyl compound **27** and releases sulfonamide **21** as the side product. When less acidic methylene moieties are present, as in “donor/acceptor” precursors, it is necessary to use a slightly stronger base. For instance, α -aryl carbonyl substrates react better with 1,8-diazabicyclo[5.4.0]-undec-7-ene (DBU)²¹ than with TEA, and for α -aryl amides stronger bases, such as LiHMDS²² and LDA,²³ are typically used. However, even with strong bases, the diazo-transfer does not occur at the α -position of simple cyclic and acyclic ketones bearing no additional EWG in β -position. To overcome this problem, Regitz and co-workers developed a deformylative diazo-transfer reaction using pre-functionalised substrates (Scheme 1.8).²⁴ The ketone **28** is activated *via* a Claisen-type condensation with ethyl formate (**29**) generating **30a**. The activated methylene group is able to undergo a 1,3-dicarbonyl cycloaddition in the presence of tosyl azide **18a** and TEA to form the triazole **31**. Next, the intermediate **31** decomposes to the α -diazoketone **6** releasing *N*-formylamide **32** as the side product.

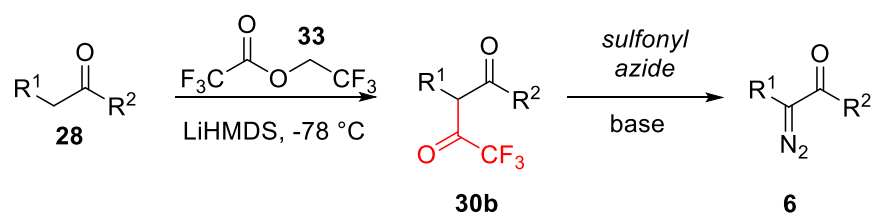
Regitz and co-workers (1968):



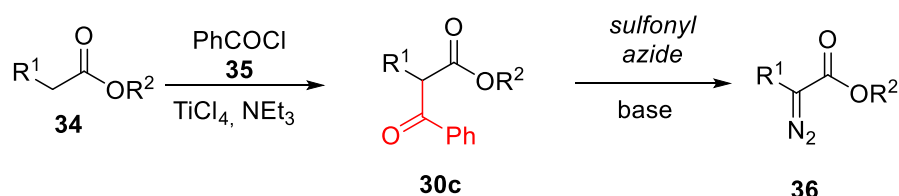
Scheme 1.8: Deformylative diazo-transfer approach.²⁴

Several modifications have been made to improve the efficiency of this reaction. For example, Danheiser and co-workers reported a two-step process using 2,2,2-trifluoroethyl trifluoroacetate (**33**) for the formation of the activated **30b** from an *in situ* generated lithium enolate for high-yielding synthesis of diazoketones **6** (Scheme 1.9).²⁵ Alternatively, Taber *et al.* reported an efficient benzoylation for the preparation of α -diazo esters **36**, which avoids the use of strong bases and cryogenic conditions.²⁶ In this case, the α -benzoyl intermediate **30c** is achieved *via* a titanium chloride-mediated benzoylation followed by a milder diazo-transfer reaction which affords the diazo compound **36** from a base-sensitive precursor **34**.

Danheiser and co-workers (1990):



Taber and co-workers (2005):



Scheme 1.9: Modification of the Regitz deformylative diazo-transfer approach.

The main drawback of the diazo-transfer approach is the potential hazards associated with the azides used as diazo-transfer reagents (Figure 1.3). The first sulfonyl azides to be used for this purpose were *p*-toluenesulfonyl azide (**18a**, TsN_3)^{20a} and mesyl azide (**18b**).²⁷ After stability studies, *p*-dodecylbenzenesulfonyl azide (**18c**, *p*-DBSA)²⁸ and 2,4,6-triisopropylbenzenesulfonyl azide (**18d**, trisyl azide)²⁹ were proposed later as safer alternatives.³⁰ Nowadays, the most commonly used diazo-transfer reagents are *p*-acetamidobenzenesulfonyl azide (**18e**, *p*-ABSA)³¹ and 4-nitrobenzenesulfonyl azide (**18f**, *p*-NBSA).³² Additional sulfonyl reagents are imidazole-1-sulfonyl azide salt **18h**,³³ ionic liquid sulfonyl azides,³⁴ as well as polystyrene-supported benzenesulfonyl azide.³⁵

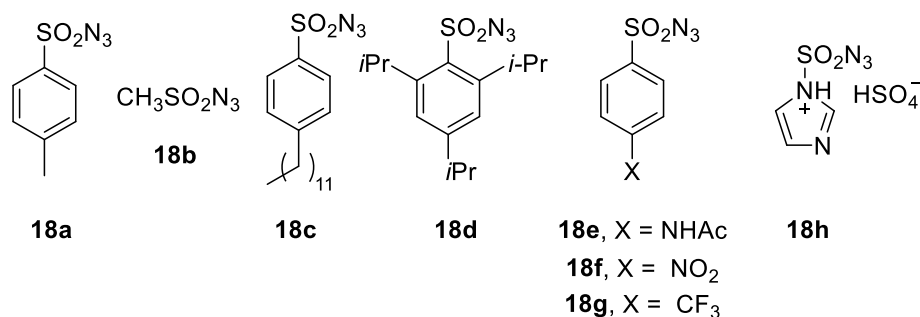
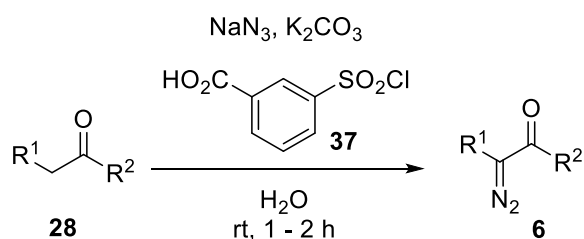


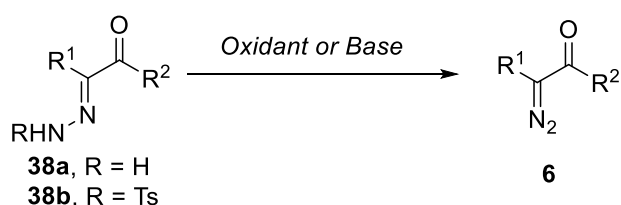
Figure 1.3: Sulfonyl azides commonly used as diazo-transfer reagents **18**.

Moreover, a sulfonyl-azide-free procedure has been recently reported where the diazo-transfer reagent is generated *in situ* using a mixture of sodium azide and *m*-carboxybenzenesulfonyl chloride **37** (Scheme 1.10).³⁶ Nevertheless, considering also the hazards linked to sodium azide, particular attention has to be taken when handling these reagents. Furthermore, some azides may be labelled as “safer” due to their less explosive nature but they can still be equally as toxic and shock-sensitive.



Scheme 1.10: 'Sulfonyl-Azide-Free' aqueous-phase diazo-transfer reaction.³⁶

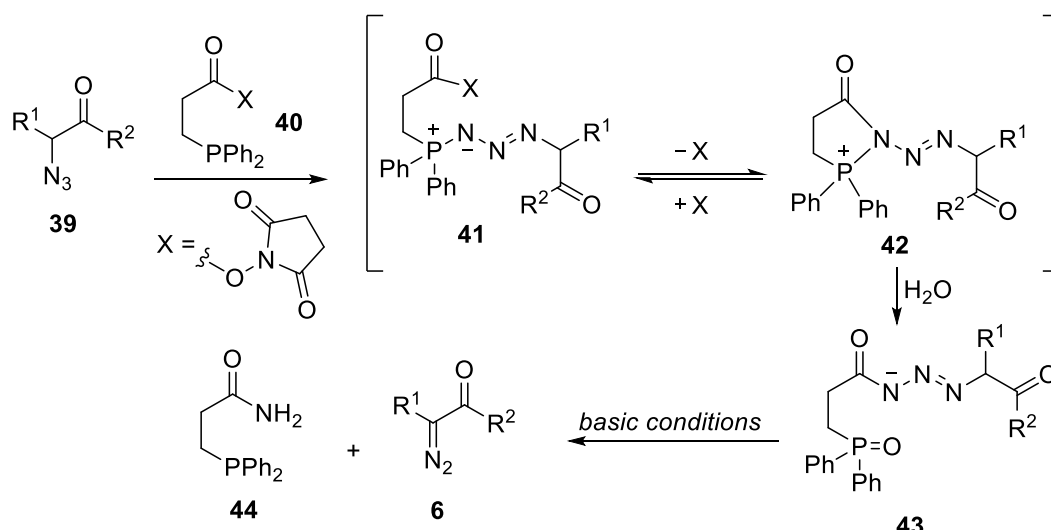
A common but mechanistically different way to prepare donor/acceptor and donor/donor diazo compounds is the dehydrogenation of hydrazones **38** (Scheme 1.11).³⁷ This procedure can be carried out on a simple hydrazone such as **38a**, using stoichiometric quantities of different oxidants such as $\text{Pb}(\text{OAc})_4$,^{37a} Ag_2O ^{37b} or more environmentally friendly "activated" DMSO ³⁸ and MnO_2 .³⁹



Scheme 1.11: Dehydrogenation of hydrazones **38a** and tosylhydrazones **38b** to generate **6**.

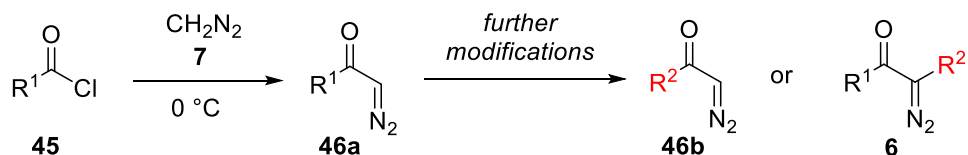
The more air stable tosylhydrazones **38b** can be also used to obtain diazo compounds *in situ* in the presence of a base *via* Bamford-Stevens type reaction.^{9c,40} Generally, the performances are drastically improved when the oxidation occurs under continuous flow conditions,¹⁰ as the reactive diazo intermediate is generated *in situ* and immediately used in a further transformation.

Over the last decade the direct conversion of azides **39** into the corresponding diazo moiety *via* triazene fragmentation has emerged as a new and efficient procedure to generate α -diazocarbonyl compounds (Scheme 1.12).⁴¹ This convenient approach, which has recently found its application in the synthesis of natural product such as aperiodine,²² was reported for the first time by Myers and Raines in 2009.⁴¹ Myers *et al.* designed the phosphine **40** in order to trap **41** into an acyl triazenenophosphonium salt such as **42**, which would then lead to acyl triazene **43** upon aqueous work-up. The following fragmentation of **43** under basic conditions (NaHCO_3 or DBU) affords the desired diazo compound **6** and the amide **44** as side product.



Scheme 1.12: Phosphine-mediated azide conversion into diazo compounds.⁴¹

A convenient way towards terminal α -diazo compounds **46** is the acylation of diazomethane (**7**) with acyl halides **45** (Scheme 1.13). It is worth mentioning that some terminal α -diazocarbonyl compounds^{13b} are stable enough to be subjected to further transformations such as substituent modifications⁴² or cross-coupling reactions.⁴³ This method provides access to various diazo compounds that are difficult to synthesise otherwise.



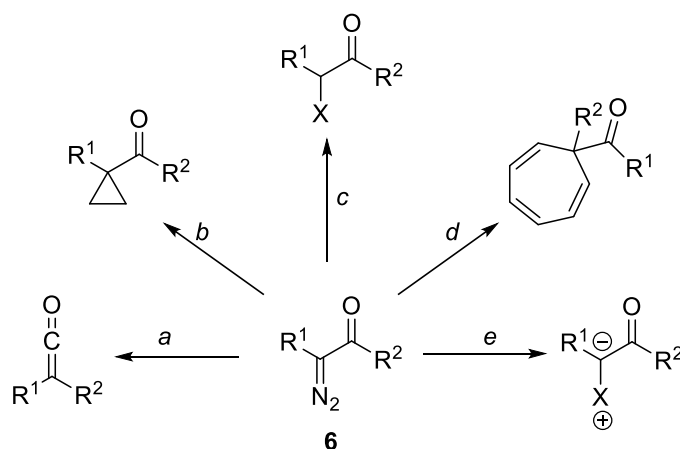
Scheme 1.13: Generation of terminal α -diazo compounds **46a** and **46b**.

In conclusion, the research of novel synthetic pathways towards α -diazocarbonyl compounds remains a hot topic in organic chemistry. During the last two decades several new reagents and procedures have been developed and enabling technologies, such as flow chemistry, provide valuable tools to successfully improve both efficiency and safety on the preparation of these versatile intermediates.^{10,13a}

1.1.2 Reactivity of α -Diazocarbonyl Compounds

The intrinsic reactivity of α -diazocarbonyl compounds driven by the release of N₂, makes them valuable precursors in organic synthesis. When exposed to heat, Brønsted acids, Lewis acids or catalytic amounts of transition metals, α -diazocarbonyl compounds react by generating useful intermediates such as free carbenes, carbenoids, enolates, ylides

or diazonium salts, which find application in various transformations: Wolff-rearrangement (a),⁴⁴ cyclopropanations (b),⁴⁵ C–X insertions (c),⁶ Buchner reaction (d)⁴⁶ and ylide formation (e) (Scheme 1.14).^{13a,47}



Scheme 1.14: General application of α -diazocarbonyl compounds **6**: a) Wolff-rearrangement, b) cyclopropanations, c) C–X insertion, d) Buchner reaction, e) ylide formation.

Among all, the most exploited reactivity of α -diazo compounds involves carbene and carbenoid-mediated reactions. Carbene species are neutral compounds characterised by a bivalent carbon having only six valence electrons ($R^1R^2C:$) and presenting three sp^2 hybridized orbitals and one p orbital. They are typically classified into singlet carbenes and triplet carbenes, depending on the localisation of the electrons (Figure 1.4).⁴⁸ Singlet carbenes have spin-paired electrons in the nonbonding sp^2 hybridized orbital while the p orbital is empty, and they show a bond angle of 100 – 110° . Differently, the triplet carbenes present a wider bond angle (130 – 150°) as result of the minor repulsion due to unpaired electrons. One of the electrons is located in the sp^2 hybridized orbital and the other in the higher energy p orbital. All carbenes can theoretically exist in both forms, however, most of them are more stable as triplets, unless they bear highly electron-donating substituents capable of interacting with the empty p orbital stabilising the singlet state.

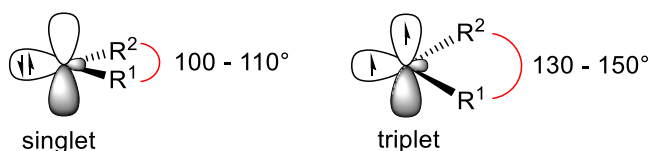
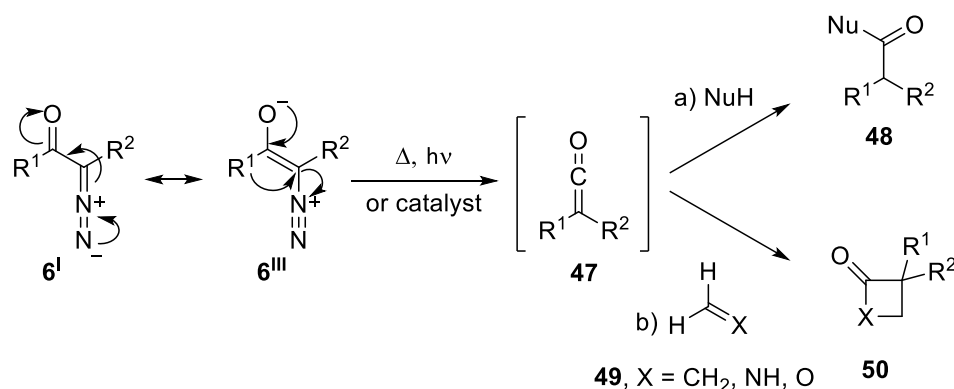


Figure 1.4: Example of carbenes species.

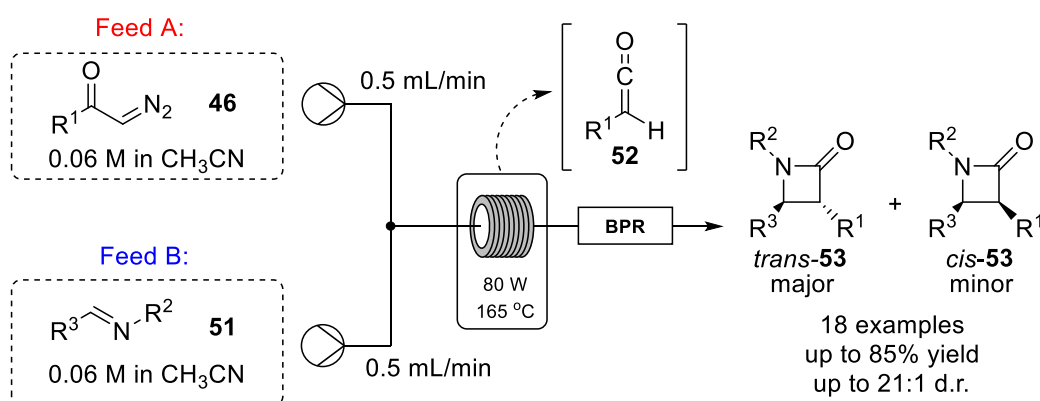
Due to their highly reactive nature, carbenes are mainly generated *in situ* through photolysis, thermal or transition metal-catalysed elimination processes, starting from precursors such as diazo compounds. When a carbene species is stabilised by a

transition metal it is referred to as a “carbenoid”. The carbenoids present a complex between the carbon bearing the lone pair and the metal, therefore the carbon structure is more like a tetravalent carbon rather than the typical bivalent carbon of a free carbene. Nevertheless, carbenes and carbenoids share similar reactivity to the point that in literature there are little distinctions and both terms are typically used as synonyms. A famous reaction involving carbene precursors is the Wolff-rearrangement, where a α -diazocarbonyl compound undergoes 1,2-migration to form a ketene **47** upon nitrogen loss (Scheme 1.15).⁴⁴ When the migration happens on a ring as starting material, the process leads to a ring contracted product.⁴⁹ The ketene intermediate **47** can undergo nucleophilic attack or [2+2] cycloaddition depending on the substrate available. When the ketene **47** is attacked by a nucleophile (NuH), the homologue carbonyl **48** is formed. This homologation reaction, named Arndt-Eistert homologation,⁵⁰ is still used nowadays to synthesise carboxylic acids or derivatives such as β -amino acids.⁵¹ Whereas in the presence of olefins, ketones or imines **49**, the ketenes **47** follow a cycloaddition pathway leading to four-membered rings such as **50**.



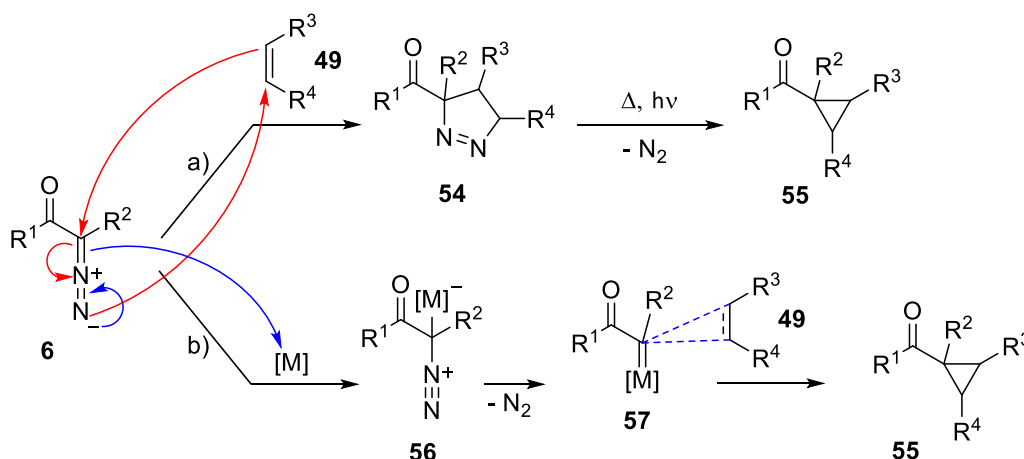
Scheme 1.15: Wolff-rearrangement to ketene **47** that undergoes a) nucleophilic attack, or b) [2+2] cycloaddition with olefins, ketones or imines **49**.

A recent example for the enantioselective generation of *trans*-configured β -lactams *via* Wolff-rearrangement enabled by flow chemistry, was reported by Ley and co-workers (Scheme 1.16).⁵² In this work a flow-microwave reactor was used to prepare primary ketenes **52** from 2-diazoketenes **46** under controlled reaction conditions. The ketene **52** reacts *in situ* with imines **51** in a [2+2] Staudinger cycloaddition affording β -lactams **53** and **54** in moderate to good yield, preferentially with *trans*-configuration. The stereochemical outcome of the [2+2] Staudinger cycloaddition is likely to be influenced by the size of the substituent at the nitrogen atom of imines **51** (R^2) or at the carbon atom (R^3).



Scheme 1.16: Microwave-assisted Wolff-Staudinger strategy with formation of β -lactams.⁵²

Another common application of α -diazo compounds is the cyclopropanation⁵³ of olefins. Considering the frequency of chiral cyclopropanes as structural motifs in pharmaceutical compounds,⁵⁴ the interest towards cyclopropanations is strong in medicinal chemistry.⁵⁵ During this reaction, a highly strained three-membered ring is formed by photochemically or thermally induced nitrogen loss from pyrazoline **54**⁵⁶ or by transition-metal catalysed decomposition of diazo compounds (Scheme 1.17).⁵³

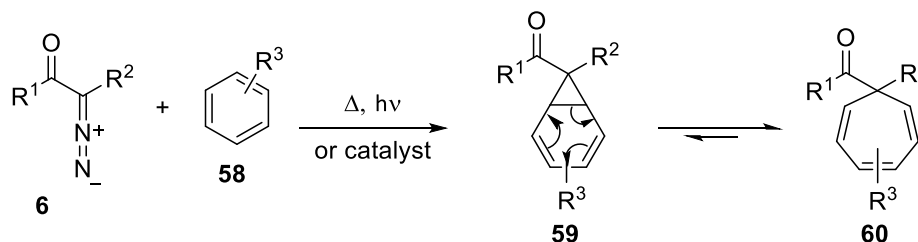


Scheme 1.17: Cyclopropanations using diazo compounds by a) photochemical or thermal denitrogenation of pyrazoline **54** or b) transition metal catalysis.

The process can occur with good stereochemical control by using chiral catalysts⁵⁷ or auxiliary directing groups,⁵⁸ and can be adapted from batch to flow mode.⁵⁹

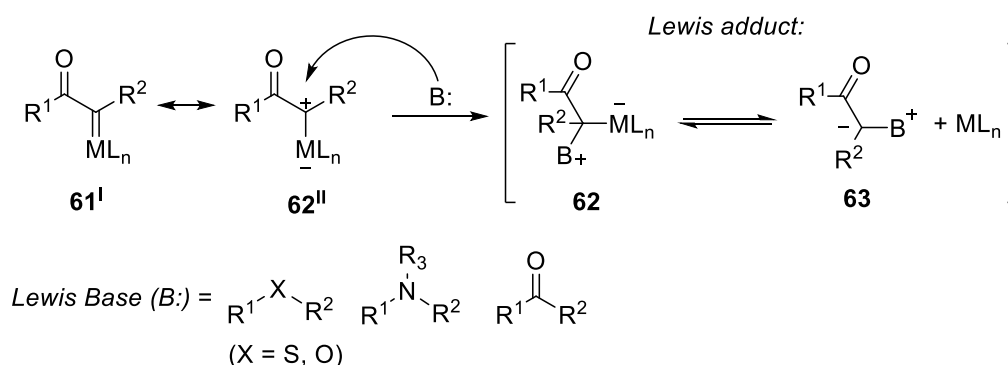
Furthermore, when the involved π -electrons belong to an aromatic ring, the cyclopropane causes a ring expansion to cycloheptatrienes **60** (Scheme 1.18).⁶⁰ In this two-step reaction, also known as the Büchner ring expansion, an aromatic ring **58** reacts with α -diazocarbonyl compound **6** generating a bicyclo[4.1.0]heptadiene derivative **59**. This undergoes a pericyclic ring expansion to generate a 7-membered ring **60**. However, the

equilibrium is shifted towards the bicycle **59** and not the 7-membered ring **60**, when the diazo compound **6** bears an EDG as substituent.⁶¹



Scheme 1.18: General scheme for Büchner ring expansion reaction.

The carbenoids are also used for their ability to form other reactive intermediates such as oxonium, sulfur, nitrogen and carbonyl ylides upon treatment with Lewis bases (Scheme 1.19).⁶² In the presence of ethers, sulfides, amines or carbonyl compounds, the carbenoid **61** acts as Lewis acid generating a Lewis adduct. Once generated, the latter can either remain as a metal-stabilised ylide **62** or it can dissociate from the metal forming a “free ylide” **63**. These intermediates are highly unstable and quickly undergo further inter- or intramolecular reactions including sigmatropic rearrangements,⁶³ dipolar cycloadditions⁶⁴ and 1,2-rearrangements.⁶⁵



Scheme 1.19: General mechanism for ylides formation from α -diazocarbonyl compounds.

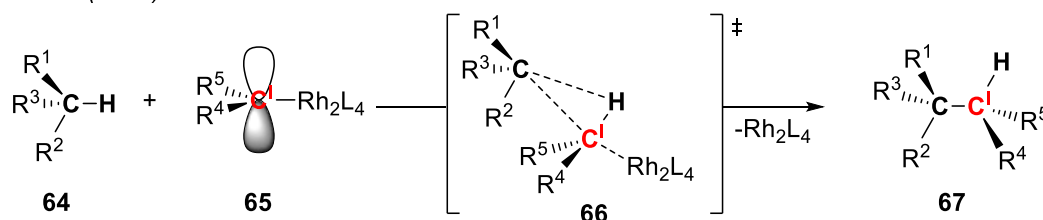
1.1.2.1 Diazo Compounds and Carbene-mediated C–X Insertions

Carbene-mediated C–X insertions from diazo compounds were reported for the first time in 1956 as an “indiscriminate” insertion of a diazomethane into *n*-pentane to form *n*-hexane, 2-methylpentane and 3-methylpentane in a 3:2:1 ratio.⁶⁶ Although thermally or photochemically generated carbenes showed unselective insertions, later work conducted by Taber and co-workers reported highly regio- and stereoselective intramolecular C–H insertions towards five-membered rings when the carbene was generated by transition metal catalysis.⁶⁷ Among all transition metals, copper⁶⁸ and

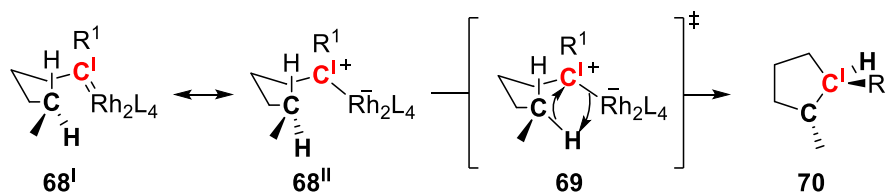
rhodium⁶⁹ were reported to efficiently catalyse this class of transformations. Especially, the dirhodium catalysts bearing carboxylate and carboxamide ligands emerged as the most efficient catalysts for chemo- and regioselective intra- and intermolecular insertions.

The reaction mechanism was proposed by Doyle *et al.* in 1993⁶⁹ and later confirmed by Nakamura and co-workers in 2002 (Scheme 1.20).⁷⁰

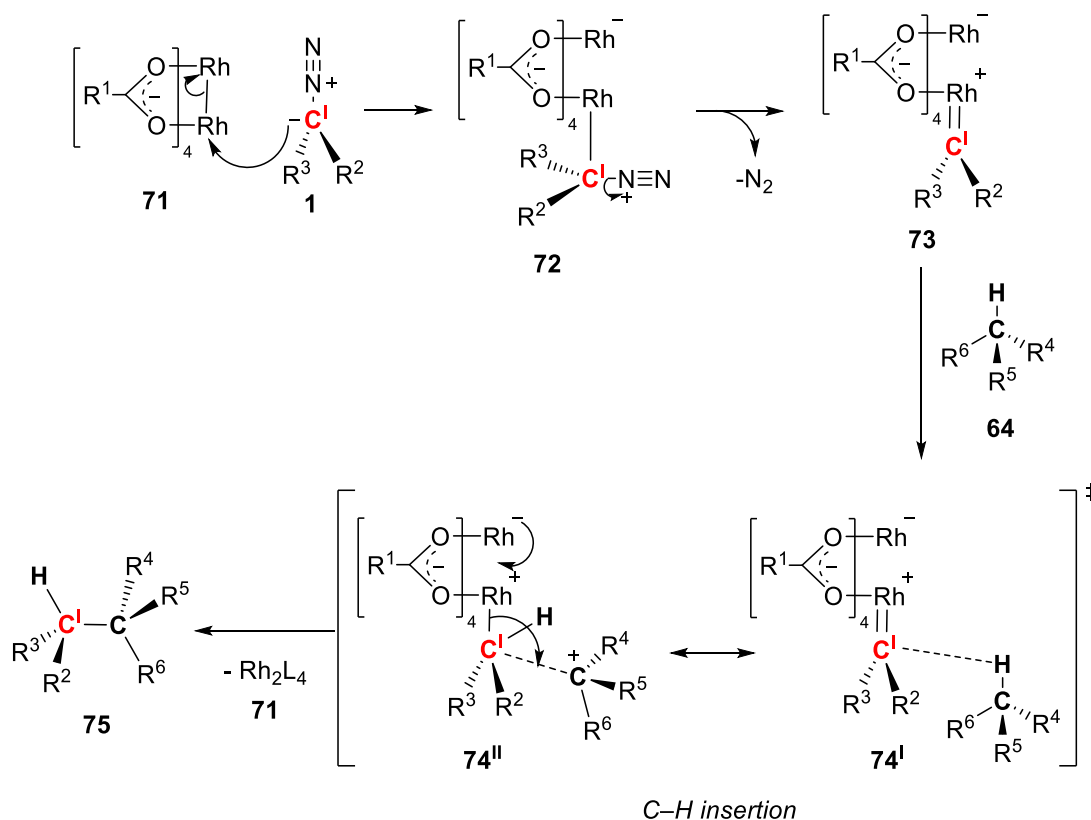
Doyle *et al.* (1993):



Taber *et al.* (1996):



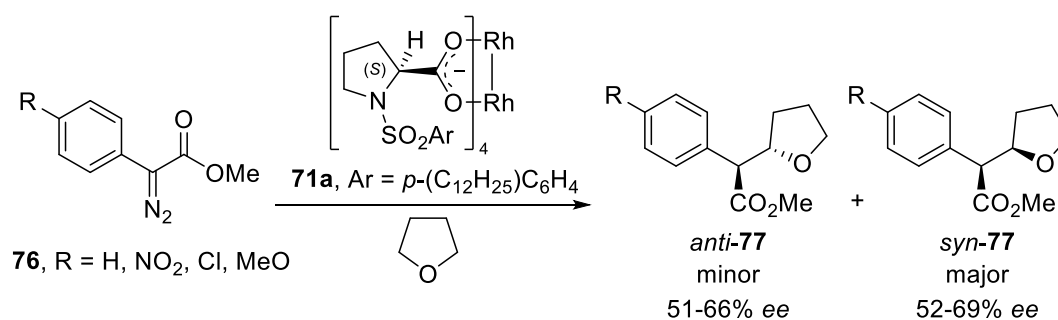
Nakamura *et al.* (2002):



Scheme 1.20: Mechanistic proposals for C-H insertion.

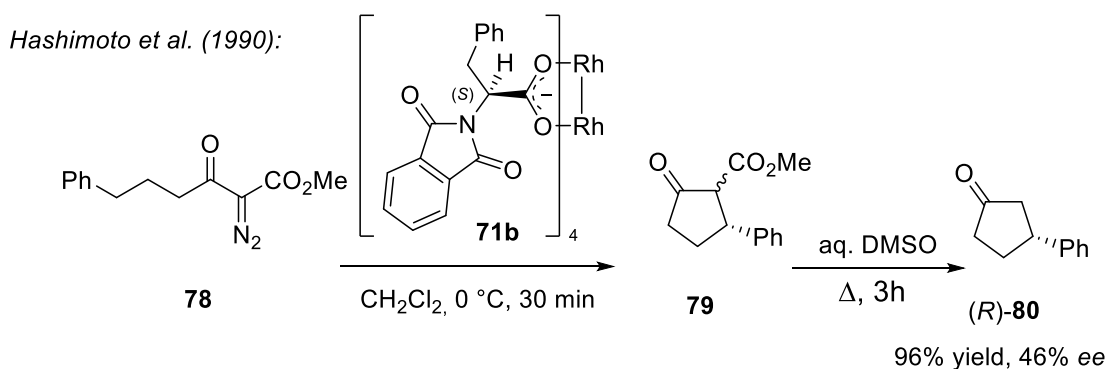
According to the Doyle proposal, the C^I-C and C^I-H bond formation between **64** and **65** bearing the carbene carbon C^I occurs as the metal dissociates passing *via* the transition state **66**. In this transition state, the different bond formations and cleavages happen at the same time but not necessarily with the same rate. Later, Taber *et al.* proposed **69** as alternative transition state in which a hydrogen atom is transferred from the C-H bond to the metal synchronous with the C-C bond formation. Product **70** is then released and the rhodium catalyst is regenerated.⁷¹ Eventually, density functional theory (DFT) calculations performed by Nakamura *et al.* in 2002 indicated a concerted but non-synchronous process⁷⁰ as previously proposed by Doyle. Once the catalyst **71** reacts with the diazo substrate **1**, a molecule of N₂ is released and the stabilised carbenoid **73** is formed allowing C-H insertions, among other chemical transformations. The carboxylate ligand acts as anchor for the dimer conferring a better stabilisation due to the presence of the nearby second rhodium atom. Moreover, the electron donation from one rhodium atom to the other assists the C-C bond formation and the catalyst regeneration. Nakamura *et al.* confirmed the additional stabilisation given by the dirhodium catalyst **71** by calculating a much lower activation energy for the C-H insertion with dirhodium(II) carboxylates catalyst (5.7 kcal/mol) compared to copper (15.6 kcal/mol) and ruthenium-carbenoids (27.6 kcal/mol).⁷⁰ The presence of electron-withdrawing substituents on the carbenoids, together with the presence of a positively charged rhodium atom, enhances the electrophilicity of the carbon centre C^I, hence the reactivity towards C-H insertion is increased.

Intuitively, when chiral ligands are used, it is possible to control diastereo- and enantioselectivity, thus, a big effort has been invested in the design of the most efficient ligands for each transformation. Both Doyle⁶⁹ and Padwa⁷² independently reported that the nature of the ligands affects the regio- and chemoselectivity of the C-H insertion reactions. Generally, the presence of an EWG increases the reactivity to the detriment of the selectivity, while sterically hindered ligands and/or carbene substituents have a stronger influence on the stereoselectivity. In the late 90s, Davies *et al.* developed the chiral dirhodium(II) tetraproline catalyst Rh₂(DOSP)₄ **71a** and reported the first highly regioselective intermolecular C-H insertions of tetrahydrofuran (THF) in the donor/acceptor diazo compound **76** (Scheme 1.21).⁷³ Moreover, the Rh₂(DOSP)₄ catalyst **71a** was found to suppress the side dimerisation reaction (see Scheme 1.2), affording exclusively the desired insertion product **77** in good to excellent yields (48–80%), with moderate stereoselectivity (up to 69% ee), preferentially as *syn*-isomer.



Scheme 1.21: First example of a stereoselective intermolecular C–H insertion.⁷³

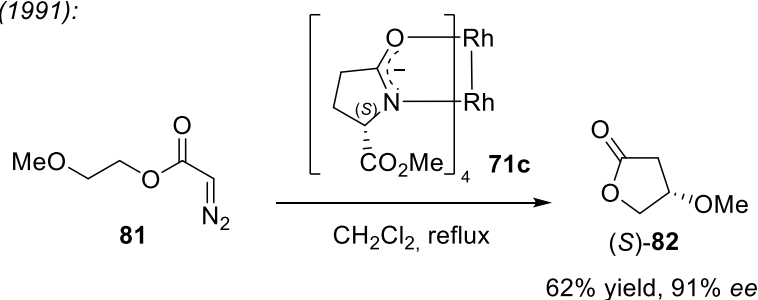
Since then, the Davies group reported several successful X–H insertions catalysed by **72a** with excellent regioselectivity of the insertions occurring in the α -position to nitrogen⁷⁴ or oxygen atoms⁷⁵ as well as in the benzylic position.⁷⁶ These afforded highly asymmetric products typically obtained *via* Mannich reaction, aldol condensation, Michael addition or Claisen rearrangement. Moreover, the Davies group expanded the library of carboxylated dirhodium catalysts to achieve site-selective and stereoselective inter-functionalisation of non-activated C–H bond into primary,⁷⁷ secondary,⁷⁸ and tertiary carbon atoms,⁷⁹ later applied to total syntheses of biologically active compounds.⁸⁰ Simultaneously with Davies *et al.*, Hashimoto *et al.*⁸¹ and McKervey *et al.*⁸² independently reported the first example of asymmetric intramolecular C–H insertion catalysed by chiral dirhodium(II) carboxylate catalysts such as **71b** (Scheme 1.22).



Scheme 1.22: Selected example of stereoselective intramolecular C–H insertions.⁸¹

Doyle then designed a series of chiral dirhodium(II) carboximidate catalysts such as Rh₂(5*S*-MEPY)₄ **71c** that catalysed highly stereoselective cyclisations providing valuable lactones such as γ -lactone **82** in 62% yield and 91% ee (Scheme 1.23).⁸³

Doyle et al. (1991):



Scheme 1.23: Selected example of stereoselective intramolecular C–H insertions.⁸³

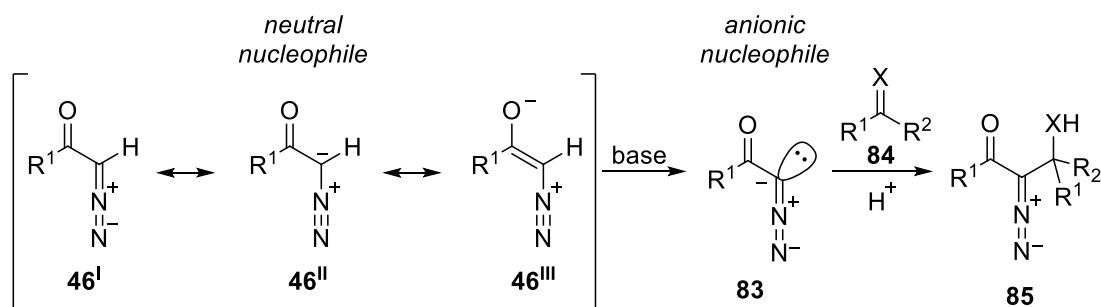
Besides C–H insertion, also N–H⁸⁴ and O–H⁸⁵ insertions have been widely investigated by using amines, carboxylic acids, alcohols and water. Moreover, when hydrogen halides, sulfur or silicon-based acids are involved, it is possible to insert a bond between an hydrogen atom and an halogen,⁸⁶ a sulfur⁸⁷ or a silicon atom.⁸⁸ Additionally, a small selection of X–Y insertion reactions have been reported, in which neither X nor Y is a hydrogen atom, which takes the name of α,α -substitutions. For instance, when diazocarbonyls are treated with molecular halogens⁸⁹ or with (dichloroiodo)benzene,⁹⁰ α,α -dihalogenated products are formed. More recently, the range of metal catalysed insertions into C–C single bonds have also been included within the scope of X–Y insertions.⁹¹

On the other hand, the carbene-functionalisation of an aromatic system has sometimes been misleadingly included within the “C–H insertion” classification, although it would be more appropriate to define them as “aromatic substitution”. In this case, the electrophilic addition of a carbene/carbenoid into an electron-rich aromatic ring generates a zwitterionic intermediate followed by proton transfer to restore the aromaticity.⁹²

Nevertheless, metal-promoted X–H and X–Y insertions of diazocarbonyl compounds represent a vast part of the applications involving diazo compounds and are still one of the main areas of modern organic research.

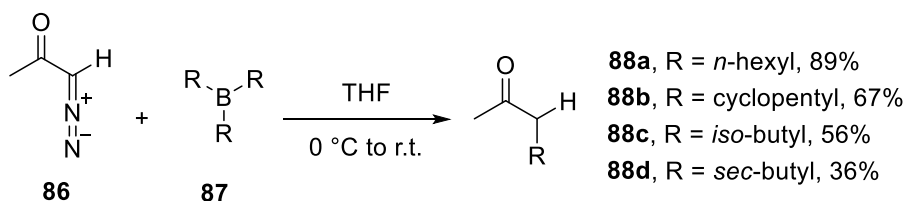
1.1.2.2 α -Diazocarbonyl Compounds and Organoboron Compounds

In all the above mentioned reactions, the diazo compounds are exploited for their electrophilic properties in order to achieve a chemical transformation. However, they possess an ambiphilic nature and can also act as nucleophiles. Moreover, some diazo compounds are usually stable enough to undergo further modifications without losing the diazo moiety, such as generating anionic nucleophiles such as **83** when treated with a base (Scheme 1.24).^{43c} The anion **83** can then react further with carbonyl or imines such as **84** forming β -hydroxy or β -amino α -diazocarbonyl compounds **85**.



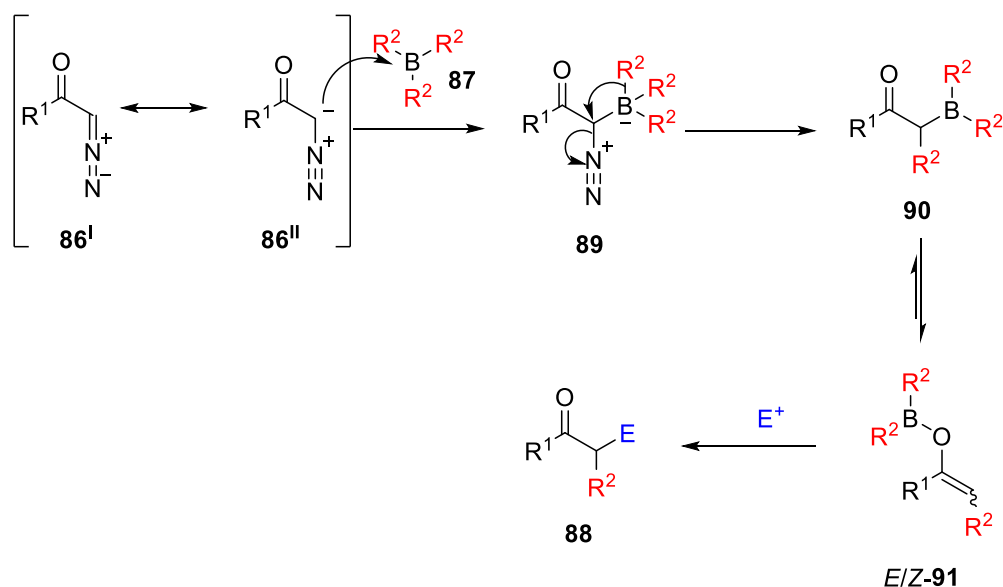
Scheme 1.24: General mechanism for diazo nucleophile addition.

One of the resonance structures of the diazo compound **46**^{II} presents a negative partial charge on the carbene atom, therefore **46** can be seen as neutral nucleophile and it can react with electron-deficient atoms such as boron atoms.⁹³ The first example of a reaction between α -diazocarbonyl compounds such as diazopropanone **86** and trialkylboranes **87** was reported by Hooz and Linke in 1968 (Scheme 1.25).⁹⁴ In this 1,2-group transfer, one of the alkyl groups migrates from the borane to the diazo compound forming products such as **88**.



Scheme 1.25: First example of reactivity between diazocarbonyl compound **86** and borane **87**.

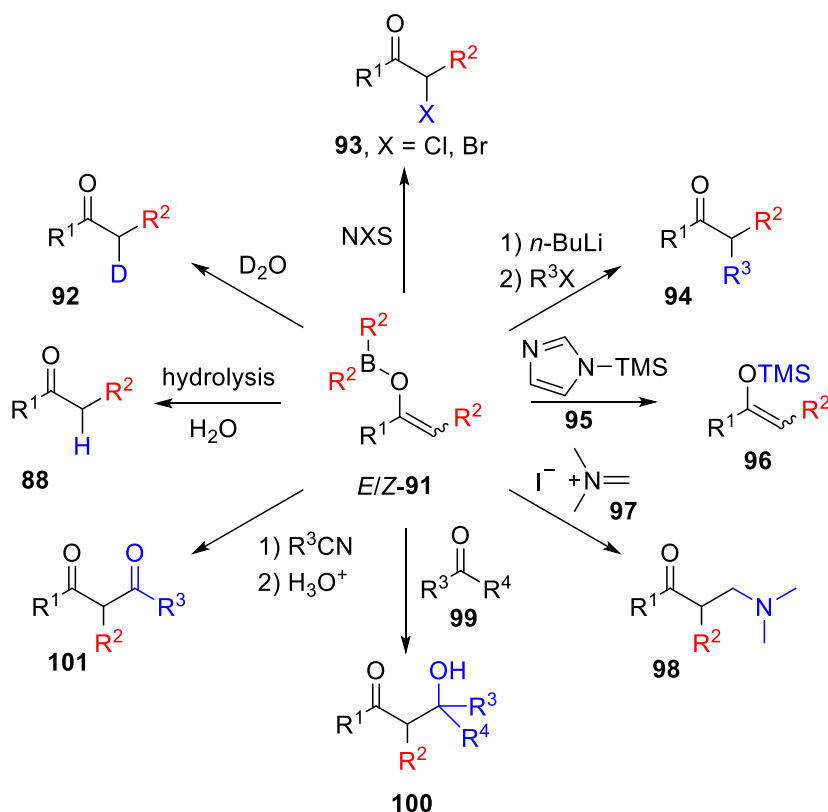
Later, Hooz and co-workers expanded the range of this metal-free 1,2-alkyl transfer to diazoketone⁹⁴ to diazoaldehydes,⁹⁵ diazonitrile,⁹⁶ and EDA,⁹⁶ however with a narrow scope limited by steric hindrance of the boranes. According to the proposed mechanism depicted in Scheme 1.26, the diazo compound **86** reacts with the borane **87** to form a tetracoordinated boron intermediate **89**. Subsequently, one of the boron-substituents (-R) migrates to the carbon atom with nitrogen gas expulsion to generate the intermediate **90**, which is in tautomeric equilibrium with its enolate form **91**.⁹⁷ Finally, the reaction with an electrophile or hydrolysis of the boron enolate **91** affords the α -functionalised product **88**.



Scheme 1.26: Proposed reaction mechanism of the 1,2-alkyl transfer from trialkylboranes **87** to α -diazocarbonyl compounds **86**.

Intuitively, different electrophiles could be trapped by the boron enolate **91**. From their pioneering work (see Scheme 1.25), Hooz and co-workers, followed by other research groups, started investigating the reactivity of enolate intermediates **91** with various reagents from inorganic bases to other electrophilic species (Scheme 1.27). Firstly, the simple hydrolysis of the boron-adducts **91** affords the α -functionalised esters or ketones such as **88** without the need for metal-catalysis. When D_2O is used to hydrolyse **91**, the α -deuterated carbonyl **92** is afforded in quantitative yields.⁹⁸ Compared to the classic acid- or base-promoted protocols, this is a unique way to form exclusively the α -monodeuterated carbonyl compound **92**. Similarly, α -monohalogenated carbonyl compounds **93** are generated in good yield as sole products when the boron enolate **91** is treated with *N*-halosuccinimide (NXS).⁹⁹ The enolate **91** can be transformed *in situ* into a lithium enolate upon treatment with *n*-BuLi, which can further react with alkyl halides or other alkylating agents such as benzyl bromide, allyl bromide and dimethyl sulfate generating α,α -disubstituted carbonyls such **94**.¹⁰⁰ Moreover, Hooz *et al.* were able to trap the boron enolate as the corresponding trimethylsilyl ether **96** by using *N*-(trimethylsilyl)-imidazole (**95**).¹⁰¹ Furthermore, imines and Eschenmoser's salt **97** can be used as electrophiles to quench the boron enolate **91** affording amine products **98** typical of a Mannich reaction, in both high regio- and stereoselectivity.¹⁰² In an analogous manner, Mukaiyama *et al.*¹⁰³ and later Hooz and co-workers¹⁰⁴ developed a three-component reaction with aldehydes and ketones, respectively, providing condensation products **100** in good yields and stereoselectivity.¹⁰⁵ This multicomponent strategy was then adopted by Miranda *et al.* for the synthesis of 1,3-diketones and β -ketoesters, which are valuable intermediates for the generation of pyrazole moieties.¹⁰⁶ The enol borane

91 was also reported to react with nitriles in a cycloaddition into boroxazines, which are easily hydrolysed to α -functionalised 1,3-diketones **101**.¹⁰⁷



Scheme 1.27: General scheme of the reactivity of boron enolate **91** with various reagents.

Although the versatile reactivity of boron enolates shows great utility in organic synthesis, it is generally limited due to the steric hindrance of the trialkylborane **87** (Figure 1.5). Further improvements were achieved by Levy *et al.* by using more reactive dialkylchloroboranes¹⁰⁸ **102** or vinyl- and aryl-dichloroboranes¹⁰⁹ **103** while alkyldichloroboranes afforded only moderate yields.

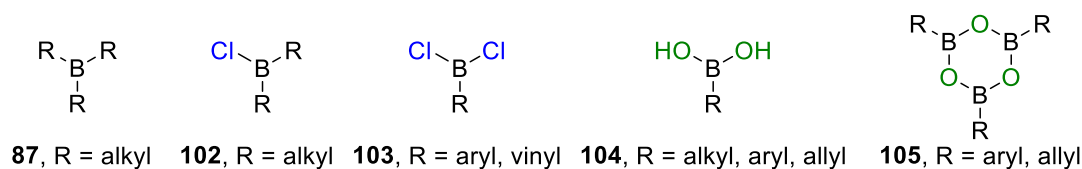


Figure 1.5: Different boranes commonly used for the α -functionalisation of carbonyls.

Nevertheless, these reagents are typically sensitive to moisture and less available, thus further studies have been made to investigate the reactivity of different organoboranes such as boronic acids **104** or boroxines **105** towards the 1,2-aryl transfer reaction. For instance, Barluenga and co-workers¹¹⁰ used more stable and less toxic boronic acids **104** and tosylhydrazones to afford coupling products similar to **88**. Alternatively, Wang

et al. used boroxines **105**, prepared from corresponding boronic acids, to functionalise α -diazocarbonyl compounds.¹¹¹

Other organoboranes that are receiving particular attention in organic synthesis as Lewis acids are represented by triarylboranes **106a–h** (Figure 1.6). In particular, tris(pentafluorophenyl)borane $B(C_6F_5)_3$ **106d** has been applied to catalyse several metal-free transformations such as cyclisation,¹¹² hydrogenation¹¹³ or hydrosilylation reactions¹¹⁴ and group migrations.¹¹⁵ Moreover, the recent works by Stephan *et al.*¹¹⁶ Oestreich *et al.*¹¹⁷ and Melen *et al.*¹¹⁸ showed how tris[3,5-bis(trifluoromethyl)-phenyl]borane (BAr^{F_3} , **106h**), tris(3,4,5-trifluorophenyl)borane **106e** and tris(2,4,6-trifluorophenyl)borane **106g** can be efficiently employed in metal-free hydroborations, with higher reactivity compared to **106d**. A recent example was published by the Melen group, in which a catalytic hydroboration protocol was developed using **106e** and microwave irradiation in order to expand the substrate scope of hydroboration to alkynes.^{118b}

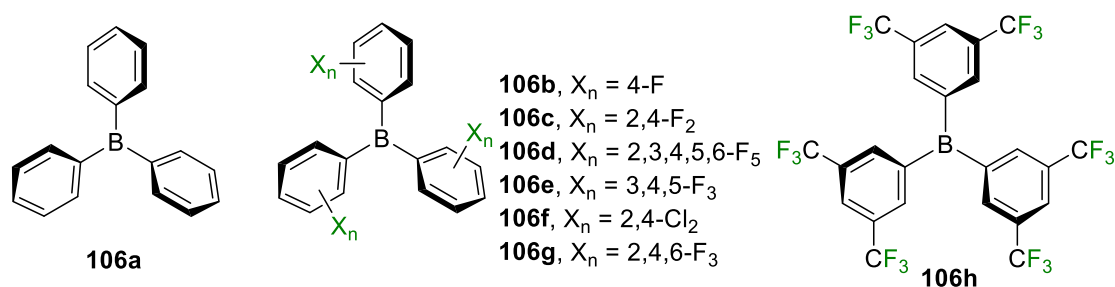
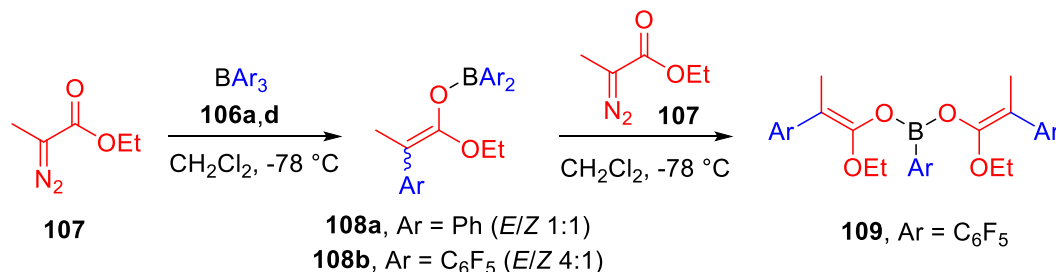


Figure 1.6: Example of aryl boranes applied in organic synthesis.

Regarding the reaction between **106** and α -diazocarbonyl compounds, Stephan *et al.* observed that, when ethyl 2-diazopropionate **107** was treated with triphenylborane **106a**, the boron enolates **108a–b** were formed as a mixture of *E/Z* isomers (Scheme 1.28).¹¹⁹ The fluorinated **108b** was found to react further with a second equivalent of **107** and, after a second aryl migration, **109** was formed.



Scheme 1.28: Example of double 1,2-aryl migration from **106b** to 2-diazopropanoate **107**.¹¹⁹

Moreover, **106d** was also recently reported to promote several C–X functionalisations into diazocarbonyl compounds, by activating molecules such as water alcohols or azides.¹²⁰

To conclude, the reaction between α -diazocarbonyl compounds and organoboranes offers an efficient and metal-free method towards novel C–C bond formation. Nevertheless, the reaction between triarylboranes and α -diazocarbonyl compounds remains still under-represented.^{102a,106} Since more Lewis acidic compounds, such as polyfluorinated triarylboranes, showed an increased reactivity, they were investigated in metal-free aryl migration towards α -functionalisation of esters, as discussed in more detail in chapter 3.

1.2 General Introduction on Enabling Technologies

The term “enabling technology” defines an invention or innovation that is applied to improve performances and capabilities of a process.¹²¹ Therefore, the concept of “enabling technologies” has a broad meaning which includes all kinds of fields, from the invention of farming tools of the classical era¹²² to the introduction of smartphones and computers in the modern era. In chemistry, it indicates those branches such as flow chemistry,¹²³ mechanochemistry,¹²⁴ electrochemistry,¹²⁵ photochemistry¹²⁶ and microwave-assisted reactions,¹²⁷ that are slowly changing the way chemical transformations are performed. More recently, within the wider concept of “enabling technology” have been included the 3D-printing,¹²⁸ automated systems,¹²⁹ machine-learning algorithms for self-optimising systems¹³⁰ as well as statistical software for Design-of-Experiment (DoE).¹³¹ These technologies, not only have allowed modern chemists to achieve different reactivities from “classic” methods and discover unknown reactions,¹³² but also helped making synthetic-protocols and industrial plants safer and more sustainable, cutting down costs and waste.¹³³

In the second part of this chapter the basics of flow chemistry and DoE are introduced, as flow chemistry was used to improve synthetic protocols and process optimisations were performed following a DoE-approach. A glossary of terminology regarding the most relevant terms about DoE can be found in Appendix A.

1.2.1 Flow Chemistry

In the last two decades continuous flow chemistry has rapidly thrived in both the academic and industrial sector due to its numerous advantages such as better mixing, heat and mass transfer and easier automation.¹²³ When a flow system is used to perform a chemical transformation, the reaction is conducted in a continuous stream. The reagents are pumped throughout chemically resistant channels of different shapes and dimension in which they meet, mix and react. The product is then collected from the outlet and its yield is strictly influenced by the residence time (t), that is the time the reagents spent in the reactor. The latter depends on the reactor volume (V) and the flow rate (Q), two parameters controlled by the operator (Equation 1).

$$\text{Residence Time } (t) = \frac{\text{Reactor Volume}}{\text{Flow Rate}} = \frac{V}{Q}$$

Equation 1

In order to have a higher residence time and to achieve better conversions, the reagents need to be pumped more slowly and/or a different reactor should be used. Nevertheless, it must be kept in mind that each design, as well as tubing size, has a different influence on the flow regime of the system and so on its mixing properties. For instance, a monophasic system in which two miscible liquids A and B are flowing in parallel without interruption follows a “laminar flow” regime and the mixing is achieved by diffusion and is defined as “passive mixing” (Figure 1.7a).^{123a}

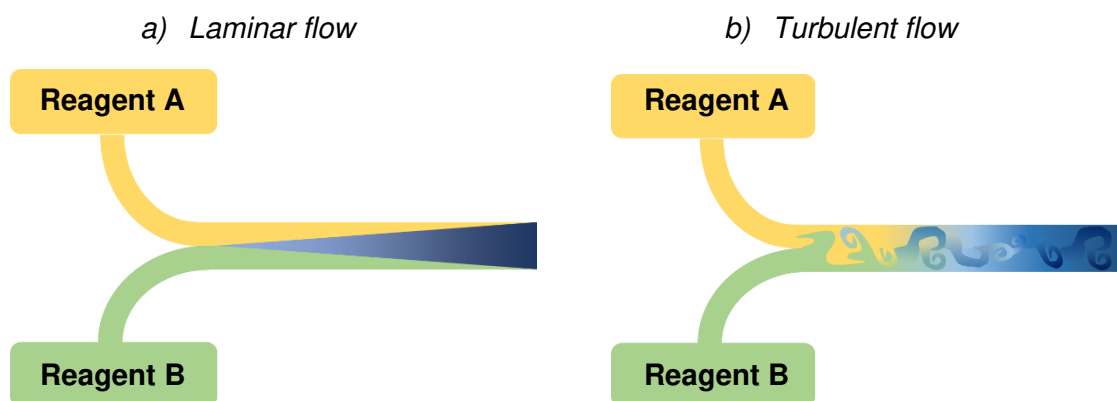


Figure 1.7: Schematic diagram showing mixing in laminar flow and turbulent flow regimes.

When the mixing happens randomly in both time and space due to inner mixers, tube lengths or rough surfaces, we talk about “turbulent flow” (Figure 1.7b). The Reynolds number (Re) is a dimensionless coefficient that can predict whether specific conditions will lead to a laminar or a turbulent flow (Equation 2).

$$Reynolds\ number\ (Re) = \frac{u * L}{\nu}$$

Equation 2

It indicates the ratio between inertial forces (fluid velocity u ($m \cdot s^{-1}$), characteristic length L (m)) and viscous forces (kinematic viscosity ν ($m^2 \cdot s^{-1}$)). For fluids flowing in pipes the Re is commonly defined as:

$$Re = \frac{Q * D}{\nu * A}$$

Equation 3

where Q is the flow rate ($m^3 \cdot s^{-1}$), D the internal diameter of the pipe (m), ν the kinematic viscosity ($m^2 \cdot s^{-1}$) and A the cross-sectional area (m^2).^{123a} Typically, for laboratory flow equipment, the tubes have an internal diameter (ID) equal to or below 1 mm, therefore the flow regime falls in the region of microfluidics. In other words, the fluids operate at

Re below 250 with laminar flow. The number of flow regimes increases when multiphasic systems are involved. For example, for gas-liquid transformations bubble, slug or annular flow can be observed depending on flow rate, whilst for solid-liquid mixtures the packed bed, fluidised bed or mixed bed are mainly used (Figure 1.8).^{123a}

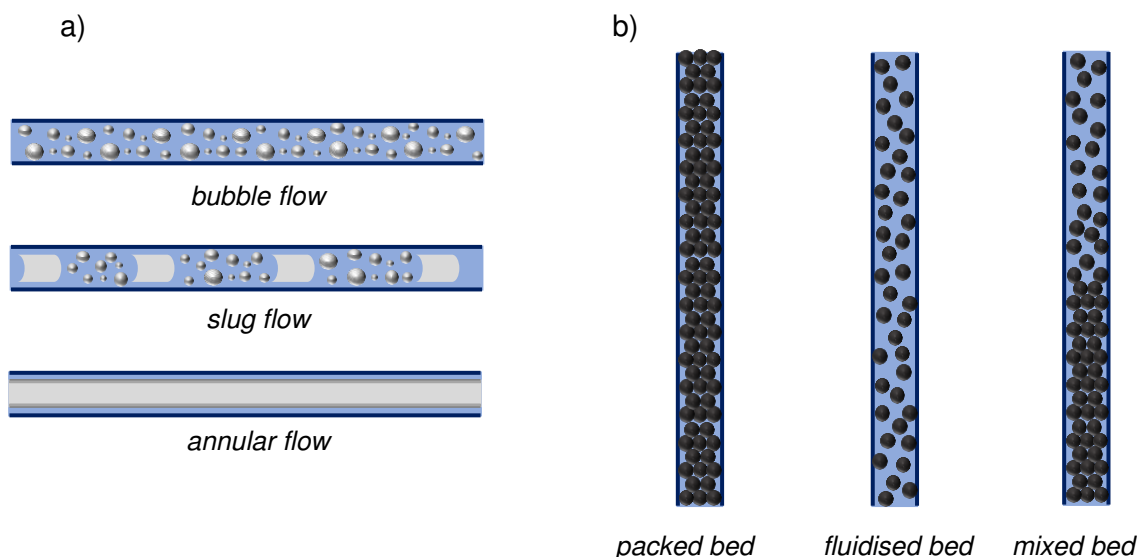


Figure 1.8: Examples of flow regimes for a) gas-liquid mixtures and b) solid-liquid mixtures.

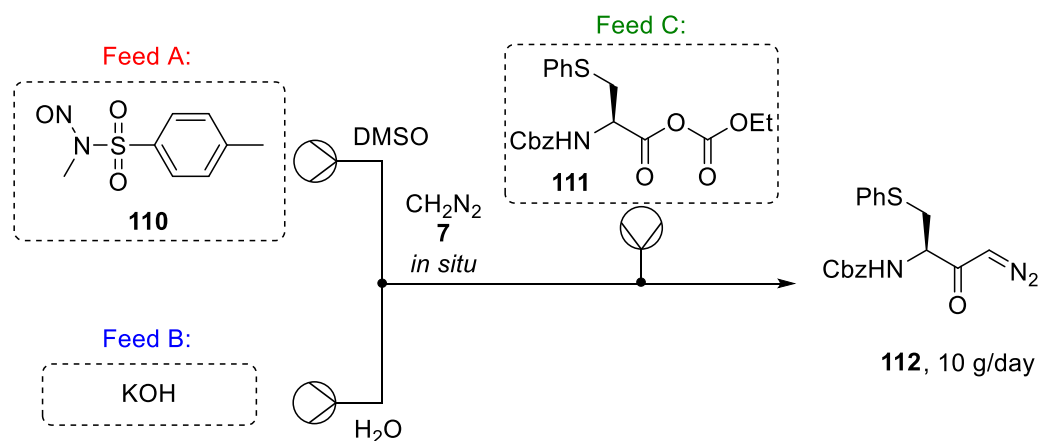
The flow technology has allowed chemists to reach a remarkable control over reaction parameters, such as temperature and mixing, that influence a reaction outcome, enhancing efficiency, reliability of the chemical processes as well as enabling new reactions.¹³² Due to the high surface to volume ratio of micro-devices and flow reactors, the mass and heat exchange is more efficient, increasing performances and allowing exothermic reactions to be performed in a safer manner.^{123g} The highly controlled generation of reactive species, together with their fast consumption in a continuous stream, avoids dangerous accumulations improving the safety profile of some reactions processes and allowing safer scale-ups.¹³⁴

Another huge advantage of continuous flow systems is their practicability in monitoring *in situ* the ongoing reactions, and their easy automation. Generally, when optimising a chemical reaction it is common practise to collect a sample and perform an “offline” analysis *via* GC-MS, LC-MS or NMR spectroscopy after work-up but with the advent of flow technologies there has been a remarkable improvement in developing “inline” and “online” monitoring techniques for a much faster optimisation. The difference between “online” and “inline” analysis, as introduced by Browne *et al.* and Cronin *et al.*,¹³⁵ lies in the different way the flow stream is sampled. The term “inline analysis” describes a system in which the whole flow stream is continuously monitored. For instance, IR and UV as well as flow-NMR kit are composed by an inline flow cell, thus are considered

“inline” devices. Whereas monitoring systems such as MS or HPLC, that use injection devices such as switching valves to isolate fractions of the flow stream, are considered “online” analysis.¹³⁵

A big drawback of flow chemistry systems is the presence of solids, such as precipitate formed during the reaction or during the inline work-up. This can cause a blockage that could lead to too high pressures, leakages and may damage the system. Another drawback of using flow chemistry is the need for the appropriate equipment that must be purchased or designed and 3D-printed *ad hoc* for the purpose and can be costly.^{123a} However, the benefits of flow chemistry often outweigh the disadvantages. The increased safety profile offered by flow systems is one of the most important characteristics, as sensitive and/or toxic intermediates can be generated *in situ* in smaller amounts avoiding dangerous accumulation of highly reactive compounds, and they can further react in the system without coming into contact with the operator.

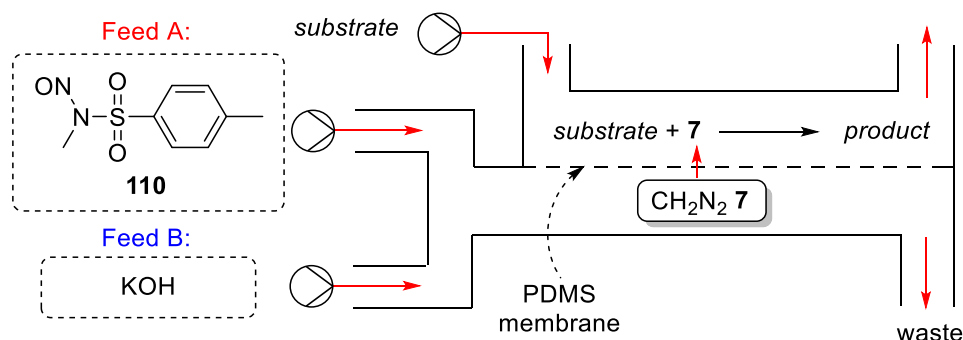
For this reason, there has been significant interest in the application of flow technology to the generation and use of diazo compounds at both laboratory and industrial scales.¹³⁶ One of the first large-scale flow system for the synthesis of diazomethane (**7**) *in situ* was reported by Proctor and Warr in 2002 (Scheme 1.29).¹³⁷ This continuous preparation/consumption of diazomethane (**7**) from Diazald® (**110**) in a mixture of DMSO and water allowed to safely produce the α -diazoketone **112**, which is an intermediate of the HIV protease inhibitor nelfinavir mesylate, in a gram-scale multi-step synthesis.



Scheme 1.29: *In situ* generation of diazomethane (**7**) for a large-scale multi-step process.¹³⁷

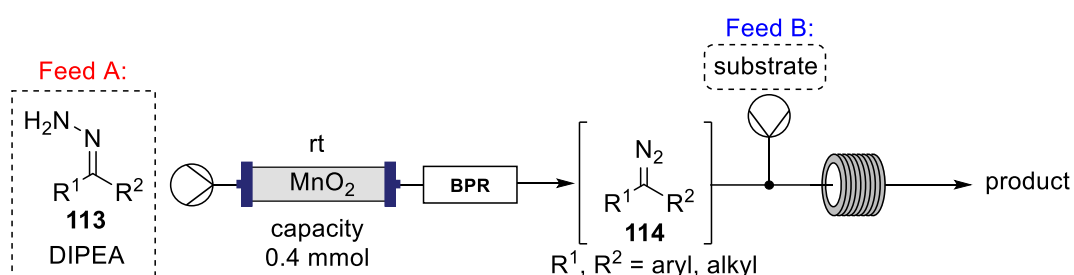
For a similar transformation, the group of Kim *et al.* designed a dual-channel micro-reactor system in which two parallel channels are separated by a thin hydrophobic membrane of poly(dimethylsiloxane) (PDMS) that prevents the passage of KOH, aqueous medium and *p*-toluenesulfonate (Scheme 1.30).¹³⁸ In the first channel an

aqueous solution of Diazald® (**110**) is used to generate diazomethane **7** that then diffuses through the membrane into the second channel where it can react with the substrate.



Scheme 1.30: Dual-channel micro reactor system for *in situ* generation, separation, and reactions of diazomethane.¹³⁸

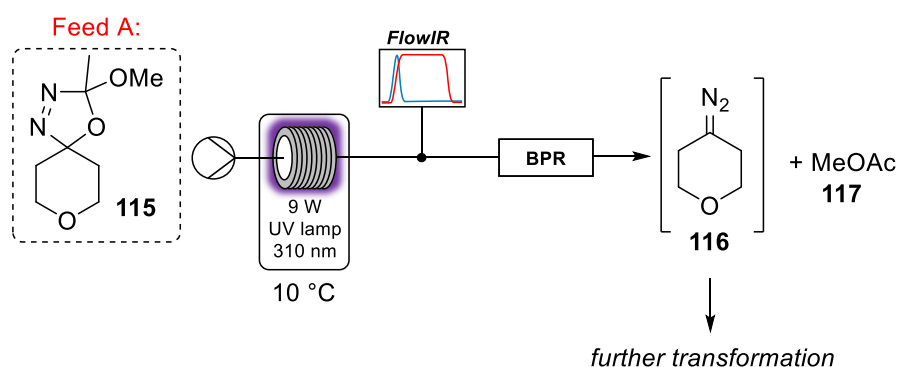
Moreover, a few years later Kappe and co-workers and more recently Koolman and co-workers further improved this protocol by applying the tube-in-tube technology to continuous multi-step synthesis of valuable α -halo ketones¹³⁹ and cyclopropylboronic esters,¹⁴⁰ respectively. The tube-in-tube technology consists of two concentric tubes separated from each other by a gas-permeable AF-2400 membrane. In this case, the diazomethane (**7**) is generated in the inner tube and diffuses through the gas-permeable membrane into the outer chamber where it reacts following a similar principle to the one showed in Scheme 1.30. More sophisticated systems such as the Vapourtec R-Series settings have also been applied to similar transformation increasing the productivity.¹⁴¹ Besides increasing the safety of diazomethane-generation, flow chemistry guarantees access to highly valuable transient reactive intermediate such as donor/donor carbene precursors. In 2014, Ley and co-workers published the *in situ* generation of diazoalkanes **114** using a pre-packed flow cartridge of MnO_2 (Scheme 1.31).¹⁴²



Scheme 1.31: Flow generation and reaction of donor/donor carbene precursors **114**. BPR = back pressure regulator.¹⁴²

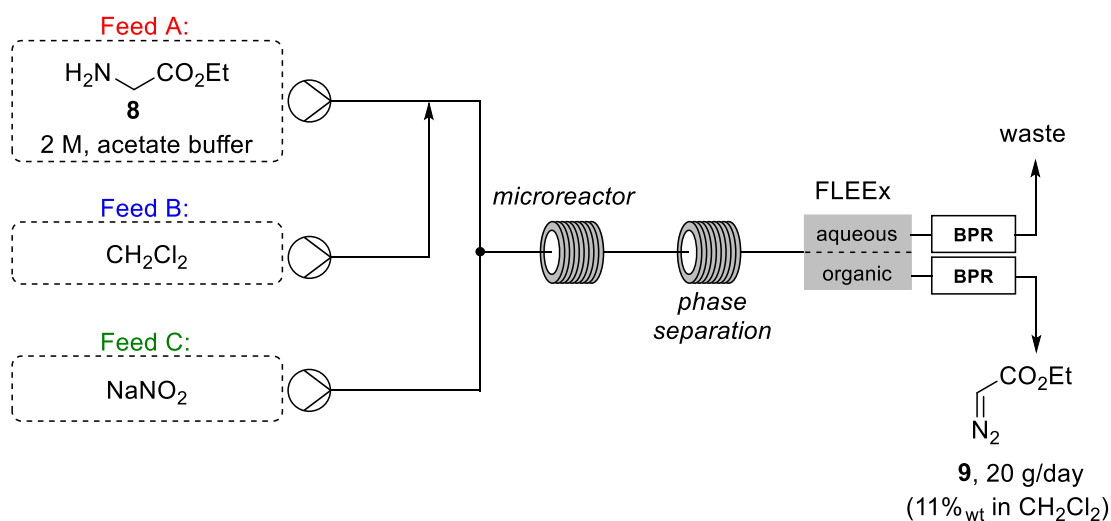
Since then, similar systems with pre-packed cartridges have been successfully applied to different transformations such as the functionalisation of boronic acids,¹⁴² Cu-catalysed allene synthesis,¹⁴³ Rh-catalysed transformations,¹⁴⁴ cyclopropanations⁵⁹ and C-C couplings.¹⁴⁵ The Ley research group has also recently reported the *in situ*

synthesis of unstable diazoalkanes using a continuous-flow photoreactor and inline IR analysis (Scheme 1.32).^{10a} The photolysis of 1,3,4-oxadiazoline **115** is a well-established method to access the “non-stabilised” diazoalkane **116**.¹⁴⁶ The novelty introduced by Ley and co-workers lies in the continuous-flow photoreactor that allows better control over the provided irradiation which ensures good yields, improved scalability and reproducibility.



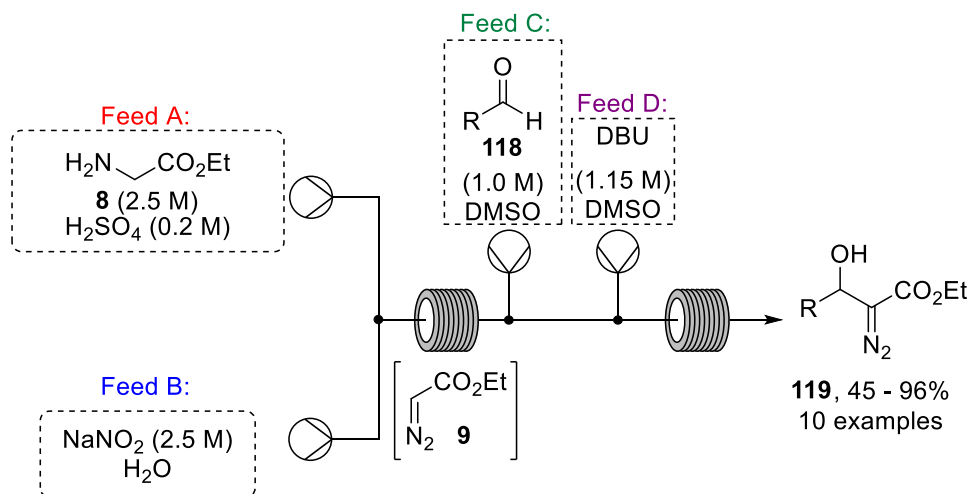
Scheme 1.32: Flow generation of non-stabilised diazo compound **116**, from oxadiazolines **115** as precursor. BPR = back pressure regulator.^{10a}

The preparation of donor and donor/acceptor carbene precursors has also been conducted in a flow setup. The first continuous flow synthesis of ethyl diazoacetate (EDA, **9**) was reported by Rutjes and co-workers (Scheme 1.33).¹⁴⁷ For this purpose, three streams were used: an aqueous buffer solution of glycine ethyl ester **8** (pH 3.5), dichloromethane to extract EDA (**9**) and an aqueous solution of sodium nitrite. The biphasic mixture is then pumped into a thermo-controlled glass-microreactor where the diazotisation occurs, then into a sector to facilitate the phase separation before the inline Flow-Liquid-Liquid-Extraction (FLLEEx) module. The organic phase is collected and the aqueous phase is recycled.



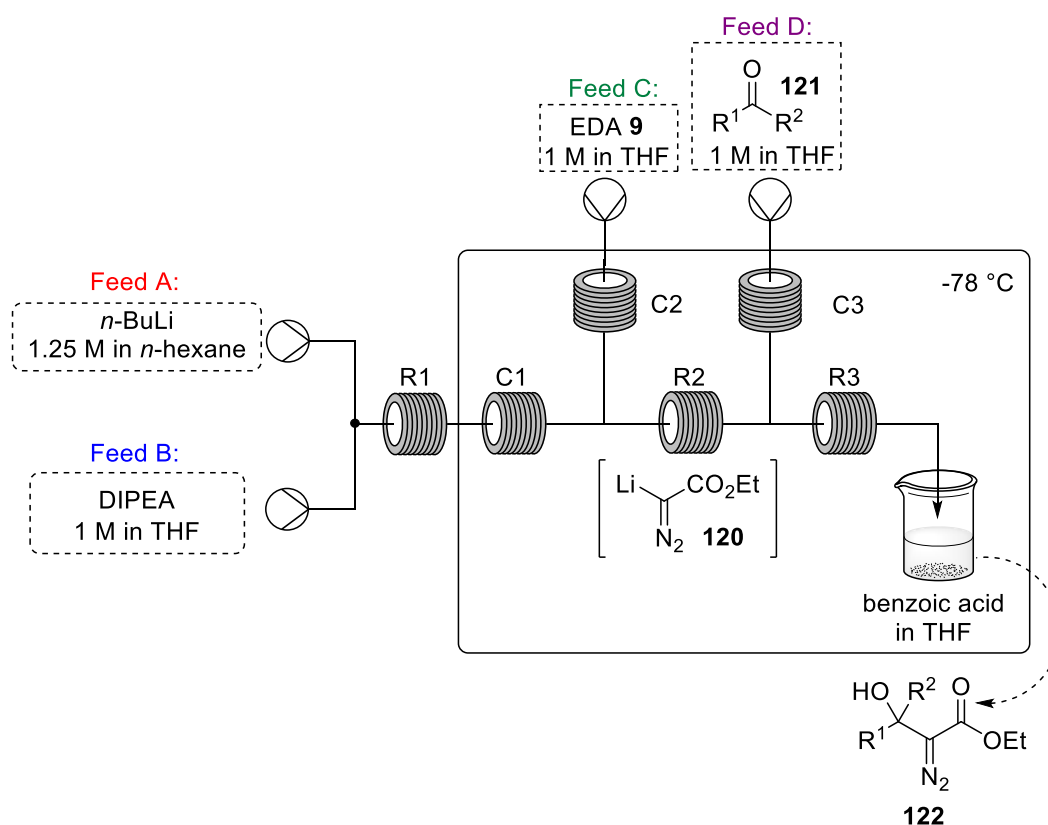
Scheme 1.33: Continuous-flow generation of EDA **9**.¹⁴⁷

Our group has also made some contributions to this topic. Indeed, not long ago, Wirth and co-workers reported the multi-step synthesis of β -hydroxy- α -diazo compounds **119** under flow conditions with the *in situ* generation of EDA (Scheme 1.34).^{43b} In this setup, EDA is generated in the first microreactor within 6 minutes *via* diazotisation, subsequently a first solution of aldehyde **118** and a second solution of DBU are added to the main stream yielding the desired β -hydroxy- α -diazo esters **119** in moderate to excellent yield with no inline extraction needed.



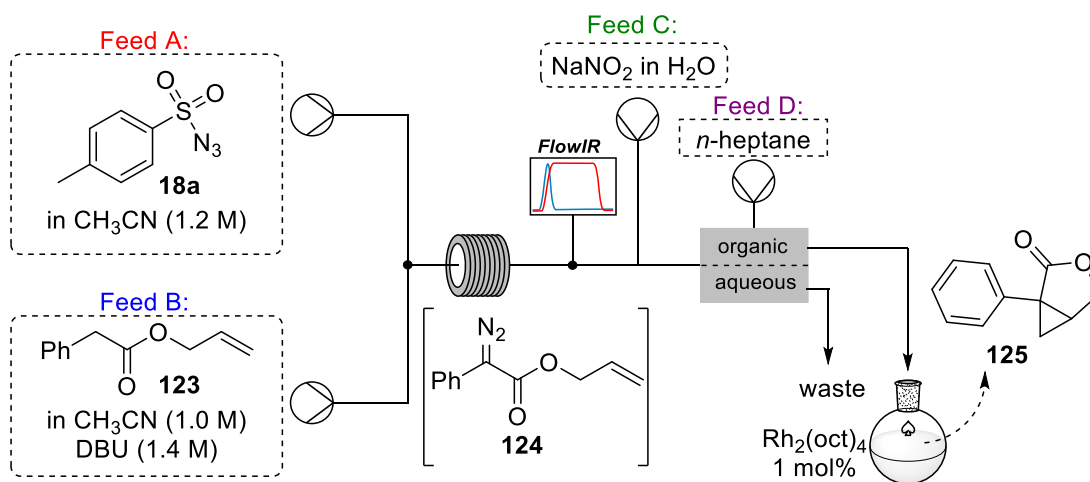
Scheme 1.34: Synthesis of β -hydroxy- α -diazo esters **119** under continuous-flow conditions.^{43b}

Moreover, with the aim of expanding the EDA addition to ketones and lactones, Wirth *et al.* developed also a temperature controlled flow system for the *in situ* generation of LDA using a Vapourtec E-series system (Scheme 1.35).^{43a} The system was dried and kept under argon¹⁴⁸ and was composed by three reactors (R) and three cooling coils (C). The base LDA was generated within 0.8 minutes in a first coil (R1), at room temperature then cooled to $-78\text{ }^{\circ}\text{C}$ for 1.3 minutes (C1) before meeting the cold stream of EDA (**9**) previously cooled for 2.6 minutes (C2) and finally mixed in R2 for 0.2 minutes to form lithium ethyldiazoacetate (**120**). This was then trapped using a pre-cooled solution of ketone **121** and the outlet was quenched with a cold ($-78\text{ }^{\circ}\text{C}$) benzoic acid solution in THF to afford the desired diazo compound **122** in good yields (up to 70%).



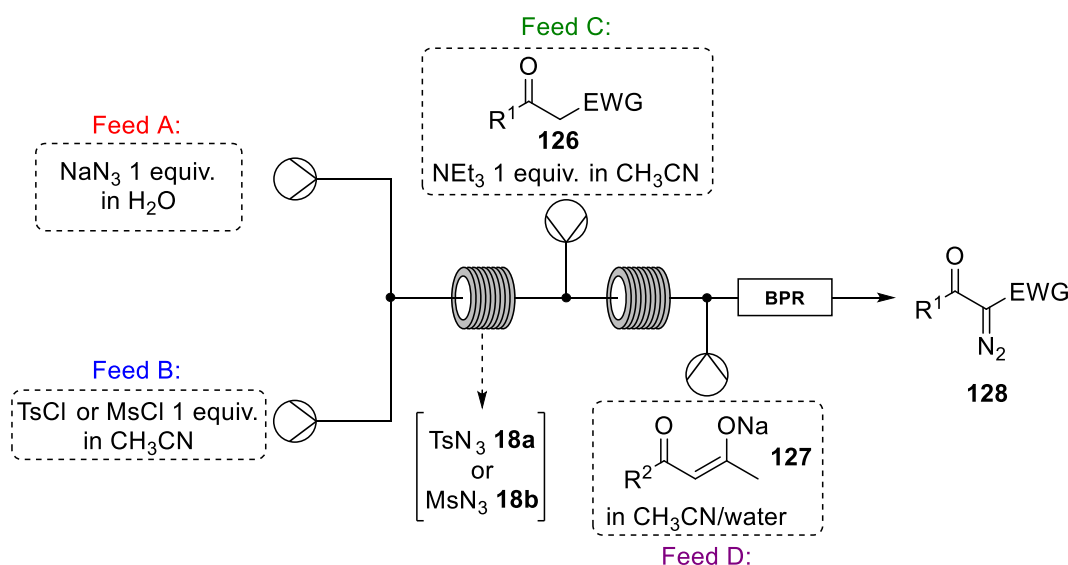
Scheme 1.35: Continuous flow system for the *in situ* generation of LDA and lithium ethyl diazoacetate **120** for the synthesis of β -hydroxy- α -diazo esters **122**. R = reactor; C = cooling coil.^{43a}

As previously mentioned, the Regitz diazo-transfer is one of the most common method to prepare α -diazocarbonyl compounds. Nevertheless, although being documented in batch, flow applications remain limited. Our group in 2015 reported a flow protocol for the synthesis of donor/acceptor diazo compounds with an inline IR spectroscopy analysis for a faster optimisation and inline work-up.¹⁴⁹ This protocol was then successfully coupled to a batch intramolecular cyclopropanation to form **125**, a key intermediate for the synthesis of Milnacipran (Scheme 1.36).¹⁵⁰ A solution of allylic ester **123** and DBU in acetonitrile was mixed together with a solution of tosyl azide (**18a**) in acetonitrile to generate the allyl α -diazoester **124**. An aqueous solution of NaNO_2 was pumped after the reactor coil to quench the reaction then the product **124** was extracted in n -heptane and the phases were separated using an inline membrane separator. The organic stream was then dropped into a round-bottomed flask containing of 1 mol% $\text{Rh}_2(\text{oct})_4$ affording **125** in 33% overall yield (8.2 g/day).



Scheme 1.36: Continuous-flow system for the generation of **125**, key intermediate of Milnacipran analogues *via* Regitz diazo-transfer reaction; oct =octanoate.¹⁵⁰

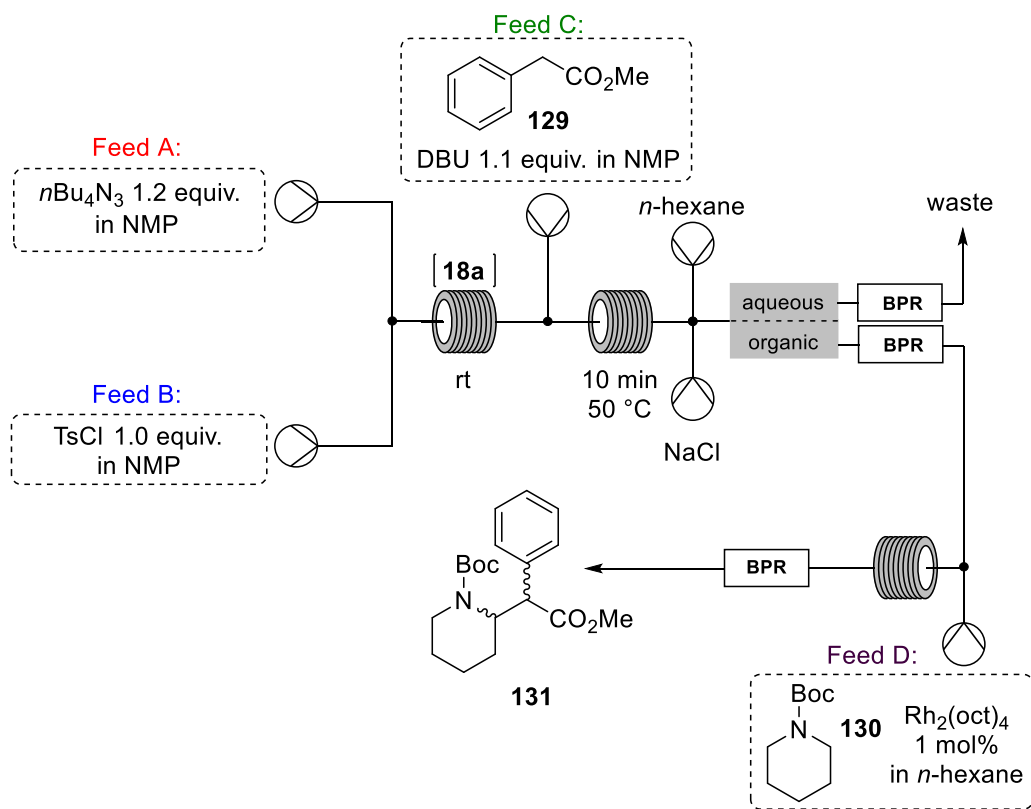
The Collins and Maguire research groups further improved this protocol including the sulfonyl azide synthesis into a continuous flow multi-step synthesis (Scheme 1.37).¹⁵¹ The hazardous tosyl and mesyl azide (**18a–b**) were safely generated *in situ* from an aqueous solution of sodium azide and a solution of either tosyl or mesyl chloride in acetonitrile. Once generated, the sulfonyl azide **18** was mixed with a stream containing the carbonyl substrate **126** and the base to afford the desired diazo compound **128** upon inline quenching with sodium acetoacetate (**127**).



Scheme 1.37: Safe continuous-flow generation of tosyl azide **18a** and mesyl azide **18b** for Regitz diazo-transfer reaction.¹⁵¹

More recently, Monbaliu *et al.* coupled the synthesis of tosyl azide **18a** reported by Maguire *et al.* to the flow diazo-transfer step reported by Wirth *et al.* and added the

intermolecular C–H insertion to the multi-step continuous-flow synthesis of *N*-Boc-protected Ritalin **131** (Scheme 1.38).¹⁵²



Scheme 1.38: Continuous-flow synthesis of Ritalin **131**; NMP = *N*-methyl-2-pyrrolidone.¹⁵²

At first, the tosyl azide (**18a**) was synthesised *in situ* from stable tetrabutylammonium azide and tosyl chloride, then mixed with methyl phenylacetoacetate (**129**) that underwent Regitz diazo-transfer under basic conditions. Subsequently, the diazo compound was extracted from the organic phase by using an inline phase separator and further combined with a stream containing the *N*-Boc piperidine **130** and dirhodium catalyst. The full telescopic strategy afforded the *N*-Boc protected Ritalin **131** in 19% overall yield with a 20 minutes of residence time including the inline separation.

In summary, since the early 2000s flow technologies provided chemists with a set of tools to overcome challenges faced during synthetic processes from the handling of hazardous compounds to scale-ups, thus the interest for developing automated systems for organic synthesis is still strongly increasing in both academia and industry.

1.2.2 Design of Experiment

Although flow chemistry has proven to be ideal to enable reactivities and cut reaction times, it certainly does not come without disadvantages. Flow systems are typically

composed by many modules which increases the complexity of the system, by adding variables that can influence the reaction outcome. Moreover, despite being a precious tool for faster high-throughput-screenings (HTS), it creates a large amount of data in a short period of time that might be hard and time-consuming to analyse. Hence, to tackle the problem self-optimising reactors¹⁵³ that combine the use of intelligent algorithms,¹⁵⁴ in/online devices and statistical software for Design-of-Experiment (DoE) have been developed. The concept of DoE was introduced for the first time by Ronald Fisher in 1926 in “The Arrangement of Field Experiments” and few years later in “The Design of Experiments”¹⁵⁵ and it has since been applied mainly in agriculture, physics and engineering process optimisation.¹⁵⁶

DoE uses a statistical approach that allows to screen many variables and to estimate the main effects with a minimum amount of experiments. Furthermore, it can identify interactions between two or more factors leading to an optimum that a traditional one-factor-at-a-time (OFAT) approach could have missed.¹⁵⁷ At first, chemists appeared to be reluctant on embracing this new approach over the classic OFAT, perhaps intimidated by the statistics and formulae, which makes the task look more complex than necessary. Although an understanding of the basics of statistical tests is encouraged to meaningfully apply a DoE, an in-depth knowledge of statistic and mathematical algorithms it is not required, given the several simplified software commercially available nowadays (Design Expert, MODDE, JMP). In 2001, Owen and co-workers published a step-by-step procedure which aimed to guide chemists through the best decision while optimising a reaction process using DoE.¹⁵⁸ Later, T. Laird with his editorial on *Org. Process Res. Dev.* spurred academia to introduce DoE trainings in undergraduate courses and to embrace the DoE system more often to identify empirical relationships within a complex system of parameters.¹⁵⁹ This resulted in a blossom of industrial applications and publications per year using DoE in the past two decades.¹⁶⁰ Nowadays, DoE found several applications in chemistry from reaction optimisation¹⁶¹ to crystallisations,¹⁶² and HPLC method development.¹⁶³ Furthermore, it finds large utility in industry, mainly drug discovery, by increasing the efficiency and minimising costs and materials, saving time and energy consumption in agreement with the twelve principle of green chemistry,¹⁶⁴ as well as validating robustness testing to ensure quality before releasing an active pharmaceutical ingredient (API).¹⁶⁵

The classic OFAT-approach consists of varying one factor within a range of values whilst the rest of n-parameters are fixed. Once the best condition for this factor is found it is kept fixed and the same process is repeated for all n-parameters in order to find the “optimum” for each factor (Figure 1.9a). This traditional approach suffers from several drawbacks. Firstly, it investigates a relatively small fraction of chemical space and finds

only one of the possible “optimum” within the given chemical space, and it is not necessary the best one. Secondly, by keeping in consideration only the “best” run per each variable, this classic method does not gain information from the discarded experiments. Finally, it is unable to uncover interactions among factors and might confuse “noises” with an actual effect, unless a significant number of repeats are made. On the other hand, DoE is composed by a set of statistically organised experiments, all equally distributed within the desired chemical space, and all of the run are necessary in order to find the local “optimum” (Figure 1.9b). Due to this organisation, DoE can distinguish signals that an OFAT-approach might miss in the noise, but mostly it can identify two-factor interactions (2FI) that are not detected with the OFAT method. Moreover, it allows to investigate even bigger and more complex chemical spaces that are too time consuming to be investigated using a traditional approach.

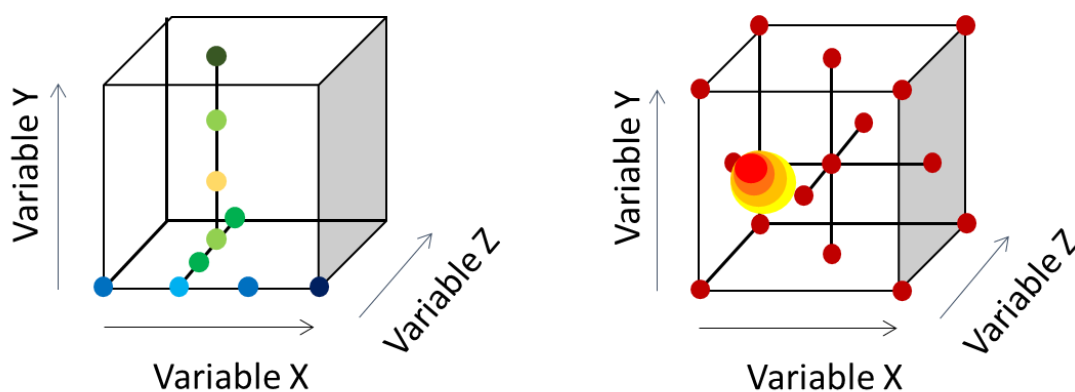


Figure 1.9: Comparison between OFAT-approach (a) and DoE-approach (b) to investigate the chemical space (x,y,z) .

One of the drawbacks of DoE is that a complex design requires a large set of experiments which need to be performed by the same operator under similar experimental conditions, therefore in a relatively short period of time to avoid errors (e.g. nuisance). However, highly automated systems and in/online analysis methods can be adopted to speed up the analysis.

The first things to do when dealing with DoE is to learn using the right terminology (Appendix A). Once familiar with the basic terms, in order to conduct a successful DoE, it is important to follow a precise work-flow:

- 1) Define the objective: it is vital to have a clear goal (e.g. screening or optimisation) in order to select the appropriate ranges and design.
- 2) Define the factors, their levels and their ranges: to define the chemical space that is going to be studied. The factors can be numeric or categoric, continuous or discrete.

- 3) Define the responses: it is necessary to have a reliable, accurate and precise method to measure the reaction outcome (e.g. yield or conversion).
- 4) Select the most appropriate experimental design: the choice depends on the prefixed objective.
- 5) Generating the experimental matrix: a matrix of experiments is generated by the software once all the above information are included. The experiments are *randomised* in order to reduce nuisance errors. Moreover, it is important to include *central point* experiments to ensure reproducibility and to detect nonlinearity.
- 6) Perform the experiments: ideally, the experiments should be performed under same experimental and analytical conditions in a randomised order and within a restricted time to reduce nuisance error. When randomisation is not possible due to hard-to-change (HTC) factors, the run can be “blocked”.
- 7) Software analysis: the most appropriate mathematical transformation (or none) is selected by the operator upon values such as adjusted and predictive R-squared terms and by evaluating the diagnostic plots. Next, the analysis of variance (ANOVA) is providing which terms are the most significant terms by looking at *p-values* < 0.05. Finally, the software creates a table of “optimal conditions” that satisfy the objectives together with a series of contour plots and 3D-surface plots. When there is more than one response to optimise, it is possible to overlap all contour plots and highlight the “sweet spot” in which all requirements are satisfied.
- 8) Confirming reactions: it is important to verify experimentally what is predicted by the model.

There are many types of experimental models and the choice depends on the dimension of the chemical space that we are interested in, thus, it is usually a compromise between the number of variables to study and the number of experiments to perform in order to have meaningful results (Figure 1.10). Among all, the simplest two-level factorial designs are the most commonly used for screening (Figures 1.10a and 1.10b). As depicted in Figure 1.10b, the Fractional Factorial Design (FFD) uses fewer experiments to explore the same chemical space of the full factorial design (FD, Figure 1.10a), hence it has a lower resolution compared to a FD. The factorial designs are reported as I^k , where I indicates the number of levels of each factor and k the number of factors. Similarly, a fractional factorial design can be reported as I^{k-p} , where I indicates the number of levels, k the number of factors, and p the size of the fraction of the FD used. In a more technical term, p represents the number of generators of the FFD. For example, in case of studying

four factors, a range of values defined by two levels, a maximum and a minimum must be selected. In coded values, these levels are indicated as “+1” or simply “+” and “-1” or “-” for the highest and the lowest level, respectively. In this case, the full factorial design is expressed as 2^4 , which represents the total number of 16 experiments required by the FD. Similarly, the factorial designs can be noted as 2^{4-1} , 2^{4-2} , 2^{4-3} and the numbers of the required experiments are 8, 4 and 2, respectively. Thus, a higher number of generators (p) leads to a lower resolved FFD. The FD and FDD, as screening designs, are using linear models to identify main effects. For this reason, to identify the presence of any curvature, it is recommended to add central points, which are reported with the coding factor level of “0”.

When a non-linear response is detected, more resolved designs are typically used for Response-Surface-Modelling (RSM) such as the Central Composite Face (CCF, Figure 1.10c) or the Circumscribed Composite Design (CCD, Figure 1.10d). However, these designs are not recommended for a high number of factors as they require a very large number of experiments. Generally, a lower resolution design is conducted first to narrow down the number of factors. Once the number of significant parameters is reduced, a higher resolution design can be performed if needed.

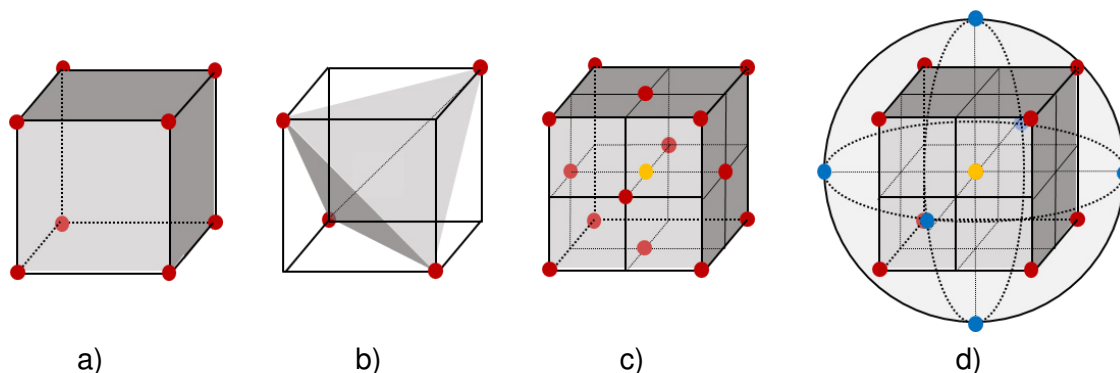


Figure 1.10: Example of models: a) Factorial Design (FD); b) Fractional Factorial Design (FFD); c) Centred Composite Face (CCF); d) Circumscribe Composite Design (CCD); The required experiments per each models are shown as dots: red = factorial points, yellow = central points; blue = axial points.

To conclude, the DoE uses a statistical approach to conduct and analyse a set of experiments offering an efficient approach towards complex systems and chemical reactions optimisation. Nevertheless, it is worth mentioning that the statistical analysis is just a tool that aims to facilitate the analysis of the data and the process optimisation. It should not replace the common sense nor the scientific knowledge of the operator, who is responsible to decide whether what it is suggested by the model is chemically sensible or dangerous to perform.

References

- 1 S. V. Heines, *J. Chem. Educ.* **1958**, *35*, 187–191.
- 2 S. P. Green, K. M. Wheelhouse, A. D. Payne, J. P. Hallett, P. W. Miller, J. A. Bull, *Org. Process Res. Dev.* **2020**, *24*, 67–84.
- 3 L. D. Proctor, A. J. Warr, *Org. Process Res. Dev.* **2002**, *6*, 884–892.
- 4 For selected examples see: a) C. Soldi, K. N. Lamb, R. A. Squitieri, M. González-López, M. J. Di Maso, J. T. Shaw, *J. Am. Chem. Soc.* **2014**, *136*, 15142–15145; b) H. M. L. Davies, R. E. J. Beckwith, *Chem. Rev.* **2003**, *103*, 2861–2904.
- 5 S. Zhu, J. A. Perman, X. P. Zhang, *Angew. Chem. Int. Ed.* **2008**, *47*, 8460–8463.
- 6 For selected examples on C–H insertion see a) M. P. Doyle, R. Duffy, M. Ratnikov, L. Zhou, *Chem. Rev.* **2010**, *110*, 704–724; b) M. P. Doyle, M. Ratnikov, Y. Liu, *Org. Biomol. Chem.* **2011**, *9*, 4007–4016; For a selected example on N–H insertion see: B. Liu, S.-F. Zhu, W. Zhang, C. Chen, Q.-L. Zhou, *J. Am. Chem. Soc.* **2007**, *129*, 5834–5835; For a selected example on O–H insertion see: C. Chen, S.-F. Zhu, B. Liu, L.-X. Wang, Q.-L. Zhou, *J. Am. Chem. Soc.* **2007**, *129*, 12616–12617.
- 7 A. Padwa, *Helv. Chim. Acta* **2005**, *88*, 1357–1374.
- 8 H. M. L. Davies, D. Morton, *Chem. Soc. Rev.* **2011**, *40*, 1857–1869.
- 9 For selected examples see: a) D. Morton, S. B. Blakey, *ChemCatChem* **2015**, *7*, 577–578; b) Q. Xiao, Y. Zhang, J. Wang, *Acc. Chem. Res.* **2013**, *46*, 236–247; c) J. R. Fulton, V. K. Aggarwall, J. de Vicente, *Eur. J. Org. Chem.* **2005**, 1479–1492.
- 10 a) A. Greb, J.-S. Poh, S. Greed, C. Battilocchio, P. Pasau, D. C. Blakemore, S. V. Ley, *Angew. Chem. Int. Ed.* **2017**, *56*, 16602–16605; b) D. N. Tran, C. Battilocchio, S.-B. Lou, J. M. Hawkinsb, S. V. Ley, *Chem. Sci.* **2015**, *6*, 1120–1125.
- 11 a) S. T. R. Müller, T. Wirth, *ChemSusChem* **2015**, *8*, 245–250; b) K. J. Hock, R. M. Koenigs, *Chem. Eur. J.* **2018**, *24*, 10571–10583.
- 12 a) X. Lei, J. A. Porco Jr., *J. Am. Chem. Soc.* **2006**, *128*, 14790–14791; b) R. S. Laufer, G. I. Dmitrienko, *J. Am. Chem. Soc.* **2002**, *124*, 1854–1855; c) S. J. Gould, *Chem. Rev.* **1997**, *97*, 2499–2509.
- 13 For general reviews see: a) A. Ford, H. Miel, A. Ring, C. N. Slattery, A. R. Maguire, M. A. McKervey, *Chem. Rev.* **2015**, *115*, 9981–10080; b) G. Maas, *Angew. Chem. Int. Ed.* **2009**, *48*, 8186–8195; c) T. Ye, M. A. McKervey, *Chem. Rev.* **1994**, *94*, 1091–1160.
- 14 T. Curtius, *Ber. Dtsch. Chem. Ges.* **1883**, *16*, 2230–2231.
- 15 V. D. Filimonov, M. Trusova, P. Postnikov, E. A. Krasnokutskaya, Y. M. Lee, H. Y. Hwang, H. Kim, K.-W. Chi, *Org. Lett.* **2008**, *10*, 3961–3964.
- 16 K. V. Kutonova, M. E. Trusova, P. S. Postnikov, V. D. Filimonov, J. Parello, *Synthesis* **2013**, *45*, 2706–2710.
- 17 O. Dimroth, *Justus Liebigs Ann. Chem.* **1910**, *373*, 336–370.
- 18 T. Curtius, W. Klavehn, *J. Prakt. Chem.* **1926**, *121*, 65–87.

- 19 a) M. Regitz, *Chem. Ber.* **1964**, *97*, 2742–2754; b) M. Regitz, *Justus Liebigs Ann. Chem.* **1964**, 676, 101–109.
- 20 a) M. Regitz, *Angew. Chem. Int. Ed. Engl.* **1967**, *6*, 733–749; b) M. Regitz, *Synthesis* **1972**, 351–373.
- 21 a) S. Chuprakov; M. Rubin; V. Gevorgyan, *J. Am. Chem. Soc.* **2005**, *127*, 3714–3715; b) W.-J. Zhao, M. Yan, D. Huang, S.-J. Ji, *Tetrahedron* **2005**, *61*, 5585–5593.
- 22 T. Wakimoto, K. Miyata, H. Ohuchi, T. Asakawa, H. Nukaya, Y. Suwa, T. Kan, *Org. Lett.* **2011**, *13*, 2789–2791.
- 23 J. M. Villalgordo; A. Enderli, A. Linden, H. Heimgartner, *Helv. Chim. Acta* **1995**, *78*, 1983–1998.
- 24 a) M. Regitz, J. Rueter, *Chem. Ber.* **1968**, *101*, 1263–1270; b) M. Regitz, F. Menz, *Chem. Ber.* **1968**, *101*, 2622–2632.
- 25 R. L. Danheiser, R. F. Miller, R. G. Brisbois, S. Z. Park, *J. Org. Chem.* **1990**, *55*, 1959–1964.
- 26 a) D. F. Taber, R. B. Sheth, R. V. Joshi, *J. Org. Chem.* **2005**, *70*, 2851–2854; b) D. F. Taber, K. You, Y. A. Song, *J. Org. Chem.* **1995**, *60*, 1093–1094.
- 27 D. F. Taber, R. E. Ruckle, M. J. Hennessy, *J. Org. Chem.* **1986**, *51*, 4077–4078.
- 28 F. W. B. G. Hazen, L. M. Weinstock, R. Connell, F. W. Bollinger, *Synth. Commun.* **1981**, *11*, 947–956.
- 29 a) L. Benati, D. Nanni, P. Spagnolo, *J. Org. Chem.* **1999**, *64*, 5132–5138; b) L. Lombardo, L. N. Mander, *Synthesis* **1980**, 368–369.
- 30 L. D. Tuma, *Thermochimica Acta* **1994**, *243*, 161–167.
- 31 J. S. Baum, D. A. Shook, H. M. L. Davies, H. D. Smith, *Synth. Commun.* **1987**, *17*, 1709–1716; b) H. M. L. Davies, W. R. Cantrell Jr., K. R. Romines, J. S. Baum, *Org. Synth.* **1992**, *70*, 93–100.
- 32 L. Benati, G. Calestani, D. Nanni, P. Spagnolo, *J. Org. Chem.* **1998**, *63*, 4679–4684; b) L. Zhou, M. P. Doyle, *J. Org. Chem.* **2009**, *74*, 9222–9224.
- 33 a) N. Fischer, E. D. Goddard-Borger, R. Greiner, T. M. Klapötke, B. W. Skelton, J. Stierstorfer, *J. Org. Chem.* **2012**, *77*, 1760–1764; b) G. T. Potter, G. C. Jayson, G. J. Miller, J. M. Gardiner, *J. Org. Chem.*, **2016**, *81*, 3443–3446.
- 34 M. K. Muthyala, S. Choudhary, A. Kumar, *J. Org. Chem.* **2012**, *77*, 8787–8791.
- 35 J. K. Rueter, O. N. Samuel, E. W. Baxter, G. C. Leo, A. B. Reitz, *Tetrahedron Lett.* **1998**, *39*, 975–978.
- 36 D. Dar'in, G. Kantin, M. Krasavin, *Chem. Commun.* **2019**, *55*, 5239–5242.
- 37 For selected examples see: a) T. L. Holton, H. Shechter, *J. Org. Chem.* **1995**, *60*, 4725–4729; b) W. Schroeder, L. Katz, *J. Org. Chem.* **1954**, *19*, 718–720; c) H. Morrison, S. Danishefsky, P. Yates, *J. Org. Chem.* **1961**, *26*, 2617–2618.
- 38 M. I. Javed, M. Brewer, *Org. Lett.* **2007**, *9*, 1789–1792.
- 39 J. R. Denton, D. Sukumaran, H. M. L. Davies, *Org. Lett.* **2007**, *9*, 2625–2628;
- 40 W. Bamford, T. Stevens, *J. Chem. Soc.* **1952**, 4735–4740.

- 41 a) E. L. Myers, R. T. Raines, *Angew. Chem. Int. Ed.* **2009**, *48*, 2359–2363; b) H.-H. Chou, R. T. Raines, *J. Am. Chem. Soc.* **2013**, *135*, 14936–14939.
- 42 For selected examples see: a) V. D. Pinho, A. C. B. Burtoloso, *J. Org. Chem.* **2011**, *76*, 289–292; b) V. D. Pinho, A. C. B. Burtoloso, *Tetrahedron Lett.* **2012**, *53*, 876–878; c) J. Barluenga, G. Lonzi, L. Riesgo, M. Tomás, L. A. López, *J. Am. Chem. Soc.* **2011**, *133*, 18138–18141; d) R. d. S. Rianelli, F. d. C. da Silva, M. C. B. V. de Souza, V. F. Ferreira, *Lett. Org. Chem.* **2006**, *3*, 73–77.
- 43 For selected example on aldol-type coupling: a) S. T. R. Müller, T. Hokamp, S. Ehrmann, P. Hellier, T. Wirth, *Chem. Eur. J.* **2016**, *22*, 11940–11942; b) S. T. R. Müller, D. Smith, P. Hellier, T. Wirth, *Synlett* **2014**, *25*, 871–875; c) Y. Zhangab, J. Wang, *Chem. Commun.* **2009**, 5350–5361; For selected example on Mannich-type coupling: a) Y. Zhao, N. Jiang, S. Chen, C. Peng, X. Zhang, Y. Zou, S. Zhang, J. Wang, *Tetrahedron* **2005**, *61*, 6546–6552; b) N. Jiang, Z. Qu, J. Wang, *Org. Lett.* **2001**, *3*, 2989–2992; For selected work on Pd-catalysed cross-coupling: a) F. Ye, S. Qu, L. Zhou, C. Peng, C. Wang, J. Cheng, M. L. Hossain, Y. Liu, Y. Zhang, Z.-X. Wang, J. Wang, *J. Am. Chem. Soc.* **2015**, *137*, 4435–4444; b) C. Eidamshaus, P. Hommes, H.-U. Reissig, *Synlett* **2012**, *23*, 1670–1674; c) C. Peng, J. Cheng, J. Wang, *J. Am. Chem. Soc.* **2007**, *129*, 8708–8709.
- 44 a) Y. Ge, W. Sun, Y. Chen, Y. Huang, Z. Liu, Y. Jiang, T.-P. Loh, *J. Org. Chem.* **2019**, *84*, 2676–2688; b) W. Kirmse, *Eur. J. Org. Chem.* **2002**, 2193–2256.
- 45 M. P. Doyle, D. C. Forbes, *Chem. Rev.* **1998**, *98*, 911–936.
- 46 S. E. Reisman, R. R. Nani, S. Levin. *Synlett* **2011**, *17*, 2437–2442.
- 47 P. Doyle, W. H. Tamblin, V. Bagheri, *J. Org. Chem.* **1981**, *46*, 5094–5102.
- 48 J. Clayden, N. Greeves, S. Warren, *Organic Chemistry*. **2012**, Ed. Oxford University Press.
- 49 H. Tomioka, H. Okuno, Y. Izawa, *J. Org. Chem.* **1980**, *45*, 5278–5283; b) W. Kirmse, H.-J. Wroblowsky, *Chem. Ber.* **1983**, *116*, 1118–1131.
- 50 a) W. E. Bachmann, W. S. Struve, *Org. React.* **1942**, *1*, 38–62; b) F. Arndt, B. Eistert, *Ber. Dtsch. Chem. Ges.* **1935**, *68*, 200–208.
- 51 V. D. Pinho, B. Gutman, C. O. Kappe, *RSC Adv.* **2014**, *4*, 37419–37422.
- 52 B. Musio, F. Mariani, E. P. Śliwiński, M. A. Kabeshov, H. Odajima, S. V. Ley, *Synthesis* **2016**, *48*, 3515–3526.
- 53 H. Pellissier, *Tetrahedron* **2008**, *64*, 7041–7095.
- 54 a) H. Lin, C. Dai, T. F. Jamison, K. F. Jensen, *Angew. Chem. Int. Ed.* **2017**, *56*, 8870–8873; b) C. A. Correia, K. Gilmore, D. T. McQuade, P. H. Seeberger, *Angew. Chem. Int. Ed.* **2015**, *54*, 4945–4948.
- 55 W. Wu, Z. Lin, H. Jiang, *Org. Biomol. Chem.* **2018**, *16*, 7315–7329.
- 56 P. Cadman, H. M. Meunier, A. F. Trotman-Dickenson, *J. Am. Chem. Soc.* **1969**, *91*, 7640–7644.
- 57 a) H. Wang, D. M. Guptill, A. Varela-Alvarez, D. G. Musaev, H. M. L. Davies, *Chem. Sci.* **2013**, *4*, 2844–2850; b) K. M. Chepiga, C. Qin, J. S. Alford, S. Chennamadhavuni, T. M.

- Gregg, J. P. Olson, H. M. L. Davies, *Tetrahedron* **2013**, 69, 27–28; c) S. Y. Shim, J. Y. Kim, M. Nam, G.-S. Hwang, D. H. Ryu, *Org. Lett.* **2016**, 18, 160–163.
- 58 P. K. Dutta, J. Chauhan, M. K. Ravva, S. Sen, *Org Lett.* **2019**, 21, 2025–2028.
- 59 N. M. Roda, D. N. Tran, C. Battilocchio, R. Labes, R. J. Ingham, J. M. Hawkins, S. V. Ley, *Org. Biomol. Chem.* **2015**, 13, 2550–2554.
- 60 A. J. Hubert, A. F. Noels, A. J. Anciaux, R. Warin, P. Teyssie, *J. Org. Chem.* **1981**, 46, 873–876.
- 61 O. A. McNamara, A. R. Maguire, *Tetrahedron* **2011**, 67, 9–40.
- 62 A. Padwa, S. F. Hornbuckle, *Chem. Rev.* **1991**, 91, 263–309.
- 63 a) M. P. Doyle, V. Bagheri, N. K. Harn, *Tetrahedron Lett.* **1988**, 29, 5119–5122; b) T. Yakura, A. Ozono, K. Matsui, M. Yamashita, T. Fujiwara, *Synlett* **2013**, 24, 65–68; c) M. Liao, L. Peng, J. Wang, *Org. Lett.* **2008**, 10, 693–696; d) E. Roberts, J. P. Sancon, J. B. A. Sweeney, *Org. Lett.* **2005**, 7, 2075–2078.
- 64 a) A. Padwa, *Tetrahedron* **2011**, 67, 8057–8072; b) A. Padwa, *Helv. Chim. Acta* **2005**, 88, 1357–1374; c) Y. Zhu, C. Zhai, L. Yang, W. Hu, *Eur. J. Org. Chem.* **2011**, 1113–1124.
- 65 a) M. P. Doyle, D. G. Ene, D. C. Forbes, J. S. Tedrow, *Tetrahedron Lett.* **1997**, 38, 4367–4370; b) J.-P. Qu, Z.-H. Xu, J. Zhou, C.-L. Cao, X.-L. Sun, L.-X. Dai, Y. Tang, *Adv. Synth. Catal.* **2009**, 351, 308–312; c) F. G. West, B. N. Naidu, *J. Am. Chem. Soc.* **1993**, 115, 1177–1178.
- 66 W. v. E. Doering, R. G. Buttery, R. G. Laughlin, N. Chaudhuri, *J. Am. Chem. Soc.* **1956**, 78, 3224–3224.
- 67 For selected examples see: a) D. F. Taber, E. H. Petty, *J. Org. Chem.* **1982**, 47, 4808–4809; b) D. F. Taber, R. E. Ruckle, *J. Am. Chem. Soc.* **1986**, 108, 7686–7693; c) D. F. Taber, R. E. Ruckle, *Tetrahedron Lett.* **1985**, 26, 3059–3062; d) D. F. Taber, K. Raman, *J. Am. Chem. Soc.* **1983**, 105, 5935–5937; e) D. F. Taber, K. Raman, M. D. Gaul, *J. Org. Chem.* **1987**, 52, 28–34; f) D. F. Taber, E. H. Petty, K. Raman, *J. Am. Chem. Soc.* **1985**, 107, 196–199.
- 68 For selected examples see: a) H.-J. Lim, G. A. Sulikowski, *J. Org. Chem.* **1995**, 60, 2326–2327; b) S. Lee, H.-J. Lim, K. L. Cha, G. A. Salikowski, *Tetrahedron* **1997**, 53, 16521–16532; c) H. Nozaki, S. Moriuti, M. Yamabe, R. Noyori, *Tetrahedron Lett.* **1966**, 59–63.
- 69 M. P. Doyle, L. J. Westrum, W. N. E. Wolthuis, M. M. See, W. P. Boone, V. Bagheri, M. M. Pearson, *J. Am. Chem. Soc.* **1993**, 115, 958–964.
- 70 E. Nakamura, N. Yoshikai, M. Yamanaka, *J. Am. Chem. Soc.* **2002**, 124, 7181–7192.
- 71 a) D. F. Taber, K. K. You, A. L. Rheingold, *J. Am. Chem. Soc.* **1996**, 118, 547–556; b) D. F. Taber, S. C. Malcolm, *J. Org. Chem.* **1998**, 63, 3717–3721.
- 72 A. Padwa, D. J. Austin, A. T. Price, M. A. Sentones, M. P. Doyle, M. N. Protopopova, W. R. Winchester, A. Tran, *J. Am. Chem. Soc.* **1993**, 115, 8669–8680.
- 73 H. M. L. Davies, T. Hansen, *J. Am. Chem. Soc.* **1997**, 119, 9075–9076.
- 74 H. M. L. Davies, C. Venkataramani, T. Hansen, D. W. Hopper, *J. Am. Chem. Soc.* **2003**, 125, 6462–6468.

- 75 a) H. M. L. Davies, G. E. Antoulinakis, *Org. Lett.* **2000**, *2*, 4153–4156; b) H. M. L. Davies, E. G. Antoulinakis, T. Hansen, *Org. Lett.* **1999**, *1*, 383–386; c) H. M. L. Davies, R. E. J. Beckwith, E. G. Antoulinakis, Q. Jin, *J. Org. Chem.* **2003**, *68*, 6126–6132.
- 76 a) H. M. L. Davies, P. Ren, *J. Am. Chem. Soc.* **2001**, *123*, 2070–2071; b) H. M. L. Davies, P. Ren, Q. Jin, *Org. Lett.* **2001**, *3*, 3587–3590.
- 77 a) K. Liao, W. Liu, Z. L. Niemeyer, Z. Ren, J. Bacsá, D. G. Musaev, M. S. Sigman, H. M. L. Davies, *ACS Catal.* **2018**, *8*, 678–682; b) C. M. Qin, H. M. L. Davies, *J. Am. Chem. Soc.* **2014**, *136*, 9792–9796; c) H. M. L.; Davies, Q. Jin, *Tetrahedron: Asymmetry* **2003**, *14*, 941–949.
- 78 K. Liao, S. Negretti, D. G. Musaev, J. Bacsá, H. M. L. Davies, *Nature* **2016**, *533*, 230–234.
- 79 a) E. Nadeau, Z. Li, D. Morton, H. M. L. Davies, *Synlett* **2009**, *1*, 151–154; b) H. M. L. Davies, T. Hansen, M. R. Churchill, *J. Am. Chem. Soc.* **2000**, *122*, 3063–3070 c) K. Liao, T.C. Pickel, V. Boyarskikh, J. Bacsá, D. G. Musaev, H. M. L. Davies, *Nature* **2017**, *551*, 609–613.
- 80 a) H. M. L. Davies, A. Ni, *Chem. Commun.* **2006**, 3110–3112; b) H. M. L. Davies, A. M. Walji, R. J. Townsend, *Tetrahedron Lett.* **2002**, *43*, 4981–4983.
- 81 S.-I Hashimoto, N. Watanabe, S. Ikegami, *Tetrahedron Lett.* **1990**, *31*, 5173–5174.
- 82 M. Kennedy, M. A. McKervey, A. R. Maguire, G. H. P. Roos, *J. Chem. Soc., Chem. Commun.* **1990**, 361–362.
- 83 M. P. Doyle, A. V. Oeveren, L. J. Westrum, M. N. Protopopova, T. W. Clayton, *J. Am. Chem. Soc.* **1991**, *113*, 8982–8984.
- 84 For selected examples see: a) I. Aviv, Z. Gross, *Chem. Commun.* **2006**, 4477–4479; b) P. Livant, Y. Jie, X. Wang, *Tetrahedron Lett.* **2005**, *46*, 2113–2116; c) R. T. Buck, P. A. Clarke, D. M. Coe, M. J. Drysdale, L. Ferris, D. Haigh, C. J. Moody, N. D. Pearson, E. Swann, *Chem. Eur. J.* **2000**, *6*, 2160–2167.
- 85 For selected examples see: a) J. Xue, H. L. Luk, M. S. Platz, *J. Am. Chem. Soc.* **2011**, *133*, 1763–1765; b) J. Busch-Petersen, E. J. Corey, *Org. Lett.* **2000**, *2*, 1641–1643; c) M. Austeri, D. Rix, W. Zeghida, J. Lacour, *Org. Lett.* **2011**, *13*, 1394–1397; d) S.-F. Zhu, X.-G. Song, Y. Li, Y. Cai, Q.-L. Zhou, *J. Am. Chem. Soc.* **2010**, *132*, 16374–16376.
- 86 S. N. Osipov, T. Lange, P. Tsouker, J. Spengler, L. Hennig, B. Kokschi, S. Berger, S. M. El-Kousy, *Synthesis* **2004**, *11*, 1821–1829.
- 87 Y.-Z. Zhang, S.-F. Zhu, Y. Cai, H.-X. Mao, Q.-L. Zhou, *Chem. Commun.* **2009**, 5362–5364.
- 88 a) H. M. L. Davies, T. Hansen, J. Rutberg, P. R. Bruzinski, *Tetrahedron Lett.* **1997**, *38*, 1741–1744; b) Y.-Z. Zhang, S.-F. Zhu, L.-X. Wang, Q.-L. Zhou, *Angew. Chem. Int. Ed.* **2008**, *47*, 8496–8498.
- 89 T. W. J. Taylor, L. A. Forscey, *J. Chem. Soc.* **1930**, 2272–2277.
- 90 J. Tao, R. Tran, G. K. Murphy, *J. Am. Chem. Soc.* **2013**, *135*, 16312–16315.
- 91 Y. Xia, Z. Liu, Z. Liu, R. Ge, F. Ye, M. Hossain, Y. Zhang, J. Wang, *J. Am. Chem. Soc.* **2014**, *136*, 3013–3015.
- 92 C. Zheng, S.-L. You, *RSC Adv.* **2014**, *4*, 6173–6214; b) S. Jia, D. Xing, D. Zhang, W. Hu, *Angew. Chem. Int. Ed.* **2014**, *53*, 13098–13101.

- 93 H. Li, Y. Zhang, J. Wang, *Synthesis* **2013**, *45*, 3090–3098.
- 94 J. Hooz, S. Linke, *J. Am. Chem. Soc.* **1968**, *90*, 5936–5937.
- 95 J. Hooz, G. F. Morrison, *Can. J. Chem.* **1970**, *48*, 868–870.
- 96 J. Hooz, S. Linke, *J. Am. Chem. Soc.* **1968**, *90*, 6891–9892.
- 97 D. J. Pasto, P. W. Wojtkowski, *Tetrahedron Lett.* **1970**, *11*, 215–218.
- 98 J. Hooz, D. M. Gunn, *J. Am. Chem. Soc.* **1969**, *91*, 6195–6196.
- 99 J. Hooz, J. N. Bridson, *Can. J. Chem.* **1972**, *50*, 2387–2390.
- 100 a) D. J. Pasto, P. W. Wojtkowski, *J. Org. Chem.* **1971**, *36*, 1790–1792; b) J. Hooz, J. Oudenes, *Synth. Commun.* **1980**, *10*, 139–145.
- 101 J. Hooz, J. Oudenes, *Tetrahedron Lett.* **1983**, *24*, 5695–5698.
- 102 a) J. Hooz, J. N. Bridson, *J. Am. Chem. Soc.* **1973**, *95*, 602–603; b) Y. Luan, J. Yu, X. Zhang, S. E. Schaus, G. Wnag, *J. Org. Chem.* **2014**, *79*, 4694–4698.
- 103 T. Mukaiyama, K. Inomata, M. Muraki, *J. Am. Chem. Soc.* **1973**, *95*, 967–968.
- 104 J. Hooz, J. Oudenes, J. L. Roberts, A. Benderly, *J. Org. Chem.* **1987**, *52*, 1347–1349.
- 105 F.J. Lopez-Herrera F. Sarabia-Garcia, *Tetrahedron Lett.* **1995**, *36*, 2851–2854.
- 106 M. A. Sanchez-Carmona, D. A. Contreras-Cruz, L. D. Miranda, *Org. Biomol. Chem.* **2011**, *9*, 6506–6508.
- 107 J. Hooz, J. Oudenes, *J. Synth. Commun.* **1982**, *12*, 189–194.
- 108 H. C. Brown, M. M. Midland, A. B. Levy, *J. Am. Chem. Soc.* **1972**, *94*, 3662–3664.
- 109 a) J. Hooz, J. N. Bridson, J. G. Calzada, H. C. Brown, M. M. Midland, A. B. Levy, *J. Org. Chem.* **1973**, *38*, 2574–2576; b) H. C. Brown, A. M. Salunkhe, *Synlett*, **1991**, *10*, 684–686.
- 110 J. Barluenga, M. Tomás-Gamasa, F. Aznar, C. Valdés, *Nat. Chem.* **2009**, *1*, 494–499.
- 111 C. Peng, W. Zhang, G. Yan, J. Wang, *Org. Lett.* **2009**, *11*, 1667–1670.
- 112 For selected examples see : a) R. L. Melen, M. M. Hansmann, A. J. Lough, A. S. K. Hashmi, D. W. Stephan, *Chem. Eur. J.* **2013**, *19*, 11928–11938; b) S. Tamke, Z.-W. Qu, N. A. Sitte, U. Flörke, S. Grimme, J. Paradies, *Angew. Chem. Int. Ed.* **2016**, *55*, 4336–4339; c) Y. Soltani, L. C. Wilkins, R. L. Melen, *Angew. Chem. Int. Ed.* **2017**, *56*, 11995–11999; d) G. Erker, *Dalton Trans.* **2005**, 1883–1890.
- 113 a) D. W. Stephan, G. Erker, *Angew. Chem. Int. Ed.* **2010**, *49*, 46–76; b) D. W. Stephan, G. Erker, *Angew. Chem. Int. Ed.* **2015**, *54*, 6400–6441.
- 114 a) D. J. Parks, W. E. Piers, *J. Am. Chem. Soc.* **1996**, *118*, 9440–9441; b) M. Oestreich, J. Hermeke, J. Mohr, *Chem. Soc. Rev.* **2015**, *44*, 2202–2220.
- 115 For selected example see: a) C. L. Wilkins, Y. Soltani, J. R. Lawson, B. Slater, R. L. Melen, *Chem. Eur. J.* **2018**, *24*, 7364–7368; b) C. Chen, G. Kehr, R. Fröhlich, G. Erker, *J. Am. Chem. Soc.* **2010**, *132*, 13594–13595; c) M. M. Hansmann, R. L. Melen, F. Rominger, A. S. K. Hashmi, D. W. Stephan, *J. Am. Chem. Soc.* **2014**, *136*, 777–782; d) C. Chen, T. Voss, R. Fröhlich, G. Kehr, G. Erker, *Org. Lett.* **2011**, *13*, 62–65;
- 116 M. Fleige, J. Möbus, T. vom Stein, F. Glorius, D. W. Stephan, *Chem. Commun.* **2016**, *52*, 10830–10833.

- 117 a) Q. Yin, S. Kemper, H. F. T. Klare, M. Ostereich, *Chem. Eur. J.* **2016**, *22*, 13840–13844; b) Q. Yin, Y. Soltani, R. L. Melen, M. Ostereich, *Organometallics* **2017**, *36*, 2381–2384.
- 118 a) J. R. Lawson, L. C. Wilkins, R. L. Melen, *Chem. Eur. J.* **2017**, *23*, 10997–11000; b) J. L. Carden, L. J. Gierlichs, D. F. Wass, D. L. Browne, *Chem. Commun.* **2019**, *55*, 318–321.
- 119 R. C. Neu, C. Jiang, D. W. Stephan, *Dalton Trans.* **2013**, *42*, 726–736.
- 120 For recent selected examples see: a) H. H. San, S.-J. Wang, M. Jiang, X.-Y. Tang, *Org. Lett.* **2018**, *20*, 4672–4676; b) Z. Yu Yongfeng, Li J. Shi, B. Ma, L. Liu, J. Zhang, *Angew. Chem. Int. Ed.* **2016**, *55*, 14807–14811; c) S. Rao, R. Kapanaiiah, K. R. Prabhu, *Adv. Synth. Catal.* **2019**, *361*, 1301–1306; d) H. H. San, C.-Y. Wang, H.-P. Zeng, S.-T. Fu, M. Jiang, X.-Y. Tang, *J. Org. Chem.* **2019**, *84*, 4478–4485.
- 121 T. F. Bresnahan, M. Trajtenberg, *J. Econometrics* **1995**, *65*, 83–108.
- 122 G. E. Fussell, *Technology and Culture* **1967**, *8*, 16–44.
- 123 For selected reviews see: a) M. B. Plutschack, B. Pieber, K. Gilmore, P. H. Seeberger, *Chem. Rev.* **2017**, *117*, 11796–11893; b) R. L. Hartman, J. P. McMullen, K. F. Jensen, *Angew. Chem. Int. Ed.* **2011**, *50*, 7502–7519; c) J. Wegner, S. Ceylan, A. Kirschning, *Adv. Synth. Catal.* **2012**, *354*, 17–57; d) I. R. Baxendale, L. Brocken, C. J. Mallia, *Green Process. Synth.* **2013**, *2*, 211–230; e) J. C. Pastre, D. L. Browne, S. V. Ley, *Chem. Soc. Rev.* **2013**, *42*, 8849–8869; f) D. T. McQuade, P. H. Seeberger, *J. Org. Chem.* **2013**, *78*, 6384–6389; g) T. Wirth, *Microreactors in Organic Chemistry and Catalysis* **2013**, Ed. Wiley-VCH.
- 124 a) J. L. Howard, Q. Cao, D. L. Browne, *Chem. Sci.* **2018**, *9*, 3080–3094; b) J. L. Howard, M. C. Brand, D. L. Browne, *Angew. Chem. Int. Ed.* **2018**, *57*, 16104–16108.
- 125 a) M. Elsherbini, T. Wirth, *Acc. Chem. Res.* **2019**, *52*, 3287–3296; b) M. Yan, Y. Kawamata, P. S. Baran, *Chem. Rev.* **2017**, *117*, 13230–13319; c) C. Kingston, M. D. Palkowitz, Y. Takahira, J. C. Vantourout, B. K. Peters, Y. Kawamata, P. S. Baran, *Acc. Chem. Res.* **2020**, *53*, 72–83.
- 126 a) Ł. W. Ciszewski, K. Rybicka-Jasińska, D. Gryko, *Org. Biomol. Chem.* **2019**, *17*, 432–448; b) P. Klán, J. Wirz, *Photochemistry of Organic Compounds: From Concepts to Practice* **2009**, Ed. Wiley-VCH.
- 127 a) T. N. Glasnov, C. O. Kappe, *Chem. Eur. J.* **2011**, *17*, 11956–11958; b) C. O. Kappe, A. Stadler, *Microwaves in Organic and Medicinal Chemistry* **2005**, Ed. Wiley-VCH.
- 128 A. J. Capel, R. P. Rimington, M. P. Lewis, S. D. R. Christie, *Nat. Rev. Chem.* **2008**, *2*, 422–436.
- 129 a) A. A. Folgueiras-Amador, K. Philipps, S. Guilbaud, J. Poelakker, T. Wirth, *Angew. Chem. Int. Ed.* **2017**, *56*, 15446–15450; b) N. Holmes, G. R. Akien, R. J. D. Savage, C. Stanetty, I. R. Baxendale, A. J. Blacker, B. A. Taylor, R. L. Woodward, R. E. Meadowse, R. A. Bourne, *React. Chem. Eng.* **2016**, *1*, 96–100; c) B. Ahmed-Omer, E. Sliwinski, J. P. Cerroti, S. V. Ley, *Org. Process Res. Dev.* **2016**, *20*, 1603–1614.
- 130 a) C. A. Shukla, A. A. Kulkarni, *Beilstein J. Org. Chem.* **2017**, *13*, 960–987; b) B. J. Reizman, K. F. Jensen, *Acc. Chem. Res.* **2016**, *49*, 1786–1796; c) V. Sans, L. Cronin, *Chem. Soc.*

- Rev.* **2016**, *45*, 2032–2043; d) D. E. Fitzpatrick, S. V. Ley, *React. Chem. Eng.* **2016**, *1*, 629–635.
- 131 S. A. Weissman, N. G. Anderson, *Org. Process Res. Dev.* **2015**, *19*, 1605–1633.
- 132 J. Hartwig, J. Metternich, N. Nikbin, A. Kirschning, S. V. Ley, *Org. Biomol. Chem.* **2014**, *12*, 3611–3615.
- 133 a) S. G. Newmana, K. F. Jensen, *Green Chem.* **2013**, *15*, 1456–1472; b) L. Vaccaro, D. Lanari, A. Marrocchi, G. Strappaveccia, *Green Chem.* **2014**, *16*, 3680–3704.
- 134 D. E. Fitzpatrick, C. Battilocchio, S. V. Ley, *ACS Cent. Sci.* **2016**, *2*, 131–138.
- 135 D. L. Browne, S. Wright, B. J. Deadman, S. Dunnage, I. R. Baxendale, R. M. Turner, S. V. Ley, *Rapid Commun. Mass Spectrom.* **2012**, *26*, 1999–2010; b) V. Sans, L. Cronin, *Chem. Soc. Rev.* **2016**, *45*, 2032–2043.
- 136 a) K. J. Hock, R. M. Koenings, *Chem. Eur. J.* **2018**, *24*, 10571–10583; b) S. T. R. Müller, T. Wirth, *ChemSusChem* **2015**, *8*, 245–50.
- 137 L. D. Proctor, A. J. Warr, *Org. Process Res. Dev.* **2002**, *6*, 884–892.
- 138 R. A. Maurya, C. P. Park, J. H. Lee, D.-P. Kim, *Angew. Chem. Int. Ed.* **2011**, *50*, 5952–5955.
- 139 V. D. Pinho, B. Gutmann, L. S. M. Miranda, R. O. M. A. de Souza, C. O. Kappe, *J. Org. Chem.* **2014**, *79*, 1555–1562.
- 140 H. F. Koolman, S. Kantor, A. R. Bogdan, Y. Wang, J. Y. Pan, S. W. Djuric, *Org. Biomol. Chem.* **2016**, *14*, 6591–6595.
- 141 H. Lehmann, *Green Chem.* **2017**, *19*, 1449–1453.
- 142 D. N. Tran, C. Battilocchio, S.-B. Lou, J. M. Hawkins, S. V. Ley, *Chem. Sci.* **2015**, *6*, 1120–1125.
- 143 J.-S. Poh, D. N. Tran, C. Battilocchio, J. M. Hawkins, S. V. Ley, *Angew. Chem. Int. Ed.* **2015**, *54*, 7920–7923.
- 144 a) S. M. Nicolle, C. J. Hayes, C. J. Moody, *Chem. Eur. J.* **2015**, *21*, 4576–4579; b) H. E. Bartrum, D. C. Blackmore, C. J. Moody, C. J. Hayes, *Chem. Eur. J.* **2011**, *17*, 9586–9589.
- 145 C. Battilocchio, F. Feist, A. Hafner, M. Simon, D. N. Tran, D. M. Allwood, D. C. Blakemore, S. L. Ley, *Nature Chem.* **2016**, *8*, 360–367.
- 146 M. W. Majchrzak, M. Bekhazi, I. Tse-Sheepy, J. Warkentin, *J. Org. Chem.* **1989**, *54*, 1842–1845.
- 147 M. M. E. Delville, J. C. M. van Hest, F. P. J. T. Rutjes, *Beilstein J. Org. Chem.* **2013**, *9*, 1813–1819.
- 148 P. R. D. Murray, D. L. Browne, J. C. Pastre, C. Butterns, D. Guthrie, S. V. Ley, *Org. Process Res. Dev.* **2013**, *17*, 1192–1208.
- 149 S. T. R. Müller, A. Murat, D. Maillos, P. Lesimple, P. Hellier, T. Wirth, *Chem. Eur. J.* **2015**, *21*, 7016–7020.
- 150 S. T. R. Müller, A. Murat, P. Hellier, T. Wirth, *Org. Process Res. Dev.* **2016**, *20*, 495–502.
- 151 a) B. J. Deadman, R. M. O'Mahony, D. Lynch, D. C. Crowley, S. G. Collins, A. R. Maguire, *Org. Biomol. Chem.* **2016**, *14*, 3423–3431; b) R. M. O'Mahony, D. Lynch, H. L. D. Hayes, E. N. Thuama, P. Donnellan, R. C. Jones, B. Glennon, S. G. Collins, A. R. Maguire, *Eur. J. Org.*

- Chem.* **2017**, 6533–6539; c) D. Lynch, R. M. O'Mahony, D. G. McCarthy, L. M. Bateman, S. G. Collins, A. R. Maguire, *Eur. J. Org. Chem.* **2019**, 3575–3580.
- 152 R. Gérardy, M. Winter, A. Vizza, J.-C. M. Monbaliu, *React. Chem. Eng.*, **2017**, *2*, 149–158.
- 153 a) A. D. Clayton, A. M. Schweidtmann, G. Clemens, J. A. Manson, C. J. Taylor, C. G. Niño, T. W. Chamberlain, N. Kapur, A. John, Blacker A. A. Lapkin, R. A. Bourne, *Chem. Eng. J.* **2020**, *384*, 123340; b) V. Sans, L. Porwol, V. Dragone, L. Cronin, *Chem. Sci.* **2015**, *6*, 1258–1264; b) V. Sans, L. Cronin, *Chem. Soc. Rev.*, **2016**, *45*, 2032–2043.
- 154 a) A. D. Clayton, J. A. Manson, C. J. Taylor, T. W. Chamberlain, B. A. Taylor, G. Clemens, R. A. Bourne, *React. Chem. Eng.*, **2019**, *4*, 1545–1554; b) D. Cortés-Borda, K. V. Kutanova, C. Jamet, M. E. Trusova, F. Zammattio, C. Truchet, M. Rodriguez-Zubiri, F.-X. Felpin, *Org. Process Res. Dev.* **2016**, *20*, 1979–1987.
- 155 R. Fisher, *The Design of Experiments* **1935**, Ed. Oliver and Boyd.
- 156 D. C. Montgomery, *Design and Analysis of Experiments* **2001**, Ed. Wiley-VCH.
- 157 H. Tye, *Drug Discovery Today* **2004**, *9*, 485–491.
- 158 M. R. Owen, C. Luscombe, L.-W. Lai, S. Godbert, D. L. Crookes, D. Emiabata-Smith, *Org. Process Res. Dev.* **2001**, *5*, 308–323.
- 159 T. Laird, *Org. Process Res. Dev.* **2002**, *6*, 33–337.
- 160 N. G. Anderson, *Org. Process Res. Dev.* **2001**, *5*, 613–621.
- 161 X. Tang, R. K. Allemann, T. Wirth, *Eur. J. Org. Chem.* **2017**, 414–418.
- 162 H. Sato, S. Watanabe, D. Takeda, S. Yano, N. Doki, M. Yokota, K. Shimizu, *Org. Process Res. Dev.* **2015**, *19*, 1655–1661.
- 163 J. Musters, L. van den Bos, E. Kellenbach, *Org. Process Res. Dev.* **2013**, *17*, 87–96.
- 164 P. T. Anastas, J. C. Warner, *Green Chemistry: theory and practice* **1998**, Oxford University Press.
- 165 D. S. Metil, S. P. Sonawane, S. S. Pachore, A. Mohammad, V. H. Dahanukar, P. J. McCormack, C. V. Reddy, R. Bandichhor, *Org. Process Res. Dev.* **2018**, *22*, 27–39.

CHAPTER 2: Synthesis of Novel *trans*-Dihydroindoles

2.1 Introduction

The 2,3-dihydroindole scaffold, also known as indoline, can be found as the main core in several biologically active compounds and natural products. For instance, naturally occurring alkaloids such as strychnine (**132**), physostigmine (**133**), oleracein (**134**), aspido-spermidine (**135**) and vinblastine (**136**) as well as drug molecule such as the Angiotensin-Converting-Enzyme (ACE) inhibitor pentopril (**137**) (Figure 2.1), present the indoline framework and therefore represents a synthetically interesting target for organic and medicinal chemists.¹

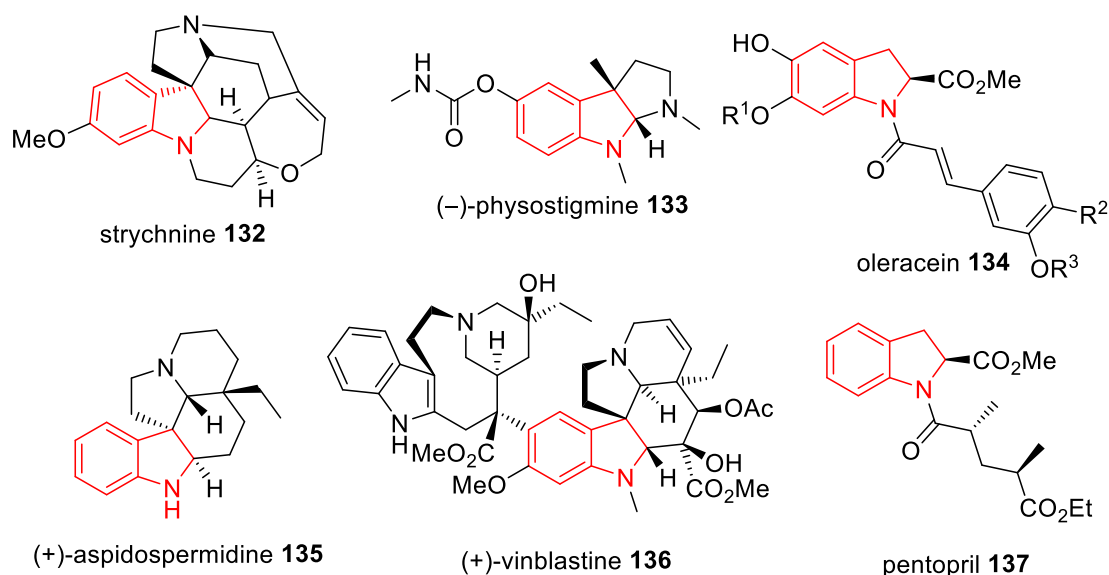
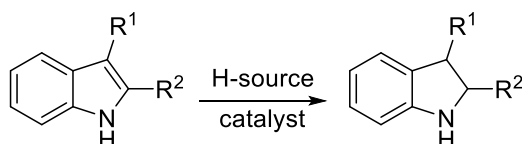
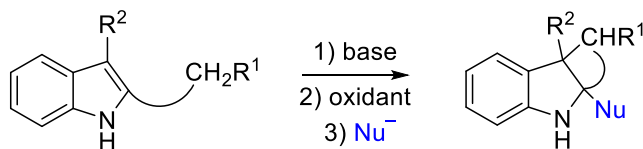
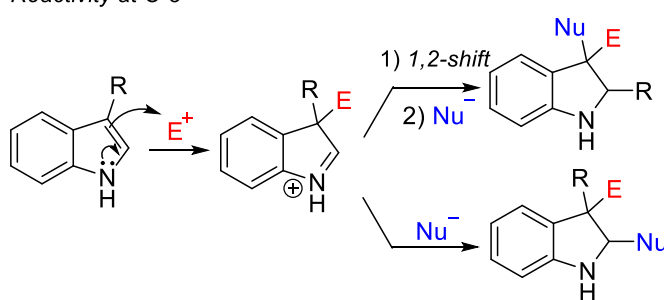


Figure 2.1: Natural products and drug molecules containing the indoline framework.

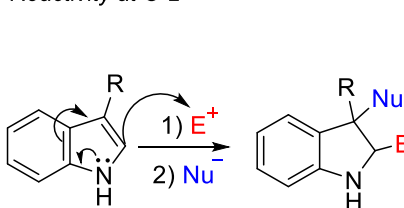
For this reason, there is an increasing interest in developing new pathways for the synthesis of optically active 2,3-dihydroindoles in both synthetic and pharmaceutical chemistry.² There are currently two main approaches towards such scaffolds. The first, is based on the dearomatisation or functionalisation of indoles (Scheme 2.1),³ which can occur through hydrogenation of the double bond,⁴ base-promoted intramolecular oxidative coupling,⁵ or by exploiting the intrinsic reactivity of the indole ring towards electrophiles.⁶ However, it is necessary to introduce/prepare the indole core in advance.⁷

Hydrogenation of Indoles:**Intramolecular Oxidative Coupling:****Indole Electrophilic Activation:**

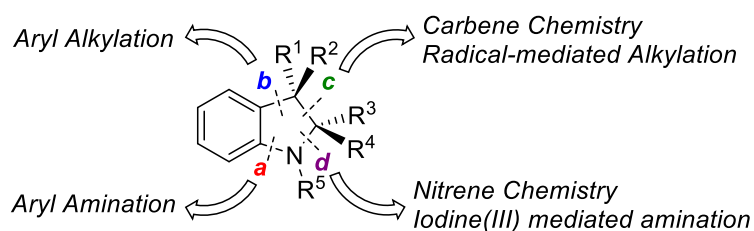
Reactivity at C-3



Reactivity at C-2

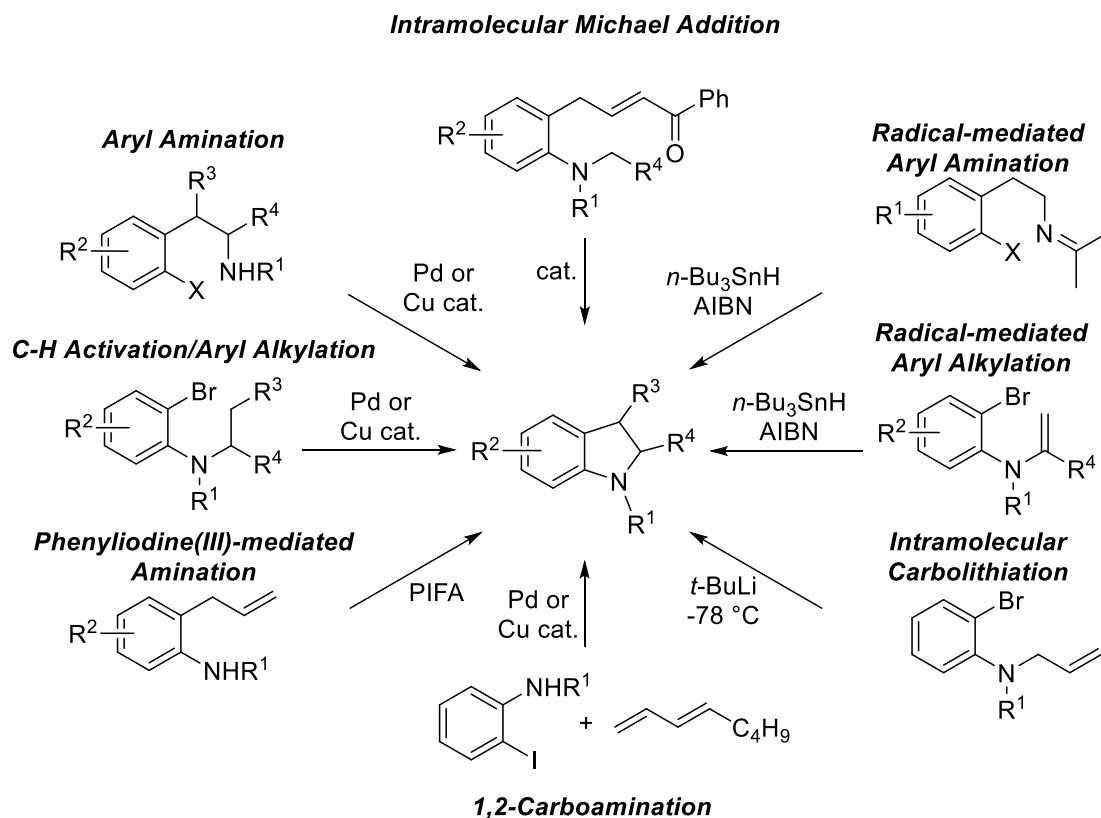
**Scheme 2.1:** Dearomatisation/functionalisation of indoles.

The second major approach relies on the construction of the nitrogen-containing five-membered ring *via* C–C and/or C–N bond formation. For this purpose, there are several available strategies depending on which of the bonds **a–d** needs to be constructed (Figure 2.2).

**Figure 2.2:** Overview of the most common retrosynthetic pathways for the *de novo* synthesis of the pyrrolidine ring.

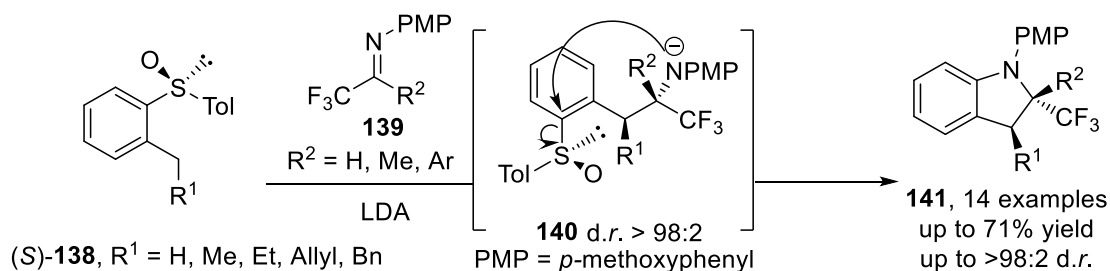
A well-established method to build the C–N bond **a** is the Pd-catalysed aryl amination.⁸ As this approach does not directly introduce new stereogenic centres the chiral backbone must be introduced in advance. On the other hand, enantioselective transition metal-catalysed C–H activation/aryl alkylations have been reported for the synthesis of bond **b** and offer the stereoselective generation of C3 and C2.⁹ Moreover, Cu-catalysed aryl and alkyl aminations¹⁰ as well as iodine(III)-mediated reactions,¹¹ present cheaper and more sustainable alternatives for the formation of bonds **a** or **d**. Additionally, intramolecular

radical aryl aminations¹² and aryl alkylations¹³ offer an efficient metal-free approach towards bonds **a** or **b**, although it is usually difficult to control the enantioselectivity. To overcome this disadvantage, metallo-radical catalysis (MRC) has been successfully applied especially for the formation of bond **c** (Scheme 2.2).¹⁴



Scheme 2.2: Overview of most common strategies towards dihydroindoles.

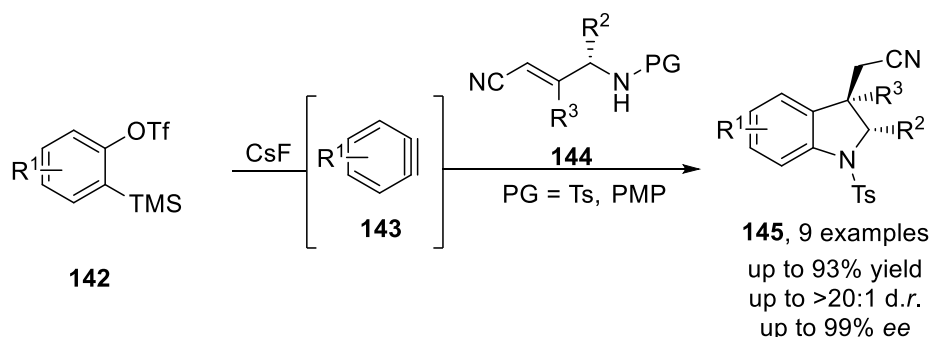
Other methods that have been successfully adopted to synthesise the indoline *de novo* include the 1,2-carboamination of dienes,¹⁵ intramolecular carbolithiation¹⁶ and intramolecular Michael addition.¹⁷ However, only a few of these reported procedures allow the direct enantio- and diastereoselective formation of C2 and C3 of the nitrogen-containing five-membered ring. In 2008, García Ruano *et al.* developed an asymmetric tandem reaction to synthesise disubstituted indolines starting from optically pure sulfoxides **138** (Scheme 2.3).¹⁸



Scheme 2.3: Anionic-anionic asymmetric tandem reaction towards optically active indolines.

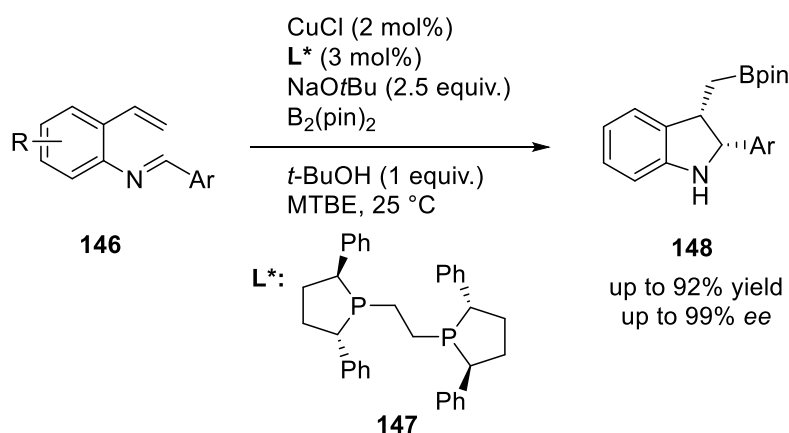
In the presence of lithium diisopropylamide (LDA), (*S*)-sulfinyl derivative **138** is deprotonated in the benzylic position and undergoes stereoselective nucleophilic addition to the activated imine **139** followed by an intramolecular nucleophilic aromatic substitution leading to chiral dihydroindoles **141** in good yields and excellent stereoselectivity (>98:2).

Another efficient protocol for the construction of enantiopure indoline nuclei is the [3+2] cycloaddition between benzyne precursors **142** and α,β -unsaturated γ -aminobutyronitriles **144** (Scheme 2.4).¹⁹ In this case the TMS-aryl triflate **142** undergoes a fluoride-induced 1,2-elimination forming the aryne intermediate **143** *in situ*, which then reacts with α,β -unsaturated γ -aminobutyronitriles **144** to afford 2,3-dihydroindoles **145** in good yields and enantioselectivity.



Scheme 2.4: Indoline **145** construction via [3+2] cycloaddition reactions between benzyne **143** and α,β -unsaturated γ -aminobutyronitriles **144**.

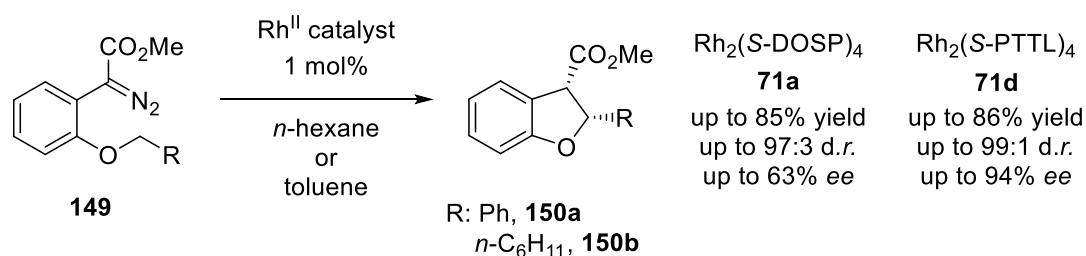
Recently, Zhang *et al.* reported the Cu-catalysed enantioselective intramolecular borylative cyclisation of 2-vinylaryl imines derivatives **146** with $B_2(\text{pin})_2$ which affords *cis*-2,3-dihydroindoles **148** bearing a Bpin moiety in excellent yields and selectivity without the need of a chiral starting material (Scheme 2.5).²⁰



Scheme 2.5: Cu-catalysed asymmetric synthesis of *cis*-2,3-dihydro-1*H*-indoles **148**.

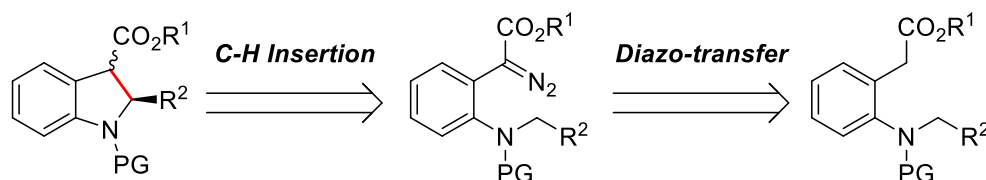
The *in situ* generated chiral copper catalyst promotes the Markovnikov addition to the vinyl moiety forming an organocuprate intermediate that is then trapped by the imine as described also by the Buchwald group in 2015.²¹

Intuitively, the formation of this C–C bond (disconnection **c**, Scheme 2.2) can be accomplished by using carbene chemistry.²² However, there are only a very few procedures using carbene-precursors for the synthesis of nitrogen-containing five-membered rings.²³ In the early 2000s Davies *et al.*²⁴ and Saito and co-workers²⁵ independently optimised the enantioselective synthesis of dihydrobenzofurans **150** *via* intramolecular rhodium-catalysed C–H insertion using 1 mol% Rh₂(S-DOSP)₄ (**71a**) and Rh₂(S-PTTL)₄ (**71d**), respectively (Scheme 2.6). In both cases the *cis*-dihydrobenzofuran was the major isomer. When Rh₂(S-DOSP)₄ was used as catalyst, the desired products **150a–b** were obtained in good yield (up to 85%) and selectivity up to 95% *de* and 63% *ee* after 72 hours at –50 °C in *n*-hexane. When Rh₂(S-PTTL)₄ was used instead, the dihydrobenzofurans **150a–b** were isolated in good yields and excellent stereocontrol (up to 98% *de* and 94% *ee*) within one hour at –78 °C in toluene.



Scheme 2.6: Synthesis of *cis*-dihydrobenzofurans **150a–b** *via* Rh^{II}-catalysed C–H insertion.

Despite these encouraging results and the advantage of installing two stereocentres in one step, the use of α -diazocarbonyl compounds as precursors for the preparation of 2,3-dihydroindoles has received limited attention. In this chapter, the development of a general synthesis for chiral 2,3-dihydro-1*H*-indoles *via* the metal-catalysed C–H insertion using diazo compounds as carbene precursors is presented (Scheme 2.7).



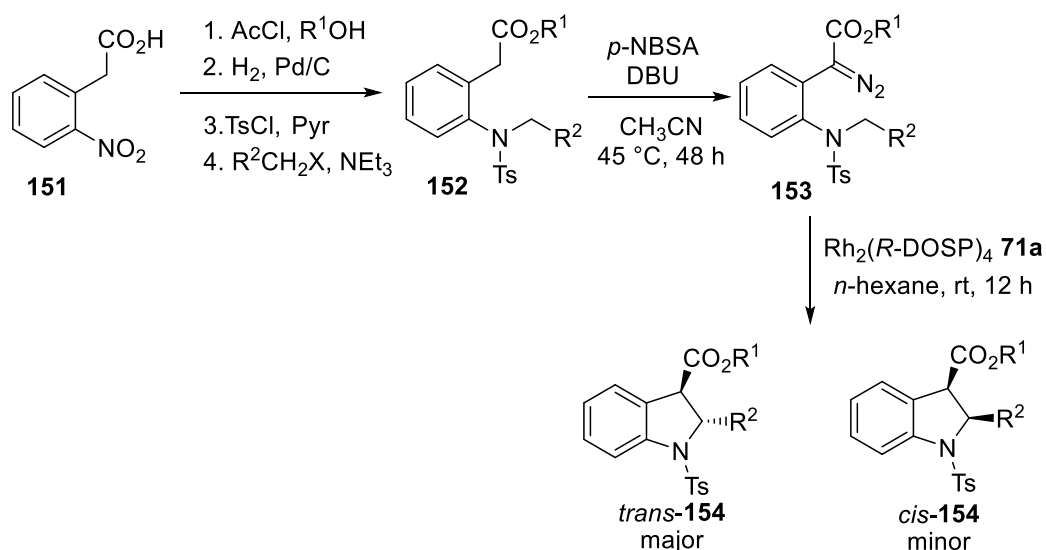
Scheme 2.7: Retrosynthetic approach toward chiral 2,3-dihydro-1*H*-indoles.

Some preliminary studies on the diazo-transfer optimisation, side product investigation and solvent screening for the C–H asymmetric insertion have already been reported by Dr. S. T. R. Müller in his PhD thesis work titled: “Diazo Compounds in Continuous Flow

Technology”.²⁶ During the work of this thesis, further optimisation studies have been carried out and the scope of diazo precursors and of *trans*-indolines have been expanded. Moreover, due to the well-known toxicity of diazo compounds, the diazo-transfer reaction was translated into a flow system using a DoE-approach for preliminary screening and optimisation. Parts of the following results are published in *Eur. J. Org. Chem.* **2017**, 1889–1893.

2.2 Results and Discussion

In Scheme 2.8 an overview of the synthetic pathways discussed in this chapter is given.



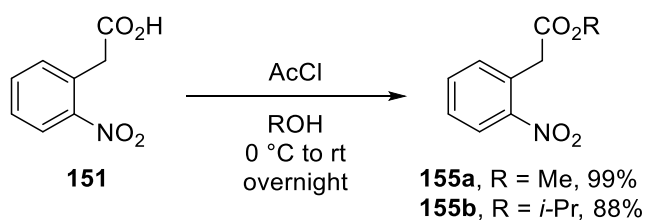
Scheme 2.8: Overview of the synthetic pathway developed to achieve indolines **154**.

Firstly, an efficient synthesis for the precursors **152** was developed. Secondly, attention was moved to the optimisation of the diazo-transfer and the optimal conditions were used to build a library of α -diazocarbonyl intermediates **153** in good yields. Moreover, the translation of the diazo-transfer reaction into a flow setup was realised using a fractional factorial design (FFD) to screen the several parameters such as temperature, equivalents of base and sulfonyl azide, time and concentration.

Finally, the effects of solvent, dirhodium catalysts and temperature on the stereoselective cyclisation were studied to afford the desired *trans*-indoles **154** as major products in good yields and enantioselectivities.

2.2.1 Synthesis of the Starting Materials

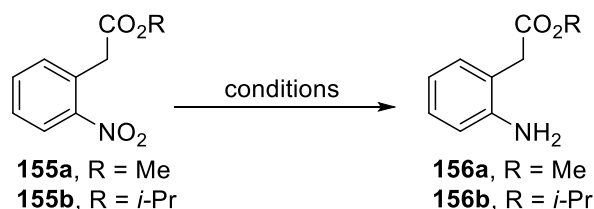
The synthesis started with the esterification of the commercially available 2-nitrophenyl acetic acid (**151**) in the presence of acetyl chloride in methanol or propan-2-ol at room temperature to afford **155a** and **155b** in excellent yields within 16 hours (Scheme 2.9).



Scheme 2.9: Esterification of 2-nitrophenyl acetic acid **151**.

Although reducing a nitroaromatic groups is a common procedure in organic chemistry, achieving a chemoselective reduction of the nitro group in presence of an ester moiety seemed to be more challenging. Hence, the reduction of the nitro group to the aryl amine was attempted following various literature protocols (Table 2.1).^{27,28}

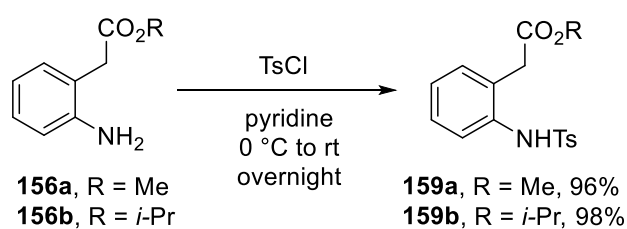
Table 2.1: Reaction conditions for the reduction of the nitro group in **155a-b**.



Entry	Conditions	Major Product	R	Yield (%)
1	NaBH ₄ , AlCl ₃ , dry THF rt, 2 h	<chem>CC(=O)OCc1ccc([N+](=O)[O-])cc1</chem>	Me (157)	17 ^a
2	HCO ₂ H, Pd/C, dry MeOH rt, 12 h	<chem>CC(=O)OCc1ccc2c(c1)nc(=O)c2</chem>	Me (158)	69
3	H ₂ (1 atm), Pd/C, dry ROH rt, 12 h	<chem>CC(=O)OCc1ccc(N)cc1</chem>	Me (156a)	99
4	H ₂ (1 atm), Pd/C, dry ROH rt, 12 h	<chem>CC(=O)OCc1ccc(N)cc1</chem>	<i>i</i> -Pr (156b)	70

^aStarting material **155a** recovered.

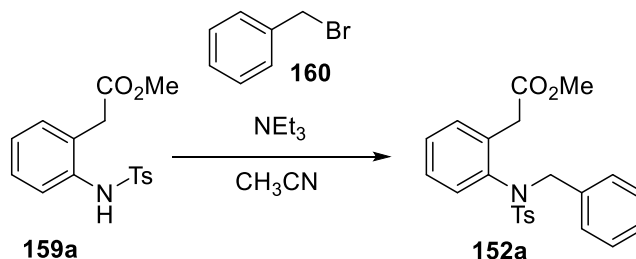
The use of a NaBH₄/AlCl₃ mixture resulted in the reduction of the ester moiety of **155a** leading to alcohol **157** in 17% with mainly starting material recovered (entry 1), despite being successfully employed for the large scale reduction of 2,4-dinitrophenyl compounds.²⁷ The catalytic hydrogenation of **155a** using Pd/C and formic acid led to the isolation of lactam **158** in 69% yield (entry 2). The formation of **158** indicated the successful reduction of the nitro to the amino group, but the acidic conditions may have activated the ester group toward intramolecular nucleophilic attack leading to the cyclised product. Finally, the desired arylamines **156a–b** were obtained in good to excellent yields using H₂ gas (1 atm) and 10% Pd/C as catalyst (entries 3,4) that are immediately tosylated in pyridine affording **159a** and **159b** to prevent their decomposition (Scheme 2.10).



Scheme 2.10: Tosylation of aryl amines **156a–b**.

Next, the further *N*-functionalisation of **159** was investigated. Treatment of **159a** with a mixture of benzyl bromide and triethylamine in acetonitrile afforded the desired product **152a** in reasonable yields (Table 2.2).

Table 2.2: Reaction conditions for the benzylation of **159a**.

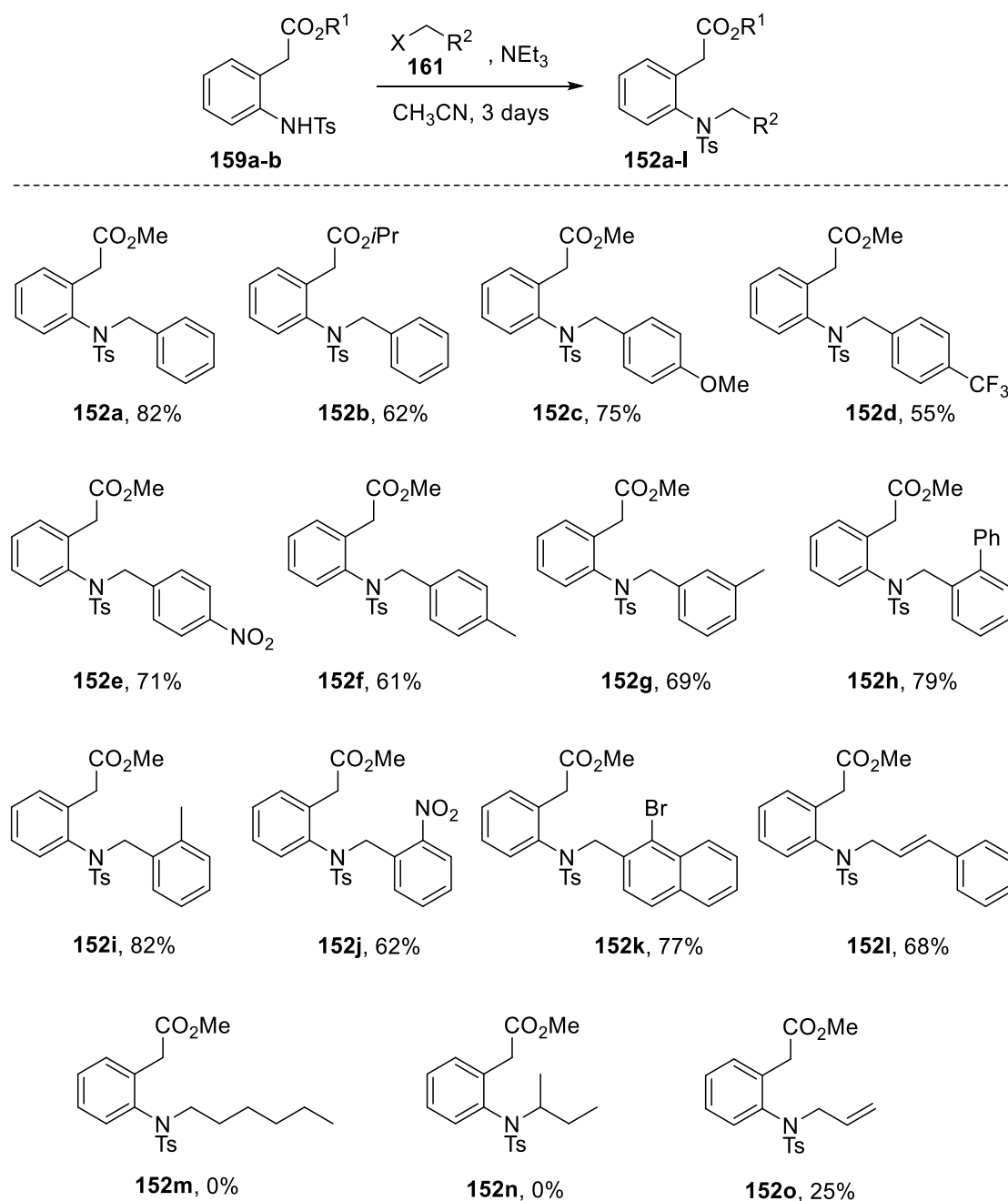


Entry	160 (equiv.)	NEt₃ (equiv.)	Conditions	152a (%)
1	2	2	48 h, rt	63
2	2	2	48 h, 45 °C	57
3	2	3	72 h, rt	73
4	3	3	48 h, rt	77–82 ^a
5	3	3	24 h, rt	42

General Procedure: Reactions performed on a 4–6 mmol scale in CH₃CN; ^aRange of four repeats.

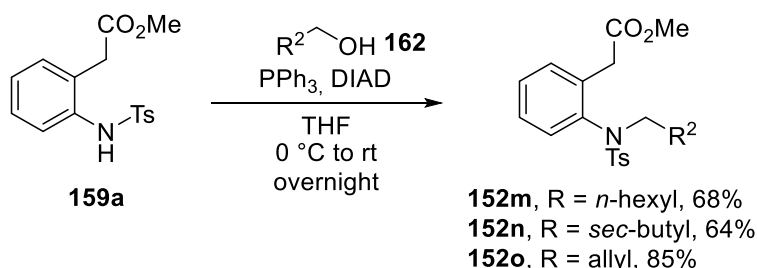
A large excess of the reagents and long reaction times were necessary to obtain **152a** in more than 60% yields (entry 1). Furthermore, increasing the temperature did not improve the reaction outcome (entry 2). Using more equivalents of triethylamine (3 equivalents) afforded **152a** in 73% yield after three days. The reaction was pushed further by increasing the amount of benzyl bromide **160** to 3 equivalents, leading to the formation of **152a** in 77–82% yield after 48 hours (entry 4). Reducing the reaction time to 24 hours led to lower yield of **152a** (42%; entry 5).

Different benzyl and alkyl halides **161** were used together with **159a–b** under the above optimised conditions (Table 2.2, entry 4) to build a library of substrates. All investigated substituents were very well tolerated, and the desired precursors **152a–i** were obtained in 62–82% yields (Scheme 2.11). When the methyl ester was replaced with an isopropyl ester, the corresponding benzylated product **152b** was isolated in 62%. Highly electron-donating groups as well as highly electron-withdrawing substituents in *para*-position showed good reactivity affording **152c**, **152d** and **152e** in 75%, 55% and 71% yield, respectively.

Scheme 2.11: Preparation of precursors **152a-l**.

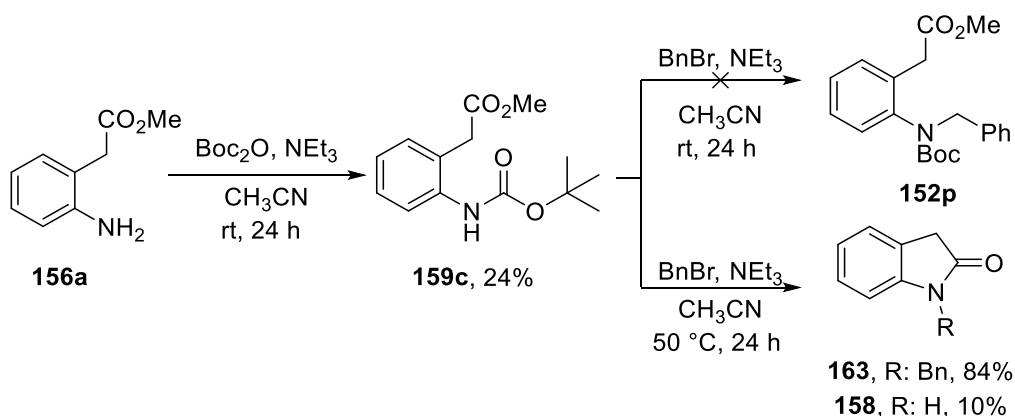
Also, substrate **152f** and **152g** moderate bearing electron-donating electrophiles in *para*- and *meta*-position were prepared in good yields (61% and 69%). A small electronic effect was noticed for the *ortho*-substituted derivatives **152h-j**. The products carrying the 2-phenyl (**152h**) and the 2-methyl (**152i**) group were afforded in higher yields (79–82%) than the 2-nitro derivative **152j** (62%). Bulkier derivatives such as 2-phenyl (**152h**) or 2-bromonaphthyl (**152k**) substituted precursor were also prepared in 79% and 77% yield, respectively. Non-benzylic electrophiles were investigated next. While (*E*)-(3-bromoprop-1-en-1-yl)benzene gave **152l** in 68% yield, and allyl bromide afforded **152o** in 25% yield, no reaction was observed between 2-bromobutane nor 1-bromohexane and the starting

material **159a**, therefore **152m** and **152n** were not formed. This is not surprising because both 2-bromobutane and 1-bromohexane are poorly reactive toward S_N2 reactions. Alternatively, treatment of **159a** with triphenylphosphine, diisopropyl azodicarboxylate (DIAD) and the corresponding alcohols **162** in a Mitsunobu reaction²⁹ afforded **152m–o**, in 68%, 64% and 85% yield, respectively (Scheme 2.12).



Scheme 2.12: Synthesis of alkyl derivatives **145m–o** via Mitsunobu reaction.

While expanding the substrate scope to other protecting groups, the *N*-Boc substituted amine **159c** was prepared using di-*tert*-butyl dicarbonate (Boc_2O) and triethylamine in acetonitrile (Scheme 2.13).^a



Scheme 2.13: Alternative route using *N*-Boc-protective group.

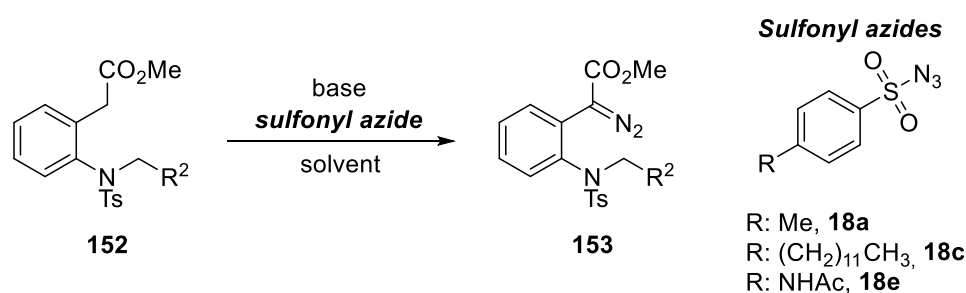
The following treatment of **159c** with benzyl bromide and triethylamine at room temperature did not lead to the desired benzylated product **152p** leaving **159c** unchanged. Performing the reaction at a higher temperature (50 °C) led to the formation of a mixture of lactams **163** and **158** in 84% and 10% yield, respectively, hence was not further investigated.

Once the diazo precursors were prepared in good yields, attention was focussed on the synthesis of the carbene-precursors, the key-intermediates of this synthetic pathway.

a. The synthesis of **159c** was carried out by Dr. S.T.R Müller

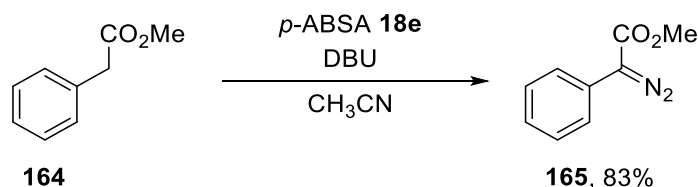
2.2.2 Synthesis of α -Diazocarbonyl Precursors

The Regitz diazo-transfer reaction³⁰ was used to synthesize the α -diazocarbonyl substrates **153** (Scheme 2.14). As mentioned in chapter 1, this base-promoted transfer into activated methylene moieties is a convenient approach for the synthesis of donor-acceptor and acceptor-acceptor carbene. The standard protocol for 1,3-dicarbonyl compounds relies on triethylamine as base and sulfonyl azides such as tosyl azide (**18a**) or the safer analogues *p*-acetamidobenzenesulfonyl azide (*p*-ABSA, **18e**) and *p*-dodecylbenzenesulfonyl (**18c**) as diazo-transfer reagents. The sulfonyl azide reagents are easily synthesized by adding sodium azide to a solution of substituted-sulfonylchloride in acetone and water,³¹ a protocol that can be easily scaled up in a flow system.³²



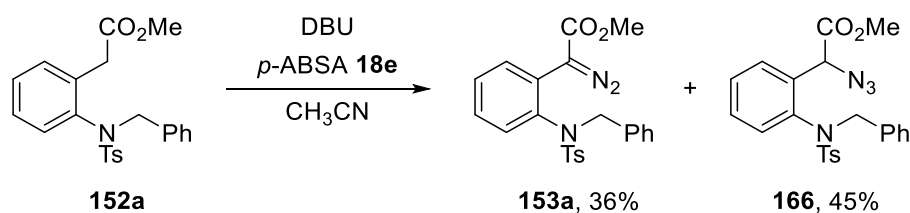
Scheme 2.14: General scheme for a classic Regitz diazo-transfer reaction.

However, for compounds containing mono-activated methylene groups, triethylamine (pK_a (CH₃CN): 18.8)³³ is not strong enough to deprotonate in α -position. Therefore, the slightly stronger 1,5-diazabicyclo[5.4.0]undec-7-ene (DBU, pK_a (CH₃CN): 24.3)³³ can be used for the synthesis of α -aryl- α -diazocarbonyl compounds³⁴ such as phenyl diazoacetate **165** (Scheme 2.15). In this case the desired α -diazo compound **165** was successfully isolated in 83% yield as orange oil after column chromatography.



Scheme 2.15: Diazo-transfer reaction of phenylacetate **164**.

Unfortunately, when the same conditions were used for on the model substrate **152a**, the desired product **153a** was isolated only as minor product in 36% yield along with the corresponding azide **166** in 45% yield (Scheme 2.16).

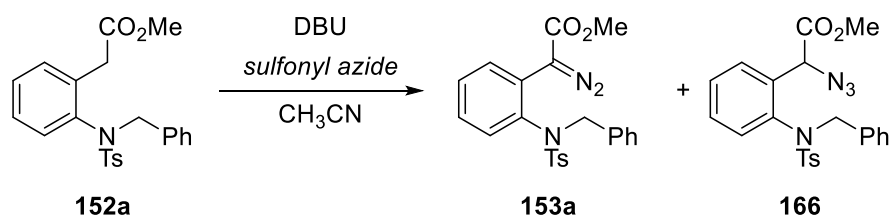


Scheme 2.16: Diazo-transfer reaction of the model substrate **152a**.

A similar azido-transfer reaction was reported for the reaction of trifluoromethanesulfonyl azide (**18g**) and β -keto carbonyl compounds,³⁵ and for the reaction of **18g** or tosyl azide (**18a**) and cyclic imides,³⁶ but received a limited attention due to its unpredictability. Optimisation screening and mechanistic investigations were carried out next, to explain the azide formation and, ideally, avoid or at least minimise its generation.

2.2.2.1 Optimisation of the Diazo-transfer Reaction in Batch

Preliminary results showed that when the reaction was performed with *p*-ABSA (**18e**) as a diazo-transfer reagent and DBU as a base in acetonitrile, the side product **166** was obtained as the major product (up to 46% yield) irrespective of the amount of base or **18e** (Table 2.3, entries 1–3). Less product (8%) was observed upon increasing either *p*-ABSA or DBU (entries 2 and 3) and no starting material was recovered, suggesting a decomposition of the desired diazo compound **153a** or the formation of other products under those conditions. Performing the reaction in THF led to a higher conversion of the starting material **152a**, however, a lower **153a/166** ratio was observed with the undesired product isolated in 62% yield (entry 4). The trend was reversed when the reaction time was significantly increased, and desired compound **153a** was obtained in a moderate yield (46%) along with 29% of the azide **166** after 7 days (entry 5). A turning point was reached once *p*-ABSA (**18e**) was replaced by *p*-NBSA (**18f**) (entry 6). In accordance with the observation of Evans and co-workers for a similar reaction,^{36a} when *p*-NBSA is used in combination with phosphate buffer as the quenching medium, an inverted chemoselectivity was observed and the desired diazo compound **153a** was formed as the major product (53%) with only 14% of side product **166**.

Table 2.3: Preliminary screening for the diazo-transfer reaction conditions on **152a**.

Entry	Sulfonyl Azide	Base	Conditions	153a (%)	166 (%)
1	<i>p</i> -ABSA (1.2)	DBU (1.7)	CH ₃ CN, 24 h, rt	36	45
2	<i>p</i> -ABSA (3)	DBU (1.7)	CH ₃ CN, 24 h, rt	8	42
3	<i>p</i> -ABSA (1.2)	DBU (4)	CH ₃ CN, 24 h, rt	8	46
4	<i>p</i> -ABSA (1.2)	DBU (1.7)	THF, 24 h, rt	20	62
5	<i>p</i> -ABSA (1.2)	DBU (1.7)	CH ₃ CN, 7 days, rt	46	29
6 ^a	<i>p</i> -NBSA (2)	DBU (2.5)	CH ₃ CN, 24 h, rt	53	14

General Procedure: Reactions performed on a 0.25–1 mmol scale of **152a** (0.5 M) and quenched with NH₄Cl saturated aqueous solution (pH = 5). ^aQuenched with 0.1 M phosphate buffer (pH = 7).

This sulfonyl azide dependent chemoselectivity can be explained by the different stabilities of the triazene intermediates **167a** and **167b** formed *in situ* during the reaction (Figure 2.3). This hypothesis was proved by performing two parallel NMR experiments, where the course of the reaction of **152a** with *p*-ABSA (a) and *p*-NBSA (b) were monitored by ¹H NMR spectroscopy over 5 days. The starting material **152a** was fully converted into the intermediate **167b** within 10 minutes in the case of *p*-NBSA, while it was still detected after 60 minutes when *p*-ABSA was used. Moreover, triazene **167b** showed a faster decomposition compared to **167a** with traces of the desired diazo compound **153a** detected after 22 hours and formed slowly over time, while **167a** proved to be more stable with no product formation after 3 days. The decomposition of **167** led to the diazo compound **153a** in accordance with the mechanism reported in literature.³⁷ To investigate the mechanism further, several attempts were made to isolate and characterise triazene **167b**. The diazo intermediate **153a** (0.24 mmol) was treated with 1.1 equivalents of *p*-NBSA and 1.1 equivalents of DBU in acetonitrile for 10 minutes before the addition of ice-cold water and extraction in dichloromethane. The protonated form of **167b** was obtained as a 1:2 mixture of rotamers (in agreement with the ratio observed *in situ* 1:1.7) together with a ~10% of unreacted starting material **152a** and DBU. Unfortunately, the pH-sensitivity and thermolability of intermediate **167b** made its isolation extremely difficult. Noteworthy, from the ¹H NMR experiment, the side product **166** was detected only in traces after one hour with no further formation during the reaction. It is intuitive that the competition between diazo compound **153a** and azide **166**

formation must come from a different behaviour of the triazenes **167a** and **167b** during their fragmentation.

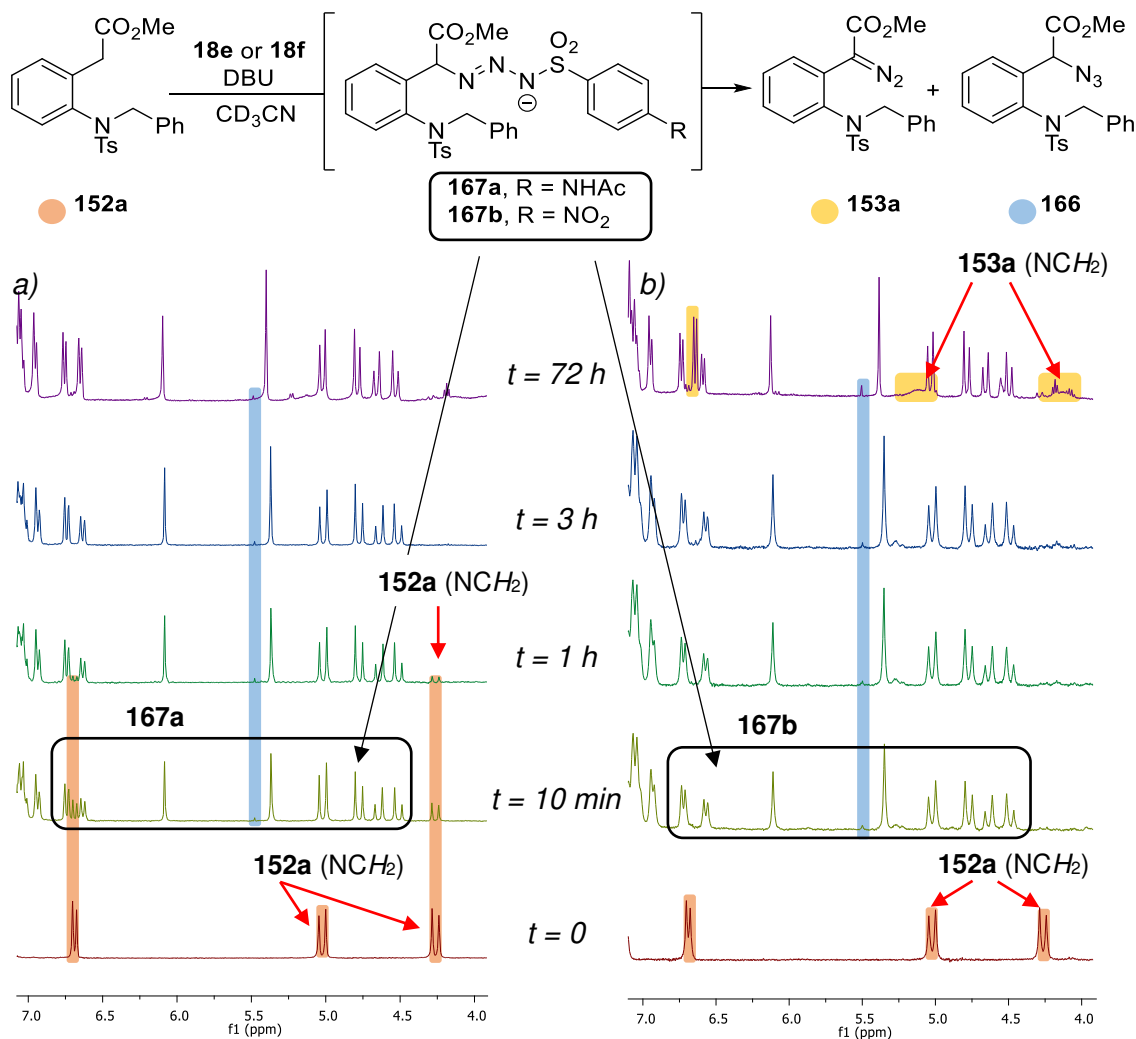
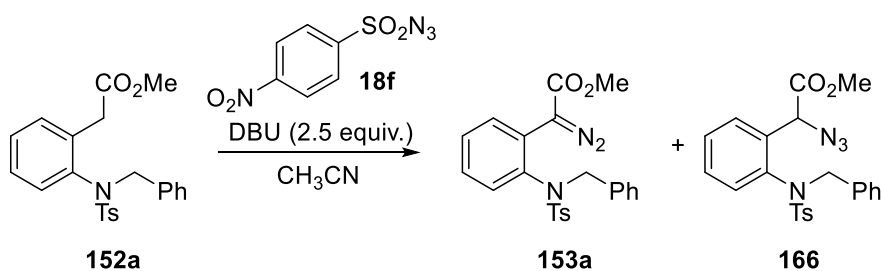


Figure 2.3: ^1H NMR spectra (300 MHz, CD_3CN) of *in situ* reaction monitoring of **152a** (0.02 mmol scale) with DBU (2.5 equiv.) and a) *p*-ABSA (**18e**, 2 equiv.) or b) *p*-NBSA (**18f**, 2 equiv.). From the bottom: reaction mixture before DBU addition ($t = 0$), reaction mixture after 10 min, 1 h, 3 h and 72 h.

Consequently, the attention moved to study the parameters that could impact the triazene cleavage: reaction time, temperature and quenching (Table 2.4). Longer reaction time (48 h) increased the yield of the desired product **153a** up to 63% with only 13% of azide **166** (entry 2). Additionally, a neutral phosphate buffer solution was preferred over acidic (NH_4Cl) or basic solution (NaHCO_3) as quenching medium, affording higher yields for **153a** (63%) and better diazo/azide ratios (entries 2–4). Increasing the temperature to 45 °C over 12 or 24 hours did not show a significant influence on the reaction outcome (entries 5–7). When the reaction was performed at 45 °C for 48 hours, the desired product was still obtained in a good yield (65%) but the formation of the side product was reduced to 5%, with 9% of recovered starting material

(entry 8). Similarly, at 65 °C only the desired diazo compound **153a** was isolated (65%). In this case, the azide **166** was not observed, but 15% of starting material **152a** was recovered (entry 9). Reactions performed at even higher temperatures (80 °C) were less selective with the formation of numerous decomposition products that lead to poor yields of **153a** (up to 46%; entries 10–13).

Table 2.4: Screening of conditions for the diazo-transfer reaction on **152a**.



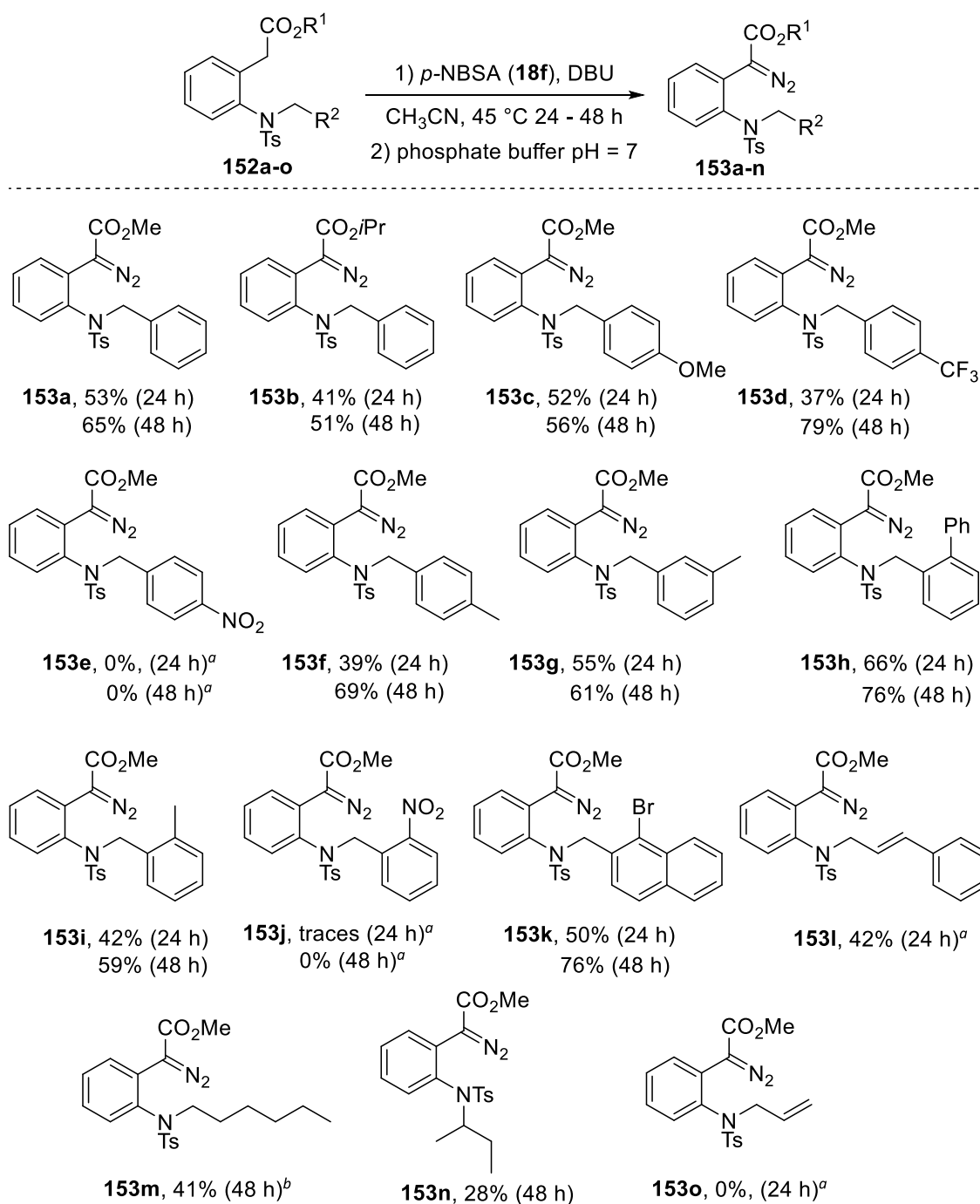
Entry	18f (equiv.)	Conditions	Quenching	153a (%)	166 (%)
1	2	24 h, rt	pH 7	53	14
2	2	48 h, rt	pH 7	63	13
3	2	48 h, rt	pH 5	50	18
4	2	48 h, rt	pH 10	53	29
5	2	24 h, 45 °C	pH 7	51	11
6	2	12 h, 45 °C	pH 7	50	13
7	4	24 h, 45 °C	pH 7	43	10
8 ^a	2	48 h, 45 °C	pH 7	65	5
9 ^a	2	24 h, 65 °C	pH 7	63	0
10 ^a	2	12 h, 80 °C	pH 7	27	0
11 ^a	4	12 h, 80 °C	pH 7	46	0
12 ^a	2	24 h, 80 °C	pH 7	40	0
13	4	24 h, 80 °C	pH 7	<i>decomposition</i>	

General Procedure: Reactions performed on a 0.17–0.25 mmol scale of **152a** (0.5 M) in acetonitrile. ^aStarting material **152a** was recovered.

Generally, the reactions carried out at 45–65 °C were more selective with little/no azide **166** formation. However, in contrast to previous reports in literature,³⁸ lower conversions were observed and the unreacted starting material **152a** was often recovered. Although the side reaction was prevented and the desired product was obtained in 63% after 24 hours compared to 53% at room temperature, a partial decomposition of triazene intermediate **167b** back to the starting material **152a** seemed to be responsible for the lower conversions. Indeed, when the reaction mixture containing **167b** in CD₃CN was

heated to 45 °C for 24 hours, the characteristic peaks of **152a** were observed by *in situ* ¹H NMR spectroscopy. Furthermore, the thermostability of the diazo compound **153a** was investigated and a full decomposition was observed when exposed to 65 °C for more than 24 hours, which explains the lower yield obtained for the reaction at 80 °C.

Therefore, 45 °C was chosen as the optimal temperature and a series of the diazo precursors **153a–n** were prepared using the optimal conditions of Table 2.4, entry 8 (Scheme 2.17). The reactions were followed by thin-layer chromatography (TLC) but the very similar R_f values for **152**, **153** and **166** made it difficult to determine the progress of the reaction by TLC, therefore the reactions in most cases were carried out twice and stopped after 24 or 48 hours. The diazo precursors **153a–k** were synthesised in good yields (51–79%) especially after 48 hours, showing that both EWG and EDG were well tolerated under the optimised conditions. The only exceptions were the nitro derivatives **152e** and **152j** which gave complex mixtures of products even under milder conditions at room temperature, and the attempts to isolate traces of product **153e** or **153j** were not successful. The cinnamic derivative **152i** and the allylic **152o** required milder conditions, as the products were highly unstable. Using 1.2 equivalents of DBU and *p*-NBSA at room temperature for 24 hours resulted in only 42% of **153i**, while **152o** led to a complex mixture but no desired product was detected. The *N*-alkyl substituted diazo compounds **153m** and **153n** were obtained in poor to moderate yields (28–41%) and were harder to purify from unreacted starting material and side products. Therefore, due to purification and or instability issues, **153l–m** were formed and used for the following step without further purifications.



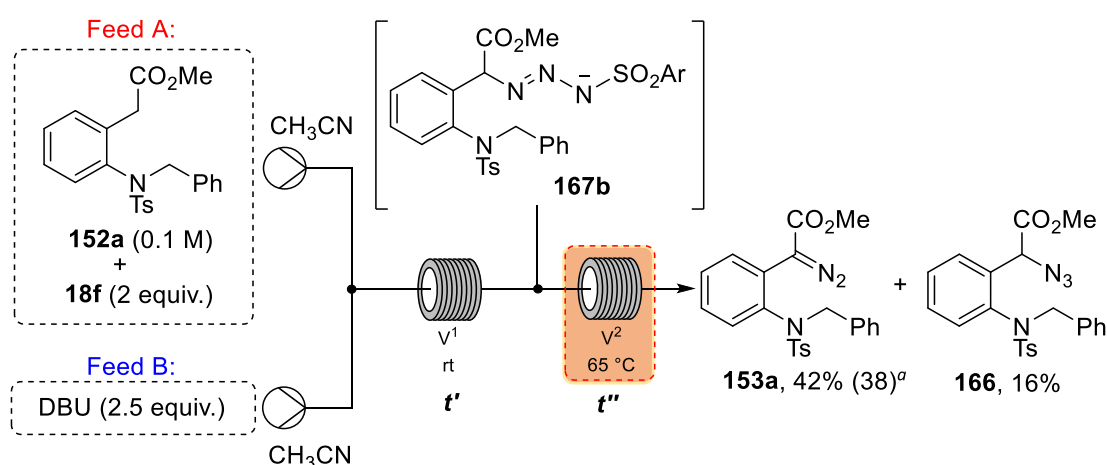
Scheme 2.17: Substrate scope of the diazo compounds **153a–n**. ^aReactions performed at room temperature using 1.2 equiv. of DBU and 1.2 equiv. of *p*-NBSA (**18f**) for 24 h; ^bYield by ¹H NMR.

2.2.2.2 Optimisation of the Diazo-transfer Reaction in a Flow Setup

Flow technologies have shown several advantages over batch techniques when it comes to handling reactive/unstable intermediates *in situ*. Thanks to the higher surface area to volume ratio in flow devices, both mass and heat are quickly and efficiently transferred avoiding prolonged exposure to higher temperature or harsh reagents.

From the ^1H NMR experiments (pg. 61) it was apparent that the starting material **152a** was fully converted into the triazene intermediate **167b** within a few minutes when *p*-NBSA (**18f**) was used. This encouraged further study of the diazo-transfer reaction in a flow system to accelerate the fragmentation of the triazene intermediate. Moreover, examples of diazo-transfer reactions have already been successfully reported in continuous flow setups.³⁹

The first flow system was designed to mimic the addition of reagents performed in batch for a reliable comparison (Scheme 2.18). For this experiment a 0.1 M solution of **152a** and 2 equivalents of *p*-NBSA (**18f**) in acetonitrile (2 mL) was prepared and loaded in a 2 mL syringe (Feed A). A second solution with DBU in acetonitrile (2 mL, 0.25 M) was prepared and loaded into a second 2 mL syringe (Feed B). A syringe pump was equipped with the two syringes, which were connected to the reactor with a T-piece mixer. The reactor consisted of a 3 mL FEP coil (i.d. = 0.5 mm) and was divided in two sections. The first part ($V^1 = 1$ mL) was left at room temperature to mimic the reaction mixture in batch during the DBU addition at room temperature and to ensure the conversion of **152a** into **167b** during t' . The second section ($V^2 = 2$ mL) was kept at 65 °C using a water bath to favour the fragmentation of **167b** into **153a** avoiding the side reaction during t'' . The two solutions were pumped at $0.2\text{ mL}\cdot\text{min}^{-1}$ through the coil where they were mixed and reacted. The solution was equilibrated for 30 minutes before being collected over 15 minutes and quenched with a 0.1 M phosphate buffer solution (pH = 7). The desired diazo compound **153a** was formed in 42% NMR yield along with 16% of side azide **166**.

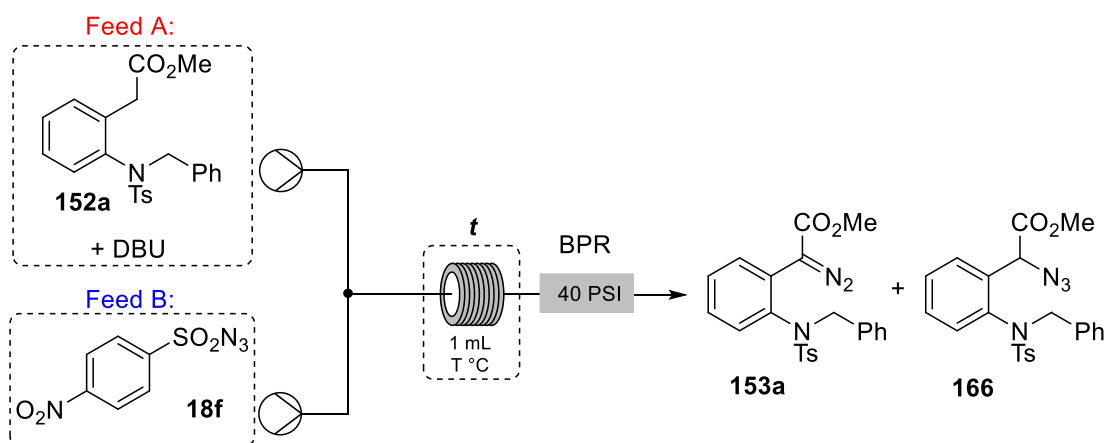


Scheme 2.18: First flow setup for the generation of **153a**; $V^1 = 1$ mL; $V^2 = 2$ mL; $t' = 5$ min; $t'' = 10$ min; the reaction was quenched with phosphate buffer (pH = 7) and the shown NMR yields were based on ^1H NMR spectroscopic analysis using 1,3,5-trimethoxybenzene as the internal standard. ^aIsolated yield after column chromatography.

When similar conditions were performed in batch, the DBU solution was added at room temperature over 5 minutes; then the solution was warmed up to 65 °C and stirred for

further 10 minutes before being quenched with a phosphate buffer solution (pH = 7). Also in this case, the desired compound **153a** was formed in 47% NMR yield along with 18% NMR yield of **166**. In both cases no complete consumption of the starting material was observed, with **152a** still present after 15 minutes in 26% and 23% NMR yield under flow and batch conditions, respectively. Despite the fact that no complete consumption was observed, this experiment showed a promising starting point for further optimisation studies.

Some modifications of the reaction setup were made to adjust the reaction conditions to flow synthesis requirements. Firstly, the sulfonyl azide **18f** was not well soluble in a 0.15 M solution of acetonitrile at room temperature together with **152a** and tended to precipitate in the syringe over time. To overcome this problem, a solution of only *p*-NBSA (**18f**) was pumped separately and combined with a pre-mixed solution of **152a** and DBU, similar to what was reported in the literature (Scheme 2.19).³⁹



Scheme 2.19: Modified flow system for the generation of diazo compounds **153a**; BPR = back-pressure regulator.

Moreover, as gas formation was observed during the reaction, a back-pressure regulator BPR (40 psi) was added at the end of the coil to pressurise the system. With the aim of finding the optimal conditions, a DoE-approach (see Chapter 1 and Appendix A for glossary) was used to identify the most significant parameters and 2-factor interactions (2FI; see Appendix A). Since a designed set of experiments is more likely to work efficiently when applied to a known system, some pilot studies were performed first to gain some experience with the reaction system and to choose the right ranges for each parameter (Table 2.5). For the experimental planning the reactor was simplified to a single sector as a 1 mL coil (i.d. = 0.5 mm). Lower concentrations (0.05 M) of **152a** compromised the yield with no reaction after 10 minutes and only 14% of **153a** after 50 minutes (entries 1–2). On the other hand, when the solution had a concentration of 0.5 M of **152a**, an inconsistent flow rate was observed due to crystallisation of *p*-NBSA

in the syringe and in the coil (entry 12). Moreover, no reaction was observed when THF was used as solvent regardless of the concentration, reaction time and temperature (entries 3, 6, 7) and when *p*-tosyl azide (**18a**) was used instead of *p*-NBSA (**18f**), **166** was formed as major product (entry 11).

Table 2.5: Pilot studies for the diazo-transfer reaction in flow.

Entry	152a (M)	18 (equiv.)	DBU (equiv.)	Solvent	T (°C)	<i>t</i> (min)	152a (%) ^a	153a (%) ^a	166 (%) ^a
1	0.05	18f (1)	2	CH ₃ CN	65	10	100	-	-
2	0.05	18f (1)	2	CH ₃ CN	22	50	73	15	7
3	0.05	18f (1)	2	THF	22	50	100	-	-
4	0.1	18f (1)	2.5	CH ₃ CN	65	10	73	14 (12) ^b	5
5	0.1	18f (1)	2	CH ₃ CN	22	50	52	24	19
6	0.1	18f (1)	2	THF	22	50	100	-	-
7	0.2	18f (1)	2	THF	65	10	100	-	-
8	0.2	18f (1)	1.5	CH ₃ CN	65	10	56	25	15
9^c	0.2	18f (1)	1.5	CH ₃ CN	65	10	53	25	10
10	0.2	18f (3)	2.5	CH ₃ CN	22	50	15	45 (40) ^b	20
11	0.2	18a (2.5)	2	CH ₃ CN	22	50	20	17	61
12^d	0.5	18f (2.5)	2.5	CH ₃ CN	65	50	(8) ^b	(51) ^b	(12) ^b

General Procedure: The reactions were performed using the flow system depicted in Scheme 2.19 with an overall flow rates of 0.1–0.02 mL·min⁻¹ and quenched with a phosphate buffer solution (pH = 7). ^aYield measured by ¹H NMR spectroscopy using 1,3,5-trimethoxybenzene as the internal standard; ^bIsolated yield; ^cReaction quenched with saturated aqueous NH₄Cl solution (pH = 5); ^dInconsistent flow rate due to *p*-NBSA precipitate.

With this information in hand the following two-levels fractional factorial design (FFD 2⁵⁻¹; see Appendix A) was designed with five numerical variables and three responses were registered (Table 2.6). The chosen parameters were: concentration of **152a** (+1 = 0.1 M; -1 = 0.05 M), *p*-NBSA (+1 = 3 equivalents; -1 = 1 equivalent), DBU (+1 = 2.5 equivalents; -1 = 1.5 equivalents), temperature (+1 = 65 °C; -1 = 22 °C) and residence time (+1 = 50 minutes; -1 = 10 minutes); the responses (starting material residue (%), diazo compound formation (%) and azide formation (%)) were measured by ¹H NMR spectroscopy using 1,3,5-trimethoxybenzene as the internal standard. The 16 experiments were performed in a random order over three days to minimise nuisance, and three central points were measured to identify any curvature. The acquired data

were fitted into the model and the three responses were analysed separately using pareto charts and half-normal plots to select the most significant factors.

Table 2.6: Matrix for the FFD 2^{5-1} with results. Factor generator for $E = A*B*C*D$.

Std	Run order	Factors					Responses		
		A: 152a (M)	B: T (°C)	C: DBU (equiv.)	D: <i>p</i> -NBSA (equiv.)	E: <i>t</i> (min)	152a (%) ^a	153a (%) ^a	166 (%) ^a
1	11	0.1	22	1.5	1	50	36	30	22
2	7	0.2	22	1.5	1	10	39	33	17
3	14	0.1	65	1.5	1	10	73	12	7
4	4	0.2	65	1.5	1	50	53	25	13
5	16	0.1	22	2.5	1	10	43	28	16
6	19	0.2	22	2.5	1	50	42	30	18
7	1	0.1	65	2.5	1	50	68	15	9
8	13	0.2	65	2.5	1	10	53	24	14
9	3	0.1	22	1.5	3	10	29	42	17
10	5	0.2	22	1.5	3	50	13	45	21
11	2	0.1	65	1.5	3	50	41	26	15
12	12	0.2	65	1.5	3	10	45	35	10
13	10	0.1	22	2.5	3	50	14	47	20
14	17	0.2	22	2.5	3	10	22	40	22
15	9	0.1	65	2.5	3	10	36	39	14
16	8	0.2	65	2.5	3	50	39	32	16
17	6	0.15	43.5	2	2	30	38	33	15
18	18	0.15	43.5	2	2	30	42	27	19
19	15	0.15	43.5	2	2	30	40	29	15

General Procedure: All reactions were performed according to Scheme 2.19. ^aYields determined by ¹H NMR spectroscopy using 1,3,5-trimethoxybenzene as the internal standard.

According to the chosen models, the concentration of **152a** (A), the amount of base (C) and the residence time (E) were not significant, which means that their influence on the outcomes was not statistically relevant within the investigated chemical space. In contrast, the impact of the temperature (B) was significant for all three responses, especially for the consumption of the starting material **152a**. In fact, a higher residue of **152a** was observed after performing the reactions at higher temperature, which resulted in lower yields for **153a** and azide **166** (Figure 2.4). As previously discussed for the batch process (pg. 61–63), despite the better yield for **153a** (65%) and a better diazo/azide ratio observed for a reaction performed at 45 °C, a small amount of starting material **152a** was recovered, and the decomposition of the triazene intermediate **167a** was suspected. Under flow conditions, due to the bigger surface area to volume ratio, the effect due to

the temperature was enhanced leading to a faster decomposition of the triazene **167a** that would explain the high amount of the starting material recovered. However, the pareto chart for the second response showed that the formation of the desired product **153a** was promoted when a higher amount of *p*-NBSA was used.

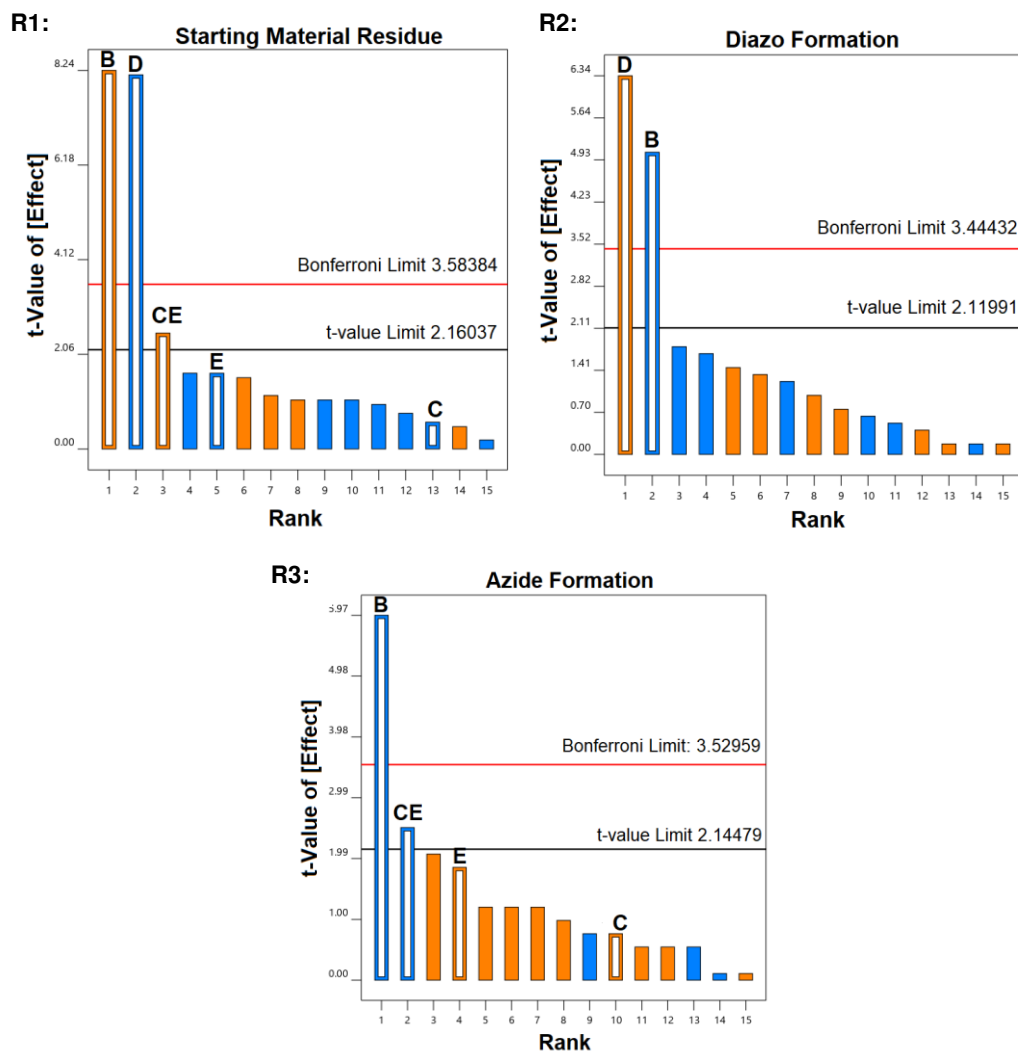


Figure 2.4: Pareto charts showing main effect for (from left to right) response R¹ (starting material residue), R² (diazo compound formation) and R³ (azide formation). A = **152a**, B = Temperature, C = Base, D = *p*-NBSA, E = time; Orange = positive effect; Blue = negative effect.

The three models were confirmed to be significant by the analysis of variance (ANOVA) with no significant curvature (see Appendix A for glossary). The models were then used to navigate the aforesaid chemical space to find optimal combinations of factors that, simultaneously, minimised the starting material residue and azide formation while maximising the formation of the desired diazo compound. The contour plots in Figure 2.5 provide a visual representation of the responses when the concentration of **152a** (A), the DBU equivalents (C) and the time (E) are kept fixed. By overlapping these contour plots, it is possible to better visualised the “sweet spot” (highlighted in yellow) in which all the

criteria are satisfied. In particular, when a solution of 0.2 M of **152a** and 2 equivalents of DBU are used with a 10 minutes residence time, the desired product **153a** is formed in more than 40% NMR yield, the residue of **152a** and azide formation are less than 25% and 20%, respectively.

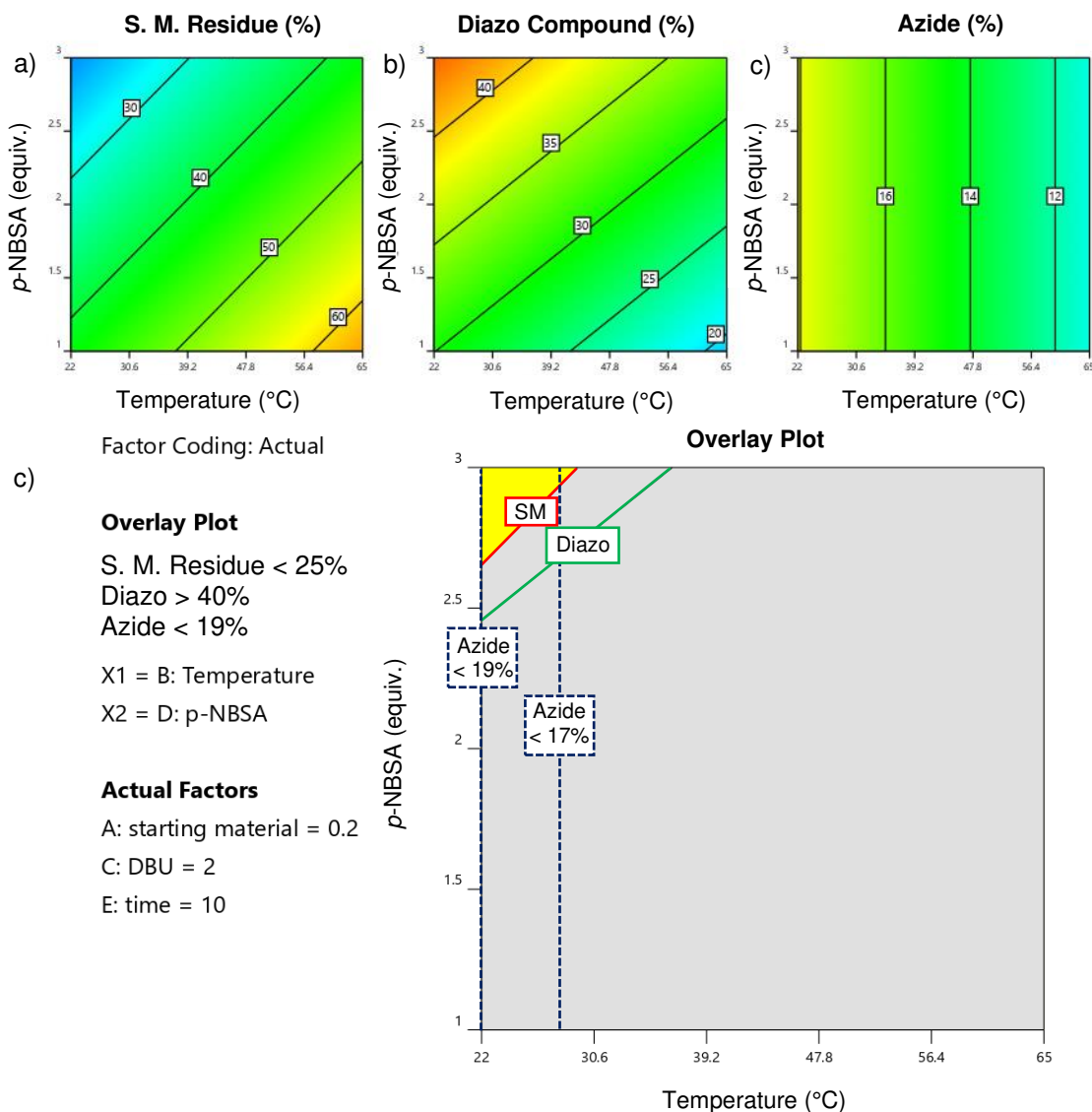
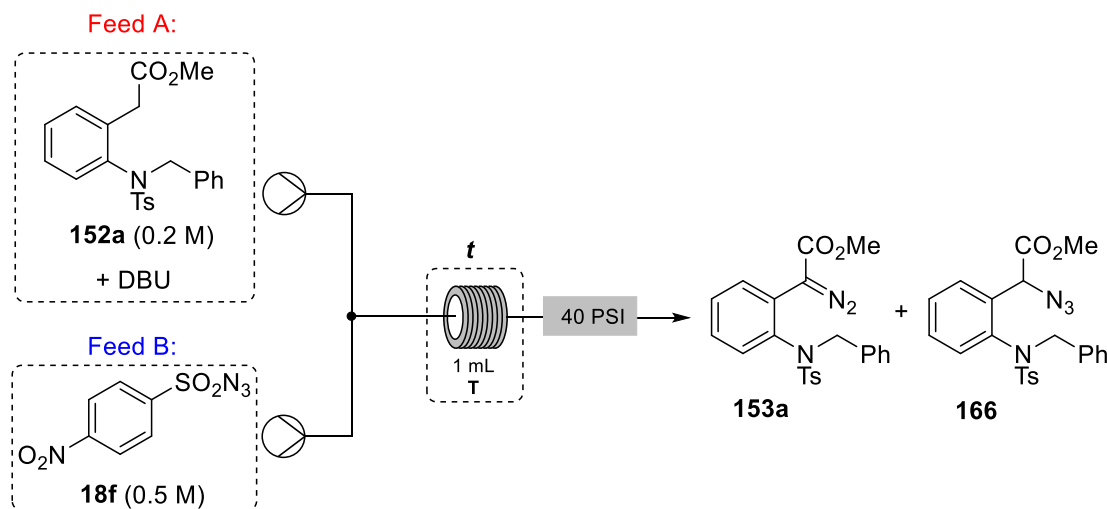


Figure 2.5: Contour plots for a) starting material residue, b) diazo and c) azide formation with **152a** = 0.2 M and DBU = 2 equiv. after 10 min; d) Overlay plot with highlighted “sweet spot” in yellow for the following criteria SM residue < 25%, diazo compound > 40% and azide < 19 or 17%.

Following that, the reaction mixture of a batch experiment was compared to the mixture obtained under flow conditions by crude ^1H NMR before and after work-up. As previously discussed (see Table 2.4), the batch reaction took 24 hours before traces of diazo **153a** were detected by ^1H NMR spectroscopy, hence the greatest part of the triazene intermediate was cleaved during the work-up and the diazo/azide ratio depended on the quenching agent. On the contrary, the products **153a** and **166** were partially formed already after 10 minutes in the flow system with no work-up. With this information in

hand, different internal diameters were modified next to investigate their influence on the mixing, and the equivalents of DBU were increased to improve the conversion of the starting material (Table 2.7).

Table 2.7: Screening of reactor internal diameters, temperatures and equivalents of DBU.



Entry	ID (mm)	DBU (equiv.)	T (°C)	time (min)	152a ^a	153a ^a	166 ^a
1	0.5	2	22	10	22	45	19
2	0.5	4	22	10	12	53 (49) ^b	27
3	1	2	22	10	20	42	32
4	1	4	22	10	13	50	31
5	1	5	22	10	12	50	35
6	0.2	4	22	10	22	47	29
7	0.5	4	45	10	19	48	25
8	0.5	4	65	10	35	45	16
9	0.5	4	22	50	13	54	28
10	0.5	4	22	5	10	52	26

General Procedure: The reactions were performed on 0.2 M of **152a** in acetonitrile using 2.5 equiv. of *p*-NBSA (**18f**); ^aDetermined by ¹H NMR spectroscopy using 1,3,5-trimethoxybenzene as the internal standard; ^bIsolated yield.

No effect was found when the internal diameter was changed from 0.5 to 1.0 mm (entries 1 and 3), however, when more equivalents of DBU were used, better conversions were achieved (80% combined yield) and the desired diazo compound **153a** was obtained in 53% and 50% NMR yield for 0.5 and 1.0 mm, respectively (entries 2 and 4). A smaller internal diameter (0.2 mm) and further addition of base did not lead to any improvement (entries 5, 6). In addition, **153a** was formed in 52%, 53% and 54% within 5, 10 and 50 minutes, respectively (entries 2, 9, 10), showing the insignificance of the residence time *t*. Hence, the optimal condition to achieve the α -diazocarbonyl intermediate **153a** in good yield were found using 4 equivalents of DBU, 0.5 mm of

internal diameter coil at room temperature (Table 2.7, entry 2). Subsequently, the Rh(II)-catalysed enantioselective cyclisation was investigated.

2.2.3 Optimisation of the C–H Insertion Reaction

The metal-catalysed C–H insertions of aryl diazo acetates have been widely investigated, especially for the synthesis of optically active heterocycles.⁴⁰ Among all, chiral Rh(II)-catalysts such as Rh₂(DOSP)₄ **71a**, Rh₂(PTTL)₄, **71d** and Rh₂(PTAD)₄ **71e** have stood out as the most efficient and selective catalysts (Figure 2.6).

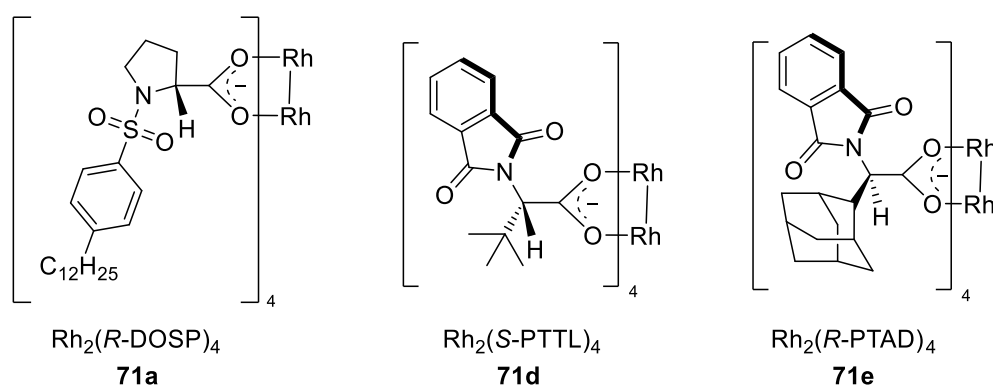
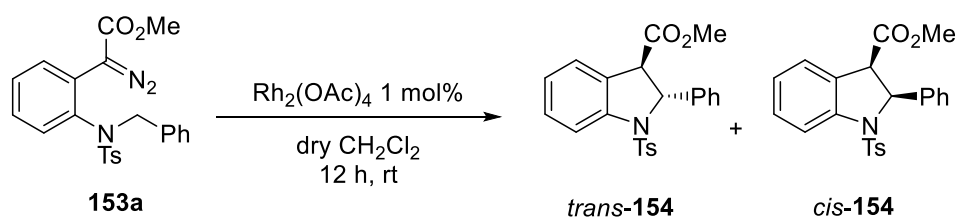


Figure 2.6: Chiral Rh(II)-catalysts most reported in the literature for asymmetric C–H insertions.

Firstly, racemic mixtures were synthesised using Rh₂(OAc)₄ as catalyst to investigate the reactivity of substrate **153a–n**. In presence of dirhodium tetraacetate catalyst in dry dichloromethane and under nitrogen atmosphere, the model diazo substrate **153a** fully converted into the desired 2,3-dihydroindoles **154** in 92% yield as a 3:1 mixture of *trans*- and *cis*-isomers within 12 hours (Scheme 2.20).



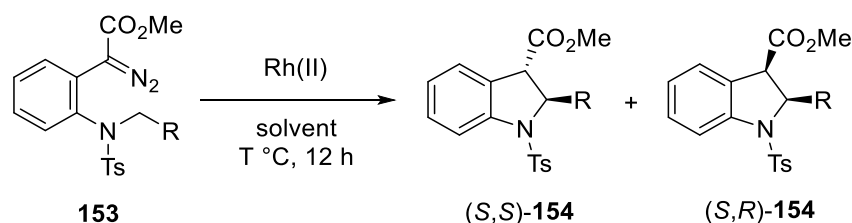
Scheme 2.20: Achiral intramolecular dirhodium-catalysed cyclisation of **153a**.

Generally, all α -diazo substrates **153a–n** formed the desired indolines in quantitative yield with high *d.r.* toward the *trans*-isomer, except *N*-sec-butyl **153n** and the *N*-allylic derivative **153o** that did not show the desired reactivity.

With the aim of optimising the stereoselectivity several solvents were screened.²⁶ Among all, *n*-hexane at room temperature provided the best *d.r.* and *ee* for the *trans*-isomer **154** when Rh₂(*R*-DOSP)₄ was used as chiral catalyst (Table 2.8). Indeed, when the

dodecylphenylsulfonylprolinate (DOSP) ligand was used at room temperature in *n*-hexane, the *trans*-**154** was obtained as the major product in good yields (up to 82%) and enantiomeric excess (up to 86% *ee*), while no stereoselectivity was detected for the *cis*-**154** (entries 2–5). Lower temperatures²⁶ showed to drastically improve the *d.r.* (>20:1) albeit lower enantiomeric excesses were observed (entry 6).

Table 2.8: Screening of conditions for the synthesis of *trans*- and *cis*-indoline **154**.



Entry	Conditions	R	Yield (%) ^a	<i>d.r.</i> ^b	(<i>S,S</i>)- 154 <i>ee</i> % ^c	(<i>S,R</i>)- 154 <i>ee</i> % ^c
1	Rh ₂ (OAc) ₄ 1 mol%, CH ₂ Cl ₂ , rt	C ₆ H ₅	92	3:1	n.a.	n.a.
2 ²⁶	Rh ₂ (<i>R</i> -DOSP) ₄ 1 mol% <i>n</i> -hexane, rt	C ₆ H ₅	72	10:1	80	6
3 ²⁶	Rh ₂ (<i>S</i> -DOSP) ₄ 1 mol% <i>n</i> -hexane, rt	C ₆ H ₅	64	9:1	76	0
4	Rh ₂ (<i>R</i> -DOSP) ₄ 1 mol% THF, rt	C ₆ H ₅	35	5.9:1	38	n.d.
5	Rh ₂ (<i>R</i> -DOSP) ₄ 0.5 mol% <i>n</i> -hexane, rt	C ₆ H ₅	82	11:1	86	0
6	Rh ₂ (<i>R</i> -DOSP) ₄ 0.5 mol% <i>n</i> -hexane, 0 °C	C ₆ H ₅	80	>20:1	73	0
7	Rh ₂ (<i>R</i> -PTAD) ₄ 1 mol% <i>n</i> -hexane, rt	C ₆ H ₅	20	1:1.1	59	40
8	Rh ₂ (<i>S</i> -PTTL) ₄ 1 mol% <i>n</i> -hexane, rt	C ₆ H ₅	63	1:4.5	11	4
9	Rh ₂ (<i>S</i> -PTTL) ₄ 1 mol% <i>n</i> -hexane, rt	4-Me-C ₆ H ₅	70	1:1.9	62	10

General Procedure: Reactions performed on a 1 mmol scale of **153**. ^aCombined yield of *trans*- and *cis*-isomers; ^bDetermined by ¹H NMR spectroscopy; ^cDetermined by chiral HPLC; n.a. = not applicable; n.d. = not determined.

Subsequently, the attention moved to other popular rhodium catalysts bearing the *N*-phthalamido-1-adamantylacetate (PTAD, **71e**) and the *N*-phthamido-1-*tert*-leucinate (PTTL, **71d**) ligands. Differently from **71a**, when **71e** or **71d** were used the *cis*-**154** was the major product formed in agreement with previous reports on dihydrobenzofurans.²⁵ In particular, the Rh₂(PTAD)₄ catalyst **71e** showed very poor diastereoselectivity and a medium enantioselectivity for both *trans*- and *cis*-**154** with 59% *ee* and 40% *ee*, respectively (entry 7). Moreover, the PTAD-ligand seems to encourage the formation of unidentified side products and only 20% of dihydroindoles **154** were isolated. On the other hand, the Rh₂(*S*-PTTL)₄ catalyst **71d** afforded the *cis*-**154** in better yield (63%) and

better diastereoselectivity (1:4.5 *trans/cis* ratio). However, the interaction between the carbene precursor **153a** and the PTTL ligand lead to a very poor selectivity for both *trans*- and *cis*-isomers (up to 11% *ee*; entry 8), while a moderate selectivity (62% *ee*) was detected when a different substrate (**153f**) was used (entry 9).

In the light of these observations, the DOSP-ligand was preferred over PTAD and PTTL for the successful synthesis of *trans*-indolines in both good yields and enantioselectivity. The absolute configuration of the major enantiomer (*2R,3R*)-2-phenyl-1-tosylindoline-3-carboxylate (**154a**) was confirmed by single crystal X-ray analysis of the product obtained after recrystallisation from *n*-hexane/2-propanol 1:1 v/v, using Rh₂(*S*-DOSP)₄ **71a** catalyst (Figure 2.7).²⁶

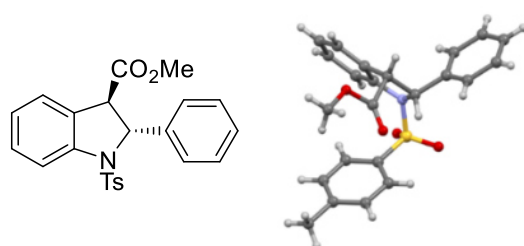
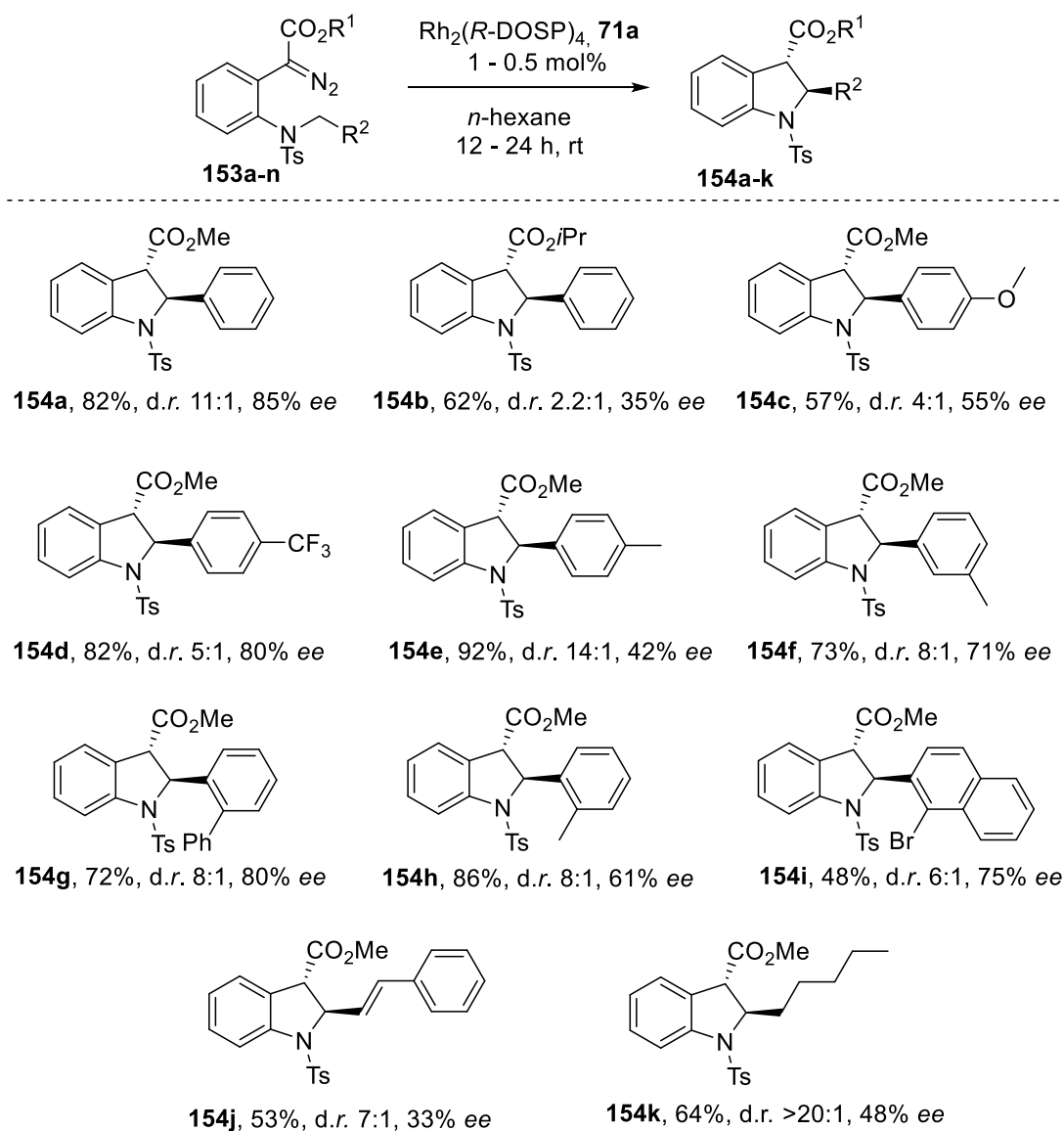


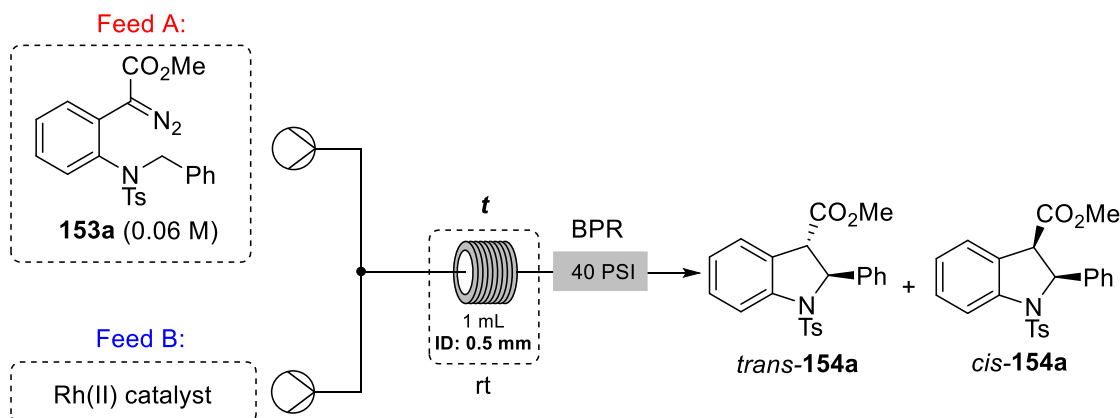
Figure 2.7: Crystal structure for (*2R,3R*)-2-phenyl-1-tosylindoline-3-carboxylate **154a**.

Subsequently, the optimal reaction conditions (Table 2.8, entry 5) were applied on various diazo precursors (**153a–n**) leading to the *trans*-products **154a–k** in good yields and in good to excellent enantiomeric excesses (Scheme 2.21). The substitution of the methyl ester with a bulkier *iso*-propyl ester decreased the selectivity with **154b** formed as a 2.2:1 diastereomeric ratio and 35% *ee*. Products **154c–f** bearing electron-donating and electron-withdrawing groups in *para*-, *meta*- and *ortho*- were obtained in good yields (up to 92%) and good to excellent selectivity (up to 80% *ee*). The bulkier 2-phenyl substituted aryl diazo derivative **153g** was slower to react, affording **154g** in 73% yield after 24 hours in 80% *ee*, while the slightly less sterically hindered **153h–i** formed **154h–i** in 86% and 48% yield and 61% and 75% *ee*, respectively, after 12 hours. Besides the benzylic-derivatives in **153a–i**, also the cinnamyl and the *n*-hexyl groups were well-tolerated under these conditions. The cinnamic-derivative showed the desired reactivity affording **154j** in 53% yield after 24 hours despite of the presence of the double bond, although with poor enantioselectivity (33% *ee*). On the other hand, the *n*-hexyl substrate **154k** was formed in good yield (64%) and excellent diastereoselectivity (>20:1) with a moderate enantiomeric excess (48% *ee*) within 12 hours.



Scheme 2.21: Substrate scope of *trans*-dihydroindoles **154a–k**. Combined yields of *trans* and *cis*-**154** are shown; diastereomeric ratio (*d.r.*) was determined by ^1H NMR spectroscopy and the enantiomeric excess (*ee*) was determined by HPLC. The absolute stereochemistries were assigned in analogy to **154a**.

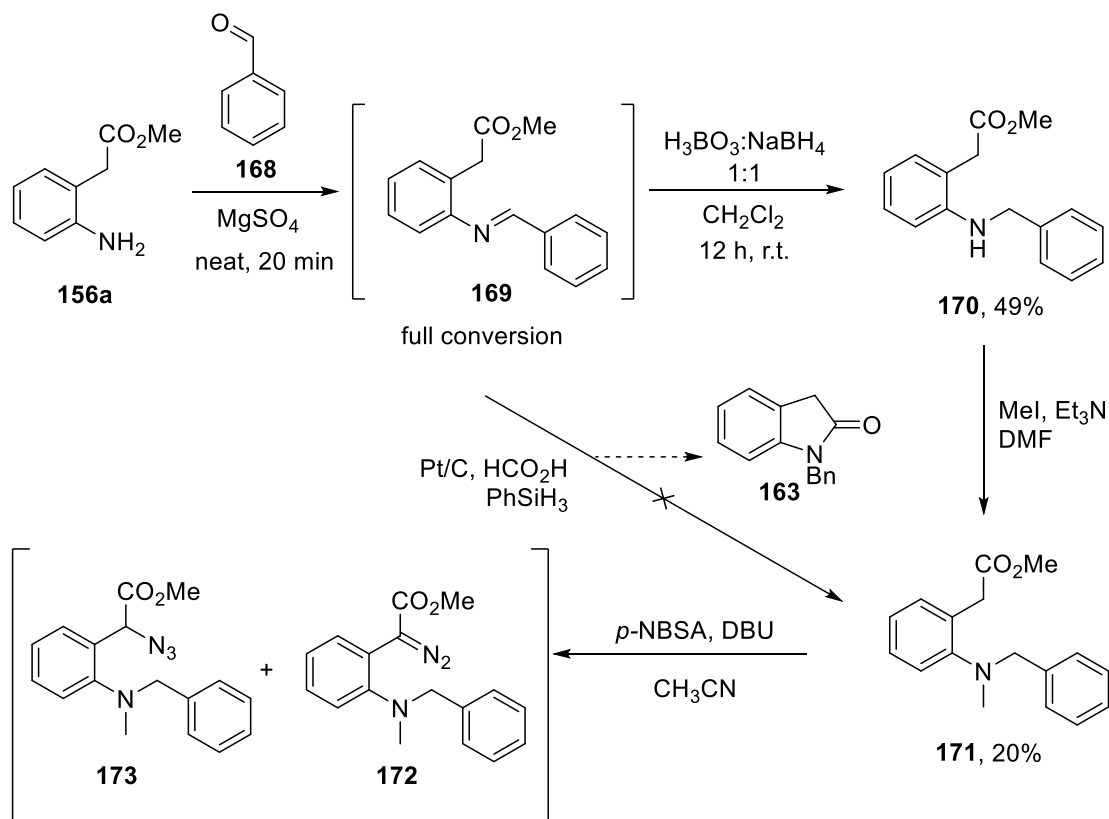
Eventually, the C–H insertion was examined in flow with the aim to combine the generation and reaction of the carbene precursor into a single continuous-flow setup. Unfortunately, there was no reaction occurring under the investigated conditions (Table 2.9) which seem to be not appropriate for flow conditions.

Table 2.9: Flow setup for intramolecular C–H insertion.

Entry	Rh(II) catalyst	Time (min)	Yield (%)
1	Rh ₂ (OAc) ₄ 1 mol%	20	no reaction
2	Rh ₂ (oct) ₄ 1 mol%	40	traces
3	Rh ₂ (<i>R</i> -DOSP) ₄ 1 mol%	40	no reaction
4	Rh ₂ (<i>R</i> -PTAD) ₄ 1 mol%	40	traces

The reaction in batch required 12–24 hours to occur completely, probably as result of the bulky tosyl group close to the C–H insertion site, making the translation into a flow system harder. Therefore, a synthesis for different *N*-substituted diazo compounds was initiated (Scheme 2.22). 2-Aminophenylacetate **156a** was quantitatively converted to the imine **169** within 10–20 minutes in the presence of benzaldehyde (**168**) and MgSO₄ under neat reaction conditions. The Pt-catalysed reduction/methylation of **169** in the presence of formic acid and phenylsilane described by Zhu *et al.*,⁴¹ provided only the undesired lactone **163** as the major product. The desired product **171** was obtained by imine reduction to **170** followed by methylation. For a successful reduction, a 1:1 mixture of boric acid and NaBH₄⁴² was used to avoid ester hydrolysis observed when only NaBH₄ was used. The secondary amine **170** was then treated with methyl iodide and triethylamine in DMF to generate the *N*-methyl derivative **171**, which was formed only in poor yield (only 16–21%) due to the competitive cyclisation to **163** (36–40% yield). Subsequently, **171** was treated with *p*-NBSA (2 equivalents) and DBU (2 equivalents) in acetonitrile at room temperature for 24 hours, but a complex mixture of unreacted **171**, desired product **172** and the side product **173** was obtained. When the crude mixture was treated with Rh₂(OAc)₄ in dichloromethane the bright yellow solution turned pale green within 5 minutes and a gas evolution was observed. The ¹H NMR spectroscopic analysis of the crude reaction mixture showed the disappearance of the diazo

precursor **172**, but the afforded reaction mixture was complex, and no product could be isolated or identified.



Scheme 2.22: Synthetic pathway to afford alternative *N*-methyl substituted indolines.

2.3 Conclusion and Outlook

In conclusion, a novel and efficient stereoselective synthesis for *trans*-indolines from α -diazocarbonyl compounds using Rh(II)-catalysed intramolecular C–H insertions was developed.

The library of carbene-precursors **153a–n** was successfully synthesised in batch in moderate to very good yields *via* Regitz diazo-transfer. Furthermore, the reaction was translated in a flow system using a DOE-approach to optimise the synthesis of the model diazo intermediate **153a** (up to 51% NMR yield). Moreover, a library of 11 new *trans*-indolines **154a–k** was built in good yields and with good to excellent selectivity.

Further work can be done to expand the substrate scope in order to include substituents on the indoline aryl ring as well as investigating different *N*-protecting groups. Moreover, future work is focused on developing a continuous flow set-up for the diazo-transfer reaction and the asymmetric cyclisation combined with an online 2D-HPLC analytic system for a faster analysis of complex mixture of isomers. Indeed, the 2D-HPLC technique proved to speed up the analysis providing information about conversion, *d.r.* and *ee* within 40 min and it presents a convenient tool to quickly analyse asymmetric transformation in a short period of time (Figure 2.8).

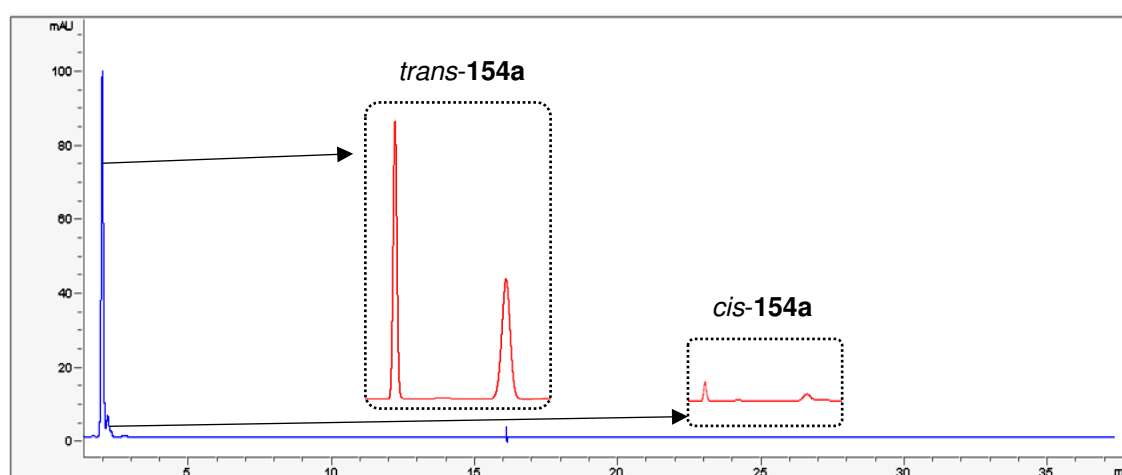
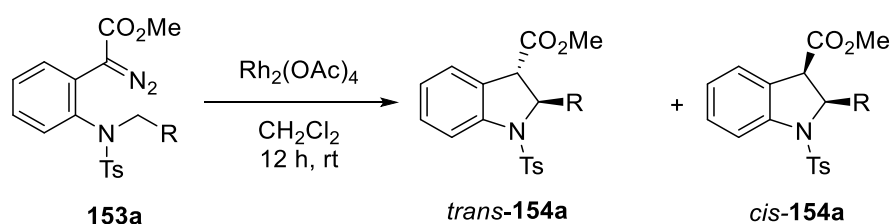


Figure 2.8: 2D-HPLC double chromatogram for the resolution of the indoline mixture ($\lambda = 254$ nm): first dimension silica column separates *trans*- from *cis*-isomer (blue line); second dimension YMC chiral column separates the enantiomers (red line).

References

- 1 For selected examples see: a) J. D. Podoll, Y. Liu, L. Chang, S. Walls, W. Wang, X Wang, *Proc. Natl. Acad. Sci.* **2013**, *110*, 15573–15578; b) R. R. Poondra, N. N. Kumar, K. Bijian, M. Prakesch, V. Campagna-Slater, A. Reayi, P. T. Reddy, A. Choudhry, M. L. Barnes, D. M. Leek, M. Daroszewska, C. Loughheed, B. Xu, M. Schapira, M. A. Alaoui-Jamali, P. Arya, *J. Comb. Chem.* **2009**, *11*, 303–309; c) Z. Gan, P. T. Reddy, S. Quevillon, S. Couve-Bonnaire, P. Arya, *Angew. Chem. Int. Ed.* **2005**, *44*, 1366–1368.
- 2 For recent reviews on indoline synthesis see: a) T.-B. Hua, C. Xiao, Q.-Q. Yang, J.-R. Chen, *Chin. Chem. Lett.* **2019**, *31*, 311–322; b) D. Liu, G. Zhao, L. Xiang, *Eur. J. Org. Chem.* **2010**, 3975–3984; c) S. Anas, H. B. Kagan, *Tetrahedron: Asymmetry* **2009**, *20*, 2193–2199.
- 3 S. P. Roche, J.-J. Y. Tendoung, B. Treguier, *Tetrahedron* **2015**, *71*, 3549–3591.
- 4 a) Y. Duan, L. Li, M.-W. Chen, C.-B. Yu, H.-J. Fan, Y.-G. Zhou, *J. Am. Chem. Soc.* **2014**, *136*, 7688–7700; b) R. Kuwano, M. Kashiwabara, *Org. Lett.* **2006**, *8*, 2653–2655; c) R. Kuwano, K. Sato, T. Kurokawa, D. Karube, Y. Ito, *J. Am. Chem. Soc.* **2000**, *122*, 7614–7615.
- 5 W. Zi, Z. Zuo, D. Ma, *Acc. Chem. Res.* **2015**, *48*, 702–711.
- 6 a) K. Kubota, K. Hayama, H. Iwamoto, H. Ito, *Angew. Chem. Int. Ed.* **2015**, *54*, 8809–8813; b) A. Awata, T. Arai, *Angew. Chem. Int. Ed.* **2014**, *53*, 10462–10465; c) D. Zhang, H. Song, Y. Qin, *Acc. Chem. Res.* **2011**, *44*, 447–457.
- 7 D. F. Taber, P. K. Tirunahari, *Tetrahedron* **2011**, *67*, 7195–7210.
- 8 a) I. Bytschkov, H. Siebeneicher, S. Doye, *Eur. J. Org. Chem.* **2003**, *15*, 2888–2902; b) S. Wagaw, R. A. Rennels, S. L. Buchwald, *J. Am. Chem. Soc.* **1997**, *119*, 8451–8458; c) J. P. Wolfe, R. A. Rennels, S. L. Buchwald, *Tetrahedron* **1996**, *52*, 7525–7546; d) B. H. Yang, S. L. Buchwald, *Org. Lett.* **1999**, *1*, 35–38; e) J. F. Hartwig, *Synlett* **1997**, 329–340; e) T.-S. Mei, D. Leow, H. Xiao, B. N. Laforteza, J.-Q. Yu, *Org. Lett.* **2013**, *15*, 3058–3061.
- 9 For selected example see: a) Z.-Y. Li, H. H. Chaminda Lakmal, X. Qian, Z. Zhu, B. Donnadiou, S. J. McClain, X. Xu, X. Cui, *J. Am. Chem. Soc.* **2019**, *141*, 15730–15736; b) D. Katayev, M. Nakanishi, T. Bürgib, E. P. Kündig, *Chem. Sci.* **2012**, *3*, 1422–1425; c) M. Nakanishi, D. Katayev, C. Besnard, E. P. Kündig, *Angew. Chem. Int. Ed.* **2011**, *50*, 7438–7441; d) A. B. Dounay, L. E. Overman, A. D. Wroblewski, *J. Am. Chem. Soc.* **2005**, *127*, 10186–10187; e) A. M. Hyde, S. L. Buchwald, *Angew. Chem. Int. Ed.* **2008**, *47*, 177–180.
- 10 a) F. Zhou, J. Guo, J. Liu, K. Ding, S. Yu, Q. Cai, *J. Am. Chem. Soc.* **2012**, *134*, 14326–14329; b) J. J. Li, T. S. Mei, J. Q. Yu, *Angew. Chem. Int. Ed.* **2008**, *47*, 6452–6455; c) A. Minatti, S. L. Buchwald, *Org. Lett.* **2008**, *10*, 2721–2724.
- 11 a) A. Correa, I. Tellitu, E. Dominguez, R. SanMartin, *J. Org. Chem.* **2006**, *71*, 8316–8319; b) L. Pouysegu, A.-V. Avenllan, S. Quideau, *J. Org. Chem.* **2002**, *67*, 3425–3436.
- 12 a) R. Viswanathan, C. R. Smith, E. N. Prabhakaran, J. N. Johnston, *J. Org. Chem.* **2008**, *73*, 3040–3046; b) J. Johnston, M. A. Plotkin, R. Viswanathan, E. N. Prabhakaran, *Org. Lett.*

- 2001**, *3*, 1009–1011; c) R. Viswanathan, E. N. Prabhakaran, M. A. Plotkin, J. N. Johnston, *J. Am. Chem. Soc.* **2003**, *125*, 163–168.
- 13 a) C. Leroi, D. Bertin, P. E. Dufils, D. Gigmes, S. Marque, P. Tordo, J. L. Couturier, O. Guerret, M. A. Ciufolini, *Org. Lett.* **2003**, *5*, 4943–4945; b) H. Fuwa, M. Sasaki, *Org. Lett.* **2007**, *9*, 3347–3350.
- 14 a) X. Wen, Y. Wang, X. P. Zhang, *Chem. Sci.* **2018**, *9*, 5082–5086; b) Y. Wang, X. Wen, X. Cui, X. P. Zhang, *J. Am. Chem. Soc.* **2018**, *140*, 4792–4796.
- 15 a) R. C. Larock, N. Berrios-Peña, K. Narayanan, *J. Org. Chem.* **1990**, *55*, 3447–3450; b) C. E. Houlden, C. D. Bailey, J. G. Ford, M. R. Gagne, G. C. Lloyd-Jones, K. I. Booker-Milburn, *J. Am. Chem. Soc.* **2008**, *130*, 10066–10067.
- 16 a) G. S. Gil, U. M. Groth, *J. Am. Chem. Soc.* **2000**, *122*, 6789–6790; b) W. F. Bailey, M. J. Mealy, *J. Am. Chem. Soc.* **2000**, *122*, 6787–6788.
- 17 a) J. Lee, K. M. Ko, S.-G. Kim, *RSC Adv.* **2017**, *7*, 56457 – 56462; b) R. Miyaji, K. Asano, S. Matsubara, *Org. Lett.* **2013**, *15*, 3658 – 3661.
- 18 J. L. García Ruano, J. Alemán, S. Catalán, V. Marcos, S. Monteagudo, A. Parra, C. d. Pozo, S. Fustero, *Angew. Chem. Int. Ed.* **2008**, *47*, 7941–7944.
- 19 a) T. Ikawa, Y. Sumii, S. Masuda, D. Wang, Y. Emi, A. Takagi, S. Akai, *Synlett* **2018**, *29*, 530–536; b) R. D. Aher, G. M. Suryavanshi, A. Sudalai, *J. Org. Chem.* **2017**, *82*, 5940–5946; c) J.-X. Pian, L. He, G.-F. Du, H. Guo, B. Dai, *J. Org. Chem.* **2014**, *79*, 5820–5826; d) C. D. Gilmore, K. M. Allan, B. M. Stoltz, *J. Am. Chem. Soc.* **2008**, *130*, 1558–1559.
- 20 a) G. Zhang, A. Cang, Y. Wang, Y. Li, G. Xu, Q. Zhang, T. Xiong, Q. Zhang, *Org. Lett.* **2018**, *20*, 1798–1801; b) D. X. Li, J. Kim, J. W. Yang, J. Yun, *Chem. Asian J.* **2018**, *13*, 2365–2368.
- 21 E. Ascic, S. L. Buchwald, *J. Am. Chem. Soc.* **2015**, *137*, 4666–4669.
- 22 a) Y. Xia, D. Qiu, J. Wang, *Chem. Rev.* **2017**, *117*, 13810–13889.
- 23 a) L. W. Souza, R. A. Squitieri, C. A. Dimirjian, B. M. Hodur, L.A. Nickerson, C. N. Penrod, J. Cordova, J. C. Fettinger, J. T. Shaw, *Angew. Chem. Int. Ed.* **2018**, *57*, 15213–15216; b) S. Lee, H.-J. Lim, K. Cha, G. A. Sulikowski, *Tetrahedron* **1997**, *53*, 16521–16532; c) H.-J. Lim, G. A. Sulikowski, *J. Org. Chem.* **1997**, *60*, 2326–2327; d) G. A. Sulikowski, S. Lee, *Tetrahedron Lett.* **1999**, *40*, 8035–8038.
- 24 H. M. L. Davies, M. V. A. Grazini, E. Aouad, *Org. Lett.* **2001**, *3*, 1475–1477.
- 25 H. Saito, H. Oishi, S. Kitagaki, S. Nakamura, M. Anada, S. Hashimoto, *Org. Lett.* **2002**, *4*, 3887–3890.
- 26 S. T. R. Müller Ph.D. Thesis **2015**, Cardiff University, “Diazo Compounds in Continuous Flow Technology”.
- 27 T. Tsung-Pei, US20120101224, **2012**.
- 28 G. D. Channe, G. Shankare, *Indian J. Chem.* **2000**, 709–711.
- 29 C.-J. Wallentin, J. D. Nguyen, P. Finkbeiner, C. R. J. Stephenson, *J. Am. Chem. Soc.* **2012**, *134*, 8875–8884.
- 30 a) M. Regitz, *Angew. Chem. Int. Ed. Engl.* **1967**, *6*, 733–749; b) M. Regitz, *Synthesis* **1972**, 351–373.

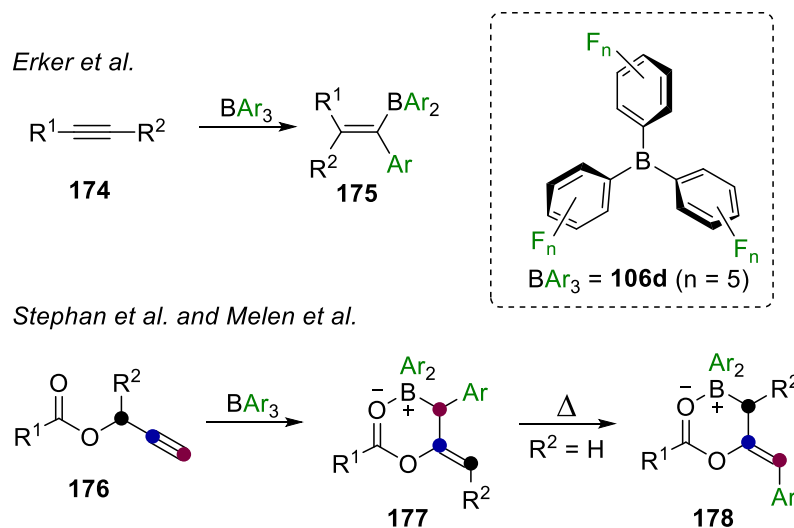
- 31 D. Das, R. Samanta, *Adv. Synth. Catal.* **2018**, *360*, 379–384.
- 32 R. M. O'Mahony, D. Lynch, H. L. D. Hayes, E. Ní Thuama, P. Donnellan, R. C. Jones, B. Glennon, S. G. Collins, A. R. Maguire, *Eur. J. Org. Chem.* **2017**, 6533–6539.
- 33 a) S. Tshepelevitsh, A. Kütt, M. Lõkov, I. Kaljurand, J. Saame, A. Heering, P. G. Plieger, R. Vianello, I. Leito, *Eur. J. Org. Chem.* **2019**, 6735 – 6748; b) I. Kaljurand, A. Kütt, L. Sooväli, T. Rodima, V. Mäemets, I. Leito, I. A. Koppel, *J. Org. Chem.* **2005**, *70*, 1019–1028.
- 34 a) S. Chuprakov, M. Rubin, V. Gevorgyan, *J. Am. Chem. Soc.* **2005**, *127*, 3714–3715; b) W.-J. Zhao, M. Yan, D. Huang, S.-J. Ji, *Tetrahedron* **2005**, *61*, 5585–5593.
- 35 G. H. Hakimelahi, G. Just, *Synth. Commun.* **1980**, *10*, 429–435.
- 36 a) D. A. Evans, T. C. Britton, J. A. Ellma, R. L. Dorow, *J. Am. Chem. Soc.* **1990**, *112*, 4011–4030; b) D. A. Evans, T. C. Britton, *J. Am. Chem. Soc.* **1987**, *109*, 6881–6883.
- 37 M. Regitz, *Angew. Chem. Int. Ed.* **1966**, *5*, 681–682.
- 38 S. T. R. Müller, A. Murat, D. Maillos, P. Lesimple, P. Hellier, T. Wirth, *Chem. Eur. J.* **2015**, *21*, 7016–7020.
- 39 a) S. T. R. Müller, T. Wirth, *ChemSusChem* **2015**, *8*, 245–250; b) S. T. R. Müller, A. Murat, P. Hellier, T. Wirth, *Org. Process Res. Chem.* **2016**, *20*, 495–502; c) B. J. Deadman, R. M. O'Mahony, D. Lynch, D. C. Crowley, S. G. Collins, A. R. Maguire, *Org. Biomol. Chem.* **2016**, *14*, 3423–3431.
- 40 a) H. M. L. Davies, A. M. Walji, *Modern Rhodium-Catalyzed Organic Reactions*, Wiley-VCH, Weinheim, **2005**, 301–340; b) T. Ye, M. A. McKervey, *Chem. Rev.* **1994**, *94*, 1091–1160; c) M. P. Doyle, M. A. McKervey, T. Ye, *Modern Catalytic Methods for Organic Synthesis with Diazo Compounds: From Cyclopropanes to Ylides*, Wiley, New York, **1998**.
- 41 L. Zhu, L.-S. Wang, B. Li, B. Fu, *Catal. Sci. Technol.* **2016**, *6*, 6172–6176.
- 42 B.T. Cho, S. K. Kang, *Tetrahedron* **2005**, *61*, 5725–5734.

CHAPTER 3: Synthesis of Fluorinated Benzofuranones

3.1 Introduction

Fluorine-containing organic molecules have an important role in both medicinal and agrochemical chemistry due to the unique properties fluorine can provide to a molecule.¹ The presence of fluorine atoms has a biological importance: it can improve the metabolic stability of the molecule as well as its binding affinity to protein targets. Moreover, it can increase the lipophilicity, which results in a better permeability of the molecule through the biological membrane.² Moreover, late stage ¹⁸F functionalisation provides access to useful radiolabel tracers that are widely used in Positron Emission Tomography (PET) imaging.³ Additionally, polyfluoroarenes play an important role in the electronics industries, as they find applications in electronic devices such as organic light-emitting diodes (OLEDs), organic thin film transistors (OFETs), photovoltaics and sensors.⁴ Therefore, the research of new methods to install halogenated aryl groups represent a hot topic in organic chemistry.⁵

Publications by Erker *et al.*⁶ as well as by Stephan *et al.*⁷ and the Melen group⁸ have shown that tris(pentafluorophenyl)borane $B(C_6F_5)_3$ **106d**, mainly used as catalyst in metal-free cyclisations,⁹ hydrogenations,¹⁰ and hydrosilylation¹¹ reactions, has the ability to undergo C_6F_5 group migration (Scheme 3.1).

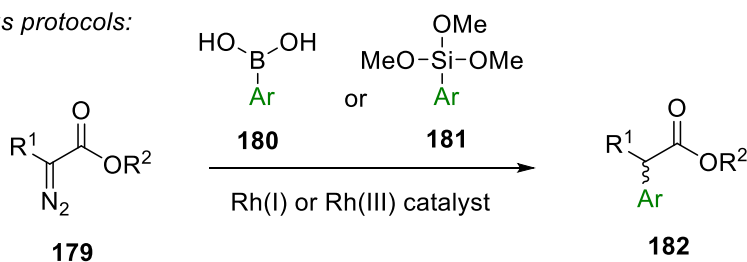


Scheme 3.1: Examples of metal-free fluoroaryl-migration using $B(C_6F_5)_3$ (**106d**).

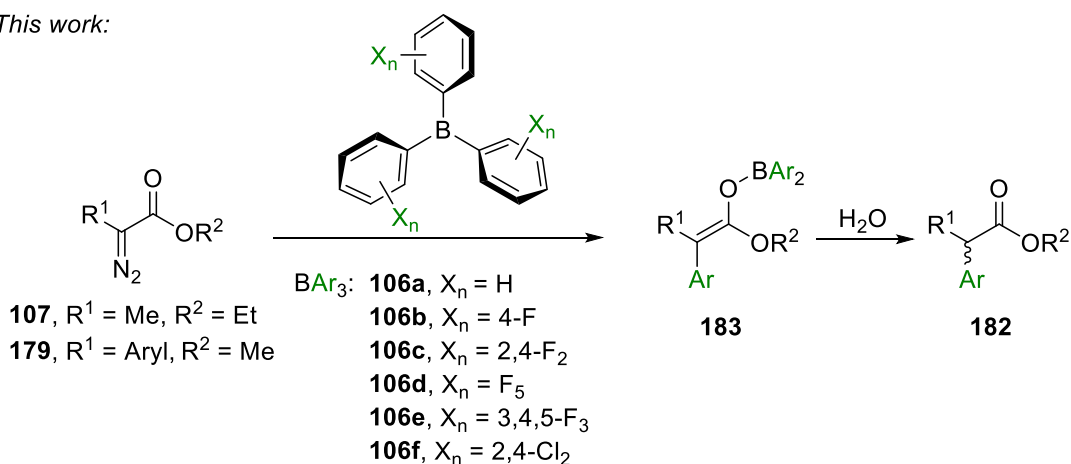
However, most approaches have been limited to the use of $B(C_6F_5)_3$ as part of a frustrated Lewis pair (FLP)^{10a} and the migratory attitude of other aryl groups from boranes is much less studied.

As mentioned earlier (Chapter 1.1.2.2), α -diazocarbonyl compounds react with trialkyl- and triarylboranes to form boron enolate intermediates which then react with various electrophiles affording α -functionalised carbonyl compounds. In this chapter the metal-free α -aryl functionalisation of esters from α -diazocarbonyl precursors **179** in the presence of halogenated and non-halogenated triarylboranes **106** is presented (Scheme 3.2).¹² The resulting α,α -diaryl esters **182**, represent a valuable class of compounds due to their role as pharmacophores,¹³ and they can be typically achieved by rhodium-mediated functionalisation of diazo compounds in the presence of arylboronic acids **180** or arylsiloxanes **181**.¹⁴

Previous protocols:

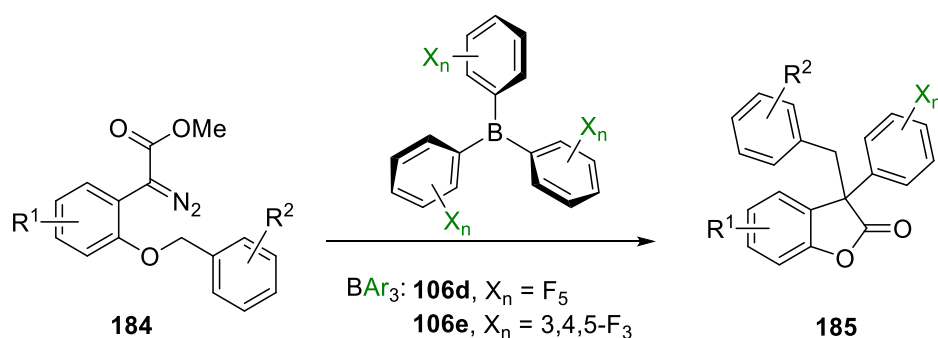


This work:



Scheme 3.2: Previous protocols for the synthesis of α -aryl esters **182** from α -diazo esters **179** catalysed by rhodium(I) or rhodium(II) (top); metal-free α -aryl functionalisation of esters from α -diazocarbonyl precursors **107** or **179** presented in this chapter (bottom).

Nevertheless, the main focus of the chapter is the development of a metal-free synthesis towards fluorinated asymmetric benzofuran-2(3*H*)-ones **159** from 2-oxygen or 2-sulfur substituted aryl- α -diazo acetates **158** in the presence of fluorinated triarylboranes **108d** and **108e** (Scheme 3.3).



Scheme 3.3: Novel metal-free synthesis of benzofuran-2(3*H*)-ones **185** using triarylboranes **106d** and **106e** presented in this chapter.

Benzofuran-2-(3*H*)-ones are oxygen-containing heterocycles which are present in many biologically active compounds such as (–)-fumimycin **186**,¹⁵ rosmadial **187**,¹⁶ yuccaol A **188**¹⁷ and abiesinol A **189** (Figure 3.1).¹⁸ Moreover, they are used as synthons for the synthesis of flavonoid-related aurones **190**¹⁹ and sesquiterpenes such as aplysin **191**.²⁰

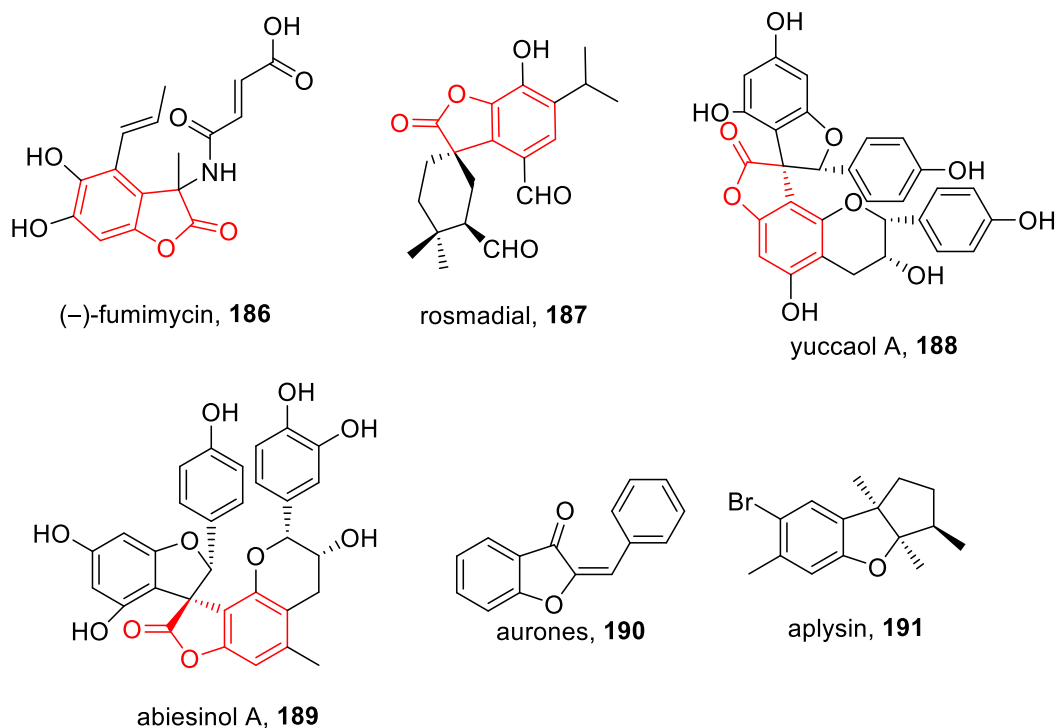
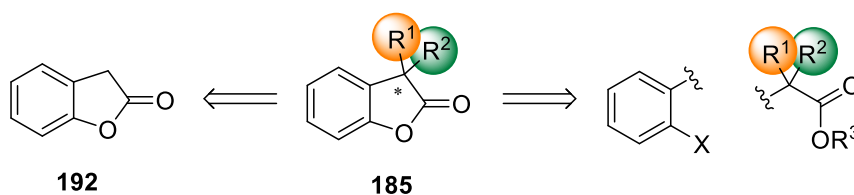


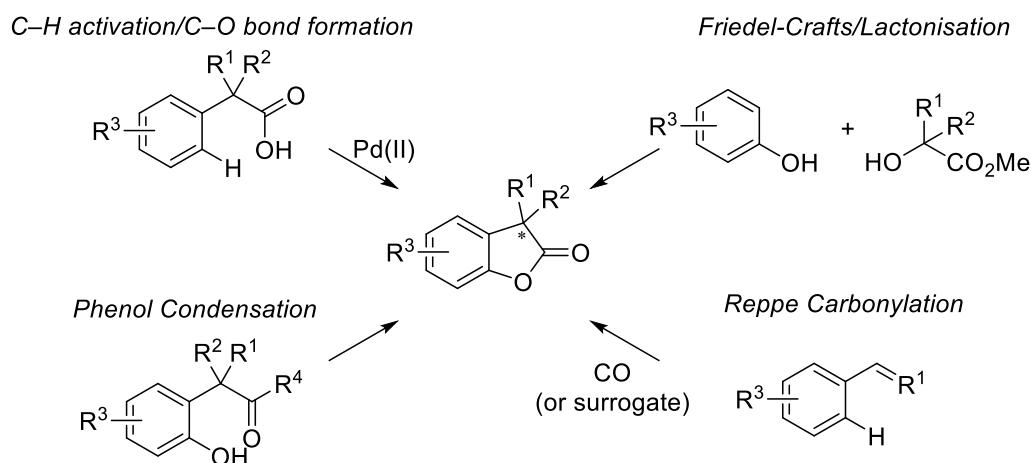
Figure 3.1: Examples of natural products containing or synthesised from benzofuranones.

The presence of a fully substituted quaternary carbon at the C-3 position is a key structural characteristic for such compounds and, to date, there are several protocols towards the asymmetric synthesis of 3,3-disubstituted benzofuranones **185** that follow two common retrosynthetic approaches (Scheme 3.4).²¹ One approach is based on the double functionalisation of benzofuranone scaffolds **192**, promoted by organo- or metal-based catalysts,²² whereas the other approach relies on the *de novo* synthesis of the lactone framework from building blocks which bear a pre-functionalised C-3 position.



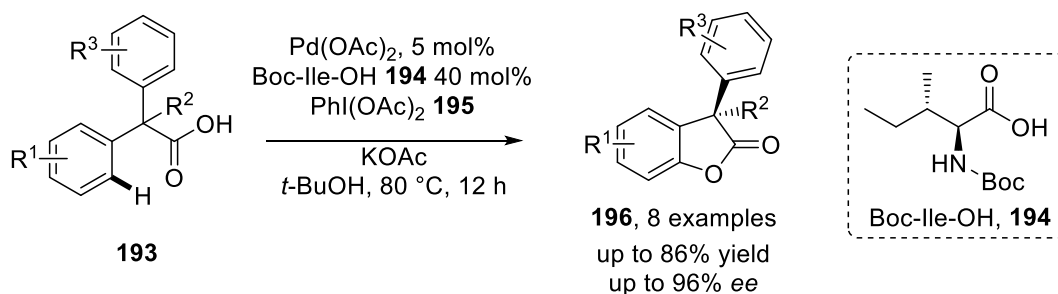
Scheme 3.4: Common retrosynthetic approaches towards 3,3-benzofuranones **185**.

For the *de novo* synthesis of the lactone core, metal-catalysed C–H activation/C–O bond formation,²³ tandem Friedel-Crafts/lactonisation,²⁴ Reppe-type cyclocarbonylation,²⁵ and condensation of phenol derivatives²⁶ have all been reported as successful strategies (Scheme 3.5). However, the protocols for the stereoselective synthesis of chiral lactones from achiral and acyclic starting materials are limited.



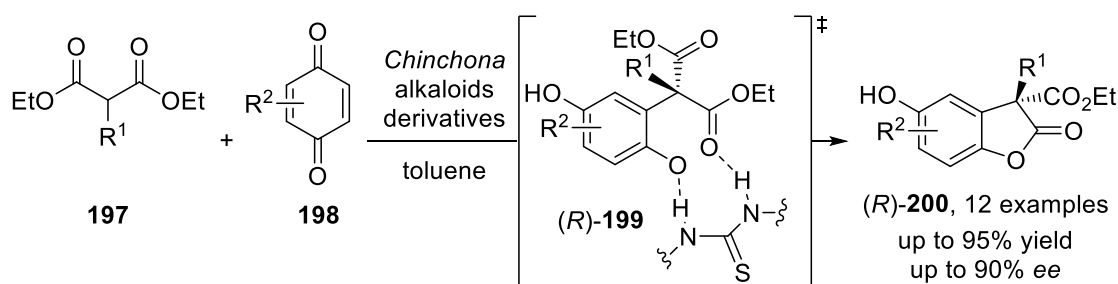
Scheme 3.5: Overview of the most common strategies towards substituted benzofuranones.

A recent example of the enantioselective synthesis of chiral benzofuranones relies on the palladium-catalysed C–H activation of 2,2-disubstituted phenylacetic acids **193**. The activation is followed by C–O bond formation in the presence of a chiral ligand **194**, which subsequently generates chiral benzofuranones **196** in good yields (up to 86%) and high enantioselectivities (up to 96% *ee*; Scheme 3.6).^{23a}



Scheme 3.6: Asymmetric Pd(II)-catalysed C–H activation/lactonisation of 2,2-disubstituted phenylacetic acid **193**.

In 2018, Bella and co-workers^{26b} developed a stereoselective synthesis for chiral 3,3-disubstituted benzofuranones **200**, *via* desymmetrisation of prochiral malonates **197** (Scheme 3.7). In the presence of *Chinchona* alkaloid derivatives, malonate **197** reacts with quinone **198** and the resulting arylated achiral malonate cyclises to give benzofuranones **200** in good yields, preferentially as the (*R*)-isomer. The intermolecular desymmetrisation is suggested to occur *via* a transition state such **199**, where the thiourea moiety of the chiral organocatalyst coordinates to both the phenolic and the carboxylic groups, favouring the formation of (*R*)-**199**.^{26b}



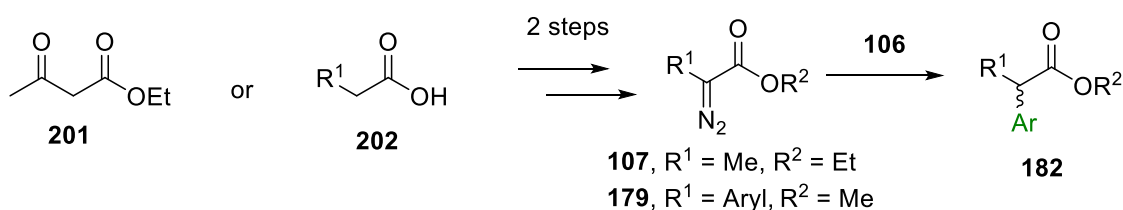
Scheme 3.7: Synthesis of chiral benzofuranones **200** *via* intramolecular desymmetrisation on malonate **197**.

In this chapter, a novel approach towards asymmetric 3,3-disubstituted benzofuranone **185** is presented. The new methodology involves α -diazo esters and highly Lewis acidic boranes, in which the lactone framework is formed and fully functionalised in the C-3 position in one single step (Scheme 3.3). Parts of the following results are published in *Angew. Chem. Int. Ed.* **2019**, *58*, 7861–7865.

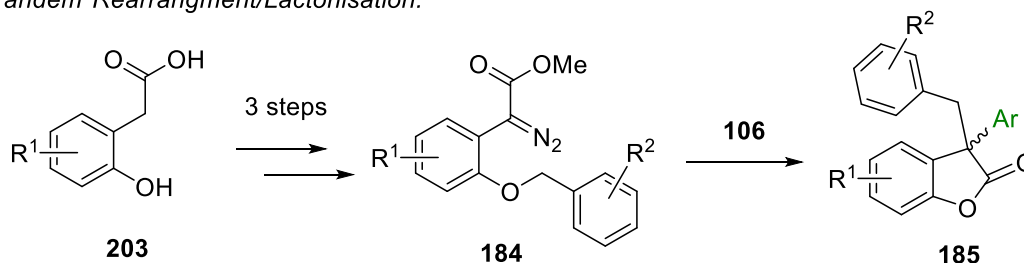
3.2 Results and Discussion

In this work, the ability of the different Lewis acids **106a–e**^a to undergo α -ester functionalisation was investigated (Scheme 3.8). A library of α -diazocarbonyl esters **107** and **179** was synthesised from ethyl acetoacetate **201** or from the corresponding carboxylic acids **202** over two steps. Moreover, α -diazo esters **184**, synthesised from 2-hydroxy phenylacetic acids **203** over three steps, were used to develop a synthesis towards asymmetric 3,3-disubstituted benzofuran-2(3*H*)-ones **185**. The relative Lewis acidity of triarylboranes **106a–e** was determined by the Gutmann-Beckett method²⁷ by Dr. Soltani and Darren M. C. Ould (Cardiff University). The Gutmann-Beckett method is an experimental method that measure the ³¹P chemical shifts of the Lewis adduct formed between a Lewis acid and triethylphosphine (Et₃PO). The difference in ³¹P chemical shifts between the adduct and the free probe is directly related to the strength of the Lewis acid and it is indicated by an Acceptor Number (AN).²⁸

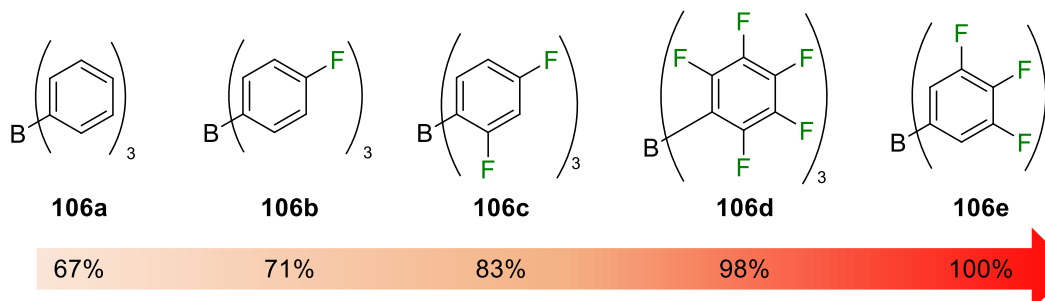
α -Aryl functionalisation of esters:



Tandem Rearrangement/Lactonisation:



Relative Lewis acidity:



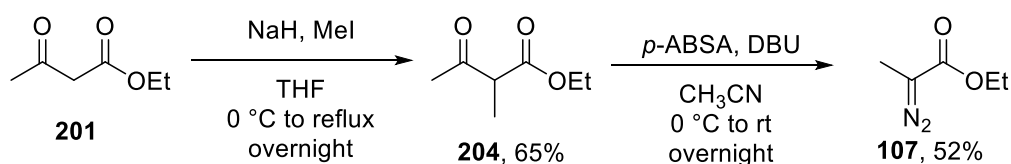
Scheme 3.8: Relative Lewis acidity scale for **106a–e**^b and an overview of the synthetic pathways developed for the metal-free α -aryl functionalisation of esters and benzofuranones **185** synthesis.

a. Except **106a**, which is commercially available, the synthesis of **106b–e** was carried out by Dr. Y. Soltani, D. M. C. Ould, Dr. J. Wenz and J. L. Carden.

b. The relative Lewis acidity was measured by Dr. Y. Soltani and D. M. C. Ould.

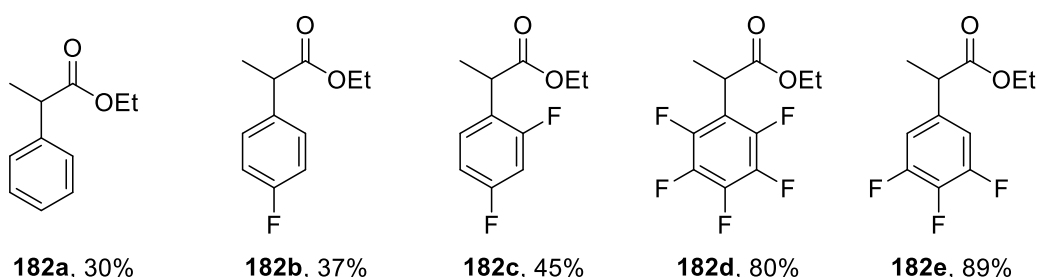
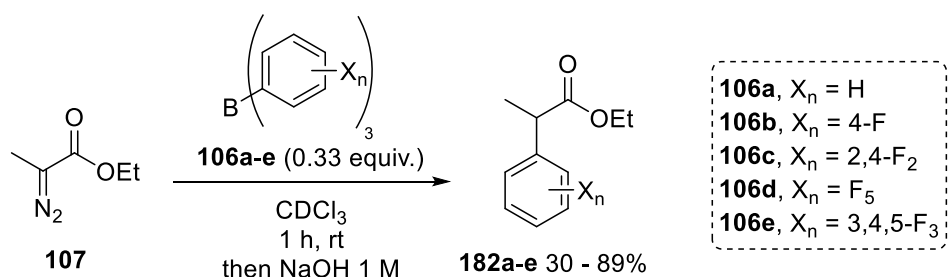
3.2.1 α -Functionalisation of Esters

Initially, the model substrate ethyl 2-diazopropanoate (**107**) was prepared to investigate the reactivity of boranes **106a–e** towards the 1,2-aryl transfer into diazo compounds reaction (Chapter 1.1.2.2, Scheme 1.26). The synthesis started with the α -methylation of ethyl acetoacetate (**201**) in the presence of methyl iodide and sodium hydride, to afford **204** in 65% yield (Scheme 3.9). Ethyl 2-diazopropanoate (**107**) was then obtained in 52% yield *via* Regitz diazo-transfer,²⁹ by treating **204** with *p*-acetamidobenzenesulfonyl azide (*p*-ABSA, **18e**) and DBU in acetonitrile.



Scheme 3.9: Preparation of ethyl 2-diazopropanoate (**107**).

Treatment of **107** with boranes **106a–e** in a 3:1 ratio, followed by aqueous basic work-up (1 M aqueous solution of NaOH) afforded ethyl 2-arylpropanoates **182a–e** in poor to very good yields (30–89%; Scheme 3.10).

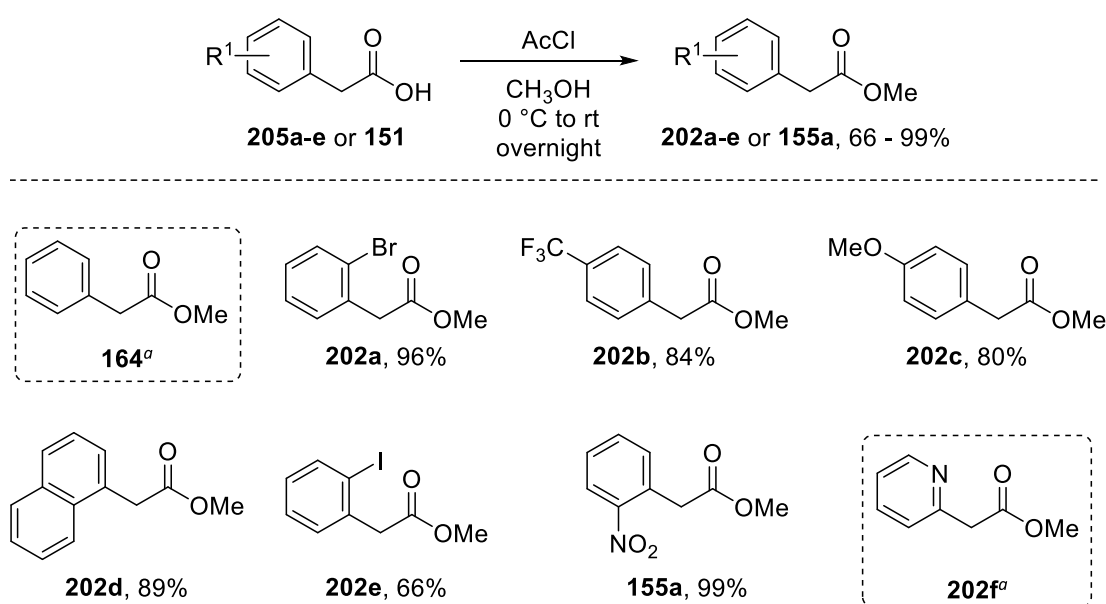


Scheme 3.10: Screening of boranes **106a–e** in the 1,2-aryl transfer reaction on the model substrate **107**. The reaction was performed on a 0.1 mmol scale using 0.33 mol% of boranes **106a–e**.

The yields of the 1,2-aryl migration reaction, in the presence of triarylboranes **106a–e**, increased with the Lewis acidity of **106a–e** (see Scheme 3.8). When the least Lewis acidic triphenylborane (**106a**) was used, **182a** was obtained in 30% yield. The more Lewis acidic fluorinated boranes **106b** and **106c** were found to be slightly more reactive

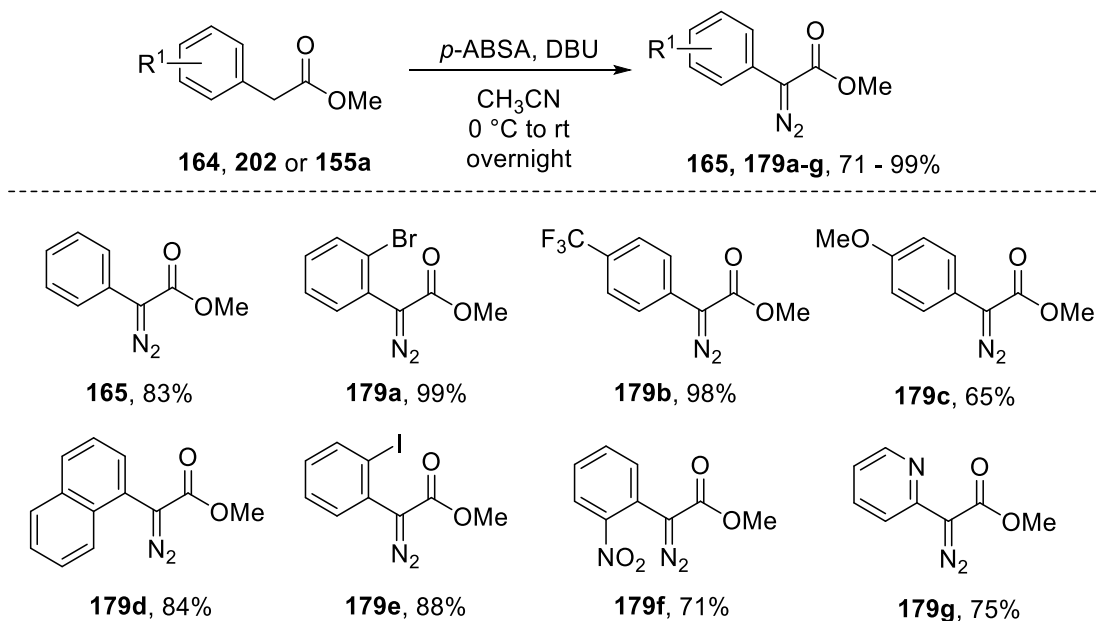
affording **182b** and **182c** in 37% and 45% yield, respectively. The more Lewis acidic $B(C_6F_5)_3$ (**106d**) or 3,4,5-fluorinated borane **106e**, on the other hand, led to good yields in product formation with **182d** and **182e** isolated in 80% and 89%, respectively. The higher reactivity of **106d–e** was clearly visible, as the characteristic bright yellow colour of the substrate solution turned colourless within 10 minutes from the borane addition, suggesting a full consumption of the diazo starting material. Moreover, a gas evolution was observed as soon as the borane reagent was added which lasted about 60 minutes, indicating the formation of nitrogen. To better follow the reaction progresses, the reactions were conducted in sealed Young NMR tubes under nitrogen atmosphere in $CDCl_3$. In the case of reactions performed using **106e**, the reaction mixtures were easily followed by *in situ* 1H NMR, showing full consumption of the starting material **107** after 60 minutes. On the other hand, when $B(C_6F_5)_3$ (**106d**) was used, both 1H and ^{19}F NMR spectra were too complex to be interpreted. Nevertheless, the yields showed that highly Lewis acidic boranes such as **106e** and **106d** were able to transfer more than two aryl groups, in agreement with what has been reported previously.³⁰ For this reason, they were preferred for further studied over less Lewis acidic boranes such as triphenylborane (**106a**) which is typically used in excess.³¹

To further investigate the reactivity of boranes **106** in the α -arylation of diazocarbonyl compounds, more sterically demanding α -aryl- α -diazo acetates **179** were prepared from the corresponding carboxylic acids over two steps. Apart from the commercially available methyl esters **164** and **205f**, the other methyl esters **205a–e** and **155a** were prepared from the corresponding carboxylic acids **202a–e** and **151** in moderate to excellent yields using acetyl chloride in methanol (Scheme 3.11).



Scheme 3.11: Preparation of ester precursors; ^aCommercially available.

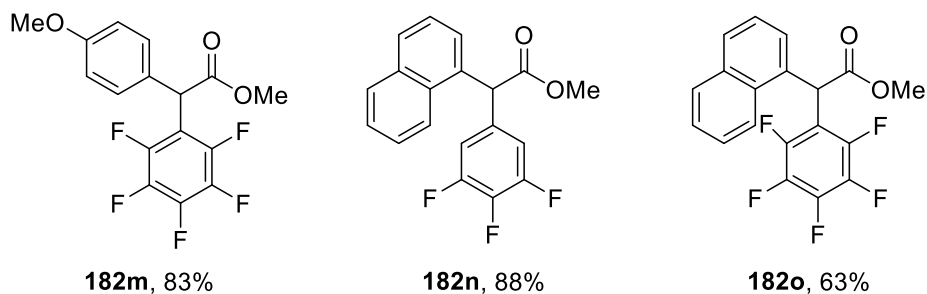
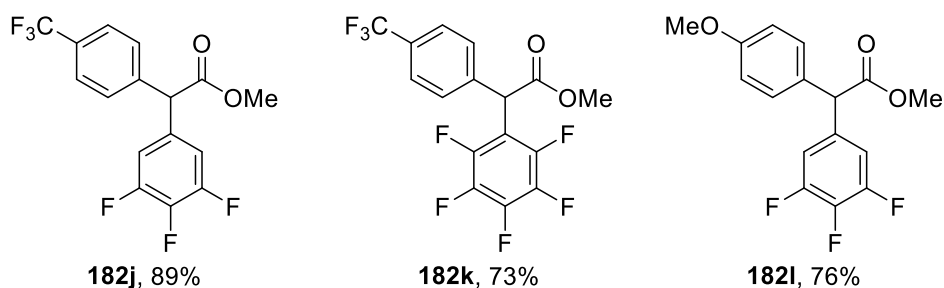
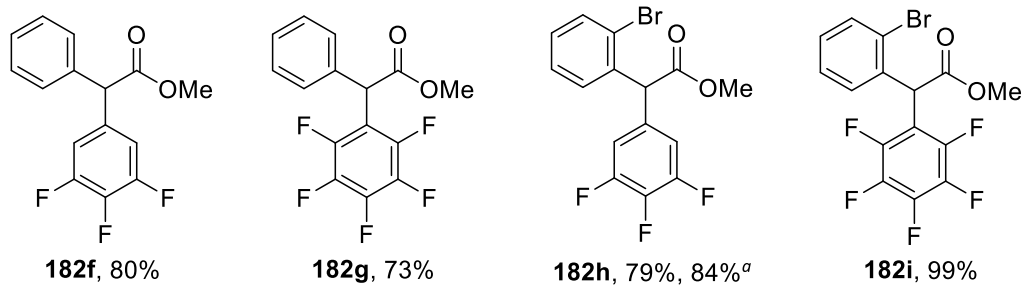
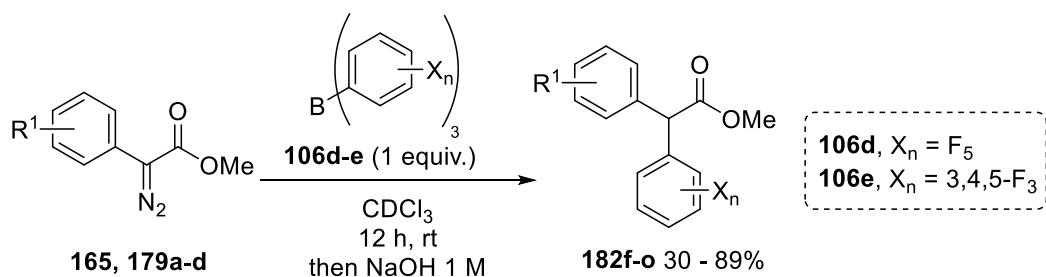
The precursors were then treated with *p*-ABSA and DBU in acetonitrile to afford the desired diazo substrates **165** and **179a–g** in very high yields (71–99%; Scheme 3.12).



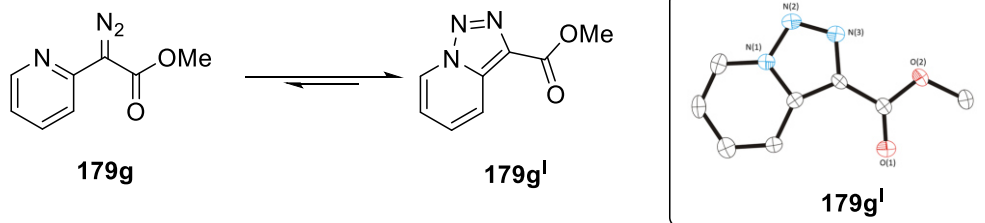
Scheme 3.12: Preparation of the diazo precursors **165**, **179a–g**.

Less Lewis acidic boranes **106a–c** did not show reactivity with α -aryl- α -diazo esters **165** and **179a** even at 50 °C,^c whereas boranes **106d** and **106e** afforded the pharmaceutically useful¹³ α,α -diaryl esters **182f–o** in moderate to excellent yields after 12 hours at room temperature (Scheme 3.13). In this case, the boron reagents **106d–e** were found to transfer only one aryl group to the α -aryl- α -diazo esters **165** and **179a–d** after 12 hours at room temperature instead of all three as observed for **107** (see Scheme 3.10). However, when the 3,4,5-fluorinated borane **106e** reacted with methyl phenyldiazoacetate (**165**) in a 1:3 ratio at 50 °C, more aryl groups were transferred from **106e** to **165**, affording **182f** in 79% yield after 7 days. Some limitations were encountered with the diazo compounds **179e–g** that did not show any reaction with boranes **106d–e**. While the low reactivity of **179e** and **179f** remains unclear, the absence of reactivity of the pyridine derivative **179g**, is probably due to the equilibrium between **179g** and its isomer 3-triazolopyridine (**179g^l**), which is shifted towards the latter (Scheme 3.14).

c. The reaction between **106a–c** and diazo compounds **165** and **179a** were performed by Dr. J. Wanz.



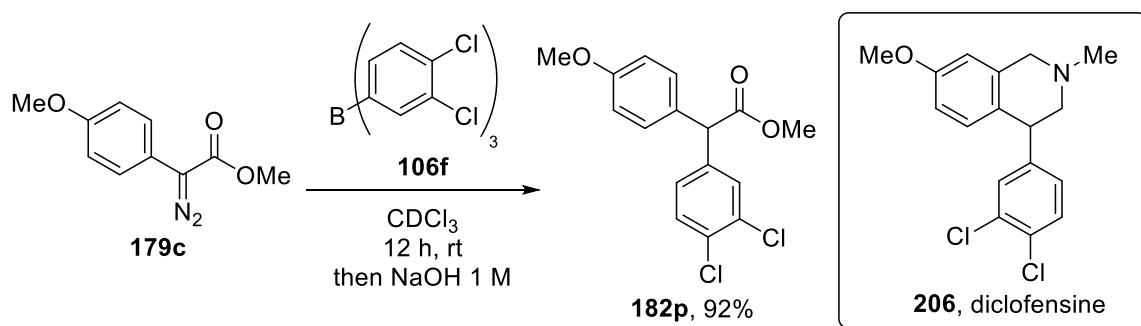
Scheme 3.13: Substrate scope of α -diarylester **182f-o**. Reactions performed on a 0.1 mmol scale using a 1:1 ratio of diazo compounds **165**, **179a-d** and boranes **106d-e**. ^aReaction performed on a 0.5 mmol scale.



Scheme 3.14: Equilibrium between the diazo compound **179g** and the triazole **179g'** and crystal structure for **179g'**.^d

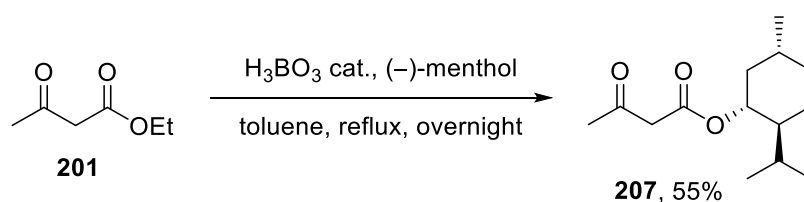
d. Crystallisation, characterisation and analysis for triazole **179g'** was performed by D. C. M. Ould.

This metal-free 1,2-aryl migration was then applied to the synthesis of **182p**, a valuable intermediate for the synthesis of diclofensine **206** (Scheme 3.15). Diclofensine (**206**) is an antidepressant drug bearing a tetrahydroisoquinoline scaffold which can be synthesised from **182p**, typically obtained by rhodium-catalysed α -functionalisation of esters.^{14b} For this reason, the 3,4-chlorinated borane **106f** was prepared^e and it was found to have a relatively high Lewis acidity (98%, acceptor number $AN = 78.06$), similar to 3,4,5-fluorinated borane (**106e**, $AN = 79.57$) and $B(C_6F_5)_3$ (**106d**, $AN = 77.49$). As expected, the reaction of **106f** with **179c** led to the precursor **182p** isolated in 92% yield after 12 hours (Scheme 3.15).



Scheme 3.15: Synthesis of **182p**, a synthetic intermediate for diclofensine **206**.

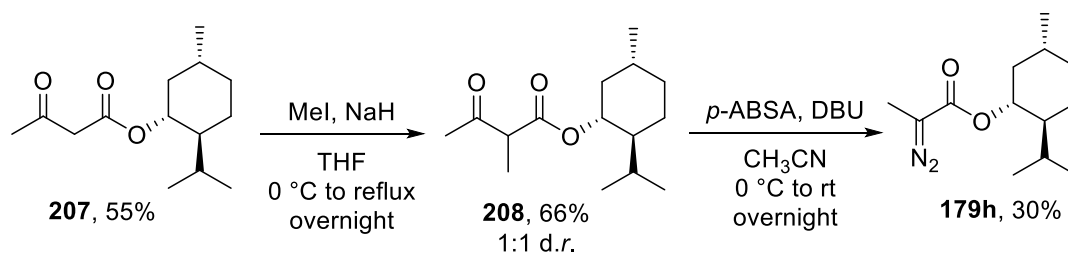
The attention was then moved to the synthesis of chiral diazo precursors **179h-j**, bearing a (-)-menthyl substituent as a chiral auxiliary, with the intention to influence the stereoselectivity of the 1,2-aryl transfer reaction.³² The (-)-menthyl group in **179h** was installed by transesterification of ethyl acetoacetate (**201**) using boronic acid as a catalyst (Scheme 3.16).³³



Scheme 3.16: Transesterification of acetoacetate **201** to the chiral **207**.

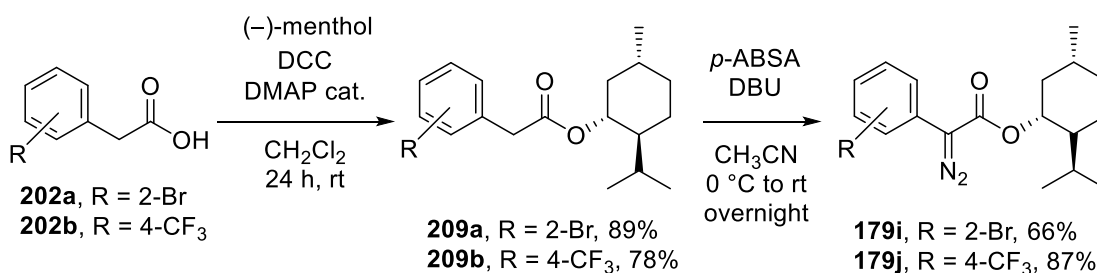
The (-)-menthyl acetoacetate (**207**) was isolated in 55% yield and treated with sodium hydride and methyl iodide in THF overnight. The obtained α -methylated precursor **208** was then used for the Regitz diazo-transfer reaction (see Chapter 1, pg. 6)²⁹ to afford the chiral diazo derivative **179h** in 30% yield (Scheme 3.17).

e. Synthesis, characterisation and Lewis acidity measurements for **106f** were performed by Dr. Y. Soltani.



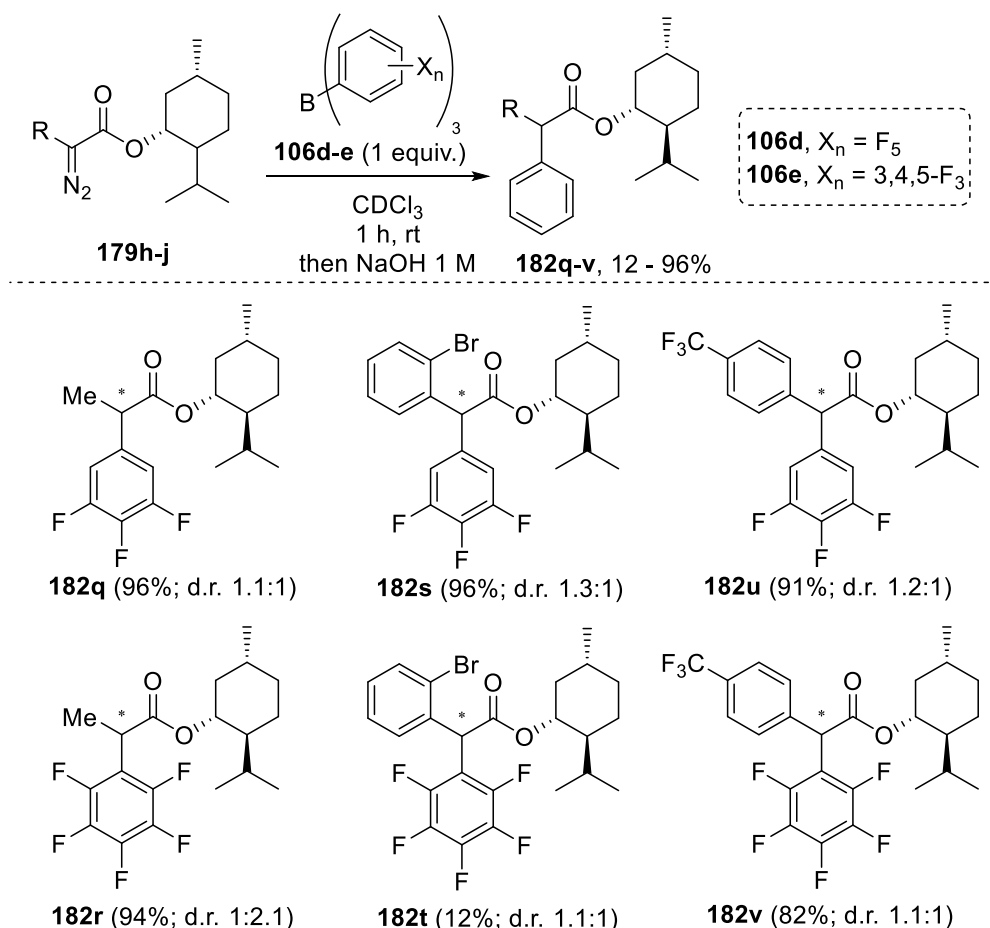
Scheme 3.17: Synthesis of chiral diazo precursor **179h**.

To synthesise the chiral α -aryl- α -diazo esters **179i** and **179j**, the corresponding carboxylic acids **202a** and **202b** were used in a Steglich esterification³⁴ in the presence of *N,N'*-dicyclohexylcarbodiimide (DCC), (-)-menthol and 4-(dimethylamino) pyridine (DMAP), to give the (-)-menthyl derivatives **209a** and **209b** in 89% and 78% yield, respectively (Scheme 3.18). The chiral derivatives **209a** and **209b** were then used in the subsequent Regitz diazo-transfer reaction²⁹ which afforded the desired chiral diazo precursor **179i** and **179j** in 66% and 87% yield, respectively.



Scheme 3.18: Synthesis of chiral diazo precursors **179i** and **179j**.

Although high yields of the α -arylated products **182q–u** (76–94%) were obtained, the observed diastereomeric ratios were extremely low (up to 1.3:1 *d.r.*; Scheme 1.19). The best result was obtained from the reaction of 2-bromo diazo derivative **179i** and **106e** which afforded **182s** in 96% yield with a 1.3:1 diastereomeric ratio. On the contrary, the reaction of **179i** and $\text{B}(\text{C}_6\text{F}_5)_3$ (**106d**) afforded a complex mixture and the desired α -diaryl ester **182t** was isolated in only 12% yield as a couple of diastereoisomers in a 1.1:1 ratio. Given the unencouraging results on inducing chirality by installing a (-)-menthyl group as a chiral auxiliary, the stereoselective α -functionalisation of menthyl esters was not further investigated.



Scheme 3.19: Stereoselective α -arylation of chiral **179h-j** using **106d-e** on a 0.1 mmol scale.

For further mechanistic insights, the reactions of 3,4,5-fluorinated borane **106e** with diazo compounds were monitored by *in situ* NMR spectroscopy. In these cases, the ^1H and ^{19}F NMR spectra showed that the diazo compounds **179** were fully converted into the corresponding boron enolates **183** as a mixture of *E/Z* isomers. After 30 minutes at room temperature, the reaction of **165** with one equivalent of **106e** in CDCl_3 showed, by ^1H NMR analysis, two sets of peaks for the methyl group in a 3:1 ratio (Figure 3.2). Similarly, the ^{19}F NMR spectrum revealed two sets of fluorine peaks, which were also found in a 3:1 ratio. In addition, a broadened ^{11}B -signal was observed at 45 ppm which supported the formation of a three-coordinated borane.³⁵ The data suggested the formation of boron enolate **183a** as a 3:1 ratio of *E/Z*-isomers, according to literature.³⁰ Similar results were also observed for the reactions of **179a**, **179b**, **179d** and **179h-j** with **106e**, which all showed the formation of two isomers (Table 3.1). When achiral methyl esters **179a**, **179b** and **179d** were used as starting materials, the isomeric ratio was influenced by the steric hindrance in the *ortho*-position (entries 1–4). In particular, the 2-bromo phenyl derivative boron enolate **183b** and the naphthyl derivative **183d** were formed in a 6:1 and 3.5:1 isomeric ratio, respectively (entries 2 and 4) while the

4-trifluoromethyl boron enolate **183c** was formed as a 1.5:1 mixture of isomers (entry 3). Similarly, for the (-)-methyl derivatives **183e–g** (entries 5–7), the highest ratio (4:1) was registered for the most sterically hindered 2-bromoaryl substituted boron enolate **183f**.

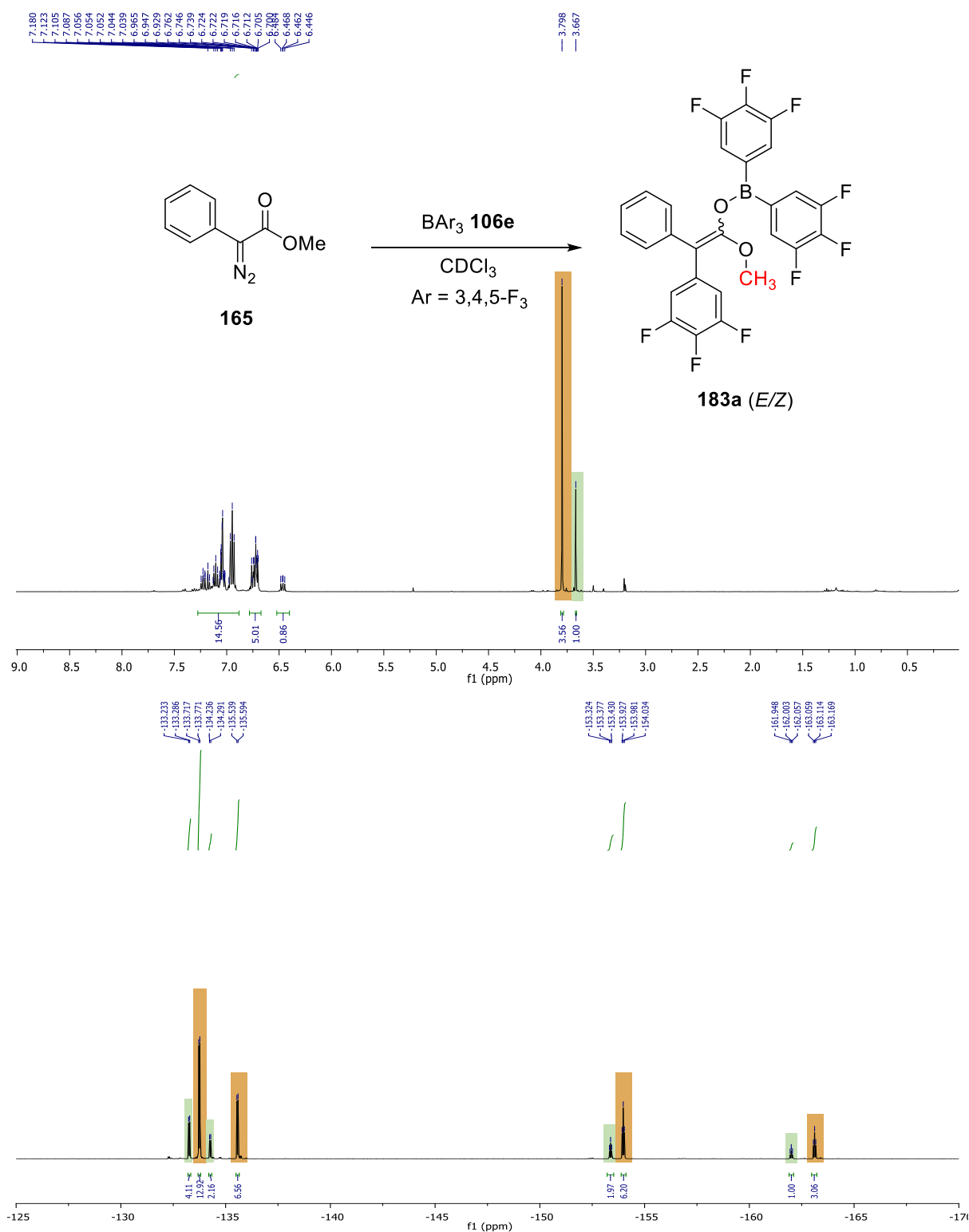
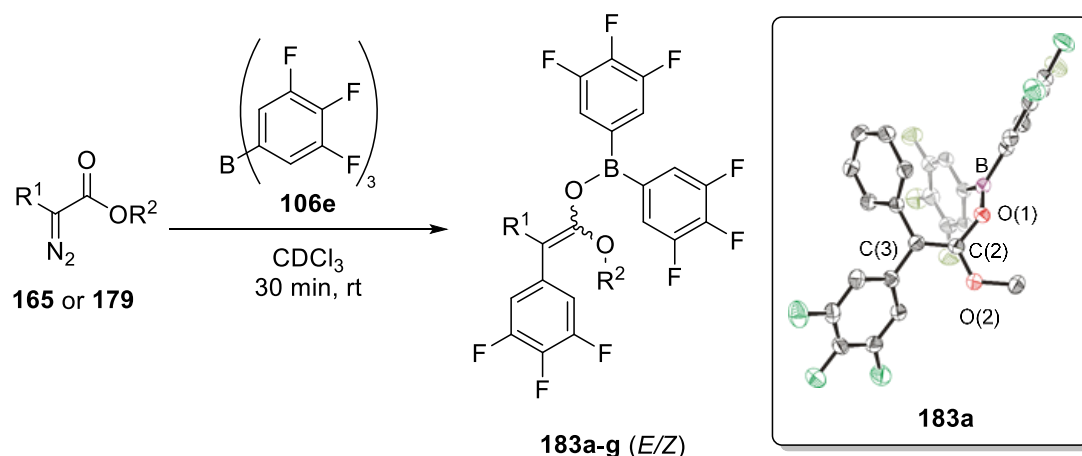


Figure 3.2: *In situ* ^1H (top) and ^{19}F NMR (bottom) spectrum of boro enolates (E/Z)-**183a**. The spectra show the presence of E/Z isomers as 3:1 mixture. (Major isomer = orange; Minor isomer = green).

Table 3.1: Isomer ratio for boron enolates (*E/Z*)-**183a–g** measured by ¹H NMR spectroscopy and crystal structure of boron enolate **183a**.^f

Entry	Starting Material	R ¹	R ²	183	Ratio ^a
1	165	C ₆ H ₅	Me	a	3:1
2	179a	2-BrC ₆ H ₄	Me	b	6:1
3	179b	4-(CF ₃)C ₆ H ₄	Me	c	1.5:1
4	179d	naphthyl	Me	d	3.5:1
5	179h	Me	(-)-menthyl	e	1.2:1
6	179i	2-BrC ₆ H ₄	(-)-menthyl	f	4:1
7	179j	4-(CF ₃)C ₆ H ₄	(-)-menthyl	g	1.5:1

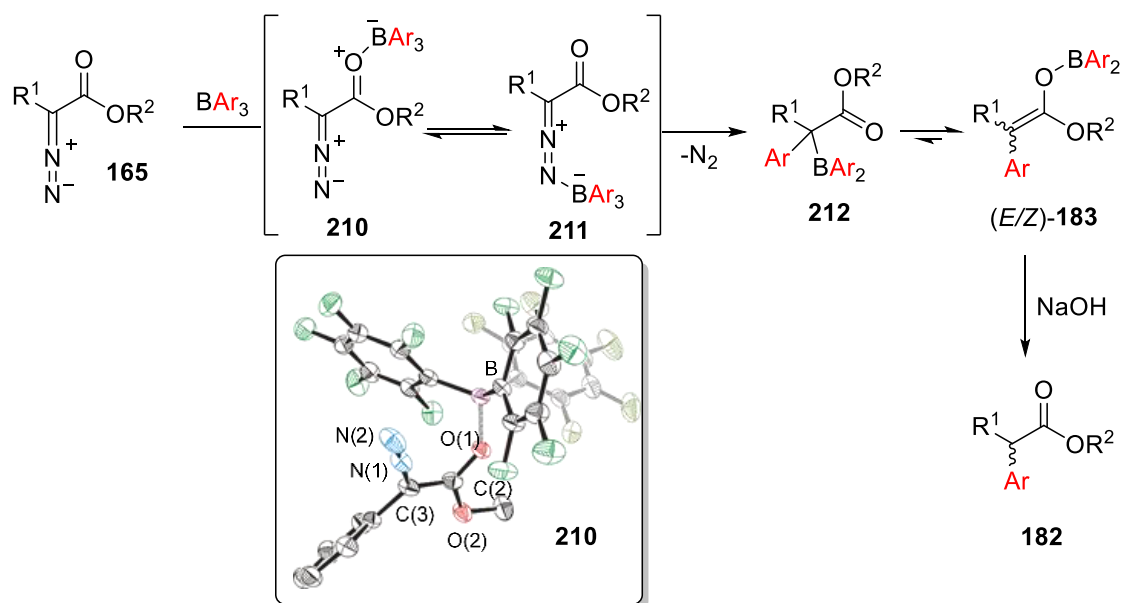
General Procedure: Reactions performed on 0.1 mmol scale in CDCl₃ under nitrogen atmosphere and monitored by ¹H and ¹⁹F NMR spectroscopy; ^aOnly the *E/Z* configuration of **183a** was assigned according to literature.

When B(C₆F₅)₃ (**106d**) was used, the NMR spectra were not clear enough to identify the *E/Z* ratio, however, regardless of the isomer for the enolate intermediate, product **182** were still formed in good yields after one hour upon basic work-up.

The (*E*)-boron enolate **183a**, derived from phenyl diazo acetate (**165**) and **106e**, could be crystallised and structurally characterised,^f providing further insight into the mechanism. Moreover, when **165** reacted with B(C₆F₅)₃ (**106d**) at -40 °C, the lower reactivity led to isolation of the adduct **210** as a colourless crystalline solid^e (Scheme 3.20). It has been recently reported by Tang *et al.* that **106d** bonds oxygen faster than the carbon attached to the diazo moiety.³⁶ For this reason, the first step is assumed to be the coordination of the triarylborane to the carbonyl group as shown by the isolation of **210**. The latter could be in equilibrium with the intermediate **211** in which the boron atom coordinates to the terminal nitrogen atom of the diazo moiety. Subsequently, upon nitrogen gas expulsion, the adduct intermediate undergoes a

f. Crystallisation, characterisation and analysis for compounds **183a** and **210** were performed by D. C. M. Ould.

1,2-aryl transfer reaction leading to the intermediate **212**, which is in tautomeric equilibrium with its enolate form **183**, as proposed in the literature.^{12b,37} In the final step, the boron enolate **183** is hydrolysed to the final product **182** during the basic work-up.

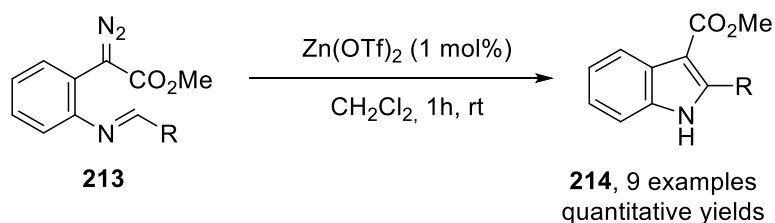


Scheme 3.20: Proposed mechanism for the 1,2-aryl transfer reaction.

Subsequently, attention was focussed on the development of a novel metal-free cyclisation mediated by Lewis acids.

3.2.2 Synthesis of α,α -Disubstituted Benzofuranones

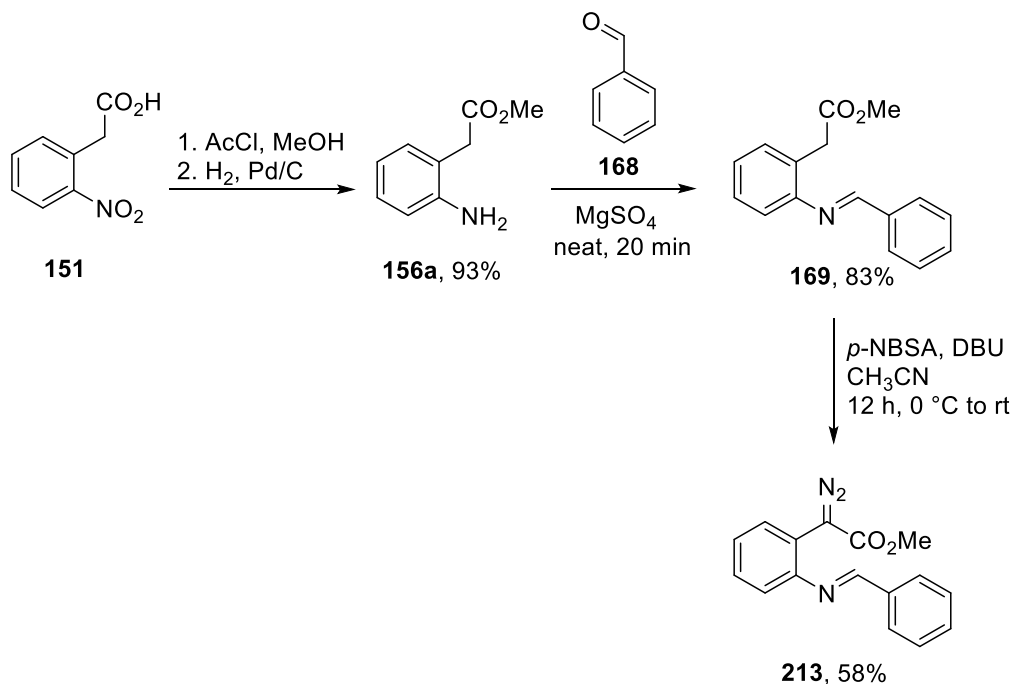
As mentioned in the previous chapters, diazo carbonyl and aryl diazocarbonyl compounds have been widely used in several cyclisation reactions such as cyclopropanations³⁸ and intramolecular C–H insertions,³⁹ especially under catalytic conditions. In 2009, Doyle and Zhou reported the Lewis acid catalysed indole synthesis from *ortho*-imino phenyl diazo acetate **213** (Scheme 3.21).⁴⁰



Scheme 3.21: Lewis acid-catalysed synthesis of indole **214**.⁴⁰

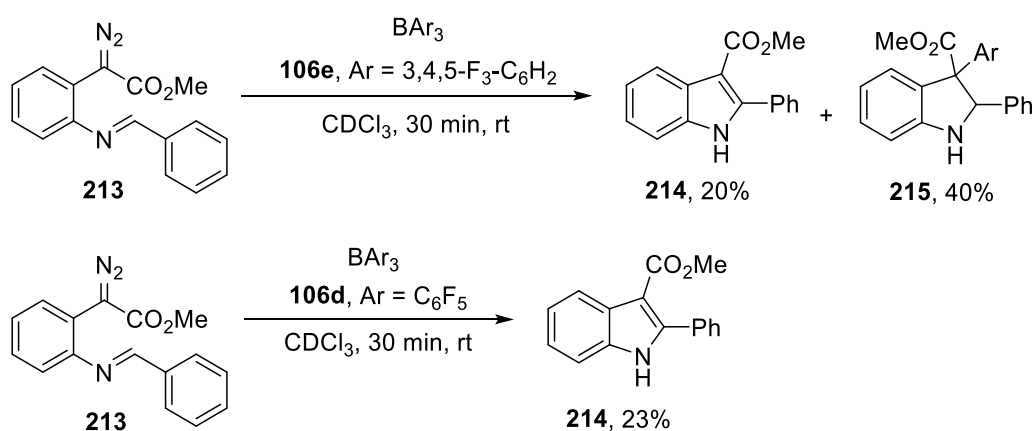
With the aim of investigating the reactivity of the fluorinated boranes **106d** and **106e** in a similar intramolecular cyclisation, the *ortho*-imine derivative **213** was synthesised from 2-nitrophenylacetic acid (**151**; Scheme 3.22). The carboxylic acid **151** was converted

quantitatively into the corresponding methyl ester using acetyl chloride in methanol. The obtained product was directly reduced in methanol using Pd/C and hydrogen gas to afford methyl 2-aminophenylacetate (**156a**) in 93% yield over the two steps. The imine **169** was then obtained by reacting **156a** with benzaldehyde **168**. The desired diazo precursor **213** was prepared in 58% yield *via* Regitz diazo-transfer²⁹ using *p*-NBSA as diazo-transfer reagent.



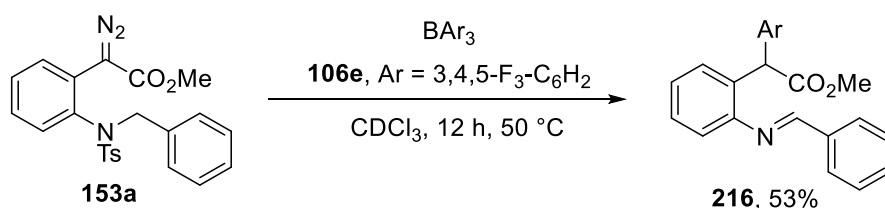
Scheme 3.22: Synthesis of the diazo precursor **213**.

In the presence of 3,4,5-fluorinated arylborane **106e** and pentafluorinated arylborane **106d** ($B(C_6F_5)_3$), the *ortho*-imino diazo compound **213** formed the indole derivative **214** in low yields (up to 23%; Scheme 3.23). Interestingly, when **106e** was used, the indoline derivative **215** was isolated as the major product in 40% yield.



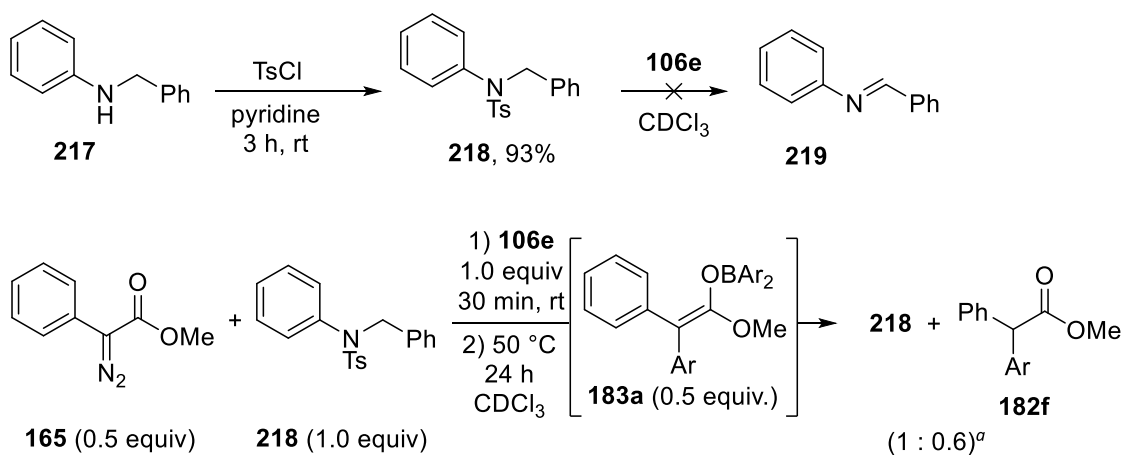
Scheme 3.23: Synthesis of indole **214** and indoline **215** using **213** and boranes **106d–e**.

The same reaction was investigated using **153a**, synthesised as described in chapter 2. At room temperature, no reaction was observed, while the α -aryl ester **216** was isolated in 53% yield after 12 hours at 50 °C (Scheme 3.24).



Scheme 3.24: Reaction between diazo compound **153a** and borane **106e**.

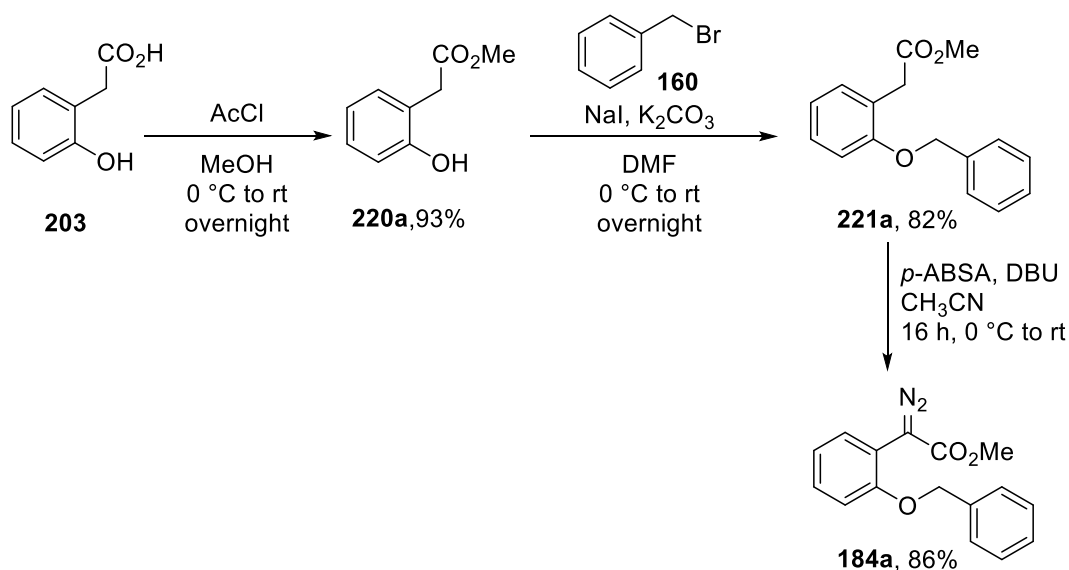
With the aim to understand and explain the formation of the detosylated product **216**, some more experiments were performed. In particular, the *N*-tosyl-*N*-benzylphenyl amine (**218**) was prepared from *N*-benzylphenyl amine (**217**), but when **218** was mixed with **106e** no detosylated product **219** was observed at room temperature, nor at 50 °C, and **218** was completely recovered (Scheme 3.25). Suspecting an involvement of the boron enolate **183a** in the detosylation reaction, 0.5 equivalents of **165** was added to a solution of borane **106e** and **218** in CDCl₃ to form **183a**. After 30 minutes at room temperature, the mixture was heated up to 50 °C for 24 hours, nevertheless, only the α -aryl ester **182f** was formed while **218** did not react. The mechanism for the detosylation and the formation of **216** formation remains unclear.



Scheme 3.25: Reactions performed to explain the formation of the detosylated product **216**; ^aNMR ratio.

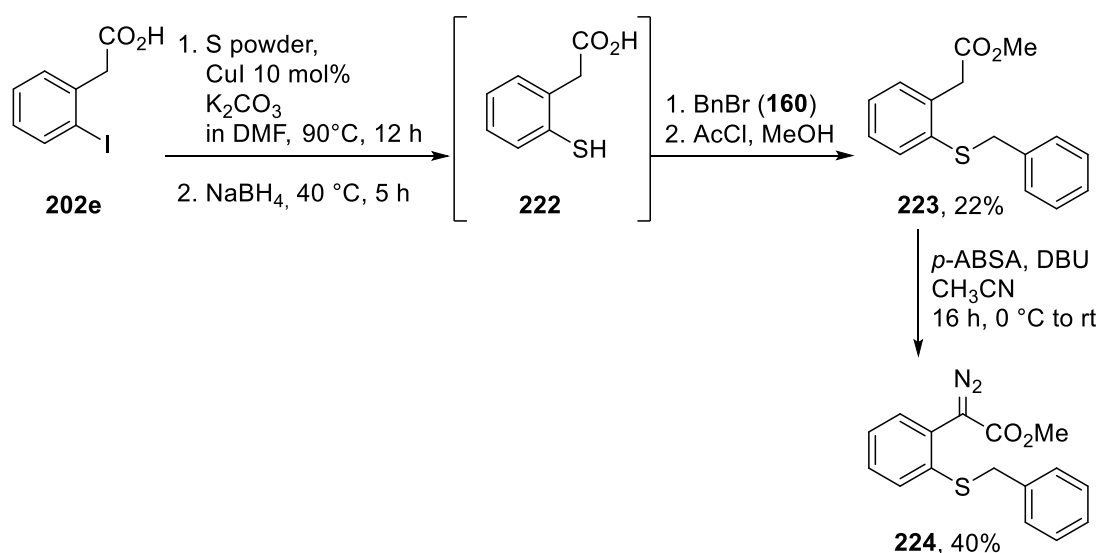
In the same context, *ortho*-substituted diazo ether **184a** and thioether **224** were prepared to investigate the borane-mediated intramolecular cyclisation further (Scheme 3.26). The oxygen-substituted diazo precursor **184a** was synthesised starting from 2-hydroxyphenylacetic acid (**203**) in three steps with 66% overall yield (Scheme 3.26). Firstly, the carboxylic acid **203** was converted quantitatively to the corresponding methyl

ester using acetyl chloride in methanol. The phenolic moiety of ester **220** was benzylated to afford ether **221a** in 82% yield. Finally, the diazo compound **184a** was obtained in 86% yield using *p*-ABSA as the diazo-transfer reagent and DBU as base in acetonitrile.



Scheme 3.26: Synthesis of the diazo precursor **184a**.

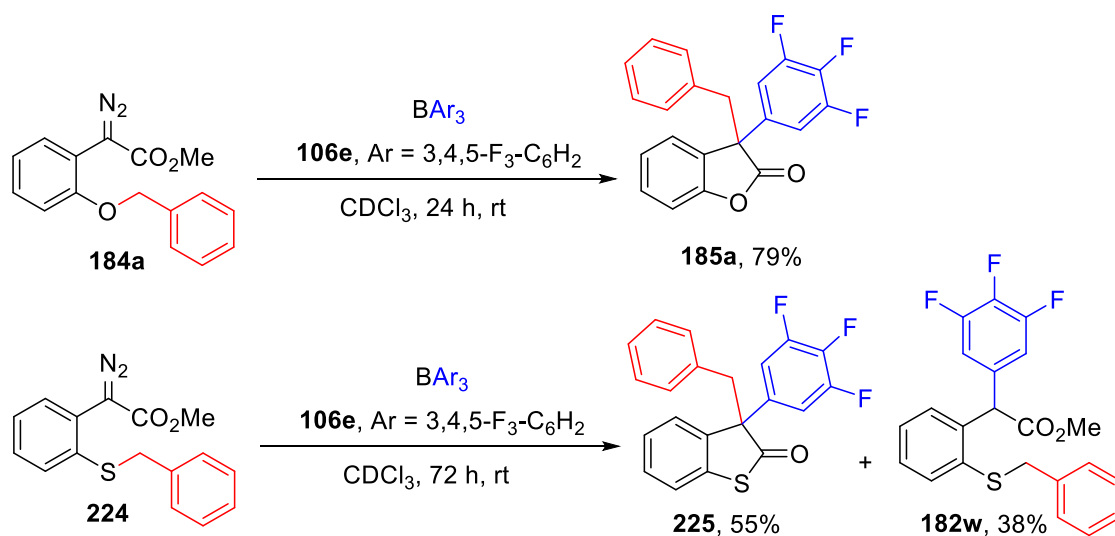
On the other hand, the sulfur analogue **224** was obtained starting from 2-iodophenylacetic acid (**202e**; Scheme 3.27).⁴¹ Treatment of the *in situ* generated thiol **222** with benzyl bromide (**160**) followed by esterification using acetyl chloride in methanol afforded the desired thioether methyl acetate **223** in 22% overall yield. The final diazo precursor **224** was obtained in 40% yield by classic Regitz diazo-transfer reaction.²⁹



Scheme 3.27: Synthesis of the diazo precursor **224**.

Interestingly, the reaction of the diazo derivative **184a** with tris(3,4,5-trifluorophenyl)borane **106e** lead to the formation of the rearranged lactone **185a** in 79% yield in

24 hours. Analogously, the rearranged thiolactone **225** was also isolated in 55% along with the α -aryl ester **182w** (38%) from the reaction of **224** with **106e** after 3 days at room temperature (Scheme 2.28).

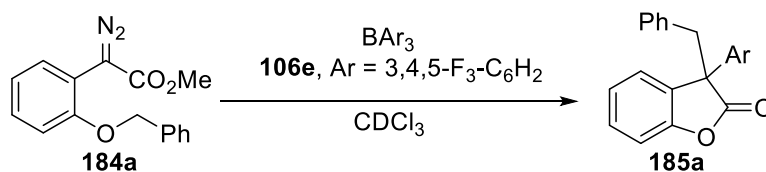


Scheme 3.28: Reaction of diazo compounds **184a** and **224** with borane **106e**.

The formation of the above rearranged products **185a** and **225**, as shown later in this chapter, is the result of a cascade reaction which starts with a 1,2-aryl transfer, followed by an aryl migration and a final lactonisation.

3.2.2.1 Benzofuranones Substrate Scope

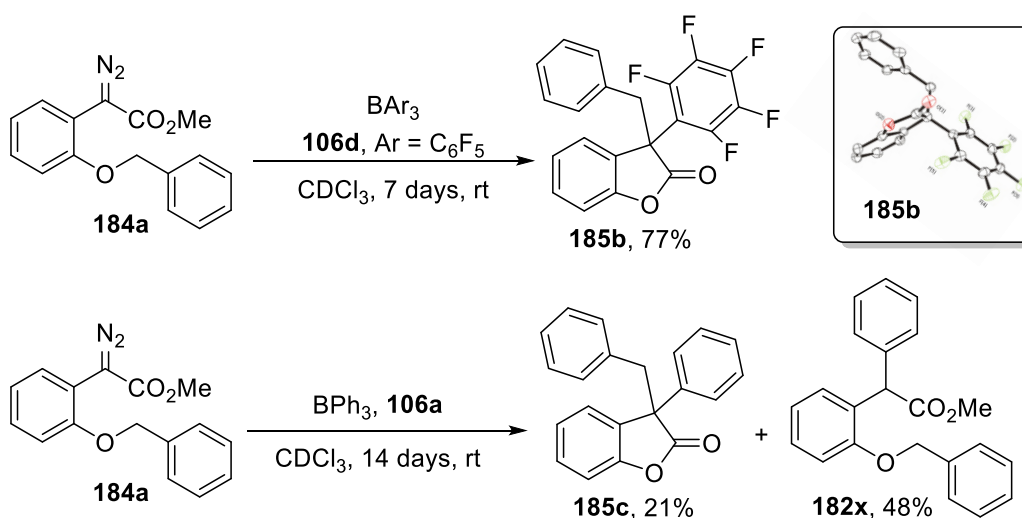
The oxygen-substituted diazo compound **184a** and the 3,4,5-fluorinated borane **106e** were chosen as model substrates for further studies (Table 3.2). Firstly, different equivalents of diazo starting material **184a** were screened while always using one equivalent of borane **106e**. A much slower reaction was observed by 1H NMR analysis when a 2:1 ratio of **184a** and **106e** was used, with lactone **185a** afforded in 45% and 63% after 24 hours or 7 days, respectively (entry 2–3). Increasing the temperature to 45 °C, did not increase the rate of lactone **185a** formation, which was formed in only 55% after 24 hours (entry 4).

Table 3.2: Screening conditions for benzofuranone **185a** formation.

Entry	184a (equiv.)	Temperature	Time	185a (%)
1	1	rt	24 h	72–79 ^a
2	2	rt	24 h	45
3	2	rt	7 d	63
4	2	45 °C	24 h	55

General Procedure: Reactions performed on a 0.1 mmol scale of **106e** in CDCl_3 under nitrogen atmosphere and followed by ^1H , ^{11}B and ^{19}F NMR spectroscopy; ^aRange of yields over six reactions.

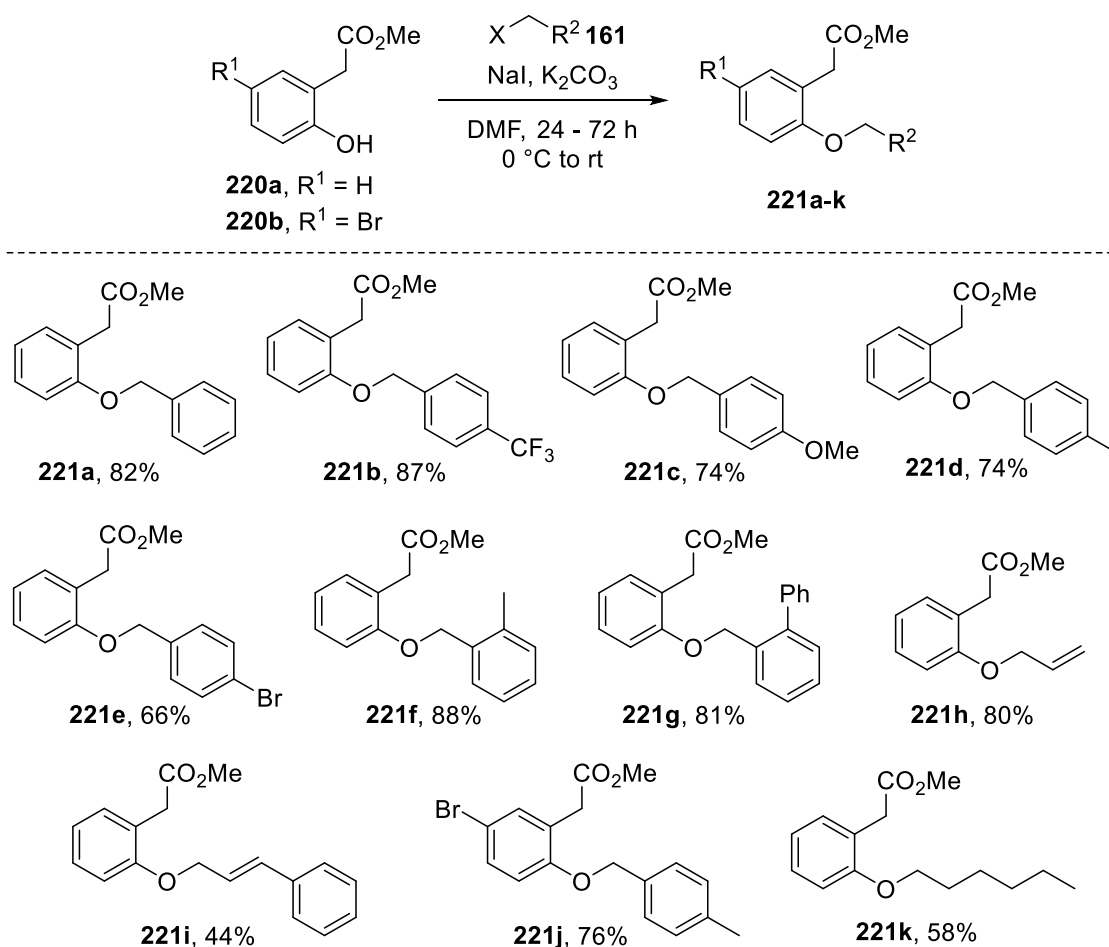
The influence of the Lewis acidity on the rearrangement/cyclisation cascade was investigated next. The model substrate **184a** was reacted with $\text{B}(\text{C}_6\text{F}_5)_3$ (**106d**) and the least Lewis acidic triphenyl borane (**106a**), and the reactions were followed by ^1H and ^{19}F NMR spectroscopy (Scheme 3.29). In the presence of $\text{B}(\text{C}_6\text{F}_5)_3$ (**106d**), the starting material **184a** was fully consumed within five minutes, however, the lactone **185b** was detected only after 4 days by ^1H NMR spectroscopy and isolated in 77% yield after 7 days at room temperature.



Scheme 3.29: Screening of boranes **106a**, and **106d** with model diazo precursor **184a**. Crystal structure for lactone **185b**.^g

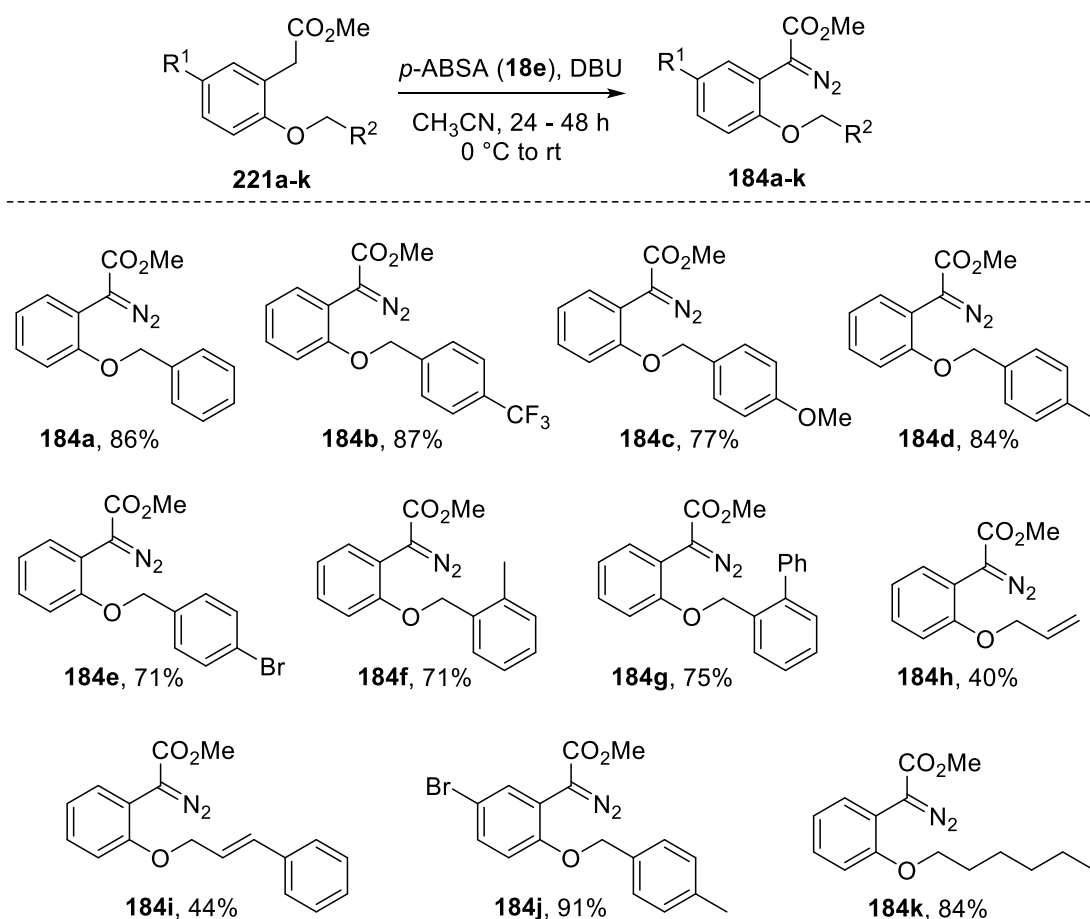
g. Crystallisation, characterisation and analysis for lactone **185b** were performed by D. C. M. Ould.

On the contrary, when the model substrate **184a** was reacted with triphenyl borane **106a**, the consumption of the starting material was slower and **184a** was still detectable after 12 hours by ^1H NMR spectroscopy. After 14 days at room temperature, the desired **185c** was isolated in 21% along with 48% yield of the corresponding α -phenyl ester **182x**. Subsequently, the influence of different substituents on the migratory aptitude was investigated. For this purpose, a library of starting materials was prepared by treating 2-hydroxyarylacetic acetates **220a–b** with sodium iodide and different aryl or alkyl halides **161** under basic reaction conditions, to afford the precursors **221a–k** in 58–88% yield within 1–3 days (Scheme 3.30). Generally, the hydroxy-functionalisation was well-tolerated by both EWG and EDG in *para*-position with **221b**, **221c**, **221d** and **221e** afforded in 87%, 74%, 74% and 66% yields, respectively. The presence of a bromo-substituent on the phenolic ring did not lower the reactivity of **220b**, which afforded **221j** in 76% yield. More sterically hindered *ortho*-substituted benzyl derivatives **221f** and **221g** were yielded also in very good yields (88% and 81%), as well as the allyl bromide, which afforded **221h** in 80% yield. On the contrary, the cinnamyl derivative **221i**, as well as the *n*-hexyl derivative **221k**, were isolated only in moderate yields (44–58%).



Scheme 3.30: Preparation of ether precursors **221a–k**.

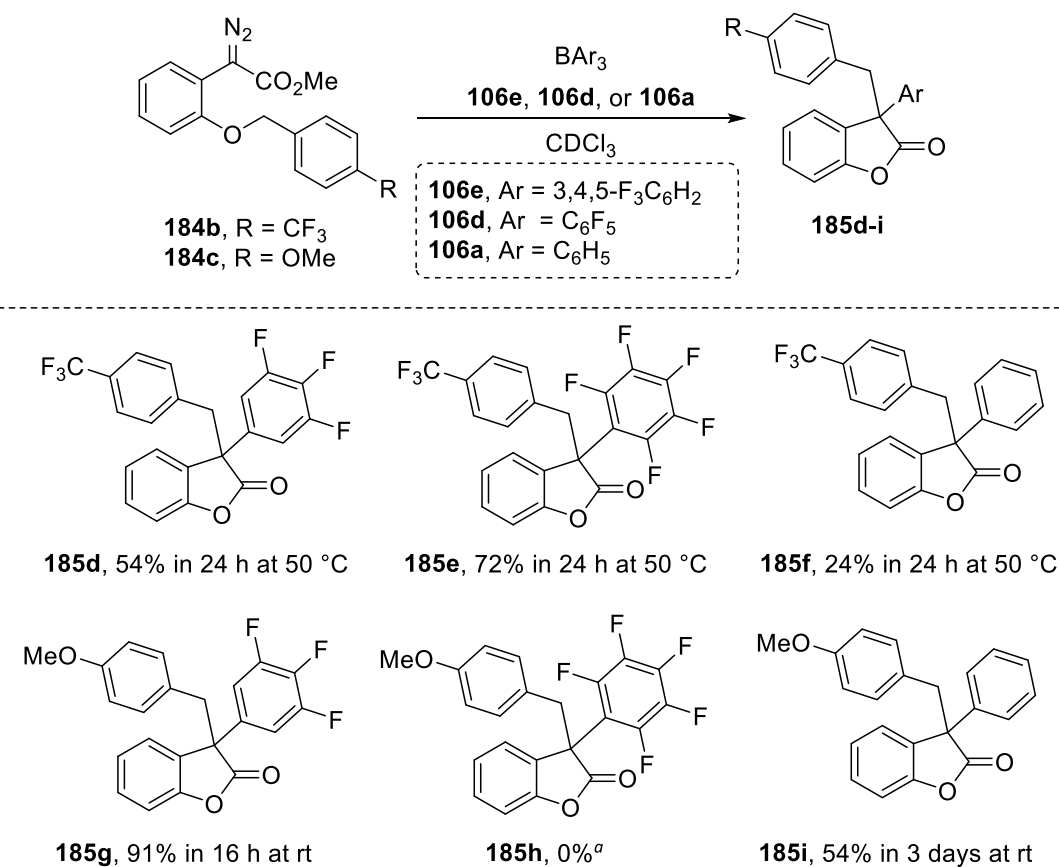
Subsequently, the precursors **221a–k** were reacted with *p*-ABSA and DBU in acetonitrile to obtain the desired diazo compounds **184a–k** in moderate to excellent yields (Scheme 3.31). Also in this case, all electron-donating substituents, as well as electron-withdrawing substituents, in *para*- and *meta*-positions showed good reactivity affording **184b–g** and **184j** in 71–91% yield. The allyl-substituted compound **184h** and the cinnamyl-derivative **184i** were formed only in moderate yields (40–44%), while the *n*-hexyl substrate **184k** was isolated in 84% yield.



Scheme 3.31: Preparation of diazo precursors **184a–k**.

The attention moved on studying the influence of different substituents in the migrating moiety in the rearrangement (Scheme 3.32). The reaction was also found to be strongly influenced by the electronic properties of the migrating group. In particular, when an electron-poor substituent was present on the migrating benzyl group, higher reaction temperatures (50 °C) were necessary in order to observe the formation of cyclised products **185d** and **185e** by ^1H NMR, which were then isolated in 54% and 72% yield, respectively, after 24 hours. On the other hand, the more electron-rich benzylic group was found to be faster in migrating, with the desired lactones **185g** and **185i** detected by ^1H NMR after a few hours at room temperature and isolated in 91% and 54% yield after

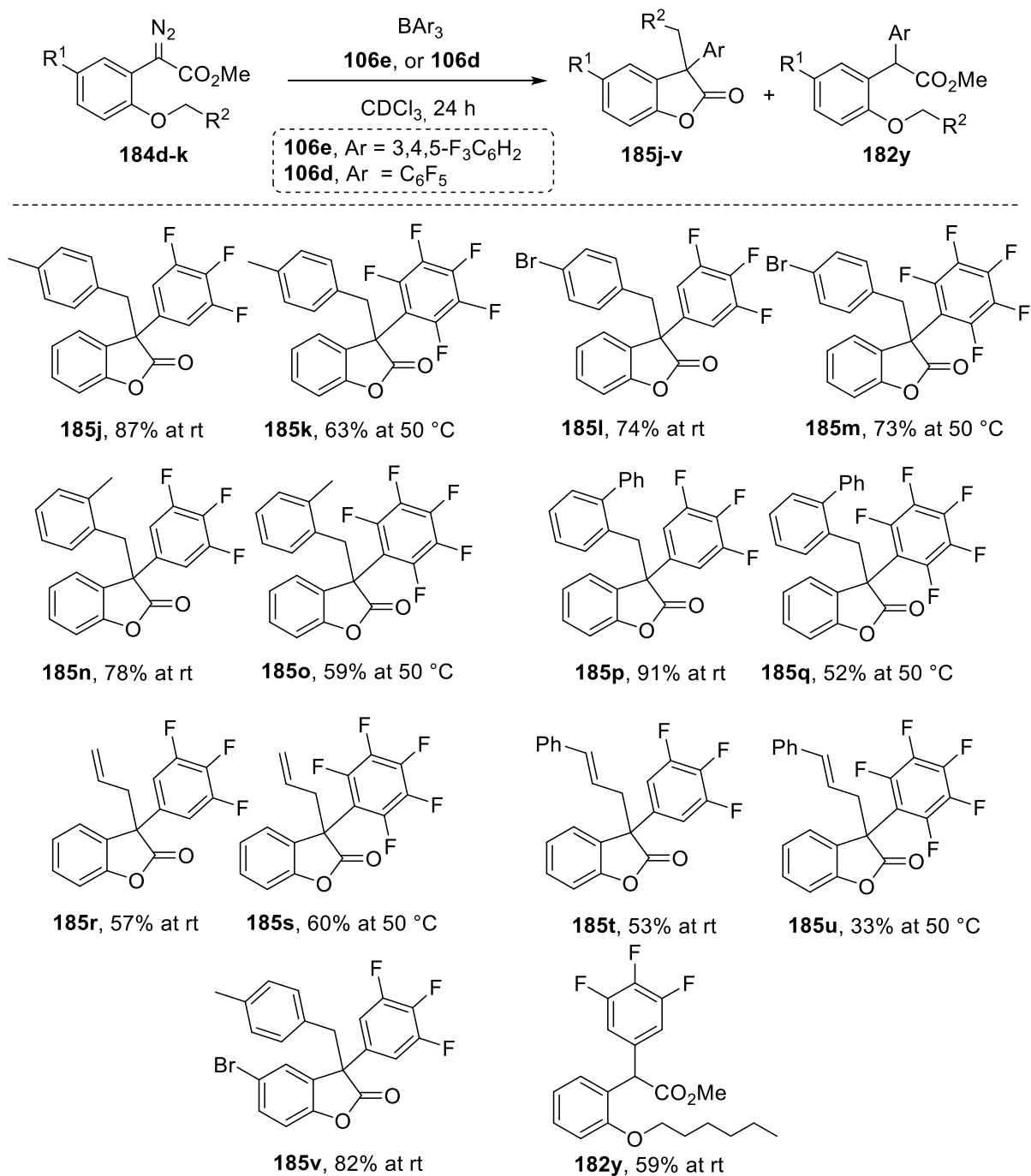
16 and 72 hours, respectively. However, when **106d** was employed, the enhanced reactivity led to a complex mixture of intermediates and no lactone **185h** could be isolated.



Scheme 3.32: Substrate scope of the reaction diazo compounds **184b–c** with boranes **106a,d,e**; ^aComplex mixture of product formed, no desired product observed by ¹H NMR spectroscopy.

The substrate scope of lactones was further expanded including moderate electron-rich benzylic and allylic migrating groups, by reacting diazo precursors **184d–k** and more Lewis acidic boranes **106e** and **106d** as starting materials (Scheme 3.33). Generally, the reactions performed using 3,4,5-fluorinated borane **106e** showed good results at room temperature in 24 hours, while B(C₆F₅)₃ **106d** was found to afford higher yields at 50 °C. Substrates **184d**, **184f**, **184g** and **184j** bearing a moderate electron-donating group in *para*- or *ortho*-position, as well as the *para*-brominated benzyl derivative **184e**, showed good reactivity with both boranes **106d–e**, generating the desired rearranged products **185j–q** and **185v** in moderate to excellent yields (52–91%). Moreover, the allyl-substituted diazo precursor **184h** reacted with both **106e** and **106d**, affording **185r** and **185s** in 57% and 60%, respectively. Similarly, the cinnamyl diazo derivative **184i** reacted

with **106e** to give **185t** in 53% yield, however, the migratory aptitude of the cinnamyl group was found to be lower when reacted with **106d**, affording **185u** in only 33% yield.



Scheme 3.33: Extended substrate scope for **185**.

A limitation was encountered when *n*-hexyl substituted diazo compound **184k** was used, as no lactone formation was observed but the reaction stopped after the 1,2-aryl transfer step, forming **182y** in 59% yield.

3.2.2.2 Mechanistic Studies

The diazo compound **184a** was used as a model substrate, along with borane **106e**, for an *in situ* NMR experiment and further mechanistic studies (Figure 3.3).

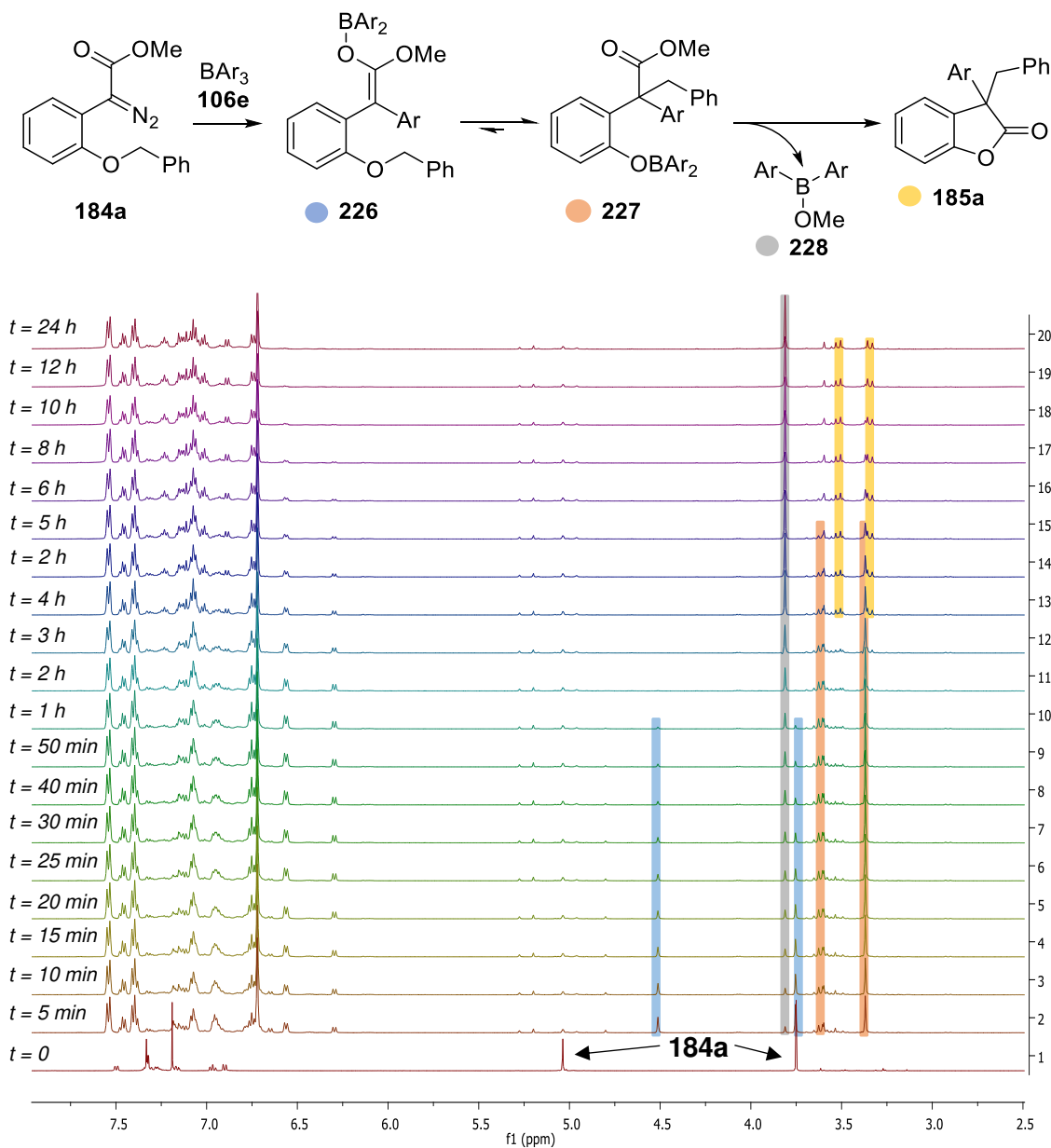


Figure 3.3: *In situ* ^1H NMR (500 MHz, CDCl_3) spectra of the reaction between **184a** (0.05 mmol) and **106e** (0.05 mmol) at different time intervals; Ar = 3,4,5- $\text{F}_3\text{C}_6\text{H}_2$.

As depicted in Figure 3.3 the ^1H NMR spectra showed that the starting material **184a** was fully consumed within 5 minutes and two main intermediates, **226** (blue) and **227** (pink), were formed. When the reaction was performed for 48 hours using mesitylene as an internal standard, the boron enolate intermediate **226** (Figure 3.4, blue) was found to be fully converted into **227** (orange) within one hour. As the reaction proceeded,

intermediate **227** was consumed forming lactone **185a** (yellow) and another side product, which was identified by NMR spectroscopy as the diarylboronic ether **228** (grey).

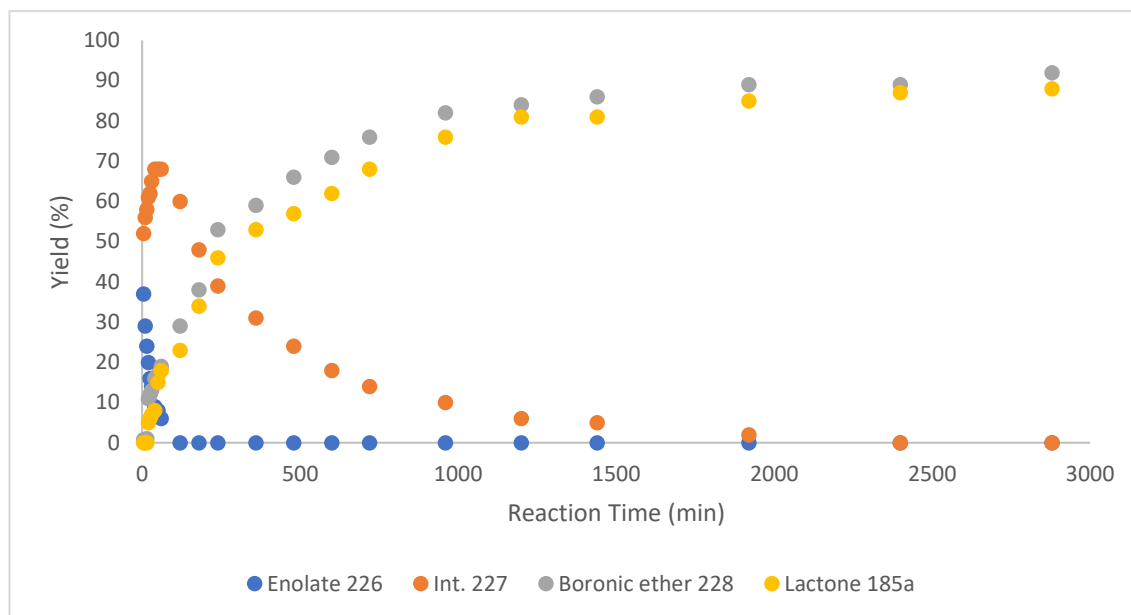
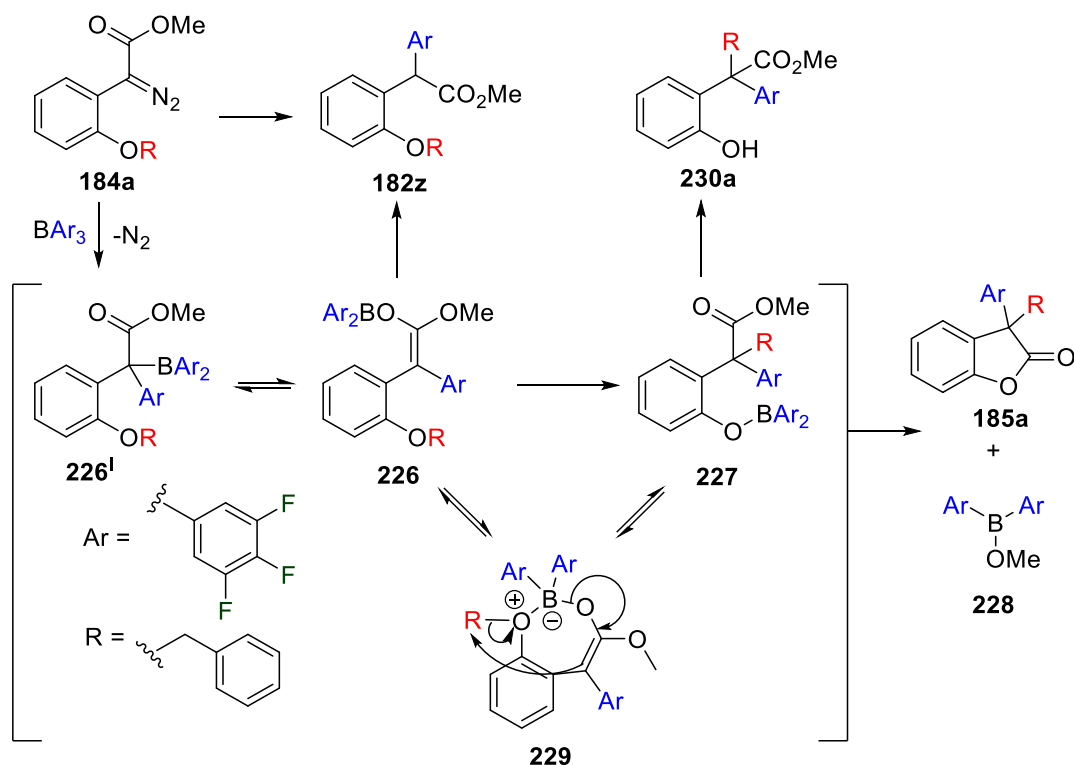


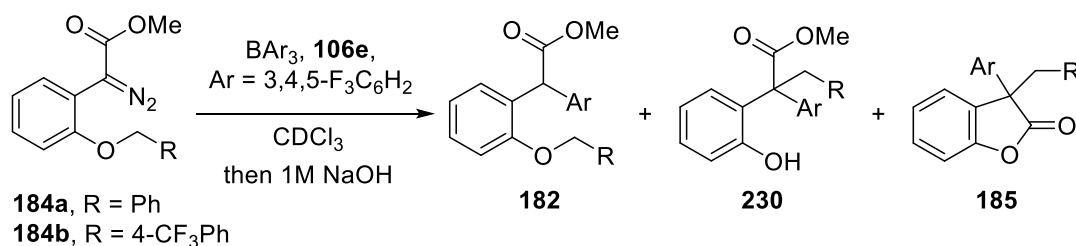
Figure 3.4: Kinetic study for the formation of lactone **185a**; mesitylene was used as the internal standard; The kinetic data are reported in Appendix B.

With this information in hand, a mechanism was proposed (Scheme 3.34). It is assumed that the diazo compound **184a** initially undergoes a 1,2-aryl shift with the borane **106e**, leading to the boron enolate **226**, with liberation of nitrogen as mentioned earlier in this chapter (see Scheme 3.20). Subsequently, the boron enolate **226** undergoes an intramolecular benzyl group migration generating **227**, possibly *via* the seven-membered ring intermediate **229**. Finally, intermediate **227** undergoes intramolecular cyclisation forming lactone **185a** and diarylboronic ether **228** as the side product within 24 hours. Evidence for the formation of **226** and **227** was found by quenching the reaction after 5, 10, 15 and 20 minutes which showed the formation of the α -aryl ester **182z** in 33%, 19%, 17% and 15% ^1H NMR yield, along with phenol **230a** in 47%, 49%, 52% and 60% ^1H NMR yield, respectively, after work-up (Table 3.3, entries 1–4). Moreover, the NMR ratio between **226** and **227** after 5 minutes ($\sim 1:1.4$) reflects the ratio between **182z** and **230a** (1:1.35) found in the crude mixture. It was also found that increasing the temperature to 50 °C accelerated the cyclisation of intermediate **227** into lactone **185** but showed no effect on the rate of rearrangement of boron enolate **226** into **227** (entries 5–6).



Scheme 3.34: Proposed mechanism for the formation of lactone **185a**.

Table 3.3: Evidence for the formation of boron enolate **226** and intermediate **227**.



Entry	Starting Material	Temperature	Time	182 ^a	230 ^a	185 ^a
1	184a	rt	5 min	33%	47%	n.o.
2	184a	rt	10 min	19%	49%	n.o.
3	184a	rt	15 min	17%	52%	n.o.
4	184a	rt	20 min	15%	60%	n.o.
5	184b	rt	24 h	20%	21%	51%
6	184b	50 °C	24 h	25%	n.o.	57%

General procedure: Reactions performed on 0.1 mmol of starting material **184a** using **106e** for 24 h at rt; ^aNMR yield, mesitylene, used as internal standard; n.o. = not observed.

Despite the reactivity of the phenolic hydroxy group, some of the phenolic intermediates **230** were stable enough to be isolated and fully characterised (See Chapter 5). The

seven-membered intermediate **229** was not observed by ^1H NMR spectroscopy, nevertheless, when **184a** and **184j** were reacted with **106e** in a 1:1:2 ratio, only **185a** and **185v** were formed in a 1:1 ratio, with no crossover reaction product **185d** observed, providing evidence for an intramolecular rearrangement (Figure 3.5).

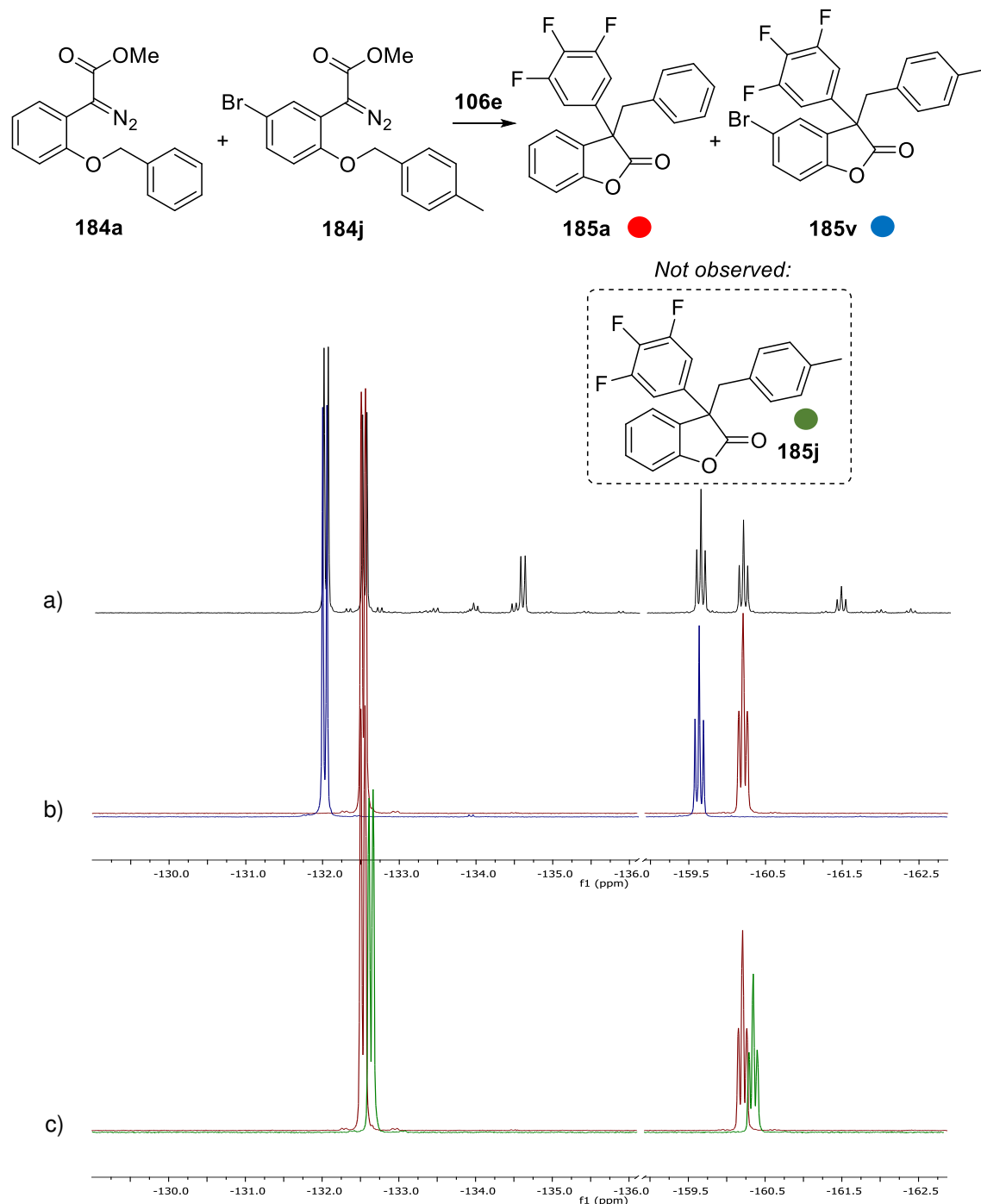


Figure 3.5: a) ^{19}F NMR (376 MHz, CDCl_3) of the crude reaction mixture of **184a** (0.1 mmol), **184j** (0.1 mmol) and **106e** (0.2 mmol) at room temperature after 48 h; b) ^{19}F NMR spectra of **185a** (red) overlapped with **185v** (blue); c) ^{19}F NMR spectra of **185a** (red) overlapped with **185j** (green); **185j** was not formed during the crossover reaction.

Although it was not possible to isolate the diaryl boronic ether **228**, it was possible to find some evidence from the *in situ* ^{19}F NMR spectra (Figure 3.6).

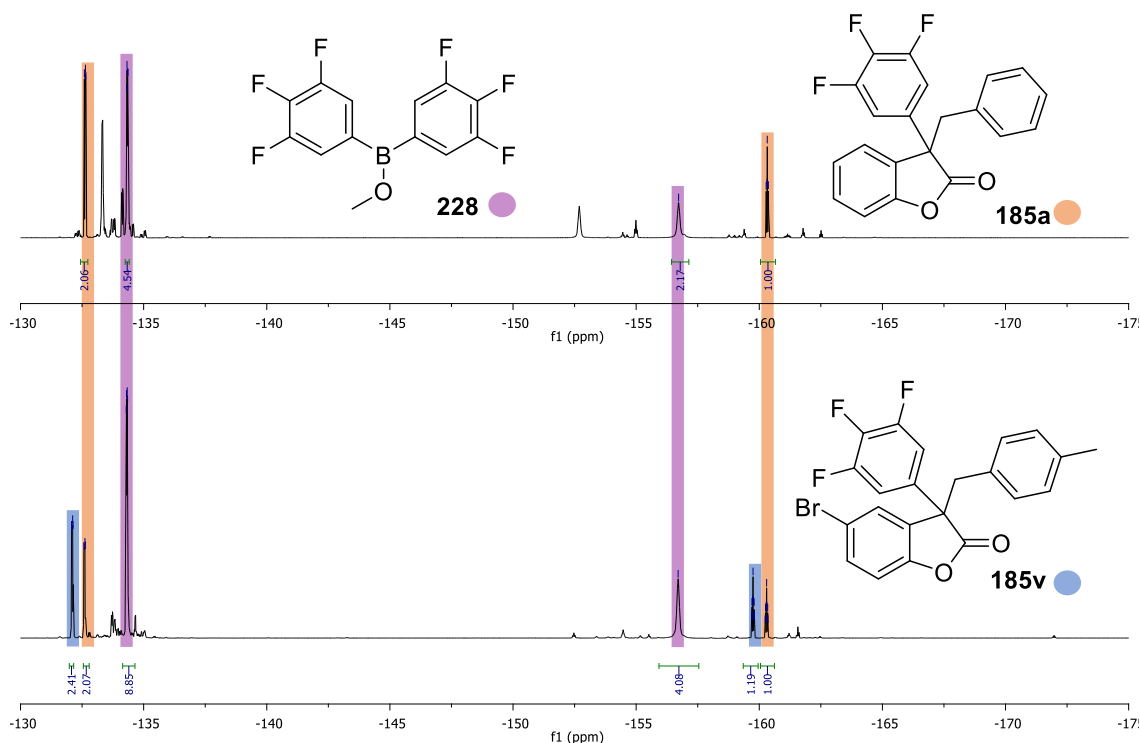
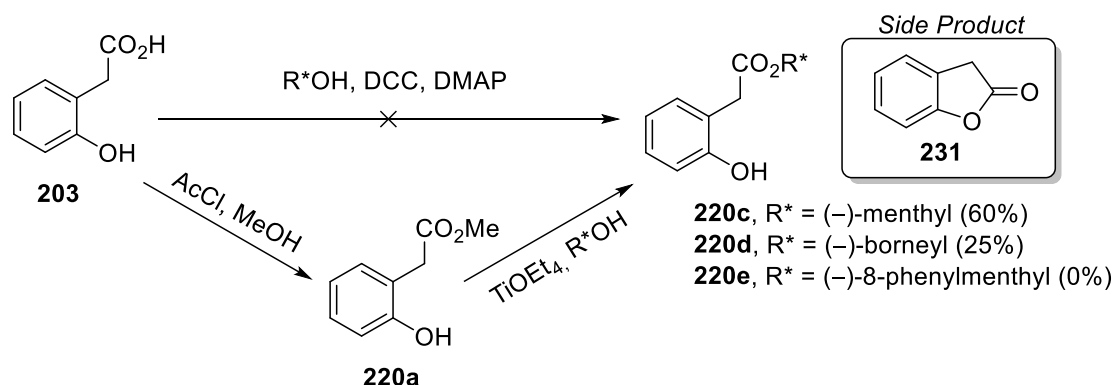


Figure 3.6: Comparison of *in situ* ^{19}F NMR (471 MHz, CDCl_3) spectra of the reaction between: a) **184a** (0.1 mmol) and **106e** (0.1 mmol) after 24 h at room temperature; b) **184a** (0.1 mmol), **184j** (0.1 mmol) and **106e** (0.2 mmol) after 24 h at room temperature; boronic ether **228** (purple), **185a** (red), **185v** (blue).

For instance, the ^{19}F NMR for the crude mixture between the model substrate **184a** and **106e** showed two sets of signals for both *meta*- and for *para*- ^{19}F which were found in a 2:1 ratio, and they were linked to **228** and **185a**, respectively. Similarly, the ^{19}F NMR of the reaction between **184a**, **184j** and **106e** showed three sets of ^{19}F signals in a 4:1:1 ratio for **228**, **185a** and **185v**, respectively. Moreover, the ^{11}B NMR spectra showed a signal at 43.0 ppm which was comparable to what was reported in the literature for similar compounds.⁴²

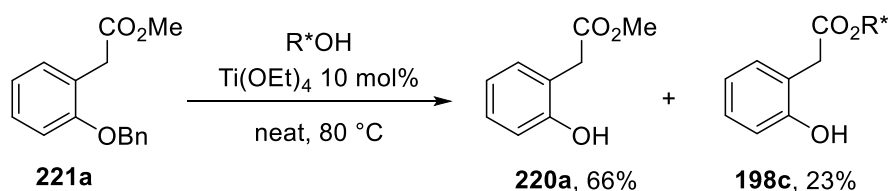
3.2.2.3 Stereoselective Lactonisation

It was then thought to stereoselectively drive the tandem rearrangement/lactonisation by introducing a chiral auxiliary at the ester moiety (Scheme 3.35). To install the chiral auxiliary, a Steglich esterification³⁴ of **203** using DCC and DMAP was investigated first but no reaction was observed. Hence, the transesterification of **220a** catalysed by $\text{Ti}(\text{OEt})_4$ was attempted next.⁴³ Despite the (-)-menthol derivative **220c**, which was obtained in good yield (60%), ester **220d** was obtained only in 25% and **220e** was not formed. In the last two cases, lactone **231** was formed as the main product instead.



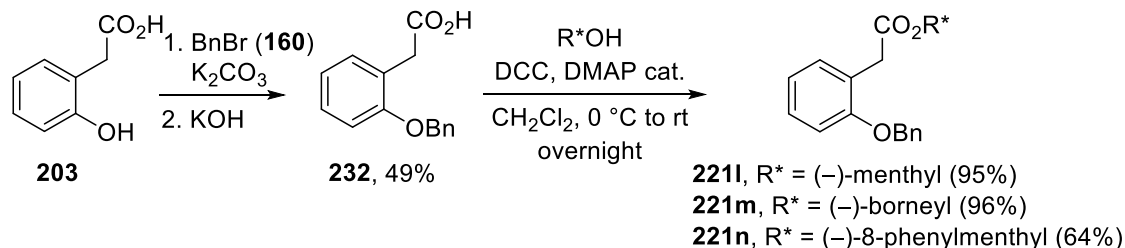
Scheme 3.35: Attempts for the synthesis of chiral esters **220c–e**.

The titanium-catalysed transesterification was then carried on using the benzylated derivative **221a** as a starting material (Scheme 3.36). However, under the described conditions the benzylic group was removed and only **220a** and **220c** were formed in 66% and 23%, respectively.



Scheme 3.36: Attempt of transesterification of **221a**.

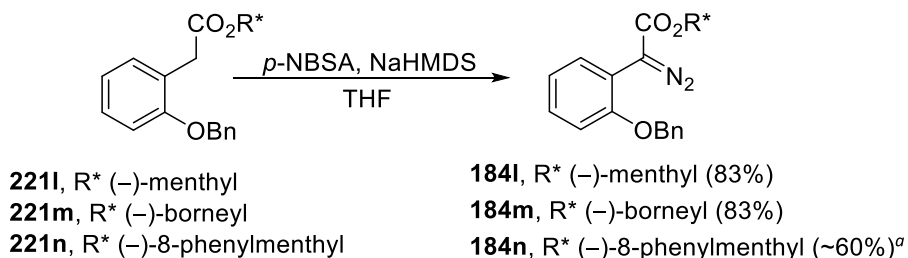
To overcome the problem, the phenolic hydroxy group of **203** was protected first, using benzyl bromide to afford the benzyl derivative **232** in 49% yield over two steps (Scheme 3.37). In this way, the chiral auxiliaries were successfully installed *via* Steglich esterification³⁴ using **232** as starting material. Both (-)-menthol substituted **221l** and (-)-borneol derivative **221m** were afforded in excellent yields (95–96%), whereas the (-)-8-phenylmenthol ester **221n** was obtained in 64% yield.



Scheme 3.37: An alternative route to chiral esters **221l–n**.

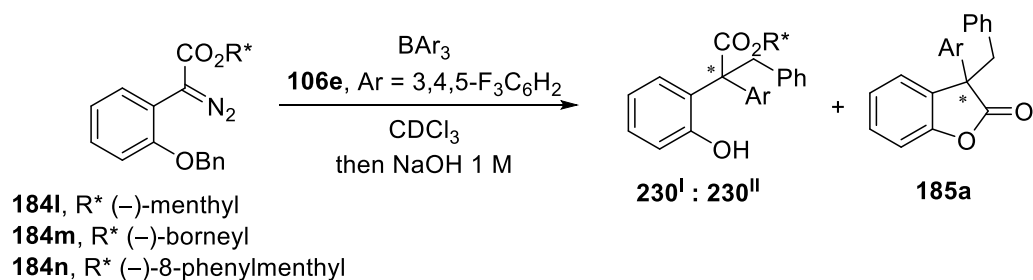
Finally, the chiral diazo precursors **184l–n** were synthesised in good yields *via* Regitz diazo-transfer reaction (Scheme 3.38).²⁹ In this case DBU did not lead to any reaction, and a stronger base such as NaHMDS was needed. While **184l** and **184m** were obtained

in very good yields (83%), the diazo precursor bearing the (-)-8-phenylmenthyl substituent **184n** was obtained in ~60% yield and it was not possible to separate it from the unreacted starting material **221n** by flash column chromatography, hence it could only be used without further purification.



Scheme 3.38: Synthesis of chiral diazo compound **184I–n**; ^aIt was not possible to separate the product from the unreacted starting material **221n**.

The chiral diazo esters **184I–n** were reacted with 3,4,5-fluorinated borane **106e** in CDCl₃ and the reaction progress was monitored by ¹H and ¹⁹F NMR spectroscopy (Table 3.4). The (-)-menthol derivative **184I** was converted to the rearranged products **230^I** and **230^{II}** in 86% yield as a 1:1.8 mixture of diastereomers after one hour, however, lactone **185a** was not observed by NMR spectroscopy nor formed after the work-up (entry 1). The diastereomeric ratio of **230** did not change when the reaction was performed for a longer time (12 hours) and at lower temperature (-78 °C, 10 days), affording **230^I** and **230^{II}** in very good yields (up to 88%) but, once again, without the formation of **185a** (entries 2 and 3). Nevertheless, when the reactions were carried out at 50 °C for seven days, the target **185a** was formed in 45% NMR yield (entries 4 and 5). The higher temperature favoured the cyclisation of both **230** isomers forming **185a**. However, it was not possible to control the selective cyclisation of only one of the two **230** isomers, and the final lactone **185a** was obtained in 41–45% yield and 21–44% ee after 7 days at 50 °C (entry 4). When (-)-borneol derivative **184m** was used, the diastereomeric ratio for **230** was inverted, with **230^I** being the major isomer formed. For the reaction performed for four days at room temperature the diastereomers **230** were formed in 83% yield with a 1:0.8 of diastereomeric ratio (entry 6). A similar result was registered for the reaction at -78 °C for 10 days (entry 8), while when the reaction was heated up at 50 °C for 3 days, 61% of **230** was converted into **185a** with 29% ee (entry 7). Despite more sterically hindered, the (-)-8-phenylmenthol ester **184n** was not found to be more selective than **184I–m**, with the two diastereomers **230** formed in good yields but with only 1:0.5 *d.r.* (entries 9 and 11). Moreover, the phenols **230^I** and **230^{II}** from **184n** were found to be more stable and only traces of **185a** were obtained after a week at 50 °C (entry 10).

Table 3.4: Enantioselective reactions between **184I–n** and Lewis acid **106e**.

Entry	Starting Material	T (°C)	Time	230 ^I :230 ^{II} ^a	185a (%) ^b	Yield (%) ^c	185a ee (%) ^d
1	184I	rt	1 h	1 : 1.8	n.d.	86	n.d.
2	184I	rt	12 h	1 : 1.8	n.d.	80	n.d.
3	184I	-78 °C	10 d	1 : 1.6	n.d.	88	n.d.
4 ^e	184I	50 °C	5 d	1 : 1.2	41–45	97	21–44
6	184m	rt	4 d	1 : 0.8	traces	83	0
7	184m	50 °C	3 d	1 : 2.2	61	90	29 ^f
8	184m	-78 °C	10 d	1 : 0.8	n.d.	85	n.d.
9	184n	rt	7 d	1 : 0.5	n.d.	74	n.d.
10 ^g	184n	50 °C	7 d	1 : 0.6	traces	n.d.	14 ^f
11	184n	-78 °C	10 d	1 : 0.5	n.d.	84	n.d.

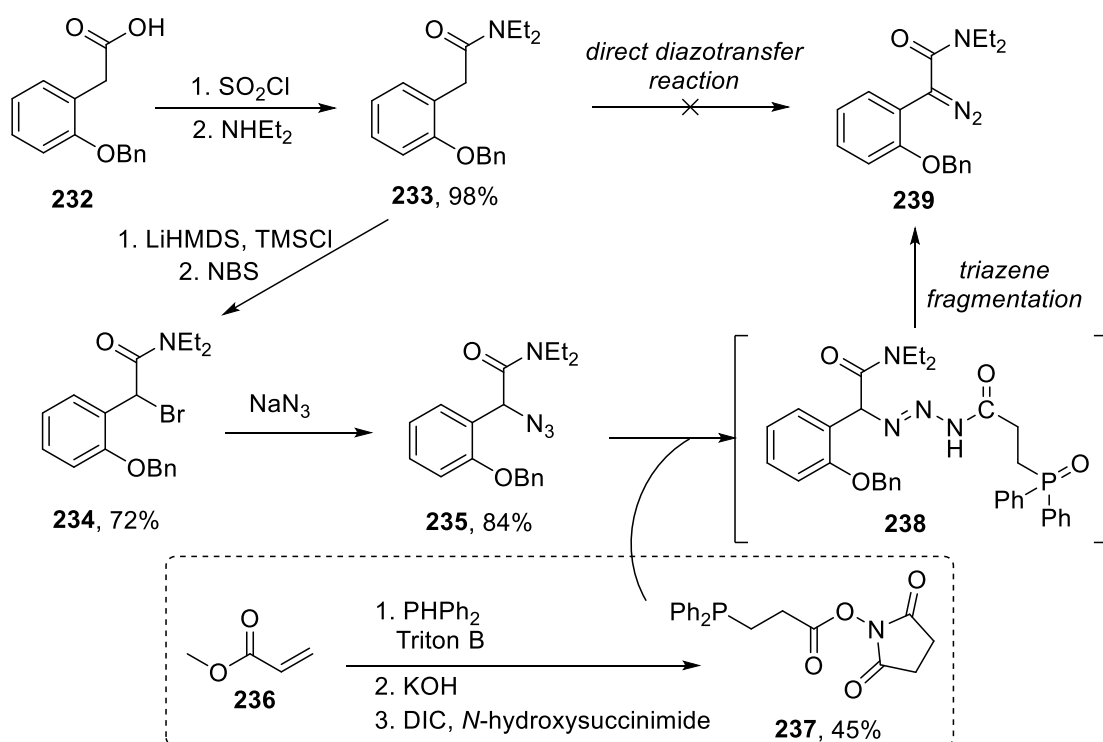
General Procedure: Reactions performed on a 0.1 mmol scale of **184** and **106e** (1 equiv.) in CDCl₃; ^aNMR ratio; ^b¹H NMR yield; ^cCombined yield of **230^I**, **230^{II}** and **185a**; ^dDetermined by 2D-HPLC analysis; ^eRange of two reactions; ^fOpposite configuration formed; ^gComplex mixture formed; n.d. = not determined.

Despite the mediocre selectivity observed, these preliminary results proved the concept that it is possible to induce a stereoselective rearrangement reaction by installing a chiral auxiliary, which will also be cleaved off during the same lactonisation step.

3.3 Conclusion and Outlook

In conclusion, a mild, metal free synthesis of α -aryl-substituted esters was achieved in high yields using halogenated triarylboranes. Importantly, when more Lewis acidic boranes were used on a less sterically hindered diazo compound, it was possible to use sub-stoichiometric amounts of boranes as more than one aryl group was transferred from the borane to the diazo substrate. Furthermore, a novel synthesis for asymmetric 3,3-disubstituted benzofuran-2(3*H*)-ones from the reaction between α -aryl- α -diazo acetates and triarylboranes was presented. After mechanistic investigations it was found that in the presence of a 2-oxy substituent on the α -aryl moiety, the initial boron enolate intermediate undergoes intramolecular rearrangement to form 3,3-disubstituted benzofuranones. To the best of my knowledge, this is the first example of lactone framework synthesis in which the C-3 position is fully substituted in a single-step under metal-free conditions.

Future work is focussed on optimising the stereoselective lactone formation, expanding the substrate scope to α -diazo amides **239** as starting material (Scheme 3.39).



Scheme 3.39: Attempts for the synthesis of the α -diazo amide **239**.

Preliminary results showed that the direct diazo-transfer reaction on **233** using *p*-ABSA (**18e**) or *p*-NBSA (**18f**) with DBU did not afford any product and the starting material was recovered. Stronger bases such as NaHMDS , or higher temperature ($50\text{ }^\circ\text{C}$) led to decomposition, therefore, the phosphine-mediated conversion of azides into diazo

compounds was investigated as a suitable approach toward **239**.⁴⁴ The azide **235** was obtained in 60% yield over two steps, after α -bromination of **233** in the presence of NBS, followed by nucleophilic substitution with sodium azide. On the other hand, the acyl phosphine **237** was synthesised in 45% yield over three steps, from methyl acrylate (**236**) and diphenylphosphine. The reaction between azide **235** and phosphine **237** generated the triazene **238**. A proper optimisation of the fragmentation of triazene **238**, as well as installing chiral amide auxiliary, will provide access to the valuable chiral α -diazo amide **239**, that can be investigated as starting materials in the stereoselective rearrangement/lactonisation reaction.

References

- 1 For selected examples see: a) H. Mei, J. Han, S. Fustero, M. Medio-Simon, D. M. Sedgwick, C. Santi, R. Ruzziconi, V. A. Soloshonok, *Chem. Eur. J.* **2019**, *25*, 11797–11819; b) S. Purser, P. R. Moore, S. Swallow, V. Gouverneur, *Chem. Soc. Rev.* **2008**, *37*, 320–330; c) K. Müller, C. Faeh, F. Diederich, *Science* **2007**, *317*, 1881–1886; c) J. Wang, M. Sánchez-Roselló, J.-L. Aceña, C. del Pozo, A. E. Sorochinsky, S. Fustero, V. A. Soloshonok, H. Liu, *Chem. Rev.* **2014**, *114*, 2432–2506.
- 2 D. O'Hagan, *Chem. Soc. Rev.* **2008**, *37*, 308–319.
- 3 S. M. Ametamey, M. Honer, P. A. Schubiger, *Chem. Rev.* **2008**, *37*, 1501–1516.
- 4 a) A. R. Murphy, J. M. J. Fréchet, *Chem. Rev.* **2007**, *107*, 1066–1096; b) F. Babudri, G. M. Farinola, F. Naso, R. Ragni, *Chem. Commun.* **2007**, 1003–1022.
- 5 a) R. Szpera, D. F. J. Moseley, L. B. Smith, A. J. Sterling, V. Gouverneur, *Angew. Chem. Int. Ed.* **2019**, *58*, 14824–14848; b) C. N. Neumann, T. Ritter, *Angew. Chem. Int. Ed.* **2015**, *54*, 3216–3221; c) M. G. Campbell, T. Ritter, *Org. Process Res. Dev.* **2014**, *18*, 474–480.
- 6 For selected example see: a) C. Chen, T. Voss, R. Fröhlich, G. Kehr, G. Erker, *Org. Lett.* **2011**, *13*, 62–65; b) F. Ge, G. Kehr, C. G. Daniliuc, G. Erker, *J. Am. Chem. Soc.* **2014**, *136*, 68–71; c) G. Kehr, G. Erker, *Chem. Sci.* **2016**, *7*, 56–65.
- 7 M. M. Hansmann, R. L. Melen, F. Rominger, A. S. K. Hashmi, D. W. Stephan, *J. Am. Chem. Soc.* **2014**, *136*, 777–782.
- 8 L. C. Wilkins, J. R. Lawson, P. Wieneke, F. Rominger, A. S. K. Hashmi, M. M. Hansmann, R. L. Melen, *Chem. Eur. J.* **2016**, *22*, 14618–14624.
- 9 For selected examples see: a) Y. Soltani, L. C. Wilkins, R. L. Melen, *Angew. Chem. Int. Ed.* **2017**, *56*, 11995–11999; b) S. Tamke, Z.-W. Qu, N. A. Sitte, U. Flörke, S. Grimme, J. Paradies, *Angew. Chem. Int. Ed.* **2016**, *55*, 4336–4339.
- 10 For reviews using B(C₆F₅)₃ see: a) D. W. Stephan, G. Erker, *Angew. Chem. Int. Ed.* **2010**, *49*, 46–76; b) D. W. Stephan, G. Erker, *Angew. Chem. Int. Ed.* **2015**, *54*, 6400–6441; c) D. W. Stephan, *J. Am. Chem. Soc.* **2015**, *137*, 10018–10032.
- 11 For selected examples see: a) S. Rendler, M. Oestreich, *Angew. Chem. Int. Ed.* **2008**, *47*, 5997–6000; b) M. Oestreich, J. Hermeke, J. Mohr, *Chem. Soc. Rev.* **2015**, *44*, 2202–2220; c) I. Chatterjee, M. Oestreich, *Angew. Chem. Int. Ed.* **2015**, *54*, 1965–1968.
- 12 a) J. Hooz, S. Linke, *J. Am. Chem. Soc.* **1968**, *90*, 5936–5937; b) H. Li, Y. Zhang, J. Wang, *Synthesis* **2013**, *45*, 3090–3098.
- 13 D. Ameen, T. Snape, *Med. Chem. Commun.* **2013**, *4*, 893–907.
- 14 a) Y. Xia, Z. Liu, S. Feng, F. Ye, Y. Zhang, J. Wang, *Org. Lett.* **2015**, *17*, 956–959; b) J. Ghorai, P. Anbarasan, *J. Org. Chem.* **2015**, *80*, 3455–3461; c) F.-N. Ng, Y.-F. Lau, Z. Zhou, W.-Y. Yu, *Org. Lett.* **2015**, *17*, 1676–1679.
- 15 Y.-J. Kwon, M.-J. Sohn, C.-J. Zheng, W.-G. Kim, *Org. Lett.* **2007**, *9*, 2449–2451.
- 16 N. Nakatani, R. Inatani, *Agric. Biol. Chem.* **1983**, *47*, 353–358.

- 17 C. Balestrieri, F. Felice, S. Piacente, C. Pizza, P. Montoro, W. Oleszek, V. Visciano, M. L. Balestrieri, *Biochem. Pharmacol.* **2006**, *71*, 1479–1487.
- 18 S.-I. Wada, T. Hitomi, H. Tokuda, R. Tanaka, *Chem. Biodiv.* **2010**, *7*, 2303–2308.
- 19 S. Venkateswarlu, G. K. Panchagnula, M. B. Guraiah, G. V. Subbaraju, *Tetrahedron* **2005**, *61*, 3013–3017.
- 20 D. C. Harrowven, M. C. Lucas, P. D. Howes, *Tetrahedron* **2001**, *57*, 791–804.
- 21 Y. Li, X. Li, J.-P. Cheng, *Adv. Synth. Catal.* **2014**, *356*, 1172–1198.
- 22 For selected recent examples, see: a) Z. Huang, X. Yang, F. Yang, T. Lu, Q. Zhou, *Org. Lett.* **2017**, *19*, 3524–3527; b) T. Cruchter, M. G. Medvedev, X. Shen, T. Mietke, K. Harms, M. Marsch, E. Meggers, *ACS Catal.* **2017**, *7*, 5151–5162; c) B. B. Dhotare, M. Kumar, S. K. Nayak, *J. Org. Chem.* **2018**, *83*, 10089–10093; d) Y. Chen, B.-D. Cui, Y. Wang, W.-Y. Han, N.-W. Wan, M. Bai, W.-C. Yuan, Y.-Z. Chen, *J. Org. Chem.* **2018**, *83*, 10465–10475; e) Y. Liu, C. Zhou, M. Xiong, J. Jiang, J. Wang, *Org. Lett.* **2018**, *20*, 5889–5893.
- 23 a) X.-F. Cheng, Y. Li, Y.-M. Su, F. Yin, J.-Y. Wang, J. Sheng, H. U. Vora, X.-S. Wang, J.-Q. Yu, *J. Am. Chem. Soc.* **2013**, *135*, 1236–1239; b) M. Yang, X. Jiang, W.-J. Shi, Q.-L. Zhu, Z.-J. Shi, *Org. Lett.* **2013**, *15*, 690–693.
- 24 a) L. Chen, F. Zhou, T.-D. Shi, J. Zhou, *J. Org. Chem.* **2012**, *77*, 4354–4362; b) B. B. Dhotare, M. K. Choudhary, S. K. Nayak, *Synth. Commun.* **2016**, *46*, 1772–1780.
- 25 a) E. Yoneda, T. Sugioka, K. Hirao, S.-W. Zhang, S. Takahashi, *J. Chem. Soc. Perkin Trans. 1* **1998**, 477–484; b) V. Hirschbeck, I. Fleischer, *Chem. Eur. J.* **2018**, *24*, 2854–2857.
- 26 a) K. Ladenburg, K. Folkers, R. T. Major, *J. Am. Chem. Soc.* **1936**, *58*, 1292–1294; b) A. Puglisi, C. Giustini, A. Ricucci, E. Perotti, L. Massaro, D. Morra, F. Ciucci, A. Zucchet, A. Antenucci, M. Moliterno, S. Placidi, F. Sciubba, L. Galantini, R. Salvio, M. Bella, *Chem. Eur. J.* **2018**, *24*, 6941–6945; c) L. Ortiz-Rojano, M. Martínez-Mingo, C. García-García, M. Ribagorda, M. C. Carreño, *Eur. J. Org. Chem.* **2018**, 1034–1040.
- 27 a) U. Mayer, V. Gutmann, W. Gerger, *Monats. Chem.* **1975**, *106*, 1235–1257; b) M. A. Beckett, G. C. Strickland, J. R. Holland, K. S. Varma, *Polymer* **1996**, *37*, 4629–4631.
- 28 J. L. Carden, A. Dasgupta, R. L. Melen, *Chem. Soc. Rev.* **2020**, *49*, 1706–1725.
- 29 a) M. Regitz, *Chem. Ber.* **1964**, *97*, 2742 – 2754; b) M. Regitz, *Justus Liebigs Ann. Chem.* **1964**, 676, 101–109.
- 30 R. C. Neu, C. Jiang, D. W. Stephan, *Dalton Trans.* **2013**, *42*, 726–736.
- 31 M. A. Sanchez-Carmona, D. A. Contreras-Cruz, L. D. Miranda, *Org. Biomol. Chem.* **2011**, *9*, 6506–6508.
- 32 S. G. Davies, A. M. Fletcher, J. E. Thomson, *Chem. Commun.* **2013**, *49*, 8586–8598.
- 33 G. C. M. Kondaiah, L. Amarnath Reddy, K. Srihari Babu, V. M. Gurav, K. G. Hüge, R. Bandichhor, P. Pratap Reddy, A. Bhattacharya, R. Vijaya Ananda, *Tetrahedron Lett.* **2008**, *49*, 106–108.
- 34 B. Neises, W. Steglich, *Angew. Chem. Int. Ed.* **1978**, *17*, 522–524.

- 35 a) P. J. Domaille, J. D. Druliner, L. W. Gosser, J. M. Read, Jr., E. R. Schmelzer, W. R. Stevens, *J. Org. Chem.* **1985**, *50*, 189–194; b) P. Jacob III, *J. Organomet. Chem.* **1978**, *156*, 101–110; c) C. S. Cundy, H. Nöth, *J. Organomet. Chem.* **1971**, *30*, 135–143.
- 36 H. H. San, S.-J. Wang, M. Jiang, X.-Y. Tang, *Org. Lett.* **2018**, *20*, 4672–4676.
- 37 D. J. Pasto, P. W. Wojtkowski, *Tetrahedron Lett.* **1970**, *11*, 215–218.
- 38 M. P. Doyle, D. C. Forbes, *Chem. Rev.* **1998**, *98*, 911–936.
- 39 M. P. Doyle, R. Duffy, M. Ratnikov, L. Zhou, *Chem. Rev.* **2010**, *110*, 704–724.
- 40 L. Zhou, M. P. Doyle, *J. Org. Chem.* **2009**, *74*, 9222–9224.
- 41 Y. Jiang, Y. Qin, S. Xie, X. Zhang, J. Dong, D. Ma, *Org. Lett.* **2009**, *11*, 5252–5253.
- 42 D. Donghi, D. Maggioni, T. Beringhelli, G. D'Alfonso, P. Mercandelli, A. Sironi, *Eur. J. Inorg. Chem.* **2008**, 1645–1653.
- 43 P. Krasik, *Tetrahedron Lett.* **1998**, *39*, 4223–4226.
- 44 E. L. Myers, R. T. Raines, *Angew. Chem. Int. Ed.* **2009**, *48*, 2359–2363.

CHAPTER 4: Synthesis of *N,O*-acetals in a Flow Electrochemical Microreactor

4.1 Introduction

The *N*-acyl-*N,O*-acetal moiety is an important functionality in organic chemistry due to its presence in bioactive molecules such as the cytotoxic agents psymbenin (**240**)¹ and pederin (**241**; Figure 4.1).² Moreover, it was reported by Floreancig and co-workers that the *N,O*-acetal moiety in **240** and **241** acts as pharmacophore, hence its presence is necessary for their bioactivity.³

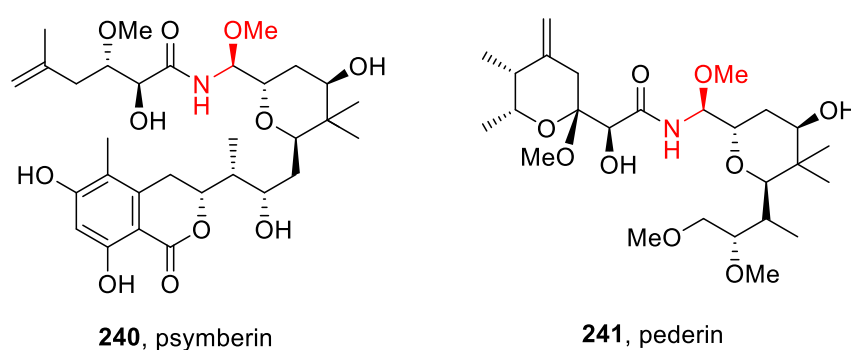
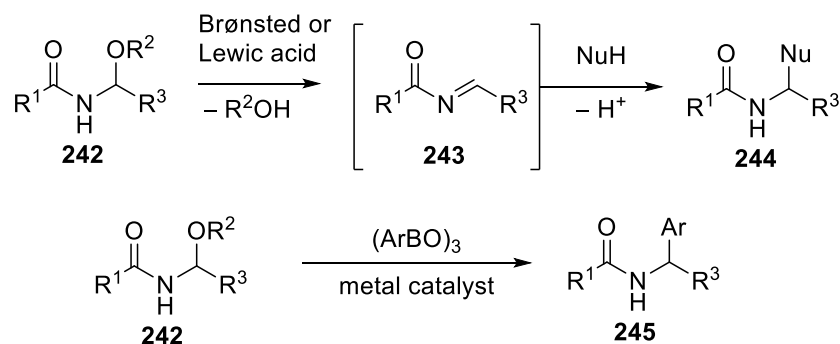


Figure 4.1: Examples of bioactive compounds bearing *N*-acyl-*N,O*-acetals.

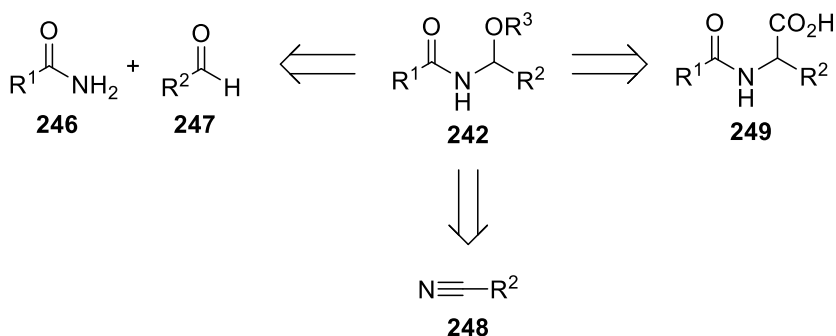
Besides being useful building blocks in organic chemistry, *N*-acyl-*N,O*-acetals are also used as valuable surrogates of unstable *N*-acylimines **243** (Scheme 4.1).⁴ While *N*-acylimines **243** are susceptible to hydrolysis in the presence of water, *N*-acyl-*N,O*-acetals **242** are air and moisture-stable. They can be readily activated by Lewis or Brønsted acids to generate reactive *N*-acylimines **243**, which then undergo nucleophilic substitution,⁴ or transition metal *catalysed* cross-coupling.⁵



Scheme 4.1: Utility of *N,O*-acetals **242** in organic synthesis.

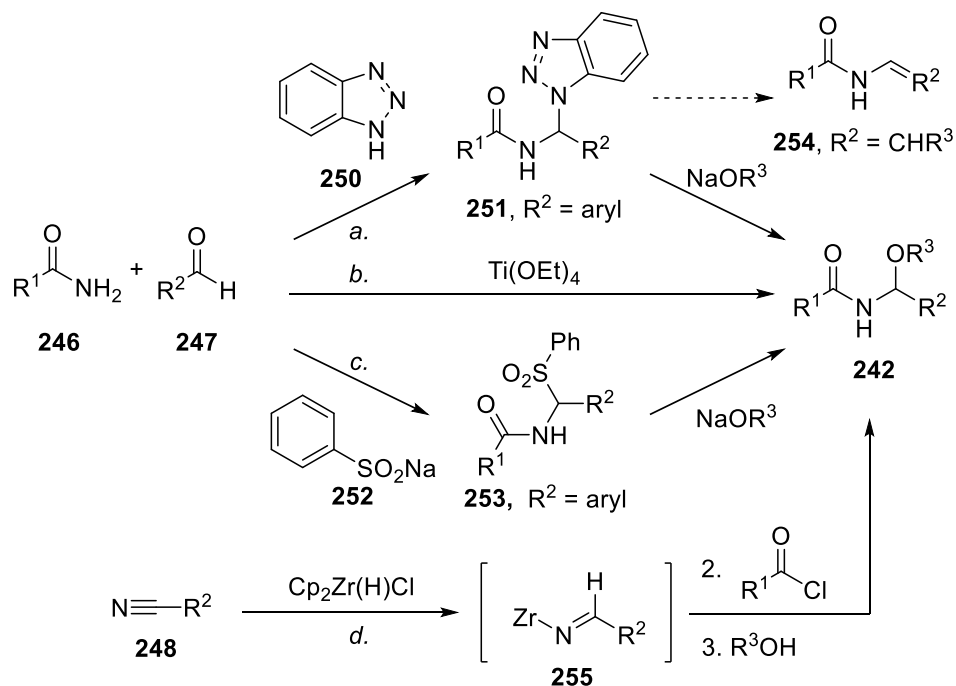
For these reasons, several protocols have been reported for the preparation of such structures. Retrosynthetically, the *N*-acetylated *N,O*-acetals **242** can be generated from

amides **246**, condensed with aldehydes **247**, from nitriles **248** or from *N*-acyl amino acid derivatives **249** (Scheme 4.2).



Scheme 4.2: Retrosynthetic approach towards *N*-acyl-*N,O*-acetals **242**.

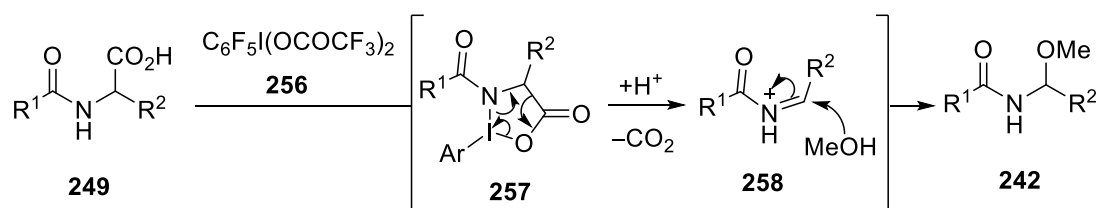
One of the classic protocols for their synthesis is the Katritzky's benzotriazole method,⁶ where an amide **246** condenses with an aldehyde **247** to generate an imine *in situ* that undergoes nucleophilic attack by benzotriazole **250** forming amide **251** (Scheme 4.3a). This α -substituted amide **251** is then treated with sodium alkoxides to install the alkoxy group on the molecule, giving the *N,O*-acetal **242**. Similarly, amide **246** and aldehyde **247** can be mixed with the benzenesulfinic acid salt **252** to afford the α -amido sulfone **253** as a *N,O*-acetal precursor (Scheme 4.3c).⁷ However, the substrate scope for these reactions is limited to aryl aldehydes, as the exclusive formation of enamides **254** was observed when alkyl-aldehyde substrates were employed.⁸



Scheme 4.3: Strategies to synthesise *N*-acyl-*N,O*-acetals **242**.

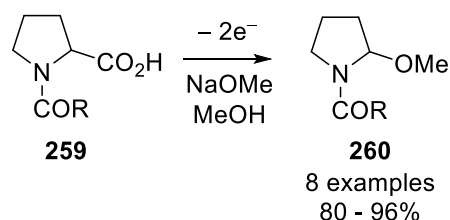
More recently, Wen and co-workers reported a concise procedure mediated by titanium ethoxide, in which *N*-acyl-*O*-ethyl *N,O*-acetals **242** are synthesised in one single step starting from the amide **246** and the aldehyde **247**, expanding the substrate scope to both aromatic and aliphatic aldehydes **247** (Scheme 4.3b).⁹ An additional method is the hydrozirconation of nitriles **248**, which leads to **242** after acylation and nucleophilic addition of alcohols to the imine intermediate **255** in a three step one-pot process (Scheme 4.3d).¹⁰

The *N,O*-acetals **242** can be also prepared by decarboxylative oxidation of amino acid derivatives **249**. For instance, the hypervalent iodine(III) reagent **256** can be used to induce an oxidative fragmentation of **249** (Scheme 4.4).¹¹ In this case, **249** reacts with the hypervalent iodine(III) reagent **256** generating the five-membered ring **257** after two consecutive ligand exchanges. The latter undergoes oxidative cleavage releasing CO₂ and forming the imine **258**, which leads to the *N*-acyl-*O*-methyl *N,O*-acetal **242** upon addition of methanol.



Scheme 4.4: Oxidative fragmentation of α -amino acids **249** using iodine(III) reagent **256**.

In addition to hypervalent iodine(III) compounds, electricity can be used as a tool to prepare *N,O*-acetals from amino acid derivatives. For example, Miyoshi *et al.* reported the electrochemical alkoxylation of proline derivatives **259** via non-Kolbe electrolysis (Scheme 4.5).¹² After the electrolysis of the *N*-acylprolines **259** in methanol with sodium methoxide acting as supporting electrolyte and base, the *N,O*-acetals **260** were afforded in very good to excellent yields.

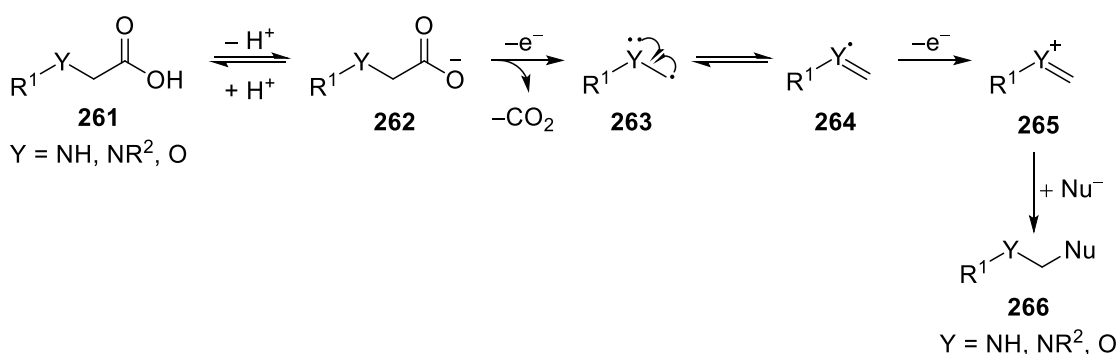


Scheme 4.5: Electrochemical synthesis of *N*-acyl-*N,O*-acetals **260**.

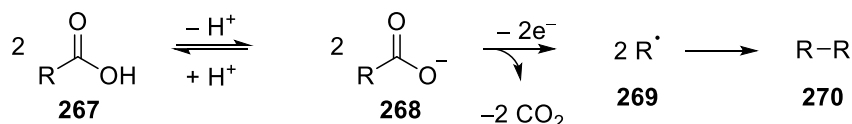
Mechanistically, in a non-Kolbe oxidation,¹³ sometimes referred to as the Hofer-Moest reaction,¹⁴ the *N*-acylated amino acid **261** undergoes a one-electron oxidation followed by decarboxylation, affording the radical intermediate **263** (Scheme 4.6). A second

one-electron oxidation leads to the formation of the *N*-acyliminium ion **265**. The intermediate **265** is then trapped by a nucleophile affording the final product **266**. Conversely, a classic Kolbe reaction affords the dimerised product **270** upon anodic decarboxylation of the carboxylate **268** and consequent coupling of two of the formed radicals **269**.¹⁵ Another electrochemical reaction which affords *N,O*-acetal as products is the anodic oxidation of unfunctionalised amides **271**, also known as the Shono oxidation.¹⁶ Similar to the non-Kolbe reaction, the starting material **271** undergoes a two-electron oxidation forming the *N*-acyliminium ion intermediate **273**, which gets trapped by a nucleophile affording the final product **274**.

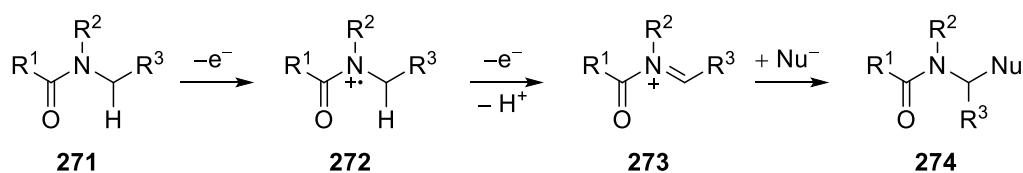
Non-Kolbe Oxidation:



Kolbe Oxidation:

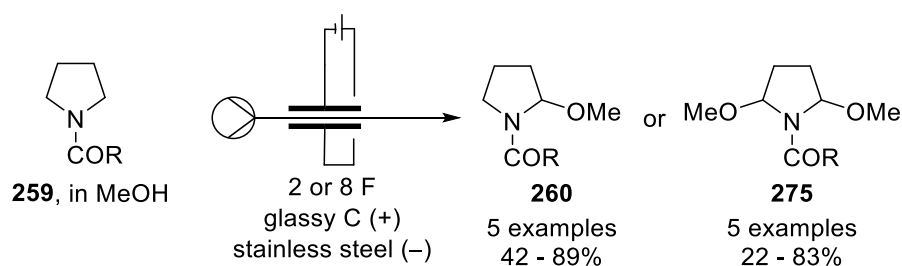


Shono Oxidation:



Scheme 4.6: Example of anodic oxidations: non-Kolbe, Kolbe and Shono oxidation.

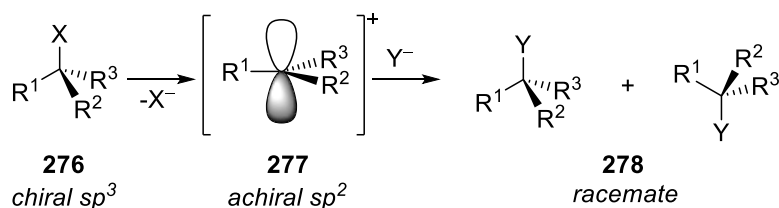
The Shono oxidation has been widely used as a test reaction, since it was found to be very successful for the synthesis of *N,O*-acetals **260**.¹⁷ Recently, the Wirth group used the Ion electrochemical reactor designed by Vapourtec to perform a regioselective methoxylation of the pyrrolidine **259** to the monoalkoxylated compound **260** (up to 86% yield) or the dialkoxylated product **275** (up to 83% yield), applying charges of 2 F or 8 F, respectively (Scheme 4.7).¹⁸



Scheme 4.7: Electrochemical synthesis of *N*-acyl-*N,O*-acetals reported by Wirth *et al.*¹⁸

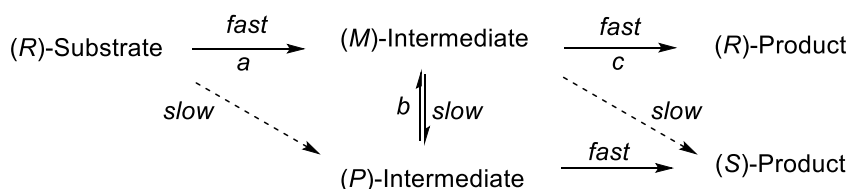
One of the advantages of flow electrochemical microreactor is the reduced distance between the anode and the cathode, which allows to minimise or even eliminate the addition of wasteful supporting electrolytes. Moreover, the use of flow microchannels improves the mass transfer, and the higher electrode surface-to-reactor volume allows the substrate to reach the reaction surface more easily compared to a batch reactor. Due to the bigger active surface available, a larger volume of solution containing the starting material gets in contact with the electrode, leading to shorter reaction times. Furthermore, as the solution is constantly pumped through the reactor, as soon the substrate reacts, the product is flushed out of the reactor avoiding side reactions.¹⁹

Given the presence of asymmetric *N,O*-acetal motifs in natural products and their function as synthons, there is a strong interest in developing stereoselective methods towards such structures. One approach is based on the employment of chiral Lewis or Brønsted acids to mediate the asymmetric *N,O*-acetalisation.²⁰ Another method is the stereoselective electrochemical oxidation of α -amino acids derivatives *via* memory of chirality. It is well-known that an enantiopure starting material such as **276**, which undergoes a chemical transformation passing *via* an achiral intermediate such as a carbocation sp^2 **277**, generates the final product **278** as a racemic mixture (Scheme 4.8).



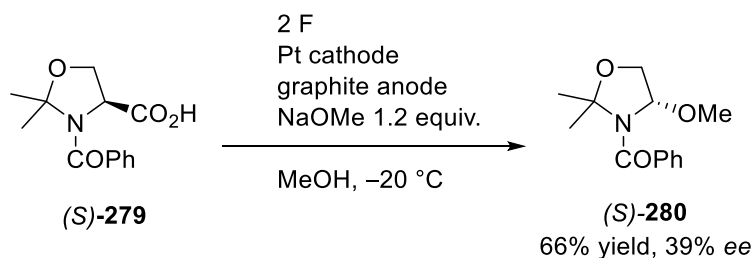
Scheme 4.8: Racemisation of a chiral starting material.

However, in some cases, the chirality in the starting material **276** bearing a chiral sp^3 carbon is preserved in the product **278**, although the reaction proceeds through an achiral intermediate such as a carbanion,²¹ a carbenium ion,²² or a monoradical²³ or a biradical species.²⁴ This phenomenon carries the name “memory of chirality” and, in order to occur, some specific requirements need to be satisfied (Scheme 4.9).²⁵



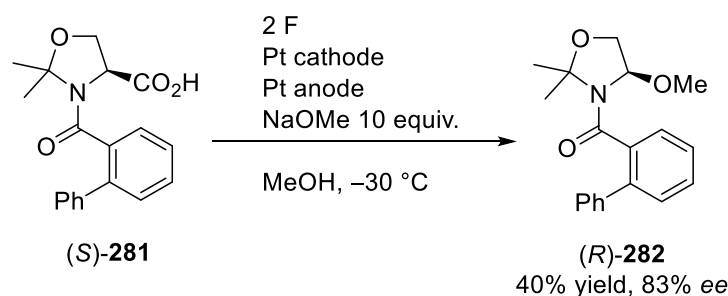
Scheme 4.9: Requirements for the memory of chirality.

Firstly, the chiral substrate undergoes a reaction at the stereogenic centre, which generates two conformationally chiral intermediates (*M*) and (*P*), and the (*M*) intermediate (*a*) is formed faster than the (*P*)-intermediate. Additionally, the racemisation rate between the two chiral intermediates (*b*) needs to be slower than the conversion of the (*M*) intermediate into the (*R*)-product (*c*), which must occur with high stereospecificity. The first example of memory of chirality *via* carbenium ion chemistry was reported by Onomura *et al.* in 2000 (Scheme 4.10).^{22a} They observed that when L-serine derivative **279** was electrochemically oxidised at $-20\text{ }^{\circ}\text{C}$ with 1.2 equivalents of NaOMe, using platinum as the cathode and graphite as the anode, the optically active α -methoxylated product **280** was afforded in good yield and with 39% of enantiomeric excess for the (*S*)-isomer.



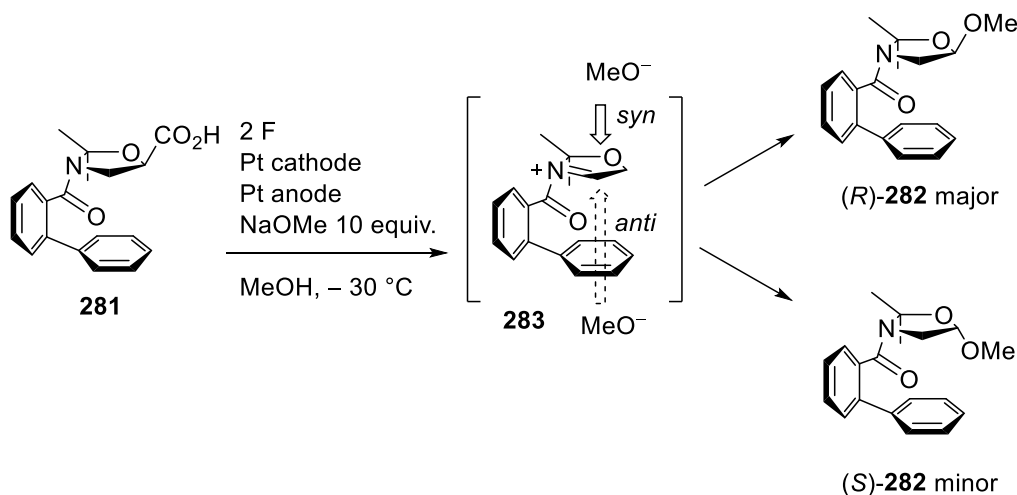
Scheme 4.10: First example of memory of chirality in carbenium ion chemistry.^{22a}

Interestingly, among all the investigated anode materials, only graphite produced optically active **280**. In particular, the substitution of the carboxyl group occurs with an inversion mechanism, possibly due to a specific interaction between the acyliminium ion intermediate and a graphite anode.^{22a} Although the exact role of the anode material on the memory of chirality it is still not clear, an interaction between the *N*-acyliminium ion intermediate **265** (Scheme 4.6) and the graphite surface was suspected. When *N*-(2-phenyl)benzyl serine derivative **281** was used for the non-Kolbe oxidation under similar conditions, the α -methoxylation occurred with retention of configuration affording the *N,O*-acetal (*R*)-**282** in moderate yields but with 72% and 83% ee when graphite or platinum were used as the anode, respectively (Scheme 4.11).^{22c}



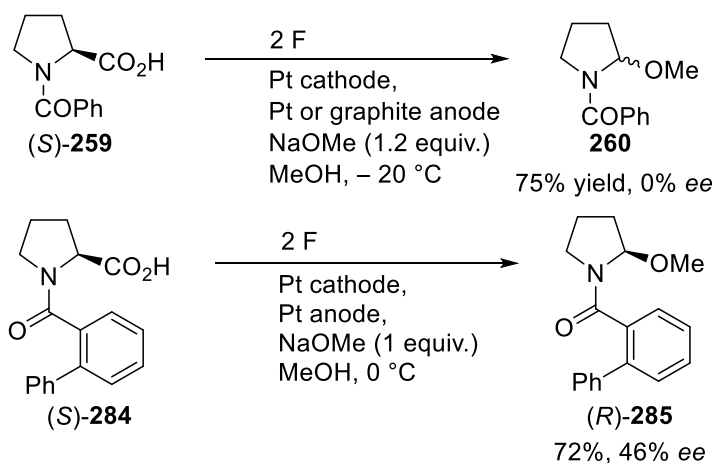
Scheme 4.11: Highly enantioselective *N,O*-acetal **282** formation via non-Kolbe electrolysis.

The same group, with the aim to explain the retained configuration, proposed a mechanism and reported **281** bearing the *ortho*-phenyl substituent underneath the carboxylic group as the most stable conformation (Scheme 4.12). According to their proposal, due to the restricted rotation caused by the bulky *ortho*-phenyl substituent, the iminium ion intermediate **283**, formed upon decarboxylation, presents one face more available towards nucleophilic attack than the other. Hence the *syn*-addition is preferred, explaining the major formation of product (*R*)-**282**.



Scheme 4.12: Proposed mechanism for the memory of chirality with retention of configuration.

When the non-Kolbe reaction is performed in a batch electrochemical cell with L-proline derivative **259**, the chirality is completely lost and the *N,O*-acetal **260** is obtained as a racemate (Scheme 4.13).^{22c} However, Onomura and co-workers found that the *N*-(2-phenyl)-benzoyl derivative **284** was able to retain some chirality, affording **285** in 72% yield and 46% ee.



Scheme 4.13: Electrochemical oxidation of L-proline derivatives (S)-259 and (S)-284.

In the following section of this thesis, the non-Kolbe oxidation of L-proline derivatives were translated into a flow electrochemical reactor setup, with the aim of optimising the memory of chirality on L-proline derivatives as well as L-acyclic amino acids derivatives. Moreover, the flow microreactor was coupled to a 2D-HPLC system for a faster analysis. Some of the following results are published in *Chem. Eur. J.* **2019**, *25*,16230–16235.

4.1.1 Continuous Flow Setup and 2D-HPLC

As illustrated in Figure 4.2, the entire continuous flow setup used for this project consisted of a syringe pump, an electrochemical microreactor connected to a power supply, a cooling system, an injecting valve (switching valve) and a 2D-HPLC.

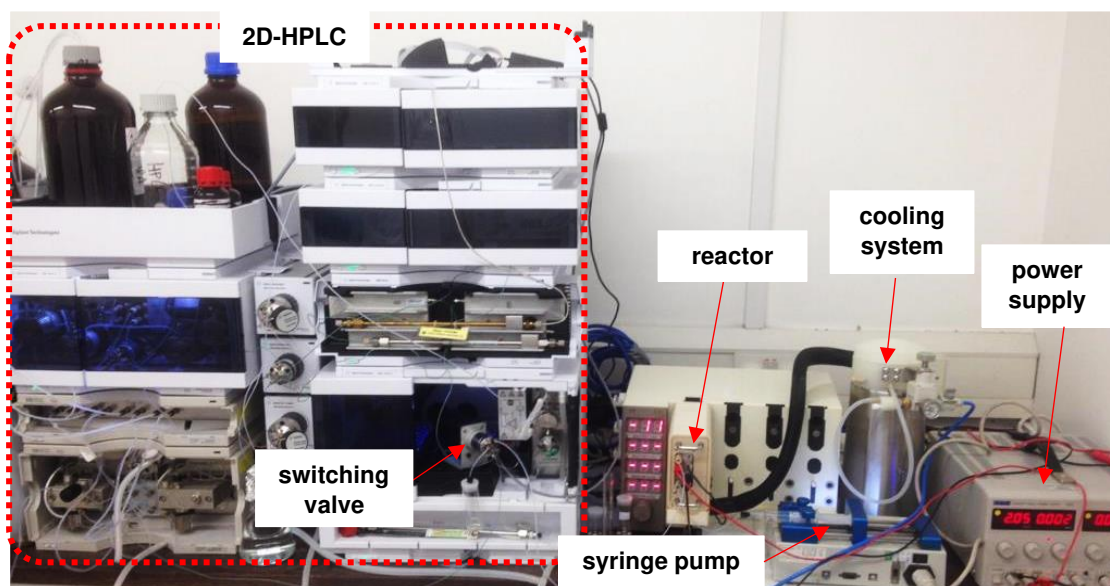


Figure 4.2: Picture of the entire continuous flow setup.

The microreactor used here was the integrated version of the Ion electrochemical reactor by Vapourtec (Figure 4.3). The reactor is composed by two electrode-carrier plates (1) supplied with a temperature sensor (2) and incorporated heat pipes (3) for temperature control. The Ion easy-clamp™ (4) holds the two electrode-carriers together allowing operations at higher pressures (up to 5 bar). Furthermore, a FEP spacer (0.5 mm thick; 5) keeps the electrodes apart and defines the reactor channel (600 μ L). The two electrodes were placed on the carriers with the FEP spacer in between, and then pressed together with the clamp. When electrodes that were supplied as a thin foil (i.e. Pt, Ni, etc.) were required, a stainless steel plate (6) was used as a backing plate to ensure the right thickness that fits into the Ion reactor and ensure a good sealing. Once assembled, the Ion reactor was located into a special housing (7) and connected with a Vapourtec E-Series. The outlet of the reactor was then connected to a 6-port switching valve bearing a 2 μ L sample loop, which was used for the online analysis.

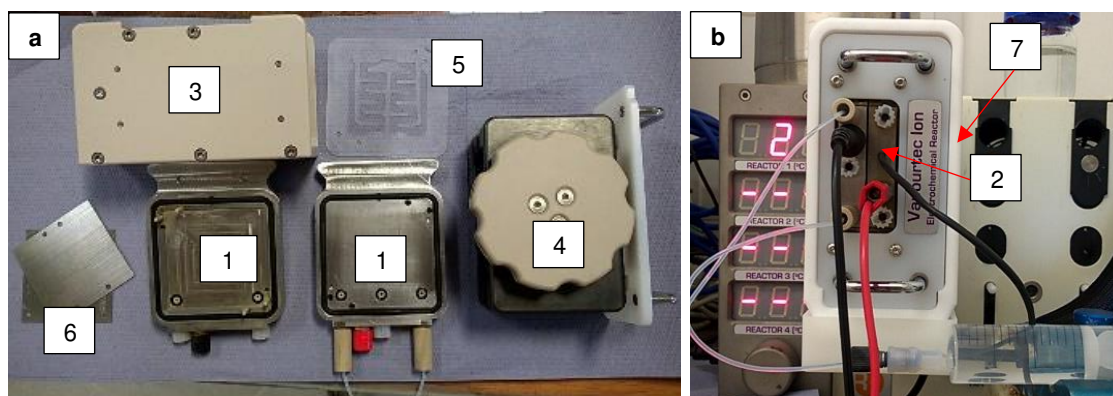


Figure 4.3: Integrated version of Ion electrochemical microreactor; a) disassembled reactor; b) operating reactor. The system is composed of: 1) two electrode-carrier plates; 2) a temperature sensor; 3) heat pipes for precise temperature control; 4) Ion easy-clamp™; 5) FEP spacer; 6) stainless steel plates; 7) housing.

4.1.2 2D-HPLC

The liquid-liquid bidimensional-chromatography (2D-LC) represents a separating technique in which the injected sample is subjected to two different separation steps. This can be achieved by using two different chromatographic columns installed in sequence with each other. The eluent is transferred from the first column into the second column, which presents a different stationary phase. Hence the elutes that were poorly resolved in the first separation can be fully separated during the second one.²⁶

The concept of liquid-liquid bidimensional separation techniques was introduced for the first time by Dent and co-workers in 1947, when they reported the separation of 19 amino acids extracted from a potato using two-dimensional paper chromatography.²⁷ However, the very first 2D-LC instrument was only developed in 1978 by Erin and Frei²⁸ and it was

until the late 1990s that the interest towards this new technique started increasing. Nowadays, 2D-HPLC is a powerful tool to resolve complex mixtures without greatly increasing the analysis time. This technique finds application in proteomics,²⁹ metabolomics³⁰ and in the pharmaceutical field.³¹

The 2D-HPLC apparatus used in this work is an Agilent Infinity 1290 2D-LC Solution, which consists of two HPLC pumps and two detectors, one for each dimension (ⁿD), an autosampler, a column oven and a set of three valves: two 14-port valves (deck A and deck B) and one 6-port valve for sampling eluent from the first dimension into the second dimension (sampler; Figure 4.4).

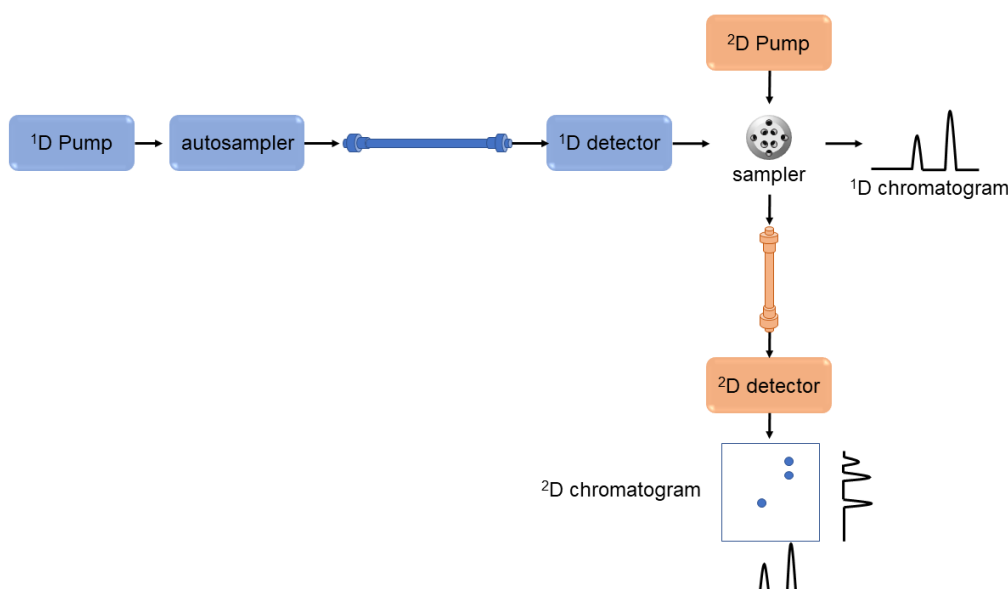


Figure 4.4: Picture of the Agilent Infinity 1290 2D-LC solution system (top) and simplified scheme of a 2D-LC system (bottom).

To perform an “offline” analysis, the samples are loaded in the autosampler, whereas for an “online” analysis a small volume of reaction mixture is injected using a 6-port valve

supplied with a sample loop and controlled by contact closure. Next, the ¹D pump pumps the sample through the ¹D column and the ¹D detector, generating a ¹D chromatogram. The ¹D eluent then reaches the sampler that, when triggered, controls which volumes from the ¹D will be analysed in the second dimension (²D) and which will go into the waste (Figure 4.5). Before going into the waste, the solution flows through deck A, continuously loading one of six loops with ¹D solution. At the same time, the ²D pump continuously flows solvent system through the valve and deck B without mixing with the ¹D solvent system. When a specific time or threshold is reached, the valve switches from the loading to the analysis position, which enables the ²D solvent system to carry the volume, contained in the loop, from deck A to the ²D column for the analysis. The amount of ¹D solvent system (40 μL) which is injected in the second dimension, can be neglected and does not contaminate the ²D eluent.

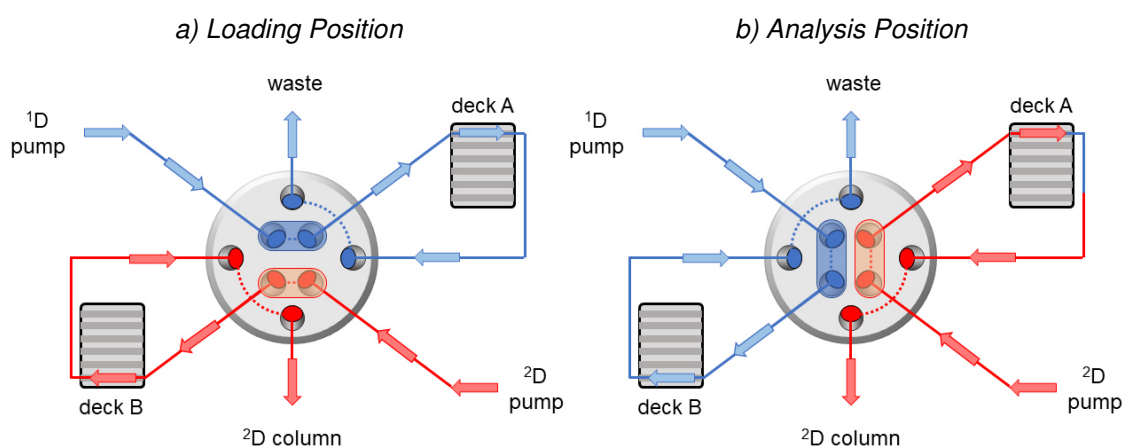


Figure 4.5: Comparison between the “loading” and the “analysis” position of the sampler.

Due to the presence of empty loops in both deck A and B, this system provides the opportunity to “park” volumes in the empty loops and analyse them in a second moment, while the second dimension is busy with a previous sample (Figure 4.6).

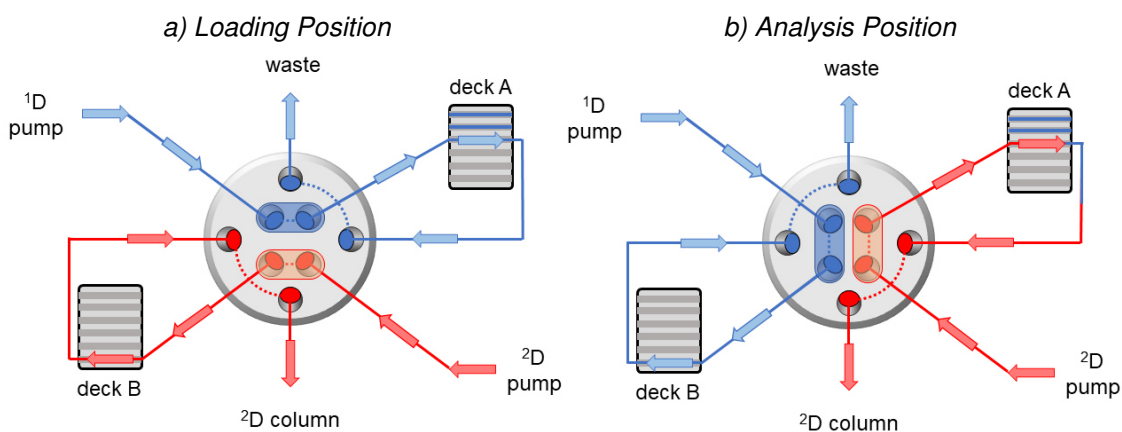


Figure 4.6: Example of “parked” volumes.

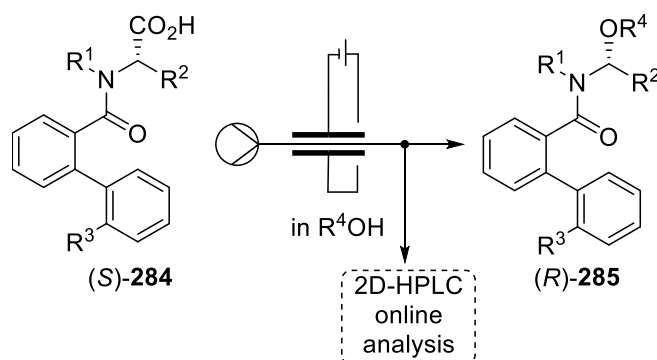
There are various ways to perform a two-dimensional analysis, depending on the reason why a 2D-LC is chosen as the separating technique. The different methods can be divided into two main groups: the comprehensive 2D-LC, also known as LC×LC, and the heart-cutting 2D-LC also known as LC-LC. During comprehensive 2D-LC (LC×LC), the ¹D eluent is continuously sampled and transferred to the second dimension, providing both ¹D and ²D analysis for the whole eluent. This technique finds application in the analysis of natural occurring complex mixtures such as natural extracts or protein mixtures.²⁹ In order to do so, the ²D analysis time must be equal or faster than the sampling time to avoid washing away samples not yet analysed. On the contrary, in the heart-cutting method (LC-LC) and multiple heart-cutting method (mLC-LC), only a few selected segments are injected into the second dimension, hence there is no time-limit for the ²D analysis. This method works better for less complex samples containing compounds with similar retention behaviour such as a mixture of isomers.

Although multi-dimensional liquid chromatography has received a lot of attention in the past decade, most applications use mainly comprehensive reverse-phase liquid chromatography (RP-LC) for highly complex mixtures,³² while the protocols using a chiral stationary phase in the second dimension for enantiomeric resolution are still limited.^{31,33}

In the following work an example of normal phase heart-cutting analysis using an achiral stationary phase in the ¹D and a chiral stationary phase in the ²D is presented.

4.2 Results and Discussion

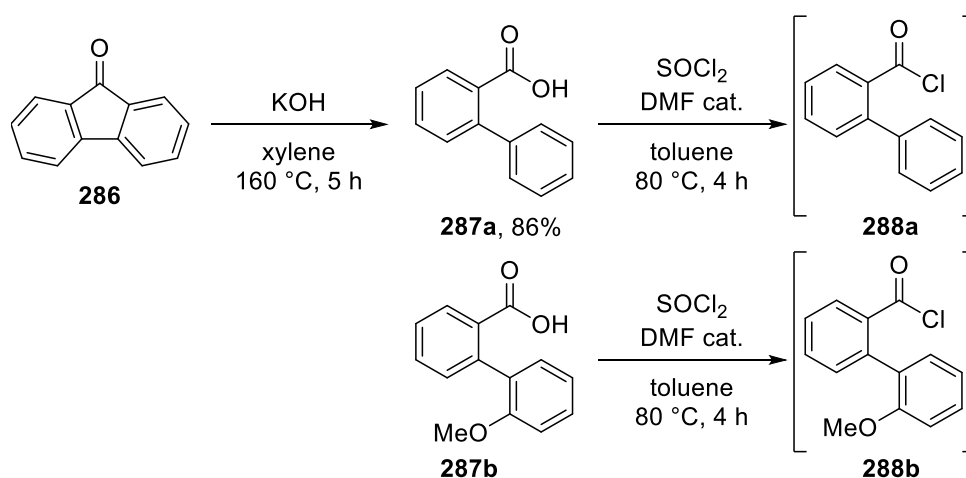
In this last chapter, the stereoselective synthesis of *N,O*-acetals **285** is presented (Scheme 4.14). The electrochemical oxidation of the *N*-protected amino acids **284** was carried out using a flow electrochemical microreactor coupled to a 2D-HPLC for online analysis. The performance of this reaction was optimised in terms of yield and the enantioselectivity using a DoE approach.



Scheme 4.14: Overview of the project for the electrochemical stereoselective synthesis of *N,O*-acetals **267** via memory of chirality.

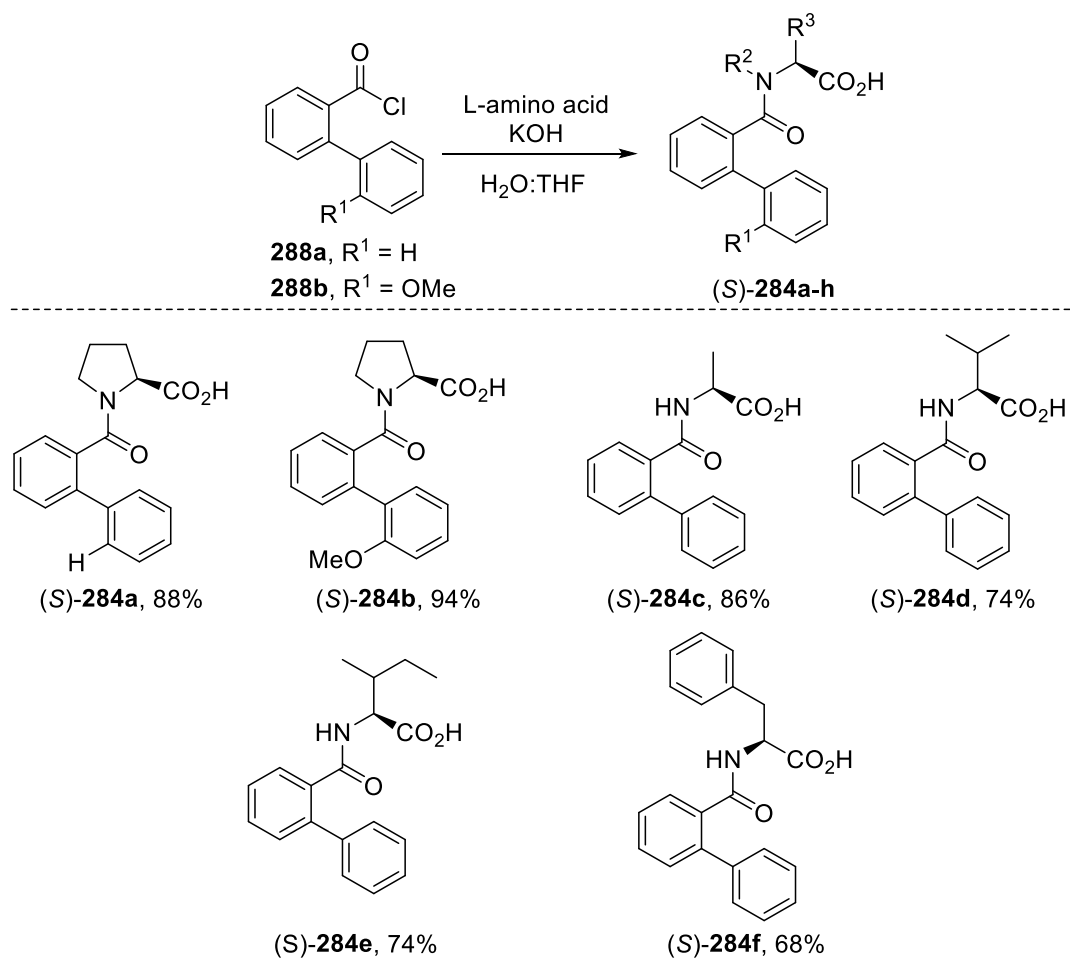
4.2.1 Synthesis of the Starting Materials and Racemates

For the synthesis of the protecting group precursor **288a**, 9-fluorenone **286** was hydrolysed using potassium hydroxide in refluxing xylene, affording the biphenyl carboxylic acid **287a** in 86% yield (Scheme 4.15). Treatment of **287a** or the commercially available **287b** with thionyl chloride and a catalytic amount of DMF, afforded the acyl chlorides **288a–b**, which were used directly for the *N*-protection step without further purification.



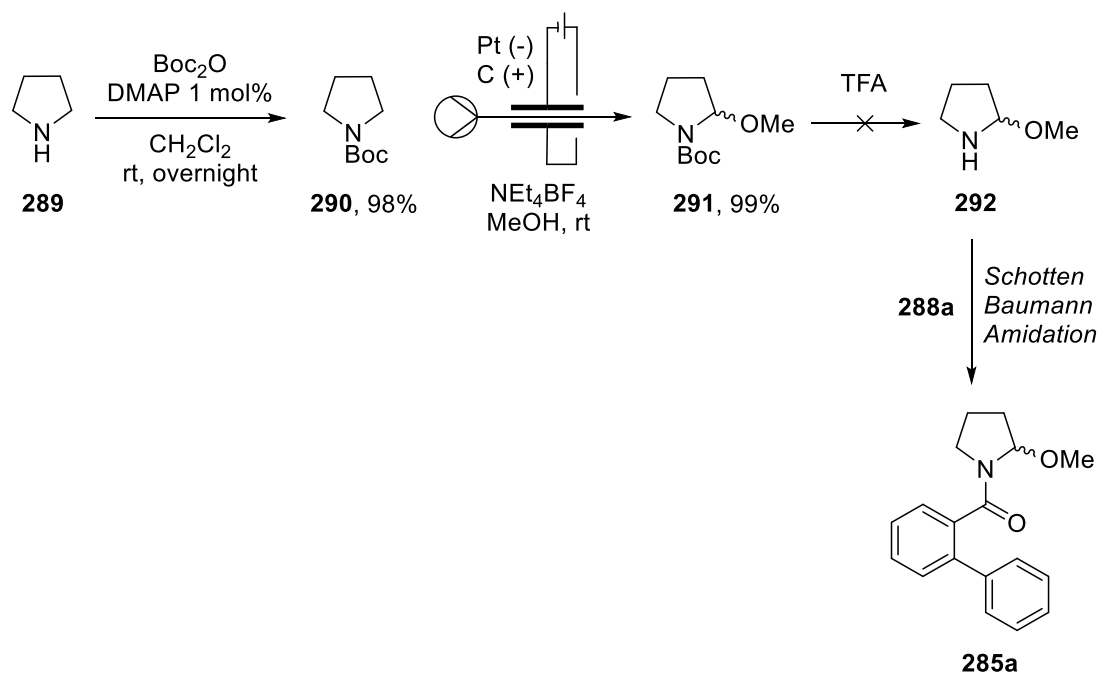
Scheme 4.15: Synthesis of *N*-protecting group precursors **288a–b**.

The chiral *N*-protected starting materials (*S*)-**284a–f** were then prepared in very good yields from the reaction of acyl chlorides **288a–b** and L-amino acids under basic conditions (Scheme 4.16).



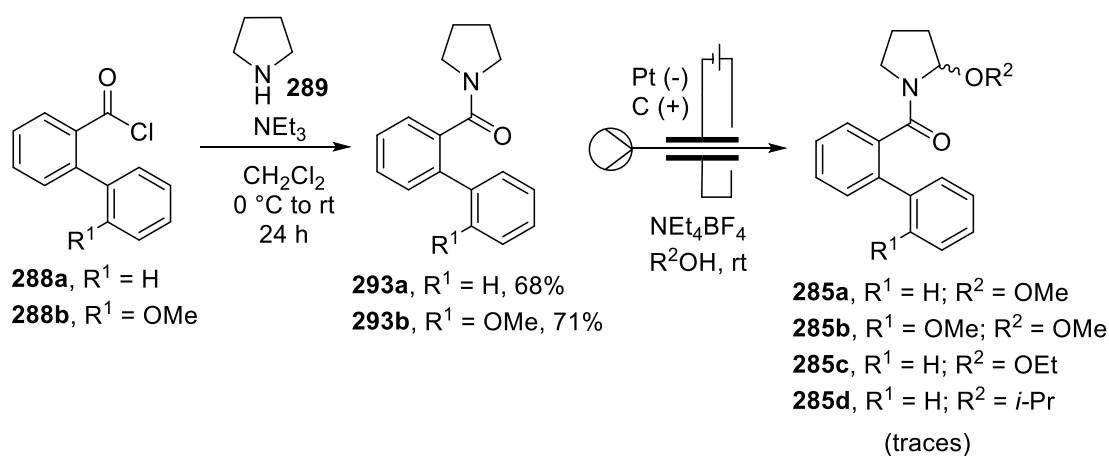
Scheme 4.16: Synthesis of chiral starting materials (*S*)-**284a–f**.

In order to find the optimal conditions for the 2D-HPLC analysis, the racemates of the final products *N,O*-acetals **285** were prepared. For the synthesis of the racemic *N*-acyl 2-methoxypyrrolidine **285a** several approaches were investigated (Scheme 4.17). First, the flow α -methoxylation of the *N*-Boc protected amine **290** was carried out, following a literature procedure.^{17c} Pyrrolidine **289** was quantitatively protected upon treatment with di-*tert*-butyl dicarbonate (Boc_2O) in the presence of a catalytic amount of DMAP. The *N*-Boc pyrrolidine **290** was then subjected to a Shono oxidation conditions in a flow microreactor, affording the α -methoxyl *N*-Boc pyrrolidine **291** also in excellent yield. However, after deprotection with trifluoroacetic acid (TFA), the α -methoxyl pyrrolidine **292** was not isolated nor detected by NMR spectroscopy, and the starting material **291** was not recovered.



Scheme 4.17: First attempts for the synthesis of racemic **285a**.

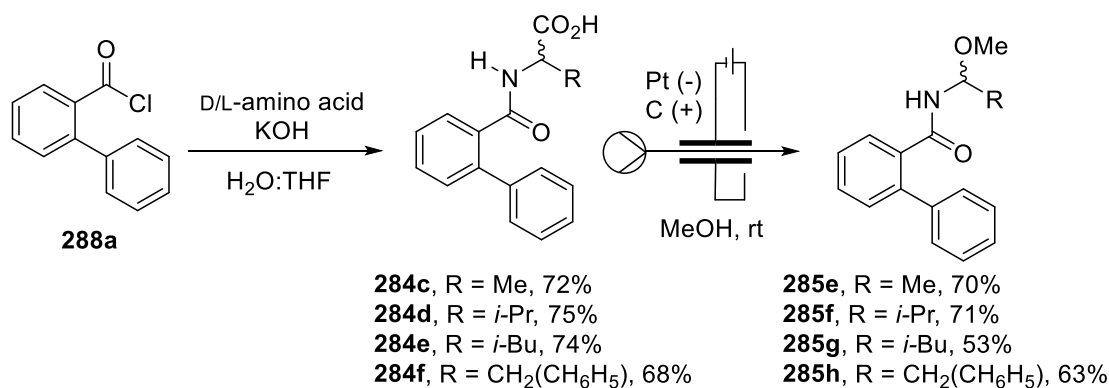
Alternatively, the Shono oxidation was carried out on the already acylated pyrrolidines **293a–b** bearing the carboxy biphenyl protecting group (Scheme 4.18).



Scheme 4.18: Second attempt for the synthesis of racemic **285a–d**.

The acyl chlorides **288a–b** were prepared as shown in Scheme 4.15 then reacted with pyrrolidine **289** affording **293a–b** in good yields. Subsequently, *N*-acyl pyrrolidines **293a–b** (0.1 M) were dissolved in methanol, ethanol or propan-2-ol and oxidised in the ion electrochemical reactor using platinum as the cathode and graphite as the anode with NEt_4BF_4 (0.02 M) as supporting electrolyte and base. The desired *N,O*-acetals **285a–d** were found only in traces together with unreacted **293a–b**, although a gas formation was observed, probably as consequence of the oxidation of the solvent as side reaction. When acyclic *N*-protected amines were investigated in the above-mentioned

Shono oxidations, no product formation was observed. Using an alternative method, the racemic *N,O*-acetals **285e–h** were afforded in moderate to good yields *via* non-Kolbe reaction from the *N*-protected amino acid **284c–f**, synthesised in good yields from the reaction of acyl chloride **288a** and D/L-alanine, D/L-valine, and D/L-phenylalanine, respectively (Scheme 4.19).



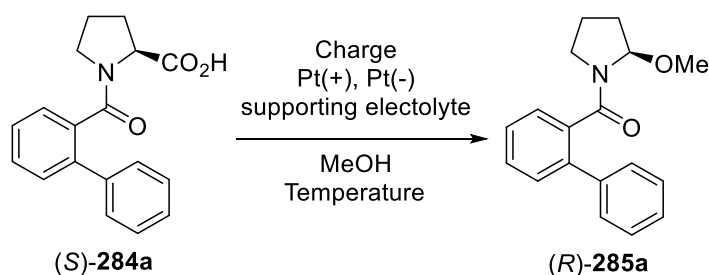
Scheme 4.19: Synthesis of racemic *N,O*-acetals **285e–h**.

4.2.2 Optimisation of Asymmetric non-Kolbe Oxidation

As previously mentioned in this chapter (Scheme 4.13), the non-Kolbe oxidations on chiral *N*-protected amino acids derivatives were found to occur with memory of chirality. With the aim of investigating the memory of chirality of a non-Kolbe oxidation in a flow electrochemical microreactor, some optimisation studies were carried out using the chiral proline derivative (*S*)-**284a** as model substrate.

When (*S*)-**284a** was reacted in a batch electrochemical cell,^a the *N,O*-acetal **285a** was formed in poor to moderate yields (up to 47%) and moderate stereoselectivity (up to 40% *ee*) when platinum was used as the anode (Table 4.1). The stereoselectivity was found to be influenced by the temperature. When the reactions were performed at –30 °C, the desired product **285a** was formed in 15% yield and 40% *ee* (entry 2). Moreover, the use of the sodium methoxide was found to be essential for the reaction in a batch electrochemical cell, as no reaction was observed without base and (*S*)-**284a** was recovered.

a. The reactions in batch were performed by Rossana Cicala.

Table 4.1: Non-Kolbe electrolysis of (*S*)-**284a** to the *N,O*-acetal **285a** in a batch electrochemical cell.^b

Entry	Base (equiv.)	T (°C)	285a yield (%) ^a	285a ee (%) ^b
1	NaOMe (10)	rt	47	30
2	NaOMe (10)	-30	15	40

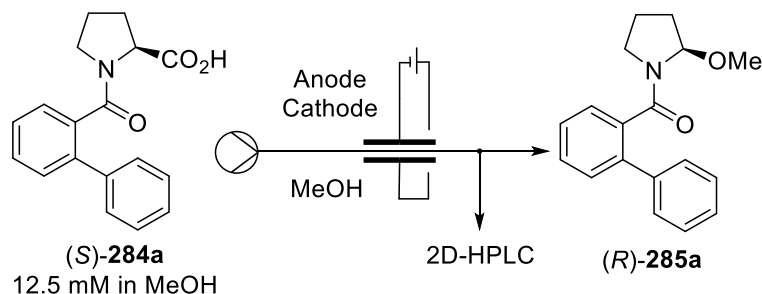
General Procedure: Reactions performed on 0.5 mmol of (*S*)-**284a** using 2 F over 1 h using 1 cm² electrodes; ^aIsolated yield; ^bDetermined by chiral HPLC; ^cOnly starting material was recovered, no current observed; ^dNo desired product formed, degradation of (*S*)-**284a** observed.

Some pilot experiments were performed using the continuous flow system in order to select the factors and the corresponding ranges to be used in the DoE (Table 4.2). When platinum was used as the anode with no supporting electrolyte or base, product **285a** was formed in poor yields (up to 12% HPLC yield) but with 32% ee which was increased to 43% ee when the reaction was carried out at -10 °C (entries 1–4). When the platinum was replaced with a graphite electrode as the anode, the *N,O*-acetal **285a** was formed in 51% HPLC yield and 31% ee. A lower concentration (6.2 mM) or a lower flow-rate (0.05 mL•min⁻¹) reduced the yield drastically (as low as 12%, entries 5–6), while at a higher flow-rate (0.2 mL•min⁻¹) **285a** was formed in 67% HPLC yield, but no effect was observed on the memory of chirality (entries 7–8). Furthermore, the reaction was found to be quantitative when the charge was doubled from 2 F to 4 F without side product formation and without losing memory of chirality (entry 9). It is worth pointing out that most of the Kolbe or non-Kolbe reactions need a base to form the active carboxylate species in order to form the final products.³⁴ Therefore, it is remarkable that quantitative yields were observed here without a base. It is suspected that in the microreactor, given the miniaturised flow conditions, the methoxide formed at the cathode was sufficient to deprotonate the starting carboxylic acid and initiate the reaction without additional base. Subsequently, different electrode materials were screened as the anode. Platinum coated on niobium showed the lowest yield with only 1% of **285a** formed although with 37% ee (entry 10). Surprisingly, when glassy carbon was used the product was formed in only 39% HPLC yield but with 65% ee of “memorised chirality” (entry 11). Other carbon-based electrodes such as

b. The reactions in batch shown in Table 4.1 were performed by Rossana Cicala.

Panasonic® Carbon, carbon on PTFE or boron doped diamond (BDD) electrodes did not show much improvements in terms of yields and stereoselectivities (entries 12–14).

Table 4.2: Pilot experiments for the asymmetric non-Kolbe oxidation of (*S*)-**284a** to **285a** in a flow microreactor using online 2D-HPLC analysis.



Entry	Anode	Cathode	Flow-rate (mL·min ⁻¹)	Charge (F)	285a (%) ^a	285a ee (%) ^b
1	Pt	Pt	0.1	2	7	32
2	Pt	Pt	0.05	2	0	-
3	Pt	Pt	0.15	2	12	32
4 ^c	Pt	Pt	0.15	2	5	43
5	graphite	Pt	0.1	2	51	31
6 ^d	graphite	Pt	0.1	2	12	27
7	graphite	Pt	0.05	2	10	30
8	graphite	Pt	0.2	2	67	30
9	graphite	Pt	0.1	4	96	30
10	Pt on Nb	Pt	0.1	2	1	37
11	glassy C	Pt	0.1	2	39	65
12	Panasonic®	Pt	0.1	2	47	19
13	C on PTFE	Pt	0.1	2	5	36
14	BDD	Pt	0.1	2	8	37
15 ^e	Pt	graphite	0.2	2	-	-
16	Pt	Pt on Ti	0.2	4	6	41
17	Pt	Pt on Nb	0.2	4	3	45

General Procedure: Reactions performed using different electrodes, FEP spacer 0.5mm thickness; reactor volume: 600 μ L, working area: 12 cm², with no additional supporting electrolyte or base; ^aHPLC yield (¹D) with α,α -trifluorotoluene as internal standard; ^bDetermined by chiral HPLC (²D); ^cReaction performed at -10 °C; ^dReaction performed on a 6.2 mM solution of (*S*)-**284a**; ^eNo reaction observed.

At last, different electrodes materials were screened at the cathode using platinum as the anode (entries 15–17). Although **285a** was formed with more than 40% *ee*, the yields were very low even when the reactions were performed at $0.2 \text{ mL}\cdot\text{min}^{-1}$ and with 4 F. Hence, the platinum electrode was chosen as the cathode for the rest of the studies whereas the anode material was included in the design as one of the factors.

After this preliminary screening, the following two-level fractional factorial design (FFD 2^{5-1} ; see Appendix A for glossary) was designed with four numeric factors (temperature, charge, flow-rate and concentration of (*S*)-**284a**) and one categoric factor (anode material). Among all the screened anodes, graphite was chosen for the better yields, while the glassy carbon was selected because despite the lower yields it was found to generate **285a** with the highest memory of chirality giving the highest *ee*. The two responses (yield and *ee*%) were measured using online 2D-HPLC analysis. In particular, the yield was measured in the first dimension on an achiral stationary phase, while the enantiomeric excess was measured in the second dimension on a chiral stationary phase. The whole design was composed of a total of 24 experiments, 16 factorial points and 8 central points, and they were performed in a random order to minimise nuisance (see Appendix A). Once the acquired data were fitted into the model, the analysis of variance (ANOVA) was carried out next. The models were found to be very complex, with numerous significant terms and some anomalies in the diagnostic plots. From one of the influential plots (Cook's distance, Figure 4.7), two factorial points (Table 4.3, entries 1 and 3) with very low yields and enantioselectivities were found to be outliers (see Appendix A), increasing the degree of complexity.

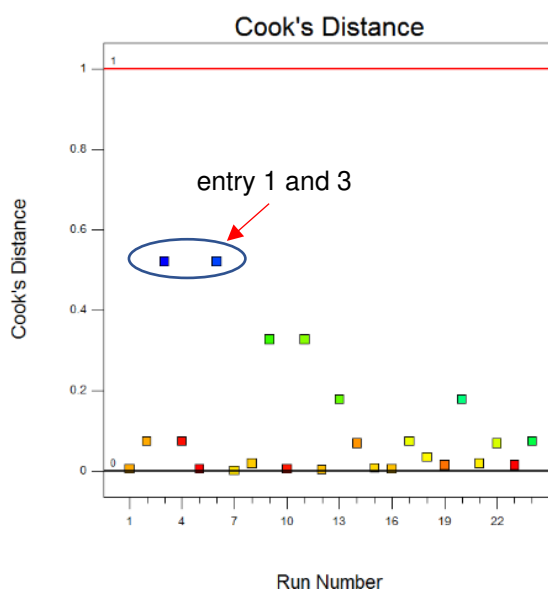


Figure 4.7: Cook's distance plot showing outliers. The different yields are represented by a scale of colours from blue (= low yields) to red (= high yields).

After several repeats of the two factorial points and a careful evaluation, it was decided to not include these two experiments (Table 4.3, entries 1 and 3) in the analysis, considering they were leading into a less interesting region of the chemical space (low yield and low enantioselectivity).

Table 4.3: Matrix for the FFD 2^{5-1} with results. Factor generator for E = A*B*C*D.

Std	Run order	Factors					Responses	
		A: (S)-284a (mM)	B: Anode	C: Flow rate (mL·min ⁻¹)	D: Charge (F)	E: T (°C)	Yield (%) ^a	ee (%) ^b
1	3	6.25	graphite	0.1	2	20	10	31
2	17	12.5	graphite	0.1	2	-10	76	24
3	6	6.25	glassy C	0.1	2	-10	16	31
4	24	12.5	glassy C	0.1	2	20	49	50
5	13	6.25	graphite	0.2	2	-10	64	25
6	11	12.5	graphite	0.2	2	20	67	29
7	20	6.25	glassy C	0.2	2	20	44	48
8	9	12.5	glassy C	0.2	2	-10	60	70
9	10	6.25	graphite	0.1	4	-10	98	23
10	4	12.5	graphite	0.1	4	20	99	27
11	16	6.25	glassy C	0.1	4	20	83	25
12	2	12.5	glassy C	0.1	4	-10	85	64
13	23	6.25	graphite	0.2	4	20	100	28
14	5	12.5	graphite	0.2	4	-10	100	25
15	19	6.25	glassy C	0.2	4	-10	90	60
16	1	12.5	glassy C	0.2	4	20	85	60
17	14	9.37	graphite	0.15	3	5	87	22
18	15	9.37	glassy C	0.15	3	5	81	57
19	21	9.37	graphite	0.15	3	5	79	20
20	22	9.37	glassy C	0.15	3	5	74	55
21	12	9.37	graphite	0.15	3	5	83	25
22	8	9.37	glassy C	0.15	3	5	82	58
23	18	9.37	graphite	0.15	3	5	78	25
24	7	9.37	glassy C	0.15	3	5	80	54
25	1	6.25	graphite	0.1	2	20	11	28
26	3	6.25	glassy C	0.1	2	-10	17	32
27	3	6.25	glassy C	0.1	2	-10	15	30
28	3	6.25	glassy C	0.1	2	-10	20	34

General Procedure: Reactions were performed according to Table 4.3; ^aHPLC yield (¹D) with α,α,α -trifluorotoluene as internal standard; ^bDetermined by chiral HPLC (²D); Light blue = these experiments were not included in the ANOVA.

Although removing two factorial points may compromise the spot-prediction ability of the model, it was possible to simplify the model and have scientifically meaningful results (Figure 4.8). From the pareto charts (see Appendix A) it emerged that the most significant parameter for the yield of the electrochemical oxidation was the charge (D; Figure 4.8a). Although a charge of 2 F should be sufficient for two consecutive single

electron-transfer reactions, the desired methoxylated amide **285a** was obtained in good to quantitative yields (>80%) when a charge of 4 F was applied. Better yields were observed when graphite was used instead of glassy carbon as the anode, which was also suggested by the ANOVA, identifying a minor effect of the type of anode (B) on the yield (Figure 4.8a).

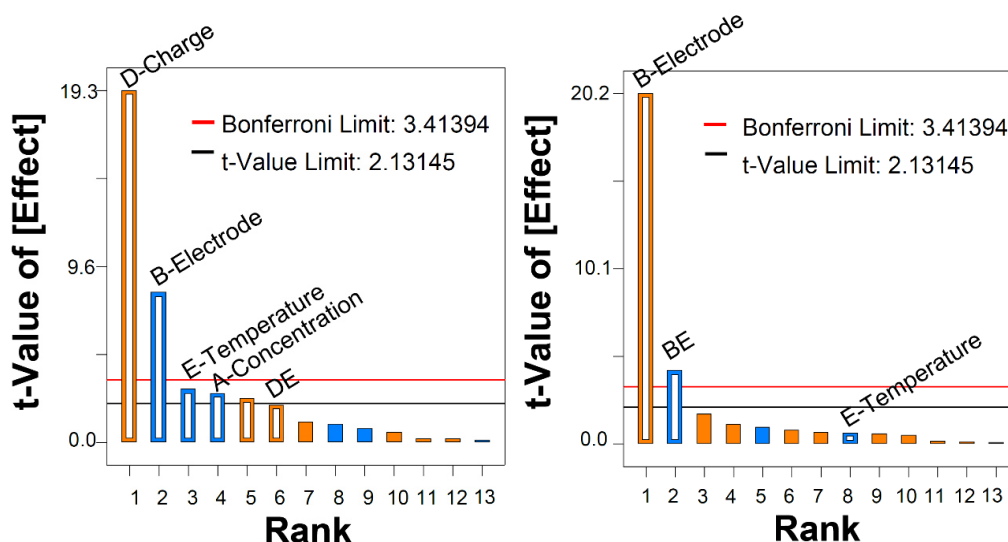


Figure 4.8: Pareto charts showing main effects for the responses a) yield % and b) ee%.

These effects can also be visualised in the 3D-surface plots for the first response (yield) with the concentration of (*S*)-**284a** and the charge as variables, and the flow rate as well as the temperature fixed (Figure 4.9). First of all, both 3D-surfaces for the yield present sharp slopes which indicates a yield improvement when the number of electrons was increased from 2 F to 4 F. Secondly, when the glassy carbon was selected as the anode, the whole surface shifted toward lower yields, highlighting the effect of the anode material on the *N,O*-acetal formation.

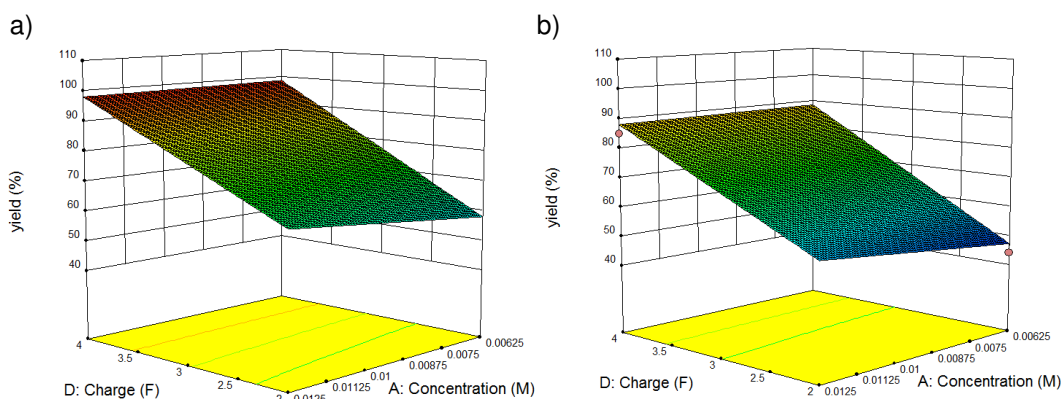


Figure 4.9: 3D-surface plots of the yield of **285a** when a) graphite or b) glassy carbon was used in the non-Kolbe oxidation at 23 °C and 0.2 mL·min⁻¹.

On the other hand, the most critical factor for the second response (enantioselectivity) was the type of material used as anode. In particular, when the oxidation of (*S*)-**284a** was performed using glassy carbon at $0.2 \text{ mL}\cdot\text{min}^{-1}$, **285a** was afforded in moderate (48% *ee*) to good enantioselectivity (70% *ee*), whereas graphite showed only moderate selectivity (up to 31% *ee*). Although the relation between anode material and memory of chirality is still unclear, this result is in agreement with previous studies in which an interaction between the carbenium ion and the electrode surface was suspected.^{22a}

On the other hand, the temperature itself (E) was not found to be significant for the memory of chirality of this transformation, in contrast with what was observed for the electrolysis in batch.²² A moderate two-factor interaction (2FI) between type of anode and temperature (BE) was observed. Figure 4.10 shows the 3D-surface plots for the second response (% *ee*) with temperature and flow-rate as variable and charge and the concentration of (*S*)-**284a** as fixed values. When graphite is selected, the surface slope remains relatively flat as the temperature decreases (Figure 4.10a), whereas by selecting the glassy carbon as anode, the surface shifts to generally better *ee*% and the memory of chirality increases as the temperature decreases (Figure 4.10b). Hence, the temperature effect changes depending on the anodic electrode.

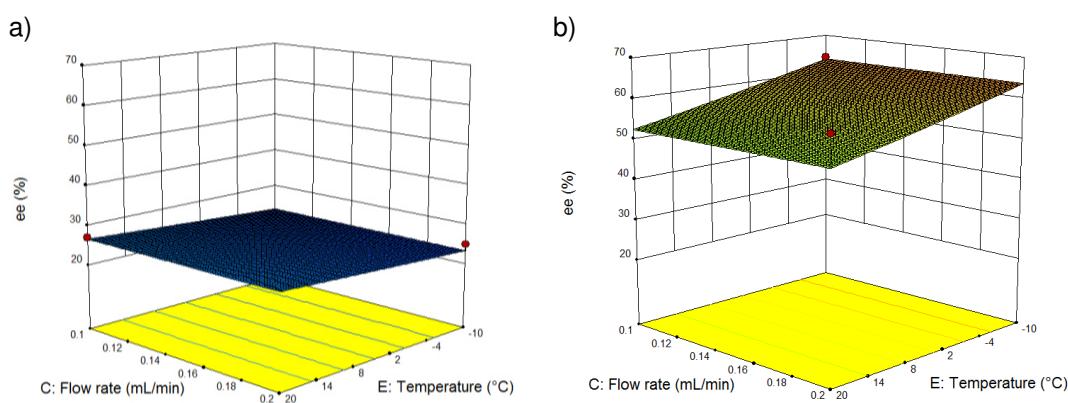
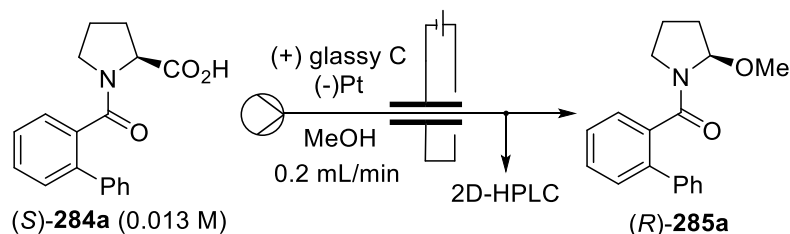


Figure 4.10: 3D-surface plots of the *ee* in % of **285a** when a) graphite or b) glassy carbon was used in the non-Kolbe oxidation performed with 12.5 mM of (*S*)-**284a** and 4 F.

Although the spot-prediction ability of these models had been compromised by ignoring two factorial points, the simplified model was still good enough to provide a set of optimal conditions, guiding towards the “sweet spot” (Table 4.4). Glassy carbon was chosen as optimal anode in order to have the highest memory of chirality, and the reactions were performed on a 12.5 mM solution of (*S*)-**284a** in methanol pumped at $0.2 \text{ mL}\cdot\text{mol}^{-1}$. When a charge of 2 F was used at room temperature or at $-10 \text{ }^\circ\text{C}$, the *N,O*-acetal **285a** was formed in 55% and 60% yield and with 64% and 70% of enantiomeric excess, respectively (entries 1 and 2). The yields were increased up to 73% and 77% by using

3 F and 4 F, respectively, in good stereoselectivity (>60% *ee*; entries 3–4). Furthermore, the desired product **285a** was formed in 81% HPLC yield and with 66% *ee* when (*S*)-**284a** was oxidised at –10 °C (entry 5).

Table 4.4: Optimised conditions for the asymmetric non-Kolbe oxidation of (*S*)-**284a**.



Entry	Charge (F)	Temperature (°C)	285a (%) ^a	285a <i>ee</i> % ^b
1	2	23	55	64
2	2	–10	60	70
3	3	23	73	62
4	4	23	77	60
5	4	–10	81	66

General Procedure: Reactions were performed using a glassy carbon anode and a Pt cathode, a FEP spacer (0.5 mm thickness; reactor volume: 600 μ L; working area: 12 cm²) with no additional supporting electrolyte or base; ^aHPLC yield (¹D) with α,α,α -trifluorotoluene as internal standard; ^bDetermined by chiral HPLC (²D).

With these results in hand other anode materials were screened under the optimised conditions at different temperatures (Table 4.5).

Table 4.5: Further screening of the anode influence on the anodic oxidation of (*S*)-**284a** to *N,O*-acetal **285a**.

Entry	Anode	Temperature (°C)	285a (%) ^a	285a <i>ee</i> % ^b
1	Pt	23	4	49
2	Pt	0	11	53
3	Pt	–10	13	51
4	Pt on Nb	23	8	48
5	Pt on Nb	–10	14	48
6	Pt on Ti	23	8	51
7	Pt on Ti	0	9	52
8	Pt on Ti	–10	12	54
9	BDD	23	51	57
10	BDD	0	58	58
11	BDD	–10	54	60

General Procedure: Reactions were performed on a 13 mM solution of (*S*)-**284a** with 4 F of charge, different electrodes as anode and Pt cathode electrodes, a FEP spacer (0.5mm thickness; reactor volume: 600 μ L; working area: 12 cm²) with no additional supporting electrolyte or base; ^aHPLC yield (¹D) with α,α,α -trifluorotoluene as internal standard; ^bDetermined by chiral HPLC (²D); BDD = boron doped diamond.

The platinum and platinum coated electrodes showed very poor yields even using higher charge, however the memory of chirality was improved to 48–54% *ee* compared to the ~30% *ee* observed in the initial pilot study (see Table 4.2). Moreover, except the platinum coated niobium, which was not affected by the temperature (Table 4.5, entries 4–5), a small improvement in *ee*% was observed for the platinum and the platinum coated titanium electrode. However, among all anodes, BDD was found to almost as efficient as the glassy carbon (entries 9–11). In fact, BDD formed the desired *N,O*-acetal **285a** in good yields (up to 58%) and in 57%, 58% and 60% *ee* for reactions performed at 20 °C, 0 °C and –10 °C, respectively.

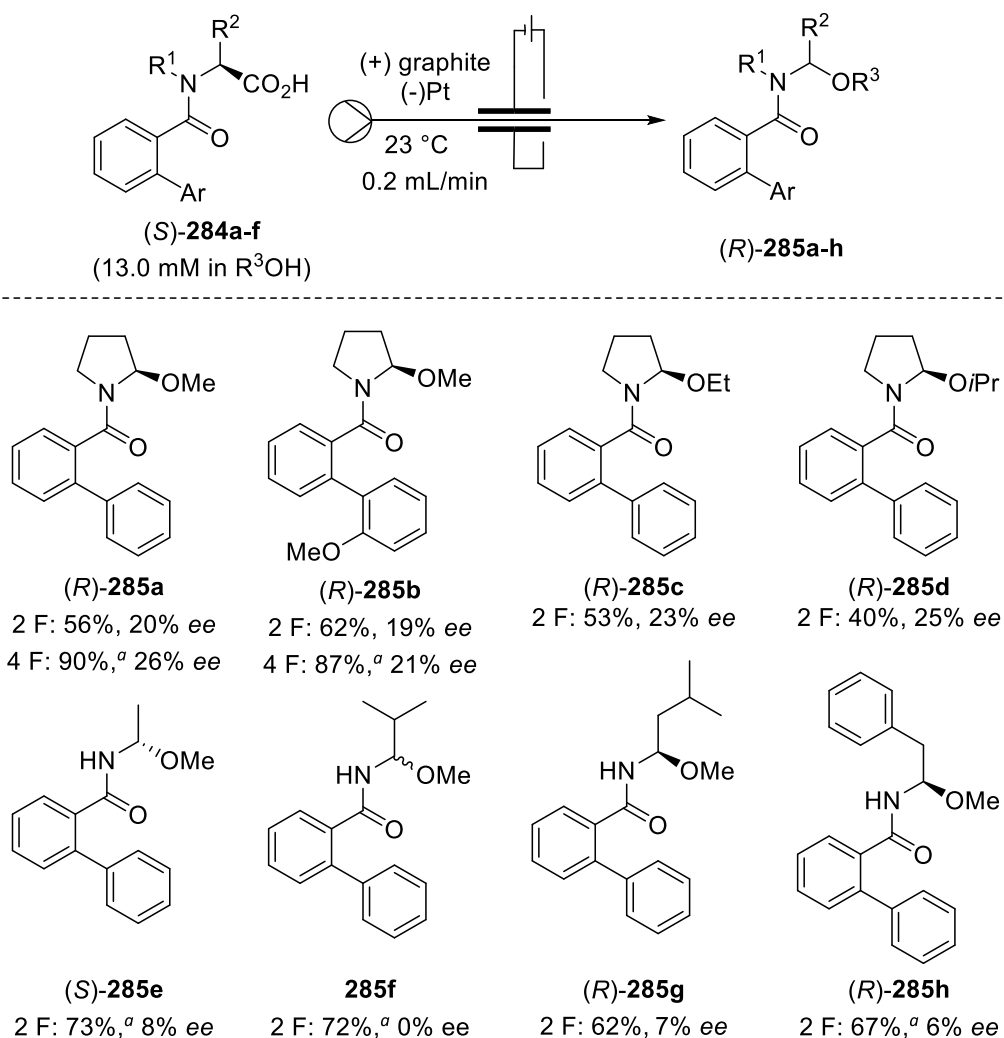
In conclusion, the final screening performed in a flow microreactor confirmed that, the memory of chirality was mainly influenced by the anodic material. However, it seemed to be less influenced by lower temperatures than what was observed in the batch process. For optimal memory of chirality results, the glassy carbon electrode was chosen as anodic material for future studies over the BDD because the latter was found to promote side reactions.

4.2.3 Substrate Scope

With the aim to study the substrate scope and to calculate the isolated yields, different *N*-protected amino acids (*S*)-**284a–f** (see Scheme 4.16) were subjected to the electrochemical oxidation using the optimal conditions suggested by the DoE.

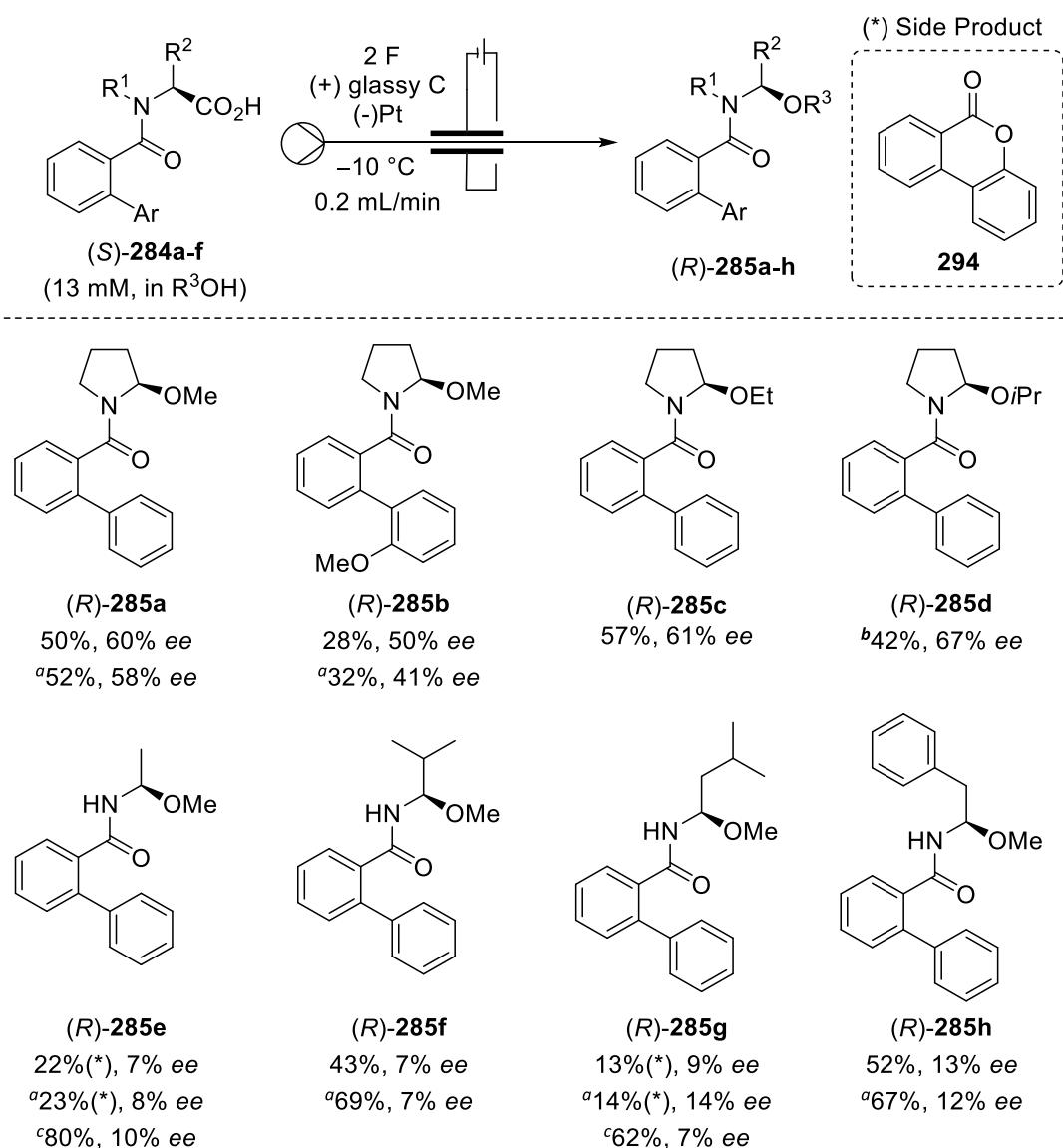
Firstly, the *N*-acyl amino acids were oxidised using graphite as optimal anodic material for the yield, with 2 F or 4 F of charge at room temperature (Scheme 4.20). The solutions of starting material were pumped at 0.2 mL·min⁻¹ and the microreactor was kept at 23 °C. The stream were equilibrated for ~20 minutes before being collected for 1.5 hours, then the *N,O*-acetals **285a–h** were isolated and the *ee*% was measured offline on the pure products. The model *N,O*-acetal **285a** and the 2-methoxyphenyl derivative **285b** were isolated in 56% and 62% yield, when 2 F were applied, and in 90% and 87% yield, when 4 F were used instead. When the electrolysis of (*S*)-**284a** was performed using 2 F in ethanol or propan-2-ol instead of methanol, the desired products **285c** and **285d** were afforded in 53% and 40% yields, respectively. When the reactions were attempted with more electricity (>2 F), remarkably high voltages were observed, probably due to the lower conductivity of the solvents, and the reactions had to be stopped. This issue may be avoided by using supporting electrolytes or a base to help the conductivity of the electrons between the electrodes. On the other hand, the acyclic amino acid derivatives (*S*)-**284c–f** were fully consumed with 2 F of charge, and the desired products **285e–h** were isolated in good yields (up to 73%). As expected, the graphite anode did not provide

great memory of chirality. In particular, the pyrrolidine derivatives **285a–d** were afforded in moderate enantioselectivities (up to 26% *ee*), whilst less constrained derivatives **285e–h** were formed with poor or no selectivity. Interestingly, when the electrolysis was performed on the sterically less hindered L-alanine derivative **284c**, the (*S*)-**285e** was found as the major isomer in 8% *ee*, in contrast with the observation for the other substrates and with what is reported in literature.^{22b,35} Nevertheless, the hypothesis of an inversion of configuration seemed possible as in agreement with what reported for substrates bearing less a bulky *N*-protecting group.^{22a} Moreover, no enantioselectivity was observed for the isopropyl-substituted **285f**, while the *N,O*-acetals **285g–h** bearing bulkier alkyl chains were formed as (*R*)-isomers, which supports the hypothesis of a relation between bulkier substrates and retention of configuration.



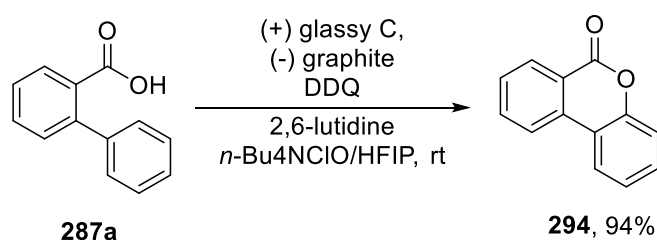
Scheme 4.20: Reactions were performed at 23 °C on a 13 mM scale of (*S*)-**284a–f** using a graphite anode and a Pt cathode, a FEP spacer (0.5mm thickness; reactor volume: 600 μ L; working area: 12 cm²) with no additional supporting electrolyte or base; Isolated yields are shown; the absolute configuration for **285a** was assigned according to literature,³⁵ and for **285b–h** were assigned in analogy to **285a**. ^aNo starting material detected by ¹H NMR.

The same library of compounds (*S*)-**284a–f** was then subjected to oxidation using the optimal conditions for the memory of chirality reported in Table 4.4, entry 2 (Scheme 4.21). The solutions of starting material were pumped at 0.2 mL•min⁻¹ and the microreactor was cooled to -10 °C. Again, the solutions were equilibrated for ~20 minutes before being collected for 1.5 hours, then the *N,O*-acetals **285a–h** were isolated and the *ee*% was measured offline on the pure products.



Scheme 4.21: Reactions were performed at -10 °C on a 0.13 mmol (13 mM solution) of (*S*)-**284a–f** using a glassy carbon anode and a Pt cathode, a FEP spacer (0.5 mm thickness; reactor volume: 600 μL; working area: 12 cm²) with no additional supporting electrolyte or base; Isolated yields are shown; the absolute configuration for **285a** was assigned according to literature,³⁵ and for **285b–h** were assigned in analogy with **285a**. ^aReaction performed on a 1.25 mmol scale (50 mM solution); ^bReaction performed at 0.1 mL•min⁻¹; ^cReactions performed on recrystallised starting materials at room temperature; (*) Reactions in which the side product **294** was formed.

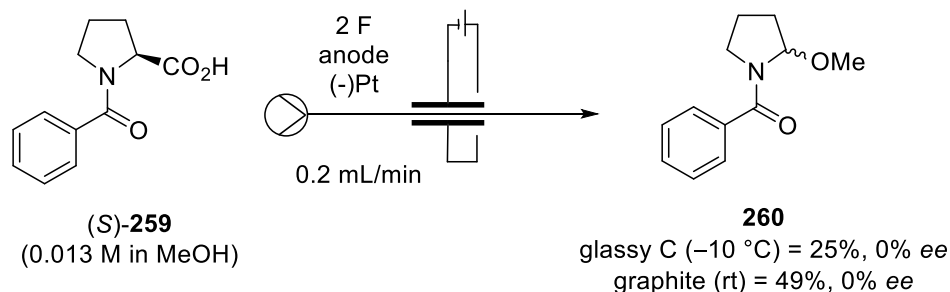
Generally, the products **285a–h** were isolated in poor to good yields and with poor to good enantioselectivity. The model substrate **285a**, was isolated in 50% yield with 60% *ee*. When a more electron-rich biphenyl group was used, the corresponding *N,O*-acetal **285b** was isolated only in 28% yield with 50% *ee*. When the electrolysis of (*S*)-**284a** was performed in ethanol or propan-2-ol instead of methanol, the desired products **285c** and **285d** were isolated in 57% and 42% yield with 61% *ee* and 67% *ee*, respectively. When the reaction was performed in propan-2-ol the flow rate was reduced to 0.1 mL·min⁻¹ to avoid an unsafe high voltage, since the conductivity was lower in this solvent. A moderate memory of chirality was also observed in non-constrained acyclic amino acids (*S*)-**284c–f**, which increased with the steric demand of the side chain with **285e–h** formed in 7–14% *ee*. Furthermore, when the oxidation was performed on L-alanine and L-leucine derivatives (*S*)-**284c** and (*S*)-**284e**, the products **285e** and **285g** were isolated only in 22% and 13% yield, respectively, along with the side product **294** isolated in 17% and 30% yield, respectively. This was not the case for L-valine and L-phenylalanine substrates (*S*)-**284d** and (*S*)-**284f**, which formed the tricyclic compound **294** in less than 10% yield, and the corresponding *N,O*-acetal **285f** and **285h** in 43% and 52% yield, respectively. The formation of benzocoumarin derivatives such as **294** was recently reported as product of the electrochemical cyclisation of 2-arylbenzoic acids such as **287a** (Scheme 4.22).³⁶



Scheme 4.22: Electrochemical C–H lactonization of aromatic carboxylic acids **287a**.³⁶

Therefore, a second recrystallisation of (*S*)-**284c** and (*S*)-**284e** was performed to remove any traces of 2-arylbenzoic acid **287a**. The recrystallised (*S*)-**284c** and (*S*)-**284e** were then subjected to electrolysis with glassy carbon at room temperature affording **285e** and **285g** in 80% and 62% yield, respectively. In this case, when the electrolysis on (*S*)-**284c** was performed with glassy carbon as the anode, the (*R*)-**285e** enantiomer was formed as the major enantiomer with 7–10% of enantiomeric excess, instead of the (*S*)-isomer which was formed as the major product with a graphite anode. For a further scale-up, higher concentrated solutions (0.05 M, 1.25 mmol scale) were used and it was possible to reproduce the same results without a remarkable loss in reactivity or enantioselectivity.

Finally, to prove the importance of the biphenyl substituent on the memory of chirality, the benzoyl L-proline **259**, prepared from benzoyl chloride and L-proline, was subjected to the non-Kolbe oxidation in the flow microreactor. As expected, **260** was obtained as racemate regardless the type of anode used. (Scheme 4.23).



Scheme 4.23: Flow non-Kolbe oxidation of (S)-**259**.

In summary, the DoE conclusions were confirmed also in the substrate scope with the graphite anodes affording the desired products in better yields and the glassy carbon anodes providing generally better *ee*. Moreover, some moderate memory of chirality was observed also in unstrained substrates, albeit still poor (up to 14% *ee*). Additionally, the presence of the biphenyl *N*-protecting group was confirmed to be fundamental for the memory of chirality in the flow process, as already reported for the batch electrolysis.^{22a}

4.3 Conclusions and Outlook

To conclude, the asymmetric electrochemical non-Kolbe oxidation of *N*-acyl L-proline was successfully translated into a flow electrochemical microreactor coupled to an online 2D-HPLC and the reaction was optimised using a DoE-approach. The short reaction times combined with a fast analysis time made it possible to rapidly screen charges as well as electrodes, flow rates, concentrations and temperatures. The graphite anodes were found to provide good to quantitative yields, while the best memory of chirality (70% *ee*) was achieved using glassy carbon anodes. The optimal conditions were then applied to the synthesis of a series of cyclic and acyclic *N,O*-acetals in moderate to good yields and enantioselectivities. These results proved the concept that the combination of a flow system coupled with an online 2D-HPLC and DoE offers an efficient method to intensively screen several parameters and quickly optimise reactions. Hence, the presented methodology might find useful applications in the optimisation of other asymmetric transformations. Future work is focussed on the complete automation of such systems with all units (reactor and HPLC) controlled by a computer.

The absolute configuration of the final products has been assigned according to literature, however the crystallisation of one of the final *N,O*-acetals could be included as part of the future work as further evidence.

Moreover, all the reactions were performed without any supporting electrolytes nor base. Although most of the Kolbe or non-Kolbe reactions need a base to form the active carboxylate species, in the flow microreactor the methoxide formed at the cathode is suspected to be enough to deprotonate the starting material and initiate the reaction. Further studies should be included in the future work to fully understand the mechanism behind this unusual base-free non-Kolbe electrolysis. Furthermore, it might be interesting to study the electrolysis in the presence of supporting electrolytes, which can be used to improve yields especially in less conductive solvents.

Future work should also investigate the role of the electrode type in the memory of chirality, which remains still unclear. For example, electrode-surface modifications might give some insights on the electrode/acyliminium ion interaction or on how to further improve the memory of chirality.

References

- 1 R. A. Mosey, P. E. Floreancig, *Nat. Prod. Rep.* **2012**, *29*, 980–995.
- 2 a) R. H. Cichewicz, F. A. Valeriote, P. Crews, *Org. Lett.* **2004**, *6*, 1951–1954; b) G. R. Pettit, J.-P. Xu, J.-C. Chapuis, R. K. Pettit, L. P. Tackett, D. L. Doubek, J. N. A. Hooper, J. M. Schmidt, *J. Med. Chem.* **2004**, *47*, 1149–1152.
- 3 S. Wan, F. Wu, J. C. Rech, M. E. Green, R. Balachandran, W. S. Horne, B. W. Day, P. E. Floreancig, *J. Am. Chem. Soc.* **2011**, *133*, 16668–16679.
- 4 For selected examples see: a) N. Yamazaki, T. Ito, C. Kibayashi, *Org. Lett.* **2000**, *2*, 465–467; b) M. Sugiura, H. Hagio, R. Hirabayashi, S. Kobayashi, *J. Am. Chem. Soc.* **2001**, *123*, 12510–12517; c) P. Gizecki, R. Dhal, C. Poulard, P. Gosselin, G. Dujardin, *J. Org. Chem.* **2003**, *68*, 4338–4344.
- 5 a) T. J. A. Graham, J. D. Shields, A. G. Doyle, *Chem. Sci.* **2011**, *2*, 980–984; b) K. T. Sylvester, K. Wu, A. G. Doyle, *J. Am. Chem. Soc.* **2012**, *134*, 16967–16970; c) T. Johnson, M. Lautens, *Org. Lett.* **2013**, *15*, 4043–4045; d) T. Johnson, B. Luo, M. Lautens, *J. Org. Chem.* **2016**, *81*, 4923–4930.
- 6 a) A. R. Katritzky, J. Pernak, W.-Q. Fan, F. Saczewski, *J. Org. Chem.* **1991**, *56*, 4439–4443; b) A. R. Katritzky, W.-Q. Fan, M. Black, J. Pernak, *J. Org. Chem.* **1992**, *57*, 547–549.
- 7 a) J. A. Murray, D. E. Franz, A. Soheili, R. Tilleyer, E. J. J. Grabowski, P. J. Reider, *J. Am. Chem. Soc.* **2001**, *123*, 9696–9698; b) S. N. George, M. Bekkaye, G. Masson, J. Zhu, *Eur. J. Org. Chem.* **2011**, 3695–3699.
- 8 A. Bayer, M. E. Maier, *Tetrahedron* **2004**, *60*, 6665–6667.
- 9 M. Li, B. Luo, Q. Liu, Y. Hu, A. Ganesan, P. Huang, S. Wen, *Org. Lett.* **2014**, *16*, 10–13.
- 10 S. Wan, M. E. Green, J.-H. Park, P. E. Floreancig, *Org. Lett.* **2007**, *9*, 5385–5388.
- 11 Y. Harayama, M. Yoshida, D. Kamimura, Y. Kita, *Chem. Commun.* **2005**, 1764–1766.
- 12 T. Iwasaki, H. Horikawa, K. Matsumoto, M. Miyoshi, *J. Org. Chem.* **1979**, *44*, 1552–1554.
- 13 H. J. Schäfer, *Top. Curr. Chem.* **1990**, *152*, 92–151.
- 14 a) J. A. Stapley, J. N. BeMiller, *Carbohydr. Res.* **2007**, *342*, 3–4; b) H. Hofer, M. Moest, *Justus Liebigs Ann. Chem.*, **1902**, *323*, 284.
- 15 a) S. D. Ross, M. Finkelstein, *J. Org. Chem.* **1969**, *34*, 2923–2927; b) H. Kolbe, *Justus Liebigs Ann. Chem.* **1849**, *69*, 257–294.
- 16 a) T. Shono, Y. Matsumura, K. Tsubata, *J. Am. Chem. Soc.* **1981**, *103*, 1172–1176; b) T. Shono, *Tetrahedron* **1984**, *40*, 811–850.
- 17 For selected examples see: a) A. M. Jones, C. E. Banks, *Beilstein J. Org. Chem.* **2014**, *10*, 3056–3072; b) J. Kuleshova, J. T. Hill-Cousins, P. R. Birkin, R. C. D. Brown, D. Pletcher, T. Underwood, *J. Electrochim. Acta* **2012**, *69*, 197–202; c) M. A. Kabeshov, B. Musio, P. D. Murray, D. L. Browne, S. V. Ley, *Org. Lett.* **2014**, *16*, 4618–4621; d) S. Suga, M. Okajima, J.-I. Yoshida, *Tetrahedron Lett.* **2001**, *42*, 2173–2176; e) R. A. Green, R. C. D. Brown, D. Pletcher, *J. Flow Chem.* **2016**, *6*, 191–197.

- 18 N. Amri, R. A. Skilton, D. Guthrie, T. Wirth, *Synlett* **2019**, *30*, 1183–1186.
- 19 D. Pletcher, R.A. Green, R. C. D. Brown, *Chem. Rev.* **2018**, *118*, 4573 – 4591.
- 20 a) S. Vellalath, I. Coric, B. List, *Angew. Chem. Int. Ed.* **2010**, *49*, 9749–9752; b) F. Saitoh, H. Nishida, T. Mukaihira, K. Aikawa, K. Mikami, *Eur. J. Org. Chem.* **2006**, 2269–2272; c) A. Koziol, J. Frelek, M. Woznica, B. Furman, M. Chmielewski, *Eur. J. Org. Chem.* **2009**, 338–341; d) G. Li, M. J. Kaplan, L. Wojtas, J. C. Antilla, *Org. Lett.* **2010**, *12*, 1960–1963.
- 21 a) T. Kawabata, K. Yahiro, K. Fuji, *J. Am. Chem. Soc.* **1991**, *113*, 9694–9696; b) K. Fuji, T. Kawabata, *Chem. Eur. J.* **1998**, *4*, 373–376.
- 22 a) Y. Matsumura, Y. Shirakawa, Y. Satoh, M. Umino, T. Tanaka, T. Maki, O. Onomura, *Org. Lett.* **2000**, *2*, 1689–1691; Y. Matsumura, T. Tanaka, G. N. Wanyoike, T. Maki, O. Onomura, *J. Electroanal. Chem.* **2001**, *507*, 71–74; c) G. N. Wanyoik, O. Onomura, T. Maki, Y. Matsumura, *Org. Lett.* **2002**, *4*, 1875–1877.
- 23 a) A. J. Buckmelter, J. P. Powers, S. D. Rychnovsky, *J. Am. Chem. Soc.* **1998**, *120*, 5589–5590; b) A. J. Buckmelter, A. I. Kim, S. D. Rychnovsky, *J. Am. Chem. Soc.* **2000**, *122*, 9386–9390.
- 24 B. Giese, P. Wettstein, C. Stähelin, F. Barbosa, M. Neuburger, M. Zehnder, P. Wessig, *Angew. Chem. Int. Ed.* **1999**, *38*, 2586–2587.
- 25 H. Zhao, D. C. Hsu, P. R. Carlier, *Synthesis* **2005**, *1*, 1–16.
- 26 a) D. R. Stoll, P. W. Carr, *Anal. Chem.* **2017**, *89*, 519–531; b) P. W. Carr, D.R. Stoll, *Two-Dimensional Liquid Chromatography: Principles, Practical Implementation and Applications*, **2015**, Agilent Technologies Primer.
- 27 C. E. Dent, W. Stepka, F. C. Steward, *Nature* **1947**, *160*, 682–683.
- 28 F. Erin, R. W. Frei, *J. Chromatogr. A* **1978**, *149*, 561–569.
- 29 a) Q. Wu, H. Yuan, L. Zhang, Y. Zhang, *Anal. Chim. Acta* **2012**, *731*, 1–10; b) J. Ren, M. A. Beckner, K. B. Lynch, H. Chen, Z. Zhu, Y. Yang, A. Chen, Z. Qiao, S. Liu, J. J. Lu, *Talanta* **2018**, *182*, 225–229.
- 30 N. L. Kuehnbaum, P. Britz-McKibbin, *Chem. Rev.* **2013**, *113*, 2437–2468.
- 31 a) C. L. Barhate, E. L. Regalado, N. D. Contrella, J. Lee, J. Jo, A. A. Makarov, D. W. Armstrong, C. J. Welch, *Anal. Chem.* **2017**, *89*, 3545–3553; b) G. Vanhoenacker, I. Vandenneede, F. David, P. Sandra, K. Sandra, *Anal. Bioanal. Chem.* **2015**, *407*, 355–366.
- 32 For selected examples see: a) S. D. Garbis, T. I. Rourmeliotis, S. I. Tyrizis, K. M. Zorpas, K. Pavlakis, C. A. Constantinides, *Anal. Chem.* **2011**, *83*, 708–718; b) P. Donato, F. Cacciola, E. Sommella, C. Fanali, L. Dugo, M. Dacha, P. Campiglia, E. Novellino, P. Dugo, L. Mondello, *Anal. Chem.* **2011**, *83*, 2485–2491; c) C. Song, M. Ye, G. Han, X. Jiang, F. Wang, Z. Yu, R. Chen, H. Zou, *Anal. Chem.* **2010**, *802*, 53–56; d) S. Dipalma, P. J. Boersema, A. J. R. Heck, S. Mohammed, *Anal. Chem.* **2011**, *83*, 3440–3447
- 33 a) E. L. Regalado, J. A. Schariter, C. J. Welch, *J. Chromatogr. A* **2014**, *1363*, 200–206; b) K. Roberta, A. Belaz, E. R. Pereira-Filho, R. V. Oliveira, *J. Chromatogr. B* **2013**, *932*, 26–33.
- 34 I. Markó, F. Chellé, *Encyclopedia of Applied Electrochemistry: Kolbe and Related Reactions*, **2014**, Springer, New York, NY.

- 35 G. N. Wanyke, Y. Matsumura, O. Onomura, *Heterocycles* **2009**, *79*, 339–345.
- 36 L. Li, Q. Yang, Z. Jia, S. Luo, *Synthesis* **2018**, *50*, 2924–2929.

CHAPTER 5: Experimental Part

5.1 General Methods

The reactions were performed using standard laboratory equipment. In all the reactions, standard reagent grade solvents and chemicals from Sigma Aldrich, Alfa Aesar, Acros Organic, and FluoroChem were used without further purification, unless otherwise specified. All air sensitive reactions were carried out under a nitrogen atmosphere using oven dried glassware. All the batch reactions were stirred using a stirrer plate and a magnetic stirrer bar and heating if necessary, over a hotplate with a temperature probe control and adapted heating block. Lower temperatures were achieved using ice/water bath (0 °C), ice/NaCl (-20 °C) and dry ice/acetone bath (-78 °C) or using a chiller to perform overnight reactions (0 to -20 °C). All reactions and manipulations of boranes were carried out under an atmosphere of dry, O₂-free nitrogen using standard double-manifold techniques with a rotary oil pump. A N₂-filled glove box (MBraun) was used to store the borane starting materials, setup reactions and sample preparation for analysis. Dry ether, acetonitrile, *n*-hexane, toluene and THF were collected from a solvent purification system (SPS) from the company MBRAUN (MB SPS-800). Dry CH₂Cl₂ was distilled over calcium hydride under nitrogen atmosphere. Büchi rotavapors were used for solvent evaporations (reduced pressure up to 8 mbar) and a high vacuum apparatus was used to further dry the products.

Thin-layer chromatography (TLC) and prep-TLC were performed on pre-coated aluminium sheets of Merck silica gel 60 F254 (0.20 mm) and visualised by UV radiation (254 nm). Manual column chromatography was performed using silica gel 60 (Merck, 230-400 mesh) under increased pressure. Automated column chromatography was performed on a Biotage[®] Isolera Four using Biotage[®] cartridges SNAP Ultra 10 g, SNAP Ultra 25 g, SNAP Ultra 50 g, SNAP Ultra 100 g. The solvents used for the purification are indicated in the text and were purchased from Fischer Scientific as laboratory grade.

The HPLC measurements were carried out on a Shimadzu apparatus or on an Agilent 1290 2D-LC Solution. The different modules of the Shimadzu apparatus: SIL-10ADVP (autoinjector), LC-10ATVP (liquid chromatograph), FCV-10ALVP (pump), DGU-14A (degasser), CTO-10ASVP (column oven), SCL-10AVP (system controller) and SPD-M10A (diode array detector). The different modules of the Agilent system: G7129A (1290 vial sampler), G1312A (1D binary pump), G1322A (degasser), G7120A (1290 high speed 2D binary pump), G1316A (1260 column oven), G7115A (1260 diode array detector),

G7114A (1260 variable wavelength detector) and G1170A (1290 valve drive). For the online analysis. For the online analysis, a Cheminert® C2-1006D switching valve was used. The solvents used were *n*-hexane, ethanol, methanol and 2-propanol and were bought from Fischer scientific as HPLC grade. The column used for the achiral separation was a Varian Si (250 × 4.6 mm, 5 μm pore size). The columns used for the chiral separation were Chiralcel® OD-H (250 × 4.6 mm, 5 μm pore size), Chiralcel® OB-H (250 × 4.6 mm, 5 μm pore size) and YMC Chiral Amylose-C (250 × 4.6 mm, 5 μm pore size) depending on the substrate.

¹H, ¹³C, and ¹⁹F NMR spectra were recorded at 298 K on Bruker DPX 300, 400 or 500 MHz apparatus and referenced to the residual proton solvent peak (H: CDCl₃, δ = 7.26 ppm; CD₃CN, δ = 1.94 ppm) and residual ¹³C signal (CDCl₃, δ = 77.2 ppm). ¹³C and ¹⁹F NMR spectra were measured as ¹H-decoupled unless otherwise stated. Chemical shifts δ were reported in ppm downfield of Si(CH₃)₄ (¹H, ¹³C), CFCl₃ (¹⁹F), multiplicity (s = singlet, d = doublet, t = triplet, q = quartet, qi = quintet, sex = sextet, hep = septet, dd = doublet of doublets, m = multiplet, br. s = broad singlet; and coupling constants (*J*) in Hertz. Yields are given as isolated yields unless noted otherwise.

Mass spectrometric measurements were performed by the EPSRC Mass Spectrometry Facility in Swansea University on a Waters Xevo G2-S and on a Thermo Scientific LTQ Orbitrap XL machine S3 or by R. Jenkins, R. Hick, T. Williams and S. Waller at Cardiff University on a Water LCR Premier XE-TOF for high resolution mass spectroscopy (HRMS). Ions were generated by the Atmospheric Pressure Ionisation Techniques (APCI), Atmospheric Solids Analysis Probe (ASAP), Electrospray (ES), Electron Ionisation (EI) or Nanospray Ionisation (NSI). The molecular ion peaks values quoted for either molecular ion (M⁺), molecular ion plus or minus hydrogen (M+H⁺, M-H⁻), molecular ion minus hydride (M-H⁺), molecular ion plus ammonium ion (M+NH₄⁺) or molecular ion plus sodium (M+Na⁺).

IR spectra were recorded on a Shimadzu FTIR Affinity-1S apparatus. Wavenumbers are quoted in cm⁻¹. All compounds were measured neat directly on the crystal of the IR machine. Melting points were measured using a Gallenkamp variable heater with samples in open capillary tubes.

Optical rotations were measured with a SCHMIDT and HAENSCH UniPol polarimeter at 20 °C in cuvette of 50–100 mm length with a sodium light (589.30 nm). HPLC grade chloroform, dichloromethane or methanol were used to prepare the solution and the concentration is indicated in the experimental section.

All the flow reactions were performed using a Chemyx Fusion 200 syringe pump and FEP tubing (OD: 1/16", ID: 0.2–1 mm). The electrochemical reactions were carried out in a galvanostatic mode using a Vapourtec Ion Electrochemical flow reactor¹ powered up by an Aim-tti bench power supply (300 Watt). The cyclic voltammogram studies were performed using an Orygalys OGF500 Potentiostat / Galvanostat with OGFPWR power supply.

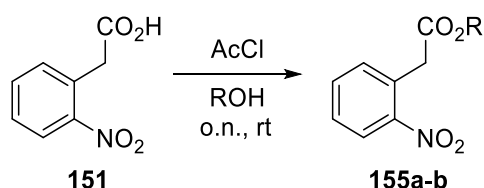
X-Ray crystallographic studies were carried out at the X-Ray Crystallography Service at Cardiff University or by Darren M. C. Ould. The structures were solved by direct methods and refined using the SHELXTL software package. In general, all non-hydrogen atoms were refined anisotropically. Hydrogen atoms were assigned at idealised locations.

5.2 Experimental Data for Chapter 2: Synthesis of novel *trans*-Dihydroindoles

The Rh(II) catalyst were purchased from Strem Chemicals. The diazo-transfer reagents *p*-ABSA (**18e**) was purchased by TCI and the *p*-NBSA (**18f**) was synthesised according to the literature procedure.²

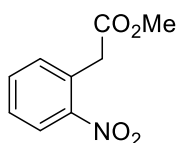
5.2.1 Synthesis of Starting Materials

General Procedure 1:



2-Nitrophenylacetic acid **151** (10.0 g, 55 mmol) was dissolved in methanol (100 mL) and the solution was cooled down to 0 °C before addition of acetyl chloride (9.8 mL, 138 mmol). The reaction was stirred overnight at room temperature and checked by TLC (*n*-hexane/ethyl acetate 4:1). The solvent was evaporated *in vacuo* and the residual oil washed with an aqueous saturated solution of NaHCO₃ (20 mL) and extracted with diethyl ether (3 × 25 mL). Subsequently, the combined organic fractions were washed with water (20 mL) and brine (20 mL), dried over MgSO₄ and concentrated *in vacuo* to afford **155a-b** as a solid or oil depending on the substrate.

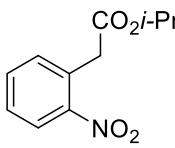
Methyl 2-(2-nitrophenyl) acetate **155a**:



Performed according to the *General Procedure 1* on a 55 mmol scale; **155a** (10.7 g, 55 mmol, 99%) was obtained as a pale-yellow oil that solidified at room temperature, m.p.: 36–40 °C.

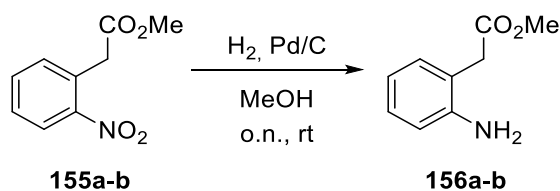
¹H NMR (300 MHz, CDCl₃): δ = 8.13 (dd, *J* = 8.1, 0.9 Hz, 1H, *ArH*), 7.62 (td, *J* = 7.5, 1.3 Hz, 1H, *ArH*), 7.49 (td, *J* = 8.1, 1.4 Hz, 1H, *ArH*), 7.37 (dd, *J* = 7.6, 1.0 Hz, 1H, *ArH*), 4.04 (s, 2H, CH₂), 3.72 (s, 3H, OCH₃) ppm; ¹³C NMR (75 MHz, CDCl₃): δ = 170.4 (C=O), 148.7 (*ArC*-N), 133.6 (*ArC*), 133.3 (*ArC*), 129.7 (*ArC*), 128.6 (*ArC*), 125.3 (*ArC*), 52.3 (OCH₃), 39.6 (CH₂) ppm. Spectroscopic data are in agreement with literature.³

Isopropyl 2-(2-nitrophenyl) acetate **155b**:

 Performed according to the *General Procedure 1* on a 13.8 mmol scale; **155b** (2.7 g, 12.3 mmol, 88%) was obtained as a pale orange oil.

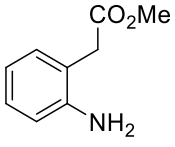
$^1\text{H NMR}$ (300 MHz, CDCl_3): δ = 7.99 (d, J = 8.1 Hz, 1H, ArH), 7.47 (td, J = 7.4, 1.0 Hz, 1H, ArH), 7.35 (t, J = 7.7 Hz, 1H, ArH), 7.23 (d, J = 7.4 Hz, 1H, ArH), 4.91 (hep, J = 6.2 Hz, 1H, $\text{OCH}(\text{CH}_3)_2$), 3.87 (s, 2H, CH_2), 1.12 (d, J = 6.2 Hz, 6H, $\text{OCH}(\text{CH}_3)_2$) ppm; $^{13}\text{C NMR}$ (75 MHz, CDCl_3): δ = 169.5 (C=O), 148.8 (ArC–N), 133.5 (ArC), 133.3 (ArC), 130.0 (ArC– CH_2), 128.5 (ArC), 125.2 (ArC), 68.9 (OCH), 40.2 (CH_2), 21.7 ($2 \times \text{CH}_3$) ppm; IR (neat) ν = 3726w, 3628w, 2981m, 2360s, 2341s, 728s, 1614m, 1579m, 1523s, 1465m, 1454m, 1344s, 1217s, 1176m, 1105s, 956m, 840m, 789m, 759m, 736m, 715s cm^{-1} ; HRMS (ASAP): exact mass calculated for $\text{C}_{11}\text{H}_{14}\text{NO}_4$ $[\text{M}+\text{H}]^+$: 224.0923, found: 224.0921.

General Procedure 2:



A two-neck flask was twice evacuated and filled with N_2 ; 10% Pd/C (233 mg) was added to the flask and the residue was washed with a small amount of dichloromethane. Methanol (20 mL) was added carefully before addition of 2-nitroaryl ester **155a–b** (4.0 g, 21 mmol) dissolved in methanol (2 mL). Subsequently, the flask was evacuated and filled with N_2 twice, evacuated again and filled with H_2 (1 atm). The reaction was stirred at room temperature for 12 hours and monitored by TLC (*n*-hexane/ethyl acetate 4:1). The mixture was filtered through Celite and the solvent was evaporated *in vacuo* to afford **156a–b** as oils.

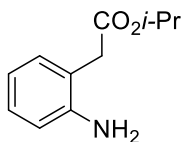
Methyl 2-(2-aminophenyl) acetate **156a**:

 Performed according to the *General Procedure 2* on a 21 mmol scale of **155a**; **156a** (3.3 g, 21 mmol, 99%) was obtained as a red oil.

$^1\text{H NMR}$ (300 MHz, CDCl_3): δ = 7.26–7.06 (m, 2H, ArH), 6.80–6.68 (m, 2H, ArH), 4.07 (br. s, 2H, NH_2), 3.71 (s, 3H, OCH_3), 3.59 (s, 2H, CH_2) ppm; $^{13}\text{C NMR}$ (75 MHz, CDCl_3): δ = 172.4 (C=O), 145.6 (ArC–N), 131.3 (ArC), 128.7 (ArC), 119.6

(ArC–CH₂), 119.1 (ArC), 116.7 (ArC), 52.3 (OCH₃), 38.4 (CH₂) ppm. Spectroscopic data are in agreement with literature.³

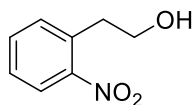
Isopropyl 2-(2-aminophenyl) acetate **156b**:



Performed according to the *General Procedure 2* on a 8.9 mmol scale of **155b**; **156b** (1.21 g, 6.26 mmol, 70%) was obtained as an orange oil.

¹H NMR (400 MHz, CDCl₃): δ = 7.12–7.08 (m, 2H, ArH), 6.77–6.70 (m, 2H, ArH), 5.00 (hep, *J* = 6.3 Hz, 1H, OCH), 4.10 (s, 2H, NH₂), 3.54 (s, 2H, CH₂), 1.24 (d, *J* = 6.3 Hz, 6H, 2 × CH₃) ppm; ¹³C NMR (75 MHz, CDCl₃): δ = 171.5 (C=O), 145.6 (ArC–N), 131.1 (ArC), 128.5 (ArC), 119.8 (ArC–CH₂), 118.9 (ArC), 116.5 (ArC), 68.5 (OCH), 38.9 (CH₂), 21.7 (2 × CH₃) ppm; IR (neat) *ν* = 3736w, 3446w, 3365w, 2980w, 2358s, 2341s, 1712s, 1627m, 1585w, 1496m, 1458m, 1373w, 1357w, 1159m, 1103s, 964m, 908m, 731s, 669m, 648m, 522m cm⁻¹; HRMS (NSI): exact mass calculated for C₁₁H₁₆NO₂ [M+H]⁺: 194.1173, found: 194.1176.

2-(2-Nitrophenyl)ethan-1-ol **157**:

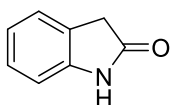


To a solution of **155a** (200 mg, 1 mmol) in dry THF (5 mL), NaBH₄ (79 mg, 2.2 mmol) and AlCl₃ (133 mg, 1 mmol) were added at 0 °C. After 2 hours the reaction was quenched with 1mL of water then filtered over

Celite. The product was extracted with Et₂O (3 × 5 mL). The combined organic layers were washed with brine and dried over MgSO₄ before being concentrated under reduced pressure. The crude was purified by column chromatography to afford **157** (28 mg, 0.17 mmol, 17%) as a colourless oil.

¹H NMR (300 MHz, CDCl₃): δ = 7.91 (d, *J* = 8.1 Hz, 1H, ArH), 7.63–7.48 (m, 1H, ArH), 7.48–7.30 (m, 2H, ArH), 3.92 (td, *J* = 6.4, 1.2 Hz, 2H, CH₂OH), 3.15 (t, *J* = 6.4 Hz, 2H, CH₂), 2.05 (br, 1H, OH) ppm; ¹³C NMR (75 MHz, CDCl₃): δ = 149.7 (ArC–N), 133.7 (ArC), 133.0 (ArC), 132.8 (ArC), 127.6 (ArC), 124.8 (ArC), 62.7 (CH₂OH), 36.1 (CH₂) ppm. Spectroscopic data are in agreement with literature.⁴

Indolin-2-one **158**:

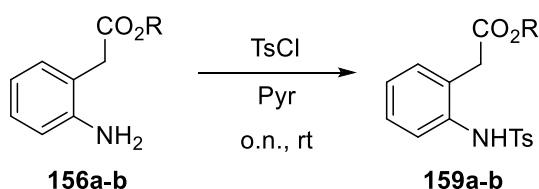


To a suspension of Pd/C 10% (50 mg, 5 mol%) in dry menthol (500 μL), a solution of **155a** (200 mg, 1 mmol) in dry methanol (2 mL) was added dropwise. The formic acid (500 μL, 5 mmol) was added and the suspension was stirred over night at room temperature. The solvent was evaporated, and the residue was washed with an aqueous saturated solution of NaHCO₃ (5 mL),

water (5 mL) and extracted with dichloromethane (3 × 5 mL). The combined organic layers were washed with brine and dried over MgSO₄ before being concentrated under reduced pressure. The crude was purified by column chromatography to afford **158** (92 mg, 0.69 mmol, 69%) as a pale pink solid, m.p.: 128–130 °C.

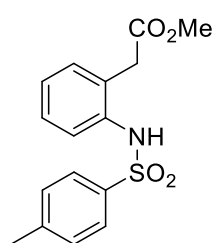
¹H NMR (300 MHz, CDCl₃) δ = 9.12 (s, 1H, NH), 7.22 (dd, *J* = 14.4, 6.9 Hz, 2H, ArH), 7.10–6.97 (m, 1H, ArH), 6.90 (d, *J* = 7.7 Hz, 1H, ArH), 3.55 (s, 2H, CH₂) ppm; ¹³C NMR (75 MHz, CDCl₃) δ = 178.7 (C=O), 142.8 (ArC–N), 128.0 (ArC), 125.4 (ArC–CH₂), 124.5 (ArC), 122.3 (ArC), 110.0 (ArC), 36.4 (CH₂) ppm. Spectroscopic data are in agreement with literature.⁵

General Procedure 3:



A solution of **156a–b** (3 g, 18 mmol) in pyridine (20 mL) was cooled down to 0 °C. *p*-Toluenesulfonyl chloride (4.16 g, 22 mmol) was added dropwise. The reaction was stirred at room temperature for 24 hours and monitored *via* TLC (*n*-hexane/ethyl acetate 4:1). An aqueous solution of HCl (1 M, 25 mL) was added and the reaction mixture was extracted with ethyl acetate (2 × 20 mL), the organic layer was washed with further aqueous solution of HCl (1 M, 20 mL), water (2 × 20 mL), brine and dried over MgSO₄. Subsequent evaporation of the solvent *in vacuo* and liquid column chromatography furnished the desired products **159a–b** as solids.

Methyl 2-(2-((4-methylphenyl)sulfonamido)phenyl) acetate **159a**:

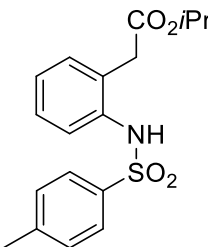


Performed according to the *General Procedure 3* on a 18 mmol scale of **156a**; **159a** (5.6 g, 17 mmol, 96%) was obtained as a pale orange solid, m.p.: 82–84 °C.

¹H NMR (300 MHz, CDCl₃): δ = 8.04 (br. s, 1H, NH), 7.60 (d, *J* = 8.3 Hz, 2H ArH), 7.29 (d, *J* = 7.9 Hz, 1H, ArH), 7.23–7.12 (m, 3H, ArH), 7.12–7.06 (m, 2H, ArH), 3.63 (s, 3H, OCH₃), 3.33 (s, 2H, CH₂), 2.34 (s, 3H, CH₃) ppm; ¹³C NMR (75 MHz, CDCl₃): δ = 172.6 (C=O), 143.7 (ArC–N), 137.2 (ArC), 135.4 (ArC), 131.1 (ArC), 129.7 (2 × ArC), 128.6 (ArC), 128.5 (ArC), 127.0 (2 × ArC), 126.5 (ArC), 125.9 (ArC), 52.5 (OCH₃), 37.7 (CH₂), 21.5 (CH₃) ppm; IR (neat) ν = 3226m, 1708s, 1597m, 1587m, 1496m, 1435m, 1417m, 1336s, 1278s, 1238w, 1157s, 1089s,

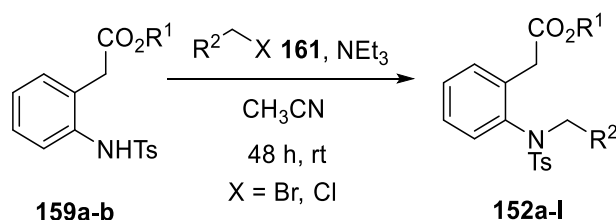
1010s, 947m, 920m, 819m, 742m, 661s cm^{-1} ; HRMS (NSI): Exact mass calculated for $\text{C}_{16}\text{H}_{21}\text{N}_2\text{O}_4\text{S}$ $[\text{M}+\text{NH}_4]^+$: 320.0951, found: 320.0955.

Isopropyl 2-(2-((4-methylphenyl)sulfonamido)phenyl) acetate **159b**:


 Performed according to *General Procedure 3* on a 6.2 mmol scale of **156b**; **159b** (2.1 g, 6.0 mmol, 98%) was obtained as a pale-yellow solid, m.p.: 74–78 °C.

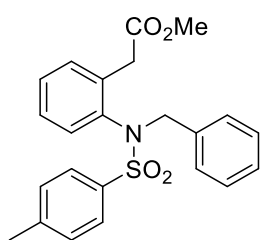
^1H NMR (400 MHz, CDCl_3): δ = 8.25 (br. s, 1H, NH), 7.68 (d, J = 8.3 Hz, 2H, ArH), 7.42 (d, J = 8.0 Hz, 1H, ArH), 7.35–7.20 (m, 3H, ArH), 7.13 (d, J = 4.1 Hz, 2H, ArH), 5.00 (hep, J = 6.2 Hz, 1H, OCH), 3.26 (s, 2H, CH_2), 2.42 (s, 3H, CH_3), 1.25 (d, J = 6.3 Hz, 6H, 2 \times CH_3) ppm; ^{13}C NMR (75 MHz, CDCl_3): δ = 172.0 (C=O), 143.7 (ArC–N), 137.7 (ArC), 135.8 (ArC), 131.2 (ArC), 129.8 (2 \times ArC), 128.8 (ArC), 128.0 (ArC), 127.0 (2 \times ArC), 126.3 (ArC), 125.5 (ArC), 69.8 (OCH), 38.9 (CH_2), 21.8 (2 \times CH_3), 21.7 (CH_3) ppm; IR (neat): ν = 3259m, 2980w, 1728m, 1707m, 1597w, 1585, 1492m, 1332s, 1290m, 1159s, 1089s, 956m, 898m, 812m, 659s, 547s, 528s cm^{-1} ; HRMS (NSI): Exact mass calculated for $\text{C}_{18}\text{H}_{25}\text{N}_2\text{O}_4\text{S}$ $[\text{M}+\text{NH}_4]^+$: 365.1530, found: 365.1532.

General Procedure 4:



A solution of starting material **159a–b** (2.6 g, 8.1 mmol) was dissolved in acetonitrile (25 mL). After the addition of triethylamine (3.2 mL, 24.3 mmol), the reaction mixture was cooled down to 0 °C. Next, aryl halide **161** was added (24.3 mmol) dropwise and the reaction mixture was stirred at room temperature for around 48–72 hours and monitored *via* TLC (*n*-hexane/ethyl acetate 4:1). Subsequently, the solvent was evaporated *in vacuo* and the residual oil was dissolved in CH_2Cl_2 (15 mL), washed with water (20 mL) and brine (20 mL). After drying over MgSO_4 , the mixture was concentrated *in vacuo* and purified *via* column chromatography to afford **152a–I** as solids.

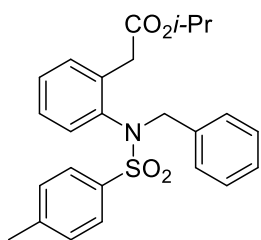
Methyl 2-(2-((*N*-benzyl-4-methylphenyl)sulfonamido)phenyl) acetate **152a**:



Performed according to *General Procedure 4* on a 2.0 mmol scale of **159a** with bromo benzene; **152a** (655 mg, 1.6 mmol, 82%) was obtained as a pale, pink solid, m.p.: 78–81 °C.

^1H NMR (300 MHz, CDCl_3): δ = 7.45 (d, J = 8.3 Hz, 2H, ArH), 7.21–6.91 (m, 10H, ArH), 6.48 (dd, J = 8.0, 1.0 Hz, 1H, ArH), 4.92 (d, J = 13.6 Hz, 1H, 1 \times NCH_2), 4.12 (d, J = 13.6 Hz, 1H, 1 \times NCH_2), 3.50–3.38 (m, 5H, $\text{CH}_2\text{CO}_2\text{Me}$ + OCH_3), 2.30 (s, 3H, CH_3) ppm; ^{13}C NMR (75 MHz, CDCl_3): δ = 171.4 (C=O), 143.7 (ArC–N), 137.6 (ArC), 136.0 (ArC), 135.4 (ArC), 135.1 (ArC), 131.3 (ArC), 129.5 (2 \times ArC), 129.3 (2 \times ArC), 128.3 (ArC), 128.2 (2 \times ArC), 128.0 (ArC), 127.9 (2 \times ArC), 127.7 (ArC), 127.4 (ArC), 56.0 (NCH_2), 51.6 (OCH_3), 35.6 (CH_2), 21.4 (CH_3) ppm; IR (neat) ν = 3062w, 3032w, 2949w, 1722s, 1597m, 1492m, 1348s, 1263s, 1161s, 1091m, 885m, 812s, 705s, 657s, 549s cm^{-1} ; HMRS (NSI): Exact mass calculated for $\text{C}_{23}\text{H}_{23}\text{NO}_4\text{S}$ $[\text{M}+\text{H}]^+$: 410.1421; found: 410.1418.

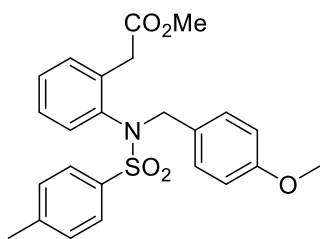
Isopropyl 2-(2-((*N*-benzyl-4-methylphenyl)sulfonamido)phenyl) acetate **152b**:



Performed according to *General Procedure 4* on a 1.47 mmol scale of **159b** with bromo benzene; **152b** (398 mg, 0.91 mmol, 62%) was obtained as a pale-yellow solid, m.p.: 88–90 °C.

^1H NMR (400 MHz, CDCl_3): δ = 7.50 (d, J = 7.9 Hz, 2H, ArH), 7.26–6.96 (m, 10H, ArH), 6.49 (d, J = 8.0 Hz, 1H, ArH), 4.93–4.81 (m, 2H, 1 \times NCH_2 + COCH), 4.27 (d, J = 13.7 Hz, 1H, 1 \times NCH_2), 3.47 (d, J = 16.8 Hz, 1H, 1 \times CH_2), 3.41 (d, J = 16.8 Hz, 1H, 1 \times CH_2), 2.38 (s, 3H, CH_3), 1.13 (t, J = 6.2 Hz, 6H, 2 \times CH_3) ppm; ^{13}C NMR (101 MHz, CDCl_3): δ = 170.9 (C=O), 143.7 (ArC–N), 137.7 (ArC), 136.5 (ArC), 135.9 (ArC), 135.4 (ArC), 131.3 (ArC), 129.6 (2 \times ArC), 129.5 (2 \times ArC), 128.6 (ArC), 128.5 (2 \times ArC), 128.1 (2 \times ArC), 128.0 (ArC), 127.3 (ArC), 68.1 ($\text{OCH}(\text{CH}_3)_2$), 56.1 (NCH_2), 36.4 (CH_2), 21.9 (2 \times CH_3), 21.7 (CH_3) ppm; IR (neat) ν = 2984w, 1716s, 1597w, 1490m, 1456m, 1344s, 1261s, 1161s, 1105m, 1089m, 1045m, 977m, 864m, 815m, 756s, 709s, 657s, 611s, 590s, 447w, 428w cm^{-1} ; HMRS (NSI): Exact mass calculated for $\text{C}_{25}\text{H}_{28}\text{NO}_4\text{S}$ $[\text{M}+\text{H}]^+$: 438.1734; found: 438.1734.

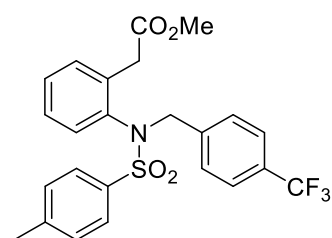
Methyl 2-(2-((*N*-(4-methoxybenzyl)-4-methylphenyl)sulfonamido)phenyl) acetate **152c**:



Performed according to *General Procedure 4* on a 0.63 mmol scale of **159a** with 4-methoxybenzyl chloride; **152c** (206 mg, 0.47 mmol, 75%) was obtained as a pale-yellow solid, m.p.: 108–110 °C.

$^1\text{H NMR}$ (300 MHz, CDCl_3): δ = 7.64–7.54 (m, 2H, ArH), 7.35–7.23 (m, 4H, ArH), 7.10 (td, J = 7.5, 1.8 Hz, 1H, ArH), 7.06–7.00 (m, 2H, ArH), 6.76–6.68 (m, 2H, ArH), 6.59 (dd, J = 8.0, 1.2 Hz, 1H, ArH), 4.97 (d, J = 13.5 Hz, 1H, 1 \times NCH_2), 4.23 (d, J = 13.5 Hz, 1H, 1 \times NCH_2), 3.75 (s, 3H, OCH_3), 3.60 (s, 3H, OCH_3), 3.55 (s, 2H, CH_2), 2.47 (s, 3H, CH_3) ppm; $^{13}\text{C NMR}$ (75 MHz, CDCl_3): δ = 171.8 (C=O), 159.4 (ArC–O), 143.7 (ArC–N), 137.8 (ArC), 136.4 (ArC), 136.0 (ArC), 131.5 (ArC), 130.8 (2 \times ArC), 129.7 (2 \times ArC), 128.5 (ArC), 128.4 (ArC), 128.2 (2 \times ArC), 127.5 (ArC), 127.4 (ArC), 113.9 (2 \times ArC), 55.7, 55.3, 51.9, 35.7 (CH_2), 21.5 ppm; IR (neat): ν = 2953w, 2835w, 1737s, 1614m, 1587m, 1514s, 1436m, 1340s, 1271m, 1244s, 1157s, 1028s, 873s, 694s, 653s, 574s cm^{-1} ; HRMS (NSI): Exact mass calculated for $\text{C}_{24}\text{H}_{29}\text{N}_2\text{O}_5\text{S}$ [$\text{M}+\text{NH}_4$] $^+$: 457.1792, found: 457.1788.

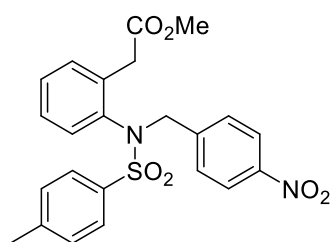
Methyl 2-(2-((4-methyl-*N*-(4-(trifluoromethyl)benzyl)phenyl)sulfonamido)phenyl) acetate **152d**:



Performed according to *General Procedure 4* on a 0.63 mmol scale of **159a** with 4-(trifluoromethyl)benzyl chloride; **152d** (162 mg, 0.34 mmol, 55%) was obtained as a pale pink solid, m.p.: 102–106 °C.

$^1\text{H NMR}$ (300 MHz, CDCl_3): δ = 7.51 (d, J = 8.2 Hz, 2H, ArH), 7.42 (d, J = 8.1 Hz, 2H, ArH), 7.30–7.16 (m, 6H, ArH), 7.06 (td, J = 8.3, 1.4 Hz, 1H, ArH), 6.56 (d, J = 7.9 Hz, 1H, ArH), 5.0 (d, J = 13.9 Hz, 1H, 1 \times NCH_2), 4.27 (d, J = 13.9 Hz, 1H, 1 \times NCH_2), 3.58 (d, J = 16.8 Hz, 1H, 1 \times CH_2), 3.53–3.35 (m, 4H, OCH_3 1 \times CH_2), 2.40 (s, 3H, CH_3) ppm; $^{13}\text{C NMR}$ (75 MHz, CDCl_3): δ = 171.5 (C=O), 144.0 (ArC–N), 139.6 (ArC), 137.7 (ArC), 136.0 (ArC), 135.3 (ArC), 131.6 (ArC), 130.0 (q, J = 32.2 Hz, ArC– CF_3), 129.7 (ArC), 129.6 (ArC), 128.7 (ArC), 128.2 (ArC), 128.0 (ArC), 127.7 (ArC), 125.3 (q, J = 3.7 Hz, ArC), 124.0 (q, J = 272.1 Hz, CF_3), 55.6 (NCH_2), 51.6 (OCH_3), 35.8 (CH_2), 21.5 ppm (CH_3); IR (neat): ν = 2954w, 2922w, 1726s, 1620w, 1595w, 1492m, 1438m, 1423m, 1348m, 1323s, 1271m, 1159s, 1109s, 1089s, 1066s, 1020s, 848m, 812m, 707m, 698m, 657m, 634m, 547s, 451w cm^{-1} ; HRMS (NSI): Exact mass calculated for $\text{C}_{24}\text{H}_{26}\text{F}_3\text{N}_2\text{O}_4\text{S}$ [$\text{M}+\text{NH}_4$] $^+$: 495.1560, found: 495.1547.

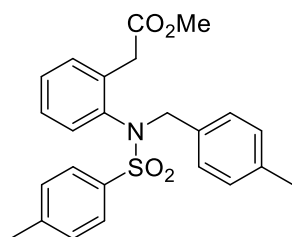
Methyl 2-(2-((4-methyl-*N*-(4-nitrobenzyl)phenyl)sulfonamido)phenyl) acetate **152e**:



Performed according to *General Procedure 4* on a 0.63 mmol scale of **159a** with 4-nitrobenzyl bromide; **152e** (291 mg, 0.45 mmol, 71%) was obtained after recrystallisation over Et₂O in *n*-hexane as a yellow solid, m.p.: 106–110 °C.

¹H NMR (400 MHz, CDCl₃): δ = 8.09 (d, *J* = 8.3 Hz, 2H, ArH), 7.58 (d, *J* = 8.0 Hz, 2H, ArH), 7.53–7.23 (m, 6H, ArH), 7.14 (t, *J* = 7.6, 1.9 Hz, 1H, ArH), 6.61 (dd, *J* = 8.0, 0.9 Hz, 1H, ArH), 5.09 (d, *J* = 14.0 Hz, 1H, 1 × NCH₂), 4.42 (d, *J* = 14.0 Hz, 1H, 1 × NCH₂), 3.83–3.41 (m, 5H, CH₂ + OCH₃), 2.47 (s, 3H, CH₃) ppm; ¹³C NMR (75 MHz, CDCl₃): δ = 171.5 (C=O), 147.6 (ArC–N), 144.3 (ArC–N), 142.9 (ArC), 137.5 (ArC), 135.9 (ArC), 134.9 (ArC), 131.7 (ArC), 130.2 (2 × ArC), 129.8 (2 × ArC), 128.9 (ArC), 128.1 (ArC), 128.0 (2 × ArC), 127.9 (ArC), 123.7 (2 × ArC), 55.4 (NCH₂), 51.9 (OCH₃), 35.9 (CH₂), 21.7 (CH₃) ppm; IR (neat): ν = 3066w, 2949w, 2854w, 1737s, 1597m, 1519s, 1435m, 1338s, 1207m, 1155s, 1105m, 1085m, 1064m, 854m, 815m, 711s, 690s, 650s, 569s, 557s cm⁻¹; HRMS (NSI): Exact mass calculated for C₂₃H₂₆N₃O₆S [M+NH₄]⁺: 472.1537, found: 472.153.

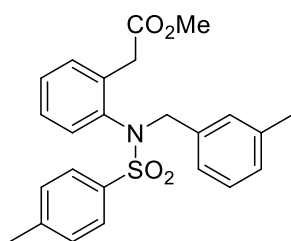
Methyl 2-(2-((4-methyl-*N*-(4-methylbenzyl)phenyl)sulfonamido)phenyl) acetate **152f**:



Performed according to *General Procedure 4* on a 0.63 mmol scale of **159a** with 4-methylbenzyl chloride; **152f** (161 mg, 0.33 mmol, 61%) was obtained as a pale white solid, m.p.: 94–96 °C.

¹H NMR (300 MHz, CDCl₃): δ = 7.60 (d, *J* = 7.4 Hz, 2H, ArH), 7.41–7.18 (m, 4H, ArH), 7.11 (t, *J* = 6.7 Hz, 1H, ArH), 7.00 (s, 4H, ArH), 6.59 (d, *J* = 7.9 Hz, 1H, ArH), 5.01 (d, *J* = 13.5 Hz, 1H, 1 × NCH₂), 4.20 (d, *J* = 13.3 Hz, 1H, 1 × NCH₂), 3.67–3.47 (m, 5H, CH₂ + OCH₃), 2.47 (s, 3H), 2.28 (s, 3H, CH₃) ppm; ¹³C NMR (75 MHz, CDCl₃): δ = 171.8 (C=O), 143.8 (ArC–N), 137.8 (ArC), 137.6 (ArC), 136.3 (ArC), 135.7 (ArC), 132.1 (ArC), 131.5 (ArC), 129.6 (ArC), 129.5 (ArC), 129.1 (ArC), 128.5 (ArC), 128.2 (ArC), 128.1 (ArC), 127.5 (ArC), 55.9 (NCH₂), 51.9 (OCH₃), 35.8 (CH₂), 21.7 (CH₃), 21.3 (CH₃) ppm; IR (neat): ν = 2364w, 1722s, 1346m, 1261m, 1159s, 1089m, 1043m, 1024m, 887w, 812s, 759w, 707m, 657s, 603m, 582s, 549s cm⁻¹; HRMS (NSI): Exact mass calculated for C₂₄H₂₆NO₄S [M+H]⁺: 424.1577, found: 424.1577.

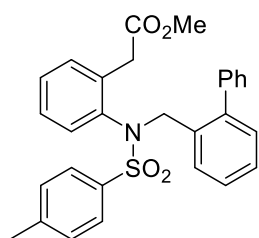
Methyl 2-(2-((4-methyl-*N*-(3-methylbenzyl)phenyl)sulfonamido)phenyl) acetate **152g**:



Performed according to *General Procedure 4* on a 0.60 mmol scale of **159a** with 3-methylbenzyl bromide; **152g** (182 mg, 0.43 mmol, 69%) was obtained as a pale white solid, m.p.: 84–86 °C.

^1H NMR (400 MHz, CDCl_3): δ = 7.54 (d, J = 8.2 Hz, 2H, *ArH*), 7.32–7.23 (m, 3H, *ArH*), 7.19 (t, J = 7.5 Hz, 1H, *ArH*), 7.09–6.90 (m, 4H, *ArH*), 6.83 (d, J = 7.3 Hz, 1H, *ArH*), 6.52 (d, J = 8.0 Hz, 1H, *ArH*), 4.98 (d, J = 13.6 Hz, 1H, 1 \times NCH_2), 4.16 (d, J = 13.6 Hz, 1H, 1 \times NCH_2), 3.62–3.42 (m, 5H, CH_2 + OCH_3), 2.41 (s, 3H, CH_3), 2.20 (s, 3H, CH_3) ppm; ^{13}C NMR (75 MHz, CDCl_3): δ = 171.6 (C=O), 143.7 (*ArC*–N), 137.9 (*ArC*), 137.7 (*ArC*), 136.1 (*ArC*), 135.4 (*ArC*), 135.1 (*ArC*), 131.3 (*ArC*), 130.0 (*ArC*), 129.5 (2 \times *ArC*), 128.5 (*ArC*), 128.3 (*ArC*), 128.1 (*ArC*), 128.0 (*ArC*), 128.0 (2 \times *ArC*), 127.4 (*ArC*), 126.3 (*ArC*), 56.0 (NCH_2), 51.8 (OCH_3), 35.8 (CH_2), 21.6 (CH_3), 21.3 (CH_3) ppm; IR (neat): ν = 3028w, 1732m, 1492w, 1344m, 1222w, 1163s, 1091w, 815w, 769s, 657m, 565m, 410m cm^{-1} ; HRMS (NSI): Exact mass calculated for $\text{C}_{24}\text{H}_{26}\text{NO}_4\text{S}$ [$\text{M}+\text{H}$] $^+$: 424.1577, found: 424.1577.

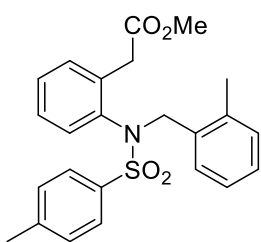
Methyl 2-(2-((*N*-([1,1'-biphenyl]-2-ylmethyl)-4-methylphenyl)sulfonamido)phenyl) acetate **152h**:



Performed according to *General Procedure 4* on a 0.63 mmol scale of **159a** with 2-(phenyl)benzyl bromide; **152h** (207 mg, 0.50 mmol, 79%) was obtained as a pale yellow solid, m.p.: 94–96 °C.

^1H NMR (300 MHz, CDCl_3): δ = 7.74 (dd, J = 7.8, 1.0 Hz, 1H, *ArH*), 7.50–7.43 (m, 2H, *ArH*), 7.36 (td, J = 7.5, 1.3 Hz, 1H, *ArH*), 7.3–7.07 (m, 8H, *ArH*), 7.02 (dd, J = 7.6, 1.2 Hz, 1H, *ArH*), 6.87 (td, J = 7.9, 1.7 Hz, 1H, *ArH*), 6.67 (dd, J = 8.0, 1.3 Hz, 2H, *ArH*), 6.12 (dd, J = 8.0, 1.0 Hz, 1H, *ArH*), 5.00 (d, J = 13.9 Hz, 1H, 1 \times NCH_2), 4.24 (d, J = 13.9 Hz, 1H, 1 \times NCH_2), 3.56–3.45 (m, 5H, CH_2 + OCH_3), 2.41 (s, 3H, CH_3) ppm; ^{13}C NMR (75 MHz, CDCl_3): δ = 171.7 (C=O), 143.7 (*ArC*–N), 142.4 (*ArC*), 140.3 (*ArC*), 137.8 (*ArC*), 136.2 (*ArC*), 135.6 (*ArC*), 133.0 (*ArC*), 131.4 (*ArC*), 130.9 (*ArC*), 130.0 (*ArC*), 129.6 (2 \times *ArC*), 129.2 (2 \times *ArC*), 128.3 (*ArC*), 128.2 (*ArC*), 128.1 (2 \times *ArC*), 127.9 (*ArC*), 127.8 (2 \times *ArC*), 127.6 (*ArC*), 127.5 (*ArC*), 126.7 (*ArC*), 52.3 (OCH_3), 47.0 (NCH_2), 35.6 (CH_2), 21.6 (CH_3) ppm; IR (neat): ν = 3062w, 3028w, 2956w, 2929w, 1743s, 1342s, 1203m, 1190m, 1153s, 1087m, 1057m, 867m, 817m, 759m, 692s, 653s, 547s cm^{-1} ; HRMS (NSI): Exact mass calculated for $\text{C}_{29}\text{H}_{31}\text{N}_2\text{O}_4\text{S}$ [$\text{M}+\text{NH}_4$] $^+$: 503.1999, found: 503.1985.

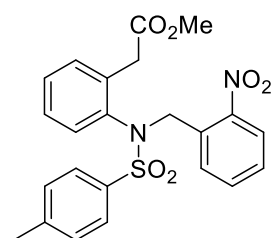
Methyl 2-(2-((4-methyl-*N*-(2-methylbenzyl)phenyl)sulfonamido)phenyl) acetate **152i**:



Performed according to *General Procedure 4* on a 0.63 mmol scale of **159a** with 2-methylbenzyl bromide; **152i** (215 mg, 0.50 mmol, 82%) was obtained as a pale white solid, m.p.: 96–98 °C.

^1H NMR (400 MHz, CDCl_3) δ = 7.60 (d, J = 8.1 Hz, 2H, ArH), 7.37–7.19 (m, 4H, ArH), 7.18–7.01 (m, 3H, ArH), 6.83 (t, J = 7.2 Hz, 1H, ArH), 6.80 (d, J = 7.6 Hz, 1H, ArH), 6.60 (d, J = 8.0 Hz, 1H, ArH), 5.19 (d, J = 13.1 Hz, 1H, 1 \times NCH₂), 4.15 (d, J = 13.1 Hz, 1H, 1 \times NCH₂), 3.55 (s, 3H, OCH₃), 3.50 (d, J = 16.8 Hz, 1H, 1 \times CH₂), 3.39 (d, J = 16.8 Hz, 1H, 1 \times CH₂), 2.47 (s, 3H, CH₃), 2.30 (s, 3H, CH₃) ppm; ^{13}C NMR (101 MHz, CDCl_3) δ = 171.5 (C=O), 143.9 (ArC–N), 137.7 (ArC), 137.6 (ArC), 136.7 (ArC), 135.3 (ArC), 132.7 (ArC), 131.5 (ArC), 131.1 (ArC), 130.6 (ArC), 129.7 (2 \times ArC), 128.5 (ArC), 128.3 (2 \times ArC), 128.2 (ArC), 127.8 (ArC), 127.4 (ArC), 125.8 (ArC), 53.6, 51.9, 35.5 (CH₂), 21.7 (CH₃), 19.0 (CH₃) ppm; IR (neat) ν = 2943w, 2362w, 1741s, 1492m, 1435m, 1338s, 1193m, 1157s, 1089m, 1037m, 879m, 823m, 746m, 727m, 694s, 655m, 569s, 547m, 536m cm^{-1} ; HRMS (NSI): Exact mass calculated for C₂₄H₂₆NO₄S [M+H]⁺: 424.1577, found: 424.1577.

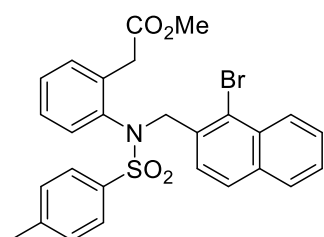
Methyl 2-(2-((4-methyl-*N*-(2-nitrobenzyl)phenyl)sulfonamido)phenyl) acetate **152j**:



Performed according to *General Procedure 4* on a 0.63 mmol scale of **159a** with 2-nitrobenzyl bromide; **152j** (174 mg, 0.38 mmol, 62%) was obtained as a yellow solid m.p.: 116–118 °C.

^1H NMR (400 MHz, CDCl_3): δ = 7.80 (d, J = 7.7 Hz, 1H, ArH), 7.71 (d, J = 8.1 Hz, 1H, ArH), 7.50 (t, J = 7.3 Hz, 1H, ArH), 7.43 (d, J = 8.2 Hz, 2H, ArH), 7.29 (t, J = 7.4 Hz, 1H, ArH), 7.34–7.22 (m, 4H, ArH), 7.02 (t, J = 7.6 Hz, 1H, ArH), 6.59 (d, J = 7.9 Hz, 1H, ArH), 5.18 (d, J = 15.7 Hz, 1H, 1 \times NCH₂), 4.82 (d, J = 15.7 Hz, 1H, 1 \times NCH₂), 3.65–3.35 (m, 5H, CH₂ + OCH₃), 2.36 (s, 3H, CH₃) ppm; ^{13}C NMR (101 MHz, CDCl_3): δ = 171.5 (C=O), 148.8 (ArC), 144.3 (ArC), 138.1 (ArC), 135.4 (ArC), 134.4 (ArC), 133.3 (ArC), 131.8 (ArC), 131.6 (ArC), 131.5 (ArC), 129.7 (2 \times ArC), 128.7 (ArC), 128.6 (ArC), 128.5 (ArC), 128.2 (2 \times ArC), 127.9 (ArC), 124.6 (ArC), 52.0 (NCH₂), 51.9 (OCH₃), 36.1 (CH₂), 21.6 (CH₃) ppm; IR (neat): ν = 2951w, 2358s, 2341s, 1735s, 1597w, 1525s, 1492m, 1435m, 1346s, 1267m, 1163s, 1091m, 1058w, 1039w, 856w, 815w, 736m, 694m, 655m, 572m cm^{-1} ; HRMS (ASAP): Exact mass calculated for C₂₃H₂₃N₂O₆S [M+H]⁺: 455.1277, found: 455.1284.

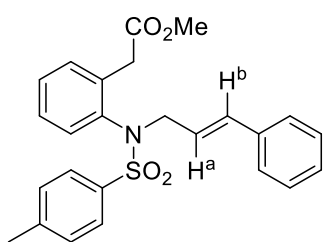
Methyl 2-(2-((*N*-((1-bromonaphthalen-2-yl)methyl)-4-methylphenyl)sulfonamido) phenyl) acetate **152k**:



Performed according to *General Procedure 4* on a 0.63 mmol scale of **159a** with 1-bromo-2-(bromomethyl)naphthalene; **152k** (262 mg, 0.49 mmol, 77%) was obtained as a pale white solid, m.p.: 140–142 °C.

$^1\text{H NMR}$ (400 MHz, CDCl_3): δ = 8.11 (d, J = 8.4 Hz, 1H, ArH), 7.68 (d, J = 7.8 Hz, 1H, ArH), 7.62 (d, J = 8.5 Hz, 1H, ArH), 7.57–7.50 (m, 3H, ArH), 7.42 (dt, J = 14.7, 6.9 Hz, 2H, ArH), 7.25 (d, J = 8.0 Hz, 2H, ArH), 7.19–7.09 (m, 2H, ArH), 7.05–6.99 (m, 1H, ArH), 6.66 (d, J = 7.9 Hz, 1H, ArH), 5.31 (d, J = 13.8 Hz, 1H, 1 \times NCH_2), 4.72 (d, J = 13.8 Hz, 1H, 1 \times NCH_2), 3.56 (d, J = 16.8 Hz, 1H, 1 \times CH_2), 3.46 (d, J = 16.8 Hz, 1H, 1 \times CH_2), 3.11 (s, 3H, OCH_3), 2.40 (s, 3H, CH_3) ppm; $^{13}\text{C NMR}$ (101 MHz, CDCl_3): δ = 171.5 (C=O), 144.0 (ArC–N), 137.6 (ArC), 136.3 (ArC), 135.1 (ArC), 134.1 (ArC), 132.8 (ArC), 132.3 (ArC), 131.4 (ArC), 129.7 (ArC), 128.6 (ArC), 128.4 (ArC), 128.3 (ArC), 128.2 (ArC), 127.9 (ArC), 127.9 (ArC), 127.5 (ArC), 127.5 (ArC), 126.9 (ArC), 124.9 (ArC), 56.3 (NCH_2), 51.5 (OCH_3), 35.9 (CH_2), 21.8 (CH_3) ppm; IR (neat): ν = 2953w, 1741s, 1593w, 1496w, 1433w, 1340s, 1157s, 1112m, 1087m, 1072m, 993w, 854m, 815s, 767m, 746m, 715m, 690m, 659s, 549s, 530m, 505m, 495m cm^{-1} ; HRMS (NSI): Exact mass calculated for $\text{C}_{27}\text{H}_{25}\text{BrNO}_4\text{S}$ [$\text{M}+\text{H}$] $^+$: 538.0682, found: 538.0678.

Methyl 2-(2-((*N*-cinnamyl-4-methylphenyl)sulfonamido)phenyl) acetate **159l**:

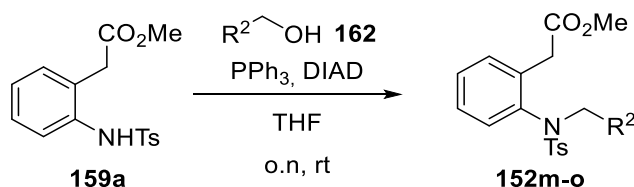


Performed according to *General Procedure 4* on a 0.94 mmol scale of **159a** with (*E*)-(3-bromoprop-1-en-1-yl)benzene; **152l** (278 mg, 0.64 mmol, 68%) was obtained as a white solid, m.p.: 106–110 °C.

$^1\text{H NMR}$ (300 MHz, CDCl_3): δ = 7.58 (d, J = 8.2 Hz, 2H, ArH), 7.41 (d, J = 7.0 Hz, 1H, ArH), 7.35–7.16 (m, 8H, ArH), 7.12 (td, J = 7.6, 1.1 Hz, 1H, ArH), 6.61 (d, J = 7.8 Hz, 1H, ArH), 6.31 (d, J = 15.8 Hz, 1H, H^b), 6.10 (dt, J = 15.7 Hz, 6.9 Hz, 1H, H^a), 4.50 (dd, J = 14.2 Hz, 6.2 Hz, 1H, 1 \times NCH_2), 4.12 (d, J = 16.4 Hz, 1H, 1 \times CH_2), 4.05 (dd, J = 14.3, 6.7 Hz, 1H, 1 \times NCH_2), 3.69 (d, J = 16.4 Hz, 1H, 1 \times CH_2), 3.55 (s, 3H, OCH_3), 2.45 (s, 3H, CH_3) ppm; $^{13}\text{C NMR}$ (75 MHz, CDCl_3): δ = 172.1 (C=O), 143.8 (ArC–N), 138.3 (ArC), 136.5 (ArC), 136.4 (ArC), 135.7 (ArC), 134.5 (ArC), 131.6 (ArC), 129.6 (2 \times ArC), 128.7 (ArC), 128.6 (2 \times ArC), 128.5 (ArC), 128.3 (2 \times ArC), 128.0 (ArC), 127.8 (ArC), 126.7 (2 \times ArC), 123.5 (ArC), 54.7 (NCH_2), 52.0 (OCH_3), 36.7 (CH_2), 21.7 (CH_3) ppm; IR (neat): ν = 3034w, 2947m, 2856w, 1730s, 1595m, 1490m, 1433m, 1313m,

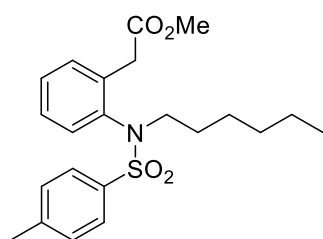
1257s, 1184m, 1153s, 881m, 657s, 580s cm^{-1} ; HRMS (NSI): Exact mass calculated for $\text{C}_{25}\text{H}_{29}\text{N}_2\text{O}_4\text{S}$ $[\text{M}+\text{NH}_4]^+$: 453.1843, found: 453.1837.

General Procedure 5:



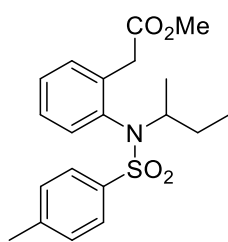
To a solution of starting material **159a** (300 mg, 0.94 mmol), triphenylphosphine (271 mg, 1.03 mmol) and alkyl alcohol **162** (128 μL , 1.03 mmol) in THF, diisopropylazodicarboxylate (DIAD, 203 μL , 1.03 mmol) was added at 0 °C. The mixture was stirred overnight refluxing and cooled to room temperature. After THF was removed under reduced pressure, the residue was purified by flash column chromatography (*n*-hexane/ethyl acetate) to afford **152m-o** as oils.

Methyl 2-(2-((*N*-hexyl-4-methylphenyl)sulfonamido)phenyl) acetate **152m**:



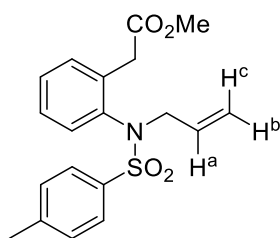
Performed according to *General Procedure 5* on a 0.94 mmol scale of **159a** with hexan-1-ol; **152m** (260 mg, 0.64 mmol, 68%) was obtained as a colourless oil.

^1H NMR (300 MHz, CDCl_3): δ = 7.43 (d, J = 8.1 Hz, 2H, ArH), 7.36 (d, J = 7.2 Hz, 1H, ArH), 7.24–7.14 (m, 3H, ArH), 7.04 (t, J = 7.2 Hz, 1H, ArH), 6.47 (d, J = 8.1 Hz, 1H, ArH), 4.01 (d, J = 16.5 Hz, 1H, 1 \times CH_2), 3.75–3.49 (m, 5H, OCH_3 + 1 \times CH_2), 3.15–2.85 (m, 1H), 2.35 (s, 3H, CH_3), 1.47–1.04 (m, 8H), 0.75 (t, J = 6.6 Hz, 3H, CH_3) ppm; ^{13}C NMR (75 MHz, CDCl_3): δ = 172.1 (C=O), 143.6 (ArC–N), 138.4 (ArC), 136.4 (ArC), 135.1 (ArC), 131.4 (ArC), 129.4 (2 \times ArC), 128.4 (ArC), 128.1 (2 \times ArC), 127.6 (ArC), 127.4 (ArC), 52.2, 51.9, 36.4, 31.4, 28.2, 26.5, 22.5, 21.6, 14.0 ppm; IR (neat): ν = 2951m, 2929m, 2856m, 1739s, 1597w, 1492m, 1452m, 1435m, 1348s, 1211w, 1165s, 1089m, 1066w, 812m, 713m, 694m, 655m, 582m cm^{-1} ; HRMS (NSI): Exact mass calculated for $\text{C}_{22}\text{H}_{30}\text{NO}_4\text{S}$ $[\text{M}+\text{H}]^+$: 404.1890, found: 404.1884.

Methyl 2-(2-((*N*-(*sec*-butyl)-4-methylphenyl)sulfonamido)phenyl) acetate **152n**:

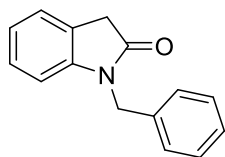
Performed according to *General Procedure 5* on a 0.94 mmol scale of **159a** with butan-2-ol; **152n** (227 mg, 0.60 mmol, 64%) was obtained as a colorless oil as a 1:1 mixture of rotamers.

$^1\text{H NMR}$ (300 MHz, CDCl_3): δ = 7.48 (dd, J = 8.2, 3.0 Hz, 4H, *ArH*), 7.39 (d, J = 7.8 Hz, 2H, *ArH*), 7.29–7.04 (m, 8H, *ArH*), 6.71 (d, J = 7.9 Hz, 1H, *ArH*), 6.63 (d, J = 7.9 Hz, 1H, *ArH*), 4.21–4.12 (m, 2H, *NCH* + *NCH*'), 3.90 (t, J = 16.5 Hz, 2H), 3.97–3.83 (m, 2H), 3.75–3.60 (m, 8H), 2.34 (s, 6H, CH_3 + CH_3), 1.65–1.31 (m, 3H), 1.21–0.91 (m, 7H), 0.91–0.76 (m, 7H), 0.76–0.65 (m, 3H) ppm; $^{13}\text{C NMR}$ (75 MHz, CDCl_3): δ = 172.2 ($\text{C}=\text{O}$), 172.1 ($\text{C}'=\text{O}$), 143.3 ($\text{ArC}-\text{N}$), 143.2 ($\text{ArC}'-\text{N}$), 138.1 (*ArC*), 137.8 (*ArC*), 137.6 (*ArC*), 137.5 (*ArC*), 134.9 (*ArC*), 134.8 (*ArC*), 131.6 (*ArC*), 131.3 (*ArC*), 129.5 (*ArC*), 129.4 (*ArC*), 128.7 (*ArC*), 128.7 (*ArC*), 127.7 (*ArC*), 127.6 (*ArC*), 127.1 (*ArC*), 126.9 (*ArC*), 58.9 (*NCH*), 58.4 (*NCH*'), 52.0 (OCH_3), 51.9 (OCH_3), 36.6, 28.6, 28.6, 21.6, 18.4, 17.9, 11.8, 11.5 ppm; IR (neat): ν = 2978w, 2881w 2394m, 2341m, 1708s, 1475w, 1419w, 1361m, 1336m, 1220m, 1174w, 1159m, 1114w, 1097w, 1082m, 1037m, 1012w, 964w, 912w, 842w, 790w, 763w cm^{-1} ; HRMS (NSI): Exact mass calculated for $\text{C}_{22}\text{H}_{26}\text{NO}_4\text{S}$ [$\text{M}+\text{H}$] $^+$: 376.1577, found: 376.1580.

Methyl 2-(2-((*N*-allyl-4-methylphenyl)sulfonamido)phenyl) acetate **152o**:

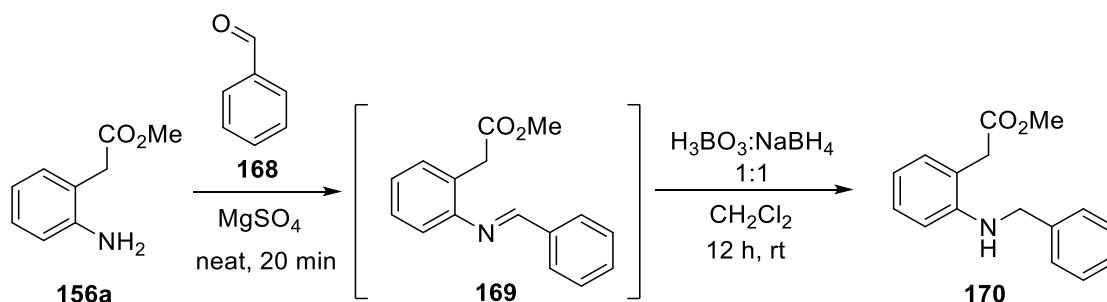
Performed according to *General Procedure 5* on a 0.93 mmol scale of **159a** and prop-2-en-1-ol; **152o** (286 mg, 0.80 mmol, 86%) was obtained as a colourless oil.

$^1\text{H NMR}$ (400 MHz, CDCl_3): δ = 7.50 (d, J = 8.1 Hz, 2H, *ArH*), 7.38 (d, J = 7.7 Hz, 1H, *ArH*), 7.25–7.22 (m, 3H, *ArH*), 7.07 (t, J = 7.7 Hz, 1H, *ArH*), 6.51 (d, J = 8.0 Hz, 1H, *ArH*), 5.77–5.62 (m, 1H, H^a), 5.07–4.80 (m, 2H, H^b + H^c), 4.32 (dd, J = 14.1, 5.9 Hz, 1H, 1 \times NCH_2), 4.04 (d, J = 16.4 Hz, 1H, 1 \times CH_2), 3.82 (dd, J = 14.1, 7.6 Hz, 1H, 1 \times NCH_2), 3.77–3.63 (m, 4H, 1 \times CH_2 + OCH_3), 2.39 (s, 3H, CH_3) ppm; $^{13}\text{C NMR}$ (101 MHz, CDCl_3): δ = 170.9 ($\text{C}=\text{O}$), 142.7 ($\text{ArC}-\text{N}$), 137.0 (*ArC*), 135.1 (*ArC*), 134.1 (*ArC*), 131.3, 130.4, 128.5 (2 \times *ArC*), 127.5, 127.2, 127.1 (2 \times *ArC*), 126.5, 118.5 ($\text{CH}=\text{CH}_2$), 53.9 (NCH_2), 50.9 (OCH_3), 35.5 (CH_2), 20.5 (CH_3) ppm.

1-Benzylindolin-2-one **163**:

To a solution of **159c^a** (200 mg, 0.75 mmol) and triethylamine (210 μ L, 1.5 mmol) in acetonitrile (3 mL) at 0 °C benzyl bromide (134 μ L, 1.1 mmol) was added and the mixture was stirred for 24 hours at 50 °C. The solution was cooled down, the solvent was concentrated, and the residual oil was dissolved in CH_2Cl_2 (10 mL), washed with water (10 mL) and then brine (10 mL). After drying over MgSO_4 , the mixture was concentrated *in vacuo* and purified *via* column chromatography to afford **163** (140 mg, 0.63 mmol, 84%) as a colourless solid, m.p.: 66–70 °C.

^1H NMR (300 MHz, CDCl_3): δ = 7.36–7.17 (m, 6H, ArH), 7.12 (td, J = 7.8, 1.2 Hz, 1H, ArH), 6.96 (td, J = 7.7, 1.0 Hz, 1H, ArH), 6.68 (d, J = 7.8 Hz, 1H, ArH), 4.87 (s, 2H, NCH_2), 3.57 (s, 2H, CH_2) ppm; ^{13}C NMR (75 MHz, CDCl_3): δ = 175.3 (C=O), 144.5 (ArC–N), 136.0 (ArC), 128.9 (2 \times ArC), 127.9 (ArC), 127.7 (ArC), 127.5 (2 \times ArC), 124.6 (ArC), 124.5 (ArC), 122.5 (ArC), 109.2 (ArC), 43.9 (NCH_2), 35.9 (CH_2) ppm. Spectroscopic data are in agreement with literature.⁶

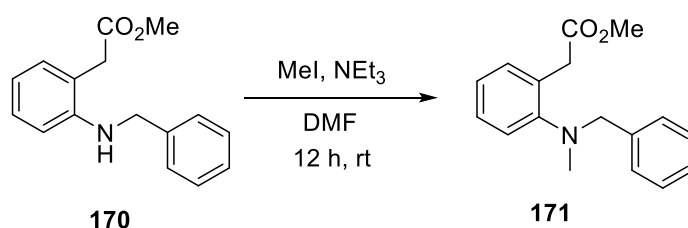
Methyl 2-(2-(benzylamino)phenyl)acetate **170**:

To neat starting material **156a** (600 mg, 3.6 mmol) benzaldehyde **168** (3.0 mmol) was added dropwise and an exothermic reaction was observed, hence some MgSO_4 (~100 mg) was added to remove the water formed. The suspension was stirred for 20 minutes then the MgSO_4 was filtered off and the product was washed off the salt with CH_2Cl_2 (5 mL). A pre-mixed solid mixture of 1:1 $\text{NaBH}_4/\text{H}_3\text{BO}_3$ (3 mmol) was added portion wise and the solution was stirred vigorously overnight at room temperature. Water was added and the phases were separated. The organic layer was washed with brine and dried over MgSO_4 and concentrated under reduced pressure. The crude was purified by column chromatography to afford **170** (450 mg, 1.7 mmol, 49% yield) as a colourless oil.

a. Synthesised by Dr. S. T. R. Müller.

^1H NMR (500 MHz, CDCl_3): δ = 7.42–7.30 (m, 4H, ArH), 7.30–7.25 (m, 1H, ArH), 7.19–7.08 (m, 2H, ArH), 6.71 (td, J = 7.4, 1.0 Hz, 1H, ArH), 6.66 (d, J = 8.1 Hz, 1H, ArH), 4.92 (br. s, 1H, NH), 4.39 (s, 2H, NCH_2), 3.67 (s, 3H, OCH_3), 3.60 (s, 2H, CH_2) ppm; ^{13}C NMR (126 MHz, CDCl_3): δ = 172.4 (C=O), 146.7 (ArC–N), 139.5 (ArC), 131.2 (ArC), 128.9 (ArC), 128.8 (2 \times ArC), 127.5 (2 \times ArC), 127.3 (ArC), 119.3 (ArC), 117.7 (ArC), 111.8 (ArC), 52.4 (OCH_3), 48.1 (NCH_2), 38.7 (CH_2) ppm; IR (neat): ν = 3385w, 3026w, 2949w, 2845w, 1720s, 1602m, 1516m, 1452m, 1261m, 1147m, 748s cm^{-1} ; HRMS (NSI): Exact mass calculated for $\text{C}_{16}\text{H}_{18}\text{NO}_2$ $[\text{M}+\text{H}]^+$: 256.1332; found: 256.1333.

Methyl 2-(2-(benzyl(methyl)amino)phenyl)acetate **171**:

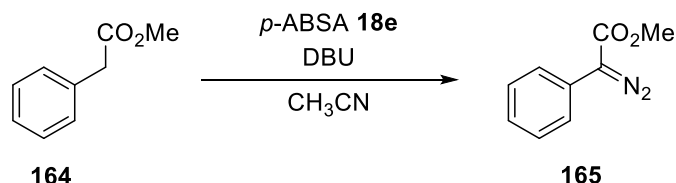


To a solution of starting material **170** (417 mg, 1.6 mmol) and triethylamine (3.2 mmol) in DMF (16 mL), methyl iodide (6.5 mmol) was added dropwise. The solution was stirred overnight at room temperature. The solution was concentrated under reduced pressure inside a fume-cupboard to remove the unreacted methyl iodide. The residue was washed with water (50 mL) and the product was extracted with Et_2O (5 \times 20 mL). The combined organic layers were washed with brine, dried over MgSO_4 and concentrated under reduced pressure. The crude was purified by column chromatography to afford **171** (86 mg, 0.32 mmol, 20% yield) as a colourless oil.

^1H NMR (300 MHz, CDCl_3): δ = 7.31–7.10 (m, 8H, ArH), 7.08–6.98 (m, 1H, ArH), 3.90 (s, 2H, CH_2), 3.76 (s, 2H, CH_2), 3.60 (s, 3H, CH_3), 2.45 (s, 3H, CH_3) ppm; ^{13}C NMR (75 MHz, CDCl_3): δ = 172.9 (C=O), 152.7 (ArC), 138.7 (ArC), 131.0 (ArC), 130.8 (ArC), 128.8 (ArC), 128.3 (ArC), 128.3 (ArC), 127.2 (ArC), 124.5 (ArC), 122.1 (ArC), 61.7, 52.0, 42.0, 36.9 ppm; IR (neat): ν = 3057w, 3032w, 2922w, 1701s, 1614s, 1466s, 1344s, 1165s, 516m cm^{-1} ; HRMS (NSI): Exact mass calculated for $\text{C}_{17}\text{H}_{20}\text{NO}_2$ $[\text{M}+\text{H}]^+$: 270.1489; found: 270.149.

5.2.2 Diazo-transfer Reaction in Batch

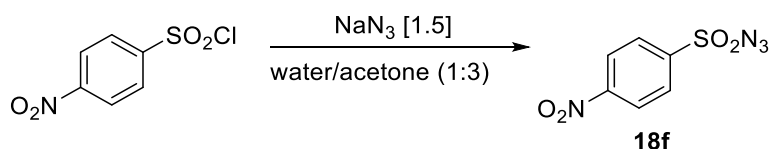
Phenyldiazoacetate **165**:



A 0.2 M solution of methyl phenylacetate **164** (600 mg, 4.0 mmol) and *p*-ABSA **18e** (1.9 g, 8 mmol) in acetonitrile (10 mL) was cooled to 0 °C before the addition of DBU (897 μL , 6 mmol). The reaction was stirred at room temperature for 12 hours and monitored by TLC (*n*-hexane/ethyl acetate). The mixture was quenched with a saturated aqueous solution of NH_4Cl and the product was extracted with CH_2Cl_2 (3 \times 5 mL). The combined organic layers were washed with water, brine, dried over MgSO_4 and concentrated under reduced pressure. The crude was purified by flash column chromatography to afford **165** as a red oil (580 mg, 3.3 mmol, 83% yield).

^1H NMR (500 MHz, CDCl_3): δ = 7.52–7.45 (m, 2H, ArH), 7.45–7.34 (m, 2H, ArH), 7.22–7.11 (m, 1H, ArH), 3.87 (s, 3H, OCH_3) ppm; ^{13}C NMR (126 MHz, CDCl_3): δ = 165.8 (C=O), 129.1 (ArC), 126.0 (ArC), 125.6 (ArC–C), 124.1 (ArC), 52.1 (OCH_3) ppm (C=N₂ not observed); IR (neat): ν = 3059w, 2953w, 2843w, 2362w, 2083s, 1699s, 1597w, 1575w, 1498m, 1435m, 1352m, 1247m cm^{-1} . Spectroscopic data are in agreement with the literature.⁷

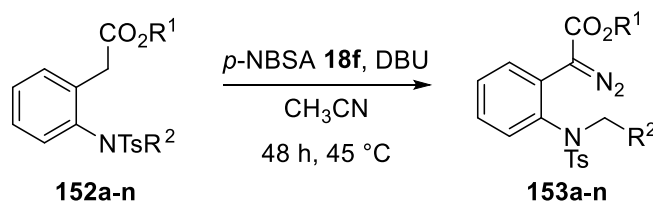
p-Nitrobenzenesulfonyl azide **18f**:²



A solution of sodium azide (290 mg, 4.5 mmol) in water (2 mL) was added dropwise to a solution of *p*-nitrobenzenesulfonyl chloride 97%_{wt} (685 mg, 3 mmol) in acetone (6 mL) cooled to 0 °C. The mixture was allowed to warm up to room temperature and stirred overnight. Acetone was then removed under reduced pressure (water bath at 25 °C). The residue was washed with water (10 mL) and Et_2O (10 mL). The organic layer was further washed with 5%_{wt} Na_2CO_3 aqueous solution, water and brine then dried over MgSO_4 and concentrated under reduced pressure (water bath at 25 °C) to afford **18f** (622 mg, 2.73 mmol, 91%) as a pale yellow solid, m.p.: 100–102 °C.

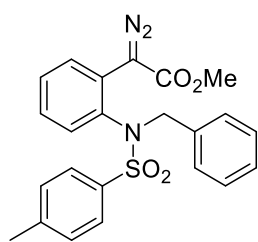
^1H NMR (500 MHz, CDCl_3): δ = 8.51–8.43 (m, 1H, ArH), 8.25–8.06 (m, 1H, ArH) ppm; ^{13}C NMR (126 MHz, CDCl_3): δ = 151.2 (ArC–N), 143.7 (ArC–S), 129.0 (2 \times ArC), 125.1 (2 \times ArC) ppm; IR (neat): ν = 3107m, 2318w, 2140s, 1604m, 1527s, 1404m, 1348s, 1155s, 1109m, 1083s, 1012m, 854s, 761s, 742s, 731s, cm^{-1} . Spectroscopic data are in accordance with the literature.⁸

General Procedure 6:



A solution containing the ester **152a–n** (1 mmol) and *p*-NBSA **18f**² (456 mg, 2 mmol) in CH_3CN (4 mL) was cooled down to 0 °C. DBU (374 μL , 2.5 mmol) was added dropwise. The reaction stirred for 48 hours at room temperature or 45 °C and checked by TLC (*n*-hexane/ethyl acetate 4:1). Then, the reaction mixture was cooled down to 0 °C and a pH 7 phosphate buffer (10 mL) was added to quench the reaction. The reaction mixture was extracted with CH_2Cl_2 (2 \times 20 mL) and the combined organic fractions were washed with pH 7 phosphate buffer (10 mL), brine (15 mL) and dried over MgSO_4 . The solvent was evaporated *in vacuo* (water temperature: 25 °C) and the crude reaction mixture was purified *via* flash column chromatography to afford **153a–n**.

Methyl 2-(2-((*N*-benzyl-4-methylphenyl)sulfonamido)phenyl)-2-diazoacetate **153a**:



Performed according to *General Procedure 6* on a 1.0 mmol scale of **152a**; **153a** (280 mg, 0.65 mmol, 65%) was obtained as a yellow solid, m.p.: 110–112 °C (N_2 loss > 80 °C).

^1H NMR (400 MHz, CDCl_3): δ = 7.64 (d, J = 8.2 Hz, 2H, ArH), 7.46 (dd, J = 7.8, 1.0 Hz, 1H, ArH), 7.33 (d, J = 8.2 Hz, 2H, ArH), 7.26 (d, J = 7.6 Hz, 1H, ArH), 7.13–7.22 (m, 3H, ArH), 7.05–7.11 (m, 3H, ArH), 6.54 (dd, J = 8.1, 1.0 Hz, 1H, ArH), 5.08 (br. s, 1H, N– CH_2), 4.07 (br. s, 1H, N– CH_2), 3.61 (s, 3H, OCH_3), 2.46 (s, 3H, CH_3) ppm; ^{13}C NMR (75 MHz, CDCl_3): δ = 166.1 (C=O), 144.1 (ArC–N), 137.0 (ArC), 135.9 (ArC), 134.5 (ArC), 131.3 (ArC), 129.8 (2 \times ArC), 129.6 (2 \times ArC), 128.8 (ArC), 128.5 (3 \times ArC), 128.4 (2 \times ArC), 128.3 (ArC), 128.1 (ArC), 127.8 (ArC), 60.6 (C= N_2), 57.0 (N CH_2), 51.9 (OCH_3), 21.8 (CH_3) ppm; IR (neat): ν = 3064w, 3032w, 2954w, 2924w, 2096s, 1693s, 1494m, 1429m, 1344s, 1242m, 1159s, 1151s,

1045m, 1029s, 858m, 812m, 717s cm^{-1} ; HRMS (NSI): Exact mass calculated for $\text{C}_{23}\text{H}_{21}\text{N}_3\text{O}_4\text{SNa}$ $[\text{M}+\text{Na}]^+$: 458.1145; found: 458.1142. The structure was confirmed by X-Ray analysis (Figure 5.1).

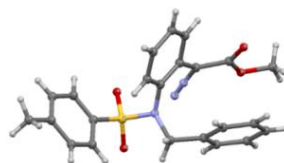
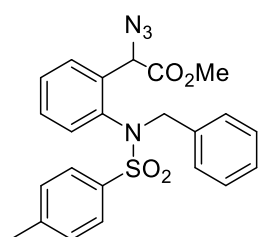


Figure 5.1: X-ray structure of **153a**.^b

Methyl 2-azido-2-(2-((*N*-benzyl-4-methylphenyl)sulfonamido)phenyl) acetate **166**:



Side product **166** (1:1:1 mixture of two rotamers) was obtained as a pale-yellow solid.

^1H NMR (300 MHz, CDCl_3): δ = 7.51 (dd, J = 8.3, 2.9 Hz, 4H, ArH), 7.17 (m, 23H, ArH), 6.57 (t, J = 7. Hz, 2H, ArH), 5.48 (s, 1H, N_3CH), 5.26 (s, 1H, N_3CH), 5.02 (d, J = 13.4 Hz, 1H, NCH_2^1), 4.90 (d, J = 13.9 Hz, 1H, NCH_2), 4.33 (d, J = 13.9 Hz, 1H, NCH_2), 4.11 (d, J = 13.4 Hz, 1H, NCH_2^1), 3.69 (s, 3H, OCH_3^1), 3.38 (s, 3H, OCH_3), 2.38 (s, 6H, 2 \times Ar- CH_3) ppm; ^{13}C NMR (75 MHz, CDCl_3): δ = 169.5 (C=O), 169.4 (C=O), 144.1 (ArC-N), 144.0 (ArC-N), 137.9 (ArC), 137.7 (ArC), 135.9 (ArC), 135.6 (ArC), 135.2 (ArC), 135.1 (ArC), 135.0 (ArC), 134.7 (ArC), 129.7 (ArC), 129.6 (ArC), 129.5 (ArC), 129.4 (ArC), 129.2 (ArC), 129.1 (ArC), 129.0 (ArC), 128.8 (ArC), 128.6 (ArC), 128.4 (ArC), 128.3 (ArC), 128.2 (ArC), 128.0 (ArC), 127.9 (ArC), 60.1 (CH- N_3), 59.9 (C 1 H- N_3), 56.3 (NCH $_2$), 56.4 (NCH $_2$), 53.0 (OCH_3), 52.8 (OCH_3), 21.6 (2 \times CH_3) ppm; IR (neat): ν = 3062w, 3030w, 2954m, 2926m, 2875w, 2850w, 2100s, 1735s, 1595m, 1490m, 1456m, 1448m, 1436m, 1354s, 1257w, 1211s, 1161s, 1089s, 1029s, 867m, 758m, 661s, 522m, 476w cm^{-1} ; HRMS: Exact mass calculated for $\text{C}_{23}\text{H}_{22}\text{N}_4\text{O}_4\text{SNH}_4$ $[\text{M}+\text{NH}_4]^+$: 468.1700; found: 468.1695. The structure was confirmed by X-Ray analysis (Figure 5.2).

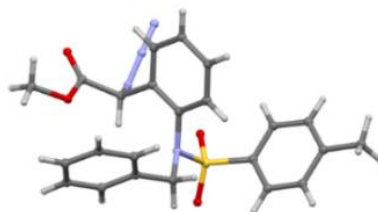
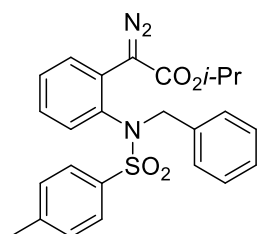


Figure 5.2: X-ray structure of **166**.^c

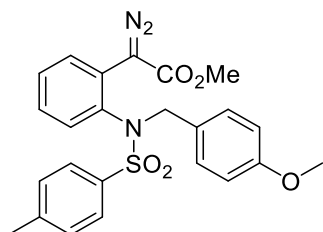
b. Measured by Dr. Benson Kariuki at Cardiff University, School of Chemistry

c. Measured by Dr. Benson Kariuki at Cardiff University, School of Chemistry

Isopropyl 2-(2-((*N*-benzyl-4-methylphenyl)sulfonamido)phenyl)-2-diazoacetate **153b**:

Performed according to *General Procedure 6* at 45 °C on a 0.37 mmol scale of **152b**; **153b** (86 mg, 0.19 mmol, 51%) obtained as yellow solid, m.p.: 86–90 °C (N₂ loss > 80 °C).

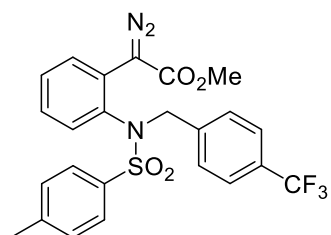
¹H NMR (300 MHz, CDCl₃): δ = 7.67 (d, *J* = 8.1 Hz, 2H, *ArH*), 7.58 (d, *J* = 7.2 Hz, 1H, *ArH*), 7.40–6.71 (m, 9H, *ArH*), 6.56 (d, *J* = 7.6 Hz, 1H), 5.23–4.70 (m, 2H, 1 × NCH₂ + OCH), 4.18 (br. s, 1H, 1 × NCH₂), 2.49 (s, 3H, CH₃), 1.16 (d, *J* = 6.1 Hz, 6H, 2 × CH₃) ppm; ¹³C NMR (75 MHz, CDCl₃): δ = 165.3 (C=O), 144.2 (ArC–N), 136.7 (ArC), 135.9 (ArC), 134.6 (ArC), 131.0 (ArC), 129.8 (2 × ArC), 129.6 (2 × ArC), 128.7 (2 × ArC), 128.5 (2 × ArC), 128.4 (2 × ArC), 128.3 (ArC), 128.2 (ArC), 127.4 (ArC), 68.5 (OCH), 60.7 (C=N₂), 56.9 (NCH₂), 22.2 (CH₃), 21.8 (CH₃) ppm; IR (neat): ν = 2916m, 2848m, 2104s, 1695s, 1595w, 1490m, 1448m, 1336s, 1238s, 1151s, 1105s, 1089s, 1012s, 910w, 856m, 817m, 715s, 698m, 659s, 615m, 586m, 561s, 547s cm⁻¹; HRMS (NSI): Exact mass calculated for C₂₅H₂₉N₂O₄S [M–N₂+NH₄]⁺: 453.1843; found: 453.1838.

Methyl 2-diazo-2-(2-((*N*-(4-methoxybenzyl)-4-methylphenyl)sulfonamido)phenyl)acetate **153c**:

Performed according to *General Procedure 6* at 45 °C on a 0.41 mmol scale of **152c**; **153c** (105 mg, 0.23 mmol, 56%) obtained as a yellow solid, m.p.: 132–135 °C (N₂ loss > 80 °C).

¹H NMR (400 MHz, CDCl₃): δ = 7.66 (d, *J* = 8.2 Hz, 2H, *ArH*), 7.50 (d, *J* = 8.1 Hz, 1H, *ArH*), 7.34 (d, *J* = 8.1 Hz, 2H, *ArH*), 7.29 (t, *J* = 7.7 Hz, 1H, *ArH*), 7.09 (td, *J* = 8.0, 1.3 Hz, 1H, *ArH*), 7.00 (d, *J* = 8.6 Hz, 2H, *ArH*), 6.70 (d, *J* = 8.6 Hz, 2H, *ArH*), 6.55 (d, *J* = 7.8 Hz, 1H, *ArH*), 5.05 (d, *J* = 11.4 Hz, 1H, 1 × NCH₂), 4.04 (d, *J* = 11.6 Hz, 1H, 1 × NCH₂), 3.74 (s, 3H, OCH₃), 3.65 (s, 3H, OCH₃), 2.48 (s, 3H, CH₃) ppm; ¹³C NMR (75 MHz, CDCl₃): δ = 166.1 (C=O), 159.5 (ArC–O), 144.1 (ArC–N), 136.9 (ArC), 136.0 (ArC), 131.2 (ArC), 130.8 (2 × ArC), 129.8 (ArC), 128.8 (ArC), 128.5 (ArC), 128.4 (2 × ArC), 128.2 (ArC), 127.7 (ArC), 126.6 (ArC), 113.8 (ArC), 56.5, 55.2, 51.8, 31.0, 21.7 (CH₃) ppm; IR (neat): ν = 2953w, 2096s, 1703s, 1612w, 1589w, 1512m, 1492m, 1435m, 1340s, 1263s, 1240s, 1149s, 1028s, 877m, 813m, 758s, 727s, 658s, 607s cm⁻¹; HRMS (NSI): Exact mass calculated for C₂₄H₂₃N₃O₄SNa [M+Na]⁺: 488.1251; found: 488.1245.

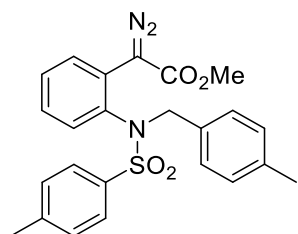
Methyl 2-diazo-2-(2-((4-methyl-*N*-(4-(trifluoromethyl)benzyl)phenyl)sulfonamido)phenyl) acetate, **153d**:



Performed according to *General Procedure 6* at 45 °C on a 0.21 mmol scale of **152d**; **153d** (84 mg, 0.17 mmol, 79%) obtained as a yellow solid, m.p.: 116–118 °C (N₂ loss > 80 °C).

¹H NMR (400 MHz, CDCl₃): δ = 7.63 (d, *J* = 8.3 Hz, 2H, ArH), 7.55–7.40 (m, 3H, ArH), 7.32 (d, *J* = 8.0 Hz, 2H, ArH), 7.28–7.21 (m, 3H, ArH), 7.10 (td, *J* = 7.9, 1.6 Hz, 1H, ArH), 6.55 (dd, *J* = 8.0, 1.2 Hz, 1H, ArH), 5.09 (br. s, 1H, 1 × NCH₂), 4.08 (br. s, 1H, 1 × NCH₂), 3.57 (s, 3H, OCH₃), 2.45 (s, 3H, CH₃) ppm; ¹³C NMR (125 MHz, CDCl₃): δ = 165.9 (C=O), 144.5 (ArC–N), 138.8 (ArC), 137.3 (ArC), 135.8 (ArC), 131.8 (ArC), 130.4 (q, *J* = 32.4 Hz, ArC–CF₃), 129.9 (2 × ArC), 129.8 (2 × ArC), 129.1 (ArC), 128.5 (2 × ArC), 128.4 (ArC), 128.2 (ArC), 128.1 (ArC), 125.3 (q, *J* = 3.7 Hz, ArC), 124.0 (q, *J* = 273.5 Hz, ArC–CF₃), 60.3 (C=N₂), 56.5 (NCH₂), 51.8 (OCH₂), 21.8 (CH₃) ppm; IR (neat): ν = 2954w, 2926w, 2096s, 1741w, 1695s, 1618w, 1597w, 1492m, 1448w, 1435m, 1421w, 1323s, 1240s, 1161s, 1111s, 1066s, 1020s, 817m, 713s, 661s, 547s cm⁻¹; HRMS (ES): Exact mass calculated for C₂₄H₂₀F₃N₃O₄SNa [M+Na]⁺: 526.1024; found: 526.0999.

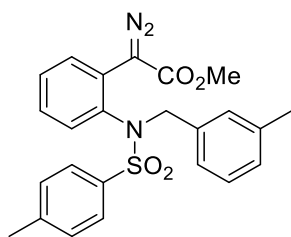
Methyl 2-diazo-2-(2-((4-methyl-*N*-(4-methylbenzyl)phenyl)sulfonamido)phenyl) acetate **153f**:



Performed according to *General Procedure 6* at 45 °C on a 0.35 mmol scale of **152f**; **153f** (108 mg, 0.24 mmol, 69%) obtained as a yellow solid, m.p.: 102–104 °C (N₂ loss > 80 °C).

¹H NMR (300 MHz, CDCl₃): δ = 7.59 (d, *J* = 8.1 Hz, 2H, ArH), 7.42 (d, *J* = 7.3 Hz, 1H, ArH), 7.39–7.17 (m, 3H, ArH), 7.02 (t, *J* = 7.0 Hz, 1H, ArH), 6.90 (s, 4H, ArH), 6.48 (d, *J* = 7.7 Hz, 1H, ArH), 4.97 (br. s, 1H, 1 × CH₂), 3.98 (br. s, 1H, 1 × CH₂), 3.57 (s, 3H, OCH₃), 2.41 (s, 3H, CH₃), 2.19 (s, 3H, CH₃) ppm; ¹³C NMR (75 MHz, CDCl₃): δ = 166.0 (C=O), 154.6 (ArC–N), 144.0 (ArC), 137.8 (ArC), 136.8 (ArC), 135.7 (ArC), 131.3 (ArC), 131.1 (ArC), 129.7 (ArC), 129.4 (ArC), 129.0 (ArC), 128.7 (ArC), 128.3 (ArC), 128.0 (ArC), 127.6 (ArC), 60.7 (C=N₂), 56.7 (NCH₂), 51.8 (OCH₃), 21.7 (CH₃), 21.2 (CH₃) ppm; IR (neat): ν = 2951w, 2918w, 2360m, 2100s, 1699s, 1597w, 1492m, 1435m, 1348s, 1290m, 1265m, 1246m, 1192w, 1161s, 1116w, 1089w, 1033m, 912m, 815w, 779w, 734s, 663m, 574s cm⁻¹; HRMS (NSI): Exact mass calculated for C₂₄H₂₇N₂O₄S [M–N₂+NH₄]⁺: 439.1686; found: 439.1682.

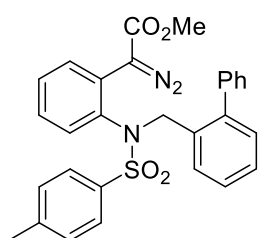
Methyl 2-diazo-2-(2-((4-methyl-*N*-(3-methylbenzyl)phenyl)sulfonamido)phenyl) acetate **153g**:



Performed according to *General Procedure 6* at 45 °C on a 0.28 mmol scale of **152g**; **153g** (78 mg, 0.17 mmol, 61%) obtained as a yellow solid, m.p.: 100–102 °C (N₂ loss > 80 °C).

¹H NMR (400 MHz, CDCl₃): δ = 7.59 (d, *J* = 8.1 Hz, 2H, ArH), 7.42 (d, *J* = 7.8 Hz, 1H, ArH), 7.37–7.12 (m, 3H, ArH), 7.10–6.92 (m, 4H, ArH), 6.72 (d, *J* = 6.1 Hz, 1H, ArH), 6.48 (d, *J* = 7.9 Hz, 1H, ArH), 5.00 (br. s, 1H, 1 × CH₂), 3.98 (br. s, 1H, 1 × CH₂), 3.56 (s, 3H, OCH₃), 2.41 (s, 3H, CH₃), 2.16 (s, 3H, CH₃) ppm; ¹³C NMR (101 MHz, CDCl₃): δ = 166.1 (C=O), 144.2 (ArC–N), 138.3 (ArC), 137.1 (ArC), 136.0 (ArC), 134.5 (ArC), 131.3 (ArC), 130.3 (ArC), 129.8 (2 × ArC), 128.8 (ArC), 128.7 (ArC), 128.5 (ArC), 128.4 (2 × ArC), 128.3 (ArC), 128.2 (ArC), 127.7 (ArC), 126.6 (ArC), 60.6 (C=N₂), 57.0 (NCH₂), 51.8 (OCH₃), 21.8 (CH₃), 21.3 (CH₃) ppm; IR (neat): ν = 2951w, 2918w, 2358m, 2341m, 2098s, 1697s, 1595m, 1492m, 1435m, 1344m, 1288s, 1246m, 1155s, 1118w, 1089m, 1049m, 752m, 723s, 705m, 661s, 565s cm⁻¹; HRMS (NSI): Exact mass calculated for C₂₄H₂₃N₃O₄SNa [M+Na]⁺: 472.1301; found: 472.1295.

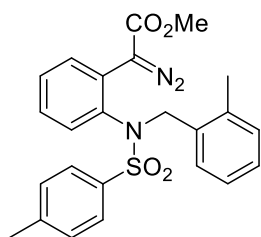
Methyl 2-(2-((*N*-([1,1'-biphenyl]-2-ylmethyl)-4-methylphenyl)sulfonamido)phenyl)-2-diazoacetate **153h**:



Performed according to *General Procedure 6* at 45 °C on a 0.30 mmol scale of **152h**; **153h** (117 mg, 0.23 mmol, 76%) was obtained as a yellow solid, m.p.: 144–146 °C (N₂ loss > 80 °C).

¹H NMR (400 MHz, CDCl₃): δ = 7.82 (d, *J* = 7.7 Hz, 1H, ArH), 7.49 (d, *J* = 8.0 Hz, 2H, ArH), 7.36–7.12 (m, 6H, ArH), 7.04–6.86 (m, 4H, ArH), 6.73 (t, *J* = 7.5 Hz, 1H, ArH), 6.51 (d, *J* = 7.2 Hz, 2H, ArH), 5.96 (d, *J* = 7.9 Hz, 1H, ArH), 4.94 (br. s, 1H, 1 × NCH₂), 4.10 (br. s, 1H, 1 × NCH₂), 3.51 (s, 3H, OCH₃), 2.35 (s, 3H, CH₃) ppm; ¹³C NMR (101 MHz, CDCl₃): δ = 166.0 (C=O), 144.0 (ArC–N), 142.3 (ArC), 140.1 (ArC), 137.6 (ArC), 136.1 (ArC), 132.5 (ArC), 131.8 (ArC), 130.5 (ArC), 129.9 (ArC), 129.8 (2 × ArC), 129.0 (2 × ArC), 128.5 (ArC), 128.3 (2 × ArC), 128.2 (ArC), 128.1 (ArC), 128.0 (ArC), 127.8 (ArC), 127.7 (2 × ArC), 127.4 (ArC), 126.4 (ArC), 60.2 (C=N₂), 53.1 (NCH₂), 51.7 (OCH₃), 21.7 (CH₃) ppm; IR (neat): ν = 3062w, 2953w, 2102s, 1693s, 1431m, 1342s, 1255m, 1238m, 1155s, 1045m, 854m, 712s, 659s, 569s, 542s cm⁻¹; HRMS (APCI): Exact mass calculated for C₂₉H₂₅N₃O₄SNa [M+Na]⁺: 534.1463; found: 534.1453.

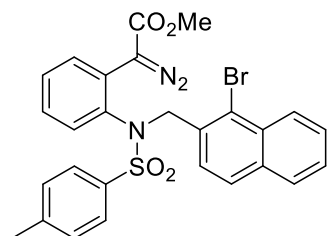
Methyl 2-diazo-2-(2-((4-methyl-*N*-(2-methylbenzyl)phenyl)sulfonamido)phenyl) acetate **153i**:



Performed according to *General Procedure 6* at 45 °C on a 0.30 mmol scale of **152i**; **153i** (79 mg, 0.17 mmol, 59%) was obtained as a yellow solid.

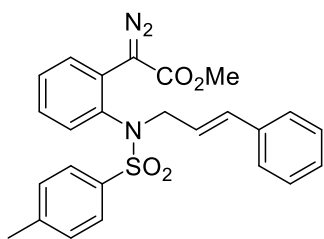
$^1\text{H NMR}$ (400 MHz, CDCl_3): δ = 7.71 (d, J = 8.1 Hz, 2H, ArH), 7.51–7.33 (m, 3H, ArH), 7.33–7.19 (m, 1H, ArH), 7.18–6.99 (m, 3H, ArH), 6.90 (t, J = 7.3 Hz, 1H, ArH), 6.76 (d, J = 7.6 Hz, 1H, ArH), 6.60 (d, J = 8.0 Hz, 1H, ArH), 5.24 (br. s, 1H, 1 \times NCH_2), 4.03 (br. s, 1H, 1 \times NCH_2), 3.59 (s, 3H, OCH_3), 2.50 (s, 3H, CH_3), 2.24 (s, 3H, CH_3) ppm; $^{13}\text{C NMR}$ (101 MHz, CDCl_3): δ = 165.9 (C=O), 144.3 (ArC–N), 138.0 (ArC), 137.4 (ArC), 135.7 (ArC), 132.1 (ArC), 131.7 (ArC), 130.9 (ArC), 130.4 (ArC), 129.9 (2 \times ArC), 128.9 (ArC), 128.8 (ArC), 128.6 (2 \times ArC), 128.2 (ArC), 127.9 (ArC), 127.8 (ArC), 125.9 (ArC), 60.4 (C=N₂), 54.7 (NCH₂), 51.8 (OCH₃), 21.8 (Ar–CH₃), 18.8 (CH₃) ppm; IR (neat): ν = 2951w, 2922w, 2858w, 2362w, 2098s, 1697s, 1595w, 1514w, 1435m, 13344s, 1155s, 1089w, 1033m, 912m, 754m, 729s, 663s, 607w, 580s, 553m cm^{-1} ; HRMS (NSI): Exact mass calculated for $\text{C}_{24}\text{H}_{27}\text{N}_2\text{O}_4\text{S}$ [$\text{M}-\text{N}_2+\text{NH}_4$]⁺: 439.1686; found: 439.1682.

Methyl 2-(2-((*N*-((1-bromonaphthalen-2-yl)methyl)-4-methylphenyl)sulfonamido)phenyl) 2-diazoacetate **153k**:



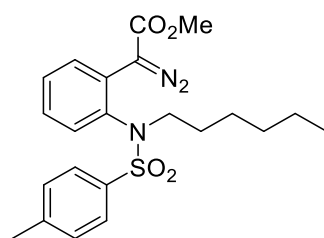
Performed according to *General Procedure 6* at 45 °C on a 0.34 mmol scale of **152k**; **153k** (146 mg, 0.26 mmol, 76%) was obtained as a yellow solid, m.p.: 136–138 °C (N_2 loss > 80 °C).

$^1\text{H NMR}$ (400 MHz, CDCl_3): δ = 8.11 (d, J = 8.4 Hz, 1H, ArH), 7.69 (t, J = 6.9 Hz, 3H, ArH), 7.61 (d, J = 8.4 Hz, 1H, ArH), 7.53–7.36 (m, 3H, ArH), 7.33 (d, J = 8.0 Hz, 2H, ArH), 7.20 (dt, J = 7.8, 7.0 Hz, 2H, ArH), 7.06 (t, J = 7.6 Hz, 1H, ArH), 6.62 (d, J = 8.0 Hz, 1H, ArH), 5.35 (br. s, 1H, 1 \times NCH_2), 4.59 (br. s, 1H, 1 \times NCH_2), 2.87 (s, 3H, OCH_3), 2.44 (s, 3H, CH_3) ppm; $^{13}\text{C NMR}$ (101 MHz, CDCl_3): δ = 165.6 (C=O), 144.4 (ArC–N), 137.9 (ArC), 134.7 (ArC), 135.9 (ArC), 134.2 (ArC), 132.2 (ArC), 132.1 (ArC), 132.0 (ArC), 129.9 (2 \times ArC), 128.9 (ArC), 128.6 (2 \times ArC), 128.5 (ArC), 128.4 (ArC), 128.2 (ArC), 128.17 (2 \times ArC), 128.16 (2 \times ArC), 127.9 (ArC), 127.5 (ArC), 126.9 (ArC), 125.4 (ArC), 60.4 (C=N₂), 57.4 (NCH₂), 51.3 (OCH₃), 20.6 (CH₃) ppm; IR (neat): ν = 2956w, 2094s, 1697s, 1597w, 1492m, 1438m, 1344s, 1247m, 1192w, 1155s, 854m, 813s, 752s, 736m, 717s, 661s, 648m, 590w, 576s, 547m, 528m cm^{-1} ; HRMS (NSI): Exact mass for $\text{C}_{27}\text{H}_{26}\text{N}_2\text{O}_4\text{SBr}$ [$\text{M}-\text{N}_2+\text{NH}_4$]⁺: 553.1009; found: 553.0786.

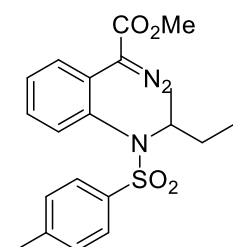
Methyl 2-(2-((*N*-cinnamyl-4-methylphenyl)sulfonamido)phenyl)-2-diazoacetate **153l**:

Performed according to *General Procedure 6* at 22 °C on a 0.62 mmol scale of **152l** with 1.2 mmol *p*-NBSA and 1.2 mmol of DBU. **153l** (116 mg, 0.25 mmol, 42%) was obtained as a yellow solid, m.p.: 106–108 °C (N₂ loss > 60 °C). The compound was unstable and decomposed during characterisation. The mixture of unreacted starting material, diazo compound and side product was used for the following step without further purification.

¹H NMR (400 MHz, CDCl₃): δ = 7.54 (d, *J* = 8.2 Hz, 2H, *ArH*), 7.26–7.10 (m, 9H, *ArH*), 7.08–7.03 (m, 1H, *ArH*), 6.59 (d, *J* = 8.0 Hz, 1H, *ArH*), 6.26 (d, *J* = 15.8 Hz, 1H, CH=CH-Ph), 6.05–5.93 (m, 1H, NCH₂CH=CH), 4.39 (br. s, 1H, 1 × NCH₂), 3.95 (br. s, 1H, 1 × NCH₂), 3.55 (s, 3H, OCH₃), 2.37 (s, 3H, CH₃) ppm; ¹³C NMR (101 MHz, CDCl₃): δ = 166.4 (C=O), 144.1 (ArC-N), 137.3 (ArC), 136.2 (ArC), 135.6 (ArC), 135.2 (ArC), 131.5 (ArC), 129.7 (2 × ArC), 128.9 (ArC), 128.6 (2 × ArC), 128.6 (ArC), 128.4 (2 × ArC), 128.1 (ArC), 126.6 (2 × ArC), 122.6 (ArC), 54.6 (NCH₂), 52.0 (OCH₃), 21.7 (CH₃) ppm; IR (neat): ν = 3038w, 2953w, 2099s, 1697s, 1491m, 1431m, 1348s, 1149s cm⁻¹. The product decomposed during mass spectrometric analysis.

Methyl 2-diazo-2-(2-((*N*-(*n*-hexyl)-4-methylphenyl)sulfonamido)phenyl) acetate **153m**:

Performed according to the *General Procedure 6* at 45 °C on a 0.24 mmol scale of **152m**. After column chromatography **153m** (41% by ¹H NMR) was still obtained as a 1.8 : 1 : 0.4 mixture of **152m**, **153m** and a side azide (rotamers 1.3 : 1). The mixture of unreacted starting material, diazo compound and side product was used for the following step without further purification.

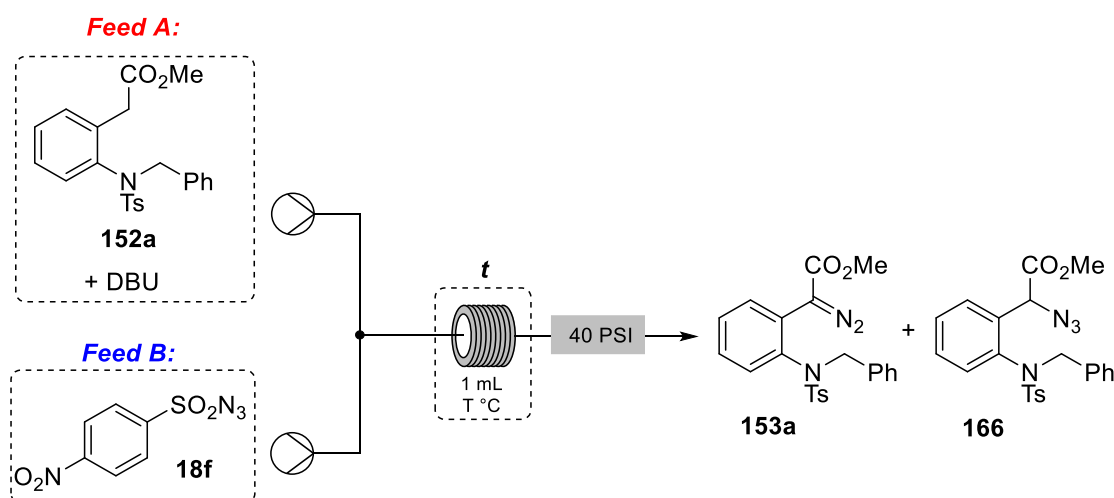
Methyl 2-diazo-2-(2-((*N*-(*sec*-butyl)-4-methylphenyl)sulfonamido)phenyl) acetate **153n**:

Performed according to *General Procedure 6* at 45 °C on a 0.15 mmol scale of **152n**; **153n** (17 mg, 0.042 mmol, 28%) was obtained as a yellow oil, 1:1.3 mixture or rotamers (air-sensitive).

¹H NMR (400 MHz, CDCl₃): δ = 7.73–7.59 (m, 3H, *ArH*), 7.39 (t, *J* = 7.7 Hz, 1H, *ArH*), 7.35–7.28 (m, 2H, *ArH*), 7.22–7.12 (m, 1H, *ArH*), 6.75 (d, *J* = 8.0 Hz, 0.4H, *ArH*), 6.69 (d, *J* = 7.9 Hz, 0.6H, *ArH*), 4.27–4.13 (m, 1H, NCH + NCH'), 3.86–3.82 (m, 3H, OCH₃ + OCH₃), 2.49–2.42 (m, 0.7H), 1.74–1.62 (m, 0.4H), 1.30–1.08 (m, 2H), 1.07–0.91 (m, 2H), 0.90–0.71 (m, 3H) ppm; ¹³C NMR (101 MHz,

CDCl₃): δ = 167.1 (C=O), 167.0 (C=O), 143.8 (ArC–N), 143.8 (ArC–N), 138.3 (ArC), 138.1 (ArC), 134.7 (ArC), 134.5 (ArC), 133.0 (ArC), 132.3 (ArC), 131.4 (ArC), 131.3 (ArC), 129.8 (2 × ArC), 129.7 (2 × ArC), 129.09 (ArC), 129.08 (ArC), 128.3 (2 × ArC), 128.1 (2 × ArC), 128.1 (ArC), 127.8 (ArC), 127.6 (2 × ArC), 59.3 (NCH), 59.1 (NCH), 52.3 (OCH₃), 28.8, 27.8, 21.7, 18.0, 11.6, 11.5 ppm; IR (neat): ν = 2960w, 2850w, 2098s, 1697s, 1358s, 1165s cm⁻¹. The isolated product decomposed during mass spectrometric analysis.

5.2.3 Diazo-transfer in Flow and DoE



The starting material **152a** (81.9–164 mg, 0.2–0.4 mmol) was dissolved in 2 mL of acetonitrile together with DBU (1.5–2.5 equiv.) and the internal standard (1,3,5-trimethoxybenzene 1 equiv.) and a HSW NORM-JECT[®] 2 mL syringe was equipped with the mixture. At the same time *p*-NBSA **18f** (1–3 equiv.) was dissolved in 2 mL of acetonitrile and a second HSW NORM-JECT[®] 2 mL syringe was equipped with this solution. Next, the two syringes were loaded on a Chemyx Fusion syringe pump and connected to a flow setup *via* a T-piece mixer and a 1 mL coil (FEP, i.d. = 0.5 mm). The pump was then set to 0.1 mL·min⁻¹ (for *t* = 10 minutes) or 0.02 mL·min⁻¹ (for *t* = 50 minutes) and the entire setup run for 25 or 100 minutes, respectively, to ensure the achievement of the steady state. Afterwards, the solution was collected for 20–60 minutes in a 0.1 M phosphate buffer solution (pH = 7) as quenching agent. Extraction was performed with CH₂Cl₂ (3 × 5 mL), the combined organic layers were washed with water, dried over a MgSO₄ plug and concentrated under reduced pressure. When isolated the desired diazo compound **153a** was purified by column chromatography (*n*-hexane / ethyl acetate 80:20). The data from the FFD 2⁵⁻¹ were analysed using a FFD and Design Expert[®] 10.⁹

Table 5.1: Real and coded values (+1 = higher level, -1 = lower level, 0 = central point) for the independent variables (k) and responses.

Factor (k)	Type	Unit	-1	0	+1
A: 152a	Numeric	M	0.1	0.15	0.2
B: Temperature	Numeric	°C	22	43.5	65
C: DBU	Numeric	equiv.	1.5	2	2.5
D: <i>p</i> -NBSA	Numeric	equiv.	1	2	3
E: Time	Numeric	min	10	30	50
Responses:		152a (%)		153a (%)	166 (%)

^aYield determined by ¹H NMR with 1,3,5-trimethoxybenzene as internal standard.

Table 5.2: Experimental Matrix of the FFD 2⁵⁻¹ in coded values and factor generator.

Std	A	B	C	D	E = A*B*C*D
1	-1	-1	-1	-1	1
2	1	-1	-1	-1	-1
3	-1	1	-1	-1	-1
4	1	1	-1	-1	1
5	-1	-1	1	-1	-1
6	1	-1	1	-1	1
7	-1	1	1	-1	1
8	1	1	1	-1	-1
9	-1	-1	-1	1	-1
10	1	-1	-1	1	1
11	-1	1	-1	1	1
12	1	1	-1	1	-1
13	-1	-1	1	1	1
14	1	-1	1	1	-1
15	-1	1	1	1	-1
16	1	1	1	1	1
17	0	0	0	0	0

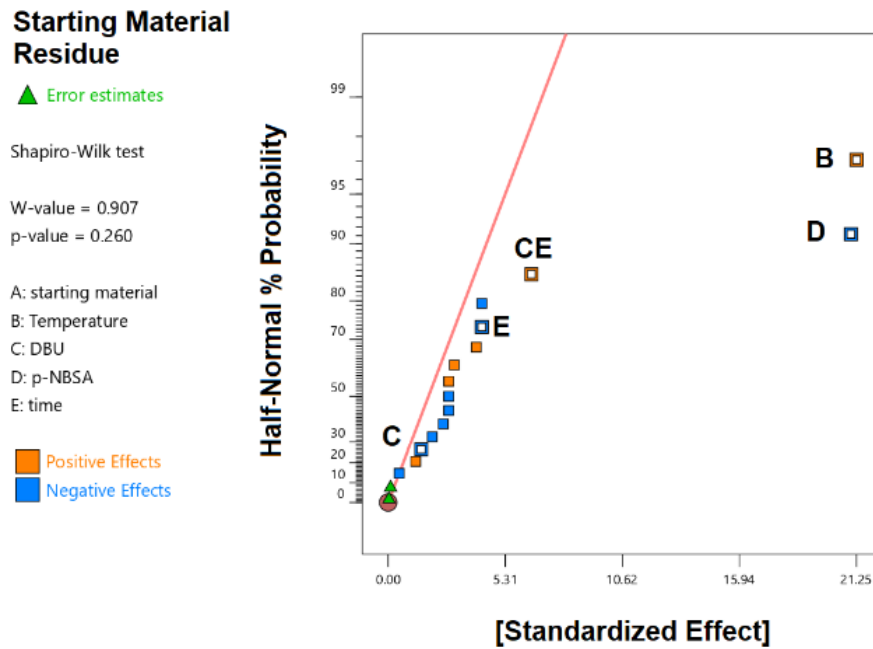


Figure 5.3: Half-normal plots for starting material **152a** left.

ANOVA for R¹: Starting Material Residue

	Sum of Squares	df	Mean Square	F-value	p-value
Model	3820.50	5	764.10	28.72	< 0.0001 significant
B-Temperature	1806.25	1	1806.25	67.89	< 0.0001
C-DBU	9.00	1	9.00	0.3383	0.5716
D-p-NBSA	1764.00	1	1764.00	66.31	< 0.0001
E-time	72.25	1	72.25	2.72	0.1253
CE	169.00	1	169.00	6.35	0.0269
Curvature	0.3553	1	0.3553	0.0134	0.9099
Residual	319.25	12	26.60		
Lack of Fit	311.25	10	31.13	7.78	0.1192 not significant
Pure Error	8.00	2	4.00		
Cor Total	4140.11	18			

Fit Statistics

Std. Dev.	5.16	R²	0.9229
Mean	40.32	Adjusted R²	0.8907
		Predicted R²	0.8032
		Adeq Precision	16.9289

Equations in Terms of Coded Values

$$\text{Starting Material Residue} = 40.375 + 10.625B - 0.75C - 10.5D - 2.125E + 3.25CE$$

Formation of Diazo Compound

▲ Error estimates

Shapiro-Wilk test

W-value = 0.952

p-value = 0.636

A: starting material

B: Temperature

C: DBU

D: p-NBSA

E: time

■ Positive Effects

■ Negative Effects

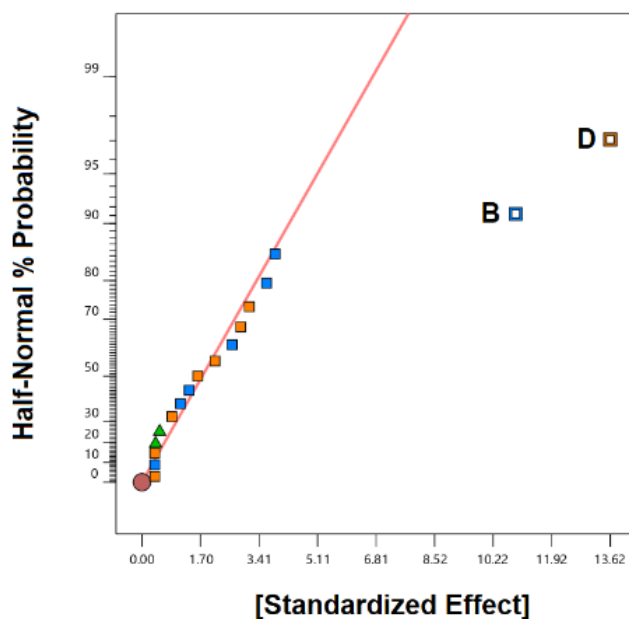


Figure 5.4: Half-normal plots for diazo compound **153a** formation.

ANOVA for R²: Formation of Diazo Compound

	Sum of Squares	df	Mean Square	F-value	p-value
Model	1215.63	2	607.81	32.92	< 0.0001 significant
B-Temperature	473.06	1	473.06	25.62	0.0001
D-p-NBSA	742.56	1	742.56	40.21	< 0.0001
Curvature	7.92	1	7.92	0.4290	0.5224
Residual	276.98	15	18.47		
Lack of Fit	258.31	13	19.87	2.13	0.3646 not significant
Pure Error	18.67	2	9.33		
Cor Total	1500.53	18			

Fit Statistics

Std. Dev.	4.30	R²	0.8144
Mean	31.16	Adjusted R²	0.7897
		Predicted R²	0.7097
		Adeq Precision	12.4261

Equation in Terms of Coded Values

$$\text{Diazo Compound Formation} = 31.4375 - 5.4375B + 6.8125D$$

Formation of Side Azide

▲ Error estimates

Shapiro-Wilk test

W-value = 0.960

p-value = 0.771

A: starting material

B: Temperature

C: DBU

D: p-NBSA

E: time

■ Positive Effects

■ Negative Effects

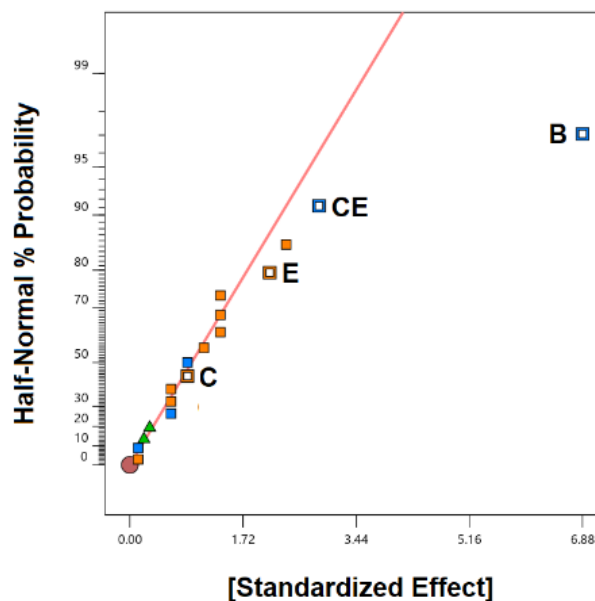


Figure 5.5: Half-normal plot for azide 166 formation.

ANOVA for R³: Formation of Azide

	Sum of Squares	df	Mean Square	F-value	p-value	
Model	243.25	4	60.81	11.48	0.0003	significant
B-Temperature	189.06	1	189.06	35.70	< 0.0001	
C-DBU	3.06	1	3.06	0.5782	0.4606	
E-time	18.06	1	18.06	3.41	0.0877	
CE	33.06	1	33.06	6.24	0.0267	
Curvature	1.05	1	1.05	0.1989	0.6629	
Residual	68.85	13	5.30			
Lack of Fit	58.19	11	5.29	0.9918	0.6038	not significant
Pure Error	10.67	2	5.33			
Cor Total	313.16	18				

Fit Statistics

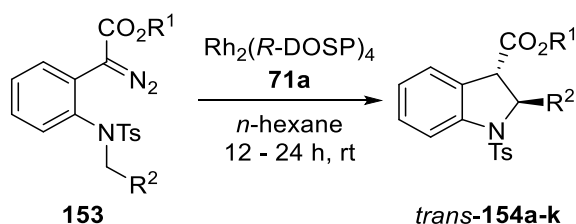
Std. Dev.	2.30	R²	0.7794
Mean	15.79	Adjusted R²	0.7115
C.V. %	14.58	Predicted R²	0.5287
		Adeq Precision	9.1821

Equations in Terms of Coded Values

$$\text{Azide Formation} = 15.6875 - 3.4375B + 0.4375C + 1.0625E - 1.4375CE$$

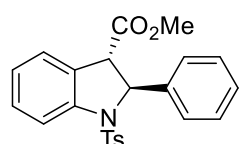
5.2.4 Synthesis of Dihydroindoles

General Procedure 7:



An oven-dried 25 mL round bottom flask was equipped with a magnetic stirring bar and flushed with argon. Molecular sieves (3 Å, 1.2 g), and $\text{Rh}_2(\text{R-DOSP})_4$ **71a** (1–0.5 mol%) were added in dry *n*-hexane. Subsequently, diazo compound **153a–k** (0.23 mmol) were added (final concentration of starting material 0.13 M) and the yellow suspension was vigorously stirred at room temperature under inert atmosphere and checked by TLC (100% CH_2Cl_2) until all diazo compound were consumed (12–24 h). The mixture was filtered through a silica-plug, washed with CH_2Cl_2 (3 × 5 mL) and concentrated under vacuum to afford the corresponding product **154a–k** as a mixture of *trans* and *cis* isomers, separated by prep-TLC or column chromatography in CH_2Cl_2 .

Methyl (2*S*,3*S*)-2-phenyl-1-tosylindoline-3-carboxylate (*S,S*)-**154a**:



Performed according to *General Procedure 7* on a 0.23 mmol scale of **153a** using 0.5 mol% of $\text{Rh}_2(\text{R-DOSP})_4$ over 12 h; (*S,S*)-**154a** (79 mg, 0.19 mmol, 82%, 11:1 *d.r.*, 85% *ee*) was obtained as a colourless solid, m.p.: 130–134 °C.

^1H NMR (300 MHz, CDCl_3): δ = 7.76 (d, J = 8.2 Hz, 1H, ArH), 7.65 (d, J = 8.3 Hz, 2H, ArH), 7.42–7.25 (m, 7H, ArH), 7.19 (d, J = 8.0 Hz, 2H, ArH), 7.08 (td, J = 7.5, 0.9 Hz, 1H, ArH), 5.78 (d, J = 3.7 Hz, 1H, N–CH), 3.91 (d, J = 3.7 Hz, 1H, CH–CO₂Me), 3.55 (s, 3H, OCH₃), 2.36 (s, 3H, CH₃) ppm; ^{13}C NMR (75 MHz, CDCl_3): δ = 170.6 (C=O), 144.1 (ArC), 142.3 (ArC), 141.9 (ArC), 134.8 (ArC), 129.6 (2 × ArC), 128.9 (2 × ArC), 128.0 (ArC), 127.7 (2 × ArC), 127.5 (ArC), 126.4 (ArC), 125.9 (2 × ArC), 124.5 (ArC), 115.8 (ArC), 67.0, 55.8, 52.8, 21.7 (CH₃) ppm; IR (neat): ν = 3032w, 2954w, 1732s, 1597m, 1477m, 1354s, 1238m, 1166s, 1155s, 1103m, 1089m, 1014m, 952m, 810m, 678s, 570s, 543s cm^{-1} ; HMRS: Exact mass calculated for $\text{C}_{23}\text{H}_{21}\text{NO}_4\text{SNH}_4$ [$\text{M}+\text{NH}_4$]⁺: 425.1530; found: 425.1525; HPLC (7:93 *e.r.*): Chiracel[®] OD-H (250 × 4.6 mm, 5 μm),

n-hexane/isopropanol 99:1 (v/v), 1.0 mL·min⁻¹, 10 °C, λ = 254 nm, retention time (*R,R*)-**154a** = 33.1 min, retention time (*S,S*)-**154a** = 36.7 min.

In a similar reaction with Rh₂(*S*-DOSP)₄ the product (*R,R*)-**154a** was obtained as the major isomer and crystallised for the determination of the X-ray structure. (*R,R*)-**154a**: [α]_D²⁰: +40° (c 0.10, CHCl₃).

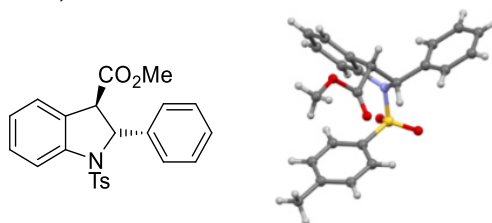
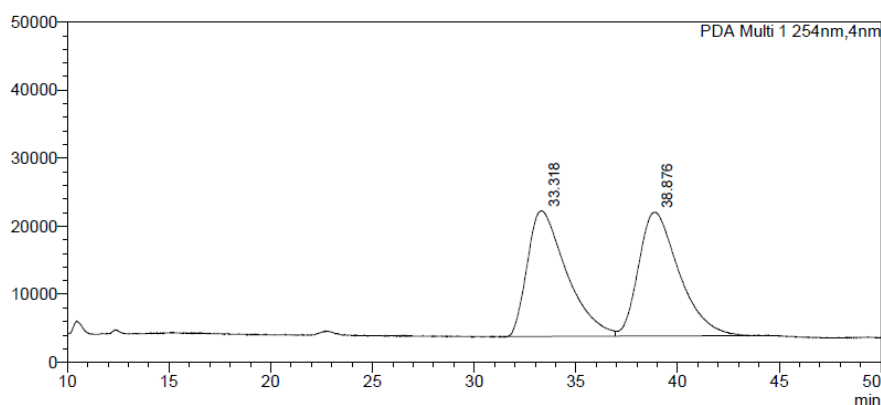
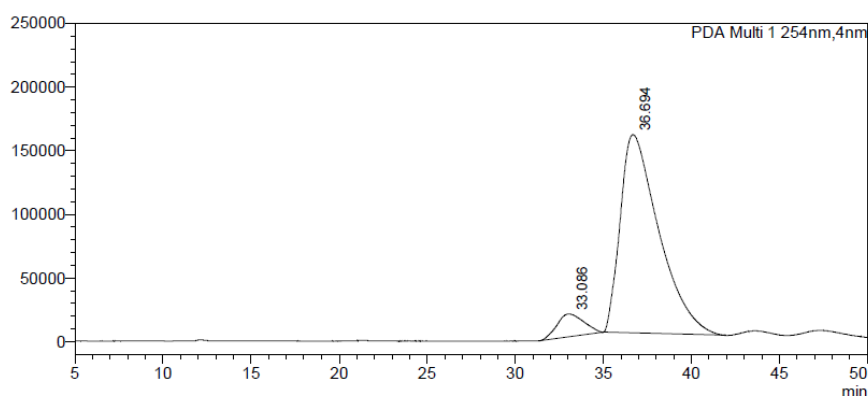


Figure 5.6: X-ray structure of (*R,R*)-**154a**.^d



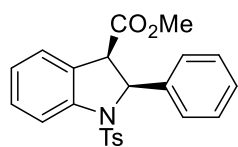
Peak #	Time (min)	Area (%)
1	33.318	49.594
2	38.876	50.406



Peak #	Time (min)	Area (%)
1	33.086	7.423
2	36.694	92.577

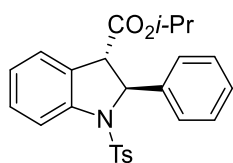
Figure 5.7: HPLC chromatograms of *trans*-**154a** enantiomers. From the top: racemic mixture, 85% ee of (*S,S*)-**154a**.

d. Measured by Dr. Benson Kariuki at Cardiff University, School of Chemistry

Methyl (2*R*,3*S*)-2-phenyl-1-tosylindoline-3-carboxylate (*R,S*)-**154a**:

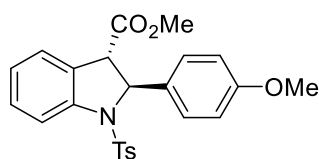
cis-**154a** was obtained as the minor product as a colourless oil after prep-TLC.

$^1\text{H NMR}$ (500 MHz, CDCl_3): δ = 7.71 (d, J = 8.2 Hz, 1H, ArH), 7.52 (d, J = 8.0 Hz, 2H, ArH), 7.34 (t, J = 7.5 Hz, 1H, ArH), 7.24–7.06 (m, 9H, ArH), 5.59 (d, J = 10.0 Hz, 1H, N–CH), 4.37 (d, J = 9.8 Hz, 1H, CH–CO₂Me), 3.22 (s, 3H, OCH₃), 2.36 (s, 3H, CH₃) ppm; $^{13}\text{C NMR}$ (126 MHz, CDCl_3): δ = 169.7 (C=O), 144.2 (ArC), 142.8 (ArC), 137.5 (ArC), 135.4 (ArC), 129.8 (2 × ArC), 129.1 (ArC), 128.7 (ArC), 128.5 (ArC), 128.3 (2 × ArC), 127.3 (2 × ArC), 127.2 (2 × ArC), 127.0 (ArC), 124.9 (ArC), 116.2 (ArC), 67.4, 52.8, 51.8, 21.7 (CH₃) ppm; IR (neat): ν = 3032w, 2954w, 1732s, 1597m, 1477m, 1354s, 1238m, 1166s, 1155s, 1103m, 1089m, 1014m, 952m, 810m, 678s, 570s, 543s cm^{-1} ; HMRS: Exact mass calculated for $\text{C}_{23}\text{H}_{21}\text{NO}_4\text{SNH}_4$ [$\text{M}+\text{NH}_4$]⁺: 425.1530; found: 425.1525; HPLC: YMC Chiral Amylose-C S (250 × 4.6 mm, 5 μm), *n*-hexane/isopropanol 90:10 (v/v), 1.0 mL·min⁻¹, 25 °C, λ = 254 nm, retention time first isomer = 17.5 min, retention time second isomer = 37.9 min.

Isopropyl (2*S*,3*S*)-2-phenyl-1-tosylindoline-3-carboxylate (*S,S*)-**154b**:

Performed according to *General Procedure 7* on a 0.10 mmol scale of **153b** using 1 mol% of $\text{Rh}_2(\text{R-DOSP})_4$ over 12 h; **154b** (27 mg, 0.062 mmol, 62%, 2.2:1 *d.r.*, 35% *ee*) was obtained as a colourless solid m.p.: 120–124 °C; $[\alpha]_D^{20}$: +5.6° (c 0.36, CHCl_3).

$^1\text{H NMR}$ (400 MHz, CDCl_3): δ = 7.64 (d, J = 8.1 Hz, 1H, ArH), 7.55 (d, J = 7.8 Hz, 2H, ArH), 7.37–7.12 (m, 7H, ArH), 7.07 (d, J = 8.1, Hz, 2H, ArH), 6.96 (t, J = 7.5 Hz, 1H, ArH), 5.69 (d, J = 4.0 Hz, 1H, N–CH), 4.78 (septet, J = 6.2 Hz, 1H, OCH), 3.77 (d, J = 3.8 Hz, 1H, CH–CO₂*i*-Pr), 2.24 (s, 3H, CH₃), 1.10 (d, J = 6.2 Hz, 3H, CH₃), 1.01 (d, J = 6.2 Hz, 3H, CH₃) ppm; $^{13}\text{C NMR}$ (101 MHz, CDCl_3): δ = 169.7 (C=O), 144.0 (ArC), 142.6 (ArC), 142.0 (ArC), 134.8 (ArC), 129.6 (2 × ArC), 129.4 (ArC), 128.9 (2 × ArC), 128.0 (ArC), 127.7 (2 × ArC), 127.6 (ArC), 126.3 (ArC), 126.0 (ArC), 124.3 (ArC), 115.6 (ArC), 69.4, 66.9, 56.0, 21.8 (CH₃), 21.6 (2 × CH₃) ppm; IR (neat): ν = 2962w, 2341s, 2262w, 1735m, 1724w, 1597w, 1477m, 1458m, 1357m, 1323w, 1259m, 1238w, 1166s, 1101s, 1010m, 908s, 864w, 798m cm^{-1} ; HRMS (NSI): Exact mass calculated for $\text{C}_{26}\text{H}_{21}\text{NO}_4\text{S}$ [$\text{M}+\text{H}$]⁺: 426.1577; found: 426.1571; HPLC (32:68) YMC Chiral Amylose-C S (250 × 4.6 mm, 5 μm), *n*-hexane / isopropanol 90:10 (v/v), 1.0 mL·min⁻¹, 25 °C, λ = 254 nm, retention time minor isomer = 9.9 min, retention time second isomer = 14.9 min. The HPLC chromatograms are reported in literature.¹⁰

Methyl (2*S*,3*S*)-2-(4-methoxyphenyl)-1-tosylindoline-3-carboxylate (*S,S*)-**154c**:

Performed according to *General Procedure 7* on a 0.14 mmol scale of **153c** using 1 mol% of $\text{Rh}_2(\text{R-DOSP})_4$ over 24 h; **154c** (32 mg, 0.080 mmol, 57%, 4:1 *d.r.*, 55% *ee*) was obtained as a pale yellow solid m.p.: 60–64 °C; $[\alpha]_D^{20}$:

+23.2° (c 0.11, CHCl_3).

$^1\text{H NMR}$ (400 MHz, CDCl_3): δ = 7.73 (d, J = 8.2 Hz, 1H, ArH), 7.63 (d, J = 8.3 Hz, 2H, ArH), 7.35–7.24 (m, 4H, ArH), 7.18 (d, J = 8.1 Hz, 2H, ArH), 7.06 (td, J = 7.5, 1.0 Hz, 1H, ArH), 6.84 (dt, J = 8.9, 2.2 Hz, 2H, ArH), 5.71 (d, J = 3.7 Hz, 1H, N–CH), 3.90 (d, J = 3.7 Hz, 1H, CH–CO₂Me), 3.78 (s, 3H, OCH₃), 3.54 (s, 3H, OCH₃), 2.35 (s, 3H, CH₃) ppm; $^{13}\text{C NMR}$ (101 MHz, CDCl_3): δ = 170.8 (C=O), 159.4 (ArC), 144.0 (ArC), 141.9 (ArC), 134.9 (ArC), 134.6 (ArC), 129.5 (2 × ArC), 127.7 (2 × ArC), 127.5 (ArC), 127.2 (2 × ArC), 126.4 (ArC), 124.4 (ArC), 115.7 (ArC), 114.3 (2 × ArC), 66.7, 55.8, 55.4, 52.7, 21.6 (CH₃) ppm; IR (neat): ν = 2937w, 1740s, 1512m, 1477m, 1460m, 1362m, 1217m, 1163s, 1105m, 1090m, 1026m, 812m, 706m, 658m cm^{-1} ; HRMS (APCI): Exact mass calculated for $\text{C}_{24}\text{H}_{23}\text{NO}_5\text{S}$ $[\text{M}+\text{H}]^+$: 438.1375; found: 438.1375; HPLC (24:76 *e.r.*): YMC Chiral Amylose-C S (250 × 4.6 mm, 5 μm), *n*-hexane/isopropanol 85:15 (v/v), 1.0 $\text{mL}\cdot\text{min}^{-1}$, 10 °C, λ = 254 nm, retention time minor isomer = 26.1 min, retention time major isomer = 62.5 min.

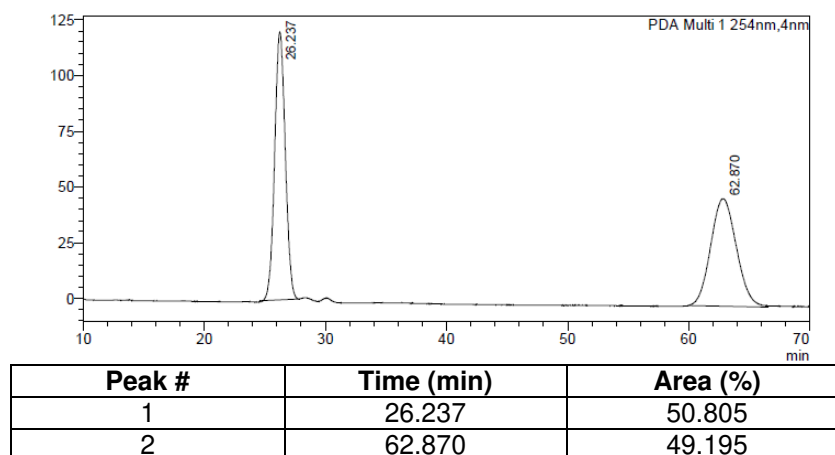
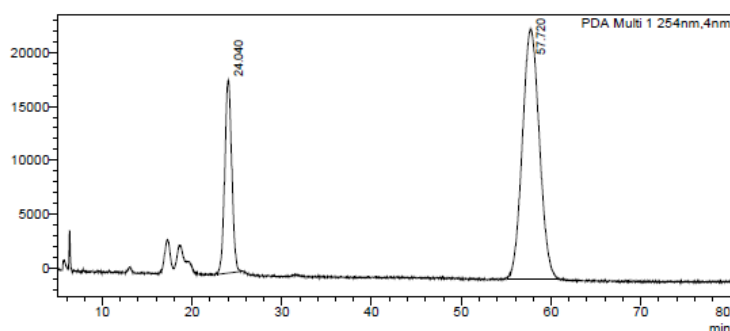


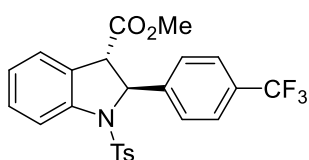
Figure 5.8: HPLC chromatograms of the racemic mixture of *trans*-**154c**.



Peak #	Time (min)	Area (%)
1	24.040	24.115
2	57.720	75.885

Figure 5.9: HPLC chromatograms of *trans*-**154c** enantiomers (55% *ee*).

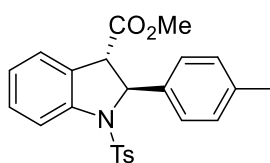
Methyl (2*S*,3*S*)-1-tosyl-2-(4-(trifluoromethyl)phenyl)indoline-3-carboxylate (*S,S*)-**154d**:



Performed according to *General Procedure 7* on a 0.12 mmol scale of **153d** using 0.5 mol% of Rh₂(*R*-DOSP)₄ over 12 h; **154d** (45 mg, 0.09 mmol, 82%, 5:1 *d.r.*, 80% *ee*) was obtained as a colourless solid m.p.: 66–70 °C; $[\alpha]_D^{20}$: +25.9° (c 0.15, CHCl₃).

¹H NMR (400 MHz, CDCl₃): δ = 7.78 (d, *J* = 8.2 Hz, 1H, ArH), 7.65 (d, *J* = 8.3 Hz, 2H, ArH), 7.59 (d, *J* = 8.3 Hz, 2H, ArH), 7.50 (d, *J* = 8.4 Hz, 2H), 7.38–7.32 (m, 1H, ArH), 7.31–7.24 (m, 1H, ArH), 7.20 (d, *J* = 8.0 Hz, 2H, ArH), 7.09 (td, *J* = 7.5, 0.9 Hz, 1H, ArH), 5.81 (d, *J* = 3.8 Hz, 1H, N–CH), 3.87 (d, *J* = 3.8 Hz, 1H, CH–CO₂Me), 3.57 (s, 3H, OCH₃), 2.35 (s, 3H, CH₃) ppm; ¹³C NMR (101 MHz, CDCl₃): δ = 170.4 (C=O), 146.1 (ArC), 144.4 (ArC), 141.7 (ArC), 134.4 (ArC), 130.0 (q, *J* = 32.6 Hz, ArC–CF₃), 129.8 (ArC), 129.7 (2 × ArC), 127.7 (2 × ArC), 126.9 (ArC), 126.5 (ArC), 126.4 (2 × ArC), 126.0 (q, *J* = 3.7 Hz, ArC), 124.6 (ArC), 123.7 (q, *J* = 222.6 Hz, CF₃), 115.8 (ArC), 66.5, 55.6, 52.9, 21.7 (CH₃) ppm; IR (neat): ν = 2955w, 2925w, 1736s, 1597w, 1477m, 1462m, 1358s, 1323s, 1161s, 1109s, 1089s, 1066m, 812m, 752m, 656m cm⁻¹; HRMS (APCI): Exact mass calculated for C₂₄H₂₁NO₄SF₃ [M+H]⁺: 476.1143, found: 476.1154; HPLC (10:90 *e.r.*): YMC Chiral Amylose-C S (250 × 4.6 mm, 5 μm), *n*-hexane/isopropanol 95:5 (v/v), 1.0 mL•min⁻¹, 10 °C, λ = 254 nm, retention time minor isomer = 25.3 min, retention time major isomer = 35.7 min. The HPLC chromatograms are reported in literature.¹⁰

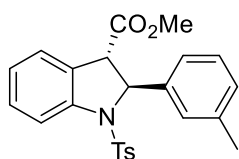
Methyl (2*S*,3*S*)-2-(*p*-tolyl)-1-tosylindoline-3-carboxylate (*S,S*)-**154e**:



Performed according to *General Procedure 7* on a 0.13 mmol scale of **153f** using 0.5 mol% of Rh₂(*R*-DOSP)₄ for 12 h; **154e** (52 mg, 0.12 mmol, 92%, 14:1 *d.r.*, 42% *ee*) was obtained as a colourless solid m.p.: 132–134 °C; $[\alpha]_D^{20}$: +33.7° (c 0.29, CHCl₃).

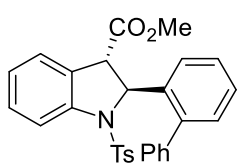
^1H NMR (400 MHz, CDCl_3): δ = 7.75 (d, J = 8.1 Hz, 1H, ArH), 7.65 (d, J = 8.2 Hz, 2H, ArH), 7.37–7.22 (m, 4H, ArH), 7.19 (d, J = 8.0 Hz, 2H, ArH), 7.13 (d, J = 7.9 Hz, 2H, ArH), 7.06 (t, J = 7.5 Hz, 1H, ArH), 5.65 (d, J = 3.6 Hz, 1H, N–CH), 3.82 (d, J = 3.4 Hz, 1H, CH–CO₂Me), 3.47 (s, 3H, OCH₃), 2.28 (s, 3H, CH₃), 2.25 (s, 3H, CH₃) ppm; ^{13}C NMR (101 MHz, CDCl_3): δ = 170.8 (C=O), 144.0 (ArC), 142.0 (ArC), 139.4 (ArC), 137.8 (ArC), 134.9 (ArC), 129.6 (2 × ArC), 129.5 (2 × ArC), 127.7 (2 × ArC), 127.5 (ArC), 126.4 (ArC), 125.9 (2 × ArC), 124.3 (ArC), 115.7 (ArC), 66.9, 55.8, 52.7, 21.6 (CH₃), 21.2 (CH₃) ppm; IR (neat): ν = 3022w, 2953w, 1735s, 1597m, 1514m, 1477m, 1460m, 1433m, 1354s, 1307w, 1238m, 1161s, 1089m, 1020m, 960m, 914m, 813s, 680s, 657s, 617m, 574s cm^{-1} ; HRMS (NSI): Exact mass calculated for $\text{C}_{24}\text{H}_{24}\text{NO}_4\text{S}$ $[\text{M}+\text{H}]^+$: 422.1426, Found: 422.1428; HPLC (29:71 *e.r.*): YMC Chiral Amylose-C S (250 × 4.6 mm, 5 μm), *n*-hexane/isopropanol 90:10 (v/v), 1.0 $\text{mL}\cdot\text{min}^{-1}$, 25 °C, λ = 254 nm, retention time minor isomer = 18.2 min, retention time major isomer = 39.2 min. The HPLC chromatograms are reported in literature.¹⁰

Methyl (2*S*,3*S*)-2-(*m*-tolyl)-1-tosylindoline-3-carboxylate (*S,S*)-**154f**:



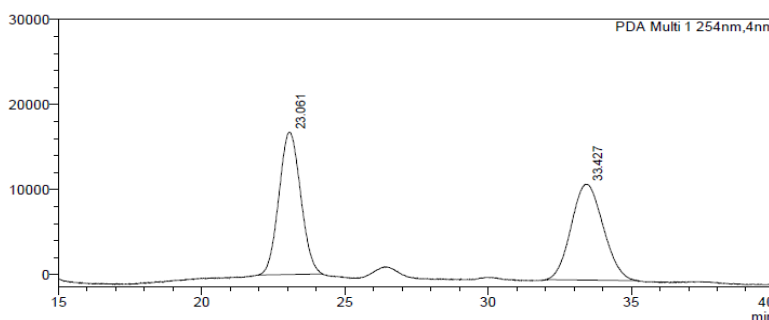
Performed according to *General Procedure 7* on a 0.08 mmol scale of **153g** using 0.5 mol% of $\text{Rh}_2(\text{R-DOSP})_4$ for 12 h; **154f** (22 mg, 0.051 mmol, 73%, 8:1 *d.r.*, 71% *ee*) was obtained as a colourless solid m.p.: 38–40 °C; $[\alpha]_D^{20}$: +24.7° (c 0.24, CHCl_3).

^1H NMR (400 MHz, CDCl_3): δ = 7.76 (d, J = 8.2 Hz, 1H, ArH), 7.64 (d, J = 7.9 Hz, 2H, ArH), 7.30–7.25 (m, 1H, ArH), 7.23–7.12 (m, 5H, ArH), 7.10–7.03 (m, 2H, ArH), 5.74 (d, J = 3.0 Hz, 1H, N–CH), 3.90 (d, J = 2.9 Hz, 1H, CH–CO₂Me), 3.55 (s, 3H, OCH₃), 2.35 (s, 3H, CH₃), 2.31 (s, 3H, CH₃) ppm; ^{13}C NMR (101 MHz, CDCl_3): δ = 170.8 (C=O), 144.0 (ArC), 142.2 (ArC), 142.0 (ArC), 138.7 (ArC), 134.9 (ArC), 129.5 (2 × ArC), 128.9 (ArC), 128.8 (ArC), 127.7 (2 × ArC), 127.5 (ArC), 126.5 (ArC), 126.4 (ArC), 124.4 (ArC), 123.0 (ArC), 115.8 (ArC), 67.0, 55.9, 52.7, 21.6 (CH₃), 21.6 (CH₃) ppm; IR (neat): ν = 3030w, 2951w, 2922w, 2850w, 1735s, 1597m, 1477s, 1460s, 1433m, 1354s, 1234m, 1163s, 1089s, 1024m, 881w, 812m, 754s, 704s, 680s, 657s cm^{-1} ; HRMS (NSI): Exact mass calculated for $\text{C}_{24}\text{H}_{27}\text{N}_2\text{O}_4\text{S}$ $[\text{M}+\text{NH}_4]^+$: 439.1686; found: 439.1682; HPLC (15:85 *e.r.*): YMC Chiral Amylose-C S (250 × 4.6 mm, 5 μm), *n*-hexane/isopropanol 90:10 (v/v), 1.0 $\text{mL}\cdot\text{min}^{-1}$, 25 °C, λ = 254 nm, retention time minor isomer = 11.6 min, retention time major isomer = 22.8 min. The HPLC chromatograms are reported in literature.¹⁰

Methyl (2*R*,3*R*)-2-([1,1'-biphenyl]-2-yl)-1-tosylindoline-3-carboxylate (*S,S*)-**154g**:

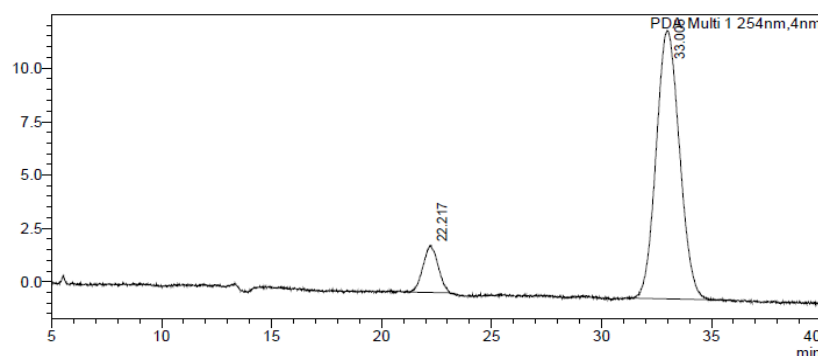
Performed according to *General Procedure 7* on a 0.10 mmol scale of **153h** using 1 mol% of $\text{Rh}_2(\text{R-DOSP})_4$ for 24 h; (*S,S*)-**154g** (35 mg, 0.072 mmol, 72%, 8:1 *d.r.*, 80% *ee*) was obtained as a colourless solid m.p.: 199–201 °C; $[\alpha]_D^{20}$: +40.0° (c 0.10, CHCl_3).

^1H NMR (400 MHz, CDCl_3): δ = 7.75 (d, J = 8.2 Hz, 1H, ArH), 7.51–7.38 (m, 8H, ArH), 7.35–7.21 (m, 4H, ArH), 7.14–7.08 (m, 3H), 7.00 (td, J = 7.5, 1.0 Hz, 1H, ArH), 5.83 (d, J = 3.6 Hz, 1H, N-CH), 3.77 (d, J = 3.6 Hz, 1H, CH-CO₂Me), 3.15 (s, 3H, OCH₃), 2.31 (s, 3H, Ar-CH₃) ppm; ^{13}C NMR (101 MHz, CDCl_3): δ = 170.1 (C=O), 143.8 (ArC), 142.1 (ArC), 140.8 (ArC), 140.6 (ArC), 140.0 (ArC), 134.6 (ArC), 130.0 (ArC), 129.9 (2 × ArC), 129.6 (ArC), 129.4 (2 × ArC), 128.4 (ArC), 128.3 (2 × ArC), 127.8 (2 × ArC), 127.6 (ArC), 127.5 (ArC), 127.3 (ArC), 125.7 (ArC), 125.6 (ArC), 124.3 (ArC), 115.4 (ArC), 64.1, 56.0, 52.2, 21.6 (Ar-CH₃) ppm; IR (neat): ν = 2983w, 1735s, 1356m, 1228.7m, 1217m, 1167m, 1091w, 959w, 752m, 692m cm^{-1} ; HRMS (APCI): Exact mass calculated for $\text{C}_{29}\text{H}_{26}\text{NO}_4\text{S}$ $[\text{M}+\text{H}]^+$: 484.1583; found: 484.1573; HPLC (10:90 *e.r.*): YMC Chiral Amylose-C S (250 × 4.6 mm, 5 μm), *n*-hexane/isopropanol 95:5 (v/v), 1.0 mL·min⁻¹, 10 °C, λ = 254 nm, retention time first isomer = 21.7 min, retention time second isomer = 32.5 min.



Peak #	Time (min)	Area (%)
1	23.061	50.273
2	33.427	49.727

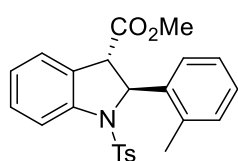
Figure 5.10: HPLC chromatograms of racemic mixture of *trans*-**154e** enantiomers.



Peak #	Time (min)	Area (%)
1	22.217	10.188
2	33.005	89.812

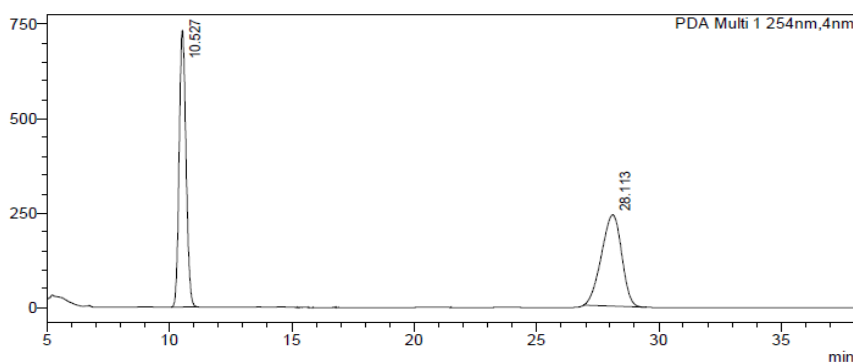
Figure 5.11: HPLC chromatograms of *trans*-**154e** enantiomers (80% *ee*).

Methyl (2*S*,3*S*)-2-(*o*-tolyl)-1-tosylindoline-3-carboxylate (*S,S*)-**154h**:

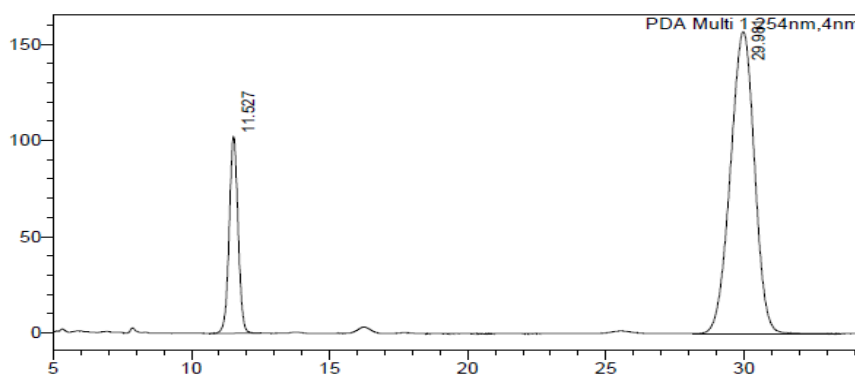


Performed according to *General Procedure 7* on a 0.08 mmol scale of **153i** using 0.5 mol% of Rh₂(*R*-DOSP)₄ for 12 h; **154h** (29 mg, 0.07 mmol, 86%, 8:1 *d.r.*, 61% *ee*) was obtained as a colourless solid m.p.: 40–42 °C; [α]_D²⁰: +22.9° (c 0.34, CHCl₃).

¹H NMR (400 MHz, CDCl₃): δ = 7.68 (d, *J* = 8.2 Hz, 1H, Ar*H*), 7.62 (d, *J* = 8.1 Hz, 2H, Ar*H*), 7.26 (t, *J* = 7.8 Hz, 1H, Ar*H*), 7.22–7.02 (m, 7H, Ar*H*), 6.98 (t, *J* = 7.5 Hz, 1H, Ar*H*), 5.94 (d, *J* = 3.4 Hz, 1H, N-CH), 3.72 (d, *J* = 3.1 Hz, 1H, CH-CO₂Me), 3.47 (s, 3H, OCH₃), 2.35 (s, 3H, CH₃), 2.29 (s, 3H, CH₃) ppm; ¹³C NMR (101 MHz, CDCl₃): δ = 170.8 (C=O), 144.0 (ArC), 142.1 (ArC), 140.5 (ArC), 135.2 (ArC), 134.1 (ArC), 130.9 (ArC), 129.6 (ArC), 129.6 (2 × ArC), 127.8 (ArC), 127.7 (2 × ArC), 127.4 (ArC), 126.7 (ArC), 126.4 (ArC), 125.9 (ArC), 124.3 (ArC), 115.4 (ArC), 64.3, 55.2, 52.7, 21.7 (CH₃), 19.6 (CH₃) ppm; IR (neat): ν = 2953w, 2922w, 1734s, 1597m, 1477s, 1460s, 1354s, 1305m, 1290s, 1089m, 1024m, 958m, 918w, 812m, 750s, 727m, 705m, 680s, 657s cm⁻¹; HRMS (NSI): Exact mass calculated for C₂₄H₂₄NO₄S [M+H]⁺: 422.1421; found: 422.1422; HPLC (19:81 *e.r.*): YMC Chiral Amylose-C S (250 × 4.6 mm, 5 μm), *n*-hexane/isopropanol 90:10 (v/v), 1.0 mL·min⁻¹, 25 °C, λ = 254 nm, retention time major isomer = 11.5 min, retention time minor isomer = 30.0 min.



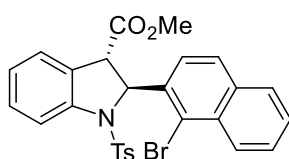
Peak #	Time (min)	Area (%)
1	10.527	50.625
2	28.113	49.375



Peak #	Time (min)	Area (%)
1	11.527	19.323
2	29.981	80.677

Figure 5.12: HPLC chromatograms of *trans*-**154f** enantiomers. From the top: racemic mixture, 61% ee.

Methyl (2*S*,3*S*)-2-(1-bromonaphthalen-2-yl)-1-tosylindoline-3-carboxylate (*S,S*)-**154i**:

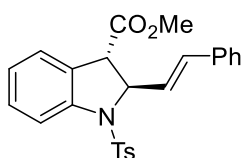


Performed according to *General Procedure 7* on a 0.048 mmol scale of **153k** using 0.5 mol% of $\text{Rh}_2(\text{R-DOSP})_4$ for 12 h; (*S,S*)-**154i** (13 mg, 0.023 mmol, 48%, 6:1 d.r, 75% ee) was obtained as a colourless oil; $[\alpha]_D^{20}$: +14.0° (c 0.14, CHCl_3).

^1H NMR (300 MHz, CDCl_3): δ = 8.34 (d, J = 8.1 Hz, 1H, ArH), 8.01–7.66 (m, 5H, ArH), 7.66–7.45 (m, 3H, ArH), 7.36 (t, J = 7.7 Hz, 1H, ArH), 7.31–7.09 (m, 3H, ArH), 7.06 (t, J = 7.4 Hz, 1H, ArH), 6.43 (d, J = 3.4 Hz, 1H, N-CH), 3.90 (d, J = 2.5 Hz, 1H, CH-CO₂Me), 3.56 (s, 3H, OCH₃), 2.39 (s, 3H, CH₃) ppm; ^{13}C NMR (126 MHz, CDCl_3): δ = 170.6 (C=O), 144.3 (ArC), 142.0 (ArC), 139.6 (ArC), 134.8 (ArC), 134.3 (ArC), 132.5 (ArC), 129.9 (ArC), 129.7 (2 × ArC), 128.7 (ArC), 128.3 (ArC), 128.0 (2 × ArC), 127.8 (ArC), 127.5 (ArC), 126.9 (ArC), 126.0 (ArC), 124.5 (ArC), 124.4 (ArC), 124.4 (ArC), 121.6 (ArC), 115.4 (ArC), 67.5, 55.3, 52.8, 21.7 (CH₃) ppm; IR (neat): ν = 3752w, 3629w, 2952w, 2917w, 2849w, 2342s, 1734s, 1596m, 1478m, 1461m, 1356s, 1326m, 1255m,

1239m, 1164s, 1108s, 1090s, 1024m, 962m, 906w, 812s, 729s, 575s cm^{-1} ; HRMS (NSI): Exact mass calculated for $\text{C}_{27}\text{H}_{23}\text{BrNO}_4\text{S}$ $[\text{M}+\text{H}]^+$: 539.0526; found: 539.0522; HPLC (12:88 *e.r.*): YMC Chiral Amylose-C S (250 \times 4.6 mm, 5 μm), *n*-hexane/isopropanol 90:10 (v/v), 1.0 $\text{mL}\cdot\text{min}^{-1}$, 25 $^\circ\text{C}$, $\lambda = 254$ nm, retention time first isomer = 24.3 min, retention time second isomer = 38.6 min. The HPLC chromatograms are reported in literature.¹⁰

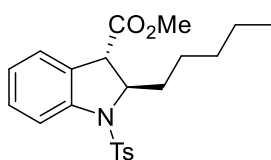
Methyl (2*S*,3*S*)-2-((*E*)-styryl)-1-tosylindoline-3-carboxylate (*S,S*)-**154j**:



Performed according to *General Procedure 7* on a 0.11 mmol scale of **153i** using 0.5 mol% of $\text{Rh}_2(\text{R-DOSP})_4$ for 24 h; **154j** (23 mg, 0.053 mmol, 53%, 7:1 *d.r.*, 33% *ee*) was obtained as a colourless solid m.p.: 52–54 $^\circ\text{C}$; $[\alpha]_D^{20}$: +7.2 $^\circ$ (c 0.28, CHCl_3).

^1H NMR (400 MHz, CDCl_3): $\delta = 7.70\text{--}7.59$ (m, 2H, ArH), 7.33–7.15 (m, 8H, ArH), 7.12 (d, $J = 8.0$ Hz, 2H, ArH), 6.98 (t, $J = 7.6$ Hz, 1H, ArH), 6.70 (d, $J = 15.6$ Hz, 1H, CH=CH–Ph), 6.16 (dd, $J = 15.8, 7.2$ Hz, 1H, CH=CH–Ph), 5.31 (dd, $J = 6.5, 3.1$ Hz, 1H, N–CH), 3.76 (d, $J = 2.9$ Hz, 1H, CH–CO₂Me), 3.46 (s, 3H, OCH₃), 2.28 (s, 3H, CH₃) ppm; ^{13}C NMR (101 MHz, CDCl_3): $\delta = 170.5$ (C=O), 144.0 (ArC), 141.4 (ArC), 136.2 (ArC), 135.2 (ArC), 131.9 (ArC), 129.6 (2 \times ArC), 129.5, 128.5 (2 \times ArC), 128.1, 128.0, 127.7 (2 \times ArC), 127.6, 126.9 (2 \times ArC), 126.4, 124.3, 116.0 (ArC), 66.1, 53.0, 52.7, 21.6 (CH₃) ppm; IR (neat): $\nu = 3026\text{w}, 2949\text{w}, 2850\text{w}, 2358\text{w}, 1735\text{s}, 1597\text{m}, 1477\text{m}, 1460\text{m}, 1435\text{m}, 1354\text{s}, 1228\text{s}, 1217\text{s}, 1163\text{s}, 1105\text{m}, 1089\text{m}, 1024\text{m}, 962\text{m}, 812\text{m}, 754\text{m}$ cm^{-1} ; HRMS (NSI): Exact mass calculated for $\text{C}_{25}\text{H}_{24}\text{NO}_4\text{S}$ $[\text{M}+\text{H}]^+$: 434.1400; found: 434.1410; HPLC (66:34 *e.r.*): Chiracel[®] OD-H (250 \times 4.6 mm, 5 μm), *n*-hexane/isopropanol 95:5 (v/v), 1.0 $\text{mL}\cdot\text{min}^{-1}$, 25 $^\circ\text{C}$, $\lambda = 254$ nm, retention time major isomer = 22.5 min, retention time minor isomer = 29.1 min. The HPLC chromatograms are reported in literature.¹⁰

Methyl (2*S*,3*S*)-2-pentyl-1-tosylindoline-3-carboxylate (*S,S*)-**154k**:



Performed according to *General Procedure 7* on a 0.09 mmol scale of **153m** using 0.5 mol% of $\text{Rh}_2(\text{R-DOSP})_4$ for 12 h; **154k** (23 mg, 0.058 mmol, 64%, >20:1 *d.r.*, 48% *ee*) was obtained as a pale yellow oil; $[\alpha]_D^{20}$: +44.1 $^\circ$ (c 0.41, CHCl_3).

^1H NMR (300 MHz, CDCl_3): $\delta = 7.67$ (d, $J = 8.1$ Hz, 1H, ArH), 7.62–7.53 (m, 2H, ArH), 7.33–7.22 (m, 2H, ArH), 7.15 (d, $J = 8.0$ Hz, 2H, ArH), 7.04 (td, $J = 7.6, 1.0$ Hz, 1H, ArH), 4.62 (ddd, $J = 8.0, 4.6, 3.1$ Hz, 1H, N–CH), 3.61 (d, $J = 2.9$ Hz, 1H, CH–CO₂Me), 3.41 (s, 3H, OCH₃), 2.33 (s, 3H, CH₃), 2.03–1.86 (m, 1H), 1.86–1.64 (m, 1H), 1.44–1.20 (m, 6H), 0.88 (t, $J = 6.9$, 3H, CH₃) ppm; ^{13}C NMR (75 MHz, CDCl_3): $\delta =$ ^{13}C NMR (101 MHz,

CDCl_3) δ = 171.1 (C=O), 143.8 (ArC), 141.6 (ArC), 134.8 (ArC), 129.4 (2 \times ArC), 129.3 (ArC), 128.7 (ArC), 127.6 (2 \times ArC), 126.4 (ArC), 124.4 (ArC), 116.7 (ArC), 65.0, 52.4, 51.5, 37.1, 31.5, 24.1, 22.6, 21.6, 14.1 ppm; IR (neat): ν = 3736w, 3601w, 3005w, 2360s, 2341s, 1707s, 1363m, 1224m, 1166w, 669m, 534m, 420w cm^{-1} ; HRMS (NSI): Exact mass calculated for $\text{C}_{22}\text{H}_{28}\text{NO}_4\text{S}$ $[\text{M}+\text{H}]^+$: 402.1734; found: 402.1728; HPLC (26:74 *e.r.*): Chiracel[®] OD-H (250 \times 4.6 mm, 5 μm), *n*-hexane/isopropanol 99:1 (v/v), 1.0 $\text{mL}\cdot\text{min}^{-1}$, 25 $^\circ\text{C}$, λ = 254 nm, retention time minor isomer = 13.4 min, retention time major isomer = 15.1 min. The HPLC chromatograms are reported in literature.¹⁰

5.2.5 *In-Situ* ^1H NMR Experiment: Temperature Effect

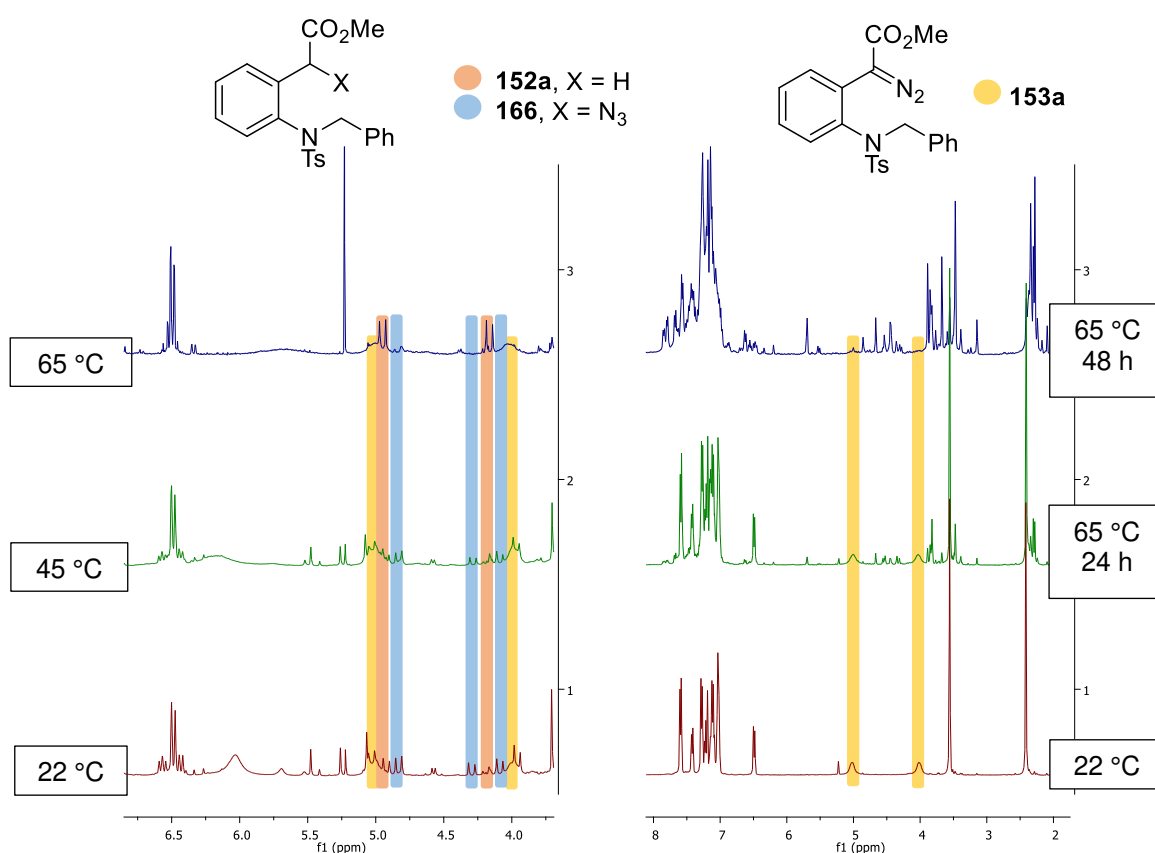


Figure 5.13: ^1H NMR (300 MHz, CD_3CN). a) Comparison of crude mixtures for reaction performed at room temperature, 45 $^\circ\text{C}$ and 65 $^\circ\text{C}$; b) Thermostability test for **153a** at 65 $^\circ\text{C}$ for 48 h.

5.2.6 Evidence for Triazene 167

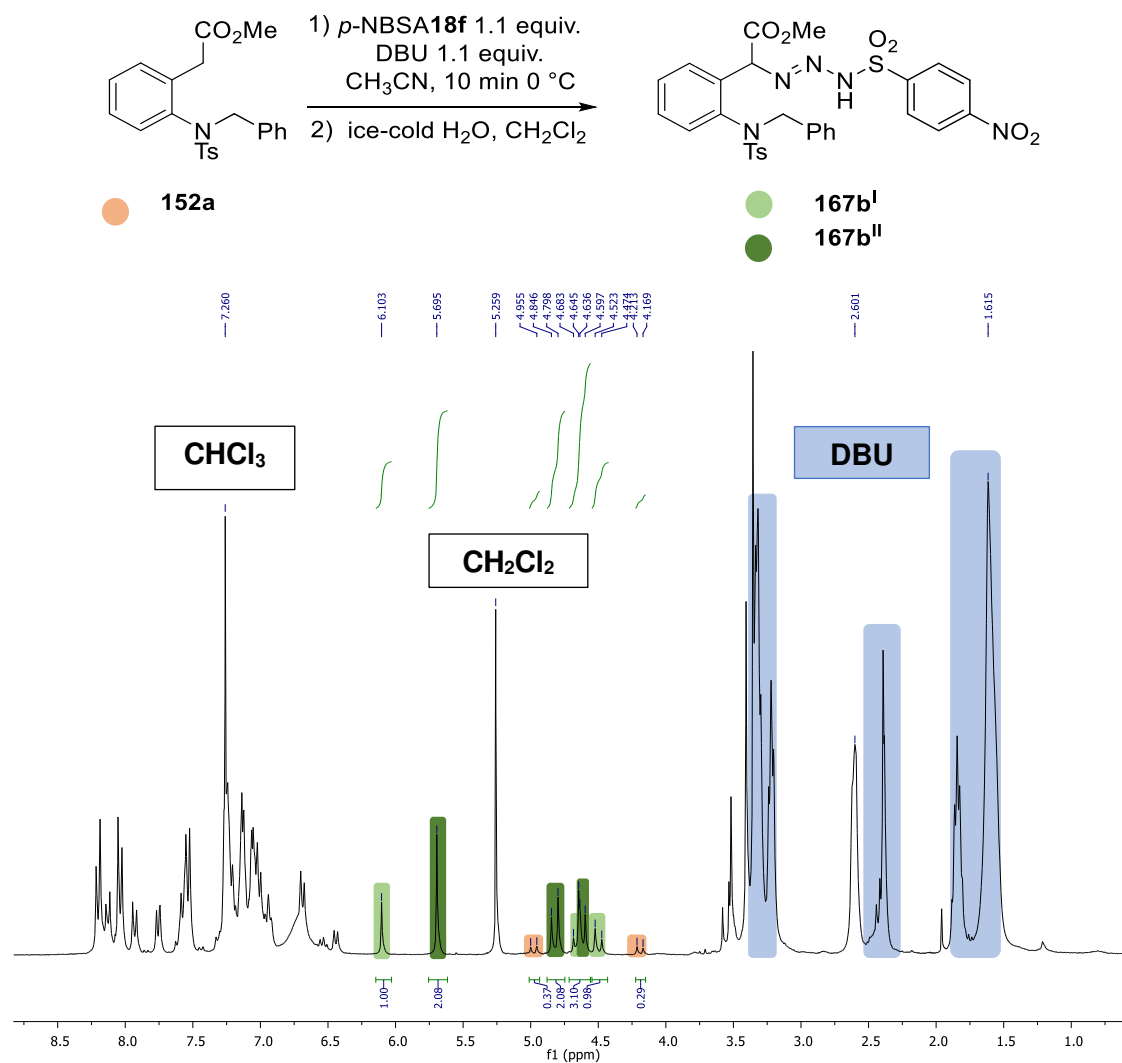


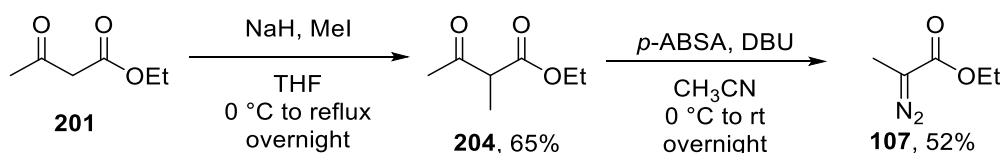
Figure 5.14: Crude NMR (300 MHz, CDCl₃) of triazene **167b** as a 1:2 mixture of rotamers. The reaction was performed on a 0.24 mmol scale of **152a** (100 mg), quenched with cold H₂O after 10 minutes and extracted with dichloromethane.

5.3 Experimental Data for Chapter 3: Synthesis of Fluorinated Benzofuranones

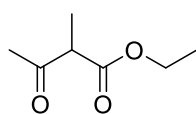
Triphenylborane **106a** was purchased from Sigma Aldrich. The synthesis of boranes **106b–f** was performed by Darren M. C. Ould, Dr. Jan Wenz, Dr. Yashar Soltani and Jamie L. Carden. The Lewis acidity was determined by Dr. Soltani according to the Gutmann-Beckett method.¹¹

5.3.1 Synthesis of Diazo Precursors

5.3.1.1 Synthesis of Diazo Compound **107**



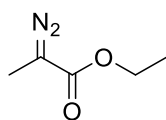
Ethyl 2-methyl-3-oxobutanoate **204**:



To a stirred suspension of NaH (60%_wt in mineral oil, 2.3 g, 60 mmol), in dry THF (40 mL), acetoacetate **201** (7.6 mL, 60 mmol), was added at 0 °C. Once the grey suspension turned into a brown clear solution, methyl iodide (2.5 mL, 40 mmol) was added and the reaction was heated under reflux overnight. A saturated solution of aqueous NH₄Cl was added at room temperature, and the product was extracted with CH₂Cl₂ (3 × 20 mL). The combined organic layers were washed with brine and dried over MgSO₄ and the solvent was evaporated under reduced pressure. The crude was purified by column chromatography to afford **204** as a colourless oil (3.8 g, 26 mmol, 65% yield).

¹H NMR (500 MHz, CDCl₃): δ = 4.29–4.12 (m, 2H, OCH₂), 3.49 (q, *J* = 7.2 Hz, 1H, CH), 2.23 (s, 3H, CH₃), 1.34 (d, *J* = 7.2 Hz, 3H, CHCH₃), 1.27 (t, *J* = 7.0 Hz, 3H, OCH₂CH₃) ppm; ¹³C NMR (126 MHz, CDCl₃): δ = 203.8 (C=O), 170.7 (C=O), 61.5 (OCH₂), 53.8 (CHCH₃), 28.5 (CH₃), 14.2 (CH₃), 12.8 (CH₃) ppm. The spectroscopic data are in agreement with the literature.¹²

Ethyl 2-diazopropanoate **107**:

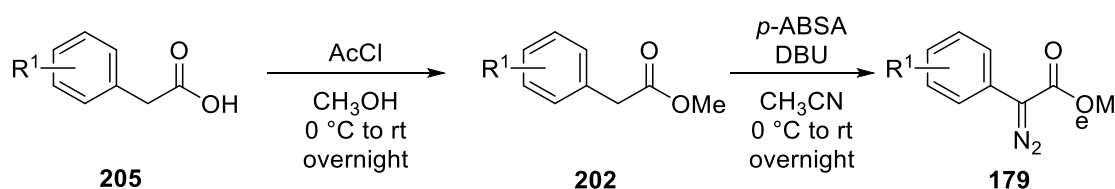


To a stirred solution of **204** (1.8 g, 12 mmol) and *p*-acetamidobenzenesulfonyl azide, (*p*-ABSA, 4.3 g, 18 mmol) in acetonitrile (30 mL) at 0 °C, 8-diazabicyclo(5.4.0)undec-7-ene (DBU,

2.7 mL, 1.8 mmol) was added dropwise. The reaction was stirred for 12 hours before quenching with a saturated aqueous solution of NH_4Cl . The product was extracted with CH_2Cl_2 (3 \times 20 mL). The combined organic layers were washed with water, brine and dried over MgSO_4 . Compound **107** was afforded as a volatile bright yellow oil (802 mg, 6.3 mmol, 52% yield) after column chromatography.

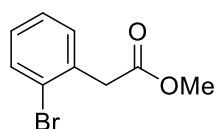
^1H NMR (500 MHz, CDCl_3): δ = 4.21 (q, J = 7.1 Hz, 2H, OCH_2), 1.95 (s, 3H, CH_3), 1.27 (t, J = 7.1 Hz, 3H, OCH_2CH_3) ppm; ^{13}C NMR (126 MHz, CDCl_3): δ = 60.9 (OCH_2), 14.7 (CH_3), 8.6 (CH_3) ppm ($\text{C}=\text{N}_2$ and $\text{C}=\text{O}$ not observed); IR (neat): ν = 2980w, 2075s, 1682s, 1304s, 1124s, 734m cm^{-1} . The spectroscopic data are in agreement with the literature.¹³

5.3.1.2 Synthesis of Diazo Compounds **179a–g**



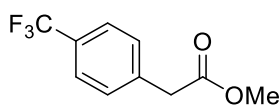
Except for **202f** which was commercially available **202a–e** were obtained following General Procedure 8: The arylacetic acid **205a–e** (4–10 mmol) was dissolved in methanol and the 0.5 M solution was cooled down at 0 °C before addition of acetyl chloride (2.5 equiv.). The reaction was stirred at room temperature for 4–12 hours and checked by TLC (*n*-hexane/ethyl acetate). The solvent was evaporated *in vacuo* and the residual oil washed with a saturated solution of NaHCO_3 and extracted with diethyl ether. Subsequently, the combined organic layers were washed with water and brine, dried over MgSO_4 and concentrated *in vacuo* to afford the pure product **202a–e** as an oil or a solid depending on the substrate.

Methyl 2-(2-bromophenyl)acetate **202a**:



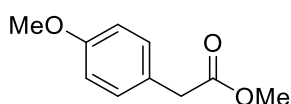
Performed according to General Procedure 8 on a 4.6 mmol scale of **205a**; **202a** (1.1 g, 4.4 mmol, 96% yield) was obtained as a pale-yellow oil.

^1H NMR (400 MHz, CDCl_3): δ = 7.54 (d, J = 7.7 Hz, 1H, *ArH*), 7.28–7.21 (m, 2H, *ArH*), 7.15–7.08 (m, 1H, *ArH*), 3.77 (s, 2H, CH_2), 3.68 (s, 3H, OCH_3) ppm; ^{13}C NMR (101 MHz, CDCl_3): δ = 171.0 ($\text{C}=\text{O}$), 134.2 (*ArC*), 132.9 (*ArC*), 131.6 (*ArC*), 128.9 (*ArC*), 127.6 (*ArC*), 125.1 (*ArC*), 52.3 (OCH_3), 41.6 (CH_2) ppm. Spectroscopic data are in accordance with the literature.¹⁴

Methyl 2-(4-(trifluoromethyl)phenyl)acetate **202b**:

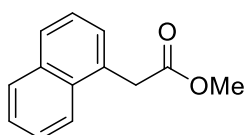
Performed according to *General Procedure 8* on a 4.9 mmol scale of **205b**; **202b** (900 mg, 4.1 mmol, 84% yield) was obtained as a colourless oil.

^1H NMR (500 MHz, CDCl_3): δ = 7.59 (d, J = 8.1 Hz, 2H, ArH), 7.40 (d, J = 8.0 Hz, 2H, ArH), 3.71 (s, 3H, OCH₃), 3.69 (s, 2H, CH₂) ppm; ^{13}C NMR (126 MHz, CDCl_3): δ = 171.3 (C=O), 138.1 (q, J = 1.3 Hz, ArC), 129.8 (2 × ArC), 129.6 (q, J = 32.5 Hz, ArC-CF₃), 125.6 (q, J = 3.8 Hz, 2 × ArC), 124.3 (q, J = 272.0 Hz, CF₃), 52.3 (OCH₃), 41.0 (CH₂) ppm; Spectroscopic data are in accordance with the literature.¹⁵

methyl 2-(4-methoxyphenyl)acetate **202c**:

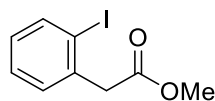
Performed according to *General Procedure 8* on a 6.0 mmol scale of **205c**; **202c** (857 mg, 4.7 mmol, 80% yield) was obtained as a colourless oil.

^1H NMR (400 MHz, CDCl_3): δ = 7.26–7.11 (m, 2H, ArH), 6.95–6.80 (m, 2H, ArH), 3.79 (s, 3H, OCH₃), 3.69 (s, 3H, OCH₃), 3.57 (s, 2H, CH₂) ppm; ^{13}C NMR (101 MHz, CDCl_3): δ = 172.5 (C=O), 158.8 (ArC-OMe), 130.4 (2 × ArC), 126.2 (ArC), 114.1 (2 × ArC), 55.4 (OCH₃), 52.1 (OCH₃), 40.4 (CH₂) ppm. Spectroscopic data are in accordance with the literature.¹⁶

Methyl 2-(naphthalen-1-yl)acetate **202d**:

Performed according to *General Procedure 8* on a 10.7 mmol scale of **205d**; **202d** (1.9 g, 9.5 mmol, 89% yield) was obtained as a colourless oil.

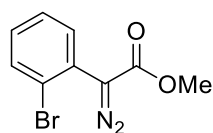
^1H NMR (400 MHz, CDCl_3): δ = 8.02–7.97 (m, 1H, ArH), 7.87 (dd, J = 8.3, 1.1 Hz, 1H, ArH), 7.81 (dd, J = 7.5, 1.7 Hz, 1H, ArH), 7.58–7.39 (m, 4H, ArH), 4.09 (s, 2H, ArCH₂), 3.69 (s, 3H, OCH₃) ppm; ^{13}C NMR (101 MHz, CDCl_3): δ = 172.2 (C=O), 133.9 (ArC), 132.2 (ArC), 130.6 (ArC), 128.9 (ArC), 128.2 (ArC), 128.2 (ArC), 126.6 (ArC), 125.9 (ArC), 125.6 (ArC), 123.9 (ArC), 52.3 (OCH₃), 39.2 (CH₂) ppm. Spectroscopic data are in accordance with the literature.¹⁷

Methyl 2-(2-iodophenyl)acetate **202e**:

Performed according to *General Procedure 8* on a 11.5 mmol scale of **205e**; **202e** (2.1 g, 7.6 mmol, 66% yield) was obtained as a colourless oil.

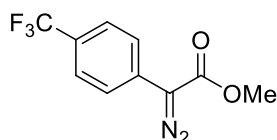
^1H NMR (400 MHz, CDCl_3): δ = 7.85 (dd, J = 7.9, 1.1 Hz, 1H, *ArH*), 7.37–7.25 (m, 2H, *ArH*), 7.03–6.87 (m, 1H, *ArH*), 3.81 (s, 2H, CH_2), 3.73 (s, 3H, OCH_3) ppm; ^{13}C NMR (101 MHz, CDCl_3): δ = 171.1 ($\text{C}=\text{O}$), 139.7 (*ArC*), 137.8 (*ArC*), 130.8 (*ArC*), 129.1 (*ArC*), 128.6 (*ArC*), 101.1 (*ArC-I*), 52.4 (OCH_3), 46.3 (CH_2) ppm. Spectroscopic data are in accordance with the literature.¹⁸

General Procedure 9: A 0.2 M solution of methyl arylacetates **202a–f** or **155a** (2–4 mmol) and *p*-ABSA (2 equiv.) in acetonitrile was cooled down to 0 °C before the addition of DBU (2.5 equiv.). The reaction was stirred at room temperature for 4–48 hours and monitored by TLC (*n*-hexane/ethyl acetate). The mixture was quenched with a saturated aqueous solution of NH_4Cl saturated solution and the product was extracted with CH_2Cl_2 . The combined organic layers were washed with water, brine, dried over MgSO_4 and concentrated under reduced pressure. The crudes were purified by flash column chromatography to afford the pure products **179a–g** as an oil or a solid depending on the substrate.

Methyl 2-(2-bromophenyl)diazoacetate **179a**:

Performed according to *General Procedure 9* on a 2.0 mmol scale of **202a**; **179a** (500 mg, 1.9 mmol, 96% yield) was obtained as a bright yellow oil.

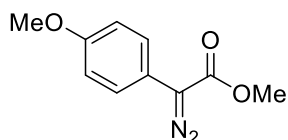
^1H NMR (500 MHz, CDCl_3): δ = 7.63 (dd, J = 8.1, 1.2 Hz, 1H, *ArH*), 7.52 (dd, J = 7.8, 1.6 Hz, 1H, *ArH*), 7.38 (td, J = 7.6, 1.3 Hz, 1H, *ArH*), 7.24–7.18 (m, 1H, *ArH*), 3.84 (s, 3H, OCH_3) ppm; ^{13}C NMR (126 MHz, CDCl_3): δ = 133.5 (*ArC*), 133.1 (*ArC*), 130.3 (*ArC*), 127.9 (*ArC*), 125.9 (*ArC-Br*), 52.4 (OCH_3) ppm ($\text{C}=\text{N}_2$ and $\text{C}=\text{O}$ not observed); IR (neat): ν = 2951w, 2100s, 1697s, 1475m, 1433m, 1350m, 1240s, 1153s, 1066s, 1022s, 914w, 752s, 642m, 441m cm^{-1} . The spectroscopic data are in agreement with the literature.¹⁹

Methyl 2-(4-(trifluoromethyl)phenyl)diazoacetate **179b**:

Performed according to *General Procedure 9* on a 3.8 mmol scale of **202b**; **179b** (941 mg, 3. mmol, 98% yield) was obtained as a bright yellow solid.

^1H NMR (400 MHz, CDCl_3): δ = 7.66–7.54 (m, 4H, ArH), 3.88 (s, 3H, OCH_3) ppm; ^{13}C NMR (126 MHz, CDCl_3): δ = 164.9 (C=O), 130.3–130.2 (m, ArC– CN_2), 129.2 (ArC), 127.7 (q, J = 33.0 Hz, ArC– CF_3), 125.5 (q, J = 3.8 Hz, 2 \times ArC), 124.15 (q, J = 271.1 Hz, CF_3), 123.5 (2 \times ArC), 52.3 (OCH_3) ppm (C= N_2 not observed); IR (neat): ν = 2960w, 2102s, 1685s, 1618m, 1521w, 1242s, 823s, 744s, 592m cm^{-1} . The spectroscopic data are in agreement with the literature.²⁰

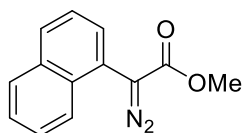
Methyl 2-(4-(methoxy)phenyl)diazoacetate **179c**:



Performed according to *General Procedure 9* on a 2.8 mmol scale of **202c**; **179c** (377 mg, 1.8 mmol, 65% yield) was obtained as a red solid.

^1H NMR (400 MHz, CDCl_3): δ = 7.42–7.31 (m, 2H, ArH), 7.01–6.88 (m, 2H, ArH), 3.84 (s, 3H, OCH_3), 3.80 (s, 3H, OCH_3) ppm; ^{13}C NMR (101 MHz, CDCl_3): δ = 166.2 (C=O), 158.2 (ArC–O), 126.0 (2 \times ArC), 116.9 (ArC– CN_2), 114.7 (2 \times ArC), 55.4 (OCH_3), 52.0 (OCH_3) ppm (C= N_2 not observed); IR (neat): ν = 3005w, 2959w, 2839w, 2085s, 1690s, 1609m, 1510s, 1437s, 1356m, 1294m, 1244s, 1028s, 833s, 739s, 606m cm^{-1} . The spectroscopic data are in agreement with the literature.²⁰

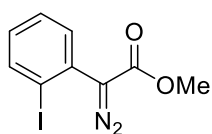
Methyl 2-(naphthalen-1-yl)diazoacetate **179d**:



Performed according to *General Procedure 9* on a 2.5 mmol scale of **202d**; **179d** (465 mg, 2.1 mmol, 84% yield) was obtained as a bright yellow oil.

^1H NMR (500 MHz, CDCl_3): δ = 7.94–7.88 (m, 2H, ArH), 7.87 (d, J = 8.4 Hz, 1H, ArH), 7.64 (dd, J = 7.2, 1.0 Hz, 1H, ArH), 7.58 (dd, J = 8.3, 1.4 Hz, 1H, ArH), 7.54 (dd, J = 12.4, 4.4 Hz, 2H, ArH), 3.86 (s, 3H, OCH_3) ppm; ^{13}C NMR (126 MHz, CDCl_3): δ = 134.1 (ArC), 131.6 (ArC), 129.8 (ArC), 129.7 (ArC), 128.9 (ArC), 126.9 (ArC), 126.3 (ArC), 125.61 (ArC), 124.3 (ArC), 122.0 (ArC), 52.4 (OCH_3) ppm (C= N_2 and C=O not observed); IR (neat): ν = 2951w, 2360w, 2083s, 1701s, 1433s, 1103s, 993w, 977w, 773s, 657m cm^{-1} . The spectroscopic data are in agreement with the literature.²⁰

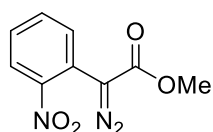
Methyl 2-(2-iodophenyl)diazoacetate **179e**:



Performed according to *General Procedure 9* on a 1.8 mmol scale of **202e**; **179e** (480 mg, 1.6 mmol, 88% yield) was obtained as a bright yellow oil.

^1H NMR (500 MHz, CDCl_3): δ = 7.88 (d, J = 8.0 Hz, 1H, ArH), 7.45 (dd, J = 7.8, 1.5 Hz, 1H, ArH), 7.38 (t, J = 7.6 Hz, 1H, ArH), 7.06–6.95 (m, 1H, ArH), 3.80 (s, 3H, OCH_3) ppm; ^{13}C NMR (126 MHz, CDCl_3): δ = 165.7 (C=O), 139.7 (ArC), 132.9 (ArC), 130.4 (ArC), 129.5 (ArC– CN_2), 128.5 (ArC), 101.0 (ArC–I), 52.2 (OCH_3) ppm (C= N_2 not observed); IR (neat): ν = 2949w, 2088s, 1693s, 1579w, 1558w, 1469m, 1431m, 1348m, 1242s, 1026s, 1006s, 752s, 638m cm^{-1} ; HRMS (NSI): Exact mass calculated for $\text{C}_9\text{H}_8\text{IN}_2\text{O}_2$ $[\text{M}+\text{H}]^+$: 302.9625, found 302.9627.

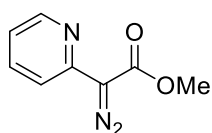
Methyl 2-(2-nitrophenyl)diazoacetate **179f**:



Performed according to *General Procedure 9* on a 1.3 mmol scale of **155a**; **179f** (200 mg, 0.90 mmol, 71% yield) was obtained as a bright yellow solid.

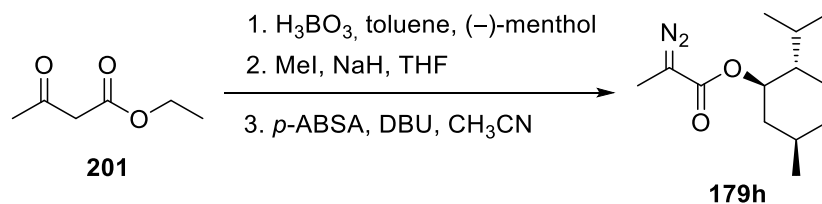
^1H NMR (500 MHz, CDCl_3): δ = 8.02 (d, J = 8.2 Hz, 1H, ArH), 7.63 (t, J = 7.6 Hz, 1H, ArH), 7.53 (d, J = 7.7 Hz, 1H, ArH), 7.46 (t, J = 7.8 Hz, 1H, ArH), 3.79 (s, 3H, OCH_3) ppm; ^{13}C NMR (126 MHz, CDCl_3): δ = 165.1 (C=O), 147.2 (ArC– NO_2), 133.3 (ArC), 131.1 (ArC), 128.9 (ArC), 125.6 (ArC), 120.9 (ArC– CN_2), 52.5 (OCH_3) ppm (C= N_2 not observed); IR (neat): ν = 2954w, 2362w, 2094s, 1697s, 1604m, 1523s, 1435m, 1352s, 1284s, 1246s, 1193s, 1161s, 1089m, 1029s, 956w, 916w, 852m, 783m, 543w, 516w cm^{-1} . The spectroscopic data are in agreement with the literature.²¹

Methyl 2-diazo-2-(pyridin-2-yl)acetate **179g**:

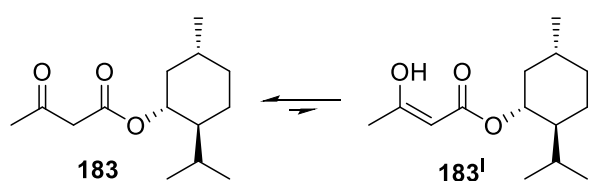


Performed according to *General Procedure 9* on a 2.0 mmol scale of commercially available **202f**; **179g** (270 mg, 1.5 mmol, 75% yield) was obtained as a white solid, m.p.: 134–138 °C.

^1H NMR (400 MHz, CDCl_3): δ = 8.84 (dt, J = 7.0, 1.0 Hz, 1H, ArH), 8.29 (dt, J = 8.9, 1.2 Hz, 1H, ArH), 7.56 (ddd, J = 8.9, 6.8, 1.0 Hz, 1H, ArH), 7.17 (td, J = 6.9, 1.2 Hz, 1H, ArH), 4.05 (s, 3H, OCH_3) ppm; ^{13}C NMR (126 MHz, CDCl_3): δ = 161.4 (C=O), 134.8 (ArC), 129.3 (ArC), 128.9 (ArC), 125.8 (ArC), 118.9 (ArC), 116.4 (ArC), 51.8 (OCH_3) ppm; IR (neat): ν = 3092m, 3044m, 2953m, 1984w, 1819w, 1693s, 1637m, 1544m, 1523s, 1215s, 1068s cm^{-1} . The spectroscopic data are in agreement with the literature.²²

5.3.1.3 Synthesis of Diazo Compound **179h**

(1*R*,2*S*,5*R*)-2-Isopropyl-5-methylcyclohexyl 3-oxobutanoate **207**:

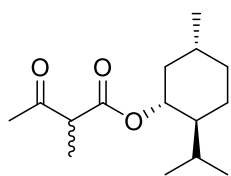


A mixture of acetoacetate **201** (1.47 mL, 12 mmol), (-)-menthol (2.8 g, 18 mmol) and catalytic amount of H_3BO_3 (74 mg, 1.2 mmol, 10 mol%) was stirred in

toluene at 115 °C and refluxed overnight for 12 hours using a Dean-Stark trap to remove the ethanol. The solvent was then removed under vacuum and the crude purified by column chromatography to afford **207** (1.58 g, 6.6 mmol, 55% yield) as a pale-yellow oil (5:1 mixture of the two tautomers **207**:**207'** by ^1H NMR spectroscopy).

^1H NMR (400 MHz, CDCl_3): δ = 12.18 (s, 0.19 H, OH^{H}), 5.05–4.89 (m, 0.19 H, $\text{C}=\text{CH}^{\text{H}}$), 4.72 (td, J = 10.9, 4.4 Hz, 1H, $\text{CO}_2\text{-CH}$), 3.42 (s, 2H, CH_2), 2.25 (s, 3H, CH_3), 2.05–1.97 (m, 1H), 1.90–1.81 (m, 1H), 1.67 (d, J = 11.6 Hz, 2H), 1.53–1.40 (m, 1H), 1.36 (t, J = 11.6 Hz, 1H), 1.11–0.80 (m, 9H), 0.75 (d, J = 7.0 Hz, 3H, CHCH_3) ppm; ^{13}C NMR (101 MHz, CDCl_3): δ = 200.8 ($\text{C}=\text{O}$), 175.4 ($\text{CH}=\text{C}^{\text{I}}$), 172.5 ($\text{C}^{\text{I}}=\text{O}$), 166.7 ($\text{C}=\text{O}$), 90.2 ($\text{C}^{\text{H}}=\text{C}$), 75.6 ($\text{CO}_2\text{-CH}$), 73.8 ($\text{CO}_2\text{-C}^{\text{H}}$), 50.7 ($\text{C}(\text{O})\text{-CH}_2\text{-CO}_2$), 47.1 (C^{I}), 47.0 (C), 41.1 (C^{H_2}), 40.8 (CH_2), 34.3 (C^{H_2}), 34.2 (CH_2), 34.3, 31.5 (C), 30.2 (C^{I}), 26.4 (C^{I}), 26.2 (C), 23.6 (C^{H_2}), 23.4 (CH_2), 22.1 (C), 21.3 (C^{I}), 20.9 (C), 20.8 (C^{I}), 16.5 (C^{I}), 16.2 (C) ppm. The spectroscopic data are in agreement with the literature.²³

(1*R*,2*S*,5*R*)-2-Isopropyl-5-methylcyclohexyl 2-methyl-3-oxobutanoate **208**:



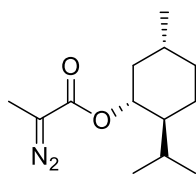
To a stirring suspension of NaH (60 wt% in mineral oil, 124 mg, 3.1 mmol), in dry THF (5 mL), **207** (750 mg, 3.1 mmol), was added at 0 °C. Once the grey suspension turned into a clear solution, methyl iodide (129 μL , 2.1 mmol) was added. The reaction was heated

under reflux overnight. A saturated aqueous solution of NH_4Cl was added at room temperature, and the product was extracted with CH_2Cl_2 (3 \times 5 mL). The combined organic layers were washed with brine and dried over MgSO_4 and the solvent was evaporated under reduced pressure. The desired product **208** was obtained as a yellow

oil (365 mg, 1.36 mmol, 66% yield, as mixture of two isomers **208:208'** *d.r.* = 1:1 by ^1H NMR spectroscopy).

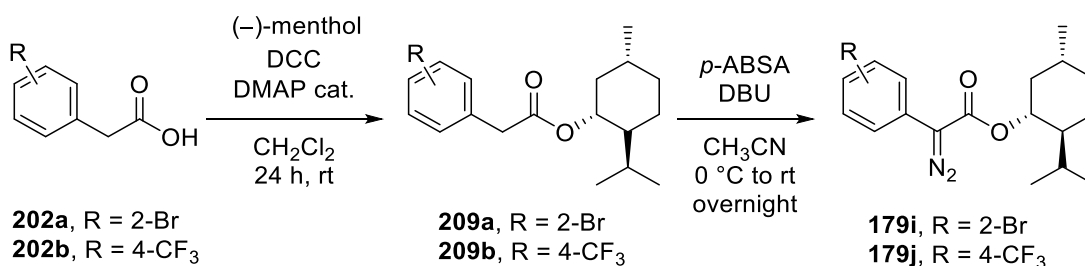
^1H NMR (500 MHz, CDCl_3): δ = 4.79–4.42 (m, 1H, $\text{CO}_2\text{-CH}$), 3.48–3.41 (m, 1H, C(O)-CHCO_2), 2.20 (s, 3H, CH_3), 1.96 (t, J = 5.9 Hz, 1H, *alkylH*), 1.89–1.72 (m, 1H, *alkylH*), 1.70–1.59 (m, 2H, *alkylH*), 1.55–1.18 (m, 5H, *alkylH*), 1.14–0.75 (m, 9H), 0.75 (dd, J = 7.0, 2.3 Hz, 3H, CH_3) ppm; ^{13}C NMR (126 MHz, CDCl_3): δ = 203.8 (C=O), 203.7 ($\text{C}'=\text{O}$), 170.3 (C=O), 170.2 ($\text{C}'=\text{O}$), 75.5 ($\text{CO}_2\text{-CH}$), 75.4 ($\text{CO}_2\text{-C}'\text{H}$), 54.2 (C(O)-CHCO_2), 54.0 ($\text{C(O)-C}'\text{HCO}_2$), 47.03 (C), 47.01 (C'), 40.7 (C), 40.6 (C'), 34.3 ($\text{C+C}'$), 31.52 (C), 31.51 (C'), 28.49 (C), 28.47 (C'), 26.4 (C), 26.2 (C'), 23.5 (C), 23.3 (C'), 22.1 ($\text{C+C}'$), 20.9 (C), 20.8 (C'), 16.3 (C), 16.1 (C'), 12.9 (C), 12.8 (C') ppm. The crude mixture was used without further purification.

(1*R*,2*S*,5*R*)-2-Isopropyl-5-methylcyclohexyl 2-diazopropanoate **179h**:



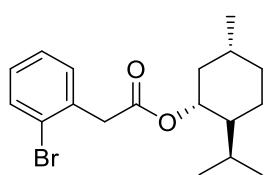
208 (300 mg, 1.2 mmol) was dissolved in acetonitrile (2 mL) and *p*-ABSA (430 mg, 1.8 mol) was added. The solution was cooled to 0 °C before the addition of DBU (300 μL , 1.8 mmol). The solution was stirred at room temperature for 12 h. A saturated aqueous solution of NH_4Cl was added and the product was extracted with CH_2Cl_2 (3 \times 5 mL). The combined organic layers were washed with water, brine and dried over MgSO_4 . The pure compound **179h** was obtained after column chromatography as a volatile yellow oil (80 mg, 0.36 mmol, 30% yield).

^1H NMR (400 MHz, CDCl_3): δ = 4.73 (td, J = 10.9, 4.4 Hz, 1H, $\text{CO}_2\text{-CH}$), 2.06–1.99 (m, 1H), 1.95 (s, 3H, CH_3), 1.90–1.82 (m, 1H), 1.71–1.62 (m, 2H), 1.54–1.43 (m, 1H), 1.42–1.32 (m, 1H), 1.13–0.86 (m, 9H), 0.77 (d, J = 7.0 Hz, 3H, CH_3) ppm; ^{13}C NMR (101 MHz, CDCl_3): δ = 74.8 ($\text{CO}_2\text{-CH}$), 47.3, 41.5, 34.4, 31.5, 26.6, 23.8, 22.2, 20.8, 16.7, 8.6 ppm (C=N_2 and C=O not observed); IR (neat): ν = 2954w, 2926w, 2870w, 2075s, 1684s, 1456w, 1303m, 1128s, 986w, 953w, 732m cm^{-1} . The spectroscopic data are in agreement with the literature.²⁴

5.3.1.4 Synthesis of Diazo Compounds **179i–j**

General Procedure 10: The arylacetic acid **202** (5 mmol) was dissolved in CH₂Cl₂, then (-)-menthol (2.5 mmol), DCC (5 mmol) and catalytic amount of DMAP (0.75 mmol, 0.3 equiv.) were added. The reaction was stirred at room temperature for 24 hours, monitored by TLC (*n*-hexane/ethyl acetate) and then filtered. The filtrate was washed with a saturated aqueous solution of NaHCO₃ and extracted with CH₂Cl₂. The combined organic layers were dried over MgSO₄ and the solvent was evaporated under vacuum. The crude was purified by column to afford the pure ester **209**.

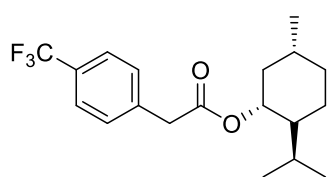
(1*R*,2*R*,5*R*)-2-Isopropyl-5-methylcyclohexyl 2-(2-bromophenyl)acetate **209a**:



Performed according to *General Procedure 10* on a 4.7 mmol scale of **202a** and 2.3 mmol of (-)-menthol; **209a** (718 mg, 2.0 mmol, 89% yield) was obtained as a colourless oil.

¹H NMR (400 MHz, CDCl₃): δ = 7.54 (d, *J* = 7.8 Hz, 1H, *ArH*), 7.31–7.20 (m, 2H, *ArH*), 7.10 (ddd, *J* = 8.0, 6.8, 2.4 Hz, 1H, *ArH*), 4.71 (td, *J* = 10.9, 4.4 Hz, 1H, CO₂–CH), 4.10–3.55 (m, 2H, Ar–CH₂–CO₂), 2.10–1.95 (m, 1H), 1.83 (dtd, *J* = 13.9, 7.0, 2.7 Hz, 1H), 1.72–1.58 (m, 2H), 1.53–1.41 (m, 1H), 1.39–1.27 (m, 1H), 1.13–0.79 (m, 9H), 0.73 (d, *J* = 7.0 Hz, 3H, CH₃) ppm; ¹³C NMR (101 MHz, CDCl₃): δ = 170.0 (C=O), 134.6 (ArC), 132.7 (ArC), 131.5 (ArC), 128.8 (ArC), 127.5 (ArC), 125.1 (ArC), 74.9 (CO₂–CH), 47.0, 42.1, 40.8, 34.3, 31.4, 26.2, 23.4, 22.1, 20.8, 16.4 ppm; IR (neat): ν = 2948m, 2860m, 1725s, 1469m, 1234s, 1163s, 1010s cm⁻¹; HRMS (NSI): Exact mass calculated for C₁₈H₂₉BrO₂N [M+NH₄]⁺: 370.1380; found: 370.1376; [α]_D²⁰: +44.1° (c 0.41, CHCl₃).

(1*R*,2*R*,5*R*)-2-Isopropyl-5-methylcyclohexyl-2-(4(trifluoromethyl)phenyl)acetate **209b**:

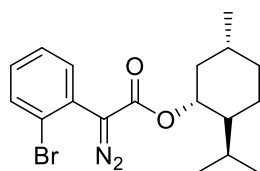


Performed according to *General Procedure 10* on a 5.0 mmol scale of **202b** and 2.5 mmol of (-)-menthol; **209b** (666 mg, 2.0 mmol, 78% yield) was obtained as a colourless oil.

¹H NMR (500 MHz, CDCl₃): δ = 7.58 (d, *J* = 8.1 Hz, 2H, Ar*H*), 7.40 (d, *J* = 8.0 Hz, 2H, Ar*H*), 4.68 (td, *J* = 10.9, 4.4 Hz, 1H, CO₂-CH), 3.65 (s, 2H, ArCH₂-CO₂), 2.09–1.92 (m, 1H), 1.76–1.62 (m, 2H), 1.56 (d, *J* = 2.6 Hz, 1H), 1.52–1.42 (m, 1H), 1.35 (ddt, *J* = 14.3, 10.9, 3.1 Hz, 1H), 1.12–0.80 (m, 9H), 0.68 (d, *J* = 7.0 Hz, 3H, CH₃) ppm; ¹³C NMR (126 MHz, CDCl₃): δ = 170.5 (C=O), 138.5 (m, ArC), 129.7 (2 × ArC), 129.5 (q, *J* = 32.5 Hz, ArC-CF₃), 125.5 (q, *J* = 3.8 Hz, 2 × ArC), 124.3 (q, *J* = 271.9 Hz, CF₃), 75.3 (CO₂-CH), 47.2, 41.7, 40.9, 34.3, 31.5, 26.3, 23.5, 22.1, 20.8, 16.4 ppm; IR (neat): ν = 2949m, 2864m, 1730s, 1323s, 1153s, 824m, 698m, 598m cm⁻¹; HRMS (ASAP): Exact mass calculated for C₁₉H₂₄O₂F [M-H₄]⁺: 341.1728; found: 341.1723; [α]_D²⁰: +44.1° (c 0.41, CHCl₃).

General Procedure 11: A 0.2 M solution of (-)-menthyl arylacetate **209** (2 mmol) and *p*-ABSA (4 mmol) in THF was cooled to 0 °C before the addition of DBU (8 mmol). The reaction was stirred at room temperature for 24 hours and monitored by TLC (*n*-hexane/ethyl acetate). The mixture was quenched with a saturated aqueous solution of NH₄Cl saturated solution and the product was extracted with ethyl acetate. The combined organic layers were washed with water, brine, dried over MgSO₄ and concentrated under reduced pressure. The crude was purified by flash column chromatography to afford the pure product **179i–j** as an oil or solid depending on the substrate.

(1*R*,2*S*,5*R*)-2-Isopropyl-5-methylcyclohexyl 2-diazo-2-(2-bromophenyl)acetate **179i**:

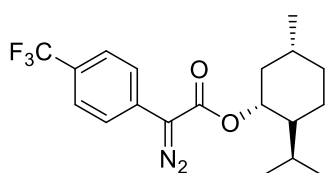


Performed according to *General Procedure 11* on a 1.3 mmol scale of **209a**; **179i** (316 mg, 0.85 mmol, 66% yield) was obtained as a bright yellow oil.

¹H NMR (400 MHz, CDCl₃): δ = 7.61 (dd, *J* = 8.1, 1.2 Hz, 1H, Ar*H*), 7.52 (dd, *J* = 7.8, 1.6 Hz, 1H, Ar*H*), 7.36 (td, *J* = 7.6, 1.3 Hz, 1H, Ar*H*), 7.19 (ddd, *J* = 8.0, 7.4, 1.7 Hz, 1H, Ar*H*), 4.85 (td, *J* = 10.9, 4.4 Hz, 1H, CO₂-CH), 2.21–2.06 (m, 1H), 1.91 (dhep, *J* = 6.9, 2.7 Hz, 1H), 1.69 (d, *J* = 11.6 Hz, 2H), 1.58–1.34 (m, 2H), 1.17–0.97 (m, 2H), 0.95–0.75 (m, 10H) ppm; ¹³C NMR (101 MHz, CDCl₃): δ = 165.2 (C=O), 133.4 (ArC), 133.0 (ArC), 130.0 (ArC), 127.7 (ArC), 126.1 (ArC), 124.6 (ArC), 75.5 (CO₂-CH), 47.2,

41.4, 34.3, 31.5, 26.7, 23.8, 22.1, 20.8, 16.8 ppm ($C=N_2$ not observed); IR (neat): $\nu = 2956m, 2868m, 2090s, 1693s, 1476m, 1236s, 1165s, 1009s, 752s, 644m \text{ cm}^{-1}$; HRMS (NSI): Exact mass calculated for $C_{18}H_{24}BrN_2O_2$ $[M+H]^+$: 379.1016, found 379.1016; $[\alpha]_D^{20}$: -54.5° (c 0.70, CH_2Cl_2).

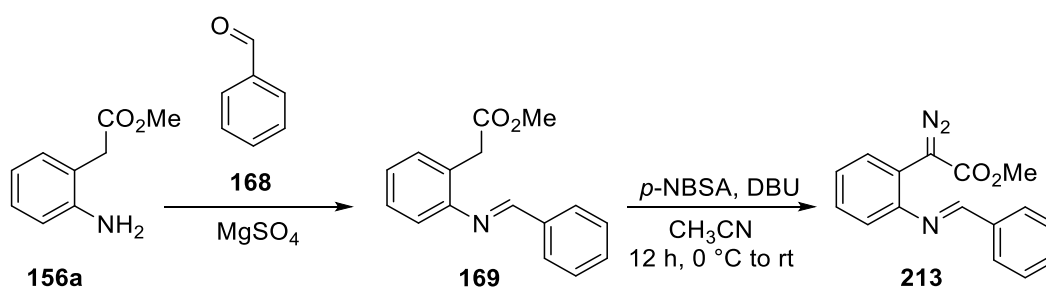
(1*R*,2*S*,5*R*)-2-Isopropyl-5-methylcyclohexyl 2-diazo-2-(4-(trifluoromethyl)phenyl)acetate **179j**:



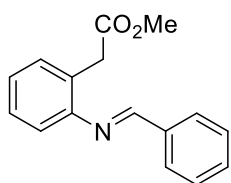
Performed according to *General Procedure 11* on a 1.7 mmol scale of **209b**; **179j** (368 mg, 1.5 mmol, 87% yield) was obtained as a bright yellow solid.

1H NMR (400 MHz, $CDCl_3$): $\delta = 7.61$ (s, 4H, ArH), 4.89 (td, $J = 10.9, 4.4$ Hz, 1H, CO_2-CH), 2.19–2.00 (m, 1H), 1.99–1.81 (m, 1H), 1.75–1.68 (m, 2H), 1.61–1.41 (m, 2H), 1.17–1.03 (m, 2H), 0.98–0.85 (m, 7H), 0.81 (d, $J = 7.0$ Hz, 3H, CH_3) ppm; ^{13}C NMR (126 MHz, $CDCl_3$): $\delta = 164.2$ ($C=O$), 130.8–130.6 (m, ArC), 127.6 (q, $J = 32.7$ Hz, ArC– CF_3), 126.0 (q, $J = 3.8$ Hz, 2 \times ArC), 124.3 (q, $J = 272.2$ Hz, CF_3), 123.6 (2 \times ArC), 75.7 (CO_2-CH), 47.3, 41.4, 34.3, 31.6, 26.7, 23.8, 22.1, 20.9, 16.7 ppm ($C=N_2$ not observed); IR (neat): $\nu = 2956m, 2930m, 2870w, 2087s, 1695s, 1616m, 1319s, 1238s, 1165s, 1115s, 1070s, 1011s, 841m \text{ cm}^{-1}$; HRMS (NSI): Exact mass calculated for $C_{19}H_{24}F_3N_2O_2$ $[M+H]^+$: 369.1784, found 369.1788; $[\alpha]_D^{20}$: -62.6° (c 0.80, CH_2Cl_2).

5.3.1.5 Synthesis of Diazo Compound **213**



Methyl (*E*)-2-(2-(benzylideneamino)phenyl)acetate **169**:

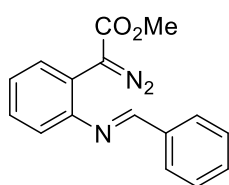


To neat aniline derivative **156a** (3 g, 18 mmol), benzaldehyde **168** (1.1 equiv.) was added dropwise. The orange solution turned into an emulsion and $MgSO_4$ was added. The suspension was stirred for 1 hour, the salt was filtered off and washed with CH_2Cl_2 and the

mixture was concentrated under *vacuo* to afford **169** as an orange oil (3.8 g, 15 mmol, 83% yield).

^1H NMR (500 MHz, CDCl_3): δ = 8.42 (s, 1H, $\text{N}=\text{CH}$), 7.92–7.86 (m, 2H, ArH), 7.51–7.43 (m, 3H, ArH), 7.35–7.28 (m, 2H, ArH), 7.21 (td, J = 7.5, 1.2 Hz, 1H, ArH), 7.04 (dd, J = 7.8, 1.0 Hz, 1H, ArH), 3.84 (s, 2H, CH_2), 3.61 (s, 3H, OCH_3) ppm; ^{13}C NMR (126 MHz, CDCl_3): δ = 172.5 ($\text{C}=\text{O}$), 160.1 ($\text{ArC}-\text{N}$), 150.7 (ArC), 136.5 (ArC), 131.5 (ArC), 130.6 (ArC), 129.2 (ArC), 129.1 (ArC), 129.0 (ArC), 128.9 (ArC), 128.6 (ArC), 126.3 (ArC), 117.7 (ArC), 52.0 (OCH_3), 37.6 (CH_2) ppm. The spectroscopic data are in agreement with the literature.²⁵

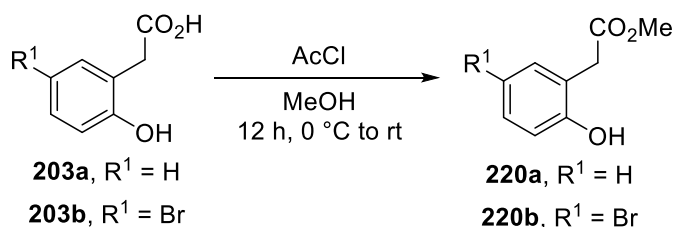
Methyl (*E*)-2-(2-(benzylideneamino)phenyl)-2-diazoacetate **213**:



A solution of **169** (340 mg, 1.3 mmol) and of *p*-NBSA **18f**² (1.5 equiv.) in acetonitrile (5 mL) was cooled to 0 °C before the addition of DBU (4 equiv.). The dark solution was stirred for 12 hours and checked by TLC (*n*-hexane/ethyl acetate). A saturated aqueous solution of NH_4Cl (10 mL) was added and the product extracted with CH_2Cl_2 (3 × 10 mL). The combined organic layers were washed with H_2O , brine, dried over MgSO_4 and concentrated under *vacuo* to afford **213** (211 mg, 0.75 mmol, 58% yield) as a yellow oil.

^1H NMR (400 MHz, CDCl_3): δ = 8.40 (s, 1H, $\text{N}=\text{CH}$), 7.99–7.88 (m, 2H, ArH), 7.75–7.67 (m, 1H, ArH), 7.57–7.46 (m, 3H, ArH), 7.34–7.27 (m, 2H, ArH), 7.14–6.98 (m, 1H, ArH), 3.84 (s, 3H, CH_3) ppm; ^{13}C NMR (101 MHz, CDCl_3): δ = 166.7 ($\text{C}=\text{O}$), 159.8 ($\text{ArC}-\text{N}$), 148.1 (ArC), 136.0 (ArC), 131.8 (ArC), 129.8 (ArC), 129.3 (ArC), 128.9 (ArC), 128.4 (ArC), 126.6 (ArC), 120.1 (ArC), 118.0 (ArC), 52.0 (OCH_3) ppm ($\text{C}=\text{N}_2$ not observed). The spectroscopic data are in agreement with the literature.²⁵

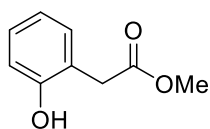
5.3.1.6 Synthesis of Diazo Compounds **184a–k**



General Procedure 12: The corresponding aryl acetic acid **203** was dissolved in methanol and the 0.5 M solution was cooled down to 0 °C before addition of acetyl chloride (2.5 equiv.). The reaction was stirred at room temperature for 16 hours and

checked by TLC (*n*-hexane/ethyl acetate). The solvent was evaporated *in vacuo* and the residual oil washed with a saturated aqueous solution of NaHCO₃ and extracted with Et₂O. Subsequently, the combined organic layers were washed with water and brine, dried over MgSO₄ and concentrated *in vacuo* to afford the pure methyl 2-hydroxyaryl acetate **220** which was used without further purification.

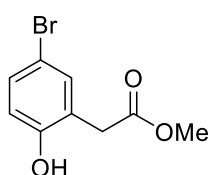
Methyl 2-(2-hydroxyphenyl)acetate **220a**:



Performed according to *General Procedure 12* on a 33 mmol scale of **203a**; **220a** (5.1 g, 31 mmol, 93% yield) was obtained as a colourless solid, m.p.: 68–70 °C.

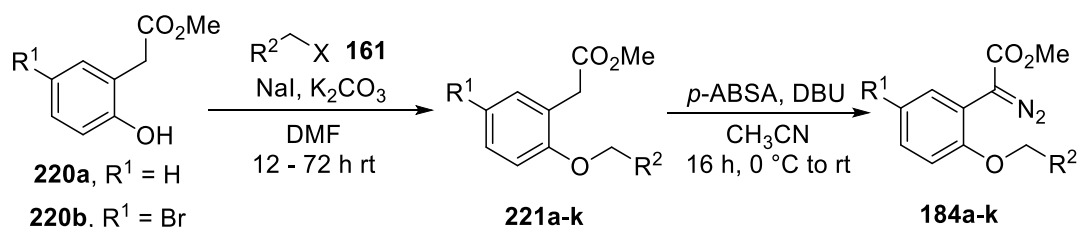
¹H NMR (500 MHz, CDCl₃): δ = 7.43 (s, 1H, OH), 7.17 (t, *J* = 7.5 Hz, 1H, ArH), 7.11 (d, *J* = 7.2 Hz, 1H, ArH), 6.96–6.75 (m, 2H, ArH), 3.74 (s, 3H, OCH₃), 3.69 (s, 2H, CH₂) ppm; ¹³C NMR (126 MHz, CDCl₃): δ = 174.3 (C=O), 155.0 (ArC–O), 131.1 (ArC), 129.1 (ArC), 120.8 (ArC), 120.7 (ArC), 117.1 (ArC), 52.7 (OCH₃), 37.2 (CH₂) ppm. The spectroscopic data are in agreement with the literature.²⁶

Methyl 2-(5-bromo-2-hydroxyphenyl)acetate **220b**:



Performed according to *General Procedure 12* on a 2.2 mmol scale of **203b**; **220b** (515 mg, 2.1 mmol, 96% yield) was obtained as a colourless solid, m.p.: 76–80 °C.

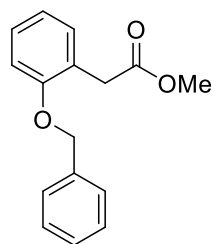
¹H NMR (500 MHz, CDCl₃): δ = 7.37 (s, 1H, OH), 7.32–7.05 (m, 2H, ArH), 6.66 (d, *J* = 8.5 Hz, 1H, ArH), 3.67 (s, 3H, OCH₃), 3.55 (s, 2H, CH₂) ppm; ¹³C NMR (126 MHz, CDCl₃): δ = 173.9 (C=O), 154.4 (ArC–O), 133.5 (ArC), 131.9 (ArC), 122.8 (ArC), 119.0 (ArC), 112.6 (ArC), 52.9 (OCH₃), 37.0 (CH₂) ppm. The spectroscopic data are in agreement with the literature.²⁷



General Procedure 13: The methyl ester **220** was dissolved in DMF (0.5 M solution), and K₂CO₃ (2.5 equiv.), NaI (1.1 equiv.) were added. The solution was cooled down to 0 °C before the addition of the corresponding halide **161** (1.2 equiv.). The reaction was performed for 12–72 hours at room temperature and checked by TLC (*n*-hexane/ethyl

acetate). The suspension was filtrate, washed with water (40 mL) and the product extracted with Et₂O (3 × 15 mL). The combined organic layers were washed with brine, dried over MgSO₄ and concentrate under vacuum and purified by column to afford the desired product **221** as an oil or solid depending on the substrate.

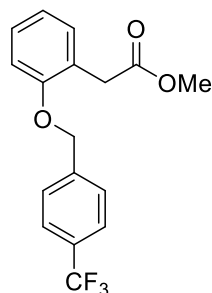
Methyl 2-(2-(benzyloxy)phenyl)acetate **221a**:



Performed according to *General Procedure 13* on a 21 mmol scale of **220a**; **221a** (4.4 g, 17 mmol, 82% yield) was obtained as a colourless solid, m.p.: 70–72 °C.

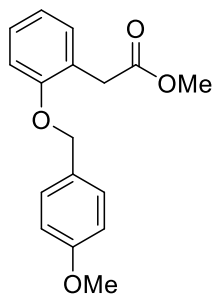
¹H NMR (400 MHz, CDCl₃): δ = 7.46–7.35 (m, 4H, ArH), 7.35–7.28 (m, 1H, ArH), 7.28–7.18 (m, 2H, ArH), 6.98–6.90 (m, 2H, ArH), 5.09 (s, 2H, OCH₂), 3.69 (s, 2H, CH₂), 3.64 (s, 3H, OCH₃) ppm; ¹³C NMR (126 MHz, CDCl₃): δ = 172.4 (C=O), 156.7 (ArC–O), 137.2 (ArC), 131.1 (ArC), 128.7 (ArC), 128.6 (2 × ArC), 127.9 (ArC), 127.2 (2 × ArC), 123.6 (ArC), 120.9 (ArC), 111.9 (ArC), 70.0 (OCH₂), 51.9 (OCH₃), 36.2 (CH₂) ppm. The spectroscopic data are in agreement with the literature.²⁸

Methyl 2-(2-((4-(trifluoromethyl)benzyl)oxy)phenyl)acetate **221b**:



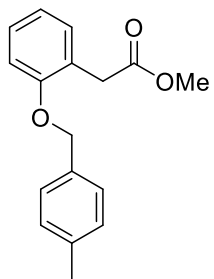
Performed according to *General Procedure 13* on a 1.5 mmol scale of **220a**; **221b** (422 mg, 1.3 mmol, 87%) was obtained as a colourless solid, m.p.: 58–60 °C.

¹H NMR (400 MHz, CDCl₃): δ = 7.60 (d, *J* = 8.2 Hz, 2H, ArH), 7.49 (d, *J* = 8.0 Hz, 2H, ArH), 7.25–7.15 (m, 2H, ArH), 6.92 (td, *J* = 7.5, 1.0 Hz, 1H, ArH), 6.84 (d, *J* = 8.1 Hz, 1H, ArH), 5.10 (s, 2H, OCH₂), 3.66 (s, 2H, CH₂), 3.60 (s, 3H, OCH₃) ppm; ¹³C NMR (101 MHz, CDCl₃): δ = 172.3 (C=O), 156.4 (ArC–O), 141.3–141.2 (m, ArC), 131.4 (ArC), 130.1 (q, *J* = 32.4 Hz, ArC–CF₃), 128.8 (ArC), 128.3 (2 × ArC), 125.6 (q, *J* = 3.8 Hz, 2 × ArC), 124.3 (d, *J* = 276.0 Hz, CF₃), 123.6 (ArC), 121.3 (ArC), 111.8 (ArC), 69.2 (OCH₂), 51.9 (OCH₃), 36.2 (CH₂) ppm; IR (neat): ν = 2949w, 1734s, 1605m, 1499m, 1452m, 1325s, 1258s, 1157s, 1107s, 820s, 754s, 696m, 586m, 565m cm⁻¹; HRMS (ES): Exact mass calculated for C₁₇H₁₆F₃O₃ [M+H]⁺: 325.1052, found 325.1047.

Methyl 2-(2-((4-methoxybenzyl)oxy)phenyl)acetate **221c**:

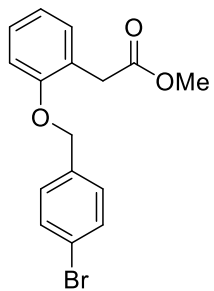
Performed according to *General Procedure 13* on a 3.0 mmol scale of **220a**; **221c** (634 mg, 2.2 mmol, 74%) was obtained as a colourless oil.

$^1\text{H NMR}$ (500 MHz, CDCl_3): δ = 7.33 (d, J = 8.3 Hz, 2H, ArH), 7.28–7.17 (m, 2H, ArH), 6.99–6.87 (m, 4H, ArH), 5.01 (s, 2H, OCH_2), 3.82 (s, 3H, OCH_3), 3.66 (s, 2H, CH_2), 3.63 (s, 3H, OCH_3) ppm; $^{13}\text{C NMR}$ (126 MHz, CDCl_3): δ = 172.4 (C=O), 159.4 (ArC–O), 156.8 (ArC–O), 131.1 (ArC), 129.8 (ArC), 128.9 (2 × ArC), 128.7, 123.6 (ArC), 120.9 (ArC), 114.0 (2 × ArC), 112.0 (ArC), 69.9 (OCH_2), 55.4 (OCH_3), 51.9 (OCH_3), 36.2 (CH_2) ppm; IR (neat): ν = 2951w, 2837w, 1735s, 1612m, 3080w, 1514s, 1454m, 1240s, 1174s, 1029s, 819s, 750s cm^{-1} ; HRMS (ES): Exact mass calculated for $\text{C}_{17}\text{H}_{18}\text{O}_4\text{Na}$ [$\text{M}+\text{Na}$] $^+$: 309.1103, found 309.1116.

Methyl 2-(2-((4-methylbenzyl)oxy)phenyl)acetate **221d**:

Performed according to *General Procedure 13* on a 1.5 mmol scale of **220a**; **221d** (302 mg, 1.1 mmol, 74% yield) was afforded as a colourless solid, m.p.: 42–44 °C.

$^1\text{H NMR}$ (300 MHz, CDCl_3): δ = 7.29 (d, J = 8.0 Hz, 2H, ArH), 7.27–7.15 (m, 4H, ArH), 6.97–6.89 (m, 2H, ArH), 5.04 (s, 2H, CH_2), 3.68 (s, 2H, CH_2), 3.64 (s, 3H, OCH_3), 2.36 (s, 3H, CH_3) ppm; $^{13}\text{C NMR}$ (101 MHz, CDCl_3): δ = 172.4 (C=O), 156.8 (ArC–O), 137.6 (ArC), 134.2 (ArC), 131.1 (ArC), 129.3 (2 × ArC), 128.7 (ArC), 127.3 (2 × ArC), 123.5 (ArC), 120.9 (ArC), 111.9 (ArC), 70.0 (OCH_2), 52.0 (OCH_3), 36.2 (CH_2), 21.3 (CH_3) ppm; IR (neat): ν = 3026w, 2949w, 2866w, 1736s, 1602m, 1589m, 1492s, 1454m, 1379w, 1242s, 1155s, 1012s, 800m, 750s cm^{-1} ; HRMS (ES): Exact mass calculated for $\text{C}_{17}\text{H}_{18}\text{O}_3\text{Na}$ [$\text{M}+\text{Na}$] $^+$: 293.1154, found 293.1157.

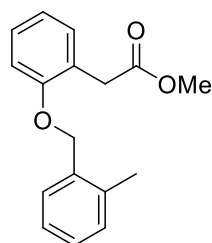
Methyl 2-(2-((4-bromobenzyl)oxy)phenyl)acetate **221e**:

Performed according to *General Procedure 13* on a 3.0 mmol scale of **220a**; **221e** (664 mg, 2.0 mmol, 66% yield) was afforded as a colourless solid, m.p.: 48–50 °C.

$^1\text{H NMR}$ (400 MHz, CDCl_3): δ = 7.50 (d, J = 8.4 Hz, 2H, ArH), 7.32–7.17 (m, 4H, ArH), 6.94 (t, J = 7.4 Hz, 1H, ArH), 6.88 (d, J = 8.2 Hz, 1H, ArH), 5.03 (s, 2H, OCH_2), 3.67 (s, 2H, CH_2), 3.63 (s, 3H, OCH_3)

ppm; ^{13}C NMR (101 MHz, CDCl_3): δ = 172.3 (C=O), 156.5 (ArC–O), 136.2 (ArC), 131.8 (2 × ArC), 131.3 (ArC), 128.8 (2 × ArC), 128.8 (ArC), 123.6 (ArC), 121.8 (ArC), 121.2 (ArC), 111.9 (ArC), 69.3 (OCH₂), 52.0 (OCH₃), 36.2 (CH₂) ppm; IR (neat): ν = 2951w, 2918w, 2864, 1743s, 1602m, 1500m, 1256s, 1157s, 1117s, 1009s, 800s, 752s cm^{-1} ; HRMS (AP): Exact mass calculated for $\text{C}_{16}\text{H}_{16}\text{O}_3\text{Br}$ $[\text{M}+\text{H}]^+$: 335.0283, found 335.0287.

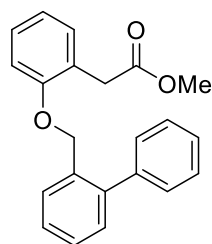
Methyl 2-(2-((2-methylbenzyl)oxy)phenyl)acetate **221f**:



Performed according to *General Procedure 13* on a 1.5 mmol scale of **220a**; **221f** (356 mg, 1.3 mmol, 88% yield) was afforded as a colourless solid, m.p.: 54–56 °C.

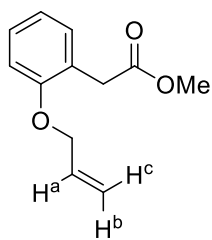
^1H NMR (400 MHz, CDCl_3): δ = 7.36 (d, J = 7.3 Hz, 1H, ArH), 7.32–7.05 (m, 5H, ArH), 7.03–6.78 (m, 2H, ArH), 4.99 (s, 2H, OCH₂), 3.62 (s, 2H, CH₂), 3.54 (s, 3H, OCH₃), 2.30 (s, 3H, CH₃) ppm; ^{13}C NMR (101 MHz, CDCl_3): δ = 172.4 (C=O), 156.8 (ArC–O), 136.3 (ArC), 135.0 (ArC), 131.1 (ArC), 130.3 (ArC), 128.7 (ArC), 128.1 (ArC), 128.1 (ArC), 126.1 (ArC), 123.5 (ArC), 120.9 (ArC), 111.6 (ArC), 68.5 (OCH₂), 51.8 (OCH₃), 36.1 (CH₂), 18.9 (CH₃) ppm; IR (neat): ν = 3076w, 2949w, 1735s, 1600m, 1498m, 1456m, 1348m, 1298m, 1250s, 1201s, 1121s, 1053s, 850m, 756s, 691s cm^{-1} ; HRMS (ES): Exact mass calculated for $\text{C}_{17}\text{H}_{18}\text{O}_3\text{Na}$ $[\text{M}+\text{Na}]^+$: 293.1154, found 293.1158.

Methyl 2-(2-([1,1'-biphenyl]-2-ylmethoxy)phenyl)acetate **221g**:



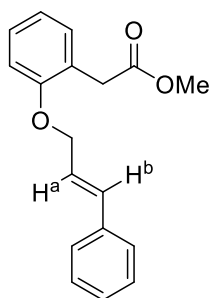
Performed according to *General Procedure 13* on a 1.5 mmol scale of **220a**; **221g** (405 mg, 1.2 mmol, 81% yield) was afforded as a colourless oil.

^1H NMR (400 MHz, CDCl_3): δ = 7.65–7.54 (m, 1H, ArH), 7.47–7.29 (m, 8H, ArH), 7.21–7.13 (m, 2H, ArH), 6.91 (td, J = 7.5, 1.0 Hz, 1H, ArH), 6.72 (d, J = 7.9 Hz, 1H, ArH), 4.96 (s, 2H, OCH₂), 3.66 (s, 2H, CH₂), 3.62 (s, 3H, OCH₃) ppm; ^{13}C NMR (126 MHz, CDCl_3): δ = 172.4 (C=O), 156.6 (ArC–O), 141.6 (ArC), 140.6 (ArC), 134.2 (ArC), 131.1 (ArC), 130.1 (ArC), 129.2 (ArC), 129.0 (ArC), 128.6 (ArC), 128.5 (ArC), 128.0 (ArC), 127.7 (ArC), 127.5 (ArC), 123.4 (ArC), 120.9 (ArC), 111.8 (ArC), 68.2 (OCH₂), 51.9 (OCH₃), 36.2 (CH₂) ppm; IR (neat): ν = 3076w, 2993w, 2949w, 2921w, 1736s, 1601m, 1589m, 1499m, 1456m, 1348m, 1298m, 1250s, 1201m, 1161s, 1121s, 1053s, 1003m, 851m, 756s, 736s, 690m cm^{-1} ; HRMS (ES): Exact mass calculated for $\text{C}_{22}\text{H}_{20}\text{O}_3\text{Na}$ $[\text{M}+\text{Na}]^+$: 355.1310, found 355.1317.

Methyl 2-(2-(allyloxy)phenyl)acetate **221h**:

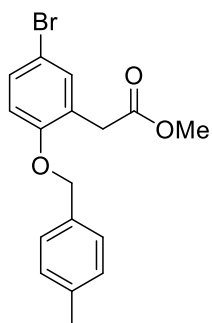
Performed according to *General Procedure 13* on a 1.5 mmol scale of **220a**; **221h** (247 mg, 1.2 mmol, 80% yield) was afforded as a colourless oil.

^1H NMR (400 MHz, CDCl_3): δ = 7.26–7.16 (m, 2H, ArH), 6.92 (td, J = 7.4, 1.1 Hz, 1H, ArH), 6.86 (d, J = 8.2 Hz, 1H, ArH), 6.02 (ddt, J = 17.3, 10.6, 4.9, 1H, CH^{A}), 5.40 (dq, J = 17.3, 1.7 Hz, 1H, CH^{B}), 5.26 (dq, J = 10.6, 1.5 Hz, 1H, CH^{C}), 4.55 (dt, J = 4.9, 1.6 Hz, 2H, OCH_2), 3.68 (s, 3H, OCH_3), 3.66 (s, 2H, CH_2) ppm; ^{13}C NMR (101 MHz, CDCl_3): δ = 172.5 (C=O) 156.6 (ArC–O), 133.3, 131.1, 128.6, 123.6, 120.9, 117.0, 111.9, 68.8 (OCH_2), 52.0 (OCH_3), 36.2 (CH_2) ppm; IR (neat): ν = 2951w, 1736s, 1603m, 1589w, 1493s, 1340m, 1244s, 1155s, 997s, 926m, 750s cm^{-1} ; HRMS (ES): Exact mass calculated for $\text{C}_{12}\text{H}_{14}\text{O}_3\text{Na}$ [$\text{M}+\text{Na}$] $^+$: 229.0841, found 229.0842.

Methyl 2-(2-(cinnamyloxy)phenyl)acetate **221i**:

Performed according to *General Procedure 13* on a 3.0 mmol scale of **220a**; **221i** (378 mg, 1.3 mmol, 44% yield) was afforded as a colourless oil.

^1H NMR (400 MHz, CDCl_3): δ = 7.34–7.30 (m, 2H, ArH), 7.27–7.21 (m, 2H, ArH), 7.19–7.10 (m, 3H, ArH), 6.89–6.79 (m, 2H, ArH), 6.64 (d, J = 16.0 Hz, 1H, H^{B}), 6.28 (dt, J = 16.0, 5.4 Hz, 1H, H^{A}), 4.61 (dd, J = 5.4, 1.6 Hz, 2H, OCH_2), 3.61 (s, 3H, OCH_3), 3.58 (s, 2H, CH_2) ppm; ^{13}C NMR (101 MHz, CDCl_3): δ = 172.4 (C=O), 156.7 (ArC–O), 136.7, 132.3, 131.1, 128.7, 128.6, 127.9, 126.6, 124.6, 123.6, 120.9, 112.0, 68.7 (OCH_2), 52.0 (OCH_3), 36.2 (CH_2) ppm; IR (neat): ν = 3026w, 2949w, 1734s, 1600m, 1589m, 1493s, 1452m, 1242s, 1155s, 1113m, 734s, 690 cm^{-1} ; HRMS (ES): Exact mass calculated for $\text{C}_{18}\text{H}_{18}\text{O}_3\text{Na}$ [$\text{M}+\text{Na}$] $^+$: 305.1154, found 305.1157.

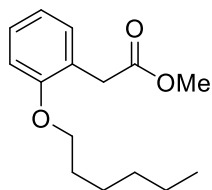
Methyl 2-(5-bromo-2-((4-methylbenzyl)oxy)phenyl) acetate **221j**:

Performed according to *General Procedure 13* on a 1.7 mmol scale of **220b**; **221j** (457 mg, 1.3 mmol, 76% yield) was afforded as a colourless solid, m.p.: 82–84 °C.

^1H NMR (500 MHz, CDCl_3): δ = 7.35 (d, J = 6.4 Hz, 2H, ArH), 7.31–7.27 (m, 2H, ArH), 7.21 (d, J = 7.7 Hz, 2H, ArH), 6.81 (d, J = 9.3 Hz, 1H, ArH), 5.04 (s, 2H, OCH_2), 3.67 (s, 3H, OCH_3), 3.65 (s, 2H, CH_2), 2.38 (s, 3H, CH_3) ppm; ^{13}C NMR (126 MHz, CDCl_3): δ = 171.7 (C=O),

156.0 (ArC–O), 137.9 (ArC), 133.8 (ArC), 133.6 (ArC), 131.3 (ArC), 129.4 (ArC), 127.3 (ArC), 125.8 (ArC), 113.6 (ArC), 112.9 (ArC), 70.4 (OCH₂), 52.1 (OCH₃), 35.8 (CH₂), 21.3 (CH₃) ppm; IR (neat): ν = 2951w, 1738s, 1493m, 1250s, 1198s, 1157s, 1124s, 1014s, 997s cm⁻¹; HRMS (ES): Exact mass calculated for C₁₇H₁₇O₃BrNa [M+Na]⁺: 371.0259, found 371.0259.

Methyl 2-(2-(hexyloxy)phenyl) acetate **221k**:

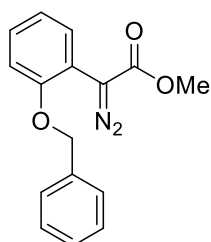


Performed according to *General Procedure 13* on a 1.5 mmol scale of **220a**; **221k** (217 mg, 0.87 mmol, 58% yield) was afforded as a colourless oil.

¹H NMR (400 MHz, CDCl₃): δ = 7.23 (td, J = 8.0, 1.8 Hz, 1H, ArH), 7.18 (dd, J = 7.4, 1.6 Hz, 1H, ArH), 6.90 (td, J = 7.4, 1.0 Hz, 1H, ArH), 6.85 (d, J = 8.2 Hz, 1H, ArH), 3.95 (t, J = 6.4 Hz, 2H, OCH₂), 3.68 (s, 3H, OCH₃), 3.63 (s, 2H, CH₂), 1.82–1.67 (m, 2H), 1.49–1.40 (m, 2H), 1.37–1.30 (m, 4H), 0.94–0.88 (m, 3H, CH₃) ppm; ¹³C NMR (101 MHz, CDCl₃): δ = 172.5 (C=O), 157.2 (ArC–O), 131.0 (ArC), 128.6 (ArC), 123.3 (ArC), 120.4 (ArC), 111.3 (ArC), 68.1 (OCH₂), 51.9 (OCH₃), 36.2, 31.7, 29.4, 25.8, 22.8, 14.2 ppm; IR (neat) ν = 2951m, 2929m, 2858w, 1738s, 1602w, 1495m, 1456m, 1244s, 1155s, 748s cm⁻¹; HRMS (ES): Exact mass calculated for C₁₅H₂₂O₃Na [M+Na]⁺: 273.1467, found 273.1469.

General Procedure 14: A 0.2 M solution of methyl arylacetate **221a–k** and *p*-ABSA (3 equiv.) in acetonitrile was cooled down to 0 °C before the addition of DBU (4 equiv.). The reaction was stirred at room temperature for 12–48 hours and monitored by TLC (*n*-hexane/ethyl acetate). The mixture was quenched with a saturated aqueous solution of NH₄Cl saturated solution and the product was extracted with CH₂Cl₂. The combined organic layers were washed with water, brine, dried over MgSO₄ and concentrated under reduced pressure (20 °C water bath). The crude was purified by flash column chromatography to afford the pure product **184a–k** as a yellow oil or solid.

Methyl 2-(2-(benzyloxy)phenyl)-2-diazoacetate **184a**:

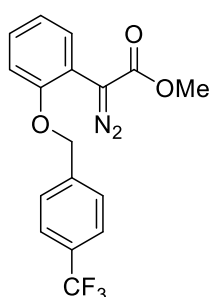


Performed according to *General Procedure 14* on a 1.4 mmol scale of **221a**; **184a** (340 mg, 1.2 mmol, 86% yield) was afforded as a bright yellow oil.

¹H NMR (400 MHz, CDCl₃): δ = 7.57 (dd, J = 7.8, 1.7 Hz, 1H, ArH), 7.44–7.32 (m, 5H, ArH), 7.27–7.21 (m, 1H, ArH), 7.04 (td, J = 7.6,

1.1 Hz, 1H, *ArH*), 6.97 (dd, $J = 8.3, 1.1$ Hz, 1H, *ArH*), 5.11 (s, 2H, OCH_2), 3.82 (s, 3H, OCH_3) ppm; ^{13}C NMR (126 MHz, CDCl_3): $\delta = 166.8$ ($\text{C}=\text{O}$), 154.8 ($\text{ArC}-\text{O}$), 136.4 (*ArC*), 130.5 (*ArC*), 128.7 (*ArC*), 128.3 (*ArC*), 127.7 (*ArC*), 121.7 (*ArC*), 114.1 (*ArC*), 112.3 (*ArC*), 70.8 (OCH_2), 52.1 (OCH_3) ppm ($\text{C}=\text{N}_2$ not observed); IR (neat): $\nu = 3032\text{w}, 2951\text{w}, 2093\text{s}, 1693\text{s}, 1494\text{m}, 1448\text{m}, 1433\text{m}, 1246\text{s}, 1149\text{s}, 1032\text{s}, 1009\text{s}, 744\text{s}, 696\text{s}$ cm^{-1} . The spectroscopic data are in agreement with the literature.²⁸

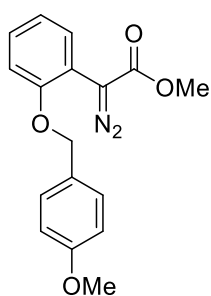
Methyl 2-(2-((4-(trifluoromethyl)benzyl)oxy)phenyl)-2-diazoacetate **184b**:



Performed according to *General Procedure 14* on a 0.9 mmol scale of **221b**; **184b** (273 mg, 0.78 mmol, 87% yield) was afforded as a bright yellow solid.

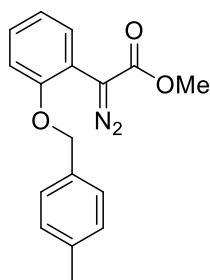
^1H NMR (400 MHz, CDCl_3): $\delta = 7.66$ (d, $J = 8.2$ Hz, 2H, *ArH*), 7.58 (dd, $J = 7.8, 1.7$ Hz, 1H, *ArH*), 7.53 (d, $J = 8.0$ Hz, 2H, *ArH*), 7.28–7.23 (m, 1H, *ArH*), 7.07 (td, $J = 7.5, 1.0$ Hz, 1H, *ArH*), 6.94 (dd, $J = 8.3, 1.0$ Hz, 1H, *ArH*), 5.16 (s, 2H, OCH_2), 3.83 (s, 3H, OCH_3) ppm; ^{13}C NMR (101 MHz, CDCl_3): $\delta = 166.6$ ($\text{C}=\text{O}$), 154.5 ($\text{ArC}-\text{O}$), 140.4 (*ArC*), 130.7 (*ArC*), 130.4 (q, $J = 32.5$ Hz, $\text{ArC}-\text{CF}_3$), 128.8 (*ArC*), 127.6 (*ArC*), 125.7 (q, $J = 3.8$ Hz, $2 \times \text{ArC}$), 124.2 (q, $J = 272.1$ Hz, CF_3), 121.9 (*ArC*), 114.2 (*ArC*), 112.3 (*ArC*), 69.9 (OCH_2), 52.1 (OCH_3) ppm ($\text{C}=\text{N}_2$ not observed); IR (neat): $\nu = 2859\text{w}, 2097\text{s}, 1693\text{s}, 1497\text{m}, 1437\text{m}, 1325\text{s}, 1248\text{s}, 1155\text{s}, 824\text{s}, 750\text{s}$ cm^{-1} ; HRMS (ES): Exact mass calculated for $\text{C}_{17}\text{H}_{14}\text{F}_3\text{O}_3$ [$\text{M}-\text{N}_2+\text{H}$] $^+$: 323.0895, found 323.0901.

Methyl 2-diazo-2-(2-((4-methoxybenzyl)oxy)phenyl)acetate **184c**:



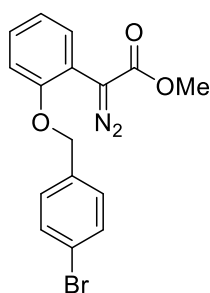
Performed according to *General Procedure 14* on a 0.52 mmol scale of **221c**; **184c** (125 mg, 0.40 mmol, 77% yield) was afforded as a bright yellow solid.

^1H NMR (400 MHz, CDCl_3): $\delta = 7.59$ (dd, $J = 7.8, 1.6$ Hz, 1H, *ArH*), 7.34 (d, $J = 8.5$ Hz, 2H, *ArH*), 7.30–7.17 (m, 1H, *ArH*), 7.05 (t, $J = 7.6$ Hz, 1H, *ArH*), 6.99 (d, $J = 8.3$ Hz, 1H, *ArH*), 6.94 (d, $J = 8.6$ Hz, 2H, *ArH*), 5.03 (s, 2H, OCH_2), 3.83 (s, 3H, OCH_3), 3.82 (s, 3H, OCH_3) ppm; ^{13}C NMR (101 MHz, CDCl_3): $\delta = 166.7$ ($\text{C}=\text{O}$), 159.6 ($\text{ArC}-\text{O}$), 154.8 ($\text{ArC}-\text{O}$), 130.4 (*ArC*), 129.4 ($2 \times \text{ArC}$), 128.6 (*ArC*), 128.4 (*ArC*), 121.4 (*ArC*), 114.1 (*ArC*), 114.0 ($2 \times \text{ArC}$), 112.3 (*ArC*), 70.5 (OCH_2), 55.3 (OCH_3), 52.01 (OCH_3) ppm ($\text{C}=\text{N}_2$ not observed); IR (neat): $\nu = 3001\text{m}, 2955\text{m}, 2839\text{w}, 2098\text{s}, 1689\text{s}, 1514\text{s}, 1435\text{s}, 1028\text{s}, 995\text{s}, 814\text{s}, 754\text{s}$ cm^{-1} . The spectroscopic data are in agreement with the literature.²⁹

Methyl 2-(2-((4-(methylbenzyl)oxy)phenyl)-2-diazoacetate **184d**:

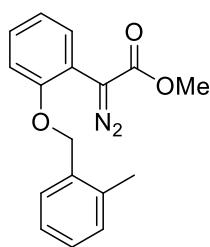
Performed according to *General Procedure 14* on a 0.55 mmol scale of **221d**; **184d** (137 mg, 0.46 mmol, 84% yield) was afforded as a bright yellow solid.

^1H NMR (400 MHz, CDCl_3): δ = 7.57 (dd, J = 7.8, 1.7 Hz, 1H, ArH), 7.30 (d, J = 8.0 Hz, 2H, ArH), 7.27–7.17 (m, 3H, ArH), 7.03 (td, J = 7.6, 1.1 Hz, 1H, ArH), 6.97 (dd, J = 8.3, 0.9 Hz, 1H, ArH), 5.06 (s, 2H, CH_2), 3.82 (s, 3H, OCH_3), 2.37 (s, 3H, CH_3) ppm; ^{13}C NMR (101 MHz, CDCl_3): δ = 166.8 ($\text{C}=\text{O}$), 154.8 (ArC–O), 138.0 (ArC), 133.4 (ArC), 130.5 (ArC), 129.4 (ArC), 128.7 (ArC), 127.8 (ArC), 121.5 (ArC), 114.1 (ArC), 112.3 (ArC), 70.7 (OCH_2), 52.1 (OCH_3), 21.3 (CH_3) ppm ($\text{C}=\text{N}_2$ not observed); IR (neat): ν = 3057w, 3030w, 2949w, 2091s, 1692s, 1429m, 1254s, 1149s, 1005s, 802s, 744s, 662m cm^{-1} . The spectroscopic data are in agreement with the literature.²⁹

Methyl 2-(2-((4-bromobenzyl)oxy)phenyl)-2-diazoacetate **184e**:

Performed according to *General Procedure 14* on a 0.89 mmol scale of **221e**; **184e** (230 mg, 0.64 mmol, 71% yield) was afforded as a bright yellow solid.

^1H NMR (400 MHz, CDCl_3): δ = 7.48 (dd, J = 7.8, 1.4 Hz, 1H, ArH), 7.41 (d, J = 8.3 Hz, 2H, ArH), 7.20–7.08 (m, 3H, ArH), 6.95 (t, J = 7.6 Hz, 1H, ArH), 6.83 (d, J = 8.3 Hz, 1H, ArH), 4.92 (s, 2H, CH_2), 3.72 (s, 3H, OCH_3) ppm; ^{13}C NMR (101 MHz, CDCl_3): δ = 166.6 ($\text{C}=\text{O}$), 154.5 (ArC–O), 135.3 (ArC), 131.8 (ArC), 130.6 (ArC), 129.2 (ArC), 128.7 (ArC), 122.2 (ArC), 121.7 (ArC), 114.1 (ArC), 112.3 (ArC), 70.0 (OCH_2), 52.1 (OCH_3) ppm ($\text{C}=\text{N}_2$ not observed); IR (neat): ν = 2988m, 2947m, 2097s, 1691s, 1495s, 1431s, 1229s, 1153s, 804s, 741s cm^{-1} . HRMS (AP): Exact mass calculated for $\text{C}_{16}\text{H}_{14}\text{O}_3\text{Br}$ [$\text{M}-\text{N}_2+\text{H}$] $^+$: 333.0126, found 333.0117.

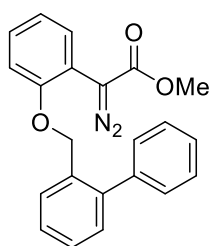
Methyl 2-diazo-2-(2-((2-methylbenzyl)oxy)phenyl)acetate **184f**:

Performed according to *General Procedure 14* on a 1.8 mmol scale of **221f**; **184f** (388 mg, 1.3 mmol, 71% yield) was afforded as a bright yellow solid.

^1H NMR (500 MHz, CDCl_3): δ = 7.53 (dd, J = 7.8, 1.6 Hz, 1H, ArH), 7.35–7.28 (m, 1H, ArH), 7.25–7.15 (m, 4H, ArH), 7.00 (td, J = 7.7, 1.1 Hz, 1H, ArH), 6.95 (dd, J = 8.3, 0.8 Hz, 1H, ArH), 5.03 (s, 2H, OCH_2), 3.76 (s, 3H,

OCH₃), 2.30 (s, 3H, CH₃) ppm; ¹³C NMR (126 MHz, CDCl₃): δ = 166.8 (C=O), 154.9 (ArC–O), 136.5 (ArC), 134.3 (ArC), 130.5 (ArC), 128.7 (ArC), 128.6 (ArC), 128.4 (ArC), 126.2 (ArC), 121.5 (ArC), 114.0 (ArC), 112.2 (ArC), 69.1 (OCH₂), 52.1 (OCH₃), 18.9 (CH₃) ppm (C=N₂ not observed); IR (neat): ν = 3055w, 2953w, 2098s, 1697s, 1497s, 1452s, 1246s, 1153s, 1003w, 733s cm⁻¹; HRMS (AP): Exact mass calculated for C₁₆H₁₄O₃Br [M–N₂+H]⁺: 333.0126, found 333.0117.

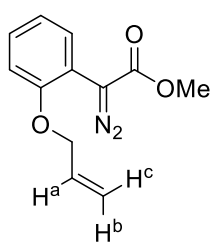
Methyl 2-(2-((2-(phenylbenzyl)oxy)phenyl)-2-diazoacetate **184g**:



Performed according to *General Procedure 14* on a 1.0 mmol scale of **221g**; **184g** (269 mg, 0.75 mmol, 75% yield) was afforded as a bright yellow oil.

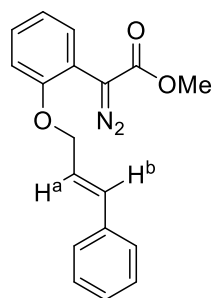
¹H NMR (300 MHz, CDCl₃): δ = 7.63–7.48 (m, 2H, ArH), 7.48–7.32 (m, 8H, ArH), 7.16 (ddd, *J* = 8.3, 7.5, 1.7 Hz, 1H, ArH), 7.01 (td, *J* = 7.6, 1.2 Hz, 1H, ArH), 6.75 (dd, *J* = 8.3, 0.9 Hz, 1H, ArH), 5.01 (s, 2H, OCH₂), 3.83 (s, 3H, OCH₃) ppm; ¹³C NMR (101 MHz, CDCl₃): δ = 166.8 (C=O), 154.7 (ArC–O), 141.8 (ArC), 140.5 (ArC), 133.5 (ArC), 130.4 (ArC), 130.2 (ArC), 129.3 (ArC), 129.2 (ArC), 128.7 (ArC), 128.5 (ArC), 128.3 (ArC), 127.8 (ArC), 127.5 (ArC), 121.5 (ArC), 114.0 (ArC), 112.4 (ArC), 68.8 (OCH₂), 52.1 (OCH₃) ppm (C=N₂ not observed); IR (neat): ν = 3059w, 2987m, 2951m, 2094s, 1697s, 1435s, 1246s, 742s, 702s cm⁻¹. HRMS (EI): Exact mass calculated for C₂₂H₁₈N₂O₃ [M]⁺: 358.1317, found 358.1320.

Methyl 2-(2-(allyloxy)phenyl)-2-diazoacetate **184h**:



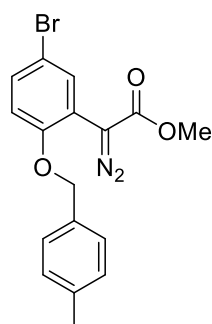
Performed according to *General Procedure 14* on a 0.97 mmol scale of **221h**; **184h** (90 mg, 0.39 mmol, 40% yield) was afforded as a bright yellow oil.

¹H NMR (500 MHz, CDCl₃): δ = 7.56 (dd, *J* = 7.8, 1.5 Hz, 1H, ArH), 7.26–7.22 (m, 1H, ArH), 7.03 (td, *J* = 7.8, 1.1 Hz, 1H, ArH), 6.90 (d, *J* = 8.3 Hz, 1H, ArH), 6.05 (ddt, *J* = 17.2, 10.5, 5.3 Hz, 1H, CH^a), 5.41 (ddd, *J* = 17.3, 3.0, 1.6 Hz, 1H, CH^b), 5.30 (dd, *J* = 10.6, 1.4 Hz, 1H, CH^c), 4.58 (dt, *J* = 5.2, 1.3 Hz, 2H, OCH₂), 3.84 (s, 3H, OCH₃) ppm; ¹³C NMR (126 MHz, CDCl₃): δ = 166.8 (C=O), 154.6 (ArC–O), 132.8, 130.4, 128.6, 121.4, 118.0, 114.0, 112.1, 69.4 (OCH₂), 52.1 (OCH₃) ppm (C=N₂ not observed); IR (neat): ν = 2953w, 2099s, 1697s, 1489s, 1450s, 1433s, 1244s, 1155s, 752s cm⁻¹; HRMS (EI): Exact mass calculated for C₁₂H₁₃O₃ [M–N₂+H]⁺: 205.0865, found 205.0870.

Methyl 2-(2-(cinnamyloxy)phenyl)-2-diazoacetate **184i**:

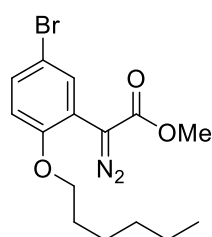
Performed according to *General Procedure 14* on a 0.88 mmol scale of **221i**; **184i** (120 mg, 0.39 mmol, 44% yield) was afforded as a bright yellow oil.

^1H NMR (500 MHz, CDCl_3): δ = 7.51 (dd, J = 7.8, 1.5 Hz, 1H, ArH), 7.39–7.32 (m, 2H, ArH), 7.30–7.24 (m, 2H, ArH), 7.24–7.06 (m, 2H, ArH), 6.97 (td, J = 7.8, 1.1 Hz, 1H, ArH), 6.88 (dd, J = 8.3, 0.6 Hz, 1H, ArH), 6.66 (d, J = 16.0 Hz, 1H, CH^b), 6.32 (dt, J = 16.0, 5.8 Hz, 1H, CH^a), 4.66 (d, J = 5.8 Hz, 2H, CH_2), 3.76 (s, 3H, OCH_3) ppm; ^{13}C NMR (126 MHz, CDCl_3): δ = 166.8 ($\text{C}=\text{O}$), 154.6 (ArC–O), 136.4, 133.3, 130.4, 129.0, 128.7, 128.7, 128.1, 126.7, 126.6, 123.9, 121.5, 114.1, 112.3, 69.3 (OCH_2), 52.1 (OCH_3) ppm ($\text{C}=\text{N}_2$ not observed); IR (neat): ν = 3025w, 2951w, 2856w, 2093s, 1695s, 1493s, 1433s, 1248, 1151s, 1031s, 964s, 733s, 690s cm^{-1} ; HRMS (AP): Exact mass calculated for $\text{C}_{18}\text{H}_{17}\text{O}_3$ [$\text{M}-\text{N}_2+\text{H}$] $^+$: 281.1178, found 281.1176.

Methyl 2-(5-bromo-2-((4-methylbenzyl)oxy)phenyl)-2-diazoacetate **184j**:

Performed according to *General Procedure 14* on a 0.88 mmol scale of **221j**; **184j** (270 mg, 0.72 mmol, 91% yield) was afforded as a bright yellow solid.

^1H NMR (400 MHz, CDCl_3): δ = 7.68 (d, J = 2.5 Hz, 1H, ArH), 7.27–7.16 (m, 3H, ArH), 7.13 (d, J = 7.9 Hz, 2H, ArH), 6.75 (d, J = 8.8 Hz, 1H, ArH), 4.95 (s, 2H, OCH_2), 3.75 (s, 3H, OCH_3), 2.30 (s, 3H, CH_3) ppm; ^{13}C NMR (101 MHz, CDCl_3): δ = 166.1 ($\text{C}=\text{O}$), 153.5 (ArC–O), 138.2 (ArC), 132.8 (ArC), 132.3 (ArC), 130.9 (ArC), 129.4 (ArC), 127.8 (ArC), 116.3 (ArC), 113.8 (ArC), 113.7 (ArC), 71.0 (OCH_2), 52.2 (OCH_3), 21.3 (CH_3) ppm ($\text{C}=\text{N}_2$ not observed); IR (neat): ν = 2951w, 2100s, 1697s, 1487s, 1435s, 1404m, 1333m, 1248s, 1153s, 1040s, 906s, 802s, 727s cm^{-1} ; HRMS (ES): Exact mass calculated for $\text{C}_{18}\text{H}_{17}\text{O}_3$ [$\text{M}-\text{N}_2+\text{H}$] $^+$: 347.0283, found 347.0283.

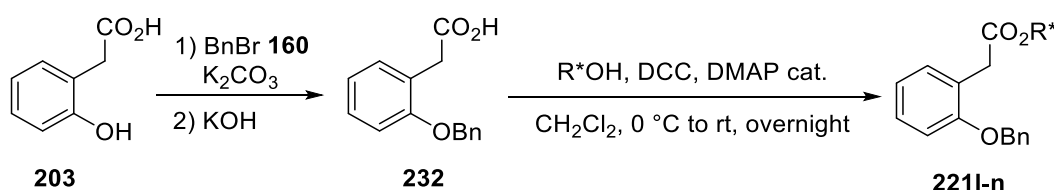
Methyl 2-(2-(hexyloxy)phenyl)-2-diazoacetate **184k**:

Performed according to *General Procedure 14* on a 0.40 mmol scale of **221k**; **184k** (93 mg, 0.34 mmol, 84%) was afforded as a bright yellow oil.

^1H NMR (400 MHz, CDCl_3): δ = 7.56 (dd, J = 7.8, 1.7 Hz, 1H, ArH), 7.23 (ddd, J = 8.3, 7.5, 1.7 Hz, 1H, ArH), 7.00 (td, J = 7.6, 1.1 Hz, 1H,

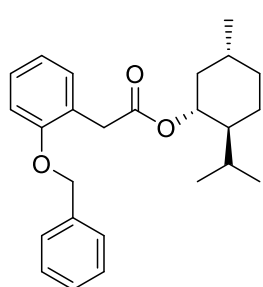
ArH), 6.88 (dd, $J = 8.3, 1.1$ Hz, 1H, *ArH*), 3.99 (t, $J = 6.5$ Hz, 2H, OCH_2), 3.84 (s, 3H, OCH_3), 1.85–1.73 (m, 2H), 1.52–1.42 (m, 2H), 1.38–1.32 (m, 4H), 0.92 (t, $J = 7.1$ Hz, 3H, CH_3) ppm; ^{13}C NMR (101 MHz, CDCl_3): $\delta = 166.9$ ($\text{C}=\text{O}$), 155.1 ($\text{ArC}-\text{O}$), 130.2 (ArC), 128.6 (ArC), 121.0 (ArC), 113.6 (ArC), 111.6 (ArC), 68.6 (OCH_2), 52.1 (OCH_3), 31.7, 29.2, 26.0, 22.7, 14.1 ppm ($\text{C}=\text{N}_2$ not observed); IR (neat): $\nu = 2951\text{m}, 2930\text{m}, 2858\text{m}, 2093\text{s}, 1701\text{s}, 1497\text{m}, 1450\text{m}, 1433\text{m}, 1248\text{s}, 1150\text{s}, 1032\text{m}, 746\text{s}$ cm^{-1} ; HRMS (ES): Exact mass calculated for $\text{C}_{15}\text{H}_{21}\text{O}_3$ [$\text{M}-\text{N}_2+\text{H}$] $^+$: 249.1491, found 249.1495.

5.3.1.7 Synthesis of Diazo Compounds **184I–n**



General Procedure 15: 2-(2-(Benzyloxy)phenyl)acetic acid **232** (4 mmol), prepared from **203** according to literature procedure,³⁰ was dissolved in CH_2Cl_2 (2 mL) and added to a solution of chiral alcohol (2 mmol) in CH_2Cl_2 (3 mL), DCC (3 mmol) and DMAP (0.6 mmol) were added. The reaction was stirred over night at room temperature. The reaction was filtered, washed with H_2O and extracted with CH_2Cl_2 (3×10 mL). The combined organic layers were washed with brine, dried over MgSO_4 and concentrated under vacuum. The crude was purified by column chromatography to afford **221I–n** as a colourless solid or an oil.

(1*R*,2*S*,5*R*)-2-Isopropyl-5-methylcyclohexyl 2-(2-(benzyloxy)phenyl)acetate **221I**:

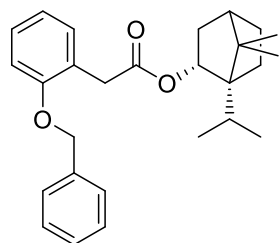


Performed according to *General Procedure 15* on a 2.0 mmol scale of (–)-menthol; **221I** (543 mg, 1.43 mmol, 95% yield) was afforded as a colourless solid, m.p.: 52–56 °C.

^1H NMR (500 MHz, CDCl_3): $\delta = 7.35$ (d, $J = 7.1$ Hz, 2H, *ArH*), 7.32–7.26 (m, 2H, *ArH*), 7.23 (t, $J = 7.3$ Hz, 1H, *ArH*), 7.18–7.10 (m, 2H, *ArH*), 6.88–6.76 (m, 2H, *ArH*), 5.11–4.87 (m, 2H, OCH_2), 4.59 (td, $J = 10.9, 4.4$ Hz, 1H, OCH), 3.60 (s, 2H, CH_2), 1.90–1.80 (m, 1H), 1.76–1.65 (m, 1H), 1.61–1.50 (m, 2H), 1.42–1.29 (m, 1H), 1.27–1.18 (m, 1H), 0.99–0.87 (m, 1H), 0.85–0.71 (m, 8H), 0.59 (d, $J = 7.0$ Hz, 3H, CH_3) ppm; ^{13}C NMR (126 MHz, CDCl_3): $\delta = 171.5$ ($\text{C}=\text{O}$), 156.7 ($\text{ArC}-\text{O}$), 137.3 (ArC), 131.1 (ArC), 128.6 (ArC), 128.5 (ArC), 127.8 (ArC), 127.1 (ArC), 123.8 (ArC), 120.8 (ArC), 111.7 (ArC), 74.5 (OCH), 69.9 (OCH_2), 47.1, 40.9, 36.6,

34.3, 31.4, 26.2, 23.5, 22.2, 20.8, 16.4 ppm; IR (neat): $\nu = 3030\text{m}, 2947\text{m}, 1730\text{s}, 1499\text{m}, 1365\text{s}, 1217\text{s}, 763\text{s}, 737\text{s}, 694\text{s} \text{ cm}^{-1}$; HRMS (ES): Exact mass calculated for $\text{C}_{25}\text{H}_{32}\text{O}_3\text{Na}$ $[\text{M}+\text{Na}]^+$: 403.2249, found 403.2266; $[\alpha]_D^{20}$: -39.5° (c 0.40, CH_2Cl_2).

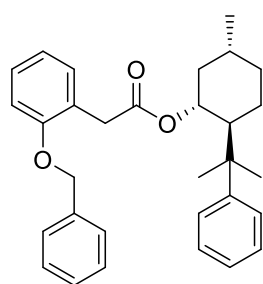
(1*R*,2*R*)-1,7,7-Trimethylbicyclo[2.2.1]heptan-2-yl 2-(2-(benzyloxy)phenyl)acetate **221m**:



Performed according to *General Procedure 15* on a 2.0 mmol scale of (-)-borneol; **221m** (545 mg, 1.44 mmol, 96% yield) was afforded as a colourless oil.

^1H NMR (500 MHz, CDCl_3): $\delta = 7.33$ (d, $J = 7.7$ Hz, 2H, ArH), 7.27 (t, $J = 7.5$ Hz, 2H, ArH), 7.20 (t, $J = 7.1$ Hz, 1H, ArH), 7.13 (dd, $J = 8.1, 3.7$ Hz, 2H, ArH), 6.87–6.79 (m, 2H, ArH), 4.98 (s, 2H, OCH_2), 4.81–4.76 (m, 1H, OCH), 3.61 (s, 2H, CH_2), 2.27–2.14 (m, 1H), 1.73–1.63 (m, 1H), 1.62–1.48 (m, 2H), 1.13–1.04 (m, 1H), 1.04–0.96 (m, 1H), 0.81 (dd, $J = 13.7, 3.3$ Hz, 2H), 0.77 (s, 3H, CH_3), 0.74 (s, 3H, CH_3), 0.65 (s, 3H, CH_3) ppm; ^{13}C NMR (126 MHz, CDCl_3): $\delta = 172.1$ (C=O), 156.7 (ArC–O), 137.2 (ArC), 131.1 (ArC), 128.6 (ArC), 128.4 (ArC), 127.8 (ArC), 127.1 (ArC), 123.9 (ArC), 120.8 (ArC), 111.7 (ArC), 80.1 (OCH), 69.9 (OCH_2), 48.8, 47.8, 44.9, 36.7, 36.5, 28.0, 27.0, 19.7, 18.9, 13.5 ppm; IR (neat): $\nu = 2951\text{m}, 2926\text{m}, 1730\text{s}, 1602\text{w}, 1589\text{w}, 1494\text{s}, 1452\text{s}, 1244\text{s}, 1153\text{s}, 1022\text{s}, 748\text{s}, 694\text{s} \text{ cm}^{-1}$; HRMS (ES): Exact mass calculated for $\text{C}_{25}\text{H}_{31}\text{O}_3$ $[\text{M}+\text{H}]^+$: 379.2268, found 379.2270; $[\alpha]_D^{20}$: -22.1° (c 1.4, CH_2Cl_2).

(1*R*,2*S*,5*R*)-5-Methyl-2-(2-phenylpropan-2-yl)cyclohexyl 2-(2-(benzyloxy)phenyl)acetate **221n**:

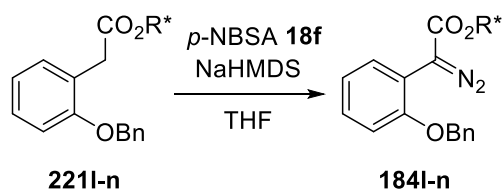


Performed according to *General Procedure 15* on a 1.59 mmol scale of (-)-8-phenylmentho; **221n** (468 mg, 1.02 mmol, 64% yield) was afforded as a colourless oil.

^1H NMR (500 MHz, CDCl_3): $\delta = 7.42$ –7.34 (m, 4H, ArH), 7.33–7.28 (m, 5H, ArH), 7.20 (t, $J = 7.8$ Hz, 1H, ArH), 7.14–7.10 (m, 1H, ArH), 7.07 (d, $J = 7.3$ Hz, 1H, ArH), 6.93–6.83 (m, 2H, ArH), 5.05 (s, 2H, OCH_2), 4.80 (td, $J = 10.6, 4.1$ Hz, 1H, OCH), 3.21 (d, $J = 16.3$ Hz, 1H, 1 \times CH_2), 3.10 (d, $J = 16.4$ Hz, 1H, 1 \times CH_2), 1.95 (t, $J = 10.5$ Hz, 1H), 1.80 (d, $J = 12.2$ Hz, 1H), 1.59 (t, $J = 10.1$ Hz, 2H), 1.46–1.34 (m, 1H), 1.28–1.13 (m, 7H), 1.08–0.94 (m, 1H), 0.92–0.76 (m, 5H) ppm; ^{13}C NMR (126 MHz, CDCl_3): $\delta = 171.0$ (C=O), 156.8 (ArC–O), 151.7 (ArC), 137.3 (ArC), 131.2 (ArC), 128.6 (ArC), 128.4 (ArC), 128.1 (ArC), 127.9 (ArC), 127.3 (ArC), 125.7 (ArC), 125.2 (ArC), 123.7 (ArC), 120.8 (ArC), 111.7 (ArC), 74.6 (OCH), 70.0 (OCH_2), 50.5, 41.7, 39.9, 36.2, 34.7, 31.3, 27.5, 26.8, 25.6, 21.9 ppm; IR (neat): $\nu =$

3030w, 2951m, 2922m, 2868w, 1730s, 1601m, 1494s, 1452s, 1242s, 987s, 748s, 696s cm^{-1} ; HRMS (ES): Exact mass calculated for $\text{C}_{31}\text{H}_{36}\text{O}_3\text{Na}$ $[\text{M}+\text{Na}]^+$: 479.2562, found 479.2564; $[\alpha]_D^{20}$: +19.2° (c 0.52, CH_2Cl_2).

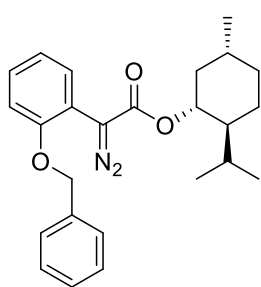
General Procedure 16:



To a solution of aryl acetate **221I-n** in dry THF (5 mL), a 2 M THF solution of NaHMDS (1.1 equiv.) was added at $-78\text{ }^\circ\text{C}$. The solution was stirred for 15 minutes before adding a solution of *p*-NBSA **18f**² (1.1 equiv.) in dry THF (1 mL) dropwise. The dark solution was stirred at $-78\text{ }^\circ\text{C}$ for 1 hour before being allowed to warm up to room temperature for 12–48 h. The reaction was quenched with pH 7 phosphate buffer, the product extracted with CH_2Cl_2 (3 × 10 mL), the combined organic layers washed with H_2O , brine and finally dried over MgSO_4 and concentrated under reduced pressure ($20\text{ }^\circ\text{C}$ water bath). The crude was purified by column chromatography to afford the products **184I-n** as yellow oils.

(1*R*,2*S*,5*R*)-2-Isopropyl-5-methylcyclohexyl 2-(2-(benzyloxy)phenyl)-2-diazoacetate

184I:

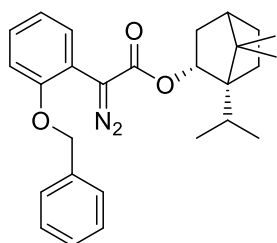


Performed according to *General Procedure 16* on a 0.63 mmol scale of **221I**; **184I** (213 mg, 0.52 mmol, 83% yield) was afforded as a bright yellow oil.

^1H NMR (500 MHz, CDCl_3): δ = 7.58 (dd, J = 7.8, 1.3 Hz, 1H, ArH), 7.39–7.26 (m, 5H, ArH), 7.18 (ddd, J = 8.5, 6.8, 3.0 Hz, 1H, ArH), 6.99 (t, J = 7.6 Hz, 1H, ArH), 6.92 (d, J = 8.3 Hz, 1H, ArH), 5.07 (s, 2H, OCH_2), 4.81 (td, J = 10.9, 4.4 Hz, 1H, OCH), 2.10–2.03 (m, 1H), 1.89 (dtd, J = 13.9, 6.9, 2.6 Hz, 1H), 1.68–1.61 (m, 1H), 1.52–1.42 (m, 1H), 1.41–1.34 (m, 1H), 1.11–0.96 (m, 2H), 0.87 (t, J = 6.5 Hz, 6H), 0.77 (d, J = 7.0 Hz, 3H, CH_3) ppm; ^{13}C NMR (126 MHz, CDCl_3): δ = 165.9 ($\text{C}=\text{O}$), 154.7 (ArC–O), 136.5 (ArC), 130.3 (ArC), 128.7 (ArC), 128.4 (ArC), 128.2 (ArC), 127.6 (ArC), 121.5 (ArC), 114.5 (ArC), 112.4 (ArC), 75.0 (OCH), 70.8 (OCH_2), 47.2, 41.5, 34.4, 31.6, 26.6, 23.8, 22.2, 20.9, 16.7 ppm ($\text{C}=\text{N}_2$ not observed); IR (neat): ν = 2953m, 2924m, 2868m, 2093s, 1690s, 1448m, 1240m, 1011s,

746s, 694m cm^{-1} ; HRMS (ES): Exact mass calculated for $\text{C}_{25}\text{H}_{31}\text{O}_3$ $[\text{M}-\text{N}_2+\text{H}]^+$: 379.2273, found 379.2272; $[\alpha]_D^{20} -49.7^\circ$ (c 0.52, CH_2Cl_2).

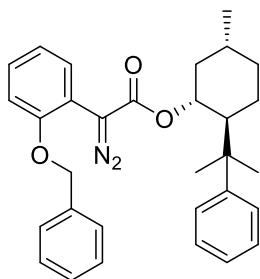
(1*R*,2*R*)-1,7,7-Trimethylbicyclo[2.2.1]heptan-2-yl 2-(2-(benzyloxy)phenyl)-2-diazoacetate **184m**:



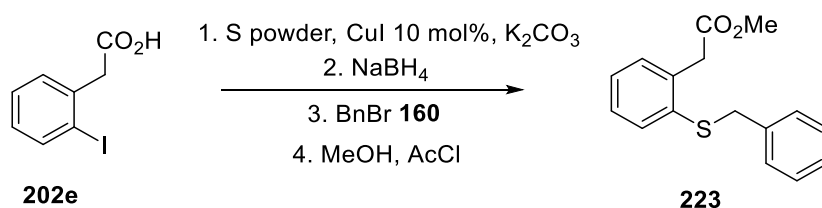
Performed according to *General Procedure 16* on a 1.1 mmol scale of **221m**; **184m** (371 mg, 0.92 mmol, 83% yield) was afforded as a bright yellow oil.

^1H NMR (500 MHz, CDCl_3): δ = 7.62 (d, J = 7.8 Hz, 1H, ArH), 7.45–7.32 (m, 5H, ArH), 7.25–7.19 (m, 1H, ArH), 7.03 (t, J = 7.6 Hz, 1H, ArH), 6.97 (d, J = 8.3 Hz, 1H, ArH), 5.12 (s, 2H, OCH_2), 5.04 (d, J = 9.7 Hz, 1H, OCH), 2.41 (td, J = 9.9, 4.9 Hz, 1H), 1.90–1.81 (m, 1H), 1.78–1.68 (m, 2H), 1.33–1.20 (m, 2H), 1.09 (dd, J = 13.7, 2.9 Hz, 1H), 0.93 (s, 3H, CH_3), 0.88 (s, 3H, CH_3), 0.87 (s, 3H, CH_3) ppm; ^{13}C NMR (126 MHz, CDCl_3) δ = 166.6 (C=O), 154.6 (ArC–O), 136.5 (ArC), 130.2 (ArC), 128.7 (ArC), 128.4 (ArC), 128.3 (ArC), 127.7 (ArC), 121.5 (ArC), 114.4 (ArC), 112.4 (ArC), 80.8 (OCH), 70.9 (OCH_2), 49.1, 47.9, 45.1, 37.1, 28.2, 27.2, 19.9, 19.0, 13.7 ppm (C=N₂ not observed); IR (neat): ν = 2953m, 2876w, 2091s, 1693s, 1497m, 1450m, 1242s, 1151s, 1022s, 746s, 694s cm^{-1} ; HRMS (ES): Exact mass calculated for $\text{C}_{25}\text{H}_{29}\text{O}_3$ $[\text{M}-\text{N}_2+\text{H}]^+$: 377.2117, found 377.2115; $[\alpha]_D^{20} -21.9^\circ$ (c 0.64, CH_2Cl_2).

(1*R*,2*S*,5*R*)-5-methyl-2-(2-phenylpropan-2-yl)cyclohexyl 2-(2-(benzyloxy)phenyl)-2-diazoacetate **184n**:



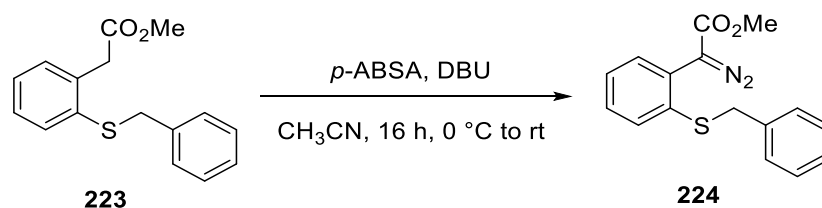
Performed according to *General Procedure 16* on a 0.63 mmol scale of **221n**; It was not possible to have full conversion nor purified **184n** from the starting material left and it was carried on as crude mixture material (product/starting material ratio = 1:0.6) for the following step.

5.3.1.8 Synthesis of Diazo Compound **224**Methyl 2-(2-(benzylthio)phenyl) acetate **223**:

An oven-dried Schlenk tube under nitrogen was loaded with 2-iodophenylacetic acid **202e** (660 mg, 2.5 mmol), CuI (10 mol%), sulfur powder (3 equiv.) and K₂CO₃ (2 equiv.). Dry DMF (5 mL) was added and the mixture was stirred at 90 °C for 16 hours under inert atmosphere. The dark brown muddy suspension was then cooled down to 0 °C before the addition of NaBH₄ (284 mg, 3 equiv.) and stirred for further 7 hours at 40 °C. The orange suspension was cooled down to 0 °C before the addition of benzyl bromide **160** (300 μL, 2 equiv.) then stirred at room temperature for 16 h. HCl 1 M was added to the dark solution until pH 2, and the product extracted with ethyl acetate (3 × 5 mL). The combined organic layers were washed with H₂O (2 × 5 mL), brine then dried over MgSO₄ and concentrated under reduced pressure to afford a yellow oil. The oil was dissolved in MeOH (8 mL), cooled to 0 °C and treated with acetyl chloride (540 μL) dropwise. The reaction was stirred at room temperature for 6 h. The solvent was removed under reduced pressure, the residue diluted with Et₂O and washed with a saturated aqueous solution of NaHCO₃ (10 mL), H₂O (10 mL) and brine. The organic layer was then dried over MgSO₄, concentrated under reduced pressure and purified by column chromatography (10% EtOAc in petroleum ether). Compound **223** was afforded as a yellow oil (152 mg, 0.55 mmol, 22% overall yield).

¹H NMR (500 MHz, CDCl₃): δ = 7.42–7.34 (m, 1H, ArH), 7.34–7.14 (m, 8H, ArH), 4.03 (s, 2H, SCH₂), 3.75 (s, 2H, CH₂), 3.69 (s, 3H, OCH₃) ppm; ¹³C NMR (126 MHz, CDCl₃): δ = 172.0 (C=O), 137.5 (ArC), 136.0 (ArC), 135.9 (ArC), 132.5 (ArC), 130.7 (ArC), 129.0 (ArC), 128.6 (ArC), 128.0 (ArC), 127.5 (ArC), 127.3 (ArC), 52.2 (OCH₃), 40.2, 39.5 ppm; IR (neat): ν = 3061w, 2949w, 1732s, 1433m, 1339m, 1213w, 1155s, 739s cm⁻¹; HRMS (ES): Exact mass calculated for C₁₆H₁₆O₂S [M]⁺: 272.0871, found 272.0867.

Methyl 2-(2-(benzylthio)phenyl) acetate **224**:

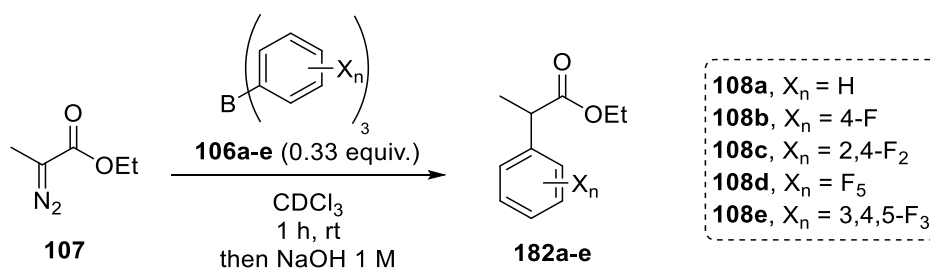


A solution of **223** (115 mg, 0.42 mmol) in dry acetonitrile (4 mL) was cooled down to 0 °C before the addition of *p*-ABSA (121 mg, 1.2 equiv.) and DBU (75 μ L, 1.2 equiv.) and stirred for 16 hours at room temperature under nitrogen and monitored by TLC (*n*-hexane/ethyl acetate, 9:1). The mixture was quenched with a saturated aqueous solution of NH_4Cl (10 mL) and the product was extracted with CH_2Cl_2 (3 \times 5 mL). The combined organic layers were washed with water, brine, dried over MgSO_4 and concentrated under reduced pressure (20 °C water bath). The crude was purified by flash column chromatography to afford **224** as a yellow oil (51 mg, 0.17 mmol, 40% yield).

^1H NMR (500 MHz, CDCl_3): δ = 7.45–7.38 (m, 1H, ArH), 7.39–7.34 (m, 1H, ArH), 7.30–7.16 (m, 7H, ArH), 4.08 (s, 2H, SCH_2), 3.81 (s, 3H, OCH_3) ppm; ^{13}C NMR (126 MHz, CDCl_3): δ = 166.6 (C=O), 137.4 (ArC), 136.9 (ArC), 132.1 (ArC), 131.0 (ArC), 129.4 (ArC), 129.0 (ArC), 128.7 (ArC), 128.6 (ArC), 127.4 (ArC), 127.2 (ArC), 127.1 (ArC), 126.1 (ArC), 52.3 (OCH_3), 39.3 (SCH_2) ppm (C=N₂ not observed); IR (neat): ν = 2951w, 2089s, 1693s, 1433s, 1344m, 1286s, 1153s, 1078m, 1028s, 914w, 754s cm^{-1} ; HRMS (ES): Exact mass calculated for $\text{C}_{16}\text{H}_{14}\text{N}_2\text{O}_2\text{S}$ [M]⁺: 298.0775, found 298.0776.

5.3.2 Synthesis of α -Aryl Esters

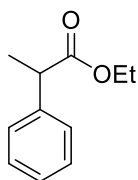
General Procedure 17:



Ethyl 2-diazopropanoate **107** (0.3 mmol) was dissolved in CDCl_3 (0.5 mL) and the triarylborane **106a–e** (0.1 mmol) was added under nitrogen and the reaction was performed for 1 hour at room temperature. A strong gas development was observed for 15–30 minutes, meanwhile the colour changed from orange to pale yellow. The reaction was monitored by NMR spectroscopy then it was quenched with 1 M aqueous solution

of NaOH (1 mL). The aqueous phase was extracted with CHCl_3 (3×1 mL). The combined organic layers were filtrated over SiO_2 plug and dried *in vacuo*, affording the products **182a–e** as a colourless oil.

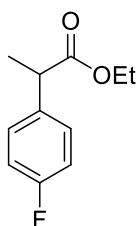
Ethyl 2-phenylpropanoate **182a**:



Performed according to *General Procedure 17* on a 0.3 mmol scale of **107** and 0.1 mmol of **106a**; **182a** (16 mg, 0.092 mmol, 30% yield) was obtained as a volatile colourless oil.

^1H NMR (500 MHz, CDCl_3): δ = 7.30–7.24 (m, 4H, ArH), 7.22–7.18 (m, 1H, ArH), 4.13–4.02 (m, 2H, OCH_2), 3.66 (q, J = 7.2 Hz, 1H, CH), 1.45 (d, J = 7.2 Hz, 3H, CHCH_3), 1.16 (t, J = 7.1 Hz, 3H, OCH_2CH_3) ppm; ^{13}C NMR (126 MHz, CDCl_3): δ = 174.7 (C=O), 140.8 (ArC–CH), 128.7 ($2 \times$ ArC), 127.6 ($2 \times$ ArC), 127.2 (ArC), 60.8 (OCH_2), 45.7 (CH), 18.7 (CH_3), 14.3 (CH_3) ppm. The spectroscopic data are in agreement with the literature.³¹

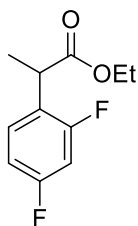
Ethyl 2-(4-fluorophenyl)propanoate **182b**:



Performed according to *General Procedure 17* on a 0.3 mmol scale of **107** and 0.1 mmol of **106b**; **182b** (20 mg, 0.11 mmol, 37% yield) was obtained as a volatile colourless oil.

^1H NMR (500 MHz, CDCl_3): δ = 7.30–7.24 (m, 2H, ArH), 7.01–6.96 (m, 2H, ArH), 4.18–4.04 (m, 2H, OCH_2), 3.69 (q, J = 7.2 Hz, 1H, CH), 1.48 (d, J = 7.2 Hz, 3H, CH_3), 1.21 (t, J = 7.1 Hz, 3H, OCH_2CH_3) ppm; ^{13}C NMR (126 MHz, CDCl_3): δ = 174.6 (C=O), 162.1 (d, J = 245.2 Hz, ArC–F), 136.5 (d, J = 8.3 Hz, ArC–CH), 129.2 (d, J = 8.0 Hz, $2 \times$ ArC), 115.5 (d, J = 21.4 Hz, $2 \times$ ArC), 61.0 (OCH_2), 44.9 (CH), 18.8 (CH_3), 14.3 (CH_3) ppm; ^{19}F NMR (471 MHz, CDCl_3): δ = –115.9 (s) ppm. The spectroscopic data are in agreement with the literature.³²

Ethyl 2-(2,4-difluorophenyl)propanoate **182c**:

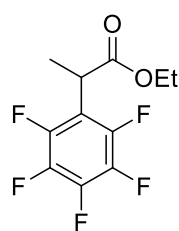


Performed according to *General Procedure 17* on a 0.35 mmol scale of **107** and 0.1 mmol of **106c**; **182c** (34 mg, 0.16 mmol, 45% yield) was obtained as a volatile colourless oil.

^1H NMR (500 MHz, CDCl_3): δ = 7.30–7.23 (m, 1H, ArH), 6.89–6.73 (m, 2H, ArH), 4.20–4.09 (m, 2H, OCH_2), 3.96 (q, J = 7.2 Hz, 1H, CH), 1.48 (d, J = 7.2 Hz, 3H, CHCH_3), 1.21 (t, J = 7.1 Hz, 3H, OCH_2CH_3) ppm; ^{13}C NMR (126 MHz, CDCl_3): δ = 173.8 (C=O), 162.3 (dd, J = 200.2, 12.0 Hz, ArC–F), 160.3 (dd, J = 201.0, 12.0 Hz,

ArC–F), 129.6 (dd, $J = 9.6, 5.7$ Hz, ArC), 124.0 (dd, $J = 15.1, 3.9$ Hz, ArC), 111.5 (dd, $J = 21.1, 3.7$ Hz, ArC), 105.9–101.8 (m, ArC), 61.2 (OCH₂), 38.1 (d, $J = 2.3$ Hz, CH), 17.7 (CH₃), 14.2 (CH₃) ppm; ¹⁹F NMR (376 MHz, CDCl₃): $\delta = -112.1$ (d, $J = 6.9$ Hz, 1F), -114.0 (d, $J = 6.9$ Hz, 1F) ppm; IR (neat): $\nu = 2916w, 1734s, 1618w, 1506s, 1194m, 964s$ cm⁻¹. HRMS (EI): Exact mass calculated for C₁₁H₁₂F₂O₂ [M]⁺: 214.0805, found 214.0807.

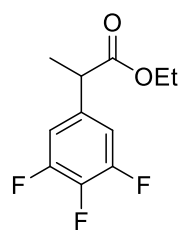
Ethyl 2-(pentafluorophenyl)propanoate **182d**:



Performed according to *General Procedure 17* on a 0.35 mmol scale of **107** and 0.1 mmol of **106d**; **182d** (64 mg, 0.25 mmol, 80% yield) was obtained as a colourless oil.

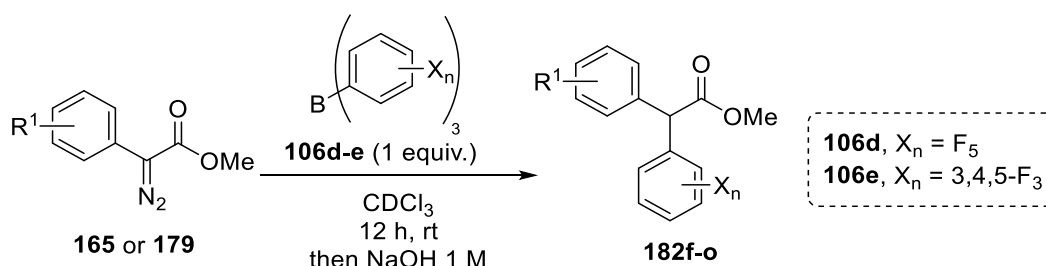
¹H NMR (500 MHz, CDCl₃): $\delta = 4.30$ – 4.10 (m, 2H, CH₂), 4.05 (q, $J = 7.3$ Hz, 1H, CH), 1.54 (d, $J = 7.4$ Hz, 3H, CH₃), 1.23 (t, $J = 7.1$ Hz, 3H, OCH₂CH₃) ppm; ¹³C NMR (126 MHz, CDCl₃): $\delta = 171.3$ (C=O), 145.4 (d, $J = 247.3$ Hz, 2 × ArC–F), 140.5 (d, $J = 247.5$ Hz, ArC–F), 137.7 (d, $J = 252.4$ Hz, 2 × ArC–F), 115.1 (dt, $J = 17.0, 4.2$ Hz, ArC–CH), 61.8 (OCH₂), 35.0 (CH), 16.3 (CH₃), 14.2 (CH₃) ppm; ¹⁹F NMR (376 MHz, CDCl₃): $\delta = -143.1$ (dd, $J = 22.0, 7.0$ Hz, 2F), -156.3 (t, $J = 20.7$ Hz, 1F), -162.4 (dt, $J = 21.1, 6.8$ Hz, 2F, m-F) ppm; IR (neat): $\nu = 2960w, 2926w, 2854w, 1739m, 1521m, 1504s, 1261s, 1012s, 970s, 800s$ cm⁻¹; HRMS (EI): Exact mass calculated for C₁₁H₉F₅O₂ [M]⁺: 268.0523, found 268.0520.

Ethyl 2-(3,4,5-trifluorophenyl)propanoate **182e**:

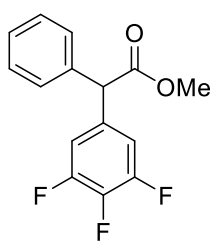


Performed according to *General Procedure 17* on a 0.35 mmol scale of **107** and 0.1 mmol of **106e**; **182e** (44 mg, 0.19 mmol, 89% yield) was obtained as a colourless oil.

¹H NMR (500 MHz, CDCl₃): $\delta = 7.03$ – 6.78 (m, 2H, ArH), 4.21– 4.06 (m, 2H, OCH₂), 3.63 (q, $J = 7.2$ Hz, 1H, CH), 1.46 (d, $J = 7.2$ Hz, 3H, CH₃), 1.22 (t, $J = 7.1$ Hz, 3H, OCH₂CH₃) ppm; ¹³C NMR (126 MHz, CDCl₃): $\delta = 173.4$ (C=O), 150.9 (ddd, $J = 249.8, 9.9, 4.1$ Hz, 2 × ArC–F), 139.0 (dt, $J = 250.0, 15.6$ Hz, ArC–F), 136.8 (td, $J = 7.4, 4.7$ Hz, 2 × ArC), 112.0– 111.7 (m, ArC–CH), 61.4 (OCH₂), 44.9 (CH), 18.5 (CH₃), 14.2 (CH₃) ppm; ¹⁹F NMR (376 MHz, CDCl₃): $\delta = -134.2$ (d, $J = 21.4$ Hz, 2F), -162.5 (t, $J = 20.5$ Hz, 1F) ppm; IR (neat): $\nu = 2986w, 1732s, 1620m, 1530s, 1447m, 1348m, 1329m, 1236m, 1211m, 1179s, 1038s, 945w, 860m, 797m, 771m$ cm⁻¹; HRMS (ES): Exact mass calculated for C₁₁H₁₀F₃O₂ [M–H]⁻: 231.0633, found 231.0644.

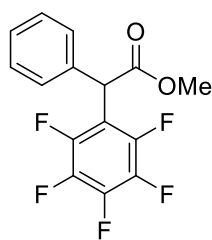
General Procedure 18:

The α -aryl- α -diazoacetates **165** or **179a–d** (0.1 mmol) was dissolved in CDCl₃ (0.5 mL) and the triarylborane **106d–f** (0.1 mmol) was added under nitrogen and the reaction was performed for 12 hours at room temperature. A strong gas development was observed for 1 hour, meanwhile the colour changed from orange to pale yellow. The reaction was monitored by NMR spectroscopy then it was quenched with 1 M aqueous solution of NaOH (1 mL). The aqueous phase was extracted with CHCl₃ (3 × 1 mL). The combined organic layers were filtrated over SiO₂ plug and the crude where purified by column chromatography, affording the products **182f–o**.

Methyl 2-Phenyl-2-(3,4,5-trifluorophenyl)acetate **182f**:

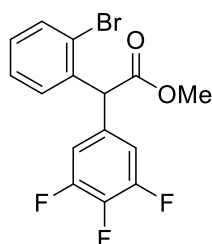
Performed according to *General Procedure 18* on a 0.12 mmol scale of **165** and 0.12 mmol of **106e**; **182f** (28 mg, 0.096 mmol, 80% yield) was obtained as a colourless oil.

¹H NMR (500 MHz, CDCl₃): δ = 7.39–7.25 (m, 5H, ArH), 6.98–6.91 (m, 2H, ArH), 4.93 (s, 1H, CH), 3.76 (s, 3H, OCH₃) ppm; ¹³C NMR (126 MHz, CDCl₃): δ = 172.0 (C=O), 151.2 (ddd, J = 250.0, 9.6, 4.2 Hz, 2 × ArC–F), 139.2 (td, J = 252.0, 15.3 Hz, ArC–F), 137.3 (ArC), 135.1–134.8 (m, ArC), 129.2 (2 × ArC), 128.5 (2 × ArC), 128.1 (ArC), 113.2–112.9 (m, 2 × ArC), 56.0 (CH), 52.8 (OCH₃) ppm; ¹⁹F NMR (376 MHz, CDCl₃): δ = –133.9 (d, J = 20.5 Hz, 2F), –162.0 (t, J = 20.3 Hz, 1F) ppm; IR (neat): ν = 2955w, 2924w, 2851w, 1735s, 1618m, 1528s, 1449m, 1435m, 1155s, 1043s, 698s cm^{–1}; HRMS (ASAP): Exact mass calculated for C₁₅H₁₁F₃O₂ [M]⁺: 280.0711, found 280.0713.

Methyl 2-phenyl-2-(pentafluorophenyl)acetate **182g**:

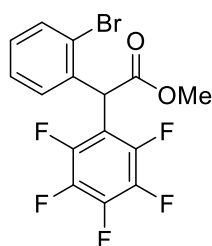
Performed according to *General Procedure 18* on a 0.12 mmol scale of **165** and 0.12 mmol of **106d**; **182g** (27 mg, 0.087 mmol, 73% yield) was obtained as a colourless oil.

^1H NMR (500 MHz, CDCl_3): δ = 7.41–7.26 (m, 5H, ArH), 5.29 (s, 1H, CH), 3.80 (s, 3H, OCH_3) ppm; ^{13}C NMR (126 MHz, CDCl_3): δ = 170.01 (C=O), 135.6 (ArC), 129.0 (2 \times ArC), 128.9–128.8 (m, 2 \times ArC), 128.2 (ArC), 53.2 (OCH_3), 46.2 (CH) ppm (ArC–F not observed); ^{19}F NMR (471 MHz CDCl_3): δ = –140.9 (dd, J = 21.7, 6.7 Hz, 2F), –155.0 (t, J = 20.9 Hz, 1F), –161.5 (dt, J = 21.0, 6.7 Hz, 2F) ppm; IR (neat): ν = 2957w, 1748s, 1522s, 1500s, 1300m, 1265m, 1205s, 1121s, 908s, 729s, 698s cm^{-1} ; HRMS (EI): Exact mass calculated for $\text{C}_{15}\text{H}_9\text{F}_5\text{O}_2$ $[\text{M}]^+$: 316.0523, found 316.0522.

Methyl 2-(2-bromophenyl)-2-(3,4,5-trifluorophenyl)acetate **182h**:

Performed according to *General Procedure 18* on a 0.11 mmol scale of **179a** and 0.12 mmol of **106e**; **182h** (31 mg, 0.86 mmol, 79% yield) was obtained as a colourless oil.

^1H NMR (500 MHz, CDCl_3): δ = 7.61 (dd, J = 7.9, 1.2 Hz, 1H, ArH), 7.39–7.27 (m, 2H, ArH), 7.19 (ddd, J = 8.0, 6.7, 2.3 Hz, 1H, ArH), 6.92 (dd, J = 8.4, 6.5 Hz, 2H, ArH), 5.42 (s, 1H, CH), 3.77 (s, 3H, OCH_3) ppm; ^{13}C NMR (126 MHz, CDCl_3): δ = 171.5 (C=O), 151.2 (ddd, J = 250.0, 9.6, 5.7 Hz, 2 \times ArC–F), 139.3 (dt, J = 252.2, 15.2 Hz, ArC–F), 136.8 (ArC), 133.6 (ArC), 133.6–133.4 (m, ArC), 129.7 (ArC), 129.6 (ArC), 128.1 (ArC), 125.1 (ArC), 113.6–113.3 (m, 2 \times ArC), 55.2 (CH), 53.0 (OCH_3) ppm; ^{19}F NMR (376 MHz, CDCl_3): δ = –133.7 (d, J = 20.5 Hz, 2F), –162.5 (t, J = 20.6 Hz, 1F); IR (neat): ν = 2954w, 2924w, 2851w, 1740s, 1620w, 1530s, 1449m, 1435m, 1348s, 1163s, 1043s, 1020s, 800.5 735s cm^{-1} ; HRMS (ASAP): Exact mass calculated for $\text{C}_{15}\text{H}_{11}\text{BrF}_3\text{O}_2$ $[\text{M}+\text{H}]^+$: 358.9895, found 358.9883.

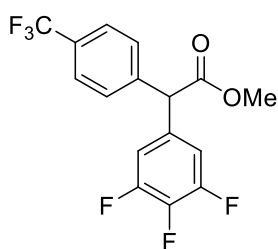
Methyl 2-(2-bromophenyl)-2-(pentafluorophenyl) acetate **182i**:

Performed according to *General Procedure 18* on a 0.11 mmol scale of **179a** and 0.12 mmol of **106d**; **182i** (46 mg, 0.12 mmol, 99% yield) was obtained as a colourless oil.

^1H NMR (500 MHz, CDCl_3): δ = 7.60 (dd, J = 8.0, 1.2 Hz 1H, ArH), 7.66–7.53 (m, 1H, ArH), 7.24–7.15 (m, 2H, ArH), 5.74 (s, 1H, CH), 3.80 (s, 3H, OCH_3) ppm; ^{13}C NMR (126 MHz, CDCl_3): δ = 168.6 (C=O), 145.5 (d, J =

245.6 Hz, $2 \times \text{ArC-F}$), 141.1 (d, $J = 254.9$ Hz, ArC-F), 137.8 (d, $J = 253.7$ Hz, $2 \times \text{ArC-F}$), 134.4 (ArC), 133.4 (ArC), 130.1 (t, $J = 3.0$ Hz, ArC), 129.9 (ArC), 127.9 (ArC), 125.1 (ArC), 112.1 (ArC), 53.4 (OCH₃), 46.5 (CH) ppm; ¹⁹F NMR (376 MHz, CDCl₃): $\delta = -139.4$ (d, $J = 18.0$ Hz, 1F), -154.0 (t, $J = 21.0$ Hz, 1F), -161.5 (t, $J = 20.7$ Hz, 2F) ppm; IR (neat): $\nu = 2955\text{w}$, 1743s , 1522s , 1472m , 1435m , 1206m , 1123s cm⁻¹; HRMS (EI): Exact mass calculated for C₁₅H₁₁BrF₃O₂ [M+H]⁺: 393.9628, found 393.9635.

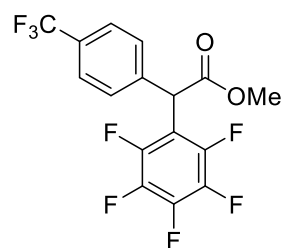
Methyl 2-(4-trifluoromethylphenyl)-2-(3,4,5-trifluorophenyl)acetate **182j**:



Performed according to *General Procedure 18* on a 0.12 mmol scale of **179b** and 0.12 mmol of **106e**; **182j** (37 mg, 0.11 mmol, 89% yield) was obtained as a colourless oil.

¹H NMR (500 MHz, CDCl₃): $\delta = 7.62$ (d, $J = 8.2$ Hz, 2H, ArH), 7.41 (d, $J = 8.2$ Hz, 2H, ArH), 6.94 (dd, $J = 8.3, 6.5$ Hz, 2H, ArH), 4.98 (s, 1H, CH), 3.78 (s, 3H, OCH₃) ppm; ¹³C NMR (126 MHz, CDCl₃): $\delta = 171.3$ (C=O), 151.3 (ddd, $J = 251.0, 9.6, 4.2$ Hz, $2 \times \text{ArC-F}$), 141.1 (ArC), 139.4 (td, $J = 252.6, 15.2$ Hz, ArC-F), 134.5–133.5 (m, ArC), 130.4 (q, $J = 32.7$ Hz, ArC-CF₃), 128.9 ($2 \times \text{ArC}$), 126.1 (q, $J = 3.7$ Hz, $2 \times \text{ArC}$), 124.0 (q, $J = 272.2$ Hz, CF₃), 113.2–112.9 (m, ArC), 55.7 (CH), 53.0 (OCH₃) ppm; ¹⁹F NMR (376 MHz, CDCl₃): $\delta = -62.7$ (s, 3F), -133.2 (d, $J = 20.5$ Hz, 2F), -161.2 (t, $J = 20.5$ Hz, 1F) ppm; IR (neat) $\nu = 3055\text{w}$, 2928w , 2855w , 1742m , 1620w , 1531m , 1325m , 1263s , 1167m cm⁻¹. HRMS (ASAP): Exact mass calculated for C₁₆H₁₀F₆O₂ [M]⁺: 348.0585, found 348.0593.

Methyl 2-(4-trifluoromethylphenyl)-2-(pentafluorophenyl)acetate **182k**:

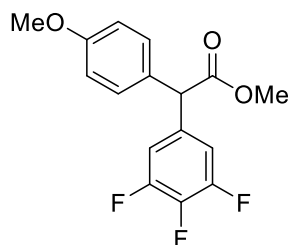


Performed according to *General Procedure 18* on a 0.12 mmol scale of **179b** and 0.12 mmol of **106d**; **182k** (33 mg, 0.087 mmol, 73% yield) was obtained as a colourless oil.

¹H NMR (500 MHz, CDCl₃): $\delta = 7.61$ (d, $J = 8.4$ Hz, 2H, ArH), 7.43 (d, $J = 8.2$ Hz, 2H, ArH), 5.33 (s, 1H, CH), 3.81 (s, 3H, OCH₃) ppm; ¹³C NMR (126 MHz, CDCl₃): $\delta = 169.4$ (C=O), 144.9 (d, $J = 248.1$ Hz, $2 \times \text{ArC-F}$), 139.4 (ArC), 137.8 (d, $J = 268.9$ Hz, $2 \times \text{ArC-F}$), 130.6 (q, $J = 31.2$ Hz, ArC-CF₃), 129.4 ($2 \times \text{ArC}$), 126.0 (q, $J = 4.1$ Hz, $2 \times \text{ArC}$), 124.0 (q, $J = 272.2$ Hz, CF₃), 123.6 (ArC), 53.4 (OCH₃), 45.7 (CH) ppm, (1 $\times \text{ArC}$ not observed); ¹⁹F NMR (376 MHz, CDCl₃): $\delta = -62.78$ (s, 3F), -140.9 (dd, $J = 20.0, 6.0$ Hz, 2F), -153.86 (t, $J = 20.9$ Hz, 1F), -160.8 (dt, $J = 21.6, 6.6$ Hz, 2F); IR (neat) $\nu = 2957\text{w}$, 2926w , 2855w , 1749m ,

1524m, 1505s, 1325s, 1265m, 1169m, 1124s, 1069s cm^{-1} ; HRMS (EI): Exact mass calculated for $\text{C}_{16}\text{H}_8\text{F}_8\text{O}_2$ $[\text{M}]^+$: 384.0397, found 384.0397.

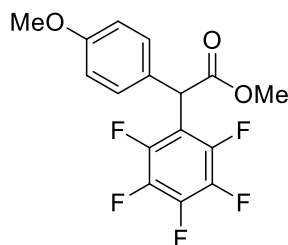
Methyl 2-(4-methoxyphenyl)-2-(3,4,5-trifluorophenyl)acetate **182l**:



Performed according to *General Procedure 18* on a 0.05 mmol scale of **179c** and 0.05 mmol of **106e**; **182l** (12 mg, 0.039 mmol, 76% yield) was obtained as a colourless oil.

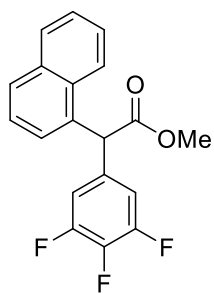
^1H NMR (500 MHz, CDCl_3): δ = 7.22–7.18 (m, 2H, ArH), 6.97–6.82 (m, 4H, ArH), 4.87 (s, 1H, CH), 3.80 (s, 3H, OCH_3), 3.75 (s, 3H, OCH_3) ppm; ^{13}C NMR (126 MHz, CDCl_3): δ = 172.3 (C=O), 159.4 (ArC–O), 151.2 (ddd, J = 250.0, 10.0, 4.1 Hz, $2 \times \text{ArC–F}$), 139.0 (dt, J = 251.6, 15.3 Hz, ArC–F), 135.3–135.1 (m, ArC), 129.6 ($2 \times \text{ArC}$), 129.3 (ArC), 114.5 ($2 \times \text{ArC}$), 113.4–111.7 (m, $2 \times \text{ArC}$), 55.5 (OCH_3), 55.2 (CH), 52.7 (OCH_3) ppm; ^{19}F NMR (376 MHz, CDCl_3): δ = –134.0 (d, J = 20.6 Hz, 2F), –162.2 (t, J = 20.6 Hz, 1F) ppm; IR (neat): ν = 2955w, 2841w, 1735s, 1611m, 1528s, 1510s, 1435m, 1155s, 1042s, 970m, 833m cm^{-1} ; HRMS (ASAP): Exact mass calculated for $\text{C}_{16}\text{H}_{14}\text{F}_3\text{O}_3$ $[\text{M}+\text{H}]^+$: 311.0895, found 311.0893.

Methyl 2-(4-methoxyphenyl)-2-(pentafluorophenyl)acetate **182m**:



Performed according to *General Procedure 18* on a 0.05 mmol scale of **179c** and 0.05 mmol of **106d**; **182m** (14 mg, 0.042 mmol, 83% yield) was obtained as a colourless oil.

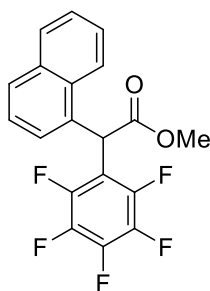
^1H NMR (500 MHz, CDCl_3) δ = 7.25–7.17 (m, 2H, ArH), 6.90–6.84 (m, 2H, ArH), 5.23 (s, 1H, CH), 3.79 (s, 6H, $2 \times \text{OCH}_3$) ppm; ^{13}C NMR (126 MHz, CDCl_3): δ = 170.4 (C=O), 159.4 (ArC–O), 144.9 (d, J = 243.6 Hz, $2 \times \text{ArC–F}$), 140.7 (d, J = 254.0 Hz, ArC–F), 137.8 (d, J = 252.1 Hz, $2 \times \text{ArC–F}$), 130.4 (ArC), 130.0 ($2 \times \text{ArC}$), 127.7 (ArC), 114.4 ($2 \times \text{ArC}$), 114.2 (ArC), 55.4 (OCH_3), 53.1 (OCH_3), 45.4 (CH) ppm; ^{19}F NMR (376 MHz, CDCl_3): δ = –141.3 (d, J = 18.4 Hz, 2F), –155.3 (t, J = 20.9 Hz, 1F), –161.5 (t, J = 19.6 Hz, 2F) ppm; IR (neat): ν = 2916w, 2849w, 1748m, 1514s, 1502s, 1252m, 1207m, 1180m, 1119m, 997m, 974m, 908w cm^{-1} ; HRMS (ASAP): Exact mass calculated for $\text{C}_{16}\text{H}_{12}\text{F}_5\text{O}_2$ $[\text{M}+\text{H}]^+$: 347.0706, found 347.0699.

Methyl 2-(naphthalen-1-yl)-2-(3,4,5-trifluorophenyl)acetate **182n**:

Performed according to *General Procedure 18* on a 0.12 mmol scale of **179d** and 0.12 mmol of **106e**; **182n** (35 mg, 0.11 mmol, 88% yield) was obtained as a colourless oil.

$^1\text{H NMR}$ (500 MHz, CDCl_3): δ = 7.92–7.82 (m, 3H, ArH), 7.56–7.44 (m, 3H, ArH), 7.39 (d, J = 7.1 Hz, 1H, ArH), 7.01–6.88 (m, 2H, ArH), 5.70 (s, 1H, CH), 3.78 (s, 3H, OCH_3) ppm; $^{13}\text{C NMR}$ (126 MHz, CDCl_3):

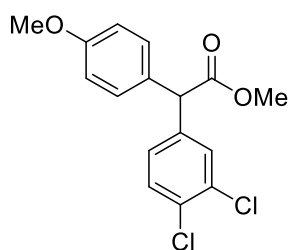
δ = 172.4 (C=O), 151.3 (d, J = 240.2 Hz, $2 \times \text{ArC-F}$), 134.5–134.4 (m, ArC), 134.3 (ArC), 132.9 (ArC), 131.3 (ArC), 129.3 (ArC), 129.1 (ArC), 127.1 (ArC), 126.2 ($2 \times \text{ArC}$), 125.6 (ArC), 123.0 (ArC), 114.4–111.7 (m, $2 \times \text{ArC}$), 52.8 (OCH_3), 52.5 (CH) ppm ($1 \times \text{ArC-F}$ not observed); $^{19}\text{F NMR}$ (376 MHz, CDCl_3): δ = -133.8 (d, J = 20.5 Hz, 2F), -161.7 (t, J = 20.5 Hz, 1F) ppm; IR (neat): ν = 3055w, 2954w, 2854w, 1740m, 1620w, 1530s, 1449w, 1435w, 1263s, 1045s cm^{-1} ; HRMS (ASAP): Exact mass calculated for $\text{C}_{19}\text{H}_{13}\text{F}_3\text{O}_2$ $[\text{M}]^+$: 330.0868, found 330.0868.

Methyl 2-(naphthalen-1-yl)-2-(pentafluorophenyl)acetate **182o**:

Performed according to *General Procedure 18* on a 0.12 mmol scale of **179d** and 0.12 mmol of **106d**; **182o** (27 mg, 0.075 mmol, 63% yield) was obtained as a colourless oil.

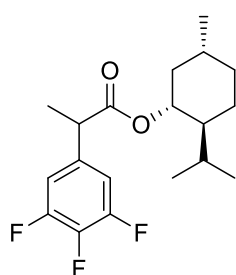
$^1\text{H NMR}$ (500 MHz, CDCl_3): δ = 8.00–7.77 (m, 3H, ArH), 7.70–7.30 (m, 4H, ArH), 6.08 (s, 1H, CH), 3.82 (s, 3H, OCH_3) ppm; $^{13}\text{C NMR}$ (126 MHz, CDCl_3): δ = 170.6 (C=O), 145.5 (d, J = 236.5 Hz, $2 \times$

ArC-F), 134.1 (ArC), 131.5 (ArC), 131.0 (ArC), 129.4 (ArC), 129.2 (ArC), 128.4 (ArC), 127.2 (ArC), 126.8 (t, J = 3.0 Hz, ArC), 126.1 (ArC), 125.4 (ArC), 122.2 (ArC), 113.0 (ArC), 53.3 (OCH_3), 43.0 (CH) ppm; $^{19}\text{F NMR}$ (376 MHz, CDCl_3): δ = -140.0 (dd, J = 18.5 Hz, 2F), -154.5 (t, J = 20.8 Hz, 1F), -161.5 (t, J = 19.8 Hz, 2F) ppm; IR (neat): ν = 3053w, 2954w, 2848w, 1742m, 1654w, 1522s, 1501s, 1468m, 986s, 908m, 775s, 731s cm^{-1} ; HRMS (EI): Exact mass calculated for $\text{C}_{19}\text{H}_{11}\text{F}_5\text{O}_2$ $[\text{M}]^+$: 366.0679, found 366.0686.

Methyl 2-(3,4-dichlorophenyl)-2-(4-methoxyphenyl)acetate **182p**:

Performed according to *General Procedure 18* on a 0.08 mmol scale of **179c** and 0.08 mmol of **106f**; **182p** (24 mg, 0.074 mmol, 92% yield) was obtained as a colourless oil.

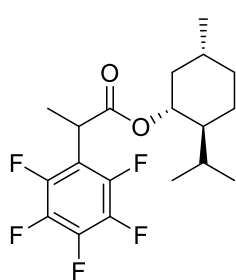
^1H NMR (500 MHz CDCl_3): δ = 7.38 (t, J = 5.6 Hz, 2H, ArH), 7.23–7.18 (m, 2H, ArH), 7.14 (dd, J = 8.3, 2.1 Hz, 1H, ArH), 6.89–6.85 (m, 2H, ArH), 4.91 (s, 1H, CH), 3.80 (s, 3H, OCH_3), 3.75 (s, 3H, OCH_3) ppm; ^{13}C NMR (126 MHz, CDCl_3): δ = 172.5 (C=O), 159.2 (ArC–O), 139.3 (ArC), 132.7 (ArC), 131.6 (ArC), 130.6 (ArC), 130.6 (ArC), 129.7 (ArC), 129.6 (2 \times ArC), 128.0 (ArC), 114.4 (2 \times ArC), 55.4, 55.3, 52.7 ppm; Spectroscopic data are in accordance with the literature.³³

(1*R*,2*S*,5*R*)-2-isopropyl-5-methylcyclohexyl-2-(3,4,5-trifluorophenyl)propanoate **182q**:

Performed according to *General Procedure 18* on a 0.11 mmol scale of **179h** and 0.11 mmol of **106e**; **182q** (36 mg, 0.11 mmol, 96% yield, 1.1:1 *d.r.*) was obtained as a colourless oil.

^1H NMR (500 MHz, CDCl_3): δ = 7.00–6.81 (m, 4H, ArH), 4.77–4.52 (m, 2H, OCH), 3.75–3.45 (m, 2H, CH), 2.02–1.93 (m, 1H), 1.88–1.80 (m, 1H), 1.79–1.59 (m, 6H), 1.51–1.40 (m, 8H), 1.41–1.26 (m, 2H), 1.13–0.80 (m, 15H), 0.77 (d, J = 7.0 Hz, 3H, CH_3), 0.73 (d, J = 7.0 Hz, 3H, CH_3), 0.59 (d, J = 7.0 Hz, 3H, CH_3) ppm; ^{13}C NMR (126 MHz, CDCl_3): δ = 173.0 (C=O), 172.9 (C=O), 151.0 (d, J = 255.3 Hz, 2 \times ArC–F), 112.5–110.4 (m, 2 \times ArC), 75.3 (OCH_2), 75.2 (OCH_2), 47.2, 47.1, 45.3, 45.2, 40.9, 40.6, 34.3, 34.3, 31.5, 31.5, 26.5, 26.2, 23.5, 23.4, 22.1, 22.1, 20.8, 20.7, 18.4, 18.3, 16.4, 16.1 ppm (1 \times ArC–F not observed); ^{19}F NMR (376 MHz, CDCl_3): δ = –134.4 (d, J = 20.4 Hz, 4F), –162.6 (t, J = 20.4 Hz, 2F) ppm; IR (neat): ν = 2957w, 2872w, 1728s, 1530s, 1449s, 1348m, 1175s, 1038s, 856m, 797m cm^{-1} ; HRMS (ASAP): Exact mass calculated for $\text{C}_{19}\text{H}_{24}\text{F}_3\text{O}_2$ $[\text{M}-\text{H}]^+$: 341.1728, found 341.1728.

(1*R*,2*S*,5*R*)-2-isopropyl-5-methylcyclohexyl 2-(pentafluorophenyl)propanoate **182r**:

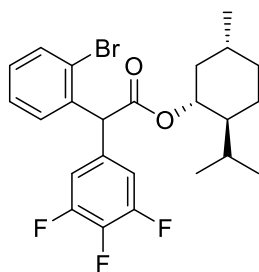


Performed according to *General Procedure 18* on a 0.06 mmol scale of **179h** and 0.06 mmol of **106d**; **182r** (22 mg, 0.058 mmol, 94% yield, 1.2:1 *d.r.*) was obtained as a colourless oil.

¹H NMR (500 MHz, CDCl₃): δ = 4.74 (td, *J* = 10.9, 4.4 Hz, 1.16H, OCH), 4.67 (td, *J* = 10.9, 4.4 Hz, 1H, OCH), 4.16–3.82 (m, 2.12H), 2.09–2.00 (m, 1H), 1.98–1.92 (m, 1.2H), 1.84–1.58 (m, 6.3H), 1.54–

1.44 (m, 10.4H), 1.36–1.21 (m, 2.4H), 1.12–0.73 (m, 23H), 0.70 (d, *J* = 7.0 Hz, 3H, CH₃) ppm; ¹³C NMR (126 MHz, CDCl₃): δ = 170.9 (C=O), 76.1 (OCH₂), 75.9 (OCH₂), 47.0, 47.0, 40.7, 40.4, 35.2, 34.3, 31.5, 31.5, 26.5, 26.2, 23.7, 23.3, 22.1, 20.8, 16.5, 16.3, 16.1, 16.0 ppm (ArC not observed); ¹⁹F NMR (376 MHz, CDCl₃): δ = -142.5 (d, *J* = 19.0 Hz, 2F), -142.8 (d, *J* = 18.6 Hz, 2.3F), -154.6– -157.3 (m, 2.16F), -160.5– -166.5 (m, 4.6F) ppm; IR (neat): ν = 2957w, 2872w, 1740m, 1521m, 1503s, 1456m, 1207m, 968s, 740m cm⁻¹; HRMS (ASAP): Exact mass calculated for C₁₉H₂₃F₅O₂ [M-H]⁺: 377.1540, found 377.1536.

(1*R*,2*S*,5*R*)-2-isopropyl-5-methylcyclohexyl 2-(2-bromophenyl)-2-(3,4,5-trifluorophenyl)acetate **182s**:



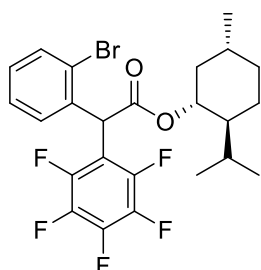
Performed according to *General Procedure 18* on a 0.07 mmol scale of **179i** and 0.07 mmol of **106e**; **182s** (32 mg, 0.067 mmol, 96% yield, 1.3:1 *d.r.*) was obtained as a colourless oil.

¹H NMR (500 MHz, CDCl₃): δ = 7.60 (d, *J* = 8.0 Hz, 2.3H, ArH), 7.35–7.21 (m, 4.6H, ArH), 7.21–7.15 (m, 2.3H, ArH), 6.97–6.86 (m, 4.6H, ArH), 5.38 (s, 1.3H, CH), 5.34 (s, 1H, CH), 4.80–4.66

(m, 2.3H, OCH), 2.06–1.98 (m, 2.3H), 1.71–1.57 (m, 6.9H), 1.53–1.43 (m, 2.3H), 1.39–1.30 (m, 2.3H), 1.10–0.79 (m, 18H), 0.78 (d, *J* = 7.0 Hz, 3H, CH₃), 0.70 (d, *J* = 7.0 Hz, 3.9H, CH₃), 0.65 (d, *J* = 7.0 Hz, 3H, CH₃) ppm; ¹³C NMR (126 MHz, CDCl₃): δ = 170.6 (C=O), 170.5 (C¹=O), 151.3 (d, *J* = 249.8 Hz, 2 × ArC–F), 139.2 (d, *J* = 252.3 Hz, ArC–F), 137.1 (ArC), 137.0 (ArC¹), 134.0–133.7 (m, ArC), 133.5 (ArC¹), 133.4 (ArC), 129.8 (ArC), 129.7 (ArC¹), 129.6 (ArC¹), 129.5 (ArC), 127.9 (ArC), 127.8 (ArC¹), 125.2 (ArC¹), 125.1 (ArC), 113.6–113.0 (m, 2 × ArC), 76.3 (OCH), 76.2 (OCH), 55.8, 55.7, 47.0, 46.9, 40.6, 40.5, 34.2, 31.6, 31.5, 26.2, 25.9, 23.4, 23.3, 22.1, 20.8, 20.7, 16.2, 16.1 ppm; ¹⁹F NMR (376 MHz, CDCl₃): δ = -133.8 (d, *J* = 20.6 Hz, 2.6F), -134.0 (d, *J* = 20.7 Hz, 2F), -161.6 (t, *J* = 20.8 Hz, 1.3F), -161.8 (t, *J* = 20.5 Hz, 1F) ppm; IR (neat): ν = 2955w, 2926w, 2870w, 1732m, 1527s, 1447m, 1348w, 1310w, 1279w, 1171s, 1045s, 739s cm⁻¹;

HRMS (ES): Exact mass calculated for $C_{24}H_{26}Br F_3O_2$ $[M-H]^-$: 481.0990, found 481.1009.

(1*R*,2*S*,5*R*)-2-isopropyl-5-methylcyclohexyl-2-(2-bromophenyl)-2-(pentafluorophenyl) acetate **182t**:

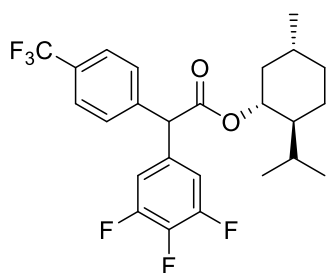


Performed according to *General Procedure 18* on a 0.10 mmol scale of **179i** and 0.10 mmol of **106d**; **182t** (10 mg, 0.019 mmol, 19% yield, 1.15:1 *d.r.*) was obtained as a colourless oil.

1H NMR (500 MHz, $CDCl_3$): δ = 7.63–7.55 (m, 2.25H, ArH), 7.33–7.15 (m, 4.7H, ArH), 5.78–5.51 (m, 2.25H, CH), 4.95–4.59 (m, 2.25H, OCH), 2.22–2.02 (m, 2.25H), 1.84–1.61 (m, 6.7H), 1.51–

1.43 (m, 2.25H), 1.33–1.25 (m, 2.25H), 1.10–0.70 (m, 27H) ppm; ^{13}C NMR (126 MHz, $CDCl_3$): δ = 168.6 (C=O), 168.5 (C=O), 135.0 (ArC), 134.9 (ArC), 133.2 (ArC), 133.2 (ArC), 130.0 (dt, J = 5.1, 2.8 Hz, ArC), 129.7 (ArC), 129.6 (ArC), 127.7 (ArC), 127.6 (ArC), 125.3 (ArC), 125.1 (ArC), 77.0 (CH) 46.9, 46.8, 40.3, 40.3, 34.2, 34.2, 31.5, 31.5, 29.9, 26.2, 26.1, 23.4, 23.2, 22.1, 20.8, 20.7, 16.2, 16.1 (ArC–F not observed) ppm; ^{19}F NMR (376 MHz, $CDCl_3$): δ = –139.1 (d, J = 18.4 Hz, 2F), –139.3 (d, J = 18.1 Hz, 2F), –154.28 (t, J = 21.1 Hz, 2.25F), –161.40– –162.02 (m, 4.5F) ppm; IR (neat): 2957w, 2926w, 2872w, 1734m, 1522m, 1503s, 1215m, 999m, 953m, cm^{-1} ; HRMS (ES): Exact mass calculated for $C_{24}H_{23}BrF_5O_2$ $[M-H]^-$: 517.0802, found 517.0798.

(1*R*,2*S*,5*R*)-2-isopropyl-5-methylcyclohexyl 2-(4-(trifluoromethyl)phenyl)-2-(3,4,5-trifluorophenyl) acetate **182u**:



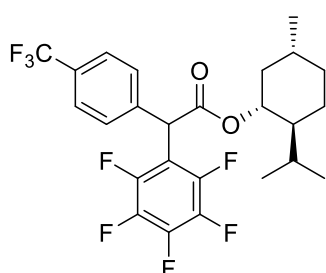
Performed according to *General Procedure 18* on a 0.13 mmol scale of **179j** and 0.13 mmol of **106e**; **182u** (56 mg, 0.12 mmol, 91% yield, 1.2:1 *d.r.*) was obtained as a colourless oil.

1H NMR (400 MHz, $CDCl_3$): δ = 7.73–7.56 (m, 4.4H, ArH), 7.47–7.31 (m, 4.4H, ArH), 6.00–6.88 (m, 4.4H, ArH), 4.95 (s,

1.2H, CH), 4.94 (s, 1H, CH), 4.81–4.68 (m, 2.2H, OCH), 2.06–1.92 (m, 2.2H), 1.74–1.30 (m, 12.5H), 1.12–0.74 (m, 20H), 0.68 (d, J = 7.0 Hz, 3.4H, CH_3), 0.62 (d, J = 6.9 Hz, 3H, CH_3^I) ppm; ^{13}C NMR (126 MHz, $CDCl_3$): δ = 170.4 (C=O), 151.3 (d, J = 250.2 Hz, 2 \times ArC–F), 141.5 (ArC), 141.4 (ArC), 139.3 (dt, J = 252.6, 15.3 Hz, ArC–F), 139.3 (dt, J = 252.6, 15.3 Hz, ArC–F), 134.4–134.1 (m, ArC), 130.4 (q, J = 32.8 Hz, ArC–CF₃), 130.3 (q, J = 32.8 Hz, ArC–CF₃), 130.0 (2 \times ArC), 129.9 (2 \times ArC), 130.9–129.6 (m, 2 \times ArC), 124.0 (q, J = 272.2 Hz, CF₃), 124.1 (q, J = 272.2 Hz, CF₃), 118.6–118.2 (m, ArC), 113.5–112.7 (m, 2 \times ArC), 76.4 (OCH₂), 56.2, 47.1, 47.07, 40.8, 40.7, 34.2, 31.6, 31.6, 26.3,

26.2, 23.4, 23.4, 22.1, 20.7, 20.7, 16.2, 16.1 ppm; ^{19}F NMR (376 MHz, CDCl_3): $\delta = -62.6$ – -62.7 (m, 6.6F), -133.3 (d, $J = 20.6$ Hz, 2.4F), -133.5 (d, $J = 20.5$ Hz, 2F), -161.3 (t, $J = 20.5$ Hz, 1.2F) 161.4 (t, $J = 20.4$ Hz, 1F) ppm; IR (neat): $\nu = 2959\text{w}$, 2930w , 2872w , 1734m , 1620m , 1530s , 1449m , 1325s , 1166s , 1128s , 1068s , 1047s , 1018m , 907s , 729s cm^{-1} ; HRMS (ES): Exact mass calculated for $\text{C}_{25}\text{H}_{25}\text{F}_6\text{O}_2$ $[\text{M}-\text{H}]^-$: 471.1759, found 471.1772.

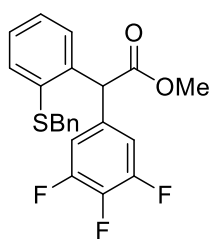
(1*R*,2*S*,5*R*)-2-Isopropyl-5-methylcyclohexyl 2-(pentafluorophenyl)-2-(4-(trifluoromethyl)phenyl)acetate **182v**:



Performed according to *General Procedure 18* on a 0.13 mmol scale of **179j** and 0.13 mmol of **106d**; **182v** (54 mg, 0.11 mmol, 82% yield, 1.1:1 *d.r.*) was obtained as a colourless oil.

^1H NMR (500 MHz, CDCl_3): $\delta = 7.61$ (dd, $J = 8.4$, 2.4 Hz, 4H, *ArH*), 7.64–7.58 (m, 4H, *ArH*), 5.30 (s, 1H, *CH*), 5.29 (s, 1H, *CH*), 4.87–4.73 (m, 2H, *OCH*'), 2.17–2.09 (m, 1H), 2.09–2.03 (m, 1H), 1.74–1.54 (m, 6H), 1.52–1.43 (m, 2H), 1.33–1.25 (m, 2H), 1.11–0.68 (m, 24H) ppm; ^{13}C NMR (126 MHz, CDCl_3): $\delta = 168.4$ ($\text{C}=\text{O}$), 145.0 (d, $J = 248.5$ Hz, $2 \times \text{ArC}-\text{F}$), 140.97 (d, $J = 253.9$ Hz, $\text{ArC}-\text{F}$), 139.7 (*ArC*), 139.6 (*ArC'*), 137.9 (d, $J = 252.4$ Hz, $2 \times \text{ArC}-\text{F}$), 131.1–129.7 (m, *ArC*), 129.4 ($2 \times \text{ArC}$), 129.3 ($2 \times \text{ArC}$), 128.4, 125.9 (q, $J = 3.8$ Hz, $2 \times \text{ArC}$), 124.0 (q, $J = 272.2$ Hz, CF_3), 113.6–112.9 (m, *ArC*), 77.2 (*OCH*), 77.1 (*OCH'*), 46.9, 46.9, 46.2, 46.2, 40.5, 40.4, 34.2, 34.2, 31.5, 26.4, 26.3, 23.5, 23.3, 22.1, 20.8, 20.7, 16.3, 16.0 ppm; ^{19}F NMR (376 MHz, CDCl_3): $\delta = -62.7$ – -62.8 (m, 6F), -140.2 (dd, $J = 18.2$ Hz, 2F), -140.5 (dd, $J = 18.3$ Hz, 2F), -154.1 (t, $J = 20.9$ Hz, 2F), -161.0 – -161.3 (m, 4F) ppm; IR (neat): $\nu = 2958\text{w}$, 2872w , 1734m , 1521m , 1504s , 1325s , 1169m , 1069m , 904s , 727s cm^{-1} ; HRMS (ES): Exact mass calculated for $\text{C}_{25}\text{H}_{23}\text{F}_8\text{O}_2$ $[\text{M}-\text{H}]^-$: 507.1570, found 507.1574.

Methyl 2-(2-(benzylthio)phenyl)-2-(3,4,5-trifluorophenyl)acetate **182w**:

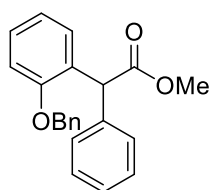


Performed according to *General Procedure 18* on a 0.083 mmol scale of **224** and 0.083 mmol of **106e**; **182w** (12 mg, 0.032 mmol, 38% yield) was obtained as a colourless oil after 72 h.

^1H NMR (500 MHz, CDCl_3): $\delta = 7.48$ – 7.41 (m, 1H, *ArH*), 7.29–7.19 (m, 6H, *ArH*), 7.18–7.11 (m, 2H, *ArH*), 6.76 (dd, $J = 8.4$, 6.6 Hz, 2H, *ArH*), 5.56 (s, 1H, *CH*), 4.02 (d, $J = 12.8$ Hz, 1H, $1 \times \text{SCH}_2$), 3.99 (d, $J = 12.9$ Hz, 1H, $1 \times \text{SCH}_2$), 3.72 (s, 3H, OCH_3) ppm; ^{13}C NMR (126 MHz, CDCl_3): $\delta = 172.0$ ($\text{C}=\text{O}$), 151.0

(ddd, $J = 250, 10.0, 4.1$ Hz, $2 \times \text{ArC-F}$), 138.9 (dt, $J = 252, 15.3$ Hz, ArC-F), 138.8 (ArC), 134.3 (ArC), 132.9 (ArC), 128.8 (ArC), 128.5 (ArC), 128.5 (ArC), 128.4 (ArC), 127.7 (ArC), 127.4 (ArC), 113.7–112.2 (m, $2 \times \text{ArC}$), 52.7 (OCH₃), 40.5 (SCH₂) ppm; ¹⁹F NMR with ¹H coupling (471 MHz, CDCl₃, 298 K) $\delta = -134.1$ (dd, $J = 20.7, 8.6$ Hz, 2F), -162.1 (tt, $J = 20.6, 6.4$ Hz, 1F) ppm; IR (neat): $\nu = 3030\text{w}, 2953\text{w}, 1736\text{s}, 1618\text{m}, 1528\text{s}, 1448\text{m}, 1435\text{m}, 1348\text{m}, 1163\text{m}, 1045\text{s}, 698\text{s}$ cm⁻¹; HRMS (ES): Exact mass calculated for C₂₁H₂₃F₃O₂S [M-H]⁻: 401.0823, found 401.0826.

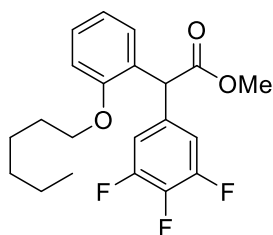
Methyl 2-(2-(benzyloxy)phenyl)-2-phenylacetate **182x**:



Performed according to *General Procedure 18* on a 0.1 mmol scale of **184a** and 0.1 mmol of **106a**; **182x** (16 mg, 0.048 mmol, 48% yield) was obtained as a colourless oil after 7 days.

¹H NMR (500 MHz, CDCl₃): $\delta = 7.28\text{--}7.17$ (m, 9 H, ArH), 7.17–7.08 (m, 2H, ArH), 7.36–7.08 (m, 1H, ArH), 6.90 (d, $J = 7.0$, 1H, ArH, ArH), 6.87–6.75 (m, 2H, ArH), 5.24 (s, 1H, CH), 4.98 (s, 2H, OCH₂), 3.50 (s, 3H, OCH₃) ppm; ¹³C NMR (126 MHz, CDCl₃): $\delta = 173.5$ (C=O), 156.1 (ArC–O), 137.6 (ArC), 137.0 (ArC), 129.3 (ArC), 128.7 (ArC), 128.6 (ArC), 128.6 (ArC), 128.2 (ArC), 128.0 (ArC), 127.4 (ArC), 127.4 (ArC), 120.9 (ArC), 111.7 (ArC), 70.2 (OCH₂), 52.2, 51.3 ppm; HRMS (ES): Exact mass calculated for C₂₂H₂₁O₃ [M+H]⁺: 333.1487, found 333.1487.

Methyl 2-(2-(hexyloxy)phenyl)-2-(3,4,5-trifluorophenyl)acetate **182y**:

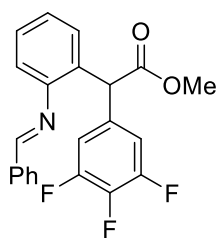


Performed according to *General Procedure 18* on a 0.1 mmol scale of **184k** and 0.1 mmol of **106e**; **182y** (22 mg, 0.059 mmol, 59% yield) was obtained as a colourless oil after 24 h.

¹H NMR (500 MHz, CDCl₃): $\delta = 7.30\text{--}7.24$ (m, 1H, ArH), 7.10 (d, $J = 7.5$ Hz, 1H, ArH), 6.97–6.90 (m, 3H, ArH), 6.87 (d, $J = 8.2$ Hz, 1H, ArH), 5.22 (s, 1H, CH), 4.01–3.89 (m, 2H, OCH₂), 3.73 (s, 3H, OCH₃), 1.78–1.68 (m, 2H), 1.39 (dd, $J = 14.2, 6.5$ Hz, 2H), 1.37–1.29 (m, 4H), 0.90 (t, $J = 6.3$ Hz, 3H, CH₃) ppm; ¹³C NMR (126 MHz, CDCl₃): $\delta = 172.5$ (C=O), 156.2 (ArC–O), 151.1 (ddd, $J = 249.0, 10.0, 4.1$ Hz, $2 \times \text{ArC-F}$), 139.1 (d, $J = 251.0$ Hz, ArC-F), 134.6–134.4 (m, ArC), 129.2 (ArC), 128.7 (ArC), 126.3 (ArC), 120.7 (ArC), 113.6–113.2 (m, ArC), 111.6 (m, ArC), 68.2 (OCH₂), 52.6, 50.3, 31.7, 29.3, 25.9, 22.7, 14.1 ppm; ¹⁹F NMR (376 MHz, CDCl₃): $\delta = -134.6$ (d, $J = 20.7$ Hz, 2F), -162.5 (t, $J = 20.5$ Hz, 1F) ppm; IR (neat): $\nu = 2955\text{m}, 2932\text{m}, 2860\text{m}, 1742\text{s}, 1618\text{m}, 1599\text{m}, 1528\text{s}, 1493\text{s}, 1449\text{s}, 1348\text{m}, 1244\text{s}, 1043\text{s}$.

750s, 675s cm^{-1} ; HRMS (EI): Exact mass calculated for $\text{C}_{21}\text{H}_{23}\text{F}_3\text{O}_3$ $[\text{M}]^+$: 380.1599, found 380.1591.

Methyl (*E*)-2-(2-(benzylideneamino)phenyl)-2-(3,4,5-trifluorophenyl)acetate **216**:

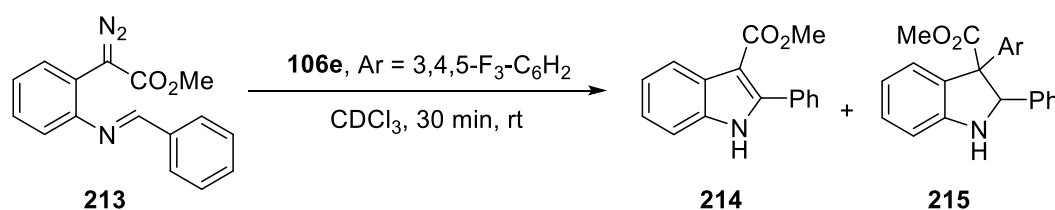


Performed according to *General Procedure 18* on a 0.1 mmol scale of **153a** and 0.1 mmol of **106e**; **216** (20 mg, 0.053 mmol, 53% yield) was obtained as a colourless oil after 12 hours at 50 °C.

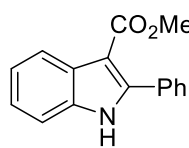
^1H NMR (500 MHz, CDCl_3): δ = 8.39 (s, 1H, N=CH), 7.89 (d, J = 7.3 Hz, 1H, ArH), 7.55–7.38 (m, 2H, ArH), 7.39–7.33 (m, 3H, ArH), 7.32–7.20 (m, 1H, ArH), 7.09 (d, J = 7.8 Hz, 2H, ArH), 6.99 (t, J = 7.4 Hz, 1H, ArH), 5.52 (s, 1H, CH), 3.67 (s, 3H, OCH_3) ppm; ^{13}C NMR (126 MHz, CDCl_3): δ = 172.5 (C=O), 160.5 (ArC–N), 151.1 (ddd, J = 250, 10.0, 4.0 Hz, 2 \times ArC–F), 140.2 (ArC), 139.2 (dt, J = 251.2, 15.3 Hz, ArC–F), 136.1, 135.2–134.3 (m, ArC), 132.6 (ArC), 131.9 (ArC), 129.1 (ArC), 129.1 (ArC), 129.0 (ArC), 128.5 (ArC), 126.7 (ArC), 118.0 (ArC), 114.1–112.9 (m, 2 \times ArC), 52.6, 51.6 ppm; ^{19}F NMR with ^1H coupling (471 MHz, CDCl_3): δ = –133.0––138.4 (m, 2F), –162.5 (ddd, J = 20.6, 13.5, 6.4 Hz, 1F) ppm; IR (neat): ν = 3017m, 1738s, 1612m, 1529s, 1472s, 1447s, 1364m, 1229s, 1043s cm^{-1} ; HRMS (ES): Exact mass calculated for $\text{C}_{22}\text{H}_{17}\text{NO}_2\text{F}_3$ $[\text{M}+\text{H}]^+$: 384.1211, found 384.1211.

5.3.3 Synthesis of Cyclised Products

5.3.3.1 Synthesis on Indole **214** and Indoline **215**

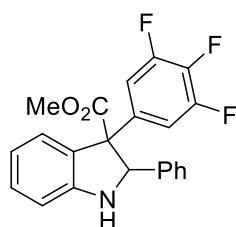


The diazo compound **213** (0.1 mmol) was dissolved in dry CDCl_3 and borane **106e** (0.1 mmol) was added. The reaction was performed under nitrogen and gas evolution was observed. After 30 minutes the reaction was quenched with aqueous solution of NaOH (0.1 M) and the crude was filtered over SiO_4 plug then purified by preparative TLC affording indole **214** and indoline **215** in 23% and 42% yields, respectively.

Methyl 2-phenyl-1*H*-indole-3-carboxylate **214**:

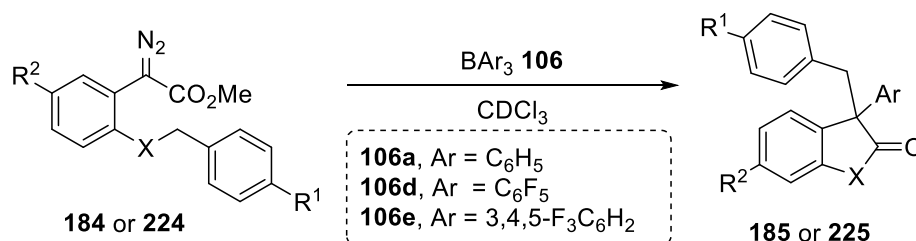
The minor product **214** (6 mg, 0.023 mmol, 23% yield) was afforded as a colourless solid.

^1H NMR (500 MHz, CDCl_3): δ = 8.49 (s, 1H, NH), 8.22 (d, J = 6.6 Hz, 1H, ArH), 7.67 (d, J = 6.5 Hz, 2H, ArH), 7.47 (d, J = 5.6 Hz, 3H, ArH), 7.40 (d, J = 6.5 Hz, 1H, ArH), 7.29 (d, J = 5.4 Hz, 2H, ArH), 3.85 (s, 3H, OCH_3) ppm; ^{13}C NMR (126 MHz, CDCl_3): δ = 165.9 (C=O), 144.7 (ArC–N), 135.2 (ArC), 132.1 (ArC), 129.7 (ArC), 129.4 (ArC), 128.4 (ArC), 127.7 (ArC), 123.4 (ArC), 122.4 (ArC), 122.3 (ArC), 111.1 (ArC), 104.7 (ArC), 51.0 (OCH_3) ppm. The spectroscopic data are in agreement with the literature.²⁵

Methyl 2-phenyl-3-(3,4,5-trifluorophenyl)indoline-3-carboxylate **215**:

The major product **215** (16 mg, 0.042 mmol, 42% yield) was afforded as a colourless oil.

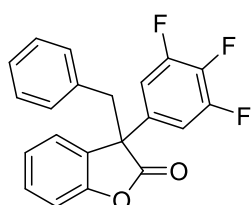
^1H NMR (500 MHz, CDCl_3): δ = 7.28 (d, J = 7.5 Hz, 1H, ArH), 7.22–7.12 (m, 6H, ArH), 7.12–7.06 (m, 2H, ArH), 6.81 (t, J = 7.3 Hz, 1H, ArH), 6.69 (d, J = 7.8 Hz, 1H, ArH), 4.99 (s, 1H, CH), 4.11 (s, 1H, NH), 3.18 (s, 3H, OCH_3) ppm; ^{13}C NMR (126 MHz, CDCl_3): δ = 170.6 (C=O), 151.0 (ddd, J = 249.2, 9.8, 4.1 Hz, $2 \times \text{ArC-F}$), 150.4 (ArC–N), 140.4 (ArC), 139.7–139.5 (m, (ArC), 139.1 (dt, J = 230.6, 15.5 Hz, Ar–F), 129.7 (ArC), 128.7 (ArC), 128.5 (ArC), 127.8 (ArC), 127.7 (ArC), 127.3 (ArC), 119.9 (ArC), 111.7–111.3 (m, $2 \times \text{ArC}$), 74.4 (N–CH), 66.6 (C– CO_2Me), 52.1 (OCH_3) ppm; ^{19}F NMR (376 MHz, CDCl_3): δ = –133.8 (d, J = 20.8 Hz, 2F), –161.8 (t, J = 20.8 Hz, 1F) ppm; IR (neat): ν = 3364w, 3032w, 2951w, 1732s, 1525s, 1431s, 1259s, 1238s, 1045s, 1028s, 736s cm^{-1} ; HRMS (ES): Exact mass calculated for $\text{C}_{22}\text{H}_{17}\text{NO}_2\text{F}_3$ $[\text{M}+\text{H}]^+$: 384.1211, found 384.1209.

5.3.3.2 Synthesis of Lactones **185** and Thiolactone **225**

General Procedure 19: The diazo compound **184a–j** or **224** (0.1 mmol) was dissolved in dry CDCl_3 and borane **106** (0.1 mmol) was added. The reaction was performed under

nitrogen and gas evolution was observed. The reaction was then quenched with aqueous solution of NaOH (0.1 M), the crude was filtered over SiO₄ plug and purified by column chromatography to afford the final lactone **185** or thiolactone **225** as solids or oils.

3-Benzyl-3-(3,4,5-trifluorophenyl)benzofuran-2(3*H*)-one **185a**:



Performed according to *General Procedure 19* on a 0.1 mmol scale of **184a** and 0.1 mmol of **106e**; **185a** (26 mg, 0.079 mmol, 79% yield) was obtained after 24 hours at room temperature as a colourless solid, m.p.: 110–112 °C.

¹H NMR (400 MHz, CDCl₃): δ = 7.34–7.27 (m, 1H, ArH), 7.26–7.03 (m, 7H, ArH), 6.96 (d, *J* = 7.9 Hz, 1H, ArH), 6.84–6.79 (m, 2H, ArH), 3.59 (d, *J* = 13.2 Hz, 1H, 1 × CH₂), 3.42 (d, *J* = 13.2 Hz, 1H, 1 × CH₂) ppm; ¹³C NMR (101 MHz, CDCl₃): δ = 176.5 (C=O), 153.1 (ArC–O), 151.3 (ddd, *J* = 251.0, 9.9, 4.1 Hz, 2 × ArC–F), 139.58 (dt, *J* = 254, 15.3 Hz, ArC–F), 134.8–134.6 (m, ArC), 133.9 (ArC), 130.1 (ArC), 130.0 (ArC), 128.3 (ArC), 127.6 (ArC), 127.5 (ArC), 126.0 (ArC), 124.5 (ArC), 112.4–111.7 (m, 2 × ArC), 111.3 (ArC), 56.6 (C), 45.5 (CH₂) ppm; ¹⁹F NMR (376 MHz, CDCl₃): δ = –132.5 (d, *J* = 20.6 Hz), –160.2 (t, *J* = 20.6 Hz) ppm; IR (neat): ν = 1790s, 1620m, 1531s, 1462s, 1435s, 1354m, 1292w, 1225m, 1120s, 1051s, 887m, 752s, 698s cm⁻¹; HRMS (ASAP): Exact mass calculated for C₂₁H₁₄F₃O₂ [M+H]⁺: 355.0946, found 355.0948; NCH₂¹D: Varian Polaris Silica (254 × 4.6 mm, 5μm), *n*-hexane/propan-2-ol: 99.9:0.1, 1.0 mL•min⁻¹, 20 °C, 210 and 254 nm, retention time **200a** = 4.1 min; ²D: YMC Chiral Amylose-C (254 × 4.6 mm, 5μm), *n*-hexane/propan-2-ol: 90:10, 1.0 mL•min⁻¹, 20 °C, 254 nm, retention time minor isomer = 4.8 min, retention time major isomer = 5.3 min.

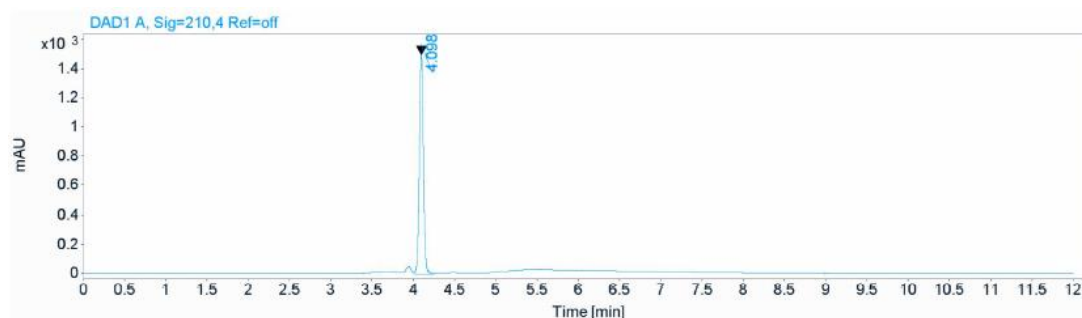
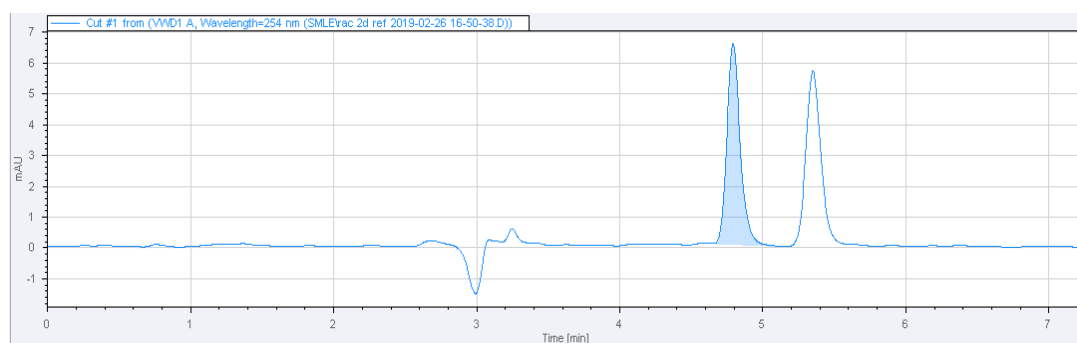
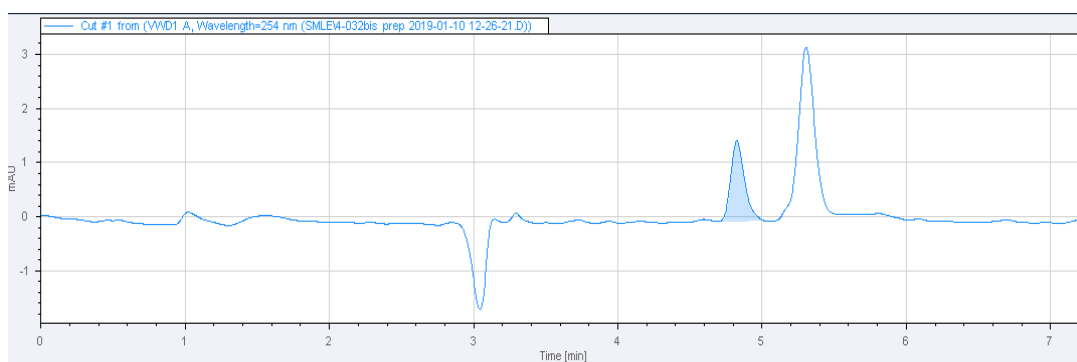


Figure 5.15: ¹D HPLC chromatograms for the enantiomers of **185a**.



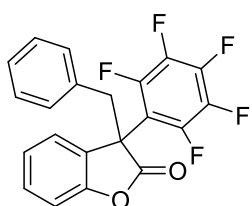
Peak#	Time	Area
1	4.797	49.745
2	5.355	50.255



Peak#	Time	Area
1	4.830	27.748
2	5.311	72.252

Figure 5.16: ²D HPLC chromatograms for the enantiomers of **185a**. From the top: racemic mixture and 44% ee mixture.

3-Benzyl-3-(pentafluorophenyl)benzofuran-2(3*H*)-one **185b**:

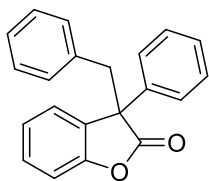


Performed according to *General Procedure 19* on a 0.1 mmol scale of **184a** and 0.1 mmol of **106d**; **185b** (30 mg, 0.077 mmol, 77% yield) was obtained after 7 days at room temperature as a colourless solid, m.p.: 148–150 °C.

¹H NMR (400 MHz, CDCl₃): δ = 7.33–7.25 (m, 2H, ArH), 7.23–7.13 (m, 2H, ArH), 7.07 (t, *J* = 7.5 Hz, 2H, ArH), 6.84 (d, *J* = 7.9 Hz, 1H, ArH), 6.73 (d, *J* = 7.4 Hz, 2H, ArH), 3.97 (dt, *J* = 12.8, 2.4 Hz, 1H, 1 × CH₂), 3.73 (d, *J* = 12.5 Hz, 1H, 1 × CH₂) ppm; ¹³C NMR (126 MHz, CDCl₃): δ = 175.2 (C=O), 153.1 (ArC–O), 146.0 (d, *J* = 250.0 Hz, 2 × ArC–F), 141.1 (d, *J* = 257.0 Hz, ArC–F), 138.2 (d, *J* = 254.1 Hz, 2 × ArC–F), 132.7 (ArC), 130.5 (ArC), 130.2 (ArC), 128.8 (ArC), 128.2 (ArC), 127.8 (ArC), 124.9 (ArC), 123.8 (ArC), 114.0–113.3 (m, 2 × ArC), 111.1 (ArC), 54.5 (C), 42.1 (t, *J* = 7.2 Hz, CH₂) ppm; ¹⁹F NMR (376 MHz, CDCl₃): δ = –36.2 (d, *J* = 18.8 Hz, 2F), –152.8 (t, *J* = 20.9 Hz, 1F), –160.4 (t, *J* = 20.8 Hz, 2F) ppm; IR (neat): ν = 1807s, 1653w, 1524s, 1485s, 1464s, 1116.8s, 1061s,

1011s, 966s, 885m, 754s, 704s, 577m cm^{-1} ; HRMS (EI): Exact mass calculated for $\text{C}_{21}\text{H}_{11}\text{F}_5\text{O}_2$ $[\text{M}]^+$: 390.0679, found: 390.0676.

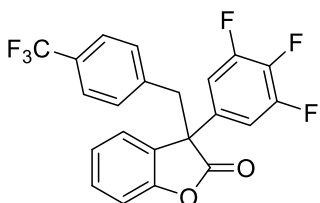
3-Benzyl-3-phenylbenzofuran-2(3*H*)-one **185c**:



Performed according to *General Procedure 19* on a 0.1 mmol scale of **184a** and 0.1 mmol of **106a**; **185c** (6.3 mg, 0.021 mmol, 21% yield) was obtained after 14 days at room temperature as a colourless solid, m.p.: 118–120 °C.

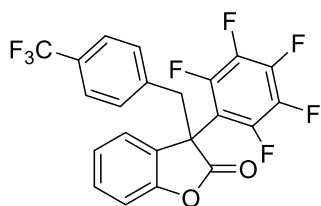
^1H NMR (400 MHz, CDCl_3): δ = 7.55–7.51 (m, 2H, ArH), 7.41–7.36 (m, 2H, ArH), 7.36–7.32 (m, 1H, ArH), 7.29–7.26 (m, 1H, ArH), 7.25–7.16 (m, 3H, ArH), 7.14–7.04 (m, 3H, ArH), 6.94 (ddd, J = 7.9, 1.1, 0.6 Hz, 1H, ArH), 6.87 (dd, J = 8.0, 1.5 Hz, 2H, ArH), 3.74 (d, J = 13.1 Hz, 1H, 1 \times CH_2), 3.53 (d, J = 13.1 Hz, 1H, 1 \times CH_2) ppm; ^{13}C NMR (126 MHz, CDCl_3): δ = 177.7 (C=O), 153.2 (ArC–O), 138.6 (ArC), 134.9 (ArC), 130.2 (ArC), 129.3 (ArC), 129.0 (ArC), 128.2 (ArC), 128.1 (ArC), 127.3 (ArC), 127.2 (ArC), 126.1 (ArC), 124.0 (ArC), 111.0 (ArC), 57.6 (C), 45.1 (CH_2) ppm; IR (neat): ν = 3030w, 2928w, 2851w, 1788s, 1618w, 1495m, 1460, 1292w, 1231m, 1063s, 951m, 881m cm^{-1} ; HRMS (EI): Exact mass calculated for $\text{C}_{21}\text{H}_{16}\text{O}_2$ $[\text{M}]^+$: 300.1150, found 300.1151.

3-(4-(Trifluoromethyl)benzyl)-3-(3,4,5-trifluorophenyl)benzofuran-2(3*H*)-one **185d**:



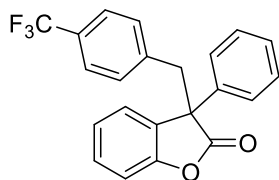
Performed according to *General Procedure 19* on a 0.1 mmol scale of **184b** and 0.1 mmol of **106e**; **185d** (24 mg, 0.054 mmol, 54% yield) was obtained after 24 hours at 50 °C as a colourless solid, m.p.: 118–120 °C.

^1H NMR (400 MHz, CDCl_3): δ = 7.39–7.32 (m, 3H, ArH), 7.32–7.14 (m, 4H, ArH), 7.00 (d, J = 8.0 Hz, 1H, ArH), 6.96 (d, J = 8.1 Hz, 2H, ArH), 3.68 (d, J = 13.2 Hz, 1H, 1 \times CH_2), 3.47 (d, J = 13.2 Hz, 1H, 1 \times CH_2) ppm; ^{13}C NMR (126 MHz, CDCl_3): δ = 176.2 (C=O), 153.1 (ArC–O), 151.4 (ddd, J = 251.1, 9.9, 4.2 Hz, 2 \times ArC–F), 139.7 (dt, J = 254.0, 15.2 Hz, ArC–F), 138.1–137.9 (m, ArC), 134.4–134.2 (m, ArC), 130.4 (2 \times ArC), 129.9 (q, J = 32.6 Hz, ArC– CF_3), 127.2 (ArC), 125.7 (ArC), 125.29 (q, J = 3.7 Hz, 2 \times ArC), 124.7 (ArC), 123.9 (q, J = 272.3 Hz, CF_3), 112.1–111.8 (2 \times ArC), 111.7 (ArC), 56.4 (C), 45.1 (CH_2) ppm; ^{19}F NMR (376 MHz, CDCl_3): δ = –62.7 (s, 3F), –132.1 (d, J = 20.4 Hz, 2F), –159.7 (t, J = 20.4 Hz, 1F) ppm; IR (neat): ν = 2922w, 1792s, 1620m, 1531s, 1466m, 1331s, 1109s, 1068s, 1045s, 1016s, 872m, 839m, 752s, 625s cm^{-1} ; HRMS (ASAP): Exact mass calculated for $\text{C}_{22}\text{H}_{13}\text{O}_2\text{F}_6$ $[\text{M}+\text{H}]^+$: 423.0820, found 423.0828.

3-(4-(Trifluoromethyl)benzyl)-3-(pentafluorophenyl)benzofuran-2(3*H*)-one **185e**:

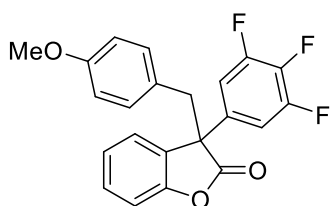
Performed according to *General Procedure 19* on a 0.1 mmol scale of **84b** and 0.1 mmol of **106d**; **185e** (33 mg, 0.072 mmol, 72% yield) was obtained after 24 hours at 50 °C as a colourless solid, m.p.: 128–130 °C.

^1H NMR (400 MHz, CDCl_3): δ = 7.37–7.29 (m, 4H, ArH), 7.25–7.19 (m, 1H, ArH), 6.89–6.83 (m, 3H, ArH), 4.02 (dt, J = 12.8, 2.2 Hz, 1H, 1 \times CH_2), 3.77 (d, J = 12.8, 1H, 1 \times CH_2) ppm; ^{13}C NMR (126 MHz, CDCl_3): δ = 174.9 (C=O), 153.0 (ArC–O), 146.0 (d, J = 250.0 Hz, 2 \times ArC–F), 141.3 (d, J = 257.1 Hz, ArC–F), 138.3 (d, J = 254.3 Hz, 2 \times ArC–F) 136.9 (ArC), 130.9 (ArC), 130.6 (ArC), 130.1 (q, J = 32.5 Hz, ArC– CF_3), 128.2 (ArC), 125.1 (ArC), 125.1 (q, J = 3.8 Hz, 2 \times ArC), 124.4 (q, J = 272.2 Hz, CF_3), 113.3 (m, ArC), 111.4 (ArC), 54.2 (C), 41.8 (t, J = 7.3 Hz, CH_2) ppm; ^{19}F NMR (376 MHz, CDCl_3): δ = –62.7 (s, 3F), –136.4 (d, J = 18.9 Hz, 2F), –152.4 (t, J = 21.1 Hz, 1F), –160.07 (t, J = 21.4 Hz, 2F) ppm; IR (neat): ν = 2924w, 2853w, 1803s, 1738m, 1531m, 1485s, 1331s, 1221m, 1119s, 970s, 885, 856m, 748s, 675m cm^{-1} ; HRMS (ASAP): Exact mass calculated for $\text{C}_{22}\text{H}_{10}\text{O}_2\text{F}_8$ [$\text{M}+\text{H}$] $^+$: 459.0631, found 459.0629.

3-(4-(Trifluoromethyl)benzyl)-3-Benzylbenzofuran-2(3*H*)-one **185f**:

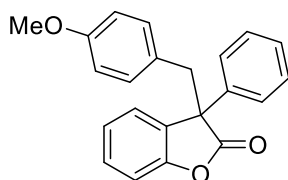
Performed according to *General Procedure 19* on a 0.1 mmol scale of **184b** and 0.1 mmol of **106a**; **185f** (9.6 mg, 0.026 mmol, 26% yield) was obtained after 24 hours at 50 °C as a colourless solid, m.p.: 112–114 °C.

^1H NMR (400 MHz, CDCl_3): δ = 7.55–7.49 (m, 2H, ArH), 7.44–7.27 (m, 6H, ArH), 7.25–7.19 (m, 2H, ArH), 7.01–6.93 (m, 3H, ArH), 3.79 (d, J = 13.2 Hz, 1H, 1 \times CH_2), 3.58 (d, J = 13.1 Hz, 1H, 1 \times CH_2) ppm; ^{13}C NMR (101 MHz, CDCl_3): δ = 177.3 (C=O), 153.1 (ArC–O), 138.1 (ArC), 130.6 (ArC), 129.7 (ArC), 129.1 (ArC), 128.7 (ArC), 128.4 (ArC), 127.1 (ArC), 125.9 (ArC), 125.1 (q, J = 3.5 Hz, ArC), 124.3 (ArC), 111.3 (ArC), 57.3 (C), 44.7 (CH_2) ppm; IR (neat): ν = 3059w, 2918w, 2848w, 1798s, 1618w, 1599m, 1462m, 1323s, 1122s, 1111s, 1064s, 879m, 844m, 754s cm^{-1} ; HRMS (ASAP): Exact mass calculated for $\text{C}_{22}\text{H}_{15}\text{O}_2\text{F}_3$ [M] $^+$: 369.1102, found 369.1102.

3-(4-Methoxybenzyl)-3-(3,4,5-trifluorophenyl)benzofuran-2(3H)-one **185g**:

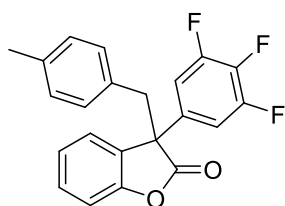
Performed according to *General Procedure 19* on a 0.1 mmol scale of **184c** and 0.1 mmol of **106e**; **185g** (35 mg, 0.091 mmol, 91% yield) was obtained after 16 hours at room temperature as a colourless solid, m.p.: 98–102 °C.

^1H NMR (400 MHz, CDCl_3): δ = 7.31 (dd, J = 7.7, 1.4 Hz, 1H, ArH), 7.28–7.14 (m, 4H, ArH), 6.98 (d, J = 8.0 Hz, 1H, ArH), 6.75–6.70 (m, 2H, ArH), 6.64–6.59 (m, 2H, ArH), 3.70 (s, 3H, OCH_3), 3.53 (d, J = 13.3 Hz, 1H, 1 \times CH_2), 3.37 (d, J = 13.3 Hz, 1H, 1 \times CH_2) ppm; ^{13}C NMR (101 MHz, CDCl_3): δ = 176.6 (C=O), 159.0 (ArC–O), 153.2 (ArC–O), 151.3 (ddd, J = 251.0, 9.9, 4.1 Hz, 2 \times ArC–F), 139.5 (dt, J = 254.2, 15.3 Hz, ArC–F), 135.1–134.5 (m, ArC), 131.2 (ArC), 130.0 (ArC), 127.6 (ArC), 126.0 (ArC), 125.9 (ArC), 124.4 (ArC), 113.7 (ArC), 112.2–111.8 (m, 2 \times ArC), 111.4 (ArC), 56.7 (C), 55.2 (OCH_3), 44.9 (CH_2) ppm; ^{19}F NMR (376 MHz, CDCl_3): δ = –132.6 (d, J = 20.3 Hz, 2F), –160.3 (t, J = 20.3 Hz, 1F) ppm; IR (neat): ν = 3076w, 2951w, 2835w, 1792s, 1616m, 1528s, 1462w, 1431m, 1248s, 1178m, 1119m, 1036s, 752s cm^{-1} ; HRMS (EI): Exact mass calculated for $\text{C}_{22}\text{H}_{15}\text{O}_3\text{F}_3$ [M] $^+$: 384.0973, found 384.0971.

3-(4-(Trifluoromethyl)benzyl)-3-benzylbenzofuran-2(3H)-one **185i**:

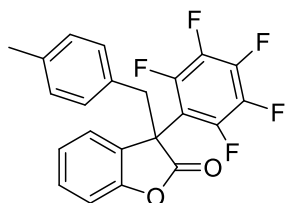
Performed according to *General Procedure 19* on a 0.1 mmol scale of **184c** and 0.1 mmol of **106a**; **185i** (18 mg, 0.054 mmol, 54% yield) was obtained after 72 hours at room temperature as a colourless solid, m.p.: 112–114 °C.

^1H NMR (500 MHz, CDCl_3): δ = 7.52 (d, J = 7.4 Hz, 2H, ArH), 7.35–7.27 (m, 2H, ArH), 7.25–7.17 (m, 2H, ArH), 6.96 (d, J = 8.0 Hz, 1H, ArH), 6.77 (d, J = 8.5 Hz, 2H, ArH), 6.61 (d, J = 8.6 Hz, 2H, ArH), 3.71 (s, 3H, OCH_3), 3.67 (d, J = 13.3 Hz, 1H, 1 \times CH_2), 3.48 (d, J = 13.4 Hz, 1H, 1 \times CH_2) ppm; ^{13}C NMR (126 MHz, CDCl_3): δ = 177.7 (C=O), 158.7 (ArC–O), 153.2 (ArC–O), 138.6 (ArC), 131.2 (ArC), 129.4 (ArC), 129.2 (ArC), 129.0 (ArC), 128.1 (ArC), 127.2 (ArC), 126.9 (ArC), 126.0 (ArC), 124.0 (ArC), 113.5 (ArC), 111.0 (ArC), 57.7 (C), 55.2 (OCH_3), 44.3 (CH_2) ppm; IR (neat): ν = 3019w, 2928w, 2841w, 1794s, 1610m, 1512m, 1460m, 1246s, 1068s, 1026s, 760s, 694s cm^{-1} ; HRMS (ES): Exact mass calculated for $\text{C}_{22}\text{H}_{17}\text{O}_3$ [$\text{M}-\text{H}$] $^-$: 329.1178, found 329.1188.

3-(4-Methylbenzyl)-3-(3,4,5-trifluorophenyl)benzofuran-2(3H)-one **185j**:

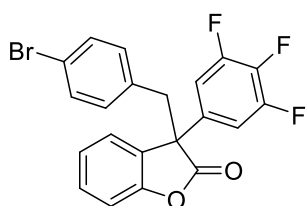
Performed according to *General Procedure 19* on a 0.1 mmol scale of **184d** and 0.1 mmol of **106e**; **185j** (32 mg, 0.087 mmol, 87% yield) was obtained after 24 hours at room temperature as a colourless solid, m.p.: 94–96 °C.

^1H NMR (400 MHz, CDCl_3): δ = 7.33 (dt, J = 7.9, 1.6 Hz, 1H, ArH), 7.26–7.17 (m, 4H, ArH), 6.99 (d, J = 8.0 Hz, 1H, ArH), 6.90 (d, J = 7.9 Hz, 2H, ArH), 6.71 (d, J = 8.0 Hz, 2H, ArH), 3.55 (d, J = 13.2 Hz, 1H, 1 \times CH_2), 3.40 (d, J = 13.2 Hz, 1H, 1 \times CH_2), 2.23 (s, 3H, CH_3) ppm; ^{13}C NMR (101 MHz, CDCl_3): δ = 176.6 (C=O), 153.2 (ArC–O), 151.3 (ddd, J = 251.1, 9.9, 4.2 Hz, 2 \times ArC–F), 139.5 (dt, J = 253.4, 15.3 Hz, ArC–F), 137.3 (ArC), 135.1–134.4 (m, ArC), 130.8 (ArC), 130.0 (ArC), 129.9 (ArC), 129.0 (ArC), 127.6 (ArC), 126.0 (ArC), 124.4 (ArC), 112.5–111.9 (m, 2 \times ArC), 111.4 (ArC), 56.6 (C), 45.2 (CH_2), 21.1 (CH_3) ppm; ^{19}F NMR (376 MHz, CDCl_3): δ = –132.6 (d, J = 19.9 Hz, 2F), –160.3 (t, J = 20.2 Hz, 1F) ppm; IR (neat): ν = 3075w, 3036w, 1794s, 1705s, 1618s, 1528s, 1464s, 1337m, 1234s, 885s, 829m, 814m, 752s, 586s, 475s cm^{-1} ; HRMS (EI): Exact mass calculated for $\text{C}_{22}\text{H}_{15}\text{F}_3\text{O}_2$ $[\text{M}]^+$: 368.1024, found 368.1027.

3-(4-Methylbenzyl)-3-(pentafluorophenyl)benzofuran-2(3H)-one **185k**:

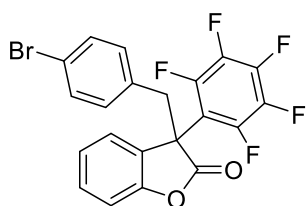
Performed according to *General Procedure 19* on a 0.1 mmol scale of **184d** and 0.1 mmol of **106d**; **185k** (25 mg, 0.063 mmol, 63% yield) was obtained after 24 hours at 50 °C as a colourless solid, m.p.: 124–126 °C.

^1H NMR (500 MHz, CDCl_3): δ = 7.32–7.25 (m, 2H, ArH), 7.23–7.16 (m, 1H, ArH), 6.89–6.83 (m, 3H, ArH), 6.60 (d, J = 8.0 Hz, 2H, ArH), 3.92 (d, J = 12.9 Hz, 1H, 1 \times CH_2), 3.68 (d, J = 12.9 Hz, 1H, 1 \times CH_2), 2.23 (s, 3H, CH_3) ppm; ^{13}C NMR (126 MHz, CDCl_3): δ = 175.3 (C=O), 153.1 (ArC–O), 146.0 (d, J = 243.3 Hz, 2 \times ArC–F), 141.1 (d, J = 257.1 Hz, ArC–F), 138.1 (d, J = 247.0 Hz, 2 \times ArC–F), 137.5 (ArC), 130.4 (ArC), 130.2 (ArC), 129.6 (ArC), 129.0 (ArC), 129.9 (ArC), 124.8 (ArC), 123.8 (ArC), 113.9–113.6 (m, ArC), 111.1 (ArC), 54.6 (C), 41.8 (t, J = 7.2 Hz, CH_2), 21.2 (CH_3) ppm; ^{19}F NMR (376 MHz, CDCl_3): δ = –136.1 (d, J = 19.4 Hz, 2F), –153.0 (t, J = 21.1 Hz, 1F), –160.4 (t, J = 21.4 Hz, 2F) ppm; IR (neat) ν = 2924w, 1803s, 1526s, 1487s, 1119s, 968s, 883s, 739s, 615m, 573s, cm^{-1} ; HRMS (ASAP): Exact mass calculated for $\text{C}_{22}\text{H}_{14}\text{O}_2\text{F}_5$ $[\text{M}+\text{H}]^+$: 405.0914, found 405.0911.

3-(4-Bromobenzyl)-3-(3,4,5-trifluorophenyl)benzofuran-2(3H)-one **185l**:

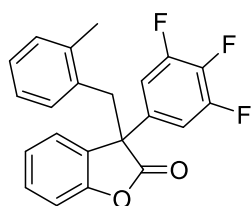
Performed according to *General Procedure 19* on a 0.1 mmol scale of **184e** and 0.1 mmol of **106e**; **185l** (32 mg, 0.074 mmol, 74% yield) was obtained after 24 hours at room temperature as a colourless oil.

^1H NMR (400 MHz, CDCl_3): δ = 7.35 (ddd, J = 8.1, 7.5, 1.6 Hz, 1H, ArH), 7.30–7.14 (m, 6H, ArH), 7.01 (d, J = 8.0 Hz, 1H, ArH), 6.74–6.61 (m, 2H, ArH), 3.57 (d, J = 13.2 Hz, 1H, 1 \times CH_2), 3.37 (d, J = 13.2 Hz, 1H, 1 \times CH_2) ppm; ^{13}C NMR (126 MHz, CDCl_3): δ = 176.3 (C=O), 153.1 (ArC–O), 151.4 (ddd, J = 251.0, 9.9, 4.1 Hz, 2 \times ArC–F), 139.6 (dt, J = 254.1, 15.3 Hz, ArC–F), 135.4–133.7 (m, ArC), 132.9 (ArC), 131.8 (ArC), 131.5 (ArC), 130.3 (ArC), 127.1 (ArC), 125.8 (ArC), 124.6 (ArC), 121.9 (ArC), 112.2–111.7 (m, 2 \times ArC), 111.7 (ArC) 56.4 (C), 44.8 (CH_2) ppm; ^{19}F NMR (376 MHz, CDCl_3): δ = –132.2 (d, J = 20.7 Hz, 2F), –159.9 (t, J = 20.7 Hz, 1F) ppm; IR (neat): ν = 3080w, 2924w, 1798s, 1529s, 1232m, 1047s, 1011s, 754s cm^{-1} ; HRMS (ES): Exact mass calculated for $\text{C}_{21}\text{H}_{11}\text{F}_3\text{O}_2\text{Br}$ $[\text{M}-\text{H}]^-$: 430.9895, found 430.9903.

3-(4-Bromobenzyl)-3-(pentafluorophenyl)benzofuran-2(3H)-one **185l**:

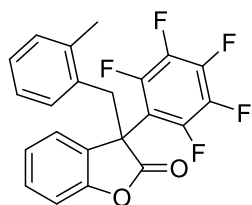
Performed according to *General Procedure 19* on a 0.1 mmol scale of **184e** and 0.1 mmol of **106d**; **185l** (34 mg, 0.073 mmol, 73% yield) was obtained after 24 hours at 50 °C as a colourless solid, m.p.: 116–118 °C.

^1H NMR (500 MHz, CDCl_3): δ = 7.33–7.27 (m, 2H, ArH), 7.23–7.17 (m, 3H, ArH), 6.89 (d, J = 8.1 Hz, 1H, ArH), 6.60 (d, J = 8.4 Hz, 2H, ArH), 3.93 (dt, J = 10.8, 2.1 Hz, 1H, 1 \times CH_2), 3.67 (d, J = 12.9 Hz, 1H, 1 \times CH_2) ppm; ^{13}C NMR (101 MHz, CDCl_3): δ = 175.0 (C=O), 153.0 (ArC–O), 146.0 (d, J = 250.1 Hz, 2 \times ArC–F), 141.23 (d, J = 262.4 Hz, ArC–F), 138.2 (d, J = 253.0 Hz, 2 \times ArC–F), 132.2 (ArC), 131.7 (ArC), 131.4 (ArC), 130.5 (ArC), 128.4 (ArC), 125.0 (ArC), 123.7 (ArC), 122.2 (ArC), 113.8–113.1 (m, ArC), 111.4 (ArC), 54.2 (C), 41.5 (m, CH_2) ppm; ^{19}F NMR (376 MHz, CDCl_3): δ = –136.3 (d, J = 18.6 Hz, 2F), –152.5 (t, J = 21.0 Hz, 1F), –160.2 (t, J = 21.2 Hz, 2F) ppm; IR (neat): ν = 2930w, 1798s, 1524s, 1487s, 1121m, 968s, 750s, 671m cm^{-1} ; HRMS (EI): Exact mass calculated for $\text{C}_{21}\text{H}_{10}\text{F}_5\text{O}_2\text{Br}$ $[\text{M}]^+$: 467.9784, found 467.9767.

3-(2-Methylbenzyl)-3-(3,4,5-trifluorophenyl)benzofuran-2(3H)-one **185n**:

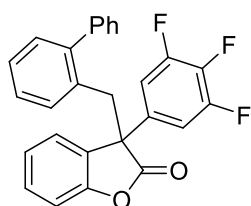
Performed according to *General Procedure 19* on a 0.1 mmol scale of **184f** and 0.1 mmol of **106e**; **185n** (29 mg, 0.078 mmol, 78% yield) was obtained after 24 hours at room temperature as a colourless solid, m.p.: 82–84 °C.

^1H NMR (500 MHz, CDCl_3): δ = 7.34 (td, J = 8.0, 1.3 Hz, 1H, ArH), 7.24–7.17 (m, 2H, ArH), 7.14 (td, J = 7.6, 0.9 Hz, 1H, ArH), 7.09–6.98 (m, 3H, ArH), 6.92–6.82 (m, 2H, ArH), 6.53 (d, J = 7.5 Hz, 1H, ArH), 3.57 (d, J = 13.9 Hz, 1H, 1 \times CH_2), 3.49 (d, J = 13.9 Hz, 1H, 1 \times CH_2), 1.96 (s, 3H, CH_3) ppm; ^{13}C NMR (126 MHz, CDCl_3): δ = 176.8 (C=O), 153.1 (ArC–O), 151.2 (ddd, J = 251.2, 9.9, 4.1 Hz, 2 \times ArC–F), 139.5 (dt, J = 254.0, 15.3 Hz, ArC–F), 137.5 (ArC), 134.5 (m, ArC), 134.6 (ArC), 134.5 (ArC), 134.5 (ArC), 134.5 (ArC), 134.5 (ArC), 134.4 (ArC), 132.5 (ArC), 130.8 (ArC), 130.1 (ArC), 129.7 (ArC), 127.8 (ArC), 127.2 (ArC), 126.4 (ArC), 125.8 (ArC), 124.3 (ArC), 113.3–111.8 (m, 2 \times ArC), 111.4 (ArC), 55.5 (C), 41.6 (CH_2), 20.0 (CH_3) ppm; ^{19}F NMR (376 MHz, CDCl_3): δ = –132.6 (d, J = 20.6 Hz, 2F), –160.2 (t, J = 20.6 Hz, 1F) ppm; IR (neat): ν = 3086w, 2924w, 2854w, 1794s, 1620m, 1526m, 1458m, 1435m, 1346m, 1232m, 760s cm^{-1} ; HRMS (ASAP): Exact mass calculated for $\text{C}_{22}\text{H}_{16}\text{O}_2\text{F}_3$ $[\text{M}+\text{H}]^+$: 369.1102, found 369.1103.

3-(2-Methylbenzyl)-3-(pentafluorophenyl)benzofuran-2(3H)-one **185o**:

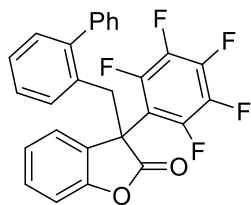
Performed according to *General Procedure 19* on a 0.1 mmol scale of **184f** and 0.1 mmol of **106d**; **185o** (24 mg, 0.059 mmol, 59% yield) was obtained after 24 hours at 50 °C as a colourless oil.

^1H NMR (500 MHz, CDCl_3): δ = 7.36–7.28 (m, 2H, ArH), 7.20 (t, J = 7.5 Hz, 1H, ArH), 7.10–7.00 (m, 2H, ArH), 6.91 (d, J = 8.0 Hz, 1H, ArH), 6.83 (t, J = 7.2 Hz, 1H, ArH), 6.43 (d, J = 7.7 Hz, 1H, ArH), 3.97 (d, J = 13.5 Hz, 1H, 1 \times CH_2), 3.89 (d, J = 13.4 Hz, 1H, 1 \times CH_2), 2.18 (s, 3H, CH_3) ppm; ^{13}C NMR (126 MHz, CDCl_3): δ = 175.4 (C=O), 153.2 (ArC–O), 146.0 (d, J = 246.0 Hz, 2 \times ArC–F), 141.1 (d, J = 257.2 Hz, ArC–F), 138.3 (d, J = 253.0 Hz, 2 \times ArC–F), 137.8 (ArC), 131.4 (ArC), 130.9 (ArC), 130.4 (ArC), 130.3 (ArC), 129.1 (ArC), 127.9 (ArC), 125.5 (ArC), 124.8 (ArC), 124.2 (ArC), 114.4–114.0 (m, ArC), 111.2 (ArC), 54.3 (C), 37.9 (t, J = 7.1 Hz, CH_2), 20.0 (CH_3) ppm; ^{19}F NMR (376 MHz, CDCl_3): δ = –135.8 (d, J = 18.6 Hz, 2F), –153.0 (t, J = 21.0 Hz, 1F), –160.37 (t, J = 20.9 Hz, 2F) ppm; IR (neat): ν = 3024w, 1807s, 1524s, 1487s, 1464s, 1121s, 968s, 883m, 677m, 478m cm^{-1} ; HRMS (ASAP): Exact mass calculated for $\text{C}_{22}\text{H}_{14}\text{O}_2\text{F}_5$ $[\text{M}+\text{H}]^+$: 405.0914, found 405.0909.

3-(2-Phenylbenzyl)-3-(3,4,5-trifluorophenyl)benzofuran-2(3H)-one **185p**:

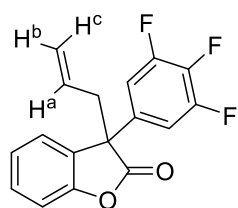
Performed according to *General Procedure 19* on a 0.1 mmol scale of **184g** and 0.1 mmol of **106e**; **185p** (39 mg, 0.09 mmol, 91%) was obtained after 24 hours at room temperature as a colourless oil.

$^1\text{H NMR}$ (400 MHz, CDCl_3): δ = 7.35–7.27 (m, 4H, ArH), 7.22 (td, J = 7.5, 1.4 Hz, 1H, ArH), 7.15 (td, J = 7.6, 1.6 Hz, 1H, ArH), 7.10–6.95 (m, 6H, ArH), 6.95–6.88 (m, 2H, ArH), 6.42 (dd, J = 7.6, 1.3 Hz, 1H, ArH), 3.84 (d, J = 13.9 Hz, 1H, $1 \times \text{CH}_2$), 3.61 (d, J = 13.9 Hz, 1H, $1 \times \text{CH}_2$) ppm; $^{13}\text{C NMR}$ (101 MHz, CDCl_3): δ = 176.8 (C=O), 153.0 (ArC–O), 151.1 (ddd, J = 250.1, 9.9, 4.1 Hz, $2 \times \text{ArC–F}$), 143.3 (ArC), 140.9 (ArC), 139.5 (d, J = 253.2 Hz, ArC–F), 134.8–134.5 (m, ArC), 131.9 (ArC), 130.9 (ArC), 129.8 (ArC), 129.7 (ArC), 128.2 (ArC), 127.6 (ArC), 127.4 (ArC), 127.2 (ArC), 126.8 (ArC), 126.7 (ArC), 124.3 (ArC), 112.2–111.8 (m, $2 \times \text{ArC}$), 111.0 (ArC), 55.9 (C), 41.1 (CH_2) ppm; $^{19}\text{F NMR}$ (376 MHz, CDCl_3): δ = –132.7 (d, J = 20.7 Hz, 2F), –160.5 (t, J = 20.7 Hz, 1F) ppm; IR (neat): ν = 3059w, 2926w, 1800s, 1618m, 1528s, 1462m, 1435, 1232m, 1121m, 1045s, 750s, 704s cm^{-1} ; HRMS (ASAP): Exact mass calculated for $\text{C}_{27}\text{H}_{18}\text{F}_3\text{O}_2$ $[\text{M}+\text{H}]^+$: 431.1259, found 431.1257.

3-(2-Phenylbenzyl)-3-(pentafluorophenyl)benzofuran-2(3H)-one **185q**:

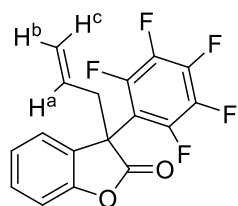
Performed according to *General Procedure 19* on a 0.1 mmol scale of **184g** and 0.1 mmol of **106d**; **185q** (24 mg, 0.052 mmol, 52% yield) was obtained after 24 hours at 50 °C as a colourless oil.

$^1\text{H NMR}$ (500 MHz, CDCl_3 , 298 K) δ = 7.41–7.28 (m, 3H, ArH), 7.21 (t, J = 7.7 Hz, 2H, ArH), 7.12 (t, J = 7.4 Hz, 1H, ArH), 7.07–6.97 (m, 4H, ArH), 6.90 (t, J = 7.6 Hz, 1H, ArH), 6.86 (d, J = 8.1 Hz, 1H, ArH), 6.57 (d, J = 7.5 Hz, 1H, ArH), 4.50 (d, J = 13.4 Hz, 1H, $1 \times \text{CH}_2$), 3.85 (d, J = 13.4 Hz, 1H, $1 \times \text{CH}_2$) ppm; $^{13}\text{C NMR}$ (126 MHz, CDCl_3): δ = 175.4 (C=O), 152.8 (ArC–O), 145.8 (d, J = 250.1 Hz, $2 \times \text{ArC–F}$), 143.6 (ArC), 140.1 (ArC), 140.9 (d, J = 256.4 Hz, ArC–F), 138.1 (d, J = 254.3 Hz, $2 \times \text{ArC–F}$), 131.0 (ArC), 131.0 (ArC), 130.3 (ArC), 130.0 (ArC), 129.7 (ArC), 128.4 (ArC), 128.2 (ArC), 127.8 (ArC), 127.2 (ArC), 127.0 (ArC), 125.0 (ArC), 124.2 (ArC), 114.7–113.9 (m, ArC), 110.7 (ArC), 54.3 (C), 36.9 (t, J = 7.4 Hz, CH_2) ppm; $^{19}\text{F NMR}$ (376 MHz, CDCl_3): δ = –136.0 (d, J = 19.6 Hz, 2F), –153.3 (t, J = 21.1 Hz, 1F), –160.5 (t, J = 21.0, 2F) ppm; IR (neat): ν = 3061w, 2924w, 2853w, 1809s, 1526s, 1487s, 1121s, 1063s, 968s, 746s, 702s cm^{-1} ; HRMS (EI): Exact mass calculated for $\text{C}_{27}\text{H}_{16}\text{O}_2\text{F}_5$ $[\text{M}+\text{H}]^+$: 467.1070, found 467.1069.

3-Allyl-3-(3,4,5-trifluorophenyl)benzofuran-2(3*H*)-one **185r**:

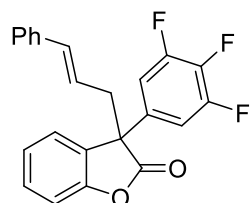
Performed according to *General Procedure 19* on a 0.1 mmol scale of **184h** and 0.1 mmol of **106e**; **185r** (17 mg, 0.057 mmol, 57% yield) was obtained after 24 hours at room temperature as a pale-yellow oil.

^1H NMR (500 MHz, CDCl_3): δ = 7.42 (t, J = 7.6 Hz, 1H, ArH), 7.34–7.28 (m, 1H, ArH), 7.26 (d, J = 9.0 Hz, 1H, ArH), 7.20 (d, J = 8.1 Hz, 1H, ArH), 7.08 (dd, J = 8.1, 6.7 Hz, 2H, ArH), 5.47–5.27 (m, 1H), 5.14–5.00 (m, 2H), 3.04–2.90 (m, 2H) ppm; ^{13}C NMR (126 MHz, CDCl_3): δ = 176.4 (C=O), 153.2 (ArC–O), 151.4 (ddd, J = 251.0, 9.9, 4.1 Hz, 2 \times ArC–F), 139.5 (dt, J = 253.1, 15.2 Hz, ArC–F), 134.4 (td, J = 7.1, 4.5 Hz), 130.4, 130.1, 128.0, 125.5, 124.8, 121.5, 112.0–111.6 (m, 2 \times ArC), 111.6 (ArC), 54.8 (C), 43.5 (CH_2) ppm; ^{19}F NMR (376 MHz, CDCl_3): δ = –132.6 (d, J = 20.1 Hz, 2F), –160.3 (t, J = 20.4 Hz, 1F) ppm; IR (neat): ν = 3068w, 2954w, 1802s, 1529s, 1229s, 754s cm^{-1} ; HRMS (ES): Exact mass calculated for $\text{C}_{17}\text{H}_{10}\text{F}_3\text{O}_2$ $[\text{M}-\text{H}]^-$: 303.0633, found 303.0644.

3-Allyl-3-(pentafluorophenyl)benzofuran-2(3*H*)-one **185s**:

Performed according to *General Procedure 19* on a 0.1 mmol scale of **184h** and 0.1 mmol of **106d**; **185s** (20 mg, 0.060 mmol, 60% yield) was obtained after 24 hours at 50 °C as a pale-yellow oil.

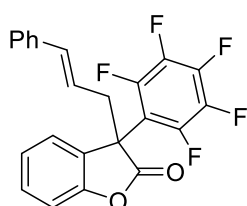
^1H NMR (500 MHz, CDCl_3): δ = 7.39–7.31 (m, 1H, ArH), 7.19–7.12 (m, 3H, ArH), 5.51–5.39 (m, 1H, ArH), 5.14–5.07 (m, 2H), 3.28 (dd, J = 13.2, 6.2 Hz, 1H, 1 \times CH_2), 3.20 (dd, J = 13.2, 8.0 Hz, 1H, 1 \times CH_2) ppm; ^{13}C NMR (126 MHz, CDCl_3): δ = 175.2 (C=O), 152.9 (ArC–O), 145.9 (d, J = 250.2 Hz, 2 \times ArC–F), 141.1 (d, J = 256.1 Hz, ArC–F), 138.2 (d, J = 254.0 Hz, 2 \times ArC–F), 130.1 (ArC), 129.6 (ArC), 129.1 (ArC), 125.1 (ArC), 123.5 (ArC), 122.2 (ArC), 114.2–112.6 (m, ArC), 111.2 (ArC), 52.6 (C), 40.8 (t, J = 6.5 Hz, CH_2) ppm; ^{19}F NMR (376 MHz, CDCl_3): δ = –136.7 (d, J = 19.7 Hz, 2F), –152.9 (t, J = 20.9 Hz, 1F), –160.4 (t, J = 20.8 Hz, 2F) ppm; IR (neat): ν = 2922w, 1807s, 1524s, 1487s, 1463s, 1291m, 1053s, 968s, 883s, 752s cm^{-1} ; HRMS (EI): Exact mass calculated for $\text{C}_{17}\text{H}_9\text{O}_2\text{F}_5$ $[\text{M}]^+$: 340.0523, found 340.0522.

3-Cinnamyl-3-(3,4,5-trifluorophenyl)benzofuran-2(3*H*)-one **185t**:

Performed according to *General Procedure 19* on a 0.1 mmol scale of **184i** and 0.1 mmol of **106e**; **185t** (20 mg, 0.053 mmol, 53% yield) was obtained after 24 hours at room temperature as a colourless oil.

^1H NMR (500 MHz, CDCl_3): δ = 7.42 (t, J = 7.7 Hz, 1H, ArH), 7.33 (d, J = 7.4 Hz, 1H, ArH), 7.31–7.10 (m, 9H, ArH), 6.40 (d, J = 15.7 Hz, 1H, CH), 5.80–5.65 (m, 1H, CH), 3.21–3.06 (m, 2H, CH_2) ppm; ^{13}C NMR (126 MHz, CDCl_3): δ = 176.4 (C=O), 153.2 (ArC–O), 151.4 (ddd, J = 251.0, 9.9, 4.1 Hz, 2 \times ArC–F), 139.6 (dd, J = 254.1, 17.1 Hz, ArC–F), 136.5, 136.2, 134.7–134.0, 130.2, 128.7, 128.0, 128.0, 126.4, 125.6, 124.9, 121.4, 112.0–111.8 (m, 2 \times ArC), 111.6 (ArC), 55.1 (C), 42.9 (CH_2) ppm; ^{19}F NMR (376 MHz, CDCl_3): δ = –132.5 (d, J = 20.8 Hz, 2F), –160.2 (t, J = 20.7 Hz) ppm; IR (neat): ν = 3030w, 1801s, 1618m, 1464s, 1232s, 1047s, 885m, 692s cm^{-1} ; HRMS (ES): Exact mass calculated for $\text{C}_{23}\text{H}_{14}\text{F}_3\text{O}_2$ $[\text{M}-\text{H}]^-$: 379.0946, found 379.0953.

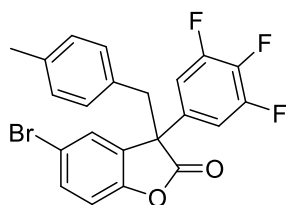
3-Cinnamyl-3-(pentafluorophenyl)benzofuran-2(3H)-one **185u**:



Performed according to *General Procedure 19* on a 0.1 mmol scale of **184i** and 0.1 mmol of **106d**; **185u** (14 mg, 0.033 mmol, 33% yield) was obtained after 24 hours at 50 °C as a colourless solid, m.p.: 114–120 °C.

^1H NMR (500 MHz, CDCl_3): δ = 7.35 (t, J = 7.3 Hz, 1H, ArH), 7.25–7.11 (m, 8H, ArH), 6.39 (d, J = 15.7 Hz, 1H, Ph–CH), 5.80 (dt, J = 15.2, 7.4 Hz, 1H, CH_2 –CH), 3.47–3.30 (m, 2H, CH_2) ppm; ^{13}C NMR (126 MHz, CDCl_3): δ = 175.3 (C=O), 152.9 (ArC–O), 145.9 (d, J = 248.0 Hz, 2 \times ArC–F), 141.0 (d, J = 261.3 Hz, ArC–F), 138.14 (d, J = 249.1 Hz, 2 \times ArC–F), 136.8, 136.6, 130.2, 129.2, 128.6, 128.0, 126.5, 125.1, 123.8, 120.6, 113.1 (ArC), 111.3 (ArC), 52.8 (C), 40.11 (t, J = 6.5 Hz, CH_2) ppm; ^{19}F NMR (376 MHz, CDCl_3): δ = –136.6 (d, J = 19.2 Hz, 2F), –152.8 (t, J = 19.7 Hz, 1F), –160.3 (t, J = 20.7 Hz, 2F) ppm; IR (neat): ν = 2922m, 2852w, 1811s, 1526s, 1491s, 1122m, 1057m, 970m, 752m cm^{-1} ; HRMS (ES): Exact mass calculated for $\text{C}_{23}\text{H}_{13}\text{O}_2\text{F}_5$ $[\text{M}-\text{H}]^-$: 415.0757, found 415.0764.

5-Bromo-3-(4-methylbenzyl)-3-(3,4,5-trifluorophenyl)benzofuran-2(3H)-one **185v**:

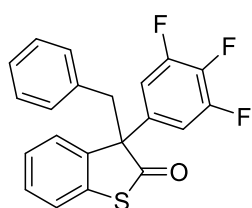


Performed according to *General Procedure 19* on a 0.1 mmol scale of **184j** and 0.1 mmol of **106e**; **185v** (37 mg, 0.082 mmol, 82% yield) was obtained after 24 hours at room temperature as a colourless oil.

^1H NMR (400 MHz, CDCl_3): δ = 7.45 (dd, J = 8.6, 2.1 Hz, 1H, ArH), 7.30 (d, J = 2.1 Hz, 1H, ArH), 7.22–7.11 (m, 2H, ArH), 6.94 (d, J = 7.9 Hz, 2H, ArH), 6.88 (d, J = 8.6 Hz, 1H, ArH), 6.71 (d, J = 8.0 Hz, 2H, ArH), 3.56 (d, J = 13.2 Hz, 1H, 1 \times CH_2), 3.38 (d, J = 13.2 Hz, 1H, 1 \times CH_2), 2.24 (s, 3H, CH_3) ppm; ^{13}C NMR (126 MHz, CDCl_3): δ = 175.8 (C=O),

152.5 (ArC–O), 151.4 (ddd, $J = 251.2, 9.9, 4.1$ Hz, $2 \times$ ArC–F), 139.7 (dt, $J = 254.1, 15.2$ Hz, ArC–F), 137.6, 134.1 (td, $J = 7.0, 4.6$ Hz, ArC), 133.0 (ArC), 130.2 (ArC), 130.1 (ArC), 130.0 (ArC), 129.9 (ArC), 129.2 (ArC), 128.9 (ArC), 117.0 (ArC), 113.0 (ArC), 112.4–111.4 (m, $2 \times$ ArC), 56.9 (C), 45.0 (CH₂), 21.1 (CH₃) ppm; ¹⁹F NMR (376 MHz, CDCl₃): $\delta = -132.0$ (d, $J = 20.7$ Hz, 2F), -159.6 (t, $J = 20.7$ Hz, 1F) ppm; IR (neat): $\nu = 2918w, 1809s, 1618m, 1526m, 1462m, 1433m, 1132m, 1053s, 814s$ cm⁻¹; HRMS (ES): Exact mass calculated for C₂₂H₁₃O₂F₃Br [M–H]⁻: 415.0757, found 415.0764.

3-Benzyl-3-(3,4,5-trifluorophenyl)benzo[b]thiophen-2(3H)-one **225**:

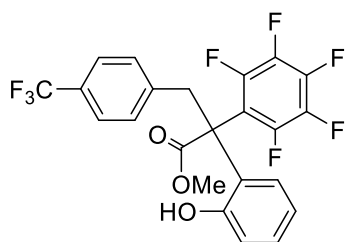


Performed according to *General Procedure 19* on a 0.083 mmol scale of **224** and 0.083 mmol of **106e**; **225** (17 mg, 0.046 mmol, 55% yield) was obtained after 72 hours at room temperature as a colorless solid, m.p.: 88–92 °C.

¹H NMR (500 MHz, CDCl₃): $\delta = 7.36$ – 7.29 (m, 2H, ArH), 7.25–7.20 (m, 1H, ArH), 7.20–7.15 (m, 1H, ArH), 7.14–7.09 (m, 1H, ArH), 7.10–7.03 (m, 2H, ArH), 7.03–6.95 (m, 2H, ArH), 6.83–6.78 (m, 2H, ArH), 3.83 (d, $J = 12.9$ Hz, 1H, $1 \times$ CH₂), 3.36 (d, $J = 12.9$ Hz, 1H, $1 \times$ CH₂) ppm; ¹³C NMR (126 MHz, CDCl₃): $\delta = 206.2$ (C=O), 152.3 (ArC–O), 151.3 (ddd, $J = 250.1, 9.8, 4.1$ Hz, $2 \times$ ArC–F), 139.3 (dt, $J = 254.0, 15.4$ Hz, ArC–F), 138.5 (ArC), 136.7 (td, $J = 6.9, 4.6$ Hz, ArC), 138.4 (ArC), 138.4 (ArC), 136.7 (ArC), 136.7 (ArC), 136.0 (ArC), 133.9 (ArC), 130.3 (ArC), 129.4 (ArC), 128.1 (ArC), 127.3 (ArC), 126.9 (ArC), 126.7 (ArC), 123.4 (ArC), 112.3–111.9 (m, $2 \times$ ArC), 67.7 (C), 44.8 (CH₂) ppm; ¹⁹F NMR (376 MHz, CDCl₃): $\delta = -132.9$ (d, $J = 20.8$ Hz, 2F), -160.5 (t, $J = 20.8$ Hz, 1F) ppm; IR (neat): $\nu = 3032w, 2926w, 1703s, 1618w, 1529s, 1435m, 1344w, 1244w, 1051s$ cm⁻¹; HRMS (ES): Exact mass calculated for C₂₂H₁₅O₃F₃ [M–H]⁻: 369.0561, found 369.0565.

5.3.4 Characterisation of Phenol Side Product **230**

Methyl 2-(2-hydroxyphenyl)-2-(perfluorophenyl)-3-phenylpropanoate **230b**:

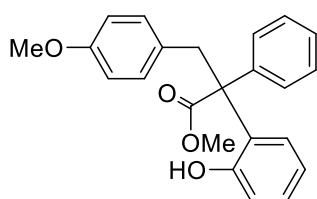


Compound **230b** was obtained as a side product after reaction of **184b** (1 equiv.) and **106d** (1 equiv.) at room temperature as a colorless oil (12 mg, 0.54 mmol, 52% yield).

¹H NMR (500 MHz, CDCl₃): $\delta = 7.49$ (dd, $J = 8.1, 1.3$ Hz, 1H, ArH), 7.33 (d, $J = 8.1$ Hz, 2H, ArH), 7.28–7.22 (m, 1H, ArH), 7.03–6.99 (m, 1H, ArH),

6.99–6.95 (m, 3H, *ArH* + *OH*), 6.90 (dd, $J = 8.1, 1.3$ Hz, 1H, *ArH*), 4.30 (d, $J = 13.4$ Hz, 1H, $1 \times \text{CH}_2$), 3.80 (s, 3H, OCH_3), 3.35 (d, $J = 13.4$ Hz, 1H, $1 \times \text{CH}_2$) ppm; ^{13}C NMR (126 MHz, CDCl_3): $\delta = 172.7$ (C=O), 155.0 (*ArC*–O), 145.2 (d, $J = 255.0$ Hz, $2 \times \text{ArC}$ –F), 140.4 (d, $J = 265.1$ Hz, *ArC*–F), 139.6 (*ArC*), 137.5 (d, $J = 246.0$ Hz, $2 \times \text{ArC}$ –F), 130.8 (*ArC*), 130.1 (*ArC*), 129.7 (q, $J = 32.6$ Hz, *ArC*– CF_3), 126.4 (*ArC*), 125.4 (*ArC*), 124.8 (q, $J = 3.7$ Hz, $2 \times \text{ArC}$), 121.6 (*ArC*), 120.0 (*ArC*), 113.7 (*ArC*), 54.8 (C), 54.1 (OCH_3), 40.8 (CH_2) ppm; ^{19}F not ^1H -decoupled (471 MHz, CDCl_3): $\delta = -62.7$ (s, 3F), -134.9 (d, $J = 15.4$ Hz, 2F), -153.7 (t, $J = 21.3$ Hz, 1F), -161.9 (td, $J = 22.0, 6.6$ Hz, 2F) ppm; IR (neat): $\nu = 3333\text{w}, 1703\text{m}, 1489\text{s}, 1122\text{s}, 995\text{s}, 739\text{s}$ cm^{-1} ; HRMS (ES): Exact mass calculated for $\text{C}_{23}\text{H}_{14}\text{O}_3\text{F}_8$ [$\text{M}+\text{H}$] $^+$: 490.0815, found 490.0811.

Methyl 2-(2-hydroxyphenyl)-2-(perfluorophenyl)-3-phenylpropanoate **230c**:



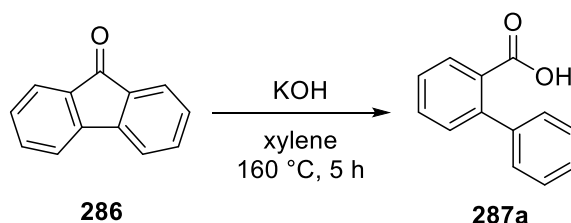
Compound **230c** was obtained as a side product after reaction of **184c** (1 equiv.) and **106a** (1 equiv.) as a colourless oil which was not stable during analysis and decomposing into **185i**.

^1H NMR (500 MHz, CDCl_3): $\delta = 7.53$ (t, $J = 7.7$ Hz, 2H, *ArH*), 7.41–7.14 (m, 7H, *ArH*), 7.01 (t, $J = 7.6$ Hz, 1H, *ArH*), 6.96 (d, $J = 7.7$ Hz, 2H, *ArH*), 6.86 (dd, $J = 8.0, 1.0$ Hz, 1H, *ArH*), 6.77 (d, $J = 8.6$ Hz, 1H, *ArH*), 6.54 (d, $J = 8.7$ Hz, 1H, *ArH*), 6.51 (d, $J = 8.7$ Hz, 2H, *ArH*), 6.51 (d, $J = 8.7$ Hz, 2H, *ArH*), 6.27 (s, 1H, *OH*), 4.08 (d, $J = 12.9$ Hz, 1H, $1 \times \text{CH}_2$), 3.80 (s, 3H, OCH_3), 3.73 (s, 3H, OCH_3), 3.20 (d, $J = 12.9$ Hz, 1H, $1 \times \text{CH}_2$) ppm; IR (neat): $\nu = 3404\text{m}, 2951\text{m}, 2835\text{m}, 1800\text{m}, 1732\text{s}, 1705\text{s}, 1610\text{s}, 1512\text{s}, 1462, 1454, 1246, 1034\text{m}, 1034, 754$ cm^{-1} ; HRMS (ES): Exact mass calculated for $\text{C}_{23}\text{H}_{21}\text{O}_4$ [$\text{M}-\text{H}$] $^-$: 361.1440, found 361.1444.

5.4 Experimental Data for Chapter 4: Synthesis of *N,O*-acetals in a Flow Microreactor

5.4.1 Synthesis of Starting Materials

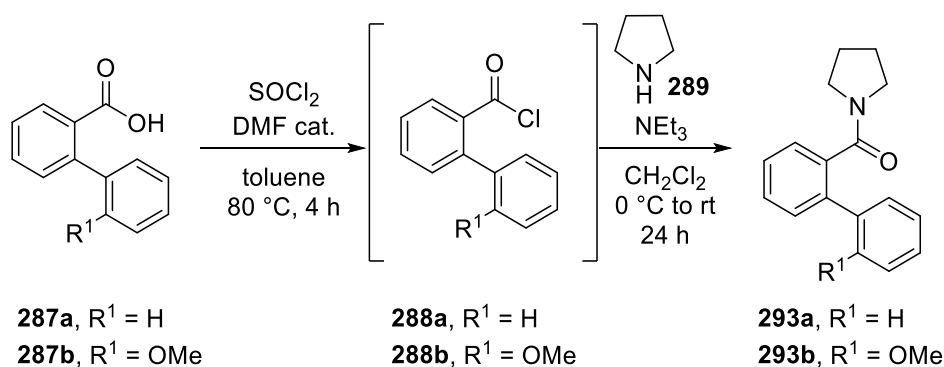
[1,1'-Biphenyl]-2-carboxylic acid **287a**:



Grounded KOH (6 g, 110 mmol) was dispersed into 50 mL of xylene and the temperature was raised to 85 °C. A solution of 9-fluorenone **286** (10 g, 55 mmol) in 50 mL of xylene was added dropwise over 30 minutes and the reaction was stirred for a further 5 hours at 160 °C. Water was added, and the phases separated. The organic phase was further washed with 1 M KOH aqueous solution (50 mL). The combined aqueous layers were acidified with 1 M HCl aqueous solution until pH = 2. The desired product **287a** (8 g, 40 mmol, 72% yield) was afforded as a colourless solid after filtration and used for the next step without further purification; m.p.: 114–116 °C (Lit. 114.3 °C).³⁴

¹H NMR (500 MHz, CDCl₃): δ = 8.11–7.79 (m, 1H, *ArH*), 7.57 (td, *J* = 7.6, 1.4 Hz, 1H, *ArH*), 7.47–7.29 m, 7H, *ArH*) ppm; ¹³C NMR (126 MHz, CDCl₃): δ = 173.5 (*C=O*), 143.5 (*ArC*), 141.1 (*ArC*), 132.2 (*ArC*), 131.3 (*ArC*), 130.8 (*ArC*), 129.4 (*ArC*), 128.6 (2 × *ArC*), 128.2 (2 × *ArC*), 127.5 (*ArC*), 127.3 (*ArC*) ppm. The spectroscopic data are in agreement with the literature.³⁴

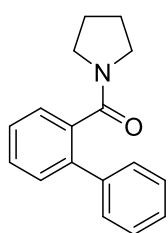
General Procedure 20:



The desired biphenylic acid **287** (2 mmol) was dissolved in 5 mL of dry toluene. Thionyl chloride (4 mmol) and 1 drop of DMF were added. The mixture was stirred for 6 hours at

60 °C under N₂. Subsequently, the solvent and excess of thionyl chloride were removed under reduced pressure. The desired acyl chloride **288** was dissolved dry CH₂Cl₂ (1 mL) and added dropwise to an ice-cold solution of pyrrolidine **289** (2.2 mmol) and triethylamine (2.6 mmol) in dry CH₂Cl₂ (1 mL). The reaction was stirred at room temperature overnight then was diluted with CH₂Cl₂ and washed with 1 M HCl aqueous solution. The collected organic layers were washed with brine, dried over MgSO₄ and concentrated under reduced pressure to afford the desired amides **293a–b** which were used for the Shono oxidation³⁵ without further purification.

[1,1'-Biphenyl]-2-yl(pyrrolidin-1-yl)methanone **293a**:

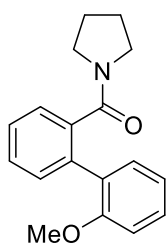


Performed according to *General Procedure 20* on a 5.8 mmol scale of **288a**; **293a** (1.0 g, 4.0 mmol, 68% yield) was obtained as a colourless oil.

¹H NMR (500 MHz, CDCl₃): δ = 7.57–7.42 (m, 2H, ArH), 7.42–7.23 (m, 7H, ArH), 3.37 (br. s, 2H, CH₂), 2.71 (br. s, 2H, CH₂), 1.60 (br. s, 2H, CH₂), 1.42 (br. s, 2H, CH₂) ppm; ¹³C NMR (126 MHz, CDCl₃): δ = 169.8 (C=O),

140.0 (ArC), 138.3 (ArC), 136.9 (ArC), 129.5 (ArC), 129.4 (ArC), 128.5 (2 × ArC), 128.4 (2 × ArC), 127.7 (ArC), 127.6 (ArC), 127.2 (ArC), 47.5 (CH₂), 45.4 (CH₂), 25.6 (CH₂), 24.2 (CH₂) ppm. The spectroscopic data are in agreement with the literature.³⁶

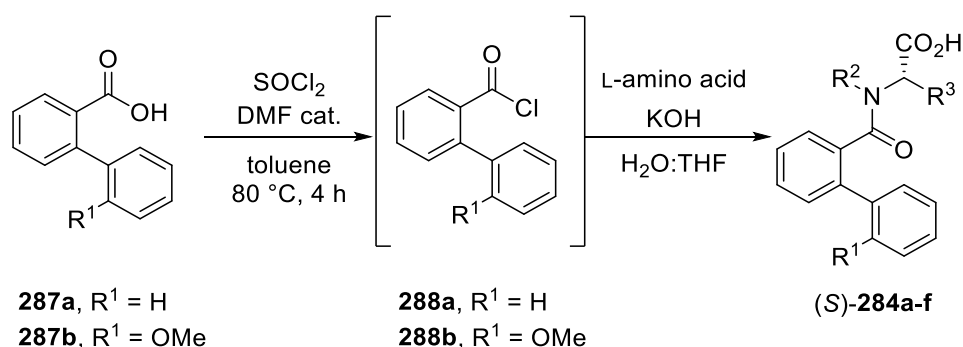
[1,1'-Biphenyl]-2-yl(pyrrolidin-1-yl)methanone **293b**:



Performed according to *General Procedure 20* on a 2.0 mmol scale of **288b**; **293b** (396 mg, 1.4 mmol, 71% yield) was obtained as a colourless oil.

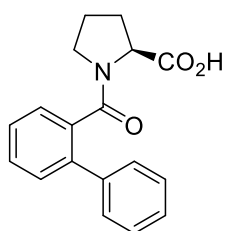
¹H NMR (500 MHz, CDCl₃): δ = 7.47–7.28 (m, 6H, ArH), 6.98 (td, *J* = 7.5, 1.0 Hz, 1H, ArH), 6.94 (d, *J* = 8.2 Hz, 1H, ArH), 3.77 (s, 3H, OCH₃), 3.36

(t, *J* = 7.0 Hz, 2H, CH₂), 2.98 (t, *J* = 6.7 Hz, 2H, CH₂), 1.75–1.47 (m, 4H, 2 × CH₂) ppm; ¹³C NMR (126 MHz, CDCl₃): δ = 169.7 (C=O), 156.3 (ArC–O), 137.9 (ArC), 135.5 (ArC), 131.6 (ArC), 131.3 (ArC), 129.2 (ArC), 128.6 (ArC), 127.5 (ArC), 127.1 (ArC), 120.7 (ArC), 110.8 (ArC), 55.6 (OCH₃), 47.9 (CH₂), 45.4 (CH₂), 25.9 (CH₂), 24.5 (CH₂) ppm.

General Procedure 21:

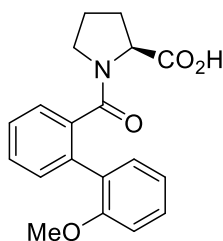
The carboxylic acid **287** (5 g, 17 mmol) was dissolved in 20 mL of dry toluene. Thionyl chloride (2.4 mL, 34 mmol) and 5 drops of DMF were added. The mixture was stirred for 6 hours at 60 °C under N₂ then the solvent and excess of thionyl chloride was removed under reduced pressure. The desired acyl chloride **288** was dissolved in dry THF (15 mL) and added dropwise to an ice-cold solution of L-amino acid (17 mmol) and KOH (2 g, 34 mmol). The solution was stirred at room temperature overnight. Once the reaction was completed, THF was removed under reduced pressure and the residue was partitioned into NaHCO₃ saturated aqueous solution (20 mL) and EtOAc (20 mL). The aqueous layer was acidified with HCl 1 M aqueous solution and the white precipitate was extracted with EtOAc (3 × 20 mL). The collected organic layers were washed with brine, dried over MgSO₄ and concentrated under reduced pressure and recrystallised from Et₂O and petroleum ether if needed. The products (*S*)-**284a-f** were isolated as colourless solids.

([(1,1'-Biphenyl]-2-carbonyl)-L-proline (*S*)-**284a**:



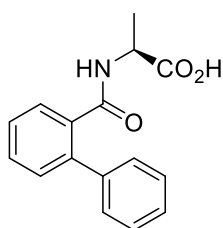
Performed according to *General Procedure 21* on a 8.5 mmol scale of **288a**; (*S*)-**284a** (2.2 g, 7.5 mmol, 88% yield) was obtained as colourless crystals, m.p: 162–164 °C; [α]_D²⁰: –83.5° (c 0.93, MeOH).

¹H NMR (500 MHz, CDCl₃): δ = 7.63–7.33 (m, 9H, ArH), 4.46 (s, 1H, N–CH), 2.88 (s, 2H, CH₂), 2.34–2.10 (m, 1H, 1 × CH₂), 1.75–1.51 (m, 2H, CH₂), 1.35 (s, 1H, 1 × CH₂) ppm; ¹³C NMR (126 MHz, CDCl₃): δ = 173.6 (C=O), 171.5 (C=O), 139.4 (ArC), 134.4 (ArC), 130.6 (ArC), 129.8 (ArC), 128.9 (ArC), 128.5 (2 × ArC), 128.3 (2 × ArC), 128.1 (ArC), 127.6 (ArC), 60.4 (N–CH), 49.0 (N–CH₂), 27.3 (CH₂), 24.3 (CH₂) ppm; The spectroscopic data are in agreement with the literature.³⁷

(2'-Methoxy-[1,1'-biphenyl]-2-carbonyl)-L-proline (*S*)-**284b**:

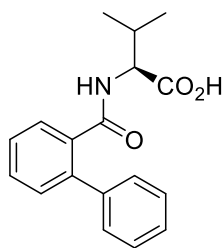
Performed according to *General Procedure 21* on a 2.2 mmol scale of **288b**; (*S*)-**284b** (672 mg, 2.1 mmol, 94% yield) was obtained as a colourless solid, m.p.: 68–70 °C; $[\alpha]_D^{20}$: -78.0° (c 0.59, MeOH).

^1H NMR (500 MHz, CDCl_3): δ = 7.54–7.48 (m, 1H, *ArH*), 7.48–7.38 (m, 3H, *ArH*), 7.35 (ddd, J = 8.3, 7.5, 1.8 Hz, 1H, *ArH*), 7.31–7.17 (m, 1H, *ArH*), 7.02 (td, J = 7.5, 1.0 Hz, 1H, *ArH*), 6.95 (d, J = 8.3 Hz, 1H, *ArH*), 4.51 (br. s, 1H, N–CH), 3.74 (s, 3H, OCH_3), 3.26 (br. s, 1H, $1 \times \text{CH}_2$), 3.11 (br. s, 1H, $1 \times \text{CH}_2$), 2.43 (br. s, 1H, $1 \times \text{CH}_2$), 1.92–1.68 (m, 2H, CH_2), 1.56 (br. s, 1H, $1 \times \text{CH}_2$) ppm; ^{13}C NMR (126 MHz, CDCl_3): δ = 173.8 (C=O), 171.1 (C=O), 156.0 (*ArC*–O), 134.9 (*ArC*), 131.6 (*ArC*), 131.3 (*ArC*), 130.2 (*ArC*), 129.9 (*ArC*), 128.2 (*ArC*), 127.5 (*ArC*), 127.0 (*ArC*), 121.0 (*ArC*), 110.9 (*ArC*), 60.5 (N–CH), 55.5 (N– CH_2), 49.6 (OCH_3), 27.1 (CH_2), 24.7 (CH_2) ppm; IR (neat): ν = 3439w, 2949m, 1730s, 1591s, 1448s, 1421s, 1022s cm^{-1} ; HRMS (ES): Exact mass calculated for $\text{C}_{19}\text{H}_{20}\text{NO}_4$ $[\text{M}+\text{H}]^+$ 326.1392; found 326.1404.

([1,1'-Biphenyl]-2-carbonyl)-L-alanine (*S*)-**284c**:

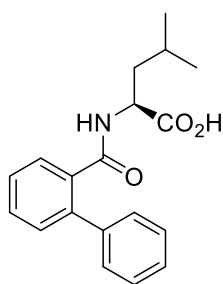
Performed according to *General Procedure 21* on a 5.0 mmol scale of **288a**; (*S*)-**284c** (1.3 g, 4.3 mmol, 86% yield) was obtained as a colourless solid, m.p.: 120–124 °C; $[\alpha]_D^{20}$: -8.5 (c 1.4, MeOH).

^1H NMR (400 MHz, CDCl_3): δ = 7.74 (dd, J = 7.6, 1.2 Hz, 1H, *ArH*), 7.51 (td, J = 7.5, 1.5 Hz, 1H, *ArH*), 7.47–7.41 (m, 2H, *ArH*), 7.41–7.32 (m, 5H, *ArH*), 5.72 (d, J = 6.7 Hz, 1H, NH), 4.49 (quin, J = 7.1 Hz, 1H, CH– CH_3), 1.10 (d, J = 7.2 Hz, 3H, CH_3) ppm; ^{13}C NMR (101 MHz, CDCl_3): δ = 175.9 (C=O), 169.7 (C=O), 140.2 (*ArC*), 140.1 (*ArC*), 134.3 (*ArC*), 130.9 (*ArC*), 130.5 (*ArC*), 129.2 (*ArC*), 128.9 (2 \times *ArC*), 128.8 (2 \times *ArC*), 128.1 (*ArC*), 127.9 (*ArC*), 48.7 (NCH), 17.3 (CH_3) ppm; IR (neat): ν = 3271m, 3057m, 1718s, 1618s, 1518s, 1448s, 744s, 698s cm^{-1} ; HRMS (ES): Exact mass calculated for $\text{C}_{16}\text{H}_{15}\text{NO}_3\text{Na}$ $[\text{M}+\text{Na}]^+$ 292.0950; found 292.0960.

([1,1'-Biphenyl]-2-carbonyl)-L-valine (*S*)-**284d**:

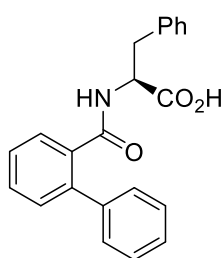
Performed according to *General Procedure 21* on a 5.0 mmol scale of **288a**; (*S*)-**284d** (1.1 g, 3.7 mmol, 74% yield) was obtained as a colourless solid, m.p.: 160–164 °C; $[\alpha]_D^{20}$: -6.0° (c 0.66, MeOH).

$^1\text{H NMR}$ (400 MHz, CDCl_3): δ = 7.75–7.69 (m, 1H, ArH), 7.49 (dt, J = 7.5, 3.8 Hz, 1H, ArH), 7.45–7.30 (m, 7H, ArH), 5.84 (d, J = 8.2 Hz, 1H, NH), 4.49 (dd, J = 8.3, 4.6 Hz, 1H, NCH), 2.07–1.93 (m, 1H, CH), 0.71 (d, J = 6.9 Hz, 3H, CH_3), 0.65 (d, J = 6.9 Hz, 3H, CH_3) ppm; $^{13}\text{C NMR}$ (101 MHz, CDCl_3): δ = 175.9 (C=O), 169.8 (C=O), 140.3 (ArC), 139.9 (ArC), 134.9 (ArC), 130.6 (ArC), 130.5 (ArC), 129.1 (2 × ArC), 128.9 (2 × ArC), 128.6 (ArC), 128.1 (ArC), 127.8 (ArC), 57.8 (NCH), 30.8 (CH), 18.8 (CH_3), 17.5 (CH_3) ppm. The spectroscopic data are in agreement with the literature.³⁸

([1,1'-Biphenyl]-2-carbonyl)-L-leucine (*S*)-**284e**:

Performed according to *General Procedure 21* on a 10 mmol scale of **288a**; (*S*)-**284e** (2.3 g, 7.4 mmol, 74% yield) was obtained as a colourless solid, m.p.: 90–94 °C; $[\alpha]_D^{20}$: -17.7° (c 1.1, MeOH).

$^1\text{H NMR}$ (400 MHz, CDCl_3): δ = 7.74–7.71 (m, 1H, ArH), 7.49 (td, J = 7.5, 1.5 Hz, 1H, ArH), 7.44–7.33 (m, 7H, ArH), 5.67 (d, J = 7.7 Hz, 1H, NH), 4.50 (ddd, J = 9.2, 7.8, 5.2 Hz, 1H, NCH), 1.53–1.35 (m, 1H, CH), 1.35–1.06 (m, 2H, CH_2), 0.79 (dd, J = 6.5, 4.1 Hz, 6H, 2 × CH_3) ppm; $^{13}\text{C NMR}$ (126 MHz, CDCl_3): δ = 176.5 (C=O), 169.9 (C=O), 140.3 (ArC), 140.0 (ArC), 134.6 (ArC), 130.7 (ArC), 130.5 (ArC), 129.2 (ArC), 128.9 (ArC), 128.0 (4 × ArC), 127.8 (ArC), 51.3 (NCH), 40.8, 24.5, 22.9, 21.9 ppm; IR (neat): ν = 3306m, 2957m, 1705s, 1636s, 1510s, 1244s cm^{-1} ; HRMS (ES): Exact mass calculated for $\text{C}_{19}\text{H}_{21}\text{NO}_3\text{Na}$ $[\text{M}+\text{Na}]^+$ 334.1419; found 334.1430.

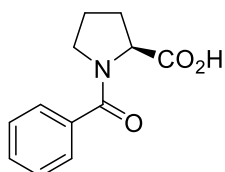
([1,1'-Biphenyl]-2-carbonyl)-L-phenylalanine (*S*)-**284f**:

Performed according to *General Procedure 21* on a 8.5 mmol scale of **288a**; (*S*)-**284f** (2.0 g, 5.8 mmol, 68% yield) was obtained as a colourless solid, m.p.: 134–136 °C; $[\alpha]_D^{20}$: $+1.8^\circ$ (c 1.1, MeOH).

$^1\text{H NMR}$ (500 MHz, CDCl_3): δ = 7.61 (d, J = 7.6 Hz, 1H, ArH), 7.48 (t, J = 7.5 Hz, 1H, ArH), 7.42–7.30 (m, 7H, ArH), 7.24–7.15 (m, 3H, ArH), 6.94–6.77 (m, 2H, ArH), 5.83 (d, J = 7.3 Hz, 1H, NH), 4.85 (q, J = 6.3 Hz, 1H, NCH),

3.17–2.74 (m, 2H, CH₂) ppm; ¹³C NMR (126 MHz, CDCl₃): δ = 175.1 (C=O), 169.8 (C=O), 140.0 (ArC), 135.5 (ArC), 134.5 (ArC), 130.8 (ArC), 130.7 (ArC), 130.6 (ArC), 129.3 (2 × ArC), 129.0 (2 × ArC), 128.9 (ArC), 128.8 (2 × ArC), 128.8 (2 × ArC), 128.1 (ArC), 127.3 (ArC), 53.6 (NCH), 37.2 (CH₂) ppm. The spectroscopic data are in agreement with the literature.³⁷

Benzoyl-L-proline (S)-**259**:



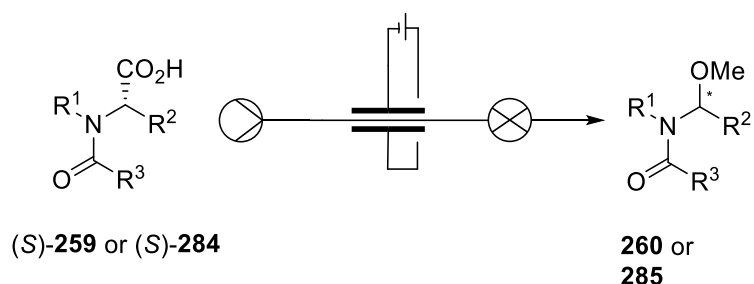
Performed according to *General Procedure 21* on a 10 mmol scale of benzoyl chloride; (S)-**259** (1.8 g, 8.2 mmol, 82% yield) was obtained as a colourless solid, m.p.: 146–148 °C; [α]_D²⁰: -94.0° (c 1.0, MeOH).

¹H NMR (500 MHz, CDCl₃): δ = 9.04 (s, 1H, CO₂H), 7.57–7.52 (m, 2H, ArH), 7.50–7.37 (m, 3H, ArH), 4.73 (dd, *J* = 7.7, 5.9 Hz, 1H, 1 × CH₂), 3.63–3.49 (m, 2H, CH₂), 2.41–2.20 (m, 2H, CH₂), 2.10–1.95 (m, 1H, 1 × CH₂), 1.95–1.85 (m, 1H, 1 × CH₂) ppm; ¹³C NMR (126 MHz, CDCl₃): δ = 174.7 (C=O), 171.2 (C=O), 135.5 (ArC), 130.7 (ArC), 128.5 (2 × ArC), 127.4 (2 × ArC), 59.8 (NCH), 50.5 (NCH₂), 28.8 (CH₂), 25.3 (CH₂) ppm; The spectroscopic data are in agreement with the literature.³⁷

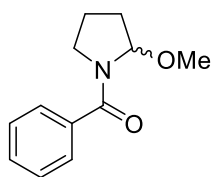
5.4.2 Synthesis of *N,O*-acetals

5.4.2.1 Enantioselective Synthesis

General Procedure 22:

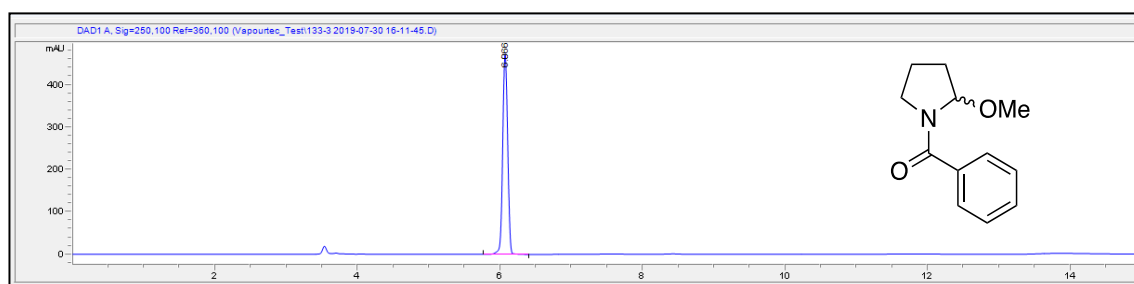


The amino acid derivative (S)-**259** or (S)-**284** was dissolved in methanol (0.012–0.05 M) and pumped through the Ion electrochemical microreactor at 0.2 mL·min⁻¹. Platinum was used as the cathode, graphite or glassy carbon as the anode (spacer: 0.5 mm; working electrode surface: 12 cm²). The current was fixed at 16–32 mA (2 F·mol⁻¹), and the temperature was maintained at -10 °C. The solution was collected over 90 minutes and the solvent was evaporated under reduced pressure. The desired *N,O*-acetals **260** or **285** were obtained after column chromatography (*n*-hexane/ethyl acetate, 8:2) as colourless oil or solid depending on the substrate.

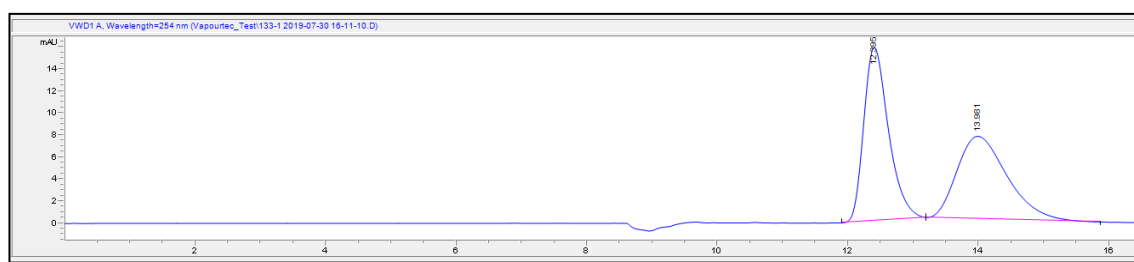
(2-Methoxypyrrolidin-1-yl)(phenyl)methanone **260**:

Performed according to *General Procedure 22* on a 0.013 M methanol solution of (*S*)-**259** using glassy carbon as anode; **260** (7.6 mg, 3.2 mM, 25% yield, 0% ee) was afforded as a colourless oil as a 1:1.5 mixture of rotamers.

^1H NMR (500 MHz, CDCl_3): δ = 7.74–7.47 (m, 2H, ArH), 7.52–7.35 (m, 3H, ArH), 5.76 (s, 0.4H, NCH), 4.73 (s, 0.6H, NCH), 3.77–3.58 (m, 1.6H), 3.49 (s, 1.2H), 3.30 (s, 0.4H), 3.06 (s, 1.8H), 2.27–1.64 (m, 4H) ppm; ^{13}C NMR (126 MHz, CDCl_3): δ = 171.5 (C=O), 171.0 (C=O), 136.7 (ArC), 130.1 (ArC), 128.2 (ArC), 127.4 (ArC), 127.2 (ArC), 90.1, 87.5, 56.4, 54.1, 48.6, 45.5, 31.3, 30.6, 23.5, 21.0 ppm; HPLC analysis: ^1D Varian Si-5 μm (250 \times 4.6 mm) *n*-hexane/isopropanol 9:1 (v/v), 1.0 mL \cdot min $^{-1}$, λ = 254 nm, retention time **260** = 6.1 min; ^2D DAICEL Chiralcel OB-H (250 \times 4.6 mm, 5 μm), *n*-hexane/isopropanol 7:3 (v/v), 1.0 mL \cdot min $^{-1}$, λ = 254 nm, overall retention time major isomer = 12.4 min, retention time minor isomer = 14.0 min. The spectroscopic data are in agreement with the literature.³⁹



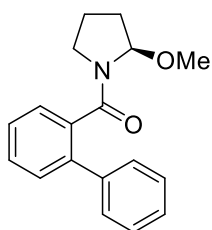
Peak #	Time (min)
1	6.066



Peak #	Time (min)	Area (%)
1	12.395	50.905
2	13.981	49.095

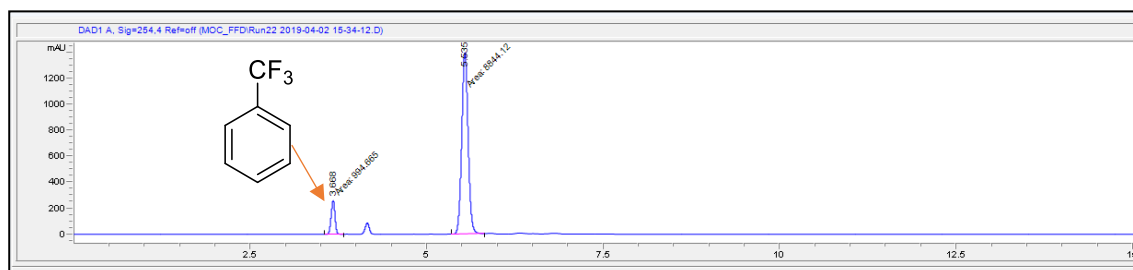
Figure 5.17: HPLC chromatograms for the enantiomers of **260**. From the top: ^1D dimension and ^2D for the racemic mixture.

(*R*)-[1,1'-Biphenyl]-2-yl(2-methoxypyrrolidin-1-yl)methanone (*R*)-**285a**:



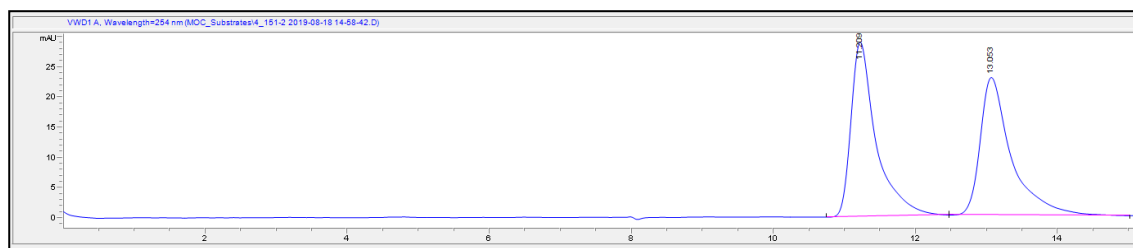
Performed according to *General Procedure 22* on a 0.05 M methanol solution of (*S*)-**284a** using glassy carbon as anode; (*R*)-**285a** (102.8 mg, 0.026 M, 52% yield, 58% *ee*) was afforded as a colourless oil as a 1:2 mixture of rotamers; $[\alpha]_D^{20}$: -16.3° (c 1.7, CH₂Cl₂).

¹H NMR (500 MHz, CDCl₃): δ = 7.62–7.30 (m, 9H, ArH), 5.46 (br. s, 0.4H, NCH), 4.31 (d, *J* = 4.1 Hz, 0.6H, NCH), 3.52 (ddd, *J* = 11.9, 9.4, 2.5 Hz, 0.7H), 3.40–3.29 (m, 1.7H), 2.78 (s, 2.2 H, OCH₃), 1.89–1.46 (m, 4H) ppm; ¹³C NMR (126 MHz): δ = 171.5 (C=O), 170.6 (C=O), 139.9 (ArC), 139.9 (ArC), 138.4 (ArC), 136.6 (ArC), 136.1 (ArC), 129.7 (ArC), 129.6 (ArC), 129.3 (ArC), 129.2 (ArC), 128.7 (ArC), 128.6 (ArC), 128.6 (ArC), 128.5 (ArC), 127.8 (ArC), 127.7 (ArC), 127.7 (ArC), 127.6 (ArC), 126.9 (ArC), 89.8 (NCH), 87.1 (NCH), 56.6 (OCH₃), 54.6 (OCH₃), 46.6 (NCH₂), 44.4 (NCH₂), 31.2, 22.5, 21.0 ppm; HPLC analysis (85:15 *e.r.*): ¹D Varian Si-5 μ m (250 \times 4.6 mm) *n*-hexane/isopropanol 9:1 (v/v), 1.0 mL \cdot min⁻¹, λ = 254 nm, retention time **285a** = 5.5 min; ²D DAICEL Chiralcel OD-H (250 \times 4.6 mm, 5 μ m), *n*-hexane/isopropanol 9:1 (v/v), 1.0 mL \cdot min⁻¹, λ = 254 nm, retention time (*R*)-**285a** = 11.2 min, retention time (*S*)-**285a** = 13.1 min. The spectroscopic data are in agreement with the literature.⁴⁰



Peak #	Time (min)
1 (Internal Standard)	3.668
2	5.535

Figure 5.18: ¹D HPLC chromatograms for **285a**.



Peak #	Time (min)	Area (%)
1	11.209	50.468
2	13.053	49.532

Figure 5.19: ²D HPLC chromatograms for the enantiomers of **285a** (racemic).

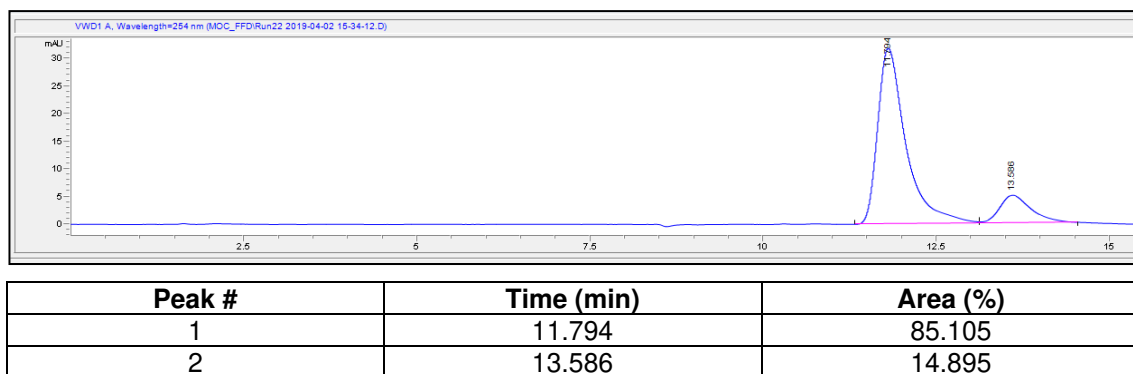
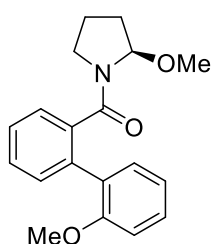


Figure 5.20: ²D HPLC chromatograms for the enantiomers of **285a** (70% *ee*).

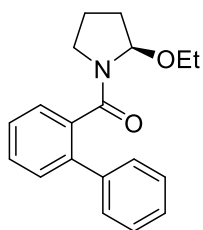
(*R*)-(2'-Methoxy-[1,1'-biphenyl]-2-yl)(2-methoxypyrrolidin-1-yl)methanone (*R*)-**285b**:



Performed according to *General Procedure 22* on a 0.013 M methanol solution of (*S*)-**284b** using glassy carbon as anode; (*R*)-**285b** (15.9 mg, 3.6 mM, 28% yield, 50% *ee*) was afforded as a colourless oil as a 1:1.5 mixture of rotamers; $[\alpha]_D^{20}$: -5.3° (c 0.38, CH₂Cl₂).

¹H NMR (500 MHz, CDCl₃): δ = 7.60–7.23 (m, 6H, ArH), 7.02–6.86 (m, 1H, 2H, ArH), 5.48 (d, *J* = 4.9 Hz, 0.4H, NCH), 4.54 (d, *J* = 4.4 Hz, 0.6H, NCH), 3.85–3.62 (m, 3H, OCH₃), 3.56–3.05 (m, 3.2H), 2.85 (s, 1.8H), 1.99–1.47 (m, 4H) ppm; ¹³C NMR (126 MHz, CDCl₃): δ = 171.4 (C=O), 170.6 (C=O), 156.2 (ArC–O), 156.2 (ArC–O), 137.3 (ArC), 136.9 (ArC), 135.7 (ArC), 135.3 (ArC), 131.6 (ArC), 131.5 (ArC), 131.4 (ArC), 131.1 (ArC), 129.4 (ArC), 129.3 (ArC), 128.8 (ArC), 128.8 (ArC), 128.7 (ArC), 128.6 (ArC), 127.4 (ArC), 127.3 (ArC), 126.7 (ArC), 120.8 (ArC), 120.7 (ArC), 110.9 (ArC), 110.8 (ArC), 89.8 (C'H), 86.9 (CH), 56.3, 55.5, 55.4, 54.8, 47.0, 44.5, 31.7, 31.4, 22.9, 21.1 ppm; IR (neat): ν = 3061w, 2926m, 2853w, 1632s, 1402s, 1254s, 1080s, 908m, 750s, 729s cm⁻¹; HRMS (ES): Exact mass calculated for C₁₉H₂₁NO₃Na [M+Na]⁺ 334.1419; found 334.1410; HPLC analysis (75:25 *e.r.*): ¹D Varian Si-5 μ m (250 × 4.6 mm) *n*-hexane/isopropanol 9:1 (v/v), 1.0 mL·min⁻¹, λ = 254 nm, retention time **285b** = 6.3 min; ²D YMC Chiral Amylose-C (250 × 4.6 mm, 5 μ m), *n*-hexane/isopropanol 85:15 (v/v), 1.0 mL·min⁻¹, λ = 254 nm, overall retention time major isomer = 13.4 min, retention time minor isomer = 14.2 min. The HPLC chromatograms are reported in literature.⁴¹

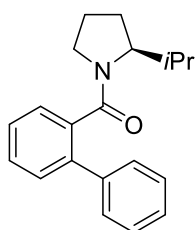
(*R*)-[1,1'-Biphenyl]-2-yl(2-ethoxypyrrolidin-1-yl)methanone (*R*)-**285c**:



Performed according to *General Procedure 22* on a 0.013 M ethanol solution of (*R*)-**284a** using graphite as anode; (*R*)-**285c** (27.6 mg, 6.9 mM, 53% yield, 23% *ee*) was afforded as a 1:2.3 mixture of rotamers; $[\alpha]_D^{20}$: -7.6° (c 0.53, CH₂Cl₂).

¹H NMR (500 MHz, CDCl₃): δ = 7.66–7.27 (m, 9H, ArH), 5.55 (br. s, 0.3H, NCH), 4.40 (br. s, 0.7H, NCH), 3.70–3.43 (m, 1.1H), 3.41–3.21 (m, 0.7H), 3.09–2.90 (m, 1H), 2.87–2.68 (m, 1H), 1.98–1.35 (m, 4H), 1.10 (br. s, 0.9H), 0.84 (t, J = 7.0 Hz, 2.1H, 3H) ppm; ¹³C NMR (126 MHz, CDCl₃): δ = 171.4 (C=O), 170.6 (C=O), 140.0 (ArC), 140.0 (ArC), 138.5 (ArC), 136.8 (ArC), 136.3 (ArC), 129.8 (ArC), 129.7 (ArC), 129.4 (ArC), 129.2 (ArC), 128.8 (ArC), 128.7 (ArC), 128.7 (ArC), 128.5 (ArC), 127.8 (ArC), 127.7 (ArC), 127.6 (ArC), 127.0 (ArC), 88.3 (NCH), 85.7 (NCH), 64.4 (OCH₂), 62.5 (OCH₂), 46.6, 44.6, 31.9, 31.7, 22.6, 21.2, 15.5, 14.8 ppm; IR (neat): ν = 3055w, 2974m, 2882w, 1630s, 1402s, 1070s, 733s, 700s cm⁻¹; HRMS (ES): Exact mass calculated for C₁₉H₂₁NO₂Na [M+Na]⁺ 318.1470; found 318.1456; HPLC analysis (80:20 *e.r.*): ¹D Varian Si-5 μ m (250 \times 4.6 mm) *n*-hexane/isopropanol 9:1 (v/v), 1.0 mL \cdot min⁻¹, λ = 254 nm, retention time **285c** = 4.9 min; ²D DAICEL Chiralcel OD-H (250 \times 4.6 mm, 5 μ m), *n*-hexane/isopropanol 9:1 (v/v), 1.0 mL \cdot min⁻¹, λ = 254 nm, overall retention time major isomer = 9.9 min, retention time minor isomer = 11.3 min. The HPLC chromatograms are reported in literature.⁴¹

(*R*)-[1,1'-Biphenyl]-2-yl(2-isopropoxypyrrolidin-1-yl)methanone (*R*)-**285d**:

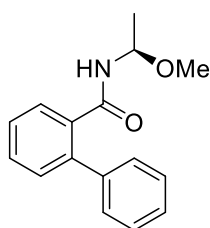


Performed according to *General Procedure 22* on a 0.013 M propan-2-ol solution of (*S*)-**284a** using graphite as anode; (*R*)-**285d** (22.6 mg, 5.2 mM, 40% yield, 42% *ee*) was afforded as a colourless oil as a 1:2 mixture of rotamers; $[\alpha]_D^{20}$: -22.7° (c 0.26, CH₂Cl₂).

¹H NMR (500 MHz, CDCl₃): δ = 7.61–7.30 (m, 9H, ArH), 5.62 (br. s, 0.3H, NCH), 4.46 (br. s, 0.7H, NCH), 3.97 (br. s, 0.3H), 3.66–3.50 (m, 0.7H), 3.27 (d, J = 9.4 Hz, 0.7H), 3.07 (hept, J = 6.1 Hz, 0.7H), 2.93 (s, 0.2H), 2.87–2.70 (m, 0.3H), 1.97–1.29 (m, 4H), 1.23–0.46 (m, 6H, 2 \times CH₃) ppm; ¹³C NMR (126 MHz, CDCl₃): δ = 170.3 (C=O), 139.9 (ArC), 36.3 (ArC), 129.6 (ArC), 129.2 (ArC), 128.7 (ArC), 128.6 (ArC), 128.5 (ArC), 128.5 (ArC), 127.7 (ArC), 127.6 (ArC), 127.6 (ArC), 126.9 (ArC), 85.8 (NCH), 67.6 (OCH), 46.4, 44.5, 32.3, 32.1, 23.4, 22.5, 22.1, 21.5, 21.0 ppm; IR (neat): ν = 2970m, 1736s, 1616s, 1416s, 741s, 700s cm⁻¹; HRMS (ES): Exact mass calculated for C₂₀H₂₃NO₂Na [M+Na]⁺ 332.1626; found 332.1631; HPLC analysis (84:16 *e.r.*):

¹D Varian Si-5 μm (250 \times 4.6 mm) *n*-hexane/isopropanol 9:1 (v/v), 1.0 mL \cdot min⁻¹, λ = 254 nm, retention time **285d** = 4.7 min; ²D DAICEL Chiralcel OD-H (250 \times 4.6 mm, 5 μm), *n*-hexane/isopropanol 9:1 (v/v), 1.0 mL \cdot min⁻¹, λ = 254 nm, overall retention time major isomer = 9.2 min, retention time minor isomer = 10.5 min. The HPLC chromatograms are reported in literature.⁴¹

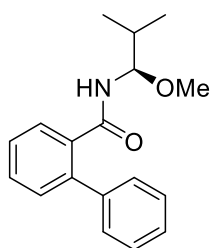
(*R*)-*N*-(1-Methoxyethyl)-[1,1'-biphenyl]-2-carboxamide (*R*)-**285e**:



Performed according to *General Procedure 22* on a 0.05 M methanol solution of (*S*)-**284c** using glassy carbon as anode; (*R*)-**285e** (39.1 mg, 0.012 M, 23% yield, 8% *ee*) was afforded as a colourless solid, m.p.: 82–84 °C; $[\alpha]_D^{20}$: +2.9° (c 0.69, CH₂Cl₂).

¹H NMR (500 MHz, CDCl₃): δ = 7.73 (ddd, *J* = 7.6, 1.5, 0.4 Hz, 1H, ArH), 7.54–7.47 (m, 1H, ArH), 7.46–7.33 (m, 7H, ArH), 5.36 (d, *J* = 9.1 Hz, 1H NH), 5.18 (dq, *J* = 9.5, 5.9 Hz, 1H, NCH), 3.19 (s, 3H, OCH₃), 0.91 (d, *J* = 5.9 Hz, 3H, CH₃) ppm; ¹³C NMR (126 MHz, CDCl₃): δ = 169.5 (C=O), 140.3 (ArC), 139.6 (ArC), 135.5 (ArC), 130.5 (ArC), 130.4 (ArC), 129.0 (ArC), 128.9 (2 \times ArC), 128.8 (2 \times ArC), 128.1 (ArC), 127.8 (ArC), 78.2 (NCH), 55.7 (OCH₃), 21.0 (CH₃) ppm; IR (neat): ν = 3289m, 3059w, 2984m, 2932m, 1647s, 1508s, 1088s, 910s, 729s, 698s cm⁻¹; HRMS (EI): Exact mass calculated for C₁₆H₁₇NO₂ [M]⁺ 255.1259; found 255.1252. HPLC analysis (55:43 *e.r.*): ¹D Varian Si-5 μm (250 \times 4.6 mm) *n*-hexane/isopropanol 9:1 (v/v), 1.0 mL \cdot min⁻¹, λ = 254 nm, retention time **267e** = 5.0 min; ²D YMC Chiral Amylose-C (250 \times 4.6 mm, 5 μm), *n*-hexane/isopropanol 85:15 (v/v), 1.0 mL \cdot min⁻¹, λ = 254 nm, overall retention time major isomer = 10.9 min, retention time minor isomer = 13.7 min. The HPLC chromatograms are reported in literature.⁴¹

(*R*)-*N*-(1-Methoxy-2-methylpropyl)-[1,1'-biphenyl]-2-carboxamide (*R*)-**285f**:

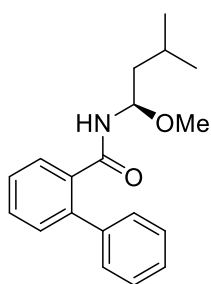


Performed according to *General Procedure 22* on a 0.05 M methanol solution of (*S*)-**284d** using glassy carbon as anode; (*R*)-**285f** (70.2 mg, 0.035 M, 69% yield, 7% *ee*) was afforded as a colourless solid, m.p.: 98–100 °C; $[\alpha]_D^{20}$: +23.5° (c 0.17, MeOH).

¹H NMR (500 MHz, CDCl₃): δ = 7.72 (ddd, *J* = 7.6, 1.5, 0.5 Hz, 1H, ArH), 7.49 (td, *J* = 7.5, 1.5 Hz, 1H, ArH), 7.46–7.39 (m, 5H, ArH), 7.39–7.33 (m, 2H, ArH), 5.48 (d, *J* = 9.7 Hz, 1H, NH), 4.89 (dd, *J* = 9.8, 5.1 Hz, 1H, NCH), 3.18 (s, 3H, OCH₃), 1.58–1.48 (m, 1H, CH) 0.66 (d, *J* = 6.9 Hz, 3H, CH₃), 0.64 (d, *J* = 6.8 Hz, 3H, CH₃) ppm; ¹³C NMR (126 MHz, CDCl₃): δ = 170.0 (C=O), 140.5 (ArC), 139.6 (ArC), 135.8 (ArC),

130.6 (ArC), 130.3 (ArC), 128.9 (2 × ArC), 128.9 (2 × ArC), 128.8 (ArC), 128.1 (ArC), 127.8 (ArC), 85.3 (NCH), 56.3 (OCH₃), 32.8(CH), 17.1 (CH₃), 17.0 (CH₃) ppm; IR (neat): $\nu = 3280\text{m}, 3057\text{w}, 2958\text{m}, 2924\text{m}, 1647\text{s}, 1502\text{s}, 1146\text{m}, 1088\text{s}, 744\text{s}, 698\text{s cm}^{-1}$; HRMS (ES): Exact mass calculated for C₁₈H₂₁NO₂Na [M+Na]⁺ 306.1470; found 306.1472; HPLC analysis (53:46 *e.r.*): ¹D Varian Si-5 μm (250 × 4.6 mm) *n*-hexane/isopropanol 9:1 (v/v), 1.0 mL•min⁻¹, $\lambda = 254\text{ nm}$, retention time **285f** = 4.0 min; ²D YMC Chiral Amylose-C (250 × 4.6 mm, 5 μm), *n*-hexane/isopropanol 85:15 (v/v), 1.0 mL•min⁻¹, $\lambda = 254\text{ nm}$, overall retention time major isomer = 9.6 min, retention time minor isomer = 11.6 min. The HPLC chromatograms are reported in literature.⁴¹

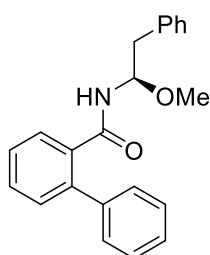
(*R*)-*N*-(1-Methoxy-3-methylbutyl)-[1,1'-biphenyl]-2-carboxamide (*R*)-**285g**:



Performed according to *General Procedure 22* on a 0.05 M methanol solution of (*S*)-**284e** using glassy carbon as anode; (*R*)-**285g** (26.7 mg, 6.9 mM, 14% yield, 14% *ee*) was afforded as a colourless solid, m.p.: 86–88 °C; $[\alpha]_D^{20}$: +4.0° (c 0.50, CH₂Cl₂).

¹H NMR (500 MHz, CDCl₃): $\delta = 7.70$ (ddd, $J = 7.6, 1.5, 0.5\text{ Hz}$, 1H, *ArH*), 7.49 (td, $J = 7.5, 1.5\text{ Hz}$, 1H, *ArH*), 7.45–7.40 (m, 5H, *ArH*), 7.39–7.34 (m, 2H, *ArH*), 5.38 (d, $J = 9.4\text{ Hz}$, 1H, *NH*), 5.11 (ddd, $J = 9.7, 7.1, 6.0\text{ Hz}$, 1H, *NCH*), 3.21 (s, 3H, *OCH*₃), 1.38 (tq, $J = 13.1, 6.5\text{ Hz}$, 1H, 1 × *CH*₂), 1.19 (dt, $J = 14.1, 7.1\text{ Hz}$, 1H, 1 × *CH*₂), 0.93 (ddd, $J = 7.8, 6.9, 3.2\text{ Hz}$, 1H, *CH*), 0.81 (dd, $J = 6.6, 0.9\text{ Hz}$, 6H, 2 × *CH*₃) ppm; ¹³C NMR (126 MHz, CDCl₃): $\delta = 169.8$ (C=O), 140.4 (ArC), 139.6 (ArC), 135.7 (ArC), 130.5 (ArC), 130.4 (ArC), 128.9 (2 × ArC), 128.9 (2 × ArC), 128.7 (ArC), 128.0 (ArC), 127.8 (ArC), 80.2 (NCH), 56.0 (OCH₃), 44.2, 24.3, 22.8, 22.5 ppm; IR (neat): $\nu = 3283\text{m}, 2955\text{m}, 1655\text{s}, 1508\text{s}, 1366\text{m}, 1148\text{m}, 1095\text{m}, 1061\text{m}, 735\text{s}, 698\text{s cm}^{-1}$; HRMS (ES): Exact mass calculated for C₁₉H₂₃NO₂Na [M+Na]⁺ 320.1626; found 320.1629; HPLC analysis (57:43 *e.r.*): ¹D Varian Si-5 μm (250 × 4.6 mm) *n*-hexane/isopropanol 9:1 (v/v), 1.0 mL•min⁻¹, $\lambda = 254\text{ nm}$, retention time **285g** = 4.0 min; ²D YMC Chiral Amylose-C (250 × 4.6 mm, 5 μm), *n*-hexane/isopropanol 85:15 (v/v), 1.0 mL•min⁻¹, $\lambda = 254\text{ nm}$, overall retention time major isomer = 8.9 min, retention time minor isomer = 11.6 min. The HPLC chromatograms are reported in literature.⁴¹

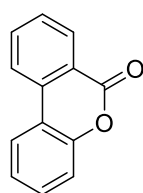
(*R*)-*N*-(1-Methoxy-3-methylbutyl)-[1,1'-biphenyl]-2-carboxamide (*R*)-**285h**:



Performed according to *General Procedure 22* on a 0.05 M methanol solution of (*S*)-**284f** using glassy carbon as anode; (*R*)-**285h** (47.4 mg, 0.033 M, 67% yield, 12% *ee*) was afforded as a colourless solid, m.p.: 118–120 °C; $[\alpha]_D^{20}$: +4.2° (c 0.95, CH₂Cl₂).

¹H NMR (500 MHz, CDCl₃): δ = 7.58 (ddd, *J* = 7.6, 1.4, 0.4 Hz, 1H, *ArH*), 7.48 (td, *J* = 7.5, 1.4 Hz, 1H, *ArH*), 7.45–7.34 (m, 7H, *ArH*), 7.26–7.18 (m, 3H, *ArH*), 7.01–6.94 (m, 2H, *ArH*), 5.50 (d, *J* = 9.5 Hz, 1H, *NH*), 5.36 (ddd, *J* = 9.6, 6.4, 4.5 Hz, 1H, *NCH*), 3.17 (s, 3H, OCH₃), 2.65 (dd, *J* = 14.0, 4.4 Hz, 1H, 1 × CH₂), 2.54 (dd, *J* = 14.0, 6.3 Hz, 1H, 1 × CH₂) ppm; ¹³C NMR (126 MHz, CDCl₃): δ = 169.9 (C=O), 140.3 (*ArC*), 139.5 (*ArC*), 135.9 (*ArC*), 135.7 (*ArC*), 130.5 (*ArC*), 130.4 (*ArC*), 129.8 (2 × *ArC*), 128.9 (2 × *ArC*), 128.8 (2 × *ArC*), 128.7 (*ArC*), 128.4 (*ArC*), 128.1 (*ArC*), 127.7 (*ArC*), 126.8 (*ArC*), 81.2 (*NCH*), 56.2 (OCH₃), 41.2 (CH₂) ppm; IR (neat): ν = 3227m, 3055m, 3022m, 2955m, 2928m, 1641s, 1530s, 1099s, 1067s, 862s, 742s, 696s cm⁻¹; HRMS (ES): Exact mass calculated for C₂₁H₁₈NO [M-OMe+H]⁺ 300.1388; found 300.1377; HPLC analysis (55:44 *e.r.*): ¹D Varian Si-5 μm (250 × 4.6 mm) *n*-hexane/isopropanol 9:1 (v/v), 1.0 mL·min⁻¹, λ = 254 nm, retention time **285h** = 4.4 min; ²D YMC Chiral Amylose-C (250 × 4.6 mm, 5 μm), *n*-hexane/isopropanol 85:15 (v/v), 1.0 mL·min⁻¹, λ = 254 nm, overall retention time major isomer = 11.7 min, retention time minor isomer = 14.8 min. The HPLC chromatograms are reported in literature.⁴¹

6*H*-Benzo[*c*]chromen-6-one **294**:



Afforded as a side product. Colourless solid, m.p.: 84–86 °C.

¹H NMR (500 MHz, CDCl₃): δ = 8.41 (ddd, *J* = 7.9, 1.4, 0.6 Hz, 1H, *ArH*), 8.18–8.09 (m, 1H, *ArH*), 8.08 (dd, *J* = 7.9, 1.5 Hz, 1H, *ArH*), 7.84 (ddd, *J* = 8.1, 7.3, 1.4 Hz, 1H, *ArH*), 7.66–7.50 (m, 1H, *ArH*), 7.52–7.44 (m, 1H, *ArH*), 7.36 (dddd, *J* = 9.2, 8.0, 4.2, 0.8 Hz, 2H, *ArH*) ppm; ¹³C NMR (126 MHz, CDCl₃): δ = 161.4 (C=O), 151.4 (*ArC*-O), 135.0, 134.9, 130.7, 130.6, 129.0, 124.7, 122.9, 121.8, 121.4, 118.2, 118.0 ppm. The spectroscopic data are in agreement with the literature.⁴²

5.4.2.2 Synthesis of Racemates:

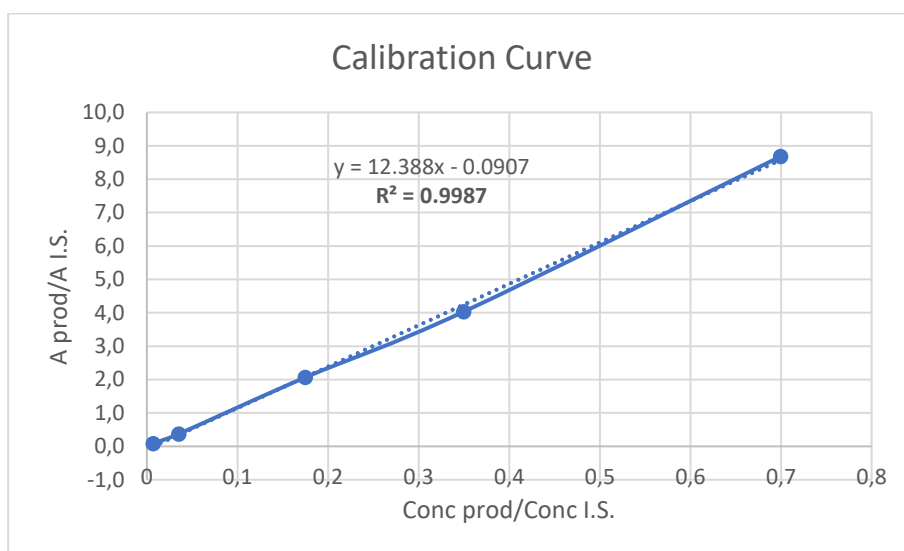
Rac-**285a,b,c** and **d** were synthesised *via* Shono oxidation from **293a–b** following the procedure reported in literature.³⁵

Rac-**285e–h** were obtained *via* non-Kolbe reaction starting from achiral **284c–f**.

5.4.3 DoE-assisted Optimisation

For the electrochemical step, an Ion Electrochemical reactor design by Vapourtec was used combined to a R-Series modular system. The solution was pumped using a Chemyx Fusion 200 syringe pump and the reactor was powered up by an Aim-tti bench power supply (300 Watt). The offline or online analysis was performed using an Agilent 1290 Infinity 2DLC system. The DoE was performed using Design Expert.⁹

Table 5.3: ¹D-HPLC calibration curve of the product **285a**.



Entry	266a (mg/mL)	Int Std ^a (µg/mL)	Area 266a (mAU)	Area Int Std (mAU)	$\frac{\text{Conc } \mathbf{266a}}{\text{Conc. Int Std}}$	$\frac{\text{Area } \mathbf{266a}}{\text{Area Int Std}}$
1	0.02	2.86	860.1	71.9	0.006993	0.0836
2	0.1	2.86	828.7	306.8	0.034965	0.3702
3	0.5	2.86	827.3	1707.45	0.1748252	2.0639
4	1	2.86	851.8	3433.35	0.3496503	4.0307
5	2	2.86	792	6872.5	0.6993007	8.6774

General HPLC protocol: Varian Si 250 × 4.6 mm, 5 µm pore size, *i*-PrOH / *n*-hexane 1:9, 1 mL·min⁻¹, 20 °C, λ = 254 nm; ^aInt Std = internal standard (*α,α,α*-trifluorotoluene as internal standard).

Table 5.4: Real and coded values (+1 = higher level, -1 = lower level, 0 = central point) for the independent variables (k) and responses.

Factor (k)	Type	Unit	-1	0	+1
A: (S)-284a	Numeric	mM	6.25	9.37	12.5
B: Anode	Categoric	-	graphite	-	glassy C
C: Flow rate	Numeric	mL•min ⁻¹	0.1	0.15	0.2
D: Charge	Numeric	F•mol ⁻¹	2	3	4
E: Temperature	Numeric	°C	-10	5	20
Responses:	285a yield (%)^a		285a ee (%)^b		

^aYield determined by ¹H NMR by HPLC using α,α,α -trifluorotoluene as internal standard;

^bDetermined by chiral HPLC.

Table 5.5: Experimental Matrix of the FFD 2⁵⁻¹ in coded values and factor generator E=A•B•C•D

Std	A	B	C	D	E = A•B•C•D
1	-1	-1	-1	-1	+1
2	+1	-1	-1	-1	-1
3	-1	+1	-1	-1	-1
4	+1	+1	-1	-1	+1
5	-1	-1	+1	-1	-1
6	+1	-1	+1	-1	+1
7	-1	+1	+1	-1	+1
8	+1	+1	+1	-1	-1
9	-1	-1	-1	+1	-1
10	+1	-1	-1	+1	+1
11	-1	+1	-1	+1	+1
12	+1	+1	-1	+1	-1
13	-1	-1	+1	+1	+1
14	+1	-1	+1	+1	-1
15	-1	+1	+1	+1	-1
16	+1	+1	+1	+1	+1
17	0	level 1	0	0	0 - level 1
18	0	level 2	0	0	0 - level 2

Table 5.4 entries 1 and 3 gave lower yield and ee% than expected, that were very influential according to the Cook's distance and other diagnostic plot, leading to a complex model with several significant terms and anomalous diagnostic plots.

Design-Expert® Software
yield
(adjusted for curvature)

Color points by value of
yield:
100
10

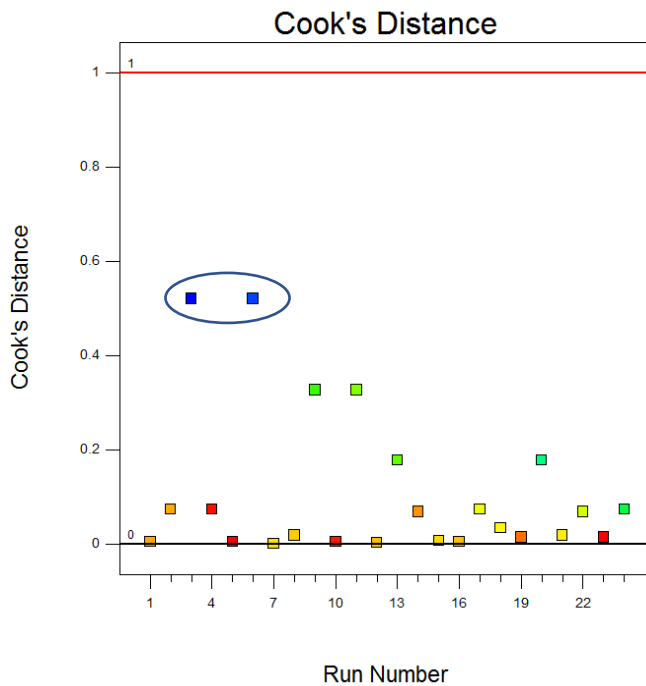


Figure 5.21: Cook's distance plot (yield).

Design-Expert® Software
yield
(adjusted for curvature)

Color points by value of
yield:
100
10

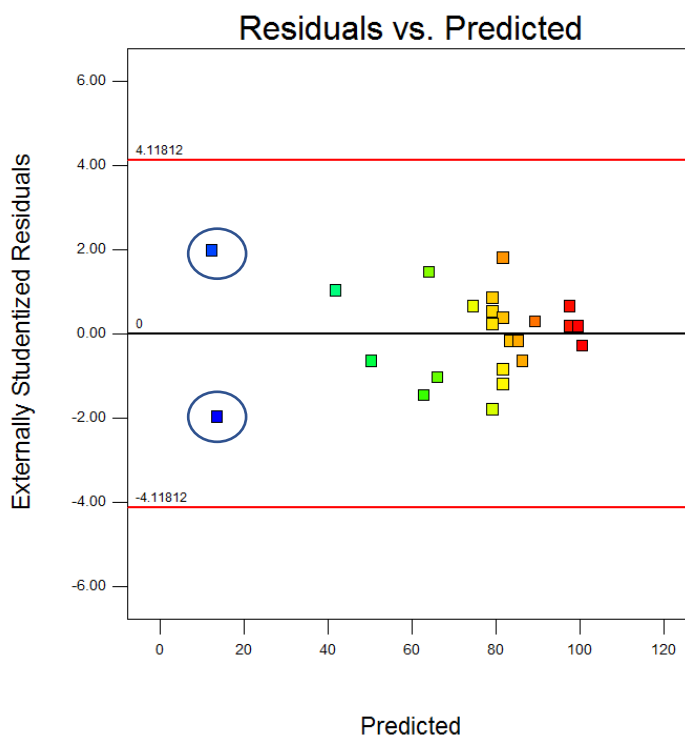


Figure 5.22: Residuals vs predicted diagnostic plot; "funnel" shape.

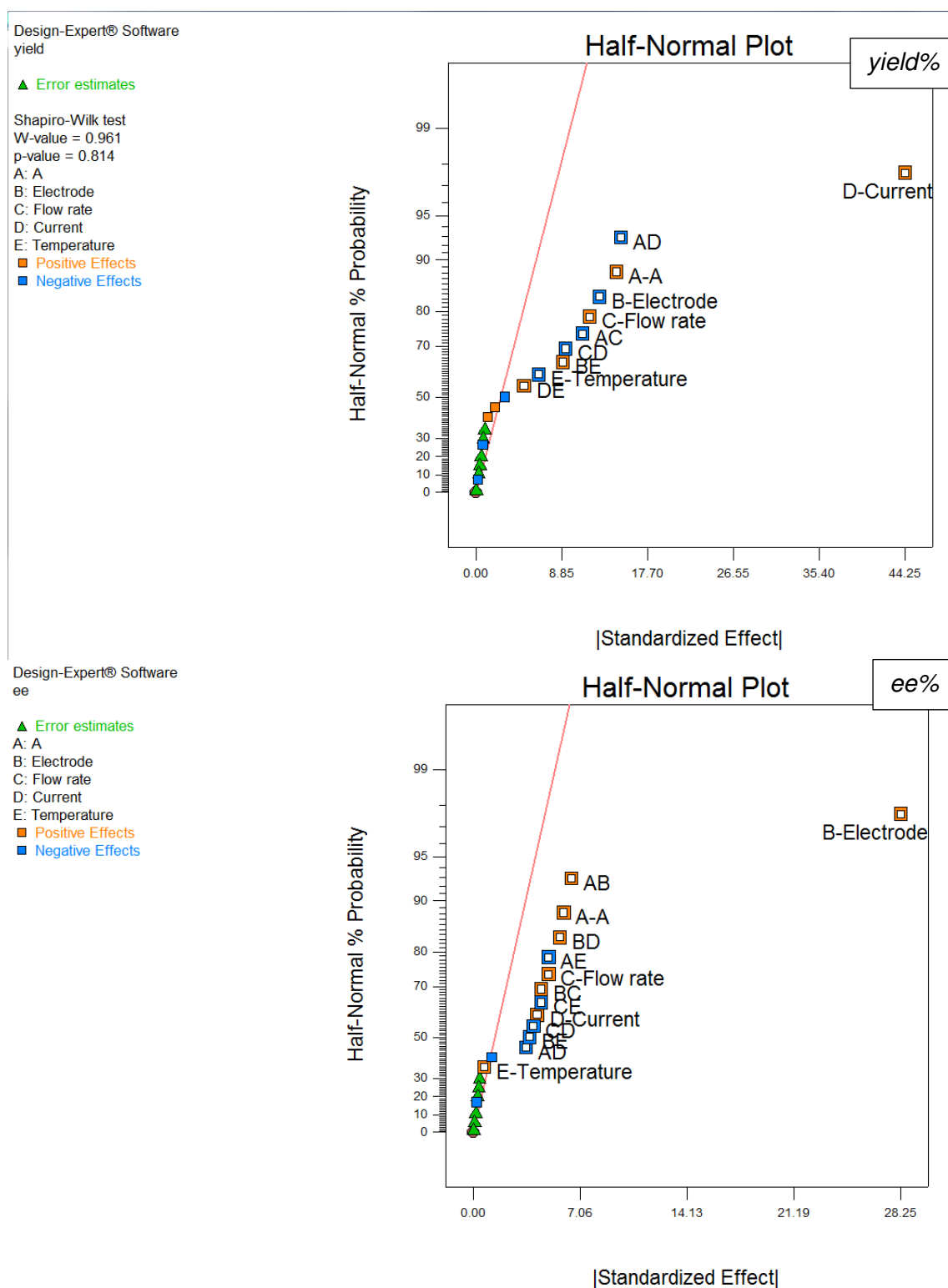


Figure 5.23: Half-normal plots for yield% and ee% considering all experiments.

After several repeats of the experiments and a careful evaluation, it was decided to not include the two experiments (Table 5.4 entries 1 and 3) as they were leading into a less interesting part of the chemical space (low yield and low ee). The ANOVA is reported in literature.⁴¹

a)

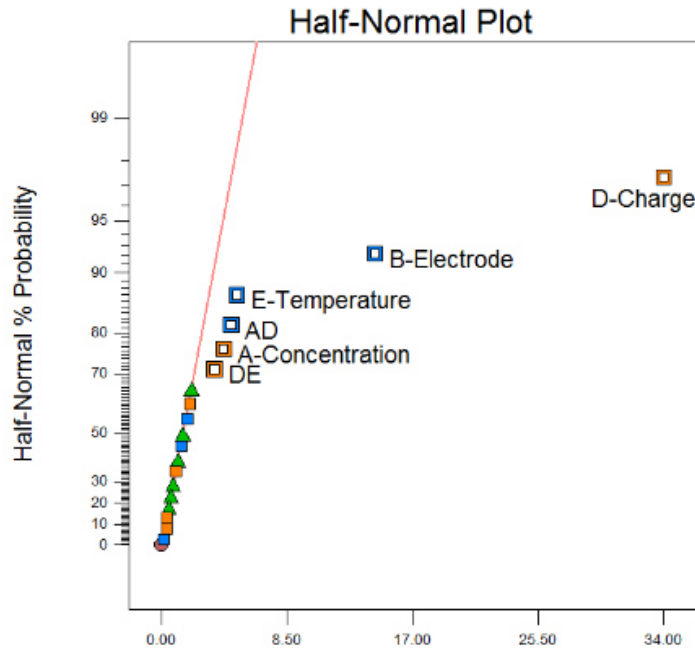
Design-Expert® Software
yield

▲ Error estimates

Shapiro-Wilk test
W-value = 0.960
p-value = 0.815

A: Concentration
B: Electrode
C: Flow rate
D: Charge
E: Temperature

■ Positive Effects
■ Negative Effects



b)

Design-Expert® Software
Log10(ee)

▲ Error estimates

Shapiro-Wilk test
W-value = 0.977
p-value = 0.947

A: Concentration
B: Electrode
C: Flow rate
D: Charge
E: Temperature

■ Positive Effects
■ Negative Effects

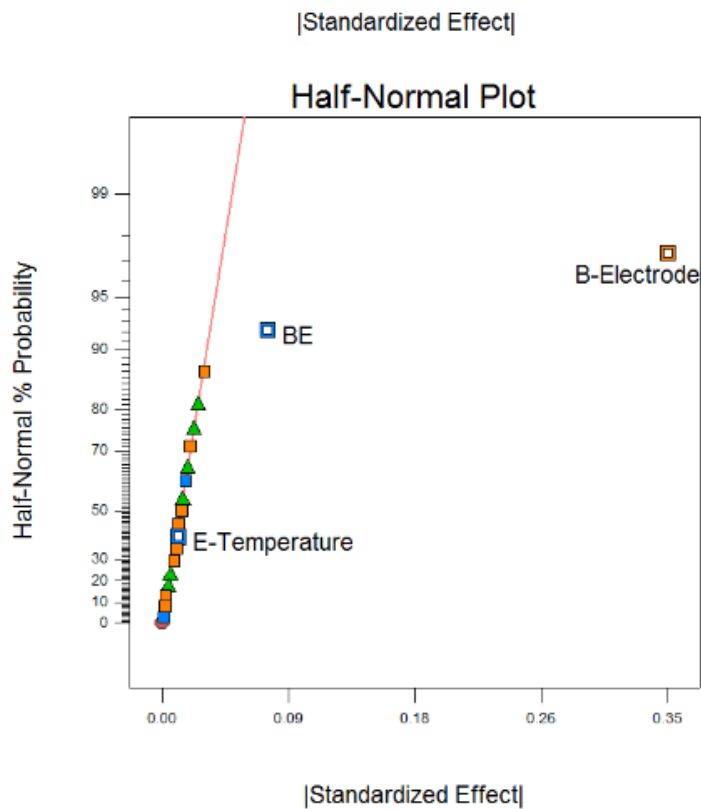


Figure 5.24: Half-normal plots for yield% and ee% without Std 1 and 3.

5.4.4 Cyclic Voltammetry

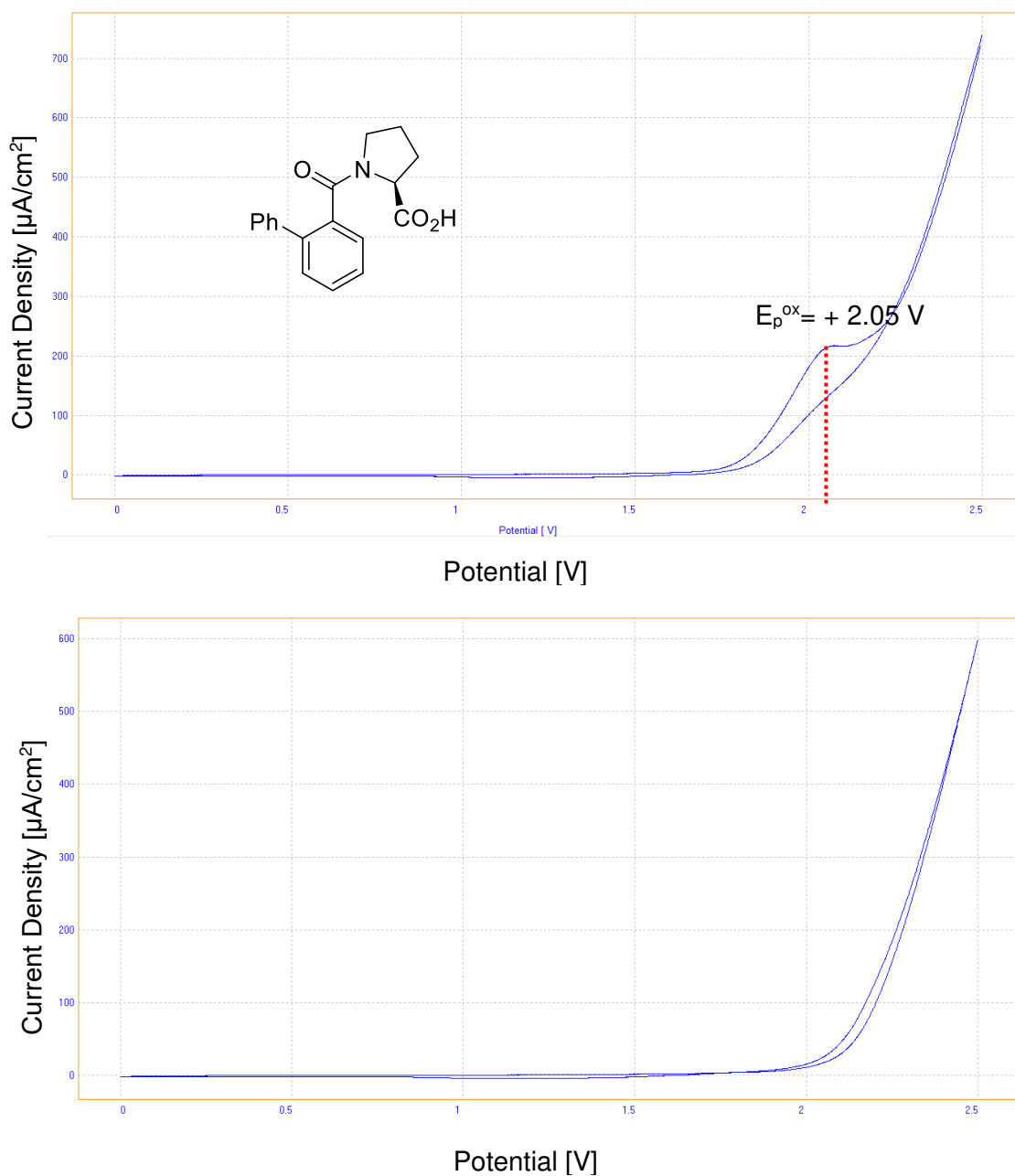


Figure 5.25: Oxidative cyclic voltammograms of the model substrate **285a** (5 mM) recorded in 0.1 M *n*-Bu₄NClO₄/MeOH electrolyte at 20 mV/s scan rate (top) and solvent background (bottom). Working electrode: glassy carbon electrode tip (3 mm diameter); Counter electrode: platinum wire; Reference electrode: Ag/AgCl in 3 M NaCl.

References

- 1 <https://www.vapourtec.com/products/flow-reactors/ion-electrochemical-reactor-features>.
- 2 J. Waser, B. Gaspar, H. Nambu, E. M. Carreira, *J. Am. Chem. Soc.* **2006**, *128*, 11693–11712.
- 3 S. Lee, H.-J. Lim, K. L. Cha, G. A. Sulikowski, *Tetrahedron*. **1997**, *53*, 16521–16532.
- 4 X. Guo, Z. Peng, S. Jiang, J. Shen, *Synth. Commun.* **2011**, *41*, 2044–2052.
- 5 Y. Motoyama, K. Kamo, H. Nagashima, *Org. Lett.* **2009**, *11*, 1345–1348.
- 6 T. Jensen, R. Madsen, *J. Org. Chem.* **2009**, *74*, 3990–3992.
- 7 W.-W. Chan, S.-H. Yeung, Z. Zhou, A. S. C. Chan, W.-Y. Yu, *Org. Lett.* **2010**, *12*, 604–607.
- 8 J. Waser, B. Gaspar, H. Nambu, E. M. Carreira, *J. Am. Chem. Soc.* **2006**, *128*, 11693–11712.
- 9 The software can be found at: <https://www.statease.com/software/design-expert>. A copy of the design files (.dpx) was submitted to Cardiff University together with this manuscript.
- 10 M. Santi, S. T. R. Müller, A. A. Folgueiras-Amador, A. Uttry, P. Hellier, T. Wirth, *Eur. J. Org. Chem.* **2017**, 1889–1893.
- 11 a) U. Mayer, V. Gutmann, W. Gerger, *Monats. Chem.* **1975**, *106*, 1235–1257; b) M. A. Beckett, G. C. Strickland, J. R. Holland, K. S. Varma, *Polymer* **1996**, *37*, 4629–4631.
- 12 H. Keipour, T. Ollevier, *Org. Lett.* **2017**, *19*, 5736–5739.
- 13 L. Huang, W. D. Wulff, *J. Am. Chem. Soc.* **2011**, *133*, 8892–8895.
- 14 J. M. Percy, H. Emerson, J. W. B. Fyfe, A. R. Kennedy, S. Maciuk, D. Orr, L. Rathouská, J. M. Redmond, P. G. Wilson, *Chem. Eur. J.* **2016**, *22*, 12166–12175.
- 15 M. Durandetti, C. Gosmini, J. Périchon, *Tetrahedron* **2007**, *63*, 1146–1153.
- 16 I. Kim, C. Lee, *Angew. Chem. Int. Ed.* **2013**, *52*, 10023–10026.
- 17 A. Dhamkshinamoorhy, A. Sharmila, K. Pitchumani, *Chem. Eur. J.* **2010**, *16*, 1128–1132.
- 18 S. M. Altermann, R. D. Richardson, T. K. Page, R. K. Schmidt, E. Holland, U. Mohammed, S. M. Paradine, A. N. French, C. Richter, A. Masih Bahar, B. Witulski, T. Wirth. *Eur. J. Org. Chem.* **2008**, 5315–5328.
- 19 H. M. L. Davies, T. Hansen, M. R. Churchill, *J. Am. Chem. Soc.* **2000**, *122*, 3063–3070.
- 20 W.-W. Chan, S.-H. Yeung, Z. Zhou, A. S. C. Chan, W.-Y. Yu, *Org. Lett.* **2010**, *12*, 604–607.
- 21 H. Tomioka, N. Ichikawa, K. Komatsu, *J. Am. Chem. Soc.* **1992**, *114*, 8045–8053.
- 22 H. M. L. Davies, R. J. Townsend, *J. Org. Chem.* **2001**, *66*, 6595–6603.
- 23 C. Y. Im, T. Okuyama, T. Sugimura, *Eur. J. Org. Chem.* **2008**, 285–294.
- 24 Y. Landais, D. Planchenaul, *Tetrahedron* **1997**, *53*, 2855–2870.
- 25 L. Zhou, M. P. Doyle, *J. Org. Chem.* **2009**, *74*, 9222–9224.
- 26 P. Fleming, D. F. O'Shea, *J. Am. Chem. Soc.* **2011**, *133*, 1698–1701.
- 27 M. J. Williams, Q. Chen, L. Codan, R. K. Dermenjian, S. Dreher, A. W. Gibson, X. He, Y. Jin, S. P. Keen, A. Y. Lee, D. R. Lieberman, W. Lin, G. Liu, M. McLaughlin, M. Reibarkh J. P. Scott, S. Strickfuss, L. Tan, R. J. Varsolona, F. Wen, *Org. Process Res. Dev.* **2016**, *20*, 1227–1238.
- 28 P.-A. Chen, K. Setthakarn, J. A. May, *ACS Catal.* **2017**, *7*, 6155–616.

- 29 H. Saito, H. Oishi, S. Kitagaki, S. Nakamura, M. Anada, S. Hashimoto, *Org. Lett.* **2002**, *4*, 3887–3890.
- 30 E. Mannekens, D. Tourwé, W. D. Lubellb, *Synthesis* **2000**, 1214–1216.
- 31 B. A. Sandoval, A. J. Meichan, T. K. Hyster, *J. Am. Chem. Soc.* **2017**, *139*, 11313–11316.
- 32 E. W. H. Ng, K.-H. Low, P. Chiu, *J. Am. Chem. Soc.* **2018**, *140*, 3537–3541.
- 33 J. Ghorai, P. Anbarasan, *J. Org. Chem.* **2015**, *80*, 3455–3461.
- 34 J. Yan, Z. Zhou, M. Zhu, *Tetrahedron Lett.* **2005**, *46*, 8173–8175.
- 35 M. A. Kabeshov, B. Musio, P. R. D. Murray, D. L. Browne, S. V. Ley, *Org. Lett.* **2014**, *16*, 4618–4621.
- 36 P. Nareddy, F. Jordana, M. Szostak, *Chem. Sci.* **2017**, *8*, 3204–3210.
- 37 T. Yamada, Y. Ozaki, M. Yamawaki, Y. Sugiura, K. Nishino, T. Morita, Y. Yoshimi, *Tetrahedron Lett.* **2017**, *58*, 835–838.
- 38 M. Branca, S. Pena, R. Guillot, D. Gori, V. Alezra, C. Kouklovsky, *J. Am. Chem. Soc.* **2009**, *131*, 10711–10718.
- 39 G. Han, M. G. LaPorte, M. C. McIntosh, S. M. Weinreb, *J. Org. Chem.* **1996**, *61*, 9483.
- 40 Y. Matsumura, T. Tanaka, G. N. Wanyoike, T. Maki, O. Onomura, *J. Electroanal. Chem.* **2001**, *507*, 71–74.
- 41 M. Santi, J. Seitz, R. Cicala, T. Hardwick, N. Ahmed, T. Wirth, *Chem. Eur. J.* **2019**, *25*, 16230–16235.
- 42 L. Li, Q. Yang, Z. Jia, S. Luo, *Synthesis* **2018**, *50*, 2924–2929.

Appendix A: Glossary of DoE Terminology

Herein a glossary of terminologies and definitions regarding Design of Experiment is reported.¹

2-Level Design: It is a set of experiments where all the factors are set at one of two levels (low = -1; high = +1).

Alias (Aliasing): When the estimate of an effect also includes the influence of one or more other effects (e.g.: high order *interactions*), and they cannot be separated and assigned. The effects are said to be “aliased”.

Analysis of Variance (ANOVA): A mathematical process that measures whether a factor contributes significantly to the variance of a response and which amount of variance is due to pure error.

Axial Point: In a Central Composite Design (CCD) are those points that distance from the centre of a cube to a star portion of the design. The star portion of the design consists of an additional set of points arranged at equal distances from the centre of the cube on radii that pass through the centre point in the face of the cube. They afford an estimate of the experimental error variance to the entity of the curvature.

Balanced Design: An experimental design where all points have the same number of observations.

Blocking: It is achieved by restricting randomisation by blocking the experiments into homogenous groups. The reason for blocking is to isolate a systematic effect (*nuisance*) and prevent it from obscuring the main effects (e.g.: blocks can be created when it is necessary to include new batches of raw material, different laboratories, etc...). The runs must be randomised within the blocks.

Central Composite Design (CCD): A 3-level design that starts with a 2-level factorial and some centre points. Used typically for quantitative factors and designed to estimate all the main effects plus the desired quadratics and two-factor interactions (2FI).

Central Point: Are design points at which all the continuous factors are run halfway between their high and low levels. The centre points can be used to check for curvature in screening designs as well as to add additional runs to experiments (*Repeats*) to estimate pure error.

Coded Value: It is generated by transforming the scale of measurement for a factor so that the high value becomes +1 and the low value becomes -1. Coding is a simple linear transformation of the original measurement scale. The coded values are used for convenience of computation and comparison of effects between different factors.

Confounding: Confusing two or more factors so their main effects cannot be separated (see *Aliasing*). Confounding designs naturally arise when full factorial designs have to be run in blocks and the block size is too small. They also occur whenever a fractional factorial design is chosen instead of a full factorial design.

Contour Plot: A plot that represents a two-dimensional grid surface similar to a topographical map. In experimental design, the contours represent the estimated level of the response variable.

Curvature: The degree of curving for a line or surface.

Design: A set of experimental runs which allows you to fit a particular model and estimate the desired effects.

Design Matrix: It is a compact representation of the experiments to run, which shows the factors level combinations and associated response values in a table.

Design of Experiment (DoE): It is a statistical technique that allows you to run the minimum number of experiments to optimise your product or process. It is defined by a list of experiments to run in order to fit the mathematical model.

Design Points: An intended experimental run.

Diagnostic Plot: is a scatterplot of the prediction errors (residuals) against the predicted values and is used to see if the predictions can be improved by fixing problems in your data.

Effect: It is the change in the average of the responses between two factor-level combinations or two experimental settings. For a factor A with two levels, scaled so that low = -1 and high = +1, the effect of A is estimated by subtracting the average response when A is -1 from the average response when A = +1 and dividing the result by 2. It gives an estimate of how changing the settings of a factor changes the response. The effect of a single factor is also called a *Main Effect*.

Error: Unexplained variation in a collection of observations.

F-Ratio: A ratio of the variance explained by a factor to the unexplained variance. If there is no effect, the associated *p*-value is close to 1.

Factor: It is a parameter (input) which is deliberately varied in an experiment in order to determine its effect on one or more responses (output). Some factors cannot be controlled by the experimenter but may affect the responses. If their effect is significant, these uncontrolled factors should be measured and used in the data analysis. The inputs can be:

Numerical: Are quantitative variables which can be:

- Continuous: Are numerical variables in which infinite number of values between two given points are accepted.
- Discrete: Are numerical variables that have a countable number of values within the limits.

Categoric: Are qualitative variables which contain a finite number of categories or distinct groups, which may not have a logical order (e.g. material types, solvent types).

Face-Centered Design (FCD): A central composite design (CCD) with three levels and with axial points at the centre of the faces of the factorial cube instead of the curve.

Factor Range: It is the range of values within the highest and the lowest levels.

Factorial Generator: Equations that indicate the columns that must be multiplied to produce the last columns in a Fractional Factorial Design (FFD).

Factorial Point: Are the points at the extremes, used to estimate the coefficients of the linear and the interaction terms.

Fractional Factorial Design (FFD): Differs from a *Full Factorial Design* (FD) as the FFD does not specify all the combinations of the factors. Instead, the operator uses a subset of a FD (number of experiments = 2^{k-n} , with k being the number of factors and n the number of *Factorial Generator*).

Full Factorial (FD): A design that combines the levels for each factor with all the levels for every other factor (number of experiments = 2^k , with k being the number of factors).

Graphical Optimisation: It is used to simultaneously optimise multiple responses by overlapping the contour plots of every response. The area in which the optimal criteria for each response is satisfied (*Sweet Spot*) is usually highlighted.

Half-Normal Plot: It is a graphical tool that uses ordered estimated effects to assess which factors are important (larger than the noise) and which are unimportant. Large effects appear on the right side of the plot.

Hard-to-Change (HTC): Are factor that are hard to change quickly and might restrict the randomisation.

Interaction Effect: Occurs when a change in the response depends on the combination of multiple factors levels. An interaction involving two factors is known as a two-factor interaction (2FI), three factors as a three-factor interaction (etc).

Lack of Fit Error: Error that occurs when the analysis omits one or more important terms or factors from the process model.

Main Effect: A measure that estimates the influence of a single factor on a response when the factor is changed from one level to another.

Model: Mathematical relationship which relates changes in a measured response to changes in one or more factors.

Noise: Any unexplained or random variability in the response.

Normal distribution: The “bell-shaped” curve distribution used to calculate probabilities of events that tend to occur around a mean value and trail off with decreasing likelihood (*Gaussian Distribution*).

Normal Plot: It is a graphical tool that uses ordered estimated effects to assess which factors are important (larger than the noise) and which are unimportant. A default plot is shown in which it is assumed there are no significant parameters, hence all the points fall on a straight line. Any points that fall away from the line indicate real effects.

Nuisance Variable: Factors that are not included or cannot be controlled in a design that will can distort the results, if not held constant or controlled through randomisation.

One factor at a time (OFAT): A method where one factor is changed while all the others are kept constant. The method ignores the possibility of interactions.

One variable at a time (OVAT): synonym of OFAT

Orthogonality: A design where the correlation between factors is zero which means that all estimates can be obtained independently of one another.

Outliner: It is a data point that does not fit the model.

p-Value: The probability value or p -value is the probability of obtaining test results at least as extreme as the results actually observed during the test, assuming that the null hypothesis is correct (p -value > 0.05 are statistically insignificant; p -value < 0.05 are statistically significant).

Pareto Chart: A graph that shows the amount of influence each factor has on the response in order of decreasing influence.

Pure Error: The sums of squares from replicated environmental runs. Pure error provides an opportunity to test for lack-of-fit in the fitted model.

Randomisation: A system of using random numbers to evenly spread the effects of factors not included in an experiment (nuisance variables). Randomisation is necessary for conclusions to be correct, unambiguous and defensible.

Repeat: Performing the same treatment combination more than once.

Replicate: Is a duplicate set of complete runs from the complete design.

Resolution: Measure of the degree of confounding. Low-resolution designs are highly confounded and can only give limited information about the system under investigation.

Response: It is the property of the system that is being measured (output). For example, yield, purity, ee%.

Response Surface Methodology (RSM): A DoE that fully explores the process window and models the responses. Note: These designs are most effective when there are less than 5 factors. Quadratic models are used for response surface designs and at least three levels of every factor are needed in the design.

Run: A set of experimental conditions in which each of the factors is held at a specific level.

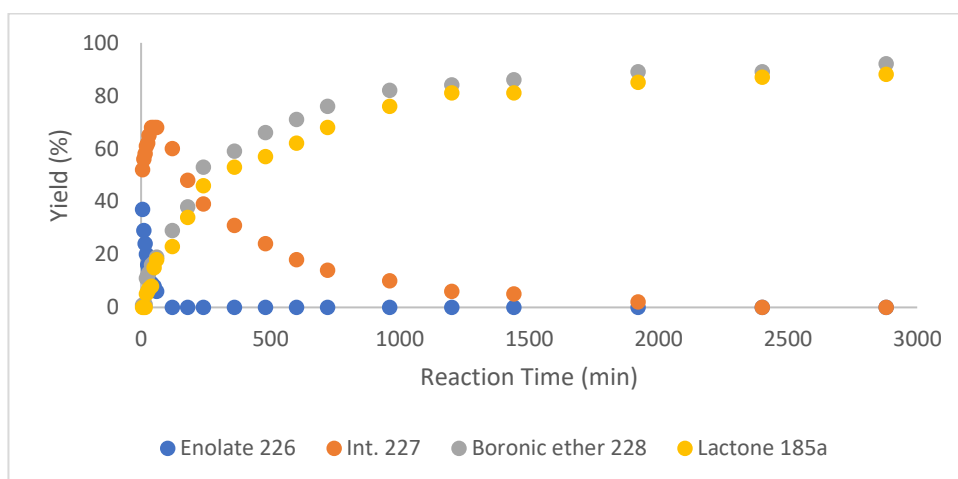
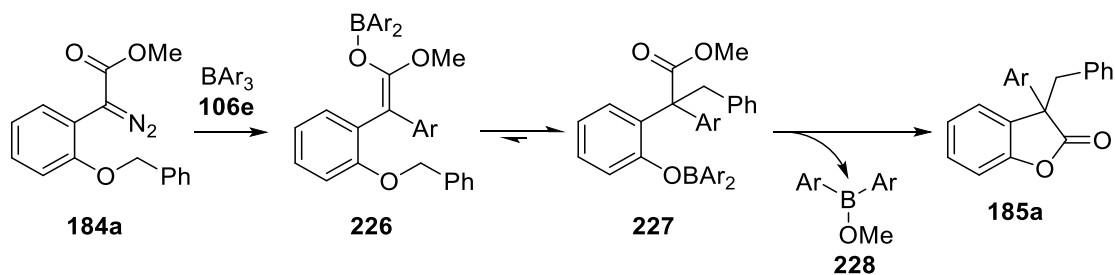
Screening Experiments: A screening experiment is used to identify the significant few factors that contribute the most to response variation.

Sweet Spot: In a graphical optimisation is the area in which the optimal criteria for each response is satisfied.

Treatment Combination: It is a set of factors and their levels; in other words, it is an entry of the design matrix.

Variable: Synonym of *Factor*

1 a) H. Tye, *Drug Discov. Today* **2004**, *11*, 485–491; b) J. A. Wass, *J. Valid. Technol.* **2010**, 49–57; c) Stat-Ease, Design of Expert v 10.01, *Handbook for Experimenters*, **2016**; d) NIST-SEMATECH, e-Handbook of Statistical Methods, <http://www.itl.nist.gov/div898/handbook/>, **2013**.

Appendix B: Kinetic Data Table for **185a** Formation

Entry	Time (min)	226 (%)	227 (%)	228 (%)	185a (%)
1	5	37	52	0,8	0
2	10	29	56	0,9	0
3	15	24	58	1	0
4	20	20	61	11	5
5	25	16	62	12	6
6	30	14	65	13	7
7	40	9	68	16	8
8	50	8	68	17	15
9	60	6	68	19	18
10	120	0	60	29	23
11	180	0	48	38	34
12	240	0	39	53	46
13	360	0	31	59	53
14	480	0	24	66	57
15	600	0	18	71	62
16	720	0	14	76	68
17	960	0	10	82	76
18	1200	0	6	84	81
19	1440	0	5	86	81
20	1920	0	2	89	85
21	2400	0	0	89	87
22	2880	0	0	92	88

Kinetic study for the formation of lactone **185a**. The reaction between **184a** (0.05 mmol) and **106e** (0.05 mmol) was run and *in situ* ¹H NMR (500 MHz, CDCl₃) spectra were measured at different time intervals using mesitylene as the internal standard; Ar = 3,4,5-F₃C₆H₂.